

STUDIES TOWARD THE TOTAL SYNTHESIS OF  
HMP-Y1 AND HIBARIMICINONE

By

Jonathan Edward Hempel

Dissertation

Submitted to the Faculty of the  
Graduate School of Vanderbilt University  
in partial fulfillment of the requirements  
for the degree of

DOCTOR OF PHILOSOPHY

in

Chemistry

May, 2013

Nashville, Tennessee

Approved:

Professor Gary A. Sulikowski

Professor Jeffrey N. Johnston

Professor Brian O. Bachmann

Professor Craig W. Lindsley

For Nicola

Mom and Dad

Amy and Jennifer



## ACKNOWLEDGEMENTS

First, I must express my sincerest thanks to Dr. Gary Sulikowski for his guidance and support throughout my graduate career. He always pushed me to continue learning, to never stop reading, and to think out of the box for problems with no readily apparent solution. His commitment to my education will certainly carry me throughout the remainder of my career, and for that I am deeply indebted.

I would like to thank my committee, Dr. Jeffrey Johnston, Dr. Brian Bachmann, and Dr. Craig Lindsley for their helpful discussions about research and other topics during my formal committee meetings and outside. Having a broad group of perspectives on research and careers has supported my education and growth as a chemist. Additionally, I am grateful to Dr. Don Stec for his extensive help with running and interpreting NMRs on which much of my research has relied.

Throughout the years, the Sulikowski group has always been a fantastic place to work and learn. Many people have come and gone, and each and every one has had an impact on my graduate school experience. Dr. Darren Engers and Dr. Bruce Melancon have provided extremely valuable guidance for me and my research, and our non-science conversations have always been a welcome diversion from the daily grind. Many other former members need acknowledgement as well, specifically Dr. Aleksandra Baranczak, Dr. Stephen Chau, Dr. Steven Townsend, Dr. Brian Smith, Dr. Jesse Teske, Dr. Ian Romaine, and Dr. Kwangho Kim, for aiding in my education as well as creating a great atmosphere to come to every morning. For these same reasons, I am appreciative of

current Sulikowski group members, Sean DeGuire, Marta Wenzler, Bobby Boer, Brendan Dutter, and Nina Collins, who have undoubtedly helped me retain my sanity.

Other members of the Vanderbilt community have helped make memories from graduate school and Nashville that I will always remember, namely Dawn Makley, Mark Dobish, Priya Mathew, Ryan Meier, Jeff Enders, Carly Enders, and Julia Dobish. I couldn't have asked for a better group of friends to spend time with in and out of lab.

I would like to acknowledge Dr. John Gupton, my undergraduate research advisor at the University of Richmond, for building the foundation of my research interests that started in my sophomore year of college. His support and encouragement led me to graduate school and ultimately to my career as a scientist.

Without question, I would not be where I am currently without the unending love and support of my family. They have always stood behind my dreams and allowed me to believe that anything was within reach with hard work. They have sacrificed much for my benefit, and I will never be able to adequately express my appreciation for everything they have given me.

Finally, I owe my sincerest gratitude to my wife, Nicola. The past five years have been a true rollercoaster of emotions, and I don't want to imagine what they would have been like without her by my side. She has been and continues to be my rock, and her unwavering love and support has been the foundation of my success in graduate school. She continually inspires me to improve myself and the world around me, and I treasure her love and friendship above all else in my life.

## TABLE OF CONTENTS

	Page
DEDICATION .....	ii.
ACKNOWLEDGEMENTS .....	iii.
LIST OF FIGURES .....	vii.
LIST OF SCHEMES .....	xv.
LIST OF ABBREVIATIONS .....	xxii.
 Chapter	
I. NATURALLY OCCURRING AROMATIC POLYKETIDES .....	1.
Secondary Metabolites and Their Medicinal Properties .....	1.
Aromatic Polyketide Biosynthesis .....	2.
Synthetic Approaches to Aromatic Polyketides .....	9.
Angelmicins A and B .....	20.
The Hibarimicin Family of Aromatic Polyketide Natural Products .....	24.
Biosynthesis of the Hibarimicins .....	28.
Atropisomerism and Natural Product Total Synthesis .....	33.
Atropisomerism and the Hibarimicins .....	42.
Conclusion .....	48.
References .....	48.
II. THE DIELS-ALDER REACTION IN NATURAL PRODUCT TOTAL SYNTHESIS .....	54.
Origin and History of the Diels-Alder Reaction .....	54.
Diels-Alder Mechanistic Details .....	55.
Applications of the Diels-Alder to Total Synthesis .....	63.
Previous Synthetic Studies Toward the Hibarimicins .....	69.
Total Syntheses of HMP-Y1 and Hibarimicinone .....	85.
Conclusion .....	96.
References .....	97.
III. A TWO DIRECTIONAL SYNTHETIC APPROACH .....	100.
Synthetic Analysis Toward HMP-Y1 and Hibarimicinone .....	100.
Romaine's Work Toward the Biaryl Core .....	101.
Engers' Work Toward the AB-Decalin .....	105.

	An Improved Route to the AB-Enone Precursor .....	115.
	Toward a Substrate-Controlled Tertiary Alcohol Formation.....	123.
	Conclusion .....	127.
	Experimental Methods .....	128.
	References.....	151.
	Appendix A1: Spectra Relevant to Chapter III.....	154.
IV.	A TRANSANNULAR DIELS-ALDER-ENABLED BIOMIMETIC DIMERIZATION APPROACH .....	173.
	Access to Single Biaryl Atropisomers .....	173.
	Biomimetic Dimerization Synthetic Analysis .....	177.
	First Generation TADA Approach.....	179.
	Second Generation TADA Approach .....	184.
	A New A-Ring Surrogate from Quinic Acid .....	190.
	The Terminal Alkyne Series for Southern Tethering .....	200.
	The Propargylic Alcohol Series for Macrocycle Formation.....	212.
	Conclusion .....	215.
	Experimental Methods .....	216.
	References.....	255.
	Appendix A2: Spectra Relevant to Chapter IV.....	259.
V.	AN INTRAMOLECULAR DIELS-ALDER-ENABLED DIMERIZATION APPROACH AND BEYOND .....	301.
	A Modified D-Ring Protecting Group and Synthetic Analysis .....	301.
	Building Block Synthesis Toward an Alkynyl IMDA Precursor .....	305.
	A Southern-Tethered Alkynyl IMDA.....	308.
	Toward a Southern-Tethered Alkenyl IMDA Substrate.....	311.
	Third Generation Southern-Tethered IMDA Approach .....	315.
	Revisiting Synthesis of a TADA Substrate.....	321.
	Future Directions .....	330.
	Conclusion .....	337.
	Experimental Methods .....	337.
	References.....	373.
	Appendix A3: Spectra Relevant to Chapter V .....	376.

## LIST OF FIGURES

Figure	Page
1.1. Historically important secondary metabolites. ....	1.
1.2. Biologically important examples of polyketide natural products. ....	4.
1.3. Examples of tetracycline family members. ....	9.
1.4. Two-dimensional structure of angelmicin B. ....	24.
1.5. Key COSY and NOE/NOESY correlations for hibarimicin B. ....	27.
1.6. The hibarimicin family of natural products. ....	28.
1.7. Important compounds exhibiting atropisomerism. ....	34.
1.8. Nomenclature standards for atropisomers. ....	35.
1.9. Computational and experimental model system CD spectra. ....	47.
2.1. Frontier molecular orbital analysis of Diels-Alder electronics. ....	56.
2.2. Diels-Alder motifs of increasing molecular complexity. ....	61.
2.3. Determination of hibarimicinone absolute stereochemistry. ....	84.
2.4. Absolute stereochemistry of hibarimicin B. ....	85.
A1.1. <sup>1</sup> H NMR spectrum (400 MHz, CDCl <sub>3</sub> ) and <sup>13</sup> C NMR spectrum (100 MHz, CDCl <sub>3</sub> ) of compound <b>3.34</b> . ....	155.
A1.2. <sup>1</sup> H NMR spectrum (400 MHz, CDCl <sub>3</sub> ) of compound <b>3.54</b> . ....	156.
A1.3. <sup>1</sup> H NMR spectrum (400 MHz, CDCl <sub>3</sub> ) and <sup>13</sup> C NMR spectrum (100 MHz, CDCl <sub>3</sub> ) of compound <b>3.55</b> . ....	157.
A1.4. <sup>1</sup> H NMR spectrum (400 MHz, CDCl <sub>3</sub> ) and <sup>13</sup> C NMR spectrum (100 MHz, CDCl <sub>3</sub> ) of compound <b>3.38</b> . ....	158.
A1.5. <sup>1</sup> H NMR spectrum (500 MHz, CDCl <sub>3</sub> ) and <sup>13</sup> C NMR spectrum (125 MHz, CDCl <sub>3</sub> ) of compound <b>3.39</b> . ....	159.

A1.6.	$^1\text{H}$ NMR spectrum (500 MHz, $\text{CDCl}_3$ ) and $^{13}\text{C}$ NMR spectrum (125 MHz, $\text{CDCl}_3$ ) of compound <b>3.64</b> .....	160.
A1.7.	$^1\text{H}$ NMR spectrum (400 MHz, $\text{CDCl}_3$ ) and $^{13}\text{C}$ NMR spectrum (100 MHz, $\text{CDCl}_3$ ) of compound <b>3.65</b> .....	161.
A1.8.	COSY spectrum (500 MHz, $\text{CDCl}_3$ ) and NOESY spectrum (500 MHz, $\text{CDCl}_3$ ) of compound <b>3.65</b> .....	162.
A1.9.	$^1\text{H}$ NMR spectrum (400 MHz, $\text{CDCl}_3$ ) and $^{13}\text{C}$ NMR spectrum (100 MHz, $\text{CDCl}_3$ ) of compound <b>3.68</b> .....	163.
A1.10.	$^1\text{H}$ NMR spectrum (600 MHz, $\text{CDCl}_3$ ) and $^{13}\text{C}$ NMR spectrum (150 MHz, $\text{CDCl}_3$ ) of compound <b>3.67</b> .....	164.
A1.11.	$^1\text{H}$ NMR spectrum (400 MHz, $\text{CDCl}_3$ ) and $^{13}\text{C}$ NMR spectrum (100 MHz, $\text{CDCl}_3$ ) of compound <b>S3.5</b> .....	165.
A1.12.	$^1\text{H}$ NMR spectrum (400 MHz, $\text{CDCl}_3$ ) and $^{13}\text{C}$ NMR spectrum (100 MHz, $\text{CDCl}_3$ ) of compound <b>S3.6</b> .....	166.
A1.13.	$^1\text{H}$ NMR spectrum (500 MHz, $\text{CDCl}_3$ ) and $^{13}\text{C}$ NMR spectrum (100 MHz, $\text{CDCl}_3$ ) of compound <b>3.70</b> .....	167.
A1.14.	$^1\text{H}$ NMR spectrum (400 MHz, $\text{CDCl}_3$ ) of compound <b>S3.7</b> and $^1\text{H}$ NMR spectrum (400 MHz, $\text{CDCl}_3$ ) of compound <b>3.78</b> .....	168.
A1.15.	$^1\text{H}$ NMR spectrum (400 MHz, $\text{CDCl}_3$ ) and $^{13}\text{C}$ NMR spectrum (100 MHz, $\text{CDCl}_3$ ) of compound <b><math>\alpha</math>-3.79</b> .....	169.
A1.16.	$^1\text{H}$ NMR spectrum (400 MHz, $\text{CDCl}_3$ ) and $^{13}\text{C}$ NMR spectrum (100 MHz, $\text{CDCl}_3$ ) of compound <b>3.80</b> .....	170.
A1.17.	$^1\text{H}$ NMR spectrum (400 MHz, $\text{CDCl}_3$ ) and $^{13}\text{C}$ NMR spectrum (100 MHz, $\text{CDCl}_3$ ) of compound <b>3.81</b> .....	171.
A1.18.	$^1\text{H}$ NMR spectrum (400 MHz, $\text{CDCl}_3$ ) and $^{13}\text{C}$ NMR spectrum (100 MHz, $\text{CDCl}_3$ ) of compound <b>3.82</b> .....	172.
A2.1.	$^1\text{H}$ NMR spectrum (400 MHz, $\text{CDCl}_3$ ) and $^{13}\text{C}$ NMR spectrum (100 MHz, $\text{CDCl}_3$ ) of compound <b>4.23</b> .....	260.
A2.2.	$^1\text{H}$ NMR spectrum (600 MHz, $\text{CDCl}_3$ ) and $^{13}\text{C}$ NMR spectrum (150 MHz, $\text{CDCl}_3$ ) of compound <b>4.24</b> .....	261.

A2.3.	$^1\text{H}$ NMR spectrum (400 MHz, $\text{CDCl}_3$ ) and $^{13}\text{C}$ NMR spectrum (100 MHz, $\text{CDCl}_3$ ) of compound <b>4.31</b> .....	262.
A2.4.	$^1\text{H}$ NMR spectrum (400 MHz, $\text{CDCl}_3$ ) and $^{13}\text{C}$ NMR spectrum (100 MHz, $\text{CDCl}_3$ ) of compound <b>4.32</b> .....	263.
A2.5.	$^1\text{H}$ NMR spectrum (400 MHz, $\text{CDCl}_3$ ) and $^{13}\text{C}$ NMR spectrum (100 MHz, $\text{CDCl}_3$ ) of compound <b>4.39</b> .....	264.
A2.6.	$^1\text{H}$ NMR spectrum (400 MHz, $\text{CDCl}_3$ ) of compound <b>4.41</b> .....	265.
A2.7.	$^1\text{H}$ NMR spectrum (400 MHz, $\text{CDCl}_3$ ) and $^{13}\text{C}$ NMR spectrum (100 MHz, $\text{CDCl}_3$ ) of compound <b>4.42</b> .....	266.
A2.8.	$^1\text{H}$ NMR spectrum (400 MHz, $\text{CDCl}_3$ ) and $^{13}\text{C}$ NMR spectrum (100 MHz, $\text{CDCl}_3$ ) of compound <b>4.40</b> .....	267.
A2.9.	$^1\text{H}$ NMR spectrum (400 MHz, $\text{CDCl}_3$ ) and $^{13}\text{C}$ NMR spectrum (100 MHz, $\text{CDCl}_3$ ) of compound <b>4.46</b> .....	268.
A2.10.	$^1\text{H}$ NMR spectrum (400 MHz, $\text{CDCl}_3$ ) and $^{13}\text{C}$ NMR spectrum (100 MHz, $\text{CDCl}_3$ ) of compound <b>4.47</b> .....	269.
A2.11.	$^1\text{H}$ NMR spectrum (400 MHz, $\text{CDCl}_3$ ) and $^{13}\text{C}$ NMR spectrum (100 MHz, $\text{CDCl}_3$ ) of compound <b>4.57</b> .....	270.
A2.12.	$^1\text{H}$ NMR spectrum (400 MHz, $\text{CDCl}_3$ ) and $^{13}\text{C}$ NMR spectrum (100 MHz, $\text{CDCl}_3$ ) of compound <b>4.61</b> .....	271.
A2.13.	$^1\text{H}$ NMR spectrum (400 MHz, $\text{CDCl}_3$ ) and $^{13}\text{C}$ NMR spectrum (100 MHz, $\text{CDCl}_3$ ) of compound <b>S4.8</b> .....	272.
A2.14.	$^1\text{H}$ NMR spectrum (400 MHz, $\text{C}_6\text{D}_6$ ) and $^{13}\text{C}$ NMR spectrum (100 MHz, $\text{C}_6\text{D}_6$ ) of compound <b>4.62</b> .....	273.
A2.15.	$^1\text{H}$ NMR spectrum (400 MHz, $\text{C}_6\text{D}_6$ ) and $^{13}\text{C}$ NMR spectrum (100 MHz, $\text{C}_6\text{D}_6$ ) of compound <b>4.74</b> .....	274.
A2.16.	$^1\text{H}$ NMR spectrum (400 MHz, $\text{CDCl}_3$ ) and $^{13}\text{C}$ NMR spectrum (100 MHz, $\text{CDCl}_3$ ) of compound <b>4.75</b> .....	275.
A2.17.	$^1\text{H}$ NMR spectrum (600 MHz, $\text{C}_6\text{D}_6$ ) and $^{13}\text{C}$ NMR spectrum (150 MHz, $\text{C}_6\text{D}_6$ ) of compound <b>S4.9</b> .....	276.

A2.18.	$^1\text{H}$ NMR spectrum (600 MHz, $\text{C}_6\text{D}_6$ ) and $^{13}\text{C}$ NMR spectrum (150 MHz, $\text{C}_6\text{D}_6$ ) of compound <b>4.80</b> .	277.
A2.19.	COSY spectrum (600 MHz, $\text{C}_6\text{D}_6$ ) and NOESY spectrum (600 MHz, $\text{C}_6\text{D}_6$ ) of compound <b>4.80</b> .	278.
A2.20.	$^1\text{H}$ NMR spectrum (400 MHz, $\text{CDCl}_3$ ) and $^{13}\text{C}$ NMR spectrum (100 MHz, $\text{CDCl}_3$ ) of compound <b>S4.10</b> .	279.
A2.21.	$^1\text{H}$ NMR spectrum (400 MHz, $\text{CDCl}_3$ ) and $^{13}\text{C}$ NMR spectrum (100 MHz, $\text{CDCl}_3$ ) of compound <b>4.81</b> .	280.
A2.22.	$^1\text{H}$ NMR spectrum (400 MHz, $\text{CDCl}_3$ ) and $^{13}\text{C}$ NMR spectrum (100 MHz, $\text{CDCl}_3$ ) of compound <b>4.83</b> .	281.
A2.23.	$^1\text{H}$ NMR spectrum (400 MHz, $\text{CDCl}_3$ ) and $^{13}\text{C}$ NMR spectrum (100 MHz, $\text{CDCl}_3$ ) of compound <b>4.84</b> .	282.
A2.24.	$^1\text{H}$ NMR spectrum (600 MHz, $\text{CDCl}_3$ ) and $^{13}\text{C}$ NMR spectrum (150 MHz, $\text{CDCl}_3$ ) of compound <b>4.85</b> .	283.
A2.25.	$^1\text{H}$ NMR spectrum (400 MHz, $\text{CDCl}_3$ ) and $^{13}\text{C}$ NMR spectrum (100 MHz, $\text{CDCl}_3$ ) of compound <b>4.86</b> .	284.
A2.26.	$^1\text{H}$ NMR spectrum (400 MHz, $\text{C}_6\text{D}_6$ ) of compound <b>4.90</b> .	285.
A2.27.	$^1\text{H}$ NMR spectrum (400 MHz, $\text{C}_6\text{D}_6$ ) and $^{13}\text{C}$ NMR spectrum (100 MHz, $\text{C}_6\text{D}_6$ ) of compound <b>4.91</b> .	286.
A2.28.	$^1\text{H}$ NMR spectrum (400 MHz, $\text{CDCl}_3$ ) and $^{13}\text{C}$ NMR spectrum (100 MHz, $\text{CDCl}_3$ ) of compound <b>4.103</b> .	287.
A2.29.	$^1\text{H}$ NMR spectrum (600 MHz, $\text{C}_6\text{D}_6$ ) and $^{13}\text{C}$ NMR spectrum (150 MHz, $\text{C}_6\text{D}_6$ ) of compound <b>S4.12</b> .	288.
A2.30.	$^1\text{H}$ NMR spectrum (400 MHz, $\text{C}_6\text{D}_6$ ) and $^{13}\text{C}$ NMR spectrum (100 MHz, $\text{C}_6\text{D}_6$ ) of compound <b>4.105</b> .	289.
A2.31.	$^1\text{H}$ NMR spectrum (400 MHz, $\text{C}_6\text{D}_6$ ) of compound <b>4.108</b> .	290.
A2.32.	$^1\text{H}$ NMR spectrum (600 MHz, $\text{C}_6\text{D}_6$ ) and $^{13}\text{C}$ NMR spectrum (150 MHz, $\text{C}_6\text{D}_6$ ) of compound <b><math>\beta</math>-4.110</b> .	291.
A2.33.	COSY spectrum (600 MHz, $\text{C}_6\text{D}_6$ ) and NOESY spectrum (600 MHz, $\text{C}_6\text{D}_6$ ) of compound <b><math>\beta</math>-4.110</b> .	292.



A2.34.	$^1\text{H}$ NMR spectrum (600 MHz, $\text{C}_6\text{D}_6$ ) and $^{13}\text{C}$ NMR spectrum (150 MHz, $\text{C}_6\text{D}_6$ ) of compound <b><math>\alpha</math>-4.110</b> .....	293.
A2.35.	COSY spectrum (600 MHz, $\text{C}_6\text{D}_6$ ) of compound <b><math>\alpha</math>-4.110</b> .....	294.
A2.36.	$^1\text{H}$ NMR spectrum (400 MHz, $\text{CDCl}_3$ ) and $^{13}\text{C}$ NMR spectrum (100 MHz, $\text{CDCl}_3$ ) of compound <b>4.112</b> .....	295.
A2.37.	$^1\text{H}$ NMR spectrum (400 MHz, $\text{CDCl}_3$ ) and $^{13}\text{C}$ NMR spectrum (100 MHz, $\text{CDCl}_3$ ) of compound <b>4.113</b> .....	296.
A2.38.	$^1\text{H}$ NMR spectrum (400 MHz, $\text{C}_6\text{D}_6$ ) of compound <b>4.114</b> .....	297.
A2.39.	$^1\text{H}$ NMR spectrum (400 MHz, $\text{C}_6\text{D}_6$ ) and $^{13}\text{C}$ NMR spectrum (100 MHz, $\text{C}_6\text{D}_6$ ) of compound <b>4.115</b> .....	298.
A2.40.	$^1\text{H}$ NMR spectrum (400 MHz, $\text{CDCl}_3$ ) and $^{13}\text{C}$ NMR spectrum (100 MHz, $\text{CDCl}_3$ ) of compound <b>4.116</b> .....	299.
A2.41.	$^1\text{H}$ NMR spectrum (400 MHz, $\text{CDCl}_3$ ) and $^{13}\text{C}$ NMR spectrum (100 MHz, $\text{CDCl}_3$ ) of compound <b>4.117</b> .....	300.
A3.1.	$^1\text{H}$ NMR spectrum (400 MHz, $\text{CDCl}_3$ ) and $^{13}\text{C}$ NMR spectrum (100 MHz, $\text{CDCl}_3$ ) of compound <b>5.3</b> .....	377.
A3.2.	$^1\text{H}$ NMR spectrum (400 MHz, $\text{CDCl}_3$ ) and $^{13}\text{C}$ NMR spectrum (100 MHz, $\text{CDCl}_3$ ) of compound <b>5.4</b> .....	378.
A3.3.	$^1\text{H}$ NMR spectrum (400 MHz, $\text{CDCl}_3$ ) and $^{13}\text{C}$ NMR spectrum (100 MHz, $\text{CDCl}_3$ ) of compound <b>5.5</b> .....	379.
A3.4.	$^1\text{H}$ NMR spectrum (600 MHz, $\text{CDCl}_3$ ) and $^{13}\text{C}$ NMR spectrum (150 MHz, $\text{CDCl}_3$ ) of compound <b>5.6</b> .....	380.
A3.5.	$^1\text{H}$ NMR spectrum (400 MHz, $\text{CDCl}_3$ ) and $^{13}\text{C}$ NMR spectrum (100 MHz, $\text{CDCl}_3$ ) of compound <b>5.10</b> .....	381.
A3.6.	$^1\text{H}$ NMR spectrum (400 MHz, $\text{CDCl}_3$ ) and $^{13}\text{C}$ NMR spectrum (100 MHz, $\text{CDCl}_3$ ) of compound <b>5.12</b> .....	382.
A3.7.	$^1\text{H}$ NMR spectrum (400 MHz, $\text{CDCl}_3$ ) and $^{13}\text{C}$ NMR spectrum (100 MHz, $\text{CDCl}_3$ ) of compound <b>5.13</b> .....	383.
A3.8.	$^1\text{H}$ NMR spectrum (600 MHz, $\text{CDCl}_3$ ) and $^{13}\text{C}$ NMR spectrum (150 MHz, $\text{CDCl}_3$ ) of compound <b>5.15</b> .....	384.

A3.9.	$^1\text{H}$ NMR spectrum (400 MHz, $\text{CDCl}_3$ ) and $^{13}\text{C}$ NMR spectrum (100 MHz, $\text{CDCl}_3$ ) of compound <b>5.17</b> .....	385.
A3.10.	$^1\text{H}$ NMR spectrum (400 MHz, $\text{CDCl}_3$ ) and $^{13}\text{C}$ NMR spectrum (125 MHz, $\text{CDCl}_3$ ) of compound <b>5.18</b> .....	386.
A3.11.	$^1\text{H}$ NMR spectrum (400 MHz, $\text{CDCl}_3$ ) and $^{13}\text{C}$ NMR spectrum (100 MHz, $\text{CDCl}_3$ ) of compound <b>5.19</b> .....	387.
A3.12.	$^1\text{H}$ NMR spectrum (400 MHz, $\text{CDCl}_3$ ) and $^{13}\text{C}$ NMR spectrum (100 MHz, $\text{CDCl}_3$ ) of compound <b>5.24</b> .....	388.
A3.13.	$^1\text{H}$ NMR spectrum (400 MHz, $\text{CDCl}_3$ ) and $^{13}\text{C}$ NMR spectrum (100 MHz, $\text{CDCl}_3$ ) of compound <b>5.26</b> .....	389.
A3.14.	$^1\text{H}$ NMR spectrum (400 MHz, $\text{CDCl}_3$ ) of compound <b>5.27</b> .....	390.
A3.15.	$^1\text{H}$ NMR spectrum (600 MHz, $\text{CDCl}_3$ ) and $^{13}\text{C}$ NMR spectrum (150 MHz, $\text{CDCl}_3$ ) of compound <b>5.28</b> .....	391.
A3.16.	COSY spectrum (600 MHz, $\text{CDCl}_3$ ) and NOESY spectrum (600 MHz, $\text{CDCl}_3$ ) of compound <b>5.28</b> .....	392.
A3.17.	$^1\text{H}$ NMR spectrum (400 MHz, $\text{CDCl}_3$ ) and $^{13}\text{C}$ NMR spectrum (100 MHz, $\text{CDCl}_3$ ) of compound <b>5.30</b> .....	393.
A3.18.	$^1\text{H}$ NMR spectrum (400 MHz, $\text{CDCl}_3$ ) and $^{13}\text{C}$ NMR spectrum (100 MHz, $\text{CDCl}_3$ ) of compound <b>5.36</b> .....	394.
A3.19.	$^1\text{H}$ NMR spectrum (400 MHz, $\text{CDCl}_3$ ) and $^{13}\text{C}$ NMR spectrum (100 MHz, $\text{CDCl}_3$ ) of compound <b>5.37</b> .....	395.
A3.20.	$^1\text{H}$ NMR spectrum (400 MHz, $\text{CDCl}_3$ ) and $^{13}\text{C}$ NMR spectrum (100 MHz, $\text{CDCl}_3$ ) of compound <b>5.38</b> .....	396.
A3.21.	$^1\text{H}$ NMR spectrum (400 MHz, $\text{CDCl}_3$ ) and $^{13}\text{C}$ NMR spectrum (100 MHz, $\text{CDCl}_3$ ) of compound <b>5.39</b> .....	397.
A3.22.	$^1\text{H}$ NMR spectrum (400 MHz, $\text{CDCl}_3$ ) and $^{13}\text{C}$ NMR spectrum (100 MHz, $\text{CDCl}_3$ ) of compound <b>5.41</b> .....	398.
A3.23.	$^1\text{H}$ NMR spectrum (400 MHz, $\text{CDCl}_3$ ) and $^{13}\text{C}$ NMR spectrum (100 MHz, $\text{CDCl}_3$ ) of compound <b>5.42</b> .....	399.

A3.24.	$^1\text{H}$ NMR spectrum (400 MHz, $\text{CDCl}_3$ ) and $^{13}\text{C}$ NMR spectrum (100 MHz, $\text{CDCl}_3$ ) of compound <b>5.43</b> .....	400.
A3.25.	$^1\text{H}$ NMR spectrum (600 MHz, $\text{CDCl}_3$ ) and $^{13}\text{C}$ NMR spectrum (150 MHz, $\text{CDCl}_3$ ) of compound <b>5.44</b> .....	401.
A3.26.	$^1\text{H}$ NMR spectrum (400 MHz, $\text{CDCl}_3$ ) and $^{13}\text{C}$ NMR spectrum (100 MHz, $\text{CDCl}_3$ ) of compound <b>5.45</b> .....	402.
A3.27.	$^1\text{H}$ NMR spectrum (400 MHz, $\text{CDCl}_3$ ) and $^{13}\text{C}$ NMR spectrum (100 MHz, $\text{CDCl}_3$ ) of compound <b>5.46</b> .....	403.
A3.28.	$^1\text{H}$ NMR spectrum (400 MHz, $\text{CDCl}_3$ ) of compound <b>5.51</b> .....	404.
A3.29.	$^1\text{H}$ NMR spectrum (400 MHz, $\text{CDCl}_3$ ) and $^{13}\text{C}$ NMR spectrum (100 MHz, $\text{CDCl}_3$ ) of compound <b>5.53</b> .....	405.
A3.30.	$^1\text{H}$ NMR spectrum (400 MHz, $\text{CDCl}_3$ ) and $^{13}\text{C}$ NMR spectrum (100 MHz, $\text{CDCl}_3$ ) of compound <b>5.56</b> .....	406.
A3.31.	$^1\text{H}$ NMR spectrum (400 MHz, $\text{CDCl}_3$ ) and $^{13}\text{C}$ NMR spectrum (100 MHz, $\text{CDCl}_3$ ) of compound <b>5.58</b> .....	407.
A3.32.	$^1\text{H}$ NMR spectrum (400 MHz, $\text{CDCl}_3$ ) and $^{13}\text{C}$ NMR spectrum (100 MHz, $\text{CDCl}_3$ ) of compound <b>5.59</b> .....	408.
A3.33.	$^1\text{H}$ NMR spectrum (600 MHz, $\text{CDCl}_3$ ) and $^{13}\text{C}$ NMR spectrum (150 MHz, $\text{CDCl}_3$ ) of compound <b>5.60</b> .....	409.
A3.34.	COSY spectrum (600 MHz, $\text{CDCl}_3$ ) and NOESY spectrum (600 MHz, $\text{CDCl}_3$ ) of compound <b>5.60</b> .....	410.
A3.35.	$^1\text{H}$ NMR spectrum (400 MHz, $\text{C}_6\text{D}_6$ ) and $^{13}\text{C}$ NMR spectrum (150 MHz, $\text{C}_6\text{D}_6$ ) of compound <b>5.64</b> .....	411.
A3.36.	$^1\text{H}$ NMR spectrum (400 MHz, $\text{C}_6\text{D}_6$ ) and $^{13}\text{C}$ NMR spectrum (100 MHz, $\text{C}_6\text{D}_6$ ) of compound <b>5.66</b> .....	412.
A3.37.	$^1\text{H}$ NMR spectrum (400 MHz, $\text{CDCl}_3$ ) and $^{13}\text{C}$ NMR spectrum (100 MHz, $\text{CDCl}_3$ ) of compound <b>5.67</b> .....	413.
A3.38.	$^1\text{H}$ NMR spectrum (400 MHz, $\text{CDCl}_3$ ) and $^{13}\text{C}$ NMR spectrum (150 MHz, $\text{CDCl}_3$ ) of compound <b>5.71</b> .....	414.

A3.39.	$^1\text{H}$ NMR spectrum (400 MHz, $\text{C}_6\text{D}_6$ ) and $^{13}\text{C}$ NMR spectrum (100 MHz, $\text{C}_6\text{D}_6$ ) of compound <b>5.77</b> .	415.
A3.40.	$^1\text{H}$ NMR spectrum (600 MHz, $\text{CDCl}_3$ ) and $^{13}\text{C}$ NMR spectrum (150 MHz, $\text{CDCl}_3$ ) of compound <b>5.78</b> .	416.
A3.41.	$^1\text{H}$ NMR spectrum (400 MHz, $\text{CDCl}_3$ ) and $^{13}\text{C}$ NMR spectrum (100 MHz, $\text{CDCl}_3$ ) of compound <b>5.81</b> .	417.
A3.42.	$^1\text{H}$ NMR spectrum (400 MHz, $\text{CDCl}_3$ ) and $^{13}\text{C}$ NMR spectrum (100 MHz, $\text{CDCl}_3$ ) of compound <b>5.82</b> .	418.

## LIST OF SCHEMES

Scheme	Page
1.1. Collie's proposed biosynthesis of orcinol.....	5.
1.2. Biosynthetic pathway of the aromatic polyketide actinorhodin. ....	8.
1.3. Myers' synthesis of (–)-tetracycline. ....	11.
1.4. Trauner's total synthesis of (–)-halenaquinone.....	13.
1.5. Corey's total synthesis of aflatoxin B <sub>2</sub> .....	15.
1.6. Harrowven's synthesis of (±)-cavicularin and (±)-riccardin C.....	16.
1.7. Nicolaou's total synthesis of kinamycin F.....	18.
1.8. Proposed biosynthetic rearrangement producing tetracycle <b>1.92</b> . ....	30.
1.9. Identification of HMP-Y1 as a biosynthetic intermediate. ....	32.
1.10. Biosynthetic pathway of hibarimicin B. ....	33.
1.11. Meyers' synthesis of atropisomerically pure ( <i>S</i> )-gossypol.....	37.
1.12. Bringmann's first synthesis of racemic bismurrayaquinone A.....	38.
1.13. Thomson's enantioselective synthesis of bismurrayaquinone A. ....	40.
1.14. Sargent's synthesis of <i>aS</i> -8'-hydroxyisodiospyrin. ....	42.
1.15. Sulikowski's model of aryl-quinone atropisomerism. ....	43.
1.16. Proposed mechanism of phenol quinone interconversion. ....	44.
1.17. Roush's aryl-quinone model system. ....	46.
2.1. The original Diels-Alder reaction. ....	54.
2.2. Regiochemical preferences in the intermolecular Diels-Alder. ....	57.
2.3. Alder and Stein's <i>cis</i> principle. ....	58.

2.4.	Stereochemical outcomes due to the Alder <i>endo</i> rule.....	59.
2.5.	Early IMDA example substrates.....	62.
2.6.	Stereochemical outcome of a representative TADA. ....	63.
2.7.	Woodward's total syntheses of cortisone and cholesterol. ....	64.
2.8.	Corey's IMDA-enabled total synthesis of forskolin.....	66.
2.9.	Rychnovsky's late-stage IMDA toward colombiasin A. ....	67.
2.10.	Schreiber's TADA toward dimethyl dynemicin A. ....	68.
2.11.	Sorensen's double TADA toward (+)-FR182877.....	69.
2.12.	Retrosynthetic consensus for early work toward hibarimicinone.....	70.
2.13.	Sulikowski's route to divergent hibarimicinone precursors. ....	71.
2.14.	Cycloetherification toward the A'B'-decalin system. ....	72.
2.15.	<i>Trans</i> diol installation and attempted cycloetherification.....	73.
2.16.	Attempted synthesis of the AB-decalin system. ....	73.
2.17.	Sulikowski's alkynyl IMDA toward the AB-decalin system. ....	74.
2.18.	Altering dienophile structure leads to different stereochemistry.....	75.
2.19.	Roush's synthesis of the A'B'-decalin system. ....	77.
2.20.	Mootoo's synthesis of the A'B'-decalin toward hibarimicinone.....	79.
2.21.	Mootoo's modified route to the AB-decalin system.....	81.
2.22.	Shair's synthesis of the AB-decalin unit.....	83.
2.23.	Hosokawa's synthesis of the AB-decalin system. ....	86.
2.24.	Synthesis of the unsymmetrical biaryl D-D' moiety. ....	88.
2.25.	Hosokawa's first total synthesis of hibarimicinone.....	90.
2.26.	Shair's synthesis of the natural AB-decalin enantiomer.....	91.

2.27.	Synthesis of a symmetrical D-D' biaryl core for bis-annulation. ....	92.
2.28.	The first total synthesis of HMP-Y1. ....	94.
2.29.	Shair's completion of the total synthesis of hibarimicinone. ....	96.
3.1.	Two-directional synthetic analysis toward HMP-Y1. ....	101.
3.2.	Biaryl core retrosynthetic analysis. ....	102.
3.3.	Romaine's synthesis of the HMP-Y1 biaryl core. ....	103.
3.4.	Annulation model systems with cyclohexenone. ....	104.
3.5.	Retrosynthetic analysis toward the AB-ring system subunit. ....	105.
3.6.	Engers' early approach toward the AB-decalin. ....	107.
3.7.	IMDA followed by attempted hydroxy-ketone installation. ....	108.
3.8.	Synthesis of the benzyl-glucopyranoside series. ....	109.
3.9.	Engers' route to the benzyl-protected dienone. ....	110.
3.10.	Engers' acrylate IMDA toward the decalinic enone. ....	111.
3.11.	Stereochemical effects in the nucleophilic addition. ....	112.
3.12.	Mechanism of RuO <sub>4</sub> -mediated ketohydroxylation. ....	114.
3.13.	Failed enone installation approach. ....	115.
3.14.	Improved route to the iodo-enone. ....	116.
3.15.	Catalytic cycle for ring closing metathesis. ....	118.
3.16.	Improved synthesis of a modified IMDA substrate. ....	119.
3.17.	Key IMDA toward the AB-decalin. ....	120.
3.18.	Failed sulfone elimination to the AB-enone. ....	121.
3.19.	An unexpected etherification of an enone intermediate. ....	122.
3.20.	A sulfone elimination model system. ....	123.

3.21.	Synthetic strategy for a substrate controlled propyl addition. ....	124.
3.22.	Encountered difficulties with a modified Suzuki coupling substrate. ....	124.
3.23.	Synthesis of the proposed decalinic enone <b>3.75</b> . ....	125.
3.24.	The reactive rotamer effect in the IMDA. ....	126.
4.1.	Brussee's deracemization of BINOL. ....	174.
4.2.	Access to pure <i>aR</i> - and <i>aS</i> -VANOL from a racemic mixture. ....	174.
4.3.	Mechanism of VANOL dynamic thermodynamic resolution. ....	176.
4.4.	Dynamic thermodynamic resolution of our model substrate. ....	177.
4.5.	A biomimetic dimerization toward HMP-Y1 and hibarimicinone. ....	178.
4.6.	A Diels-Alder-enabled strategy to tetracycle <b>4.12</b> . ....	179.
4.7.	Synthetic analysis for assembly of a TADA precursor. ....	180.
4.8.	Synthesis of the D-ring aryl aldehyde. ....	180.
4.9.	Nicolaou's "stitching-cyclization" method for rapamycin. ....	181.
4.10.	Unsuccessful Stille coupling toward the northern tether. ....	182.
4.11.	Singleton's chemoselective hydroboration. ....	183.
4.12.	Failed alkyne hydroboration for Suzuki coupling. ....	183.
4.13.	Second generation TADA synthetic analysis. ....	185.
4.14.	Synthesis of the aryl bromide. ....	185.
4.15.	Synthesis of the tethered A-ring. ....	186.
4.16.	Improved synthesis of the A-ring aldehyde and tethering. ....	187.
4.17.	Vaultier's arylzinc addition to aldehyde <b>4.36</b> . ....	188.
4.18.	Alternate order for northern tethering. ....	189.
4.19.	TADA synthetic analysis from (–)-quinic acid. ....	191.



4.20.	Synthesis of a (–)-quinic acid-derived iodo-enone. ....	192.
4.21.	Selective C-13 stereocenter formation. ....	193.
4.22.	Northern tether formation with the (–)-quinic acid-derived A-ring. ....	194.
4.23.	Improved synthesis of the A-ring aldehyde and tethering. ....	195.
4.24.	Mechanism of Suzuki cross coupling of vinyl halides. ....	196.
4.25.	Sieburth’s silyl-tethered IMDA/Tamao-Fleming sequence. ....	197.
4.26.	Failed attempts toward southern tether formation. ....	199.
4.27.	Incorrect C-9 stereochemistry from a northern-tethered IMDA. ....	200.
4.28.	Aryl alkyne synthesis and functionalization. ....	202.
4.29.	Attempted northern tether formation with functionalized alkynes. ....	203.
4.30.	Successful northern tethering with terminal alkyne functionality. ....	204.
4.31.	Failed attempts at alkyne functionalization. ....	205.
4.32.	Proposed mechanism of alkyne carbonylation. ....	206.
4.33.	Ogasawara’s carbonylative macrolactonization. ....	207.
4.34.	Alternate macrolactonization attempts. ....	208.
4.35.	Nicolaou’s nucleophilic opening of a cyclic carbonate. ....	209.
4.36.	Alkyne functionalization and an unexpected IMDA. ....	211.
4.37.	Synthesis of an aryl propargylic alcohol. ....	213.
4.38.	Synthesis of a deactivated alkynyl ester. ....	214.
5.1.	Retrosynthesis reflecting new stereochemical knowledge. ....	302.
5.2.	Synthesis of an orthogonally-protected D-ring. ....	303.
5.3.	Revisiting possible Diels-Alder-enabled routes to tetracycle <b>4.12</b> . ....	304.
5.4.	Synthetic analysis of an IMDA approach. ....	304.

5.5.	Synthesis of the alkynyl acid D-ring building block. ....	306.
5.6.	Regioselectivity evaluation of a model esterification. ....	307.
5.7.	Synthesis of a differentially functionalized A-ring. ....	307.
5.8.	Proposed installation of <i>trans-trans</i> triol functionality. ....	308.
5.9.	Formation of a southern-tethered alkynyl ester. ....	309.
5.10.	Arrival at a southern-tethered IMDA precursor. ....	310.
5.11.	A southern-tethered IMDA leads to desired C-9 stereochemistry. ....	310.
5.12.	Attempted southern tethering of an $\alpha,\beta$ -unsaturated acid. ....	312.
5.13.	Cross-metathesis route to the southern tether. ....	313.
5.14.	Failed southern-tethered IMDA. ....	314.
5.15.	Synthesis of the benzyl series acrylate ester. ....	315.
5.16.	Failed IMDA route with the benzyl series. ....	316.
5.17.	Conformational analysis of the benzyl series IMDA substrate. ....	317.
5.18.	Unsuccessful cross metatheses of alternate vinyl A-ring substrates. ....	319.
5.19.	An attempted diene-truncated IMDA. ....	320.
5.20.	Successful dienophile-truncated IMDA. ....	321.
5.21.	An improved TADA synthetic analysis. ....	322.
5.22.	Northern tethering and first generation cross metathesis. ....	324.
5.23.	Diverging metathesis pathways. ....	325.
5.24.	Unsuccessful deprotection to an aldehyde triol intermediate. ....	326.
5.25.	Kozmin's spontaneous macrolactolization. ....	327.
5.26.	<i>Tert</i> -butyl acrylate cross metathesis and attempted deprotection. ....	328.
5.27.	Synthesis of a macrolactonization precursor. ....	329.

5.28.	Remaining steps to the ABCD tetracycle. ....	330.
5.29.	Possible base-promoted pathways for TADA product <b>5.85</b> . ....	331.
5.30.	Proposed B- and C-ring oxidation sequence.....	332.
5.31.	Proposed installation of the A-ring <i>trans-trans</i> triol system. ....	333.
5.32.	Completion of the protected tetracyclic monomer <b>5.99</b> .....	334.
5.33.	Romaine's preliminary work toward oxidative dimerization. ....	334.
5.34.	Endgame strategy for completion of <i>aR</i> HMP-Y1. ....	335.
5.35.	Proposed completion of hibarimicinone. ....	336.

## LIST OF ABBREVIATIONS

)))	sonication
2,2-DMP	2,2-dimethoxypropane
18-c-6	18-crown-6
Ac	acetyl
Ac <sub>2</sub> O	acetic anhydride
AcOH	acetic acid
ACP	acyl carrier protein
AIBN	azobisisobutyronitrile
AM	amicetopyranose
app	apparent
ARO	aromatase
AT	acyltransferase, acetyl trideoxyhexopyranose
ATP	adenosine triphosphate
AX	acetyl dideoxyxylohexopyranose
BHT	butylated hydroxytoluene
Bn	benzyl
BnBr	benzyl bromide
br	broad
Bz	benzoyl
BzCl	benzoyl chloride
°C	degrees Celsius
CAM	ceric ammonium molybdate
cAMP	cyclic adenosine monophosphate
CAN	ceric ammonium nitrate
CD	circular dichroism
CH <sub>2</sub> Cl <sub>2</sub>	dichloromethane
(CH <sub>2</sub> O) <sub>n</sub>	paraformaldehyde
CLF	chain length factor
CoA	coenzyme A
COSY	correlation spectroscopy
CSA	camphorsulfonic acid
Cy	cyclohexyl
CYC	cyclase
d	doublet
DABCO	1,4-diazabicyclo[2.2.2]octane
DBN	diazabicyclononene
DBU	1,8-diazabicyclo[5.4.0]undec-7-ene
DCC	<i>N,N'</i> -dicyclohexylcarbodiimide
DCE	1,2-dichloroethane
DDQ	2,3-dichloro-5,6-dicyano-1,4-benzoquinone
DEAD	diethyl azodicarboxylate
Δ	heat

$\delta$	chemical shift in ppm
DG	digitoxopyranose
DH	dehydratase
DIBAL	diisobutylaluminum hydride
DIPEA	diisopropylethyl amine
DMAP	4-dimethylaminopyridine
DMDO	dimethyldioxirane
DMF	dimethylformamide
DMP	Dess-Martin periodinane
DMSO	dimethylsulfoxide
DMTSF	dimethyl(methylthio)sulfonium tetrafluoroborate
DTBC	di- <i>tert</i> -butylcatechol
DTBMP	di- <i>tert</i> -butyl-4-methylpyridine
EDCI	1-ethyl-3-(3-dimethylaminopropyl)carbodiimide
eq	equivalent
ER	enoyl reductase
ESI	electrospray ionization
Et <sub>2</sub> O	diethyl ether
Et <sub>3</sub> N	triethylamine
EtOH	ethanol
EtOAc	ethyl acetate
FDA	United States Food and Drug Administration
FMO	frontier molecular orbital
g	gram
h	hour
HMBC	heteronuclear multiple bond correlation spectroscopy
HMDS	bis(trimethylsilyl)amide
HMT	hexamethylenetetramine
HOMO	highest occupied molecular orbital
HPLC	high-performance liquid chromatography
HRMS	high-resolution mass spectrum
HWE	Horner-Wadsworth-Emmons reaction
Hz	hertz
IBX	2-iodoxybenzoic acid
IC <sub>50</sub>	half maximal inhibitory concentration
IMDA	intramolecular Diels-Alder
ImH	imidazole
<i>i</i> -PrOH	isopropanol
IR	infrared spectroscopy
<i>J</i>	coupling constant
KHMDS	potassium bis(trimethylsilyl)amide
KR	ketoreductase
KS	ketosynthase
L	liter
LAH	lithium aluminum hydride
LDA	lithium diisopropylamide

LHMDS	lithium bis(trimethylsilyl)amide
LiTMP	lithium tetramethylpiperidine
LUMO	lowest unoccupied molecular orbital
M	molar concentration
m	milli, multiplet
<i>m</i> -CPBA	meta-chloroperoxybenzoic acid
Me	methyl
MeCN	acetonitrile
MeI	methyl iodide
MeNO <sub>2</sub>	nitromethane
MeOH	methanol
MHz	megahertz
MIC	minimum inhibitory concentration
min	minute
μ	micro
μW	microwave
mol	mole
MOM	methoxy methyl ether
MOMCl	chloromethyl methyl ether
MP	melting point
MS	molecular sieves
Ms	methanesulfonate
MsCl	methanesulfonyl chloride
MTPA	α-methoxy-α-trifluoromethylphenylacetic acid
N	normal concentration
n	nano
NaHMDS	sodium bis(trimethylsilyl)amide
NBS	<i>N</i> -bromosuccinimide
NBT	nitro blue tetrazolium chloride
<i>n</i> -BuLi	<i>n</i> -butyllithium
NMO	<i>N</i> -methylmorpholine- <i>N</i> -oxide
NMP	<i>N</i> -methyl-2-pyrrolidone
NMR	nuclear magnetic resonance
NOE	nuclear Overhauser effect
NOESY	nuclear Overhauser effect spectroscopy
NTG	<i>N</i> -methyl- <i>N</i> '-nitro- <i>N</i> -nitrosoguanidine
OAc	acetoxyl
Oxone	potassium peroxymonosulfate
p	pentet
PCC	pyridinium chlorochromate
Ph	phenyl
PIDA	phenyliodonium diacetate
Piv	pivaloate
PivCl	pivaloyl chloride
PKS	polyketide synthase
ppm	parts per million

PPTS	pyridinium <i>para</i> -toluenesulfonate
<i>p</i> -TSA	<i>para</i> -toluenesulfonic acid
PyBroP	bromotripyrrolidinophosphonium hexafluorophosphate
q	quartet
RT	room temperature
s	singlet
<i>s</i> -BuLi	<i>sec</i> -butyllithium
sept	septet
t	triplet
TADA	transannular Diels-Alder
TBAB	tetra- <i>n</i> -butylammonium bromide
TBAF	tetra- <i>n</i> -butylammonium fluoride
TBAI	tetra- <i>n</i> -butylammonium iodide
TBAT	tetra- <i>n</i> -butylammonium difluorotriphenylsilicate
TBDPS	<i>tert</i> -butyldiphenylsilyl
TBDPSCI	<i>tert</i> -butyldiphenylsilyl chloride
TBS	<i>tert</i> -butyldimethylsilyl
TBSCI	<i>tert</i> -butyldimethylsilyl chloride
TBSOTf	<i>tert</i> -butyldimethylsilyl trifluoromethanesulfonate
<i>t</i> -BuLi	<i>tert</i> -butyllithium
<i>t</i> -BuOK	potassium <i>tert</i> -butoxide
TE	thioesterase
TES	triethylsilyl
TESCI	triethylsilyl chloride
TESOTf	triethylsilyl trifluoromethanesulfonate
TFA	trifluoroacetic acid
TFE	trifluoroethanol
Tf <sub>2</sub> O	trifluoromethanesulfonic anhydride
THF	tetrahydrofuran
TIPS	triisopropylsilyl
TIPSCI	triisopropylsilyl chloride
TIPSOTf	triisopropylsilyl trifluoromethanesulfonate
TMEDA	tetramethylethylenediamine
TMS	trimethylsilyl
TMSCI	trimethylsilyl chloride
TMSTFA	trimethylsilyl trifluoroacetate
TNF	tumor necrosis factor
TOCSY	total correlation spectroscopy
TPAP	tetra- <i>n</i> -propylammonium perruthenate
UV	ultraviolet
VO(acac) <sub>2</sub>	vanadyl acetylacetonate

## CHAPTER I

### NATURALLY OCCURRING AROMATIC POLYKETIDES

#### Secondary Metabolites and Their Medicinal Properties

The medicinal properties of secondary metabolites have been known for thousands of years.<sup>1</sup> The Inca civilization chewed the leaves of coca plants, which produce cocaine (**1.1**) and cause feelings of intense euphoria.<sup>1</sup> Secretions of the opium poppy, which produces morphine (**1.2**), codeine, and other alkaloid metabolites, have found use as analgesics and anxiolytics since the time of Homer, and pure morphine, first isolated in 1806 by Friedrich Wilhelm Adam Sertürner, aided minor surgical procedures beginning in the mid-nineteenth century.<sup>2</sup> In 1928, Alexander Fleming noted the absence of *Staphylococcus aureus* colonies surrounding the mould *Penicillium notatum*, the now famous producer of penicillin G (**1.3**), and thus began the modern era of antibiotic drug treatment.<sup>3</sup> Many subsequent anecdotes similar to these have shaped the history of medicine, and microbial secondary metabolism remains an important source of treatments for prominent twenty-first century diseases.

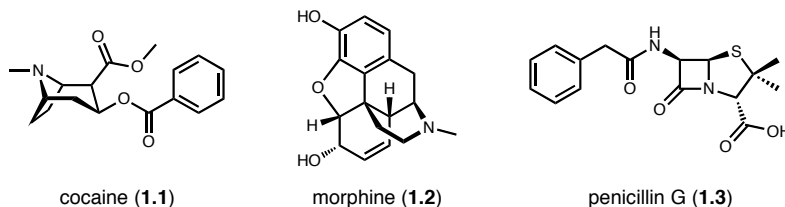


**Figure 1.1.** Historically important secondary metabolites.



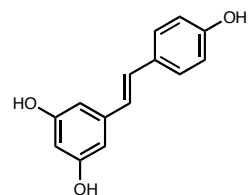
Organisms synthesize natural products through secondary metabolism which exists as a close extension of primary metabolism. The pathways responsible for converting key dietary components such as carbohydrates, sugars, fats, and proteins into energy are described as primary metabolic pathways and are common to all organisms.<sup>4</sup> In contrast, secondary metabolism produces compounds of varying amount and utility under specific environmental conditions and lacks consistency across species. While few compounds have known purposes, self-defense, mating, and camouflage are among the common elucidated uses for certain classes of secondary metabolites. Compounds involved in and produced by primary metabolism provide many of the biosynthetic intermediates necessary for secondary metabolism, and acetyl coenzyme A (CoA), shikimic acid, and mevalonate are important examples.<sup>4</sup>

Specifically, the acetate pathway for secondary metabolism utilizes acetyl CoA to synthesize natural products such as polyketides, phenols, prostaglandins, and fatty acids.<sup>4</sup> These classes of natural products have found many uses as medicinal therapies such as antibiotics, immunosuppressants, and antitumor agents.<sup>5</sup> Acetyl CoA is produced through oxidative decarboxylation of pyruvic acid *via* the glycolytic pathway, which utilizes dietary D-glucose as its input.<sup>4</sup> Cellular machinery then uses acetyl CoA as a key building block for production of important secondary metabolites.

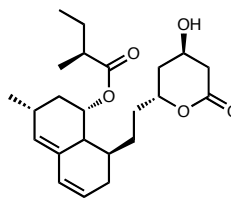
### **Aromatic Polyketide Biosynthesis**

Polyketides are a large and diverse class of natural products that can be divided into subcategories including macrolides (erythromycin, **1.10**), polyenes (amphotericin,

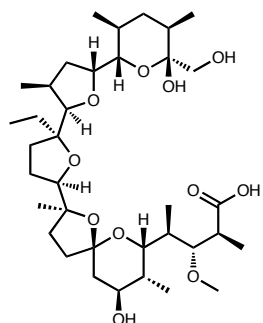
**1.7** and rapamycin, **1.9**), polyethers (monensin, **1.6**), and aromatics (tetracycline, **1.8**) as shown in Figure 1.2 and the selected polyketides have a rich history of clinical use.<sup>6</sup> Erythromycin (**1.10**), a common broad-spectrum antibiotic, has been used in the treatment of upper and lower respiratory infections for more than 50 years, and it is a common alternative for penicillin-allergic patients.<sup>7</sup> Monensin (**1.6**) and tetracycline (**1.8**) are commercially marketed antibiotic therapies, while amphotericin is a widely used antifungal treatment.<sup>8</sup> Rapamycin (**1.9**) is an immunosuppressant utilized to prevent transplanted organ rejection, and lovastatin (**1.5**) is a cholesterol-lowering agent.<sup>8</sup> Resveratrol (**1.4**), a stilbene polyketide found in red wine, has produced much debate over its reported anti-aging effects, and calicheamicin  $\gamma_1$  (**1.11**), one of the most potent antitumor agents known, is an enediyne natural product that has been developed as part of several monoclonal antibody constructs for cancer treatment.<sup>9,10</sup> The classification of polyketides arises from the biosynthetic machinery utilized in their synthesis, all of which derive from the acetate pathway of secondary metabolism.



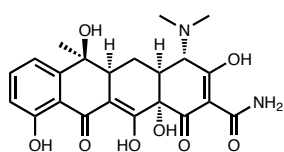
resveratrol (1.4)



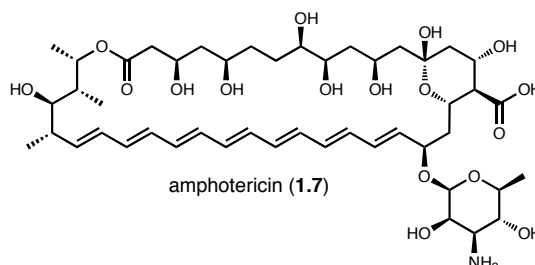
lovastatin (1.5)



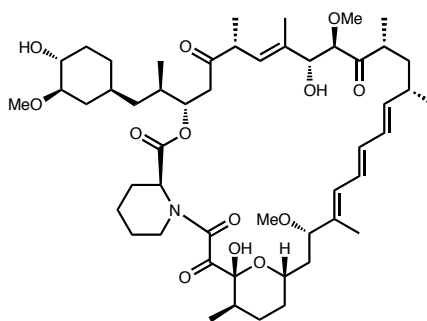
monensin (1.6)



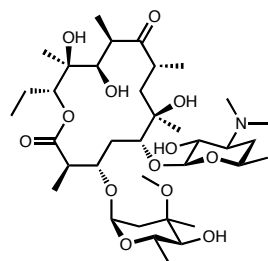
tetracycline (1.8)



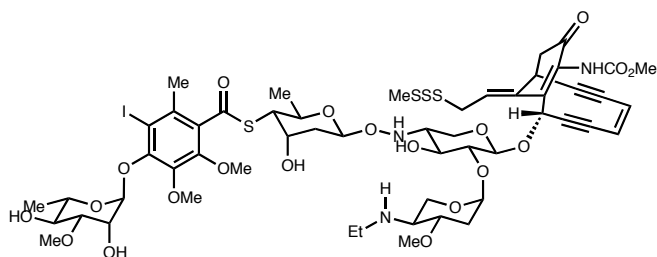
amphotericin (1.7)



rapamycin (1.9)



erythromycin (1.10)

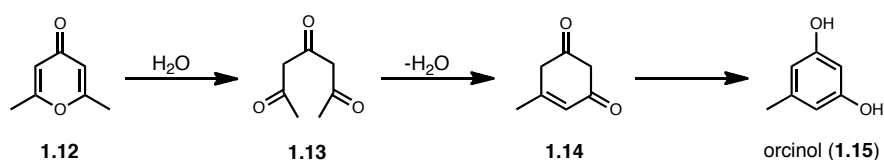


calicheamicin (1.11)

**Figure 1.2.** Biologically important examples of polyketide natural products.

The original biosynthetic hypothesis for polyketides arose from James Collie's studies at the beginning of the twentieth century.<sup>12</sup> While working toward proving the structure of the dehydroacetic acid **1.12**, reaction with barium hydroxide and acidic

workup surprisingly led to the aromatic compound orcinol (**1.15**). While simply determining the structure of the reaction product was no small task at the time, the key point to his groundbreaking hypothesis involved proposing the triketone **1.13** as an intermediate in the transformation. Thus, the biosynthetic pathway was proposed to involve addition of water followed by dehydration and tautomerization to the aromatic product. Despite the importance of Collie's findings, acceptance of his hypothesis did not come until Robert Robinson revived the conversation with his publication of the biosynthesis of tropinone.<sup>12</sup> Arthur Birch also played an important role in developing the basis for polyketide biosynthesis in the 1950's.<sup>12</sup> Birch hypothesized that the polyketone intermediate proposed by Collie could arise from the condensation of acetate units, and he confirmed his theory by determining the pattern of acetate incorporation into the natural product 6-methylsalicylic acid with isotopic labeling. These studies laid the groundwork for the extensive research that followed and formed the basis of our current understanding of polyketide biosynthesis.



**Scheme 1.1.** Collie's proposed biosynthesis of orcinol.

Analogous in many ways to fatty acid biosynthesis, polyketide biosynthesis can be subdivided into three categories. Enzymes and enzyme complexes involved are termed polyketide synthases, which can exist as large complexes or discrete enzymes functioning

in unison. Type I polyketide synthases (PKS) are large proteins with many enzymatic active sites performing all necessary functions for metabolite synthesis.<sup>11</sup> Type I PKS's have been identified in bacteria, plants, and fungi, and the type I PKS mechanism produces macrolides, polyethers, and polyenes.<sup>6</sup> The minimal domains necessary for type I synthesis include ketosynthase (KS), acyltransferase (AT), and acyl carrier protein (ACP).<sup>12</sup> Optional subunits provide variation along the growing linear chain, which include ketoreductase (KR), dehydratase (DH), and enoyl reductase (ER).<sup>12</sup> The type I PKS builds a linear chain with a terminal  $\beta$ -diketone through a decarboxylative condensation between enzyme-associated starter and extender units, acetyl CoA being the simplest.<sup>13</sup> Through each round of chain extension, varying levels of ketone reduction occur based on the use of optional domains listed above.<sup>6</sup> In this way, the level of oxidation in type I products directly correlates to the domains utilized in their synthesis; however, post-PKS modification can alter the oxidation state of the final product.<sup>13</sup> Finally, a thioesterase (TE) enzyme is responsible for releasing the polyketide chain from the complex with either an acid or acyl ester terminus.<sup>12</sup>

In contrast to the type I PKS enzyme complex, type II polyketides arise from the coordinated action of individual enzymes acting as a large complex and are generally produced by bacteria.<sup>6</sup> Aromatic polyketides are produced by type II PKS machinery, and the minimal type II PKS complex includes KS, ACP, and chain length factor (CLF).<sup>11</sup> Unlike the varying states of reduction found along the extending chain in type I PKS synthesis, the linear polyketide chain associated with the type II PKS often remains in the ketone oxidation state and is stabilized by a complex between the CLF and KS, which allows for ultimate cyclization and aromatization.<sup>11</sup> Synthetic studies by Tom and

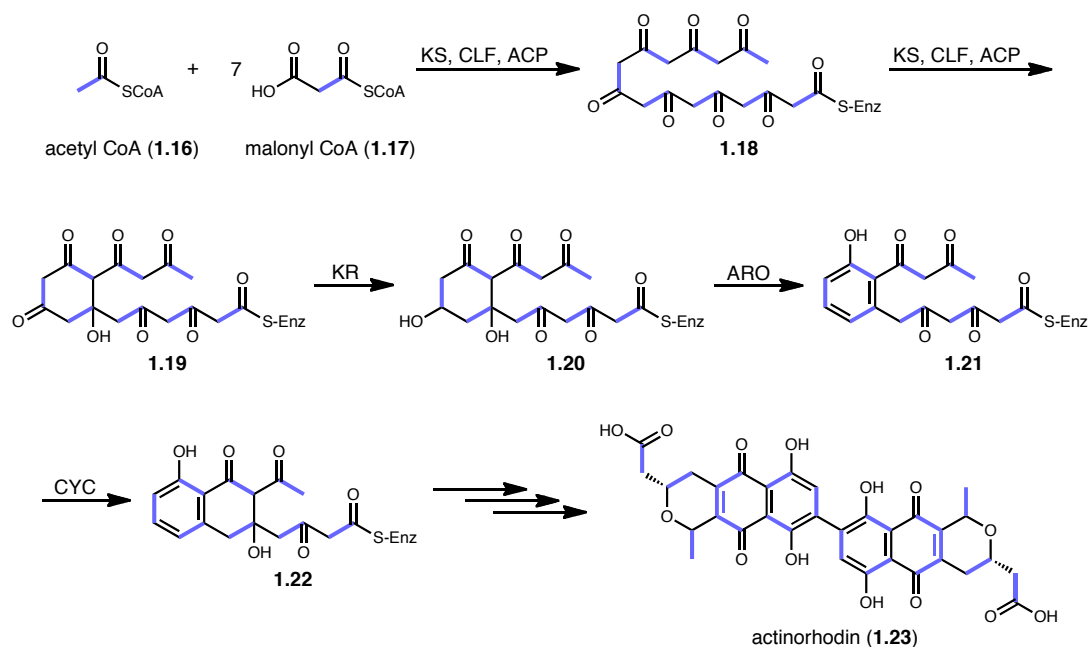
Constance Harris in 1977, in which they prepared linear polyketone chains through polyanion additions to polyketoesters, importantly confirmed that the biosynthetic cyclization of these linear chains must be under enzymatic control due to the formation of isomeric products in solution.<sup>14</sup> In addition to the optional enzymes involved in type I PKS's, type II synthesis utilizes enzymes such as cyclases (CYC) and aromatases (ARO) to effect formation of the hallmark fused aromatic polycyclic structures of aromatic polyketides.<sup>6</sup>

The final subgroup of polyketides is synthesized by chalcone and stilbene synthases which are categorized as type III PKS's. These PKS's exist primarily in plants but also in bacteria, and fungi.<sup>5</sup> Type III PKS's do not utilize an ACP in contrast to the first two types and function as iterative homodimers in the production of aromatic polyketides.<sup>15</sup> Importantly, consideration must be given to the numerous examples that do not strictly follow the paradigm laid out by the rather rigid definitions of the type I, II, and III PKS's.<sup>15</sup>

Actinorhodin (**1.23**), a blue-pigmented antibiotic, is a classic example of a type II aromatic polyketide.<sup>16</sup> Isolated from the actinomycete *Streptomyces coelicolor* A3, actinorhodin is the first antibiotic for which its entire gene cluster was cloned.<sup>16</sup> These studies determined that actinorhodin is produced iteratively by a single set of biosynthetic enzymes, and therefore it has become one of the most well studied type II PKS systems.<sup>16</sup>

The initial steps involved in actinorhodin biosynthesis are shown in Figure 1.3. The minimal type II PKS system, which consists of KS, CLF, and ACP, utilizes acetyl CoA as the starter unit and seven malonyl CoA extender units to synthesize the linear polyketide chain **1.18**, where bolded bonds indicate the two-carbon unit incorporation

pattern.<sup>12</sup> The minimal PKS machinery has also been implicated in the first cyclization step, which yields **1.19**, and KR then regioselectively effects ketone reduction in preparation for aromatization.<sup>12</sup> Aromatase forms the phenol **1.21** which then undergoes a second cyclization performed by CYC. From **1.22**, the biosynthetic steps are less well characterized; however, stereoselective reduction of the  $\beta$ -keto-thioester in **1.22** by KR provides the first chiral intermediate leading to the outer ring stereochemistry.<sup>16</sup> Actinorhodin biosynthesis provides a relatively general template for the assembly of many related aromatic polyketides, in which a linear polyketide undergoes a series of reductions, cyclizations, and aromatizations.



**Scheme 1.2.** Biosynthetic pathway of the aromatic polyketide actinorhodin.

## Synthetic Approaches to Aromatic Polyketides

Following seminal work by Collie and Birch, much of the early synthetic research toward aromatic polyketides involved accessing clinically relevant compounds. Notably, the tetracycline family of antibiotics, which represent canonical aromatic polyketides with their linear tetracyclic backbone, garnered much attention in the 1950's and 1960's following their isolation from various strains of *Streptomyces* actinobacteria.<sup>17</sup> Aureomycin (**1.24**), also termed chlorotetracycline, was the first family member to be isolated and identified as a potent antibacterial agent, and Lloyd Conover at the Charles Pfizer Co., Inc. first produced tetracycline (**1.8**) through catalytic hydrogenation of aureomycin. Following fevered studies, Pfizer in collaboration with R. B. Woodward determined the structure of terramycin (**1.25**), also known as oxytetracycline. Tetracycline (**1.8**) was approved by the FDA in 1954 and has enjoyed widespread success as a broad-spectrum antibiotic since its first use in the clinic.<sup>17</sup>

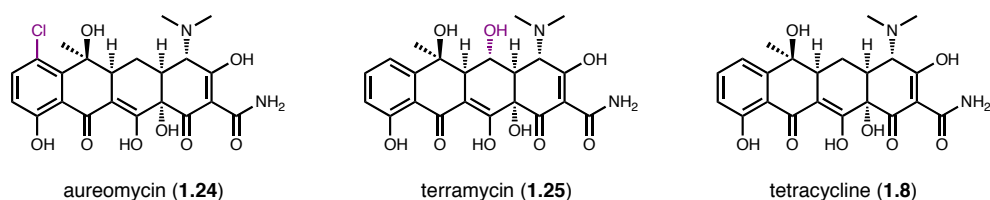


**Figure 1.3.** Examples of tetracycline family members.

Due to the importance of the tetracyclines and the inaccessibility of various derivatives from fermentation, numerous groups across the globe launched efforts toward their total synthesis. Ultimately, work by Muxfeldt in Germany, Shemyakin in Russia,

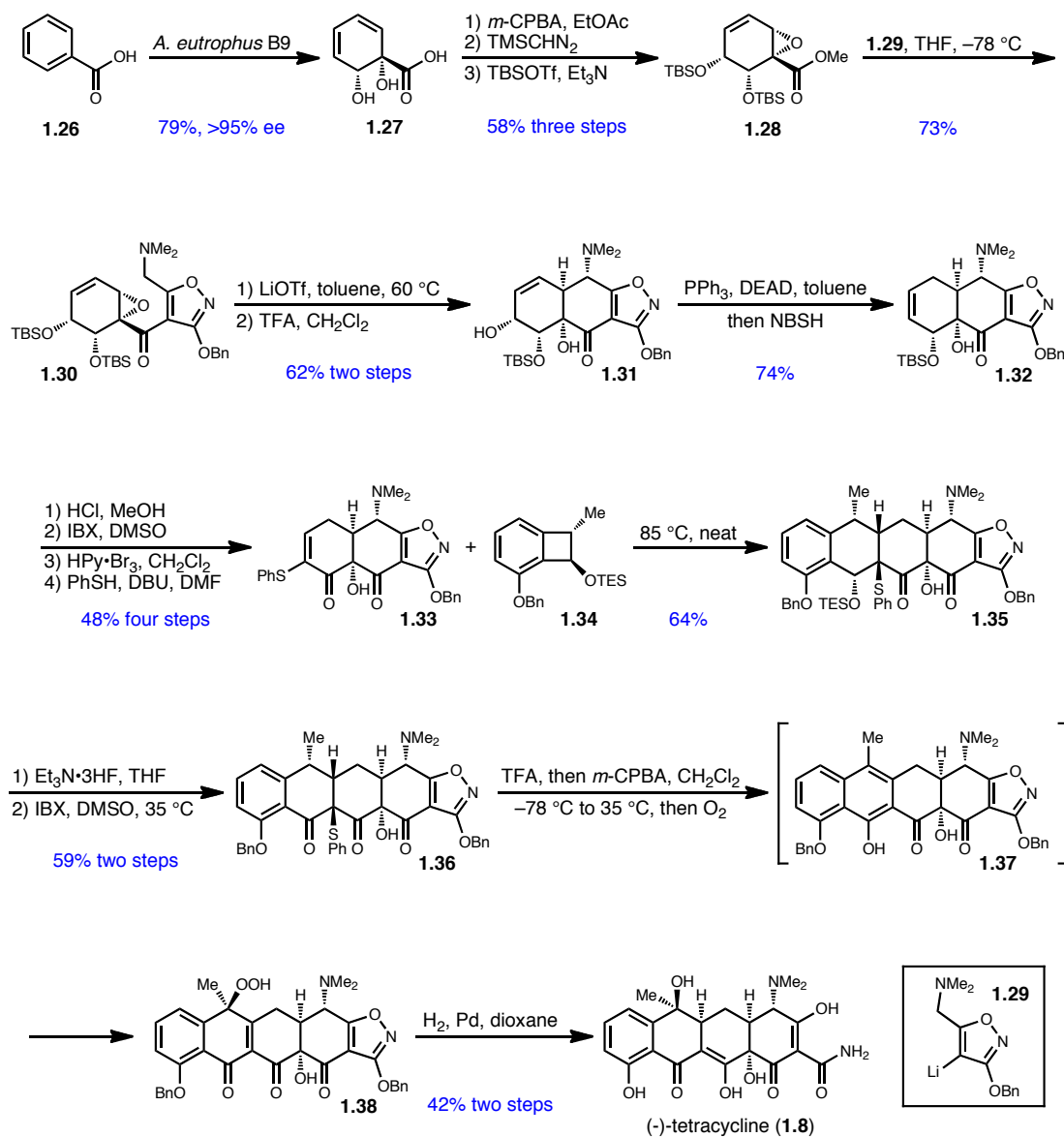


and Fields, Kende, and Boothe in the United States was superseded by completion of the total synthesis of 6-demethyl-6-deoxytetracycline by R. B. Woodward in 1962.<sup>18</sup> Woodward's synthesis was quickly followed by Shemyakin's synthesis of tetracycline (**1.8**) in 1963 and Muxfeldt's assembly of 6-demethyl-6-deoxytetracycline in 1965. Later, Muxfeldt succeeded in the total synthesis of the much more complicated terramycin (**1.25**) in 1968.

Owing to their importance as medicinal agents and their often-scarce availability, many other aromatic polyketides have been the subjects of many modern total synthesis efforts. While the aldol reaction is the linchpin reaction for synthesis of macrocyclic polyketide type I natural products and the Dieckmann condensation the linchpin of aromatic polyketide biosynthesis, a wide variety of approaches have been utilized for the total synthesis of type II aromatic polyketides, and an examination of the key backbone-forming reactions can provide insight into the most effective methods for consideration in synthetic planning. The fused polycyclic structures lend themselves to a range of ring formation methodologies, including Diels-Alder, electrocyclization, radical ring closure, and multi-step cyclizations. Examples shown encompass the recent literature and focus on the enabling step in ring-structure formation.

After a half-century of clinical use, tetracycline antibiotic resistance has become a serious issue, and Myers and co-workers have led the field in producing synthetic routes to tetracycline derivatives aimed at circumventing resistance.<sup>19</sup> Key to their approach is the unification of two halves through an electrocyclic ring opening of a benzocyclobutane followed by intermolecular Diels-Alder cycloaddition. This method has proven rather general toward accessing aromatic polyketides and has been implemented in numerous

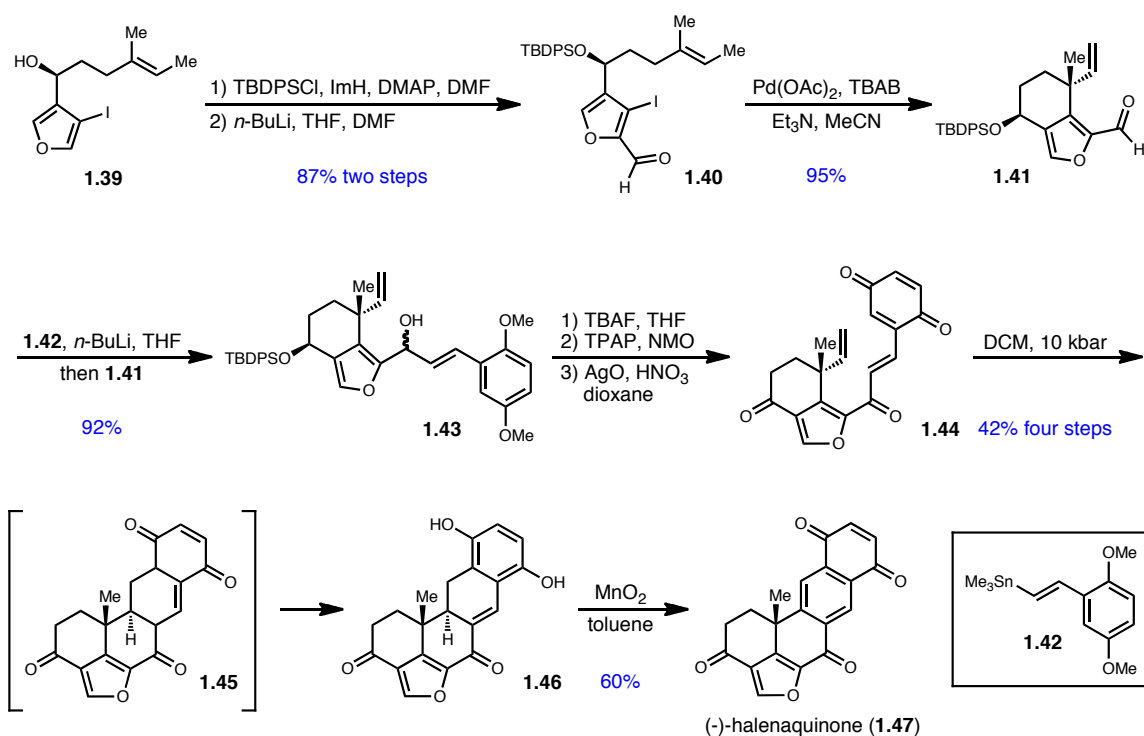
other syntheses. Therefore, Myers' total synthesis of (–)-tetracycline truly set the state of the art by introducing important alternative methods for the antibiotic's production.



Scheme 1.3. Myers' synthesis of (–)-tetracycline.

Starting with large-scale microbial whole-cell dihydroxylation of benzoic acid (**1.26**), optically pure **1.27** was then regio- and stereoselectively epoxidized with *m*-CPBA.<sup>19</sup> Methyl ester formation was followed by treatment with TBSOTf under basic conditions which effected epoxide rearrangement and subsequent bis-silylation to arrive at **1.28**. Nucleophilic addition of the lithiated isoxazole **1.29** into the methyl ester yielded ketone **1.30**, which set the stage for the first ring closure step. Heating in the presence of LiOTf caused S<sub>N</sub>2' epoxide opening by the tertiary amine functionality followed by a [2,3]-sigmatropic rearrangement of the resultant nitrogen ylide to arrive at the tricyclic **1.31**. Reductive olefin transposition successfully installed the necessary olefin regioisomer for upcoming Diels-Alder unification. Silyl deprotection and oxidation to the enone produced a common intermediate utilized by Myers for synthesis of a large number of tetracycline derivatives, whereas continuation in Scheme 1.2 describes the group's route to the natural (–)-tetracycline (**1.8**).<sup>20</sup> Installation of an α-thiophenyl enone set the stage for intermolecular Diels-Alder reaction with the stereochemically-defined benzocyclobutane **1.34** which provided the highly-elaborated **1.35** in good yield. TES-ether deprotection was followed by IBX oxidation, and *m*-CPBA oxidation of the thiophenyl group to a sulfoxide then led to sulfoxide elimination and air oxidation to hydroperoxide **1.38**. Finally, global hydrogenolysis led to (–)-tetracycline (**1.8**) through benzyl ether deprotection, isoxazole cleavage, and hydroperoxide reduction. Myers' clever approach allowed rapid buildup of complexity with an efficient route to the broad-spectrum antibiotic tetracycline and opened access to a wide range of analogs to combat problems of antibiotic resistance.

Isolated in 1983 from the tropical marine sponge *Xestospongia exigua*, halenaquinone (**1.47**) exhibits in vitro biological activity against *Staphylococcus aureus* and *Bacillus subtilis* and represents a unique pentacyclic polyketide-derived structure.<sup>21</sup> Although it had succumbed to total synthesis three times prior, Trauner and co-workers offered an elegant entry into the pentacyclic core of halenaquinone through a unique vinyl-quinone Diels-Alder.<sup>22</sup>

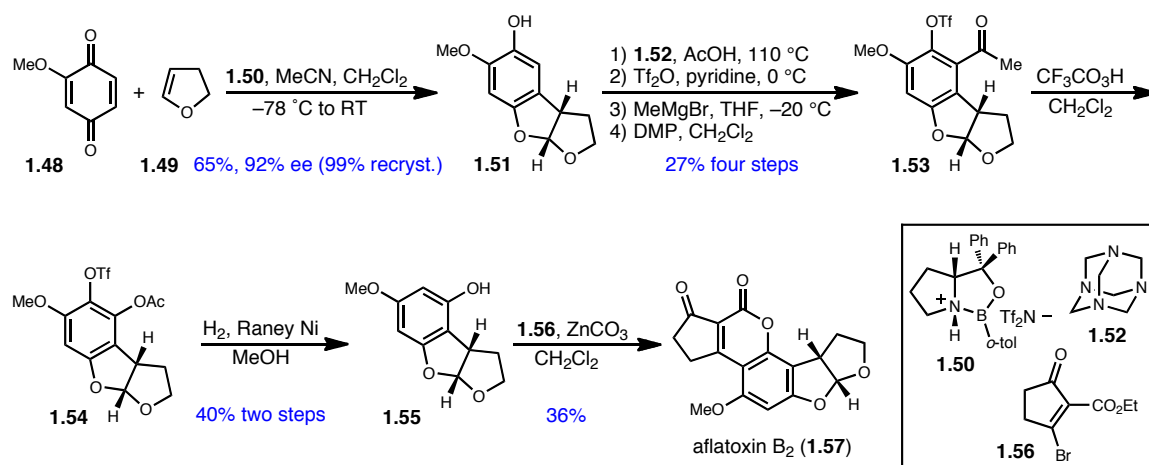


**Scheme 1.4.** Trauner's total synthesis of (-)-halenaquinone.

Starting from the enantiomerically pure iodofuran **1.39**, silyl protection of the secondary alcohol was followed by regioselective deprotonation and formylation with DMF to provide **1.40**. In a key step, an intramolecular Heck reaction stereoselectively

installed the quaternary center with the pendant vinyl dienophile found in **1.47**. Tin-lithium exchange with **1.42** and addition into the furanal **1.41** afforded the advanced intermediate as an inconsequential mixture of diastereomers. Silyl deprotection, bis-oxidation under Ley conditions, and oxidation to the vinyl quinone produced the Diels-Alder precursor **1.44**. The key pentacycle-forming step involved a high-pressure inverse-demand intramolecular Diels-Alder reaction with concomitant tautomerization to the vinyl hydroquinone **1.46**. Lastly, oxidation with MnO<sub>2</sub> completed the synthesis of (–)-halenaquinone (**1.47**). Trauner's use of the intramolecular Diels-Alder reaction for multicyclic ring system installation exemplifies one major strategy for the assembly of aromatic polyketide natural products.

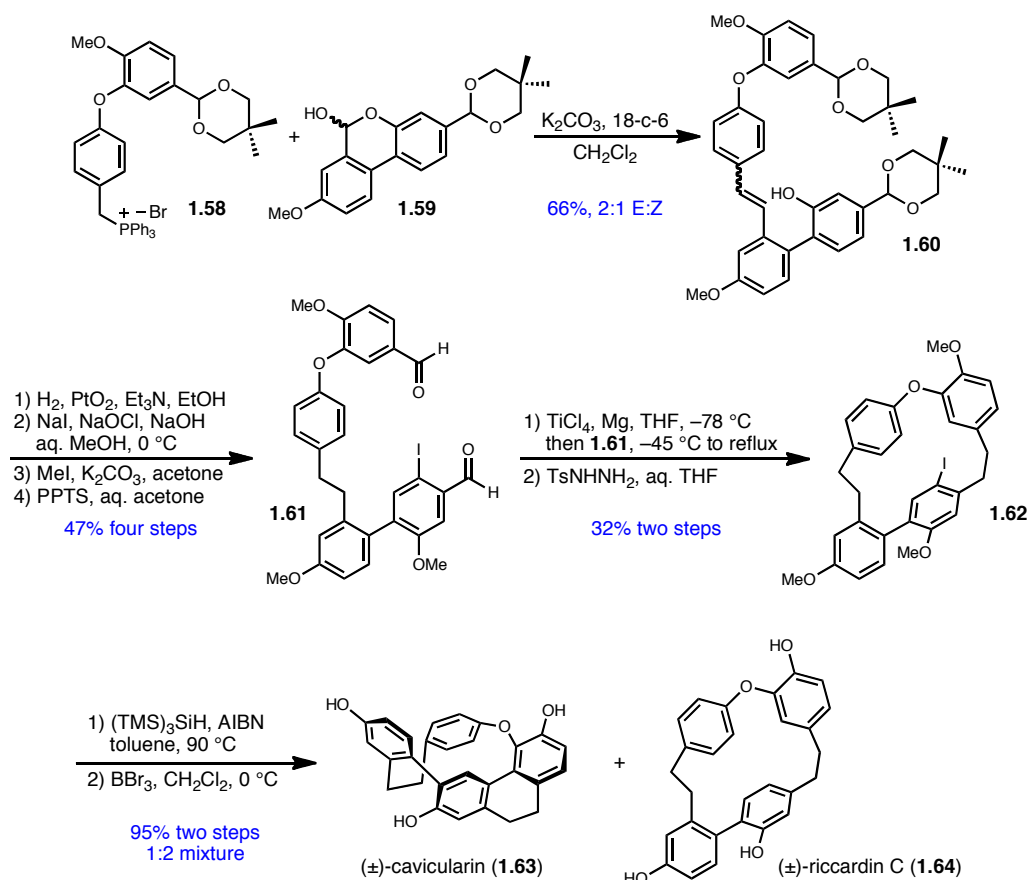
The aflatoxin family of mycotoxins was originally identified in 1960 as the common mutagens produced by a number of *Aspergillus* molds that contaminate grains and nuts in the food supply.<sup>23</sup> Aflatoxin B<sub>1</sub> (not shown), the most toxic of the family, undergoes P450-mediated epoxidation at the outer ring dihydrofuran moiety which readily undergoes DNA alkylation. Numerous syntheses of aflatoxin family members preceded Corey's enantioselective route in 2005, but the simplicity of an asymmetric [3+2] cyclization to establish three of the five rings sets this approach apart from others in addition to its brevity.<sup>24</sup>



**Scheme 1.5.** Corey's total synthesis of aflatoxin B<sub>2</sub>.

Key to Corey's synthesis is the enantioselective [3+2] electrocyclization between 2-methoxy-1,4-benzoquinone (**1.48**) and 2,3-dihydrofuran (**1.49**) catalyzed by (*R*)-oxazaborolidinium triflimide **1.50** to yield the desired adduct in 65% yield and 92% ee. Following one crystallization, 99% ee can be obtained. Regioselective formylation with HMT, phenol triflation, methyl Grignard addition to the aldehyde, and subsequent oxidation to the methyl ketone provided the advanced intermediate **1.53** in a four-step yield of 27%. Baeyer-Villiger oxidation of the methyl ketone installed the necessary acetate-protected phenol in **1.54**, which was deacetylated along with hydrogenolysis of the aryl triflate to provide **1.55**. In one final step, construction of the final two rings occurred with β-bromo-cyclopentenone **1.56** and ZnCO<sub>3</sub> to complete the synthesis of aflatoxin B<sub>2</sub> (**1.57**) in 36% yield. The effectiveness of an electrocyclization step in the synthesis of a complex aromatic polyketide is evident in Corey's route to aflatoxin B<sub>2</sub>, which allowed for rapid assembly of molecular architecture in a single step.

One of the more unusual aromatic polyketides known, caviclarin (**1.63**) was isolated from the liverwort *Cavicularia densa* and possesses a dihydrophenanthrene moiety within a macrocyclic structure containing two other aryl rings.<sup>25</sup> Interestingly, the immense macrocyclic ring strain causes the ether-linked arene to adopt a boat-like conformation, and this fact played a large part in Harrowven's synthetic design. To this point, an ingenious radical-mediated transannular ring contraction was planned to alleviate issues related to ring strain until the final steps of the synthesis.

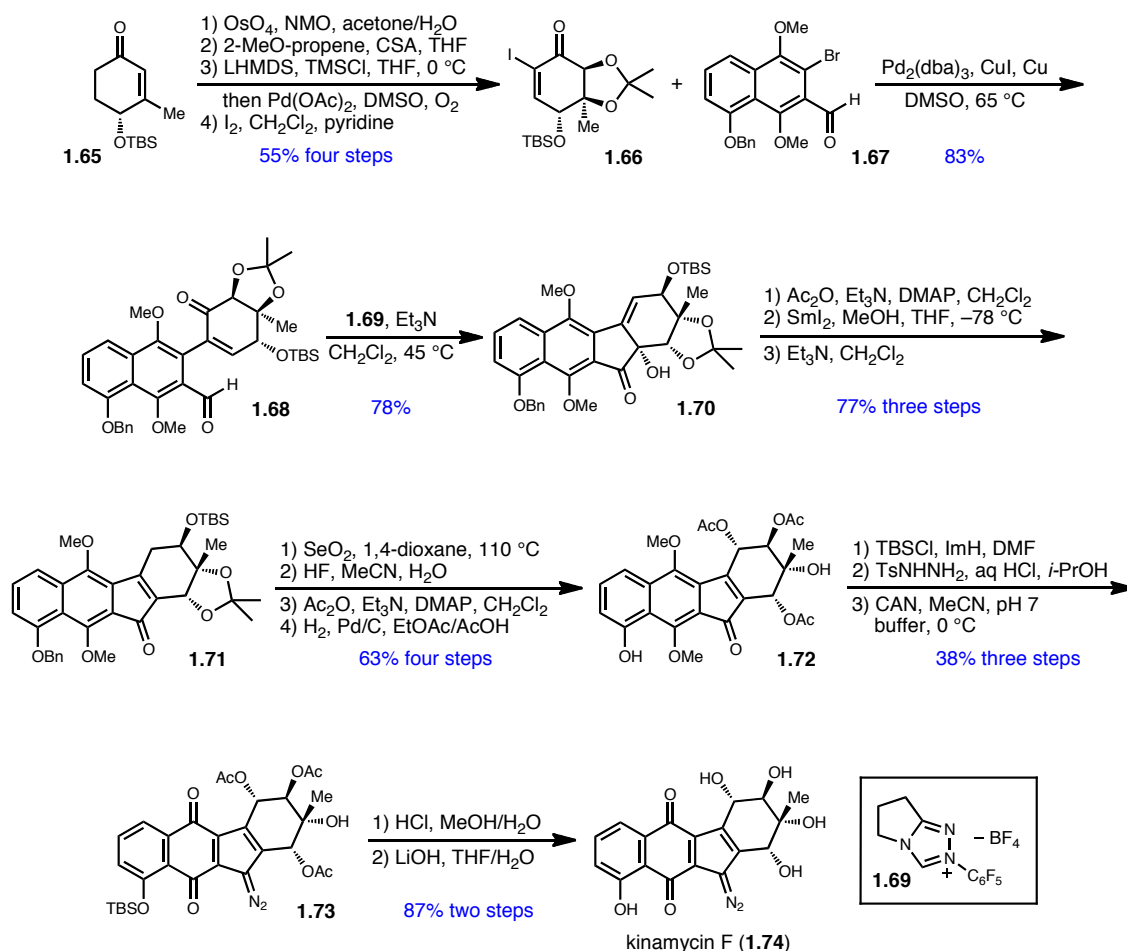


**Scheme 1.6.** Harrowven's synthesis of (±)-caviclarin and (±)-riccardin C.

Thus, starting from the two advanced building blocks **1.58** and **1.59**, synthesized in six and four steps respectively, a modified Wittig protocol provided the stilbene **1.60** as an inconsequential mixture of *E* and *Z* isomers. Hydrogenation of the resultant olefin was followed by regioselective basic aryl iodination, phenol methylation, and bis-acetal deprotection to arrive at **1.61** in high yield. Macrocyclization under McMurray-type conditions was followed by diimide reduction to provide **1.62**, which was set up for the key ring contraction reaction. Radical initiation with tris(trimethylsilyl)silane and AIBN successfully effected transannular ring contraction at 90 °C through radical combination into the adjacent aryl ring, although a large majority of the material underwent dehalogenation toward riccardin C (**1.64**). The inseparable mixture was subjected to demethylation conditions which led to a separable mixture of (±)-cavicularin (**1.63**) and (±)-riccardin C (**1.64**) in a 1:2 ratio. Harrowven's use of a radical-mediated ring contraction truly enabled the assembly of this highly strained macrocyclic system.

The kinamycin family of aromatic polyketides, whose original members A-D were isolated by Ōmura from *Streptomyces murayamaensis*, contains a unique diazotetrahydrobenzo[*b*]fluorene skeleton and includes numerous other members varying in alcohol acetylation level.<sup>26</sup> The kinamycins exhibit potent anticancer activity across a range of cell lines and have been shown to act as DNA damaging agents. Although various kinamycin family members have succumbed to synthesis, Nicolaou's approach to kinamycin F highlights the usefulness of multi-step cyclization sequences in the assembly of aromatic polyketides.<sup>27</sup>





**Scheme 1.7.** Nicolaou's total synthesis of kinamycin F.

Toward synthesis of kinamycin F (**1.74**), stereoselective dihydroxylation of the readily available enantiopure **1.65** was followed by acetone protection, Saegusa oxidation, and enone iodination to arrive at **1.66** in high yield over four steps. Iodo enone **1.66** and naphthalene bromide **1.67** constitute three of the four rings of the kinamycins, and their unification to produce the remaining five-membered ring was initiated through an Ullmann coupling to provide **1.68**. To complete the multi-step cyclization, a benzoin-like condensation with the Rovis catalyst (**1.69**) effectively formed the acyloin **1.70** in

78% yield. With the kinamycin backbone synthesized, functional group manipulation began with tertiary alcohol acetylation and reduction, which was followed by base-mediated olefin isomerization to provide **1.71**. Stereoselective allylic oxidation with  $\text{SeO}_2$  installed the final oxygen functionality, and the sequence of concomitant silyl and acetonide deprotection, triacetylation, and benzyl deprotection arrived at **1.72** in excellent yield. Phenol silylation set up for diazo moiety incorporation, which was effected by formation of the tosyl-hydrazone and CAN oxidation to form the protected kinamycin product **1.73**. Finally, silyl and acetate group deprotection led to kinamycin F (**1.74**). While utility overrules elegance in the two-step cyclization approach to aromatic polyketides, Nicolaou and co-workers effectively demonstrated the importance of its consideration during synthetic planning through their successful assembly of kinamycin F (**1.74**).

Aromatic polyketide natural products have played an important role as medicinal agents, and thus synthetic access holds the potential to continue impacting human health. While many structural scaffolds exist, all aromatic polyketides can be related by common biosynthetic synthesis by type II polyketide synthases. Numerous strategies for their synthetic assembly have emerged, and the examples shown above seek to highlight the main methods used as key cyclization steps. Myers' use of an intermolecular Diels-Alder reaction toward (–)-tetracycline (**1.8**) allowed for rapid unification of two highly functionalized subunits, while Trauner's synthesis of halenaquinone (**1.47**) showcases the power of the intramolecular Diels-Alder reaction to build multi-ring systems in one single step. The linchpin [3+2]-electrocyclization in Corey's approach to aflatoxin B<sub>2</sub> (**1.57**) highlights the value of simplicity in the first synthetic step which provided three of the

five rings found in the natural product with the correct functionalization and stereochemistry. The unusual natural product caviularin (**1.63**) shows the wide range of possible aromatic polyketides synthesized by microorganisms, and Harrowven's elegant implementation of a radical-mediated macrocyclic ring contraction overcame innate structural limitations to arrive at the desired product. Finally, Nicolaou's approach to kinamycin F (**1.74**) underscores the value and utility of multi-step ring formation, as its use can be equally successful in comparison with single-step cyclizations such as the Diels-Alder. With the importance of aromatic polyketide and methods for their formation in mind, the hibarimicin aromatic polyketide natural products constitute an important family of biologically important compounds in which a total synthetic effort holds promise in furthering the field of natural product therapeutics.

### **Angelmicins A and B**

Oncogene-transformed cells exhibit lower growth requirements and continue to grow and thrive in a serum-free medium, while normal cells require specific growth factors for proliferation.<sup>28</sup> Therefore, selective inhibitors of oncogenesis should display growth inhibition of transformed cells in serum-free medium but not in serum-containing medium, and an IC<sub>50</sub> shift should be observable. Using this paradigm, Uehara and co-workers screened the culture broth of a rare actinomycete *Microbispora* sp. AA9966 for selective growth inhibition and in 1993 reported the isolation of substances that potently inhibited the growth of *src* and *abl* oncogene-transformed NIH3T3 cells.<sup>29</sup> The microorganism was isolated from a soil sample collected at Mt. Tennyō in Gunma

Prefecture, Japan, and the substances were termed angelmicins A and B (**1.75**). The red powders were determined to have molecular formulae of  $C_{85}H_{112}O_{38}$  and  $C_{85}H_{112}O_{37}$  respectively and were determined to have general structures including one anthraquinone and six sugar moieties for each compound.

Angelmicin B was found to shift  $IC_{50}$  values of growth inhibition of *src* and *abl*-transformed mouse NIH3T3 cells between serum-free and serum-containing media 7- and 10-fold respectively, while in *ras*-transformed cells, angelmicin B caused only a 2.5-fold change in  $IC_{50}$ .<sup>29</sup> Comparatively, common chemotherapeutics such as doxorubicin and vinblastine showed no such selectivity in the developed assay indicating that the activity of angelmicins may be attributed to novel modes of action directly involving oncogenic signaling pathways. To further validate the activity of angelmicins on oncogene-derived signaling,  $p60^{v-src}$  autophosphorylation was probed, and it was determined that angelmicins reduced activity in a dose dependent manner. Thus, angelmicins selectively inhibit the growth of oncogene-transformed cells without affecting the growth of normal cells, and through a single assay testing for direct inhibition of various protein kinases, angelmicins were characterized as selective inhibitors of tyrosine kinase without affecting protein kinase A or C.

With knowledge of its activity toward *src* tyrosine kinase, it was postulated that angelmicin B could be utilized as a differentiation agent for acute leukemia.<sup>30</sup> This indication is based on the premise that unchecked cell proliferation results from aberrant signaling due to the action of oncogenes, and chemical agents can induce terminal differentiation of immature malignant cell lines to abate cancerous growth. Therefore, because *src* is known to be a proto-oncogene implicated in numerous forms of cancer,

angelmicin B could potentially act as a chemotherapeutic, and the HL-60 leukemia cell line was chosen based on its previously reported ability to differentiate into a mature lineage with the addition of chemical agents. Thus, angelmicin was determined to inhibit HL-60 cell line growth with an  $IC_{50}$  of 58 nM while other leukemia cell lines were less responsive. Differentiation induction was also evaluated, and angelmicin B showed significant ability to effect differentiation of the HL-60 cell line which is indicated by NBT reduction and morphological changes, at a concentration of approximately 175 nM. Additionally, angelmicin B was found to act synergistically in effecting HL-60 differentiation when co-treated with retinoic acid,  $TNF\alpha$ , and vitamin  $D_3$ . And while most chemotherapeutics effect differentiation at cytotoxic concentrations, all angelmicin B-treated cells that underwent differentiation were not apoptotic, indicating that the mechanism of differentiation induction may be novel and may implicate angelmicin B as an effective therapy for myeloid leukemia.

Several other angelmicin family members that were isolated from the same actinomycete culture broth but not reported in the initial isolation paper, which include angelmicins  $A_1$ ,  $A_2$ , C, and D, were also tested for their ability to inhibit HL-60 cell growth and differentiation.<sup>30</sup> Angelmicin B most potently inhibited tyrosine kinase activity and HL-60 growth, while angelmicin  $A_2$  was determined to be the most effective differentiation inducer. Also, from these studies, some important inconsistencies regarding the activity of angelmicin B arose. Most importantly, the concentrations of angelmicin B required for *src* tyrosine kinase inhibition were 20 to 200-fold higher than the concentrations necessary for growth inhibition. This indicates that tyrosine kinase may not be the responsible mechanism for the observed growth inhibition; however,

these events may be closely linked through a yet unknown pathway. Additionally, topoisomerase II was postulated as an alternative target that could be responsible for HL-60 growth inhibition, of which known tyrosine kinase inhibitors have been shown to also effect topoisomerase inhibition. Finally, angelmicin B was studied as a differentiation inducer in freshly isolated leukemia cells, and while angelmicin B alone did not effect differentiation, it greatly improved the differentiation induction in unison with retinoic acid in acute promyelocytic leukemia.

Three years removed from the publication of angelmicin isolation and characterization as selective tyrosine kinase inhibitors, the structure of angelmicin B was reported.<sup>31</sup> Based on UV and visible spectra, which indicated absorbance at 511 nm that disappeared in a basic methanol solution, and an IR spectrum with peaks at 3450, 1705, and 1620  $\text{cm}^{-1}$ , angelmicin B was identified as containing a phenolic quinone structure. Beyond these studies, extensive 1D and 2D NMR spectroscopy was utilized to determine the complete carbon structure. The presence of six anomeric methine carbons indicated six sugar moieties, while two similar halves of the aglycon were assigned based on COSY and HMBC spectra. Each half contained a tertiary *n*-propyl unit, of which the tertiary oxygen of one half formed an ether bridge. Through NOESY and HMBC spectra, the sugar incorporation appeared symmetrical with equivalent disaccharides attached at both C-12 and C-12' and a monosaccharide connected to C-10 and C-10'. Specifically, angelmicin B contains a  $\beta$ -amicetopyranose (AM) directly attached to the C-12 and C-12' hydroxyl groups and an  $\alpha$ -4-*C*-acetyl-2,3,6-trideoxyhexopyranose (AT) linked to both AM's. Connected to the C-10 and C-10' hydroxyl groups is an  $\alpha$ -digitoxopyranose (DG) moiety. Anomeric configurations were determined by coupling constants and relative

sugar stereochemistry was reported; however, absolute sugar configurations were not determined. Three aryl methoxy groups reside on the A-ring, and the remaining methoxy group was assigned to the C-3' quinone carbon based on comparison with a similar compound, *O*-methyllapachol. Finally, the remaining assignment involved attachment of the two similar halves through a carbon-carbon bond between the aryl C-2 and quinone C-2'. The originally assigned two-dimensional structure of angelmicin B, which did not include relative or absolute stereochemical assignments, is shown in Figure 1.4.

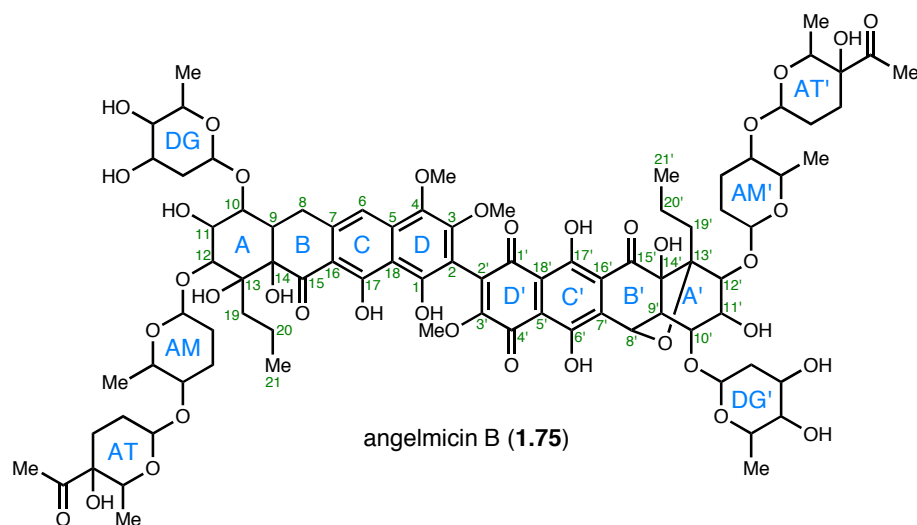


**Figure 1.4.** Two-dimensional structure of angelmicin B.

### The Hibarimicin Family of Aromatic Polyketide Natural Products

In 1998, while searching for tyrosine kinase inhibitors based on the aforementioned multi-kinase assay, Kajiura and co-workers reported the isolation of a family of natural products produced by the actinomycete *Microbispora rosea* subsp.

*hibaria* TP-A0121.<sup>32</sup> The microorganism was isolated from a soil sample collected at Hibari, Toyama Prefecture, Japan, in 1995, and the species was identified based on growth characteristics and DNA-DNA homology studies. Fermentation, ethyl acetate extraction, and chromatographic separation yielded more than ten components which were termed hibarimicins. Of these ten hibarimicins, physicochemical properties were reported for hibarimicins A, B, C, D, and G, all of which were red powders with an indicative UV absorbance at 511 nm in MeOH, properties that for B and D were noted in the publication to be identical to angelmicins B and A.

The multi-kinase assay utilized in the isolation of the hibarimicins involved detection of protein kinase A, protein kinase C, protein tyrosine kinase, and calmodulin-dependent protein kinase III. By screening all four kinases within the same assay, Kajiura and co-workers were able to determine that the hibarimicins were selective inhibitors of protein tyrosine kinase activity without inhibiting the activity of protein kinases A or C. In vitro IC<sub>50</sub> values for hibarimicins A-D were reported to range from 580 nM (hibarimicin A) to 2.32  $\mu$ M (hibarimicin B) against *src* tyrosine kinase. And MIC's for in vitro inhibitory activity against Gram-positive bacteria for hibarimicins A-D ranged from 464 nM to 7.25  $\mu$ M. Finally, in vitro cytotoxicity against B16-F10 (murine melanoma) and HCT-116 (human colon carcinoma) cells ranged from 406 nM to 1.01  $\mu$ M. Therefore, the hibarimicin natural products exhibit a broad range of biological activity that centers around their roles as protein tyrosine kinase inhibitors.

The second publication in the series with Kajiura's report in 1998 involved the structural determination of hibarimicins A-D and G highly relying on 1-D and 2-D NMR spectroscopic techniques.<sup>33</sup> Based on the identically characteristic UV absorbances and



IR stretches across the family, the determination was made that the compounds all contained the same chromophore. Basic NMR spectroscopy identified the presence of carbohydrate moieties, and further investigation indicated their attachment in pairs for a total of six sugars. Thus, utilizing COSY, HMBC, NOESY, and TOCSY NMR, the sugars and their connectivities were assigned as  $\beta$ -amicetosyl (2,3,6-trideoxy- $\beta$ -*erythro*-hexopyranose),  $\alpha$ -digitoxosyl (2,6-dideoxy- $\alpha$ -*ribo*-hexopyranose), and 4-*C*-acetyl-2,3,6-trideoxy-*threo*-hexopyranose moieties. While the relative stereochemistry of the sugars was determined through coupling constants and comparison with synthetic versions, the absolute stereochemistry of all sugars remained undetermined.

Assignment of the hibarimicin aglycon again involved extensive 2-dimensional NMR spectroscopy. The molecule was divided roughly into halves, and two spin systems for each side were determined through COSY correlations. Complimentary HMBC established the carbon framework, and NOE and NOESY experiments confirmed these connectivities. Importantly, the six and seven contiguous stereocenters of the western and eastern tetracycles, respectively, were assigned primarily by coupling constants, which confirmed the *cis* relationship of the decalin ring systems and the *trans-trans* orientation of the triol systems. NOE and NOESY correlations further reinforced these stereochemical findings. And while the ether linkage in the eastern tetracycle aided in assigning the relative stereochemistry of the C-13' center, no related assignment could be made at C-13 purely based on spectroscopic data. Additionally, although relative stereochemistry for the aglycon was successfully determined, the absolute configuration remained to be elucidated.

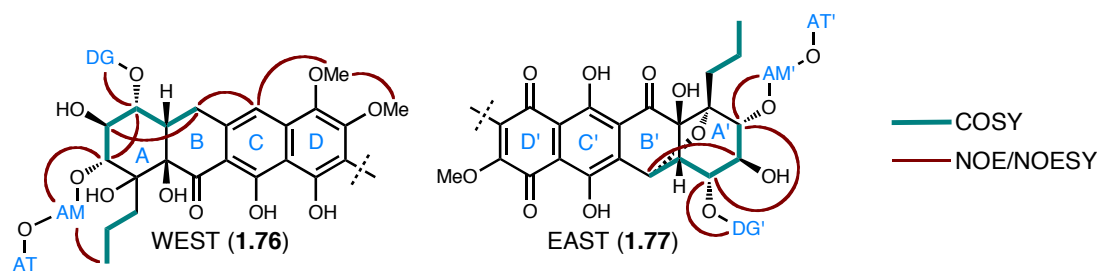


**Figure 1.5.** Key COSY and NOE/NOESY correlations for hibarimicin B.

With the carbohydrates and aglycon for hibarimicin B (**1.78**) assigned, it was confirmed that hibarimicin B was identical to the previously reported angelmicin B. And from the structural knowledge of hibarimicin B, the final assignments were made for the remaining members of the family. Ultimately, it was determined that the hibarimicins all retained the same aglycon core and AM and DG sugar patterning while differentiation occurred at the terminal carbohydrate moieties X and Y, as shown in Figure 1.6. Hibarimicins A, B, C, D, and G were reported in the 1998 structure elucidation paper, and E, H, and I were disclosed in a later publication. As shown, a few structural features are worth noting. While the absolute stereochemistry was not determined for the aglycon, the relative stereochemistry was initially represented in early reports as the enantiomer shown in Figure 1.6. Importantly, the tetra ortho-substituted aryl-quinone bond connecting the western and eastern halves of the aglycon has the potential to exhibit hindered rotation due to steric repulsion of the ortho substituents (atropisomerism); however, this possibility was not addressed in the structure elucidation paper. Nevertheless, one could reasonably assume that any isolated mixture of atropisomers would relay to a mixture of diastereomers visualized in the proton NMR spectrum, or readily interconvertible atropisomers would potentially cause line broadening. Thus, if

the hibarimicins do display atropisomerism, a single natural atropisomer would be a fair assumption for the family.

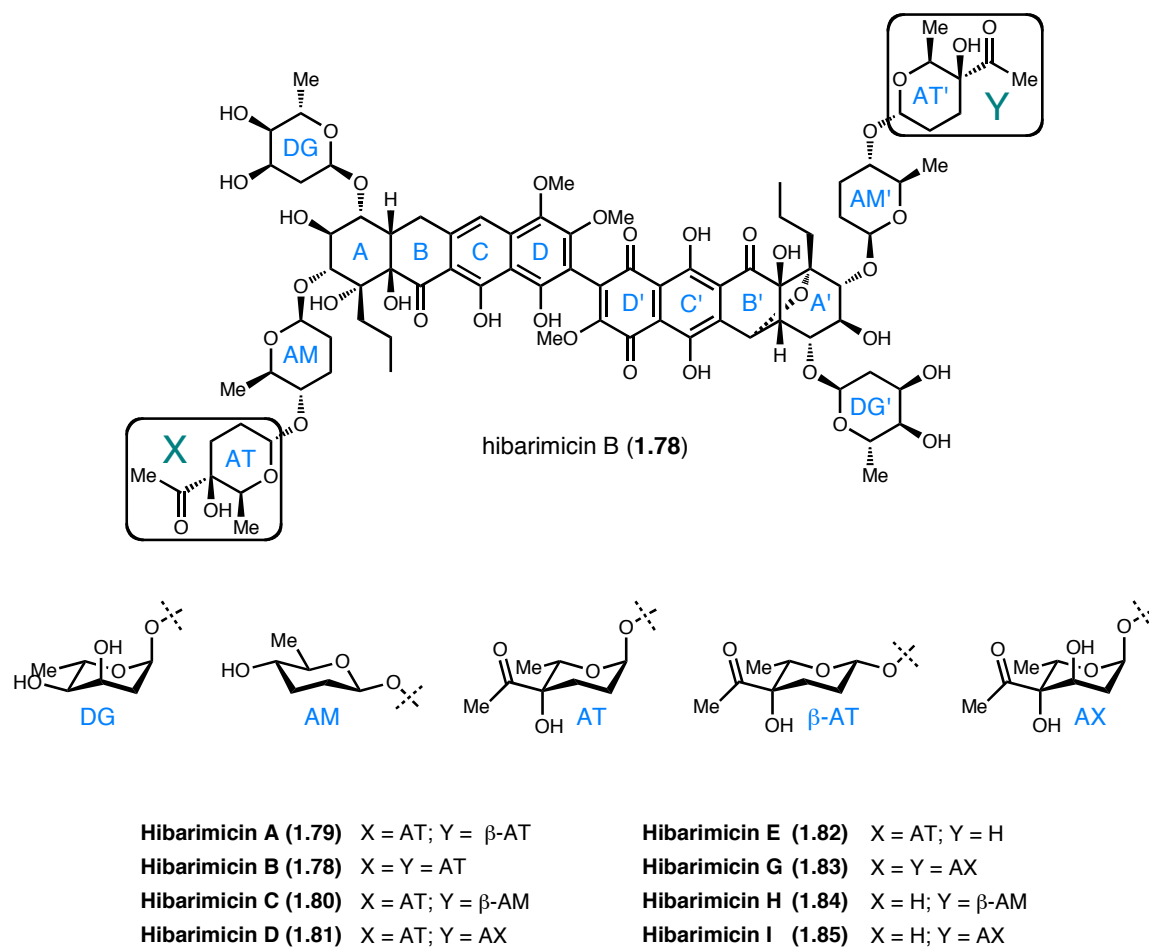


**Figure 1.6.** The hibarimicin family of natural products.

### Biosynthesis of the Hibarimicins

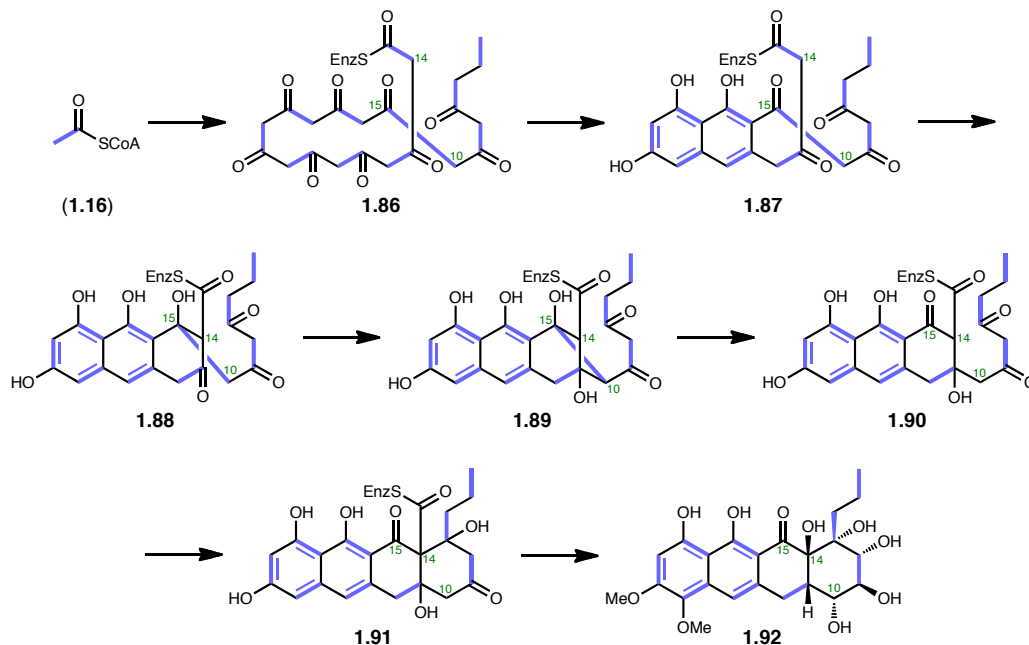
The hibarimicins are some of the most complex type II aromatic polyketide natural products to have been isolated, and because their structures do not purely adhere

to simple aromatic PKS patterning, determining their biosynthetic pathway remained an intriguing proposal. In 2002, led by Hori, Kajiura, and Igarashi, a series of three publications addressed this interest through two different approaches.

Utilizing the methodology originally developed by Birch, Hori and co-workers reported the use of isotopic labeling of precursor units to unravel important portions of the pathway.<sup>34</sup> By fermentation of *Microbispora rosea* subsp. *hibaria* TP-A0121 with [1-<sup>13</sup>C], [2-<sup>13</sup>C], or [1,2-<sup>13</sup>C<sub>2</sub>] acetates, isotopically labeled hibarimicin B was produced and analyzed by <sup>13</sup>C NMR. These studies revealed that aside from three methoxy carbons and the carbohydrate moieties, all carbons of the hibarimicin B aglycon were derived from acetate units and thus confirming its biosynthesis from a polyketide pathway. Incorporation patterns indicated two symmetric polyketide chains attached at the C-2/C-2' aryl-quinone bond, which supports a pathway involving oxidative dimerization of two half-fragments, biosynthesized from a linear undecaketide, to provide the bis-tetracyclic carbon framework. Additionally, irregular two carbon unit incorporation was observed at carbons 10, 14, and 15, implying the possibility of a rearrangement and decarboxylation sequence. Specifically, C-10 and C-15 were proposed to be derived from a single acetate, while decarboxylation at C-14 would account for the remaining missing carbon. Importantly, by proposing an oxidative dimerization of two equal tetracycles, the assumption can be made that the previously unassigned C-13 tertiary center should exhibit the same stereochemistry as the C-13' tertiary ether.

The hypothesized rearrangement necessary to account for the results of isotope labeling studies is shown in Scheme 1.8. From acetyl CoA (**1.16**) fragments, a linear undecaketide **1.86** is assembled, in which purple bolded bonds represent the

incorporation of a single acetate. Cyclization and aromatization of the first two rings occurs with standard Claisen condensation reactions and ketone tautomerization. Intermediate **1.87** has been shown suggestively to account for C-10/C-15 incorporation from a single acetate unit, and Claisen condensation of C-14 onto the C-15 ketone is proposed to initiate the rearrangement cascade to provide **1.88**. A second Claisen of C-10 onto the C-9 ketone provides an unstable four membered ring that should undergo a retro-Claisen to arrive at **1.90**. Finally, addition of C-14 to the C-13 ketone forms the A ring and is followed by C-14 decarboxylation and further oxidation steps to arrive at the monomeric unit (**1.92**) utilized in the proposed oxidative dimerization.

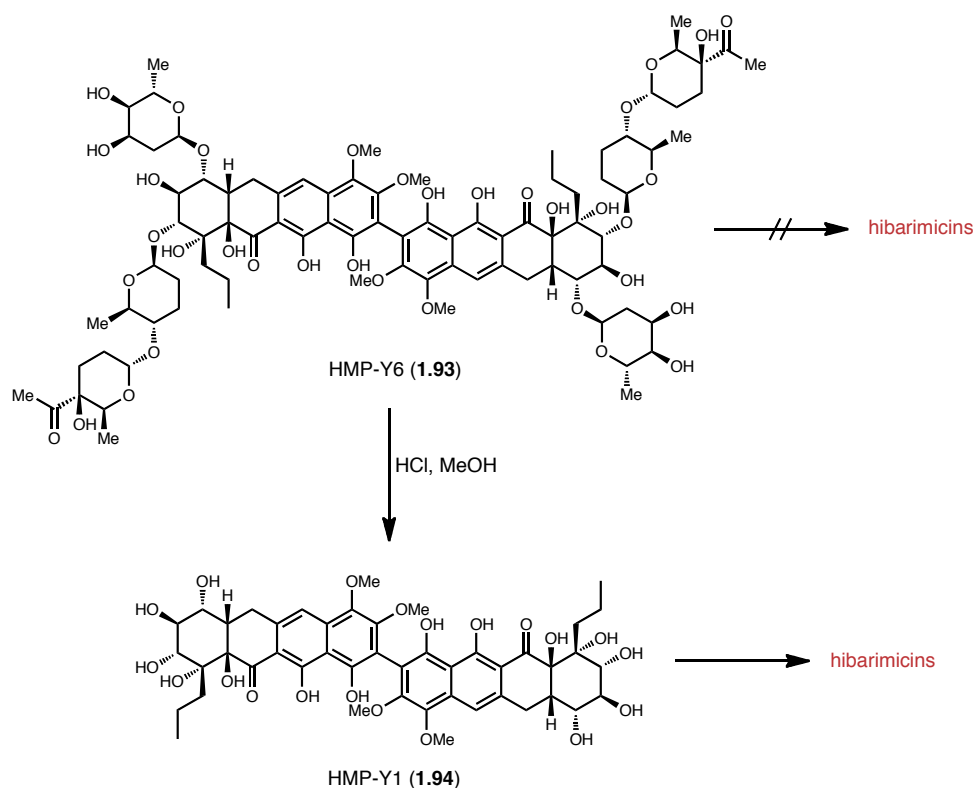


**Scheme 1.8.** Proposed biosynthetic rearrangement producing tetracycline **1.92**.

The second complimentary biosynthetic study involved random mutagenesis of the hibarimicin-producing bacteria with N-methyl-N'-nitrosoguanidine (NTG).<sup>35</sup> After

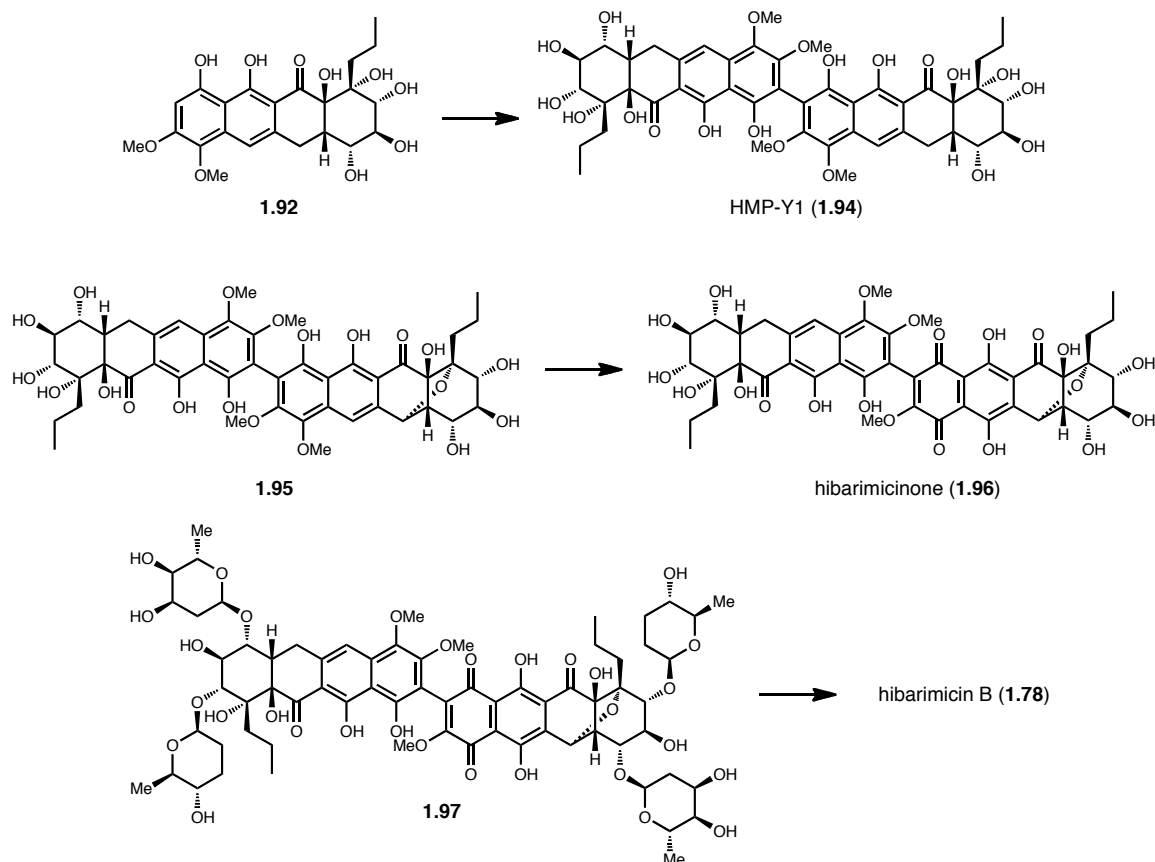
incubation of strain TP-A0121 with NTG, the surviving spores were further incubated for 14 days to produce colonies that were chosen based on pigment color. Fermentation of the chosen colonies produced mutant products that provided insight into the order of dimerization and glycosylation.

Of the stable isolated mutant lines, mutant AN-0416 produced the most important blocked mutant compound which was termed HMP-Y6 (**1.93**). HMP-Y6, where Y describes the color of the product (yellow), was determined to be a dimer of the west half of hibarimicin B, where presumably mutagenesis affected PKS enzymes responsible for the east half oxidation state.<sup>36</sup> HMP-Y6 was converted to HMP-Y1 (**1.94**) by acidic methanolysis to provide the aglycon, and one of these two metabolites was proposed as a biosynthetic intermediate to hibarimicin B. To test this hypothesis, cosynthesis, or direct addition of HMP-Y6 and HMP-Y1 to the fermentation broth of mutant strains, was performed with the expectation that a true intermediate would be indicated by the production of hibarimicins. With HMP-Y6 and HMP-Y1, cosynthesis experiments confirmed that HMP-Y1, not the glycosylated form HMP-Y6, was a biosynthetic intermediate of the hibarimicins. Additionally, the HMP-Y6 producing strain was further mutated to glean insight into the order of cyclization to produce the tetracycle **1.92**. Isolated mutant products confirmed that cyclization of the aromatic rings occurs under the traditional Claisen cyclization paradigm and is followed by rearrangement and decarboxylation.



**Scheme 1.9.** Identification of HMP-Y1 as a biosynthetic intermediate.

The resulting biosynthetic pathway for the hibarimicins is proposed in Scheme 1.10. From the monomeric tetracycle **1.92**, oxidative dimerization arrives at the  $C_2$ -symmetric intermediate HMP-Y1 (**1.94**). Because HMP-Y1 and not HMP-Y6 produced hibarimicins in the cosynthesis experiment, dimerization and oxidation were confirmed to occur prior to glycosylation. Thus, HMP-Y1 undergoes ether-bridge formation and oxidation to the naphthoquinone to provide the hibarimicin aglycon, which was termed hibarimicinone (**1.96**). Hibarimicinone undergoes a first round of glycosylation, installing amictoses at C-12 and C-12' and digitoxoses at C-10 and C-10', then the second round of glycosylation provides the hibarimicin family of natural products.



**Scheme 1.10.** Biosynthetic pathway of hibarimicin B.

### Atropisomerism and Natural Product Total Synthesis

Due to the scarcity of natural products displaying the tetra-ortho substituted aryl-quinone bond found in the hibarimicins, minimal precedent exists for evaluating the possibility of atropisomerism in this system. However, axial chirality is a prevalent feature of natural products, drug molecules, and ligands such as BINAP (**1.99**), which most commonly exist in biaryls and trisubstituted amide functionalities.<sup>37,38</sup> The natural product vancomycin (**1.98**) has been used in the clinic as the antibiotic of last resort since its isolation in 1953, while BINAP continues to play an instrumental role in the



generation of enantiomerically pure materials, initially used in pioneering work by Ryōji Noyori in his development of an asymmetric hydrogenation reaction that garnered him a Nobel Prize in 2001. Atropisomerism also plays an important role within drug molecules, exemplified by telenzepine (**1.100**), which exhibits atropisomerism about its trisubstituted amide bond that undergoes conversion between isomers with a half life of 1000 years.<sup>37</sup>

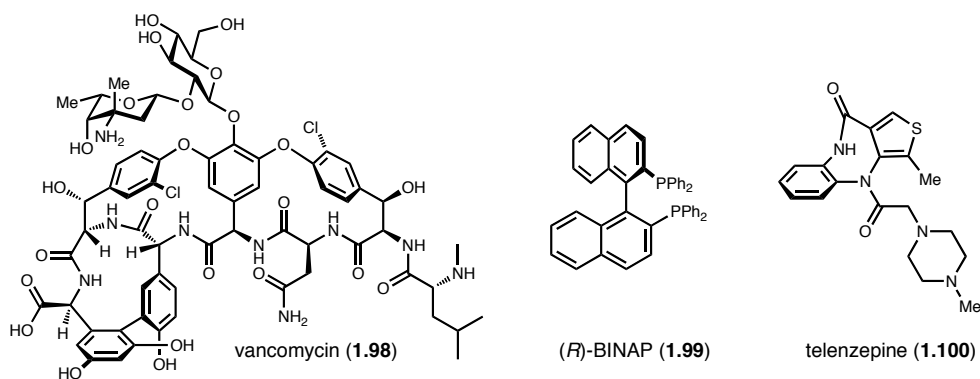


**Figure 1.7.** Important compounds exhibiting atropisomerism.

Atropisomerism is defined as the restricted bond rotation about a covalent bond that arises from steric strain during interconversion resulting in the existence of stereoisomers. In the case of biaryls, most tetra-ortho substituted systems can exhibit this type of stereoisomerism, where the size of the ortho substituents can determine the barrier to rotation, and require elevated temperatures for interconversion. Generally, as the number of ortho substituents (or their size) decreases, the temperatures at which they become no longer distinguishable also decreases, and often tri-ortho substituted systems racemize at or slightly above room temperature. The commonly accepted standard for considering rotation sufficiently hindered to cause atropisomerism is a half life for

interconversion of 1000 seconds, or 16.7 minutes at a certain temperature.<sup>39</sup> This roughly correlates to an energy barrier of  $\Delta G = 22.3$  kcal/mol at 27 °C.

Two related naming conventions exist for indicating axial chirality. The most common notation utilizes the standard *R* and *S* nomenclature used for linear chirality, which is denoted by *aR* and *aS* for atropisomers. By viewing the Newman projection of the biaryl bond, the ortho substituents are assigned Cahn-Ingold-Prelog priorities, and a 270 ° path from the highest priority substituent of the front ring to the highest priority substituent on the back ring in a clockwise direction denotes the *aR* configuration, while the counter-clockwise direction indicates the *aS* configuration. Conversely, a direct 90 ° path from highest priority substituent on the front ring to the highest priority substituent on the back ring in a counter-clockwise direction is defined as the M (minus) orientation, and the clockwise direction indicates the P (plus) orientation. For the remainder of this document, the *aR/aS* notation will be utilized exclusively.

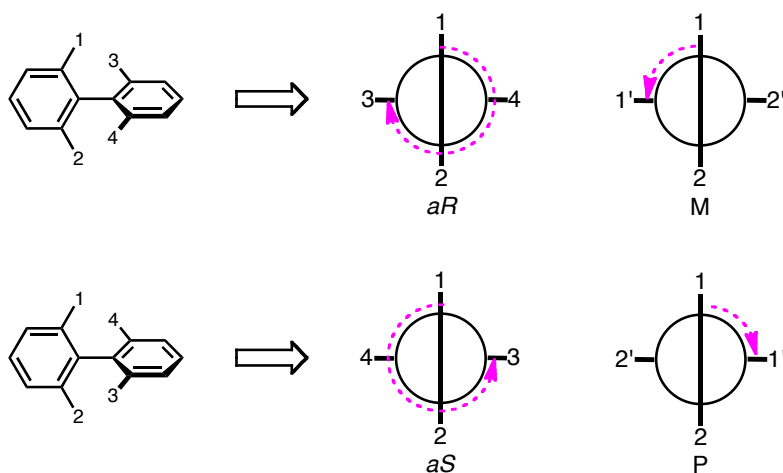
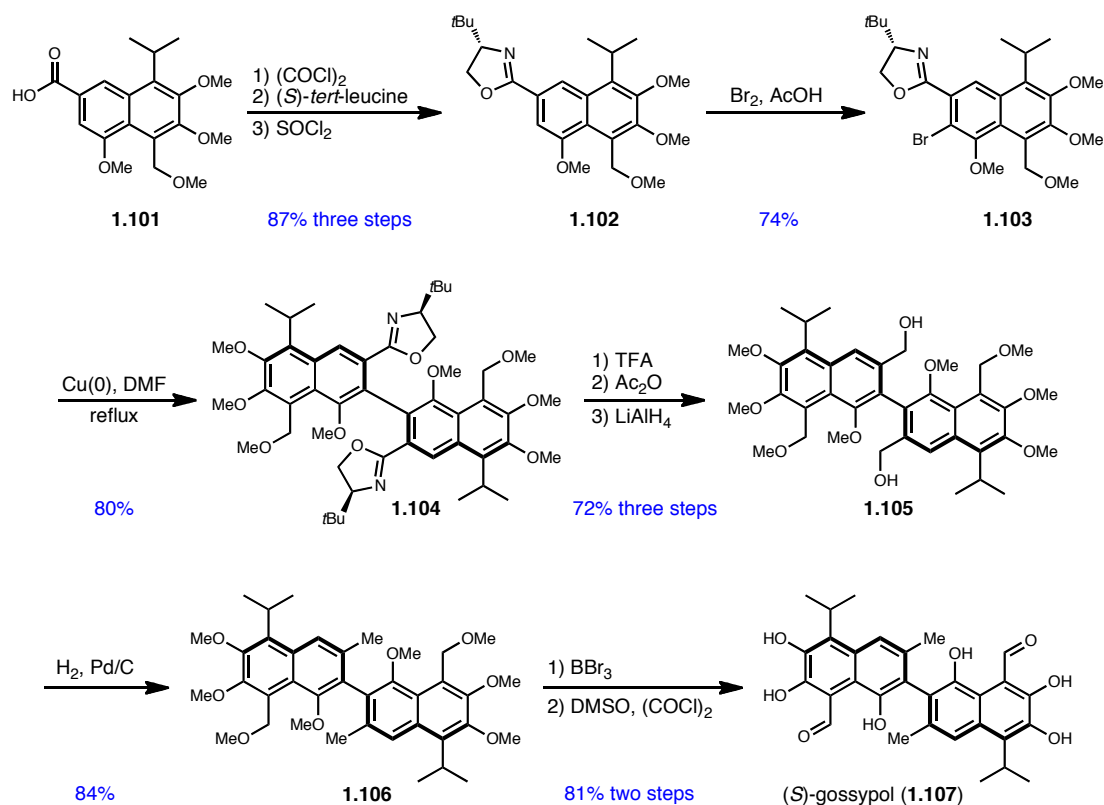


**Figure 1.8.** Nomenclature standards for atropisomers.

Gossypol is one of the most well known atropisomeric natural products, which exhibits antispermatic, antimalarial, and antitumor properties based on its atropisomeric orientation.<sup>40</sup> Originally isolated in 1886 by Longmore, its structure wasn't determined until 1938 by Adams and ultimately not confirmed until Edwards published its first total synthesis in 1957.<sup>41</sup> Its  $C_2$ -symmetric bis-naphthalene structure represents one of the most common and simplest forms of biaryl atropisomerism. And its atroposelective synthesis by Meyers in 1997 represents one of the key synthetic approaches to enantiopure atropisomers.

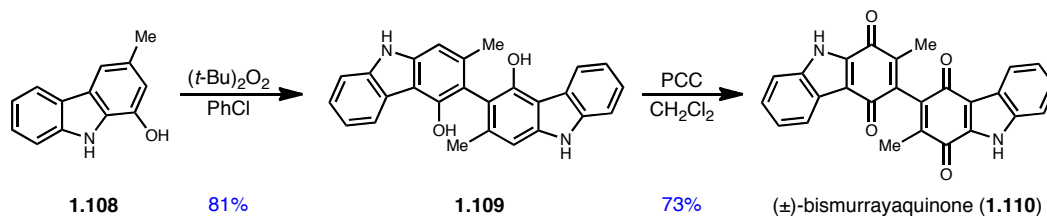
From naphthalene acid **1.101**, formation of the oxazoline auxiliary with the acid chloride and (*S*)-*tert*-leucine was followed by regioselective bromination to arrive at **1.103**. Refluxing this compound in DMF with Cu(0) effected asymmetric Ullmann coupling to arrive at a 17:1 diastereomeric mixture of **1.104**, where the use of a removable auxiliary successfully effected the formation of a single isomer. Three step removal of the oxazoline functionality provided the primary alcohol, which was converted to the bis-tolyl product **1.106** under hydrogenolysis conditions. Finally, global demethylation and Swern oxidation yielded essentially atropisomerically pure gossypol (**1.107**) as a 99.2:0.8 mixture of *aS* to *aR* conformations. This method provides a powerful approach for the synthesis of single atropisomers, and the substitution of (*R*)-*tert*-leucine for the (*S*)-form should switch the selectivity of the asymmetric Ullmann coupling.



**Scheme 1.11.** Meyers' synthesis of atropisomerically pure (*S*)-gossypol.

In contrast to the bis-phenolic structure of gossypol, bismurrayaquinone A (**1.110**) exemplifies the possibility of atropisomerism across an ortho-substituted diquinone bond. Isolated from the southeast Asian *Murraya* plants, bismurrayaquinone A is one of many metabolites produced by the plant that is commonly used for food flavoring in India as well as treating dermatological problems.<sup>42</sup> Prior to its total synthesis, the possibility of atropisomerism had not been addressed, and Bringmann's first synthesis led to quantities of the natural product for these studies. Starting from the functionalized carbazole **1.108**, oxidative dimerization under radical conditions effected regioselective coupling yielded the biaryl bis-phenol **1.109**, which was cleanly oxidized to bismurrayaquinone (**1.110**)

with PCC.<sup>42,43</sup> The two atropisomeric enantiomers were separated by chiral HPLC, thus confirming the existence of a stable stereoisomeric bis-quinone bond, and the experimental circular dichroism (CD) spectra were compared with computationally generated CD spectra to assign the absolute orientation of each enantiomer. This method of separating a racemic mixture of atropisomers and correlation with either a natural sample or a computational experiments has played an important role in the assignment of many axially chiral natural products. Additionally, the oxidative dimerization method for synthesizing biaryl bonds represents one of the major approaches to these types of natural products.



**Scheme 1.12.** Bringmann's first synthesis of racemic bismurrayaquinone A.

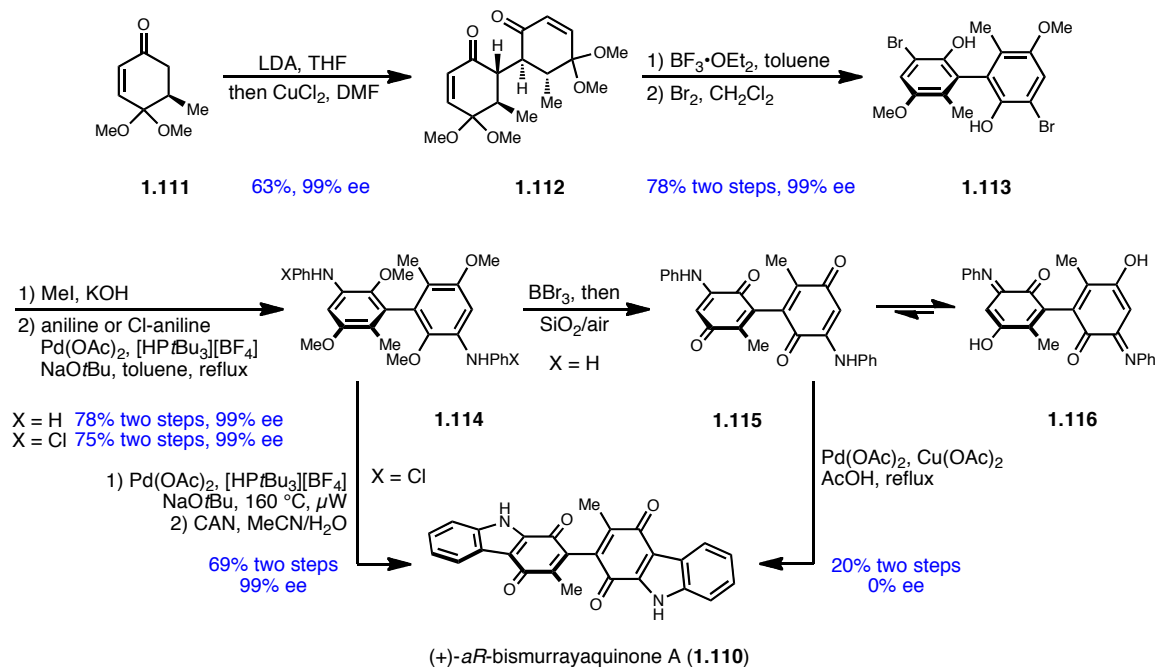
Only recently did bismurrayaquinone A succumb to enantioselective total synthesis by Thomson and co-workers, and their approach highlights another key method for assembling symmetric molecules.<sup>44</sup> Through Thomson's "traceless stereochemical exchange" method, stereoselective Feringa conjugate addition relayed chirality through the following oxidative dimerization of the pre-formed enolate with  $\text{CuCl}_2$  to arrive at enantiomerically pure **1.112**. Then through an oxidation/tautomerization transformation and dibromination, the chirality of **1.112** relays to axial chirality with the formation of

**1.113** as a single atropisomer determined by the stereochemistry of the conjugate addition. This approach to the natural product also hinged upon a contrasting approach to Bringmann's original synthesis shown above. By forming the central bond first, as opposed to Bringmann's late-stage oxidative dimerization, Thomson demonstrated the use of a two-directional synthesis, where each transformation after forming a central core occurs at both ends of the molecule.

From the bis-phenol **1.113**, phenol methylation was followed by Buchwald-Hartwig amination, first with aniline to cleanly provide **1.114** (X = H). By performing demethylation and air oxidation of **1.114** first, the bis-quinone was finally transformed to bismurrayaquinone A by palladium-catalyzed C-C bond formation. However, upon product analysis, it was determined that the product had racemized along the synthetic route. Ultimately, it was determined that **1.115** could undergo room-temperature racemization through the N-O tautomer (**1.116**) on the order of weeks at room temperature, and the refluxing conditions of the final step highly increased the rate of racemization.

Thomson and co-workers reasoned that because the bis-phenol intermediate did not undergo racemization, palladium-catalyzed C-C bond formation could occur first followed by oxidation. Utilizing chloro-aniline in the Buchwald-Hartwig amination to improve the reactivity of the bis-phenol **1.114** (X = Cl) toward C-C bond formation, the two step sequence provided (+)-*aR*-bismurrayaquinone A in 99% ee. Ultimately, it was determined that a combination of shorter C-O bond lengths between the quinones and phenols respectively and an out-of plane distortion of the biquinone bond in **1.115** compared to that in bismurrayaquinone A accounted for the differences in racemization

potential. Finally, Thomson and co-workers determined that the barrier to rotation in bismurraquinone A (**1.110**) was 54 kcal/mol whereas that of a model biquinone was 13 kcal/mol and a model biphenol was essentially inert to racemization.



**Scheme 1.13.** Thomson's enantioselective synthesis of bismurraquinone A.

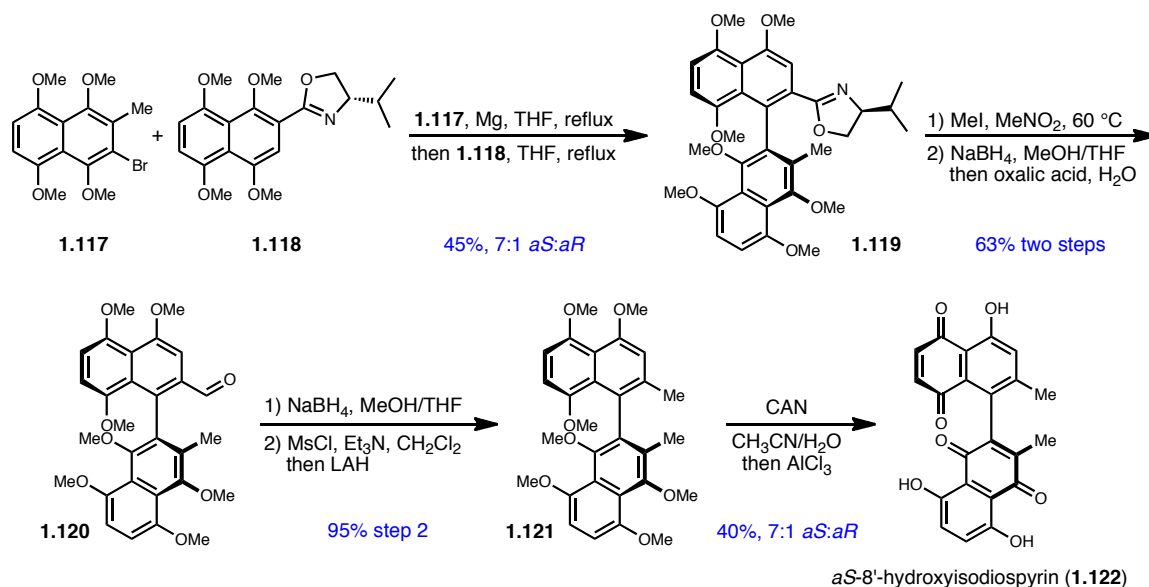
Lessons from Meyers' synthesis of gossypol as well as Bringmann's and Thomson's syntheses of bismurraquinone A can apply to synthetic considerations necessary for that of the hibarimicins. First, approaches involving oxidative homodimerization necessarily require a proximate chiral element to effect selective biaryl formation (modest relay of remote internal chirality is possible, as exemplified by Shaw's synthesis of viriditoxin; however this effect cannot reliably be applied as a method for atroposelective homodimerization), where Meyers' internal oxazoline auxiliary imparted

stereoselectivity and Bringmann's lack of a chiral element led to a racemic mixture.<sup>45</sup> Next, two major approaches to symmetric natural products are highlighted by Meyers' and Bringmann's dimerizations and Thomson's two-directional synthesis. Finally, while many tetra-ortho substituted biphenols exhibit stable atropisomerism, other mechanisms evident in Thomson's synthesis lead to a case-by-case evaluation of the stability of compounds such as biquinones.

Very few aryl-quinone natural products have been identified to date. In fact, to the author's knowledge, only three other natural products contain this motif, namely 8'-hydroxyisodiospyrin (**1.122**), the xanthoviridicatin family (not shown), and the belamcandaquinone family (not shown).<sup>46,47</sup> In contrast to the xanthoviridicatin and belamcandaquinones, which were not investigated for the possibility of atropisomerism, 8'-hydroxyisodiospyrin (**1.122**) has been isolated separately in both atropisomeric forms from the *Diospyros* and *Euclea* species but had not undergone studies to probe the stability of aryl-quinone atropisomers.<sup>48</sup> In 1998, Sargent and co-workers reported the atroposelective synthesis and absolute stereochemical confirmation of (+)-*aS*-8'-hydroxyisodiospyrin (**1.122**) by regioselective nucleophilic aromatic substitution with an internal Meyers' chiral oxazoline auxiliary to arrive at a 7:1 biaryl mixture of *aS* and *aR* atropisomers **1.119**. Four step conversion of the oxazoline auxiliary to the tolyl moiety in **1.121** led to completion of the synthesis by CAN oxidation to provide a 7:1 mixture of *aS*:*aR* 8'-hydroxyisodiospyrin. Importantly, while the tetra-ortho substituted biaryl **1.121** would be expected to exist as a stable atropisomer, conversion to the aryl-quinone product **1.122** retained the same mixture and thus confirmed the stable axially chiral aryl-quinone linkage. However, despite 8'-hydroxyisodiospyrin sharing a similar structural



feature with the hibarimicins, applying lessons of its atropisomeric stability to the hibarimicin system may be of limited value considering the differences in symmetric versus unsymmetric linkages.



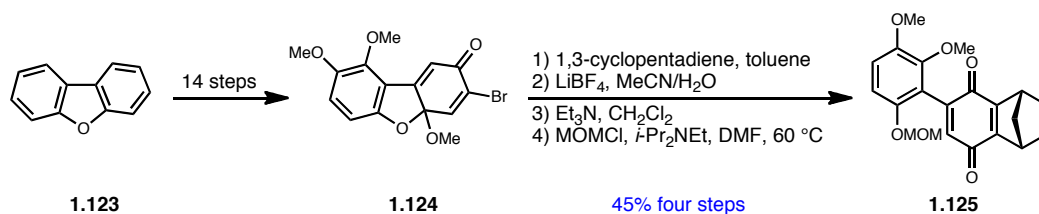
**Scheme 1.14.** Sargent's synthesis of *aS*-8'-hydroxyisodiospyrin.

## Atropisomerism and the Hibarimicins

Synthetic interest in the hibarimicins had grown by the beginning of the new millennium, and in light of the previously highlighted investigations into atropisomerism stability, interest existed to determine the properties of the aryl-quinone bond found in the hibarimicins. No mention had been made regarding the possibility for atropisomerism in the isolation reports for either the angelmicins or the hibarimicins, and therefore, our laboratory initiated this study with the synthesis of an aryl-quinone model system.<sup>49</sup> By

targeting a D-D' model system that incorporated stereogenic centers, the evaluation of axial chirality would thus be simplified by the existence of atropodiastereomers that could be easily visualized by proton NMR.

Although transition metal-mediated cross couplings are the method of choice for forming the biaryl functionality, formation of highly hindered biaryl bonds with this approach is often difficult, and thus another method was utilized. Starting from dibenzofuran (**1.123**), fourteen steps arrived at the functionalized monoketal quinone **1.124**. Using 1,3-cyclopentadiene, room temperature intermolecular Diels-Alder provided the bridged bicyclic monoketal, which was hydrolyzed with  $\text{LiBF}_4$  in aqueous acetonitrile to provide the quinone phenol. Finally, MOM protection of the free phenol provided the aryl-quinone model system **1.125**.

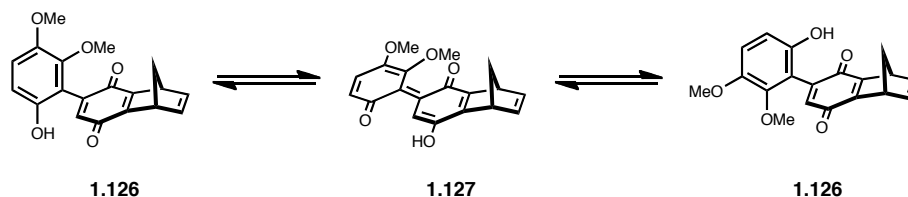


**Scheme 1.15.** Sulikowski's model of aryl-quinone atropisomerism.

Interestingly, upon generation of the phenol quinone prior to MOM protection, NMR analysis indicated a single isomer at room temperature, which would indicate rapid interconversion between the two possible isomers. Conversely, the MOM-protected model **1.125** was observed as an approximately 1:1 mixture of interconverting atropisomers. Spectroscopically, heating of a mixture of atropisomers to the temperature

at which they can freely rotate between isomers should result in observation of a single set of peaks as seen with the free phenol. However, heating the MOM-protected model **1.125** to a temperature of 148 °C did not result in coalescence of the diastereomeric mixture, which was taken to imply that **1.125** does exhibit atropisomerism with a barrier to rotation of approximately 20-25 kcal/mol.

When the high rate of interconversion for the phenol quinone was compared to the relative stability of **1.122** atropodiastereomers, it was unlikely that the extra steric hindrance provided by the MOM-ether can fully account for these differences. Thus, a tautomeric pathway, as shown in Scheme 1.16, was proposed that should greatly lower the activation energy necessary for aryl-quinone bond rotation. And because the MOM-ether **1.125** cannot access this tautomeric pathway, the difference in interconversion between the two compounds could be rationalized. While these studies do indicate the potential for alternate aryl-quinone racemization pathways, it remained unknown what insights from the model **1.125** could be applied to the atropisomeric stability of the hibarimicins considering **1.125** lacks their C-3' methoxy group.

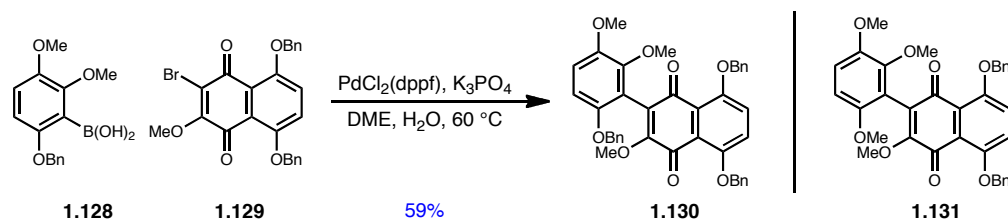


**Scheme 1.16.** Proposed mechanism of phenol quinone interconversion.

In 2004, Roush and co-workers reported the synthesis of a similar model system to evaluate the possibility of a late-stage aryl-quinone bond formation strategy and related

concerns regarding atropisomerism.<sup>50</sup> As previously mentioned, metal-catalyzed cross coupling reactions of sterically hindered and highly electron rich aryl rings for biaryl bond formation is commonly met with difficulty, and thus Roush and co-workers were unsuccessful at performing Suzuki, Stille, and Ullmann couplings between a variety of functionalized naphthalene partners. In contrast, synthesis of bromoquinone **1.129** impressively provided a suitable partner with favorable electronics for oxidative insertion, which provided aryl-quinone **1.130** through Suzuki coupling with the aryl boronic acid **1.128** in good yield.

With aryl-quinone **1.130** in hand, evaluation of its atropisomeric stability commenced. Although no other chiral centers exist in **1.130** to produce spectroscopically discernable diastereomers, the splitting pattern observed for the aryl benzyl methylene existed as an AB quartet which indicated some amount of asymmetry present and allowed for variable temperature NMR studies. Heating **1.130** to 150 °C did not cause any change in the splitting pattern, and thus the barrier to rotation was estimated to be greater than 22 kcal/mol, or roughly in agreement with Sulikowski's estimate. Additionally, computational studies were carried out with the slightly modified methyl ether **1.131**, and the barrier to rotation was calculated to be 25.6 kcal/mol. Considering this information in concert with Sulikowski's estimates, it appeared that the hibarimicins should exhibit reasonable atropisomeric stability to allow for resolution at room temperature; however, the contribution of alternate tautomerization pathways remained to be determined with the nature product family itself.



**Scheme 1.17.** Roush's aryl-quinone model system.

The model system studies by Sulikowski and Roush were followed by numerous efforts toward hibarimicin fragments, which will be discussed in further detail in the following chapter. These studies generally focused on the synthesis of the A'B' ring system and did not discuss issues of atropisomerism. Finally, our laboratory published the determination of the natural hibarimicin atropisomer in 2011 by utilizing a chromophore model system of HMP-Y6 **1.132**.<sup>51</sup>

Circular dichroism (CD) measures the differential absorption of plane polarized light by a chiral molecule and thus operates based on the absorption of molecular chromophores. This method is well suited for observation of axial chirality, where atropisomeric biaryls show opposing CD spectra. With this method, we reasoned that synthesis of a suitably similar model system of HMP-Y6, whose CD spectrum was available through correspondence with Professors Hori and Igarashi, would enable comparison of a known model atropisomer with the HMP-Y6 spectrum to unequivocally assign the hibarimicin atropisomer. The synthesis of (+)-*aR*-**1.132** and (–)-*aS*-**1.132**, which will be addressed in chapter III, was followed by recording of each compound's CD spectrum, as shown in Figure 1.9. Although an intermediate of *aS*-**1.132** was confidently assigned an absolute configuration through X-ray crystallography, we also

confirmed the correlation of the computational CD spectrum of *aR*-**1.132** with its experimental spectrum prior to using this data for drawing conclusions. A negative Cotton effect (negative band on the long wavelength side and a positive band on the short wavelength side) was observed for *aR*-**1.132**, and a positive Cotton effect was observed for *aS*-**1.132**. The computational data for *aR*-**1.132** were in agreement with experimental data, predicting a negative Cotton effect.

With this data in hand, we then compared both the *aR*-**1.132** and *aS*-**1.132** CD spectra to the CD spectrum for HMP-Y6 (**1.93**, not shown), which exhibited a negative Cotton effect. Therefore, the CD spectrum of HMP-Y6 matched the torsional angle of *aR*-**1.132**, and HMP-Y6 could be assigned as having the *aR* configuration. This assignment could be applied directly to HMP-Y1 which presumably exists as the biosynthetic precursor of the blocked mutant HMP-Y6. And assuming atropisomeric retention in the conversion of HMP-Y1 to hibarimicin B and the rest of the family members, hibarimicin B could be assigned a configuration of *aS*.

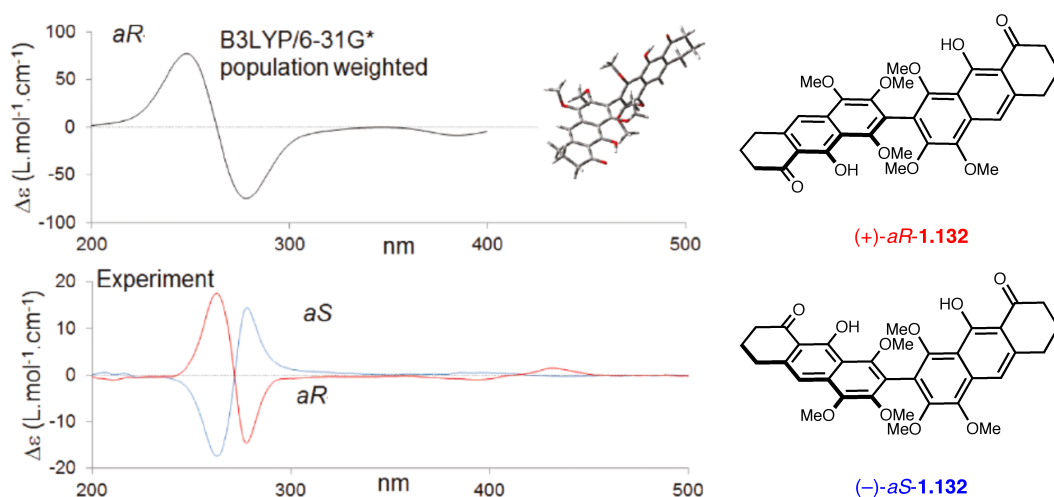


**Figure 1.9.** Computational and experimental model system CD spectra.

## Conclusion

Secondary metabolites have a rich history as medicinal agents, and aromatic polyketides have greatly contributed to the treatment of human disease. The biosynthesis of aromatic polyketides generally utilizes the acetate pathway, and many diverse structures can be produced through this biosynthetic mechanism. Despite their biological importance, scant natural quantities of many aromatic polyketides preclude their medicinal use, and thus total synthetic efforts have attempted to alleviate this issue. Various synthetic approaches have been developed for the assembly of aromatic polyketides, and the Diels-Alder reaction has found great utility for this purpose. Hibarimicin B is one of the most complicated aromatic polyketides isolated to date, and its interesting biological activity makes it an intriguing candidate for a total synthesis effort. Its biosynthesis goes through a homodimerization step to form the key intermediate HMP-Y1, and the hibarimicins have been determined to exist as stable atropisomers.

## References

1. Dickschat, J. S. "Biosynthesis and function of secondary metabolites" *Beilstein J. Org. Chem.*, **2011**, 7, 1620-1621.
2. Brownstein, M. J. "A brief history of opiates, opioid peptides, and opioid receptors" *Proc. Natl. Acad. Sci. USA*, **1993**, 90, 5391-5393.
3. Hare, R. "New light on the history of penicillin" *Medical History*, **1982**, 26, 1-24.

4. Dewick, P. M. *Medicinal Natural Products: A Biosynthetic Approach*, **2002**, John Wiley & Sons, Ltd., New York City, 507 p.
5. Hertweck, C. "The biosynthetic logic of polyketide diversity" *Angew. Chem. Int. Ed.*, **2009**, *48*, 4688-4716.
6. Shen, B. "Biosynthesis of aromatic polyketides" *Top. Curr. Chem.*, **2000**, *209*, 1-51.
7. Pal, S. "A journey across the sequential development of macrolides and ketolides related to erythromycin" *Tetrahedron*, **2006**, *62*, 3171-3200.
8. Weissman, K. J. "Polyketide biosynthesis: understanding and exploiting modularity" *Phil. Trans. R. Soc. London A*, **2004**, *362*, 2671-2690.
9. Jang, M.; Cai, L.; Udeani, G. O.; Slowing, K. V.; Thomas, C. F.; Beecher, C. W. W.; Fong, H. H. S.; Farnsworth, N. R.; Kinghorn, A. D.; Mehta, R. G.; Moon, R. C.; Pezzuto, J. M. "Cancer chemopreventive activity of resveratrol, a natural product derived from grapes" *Science*, **1997**, *275*, 218-220.
10. Ellestad, G. A. "Structural and conformational features relevant to the anti-tumor activity of calicheamicin  $\gamma_1$ " *Chirality*, **2011**, *23*, 660-671.
11. Schneider, G. "Enzymes in the biosynthesis of aromatic polyketides" *Curr. Opin. Struct. Biol.*, **2005**, *15*, 629-636.
12. Staunton, J.; Weissman, K. J. "Polyketide biosynthesis: a millennium review" *Nat. Prod. Rep.*, **2001**, *18*, 380-416.
13. Carreras, C. W.; Pieper, R.; Khosla, C. "The chemistry and biology of fatty acid, polyketide, and nonribosomal peptide biosynthesis" *Top. Curr. Chem.*, **1997**, *188*, 85-126.
14. Harris, T. M.; Harris, C. M. "Synthesis of polyketide-type aromatic natural products by biogenetically modeled routes" *Tetrahedron*, **1977**, *33*, 2159-2185.
15. Shen, B. "Polyketide biosynthesis beyond the type I, II and III polyketide synthase paradigms" *Curr. Opin. Chem. Biol.*, **2003**, *7*, 285-295.
16. Okamoto, S.; Taguchi, T.; Ochi, K.; Ichinose, K. "Biosynthesis of actinorhodin and related antibiotics: discovery of alternative routes for quinone formation encoded in the *act* gene cluster" *Chem. Biol.*, **2009**, *16*, 226-236.



17. Nelson, M. L.; Levy, S. B. "The history of the tetracyclines" *Ann. N.Y. Acad. Sci.*, **2011**, *1241*, 17-32.
18. Woodward, R. B. "The total synthesis of a tetracycline" *Pure Appl. Chem.*, **1963**, *6*, 561-573.
19. Charest, M. G.; Lerner, C. D.; Brubaker, J. D.; Siegel, D. R.; Myers, A. G. "A convergent route to structurally diverse 6-deoxytetracycline antibiotics" *Science*, **2005**, *308*, 395-398.
20. Charest, M. G.; Siegel, D. R.; Myers, A. G. "Synthesis of (-)-tetracycline" *J. Am. Chem. Soc.*, **2005**, *127*, 8292-8293.
21. Roll, D. M.; Scheuer, P. J.; Matsumoto, G. K.; Clardy, J. "Halenaquinone, a pentacyclic polyketide from a marine sponge" *J. Am. Chem. Soc.*, **1983**, *105*, 6177-6178.
22. Kienzler, M. A.; Suseno, S.; Trauner, D. "Vinyl quinones as Diels-Alder dienes: concise synthesis of (-)-halenaquinone" *J. Am. Chem. Soc.*, **2008**, *130*, 8604-8605.
23. Minto, R. E.; Townsend, C. A. "Enzymology and molecular biology of aflatoxin biosynthesis" *Chem. Rev.*, **1997**, *97*, 2537-2555.
24. Zhou, G.; Corey, E. J. "Short, enantioselective total synthesis of aflatoxin B<sub>2</sub> using an asymmetric [3+2]-cycloaddition step" *J. Am. Chem. Soc.*, **2005**, *127*, 11958-11959.
25. Harrowven, D. C.; Woodcock, T.; Howes, P. D. "Total synthesis of cavicularin and riccardin C: addressing the synthesis of an arene that adopts a boat configuration" *Angew. Chem. Int. Ed.*, **2005**, *44*, 3899-3901.
26. Herzon, S. B.; Woo, C. M. "The diazofluorene antitumor antibiotics: structural elucidation, biosynthetic, synthetic, and chemical biological studies" *Nat. Prod. Rep.*, **2012**, *29*, 87-118.
27. Nicolaou, K. C.; Li, H.; Nold, A. L.; Pappo, D.; Lenzen, A. "Total synthesis of kinamycins C, F, and J" *J. Am. Chem. Soc.*, **2007**, *129*, 10356-10357.
28. Li, P.-M.; Fukazawa, H.; Yamamoto, C.; Mizuno, S.; Tanaka, K.; Hori, M.; Yaginuma, S.; Saito, T.; Uehara, Y. "Method of identifying inhibitors of oncogenic transformation: selective inhibition of cell growth in serum-free medium" *Oncogene*, **1993**, *8*, 1731-1735.

29. Uehara, Y.; Li, P.-M.; Fukazawa, H.; Mizuno, S.; Nihei, Y.; Nishio, M.; Hanada, M.; Yamamoto, C.; Furumai, T.; Oki, T. "Angelmicins, new inhibitors of oncogenic *src* signal transduction" *J. Antibiotics*, **1993**, *46*, 1306-1308.
30. Yokoyama, A.; Okabe-Kado, J.; Uehara, Y.; Oki, T.; Tomoyasu, S.; Tsuroka, N.; Honma, Y. "Angelmicin B, new inhibitor of oncogenic signal transduction, inhibits growth and induces myelomonocytic differentiation of human myeloid leukemia HL-60 cells" *Leukemia Res.*, **1996**, *20*, 491-497.
31. Hori, H.; Higashi, K.; Ishiyama, T.; Uramoto, M.; Uehara, Y.; Oki, T. "Structure of angelmicin B, a novel *src* signal transduction inhibitor" *Tet. Lett.*, **1996**, *37*, 2785-2788.
32. Kajiura, T.; Furumai, T.; Igarashi, Y.; Hori, H.; Higashi, K.; Ishiyama, T.; Uramoto, M.; Uehara, Y.; Oki, T. "Signal transduction inhibitors, hibarimicins A, B, C, D and G produced by *Microbispora*: I. Taxonomy, fermentation, isolation and physico-chemical and biological properties" *J. Antibiotics*, **1998**, *51*, 394-401.
33. Hori, H.; Igarashi, Y.; Kajiura, T.; Furumai, T.; Higashi, K.; Ishiyama, T.; Uramoto, M.; Uehara, Y.; Oki, T. "Signal transduction inhibitors, hibarimicins A, B, C, D and G produced by *Microbispora*: II. Structural studies" *J. Antibiotics*, **1998**, *51*, 402-417.
34. Hori, H.; Kajiura, T.; Igarashi, Y.; Furumai, T.; Higashi, K.; Ishiyama, T.; Uramoto, M.; Uehara, Y.; Oki, T. "Biosynthesis of hibarimicins: I. <sup>13</sup>C-Labeling experiments" *J. Antibiotics*, **2002**, *55*, 46-52.
35. Kajiura, T.; Furumai, T.; Igarashi, Y.; Hori, H.; Higashi, K.; Ishiyama, T.; Uramoto, M.; Uehara, Y.; Oki, T. "Biosynthesis of hibarimicins: II. Elucidation of biosynthetic pathway by cosynthesis using blocked mutants" *J. Antibiotics*, **2002**, *55*, 53-60.
36. Igarashi, Y.; Kajiura, T.; Furumai, T.; Hori, H.; Higashi, K.; Ishiyama, T.; Uramoto, M.; Uehara, Y.; Oki, T. "Biosynthesis of hibarimicins: III. Structures of new hibarimicin-related metabolites produced by blocked mutants" *J. Antibiotics*, **2002**, *55*, 61-70.
37. Lloyd-Williams, P.; Giralt, E. "Atropisomerism, biphenyls and the Suzuki coupling: peptide antibiotics" *Chem. Soc. Rev.*, **2001**, *30*, 145-157.
38. Clayden, J.; Moran, W. J.; Edwards, P. J.; LaPlante, S. R. "The challenge of atropisomerism in drug discovery" *Angew. Chem. Int. Ed.*, **2009**, *48*, 6398-6401.

39. Bringmann, G.; Price Mortimer, A. J.; Keller, P. A.; Gresser, M. J.; Garner, J.; Breuning, M. "Atroposelective synthesis of axially chiral biaryl compounds" *Angew. Chem. Int. Ed.*, **2005**, *44*, 5384-5427.
40. Bringmann, G.; Gulder, T.; Gulder, T. A. M.; Breuning, M. "Atroposelective total synthesis of axially chiral biaryl natural products" *Chem. Rev.*, **2011**, *111*, 563-639.
41. Meyers, A. I.; Willemsen, J. J. "The synthesis of (*S*)-(+)-gossypol via an asymmetric Ullmann coupling" *Chem. Comm.*, **1997**, 1573-1574.
42. Bringmann, G.; Ledermann, A.; Stahl, M.; Gulden, K.-P. "Bismurrayaquinone A: synthesis, chromatographic enantiomer resolution, and stereoanalysis by computational and experimental CD investigations" *Tetrahedron*, **1995**, *51*, 9353-9360.
43. Bringmann, G.; Ledermann, A.; François, G. "Dimeric murrayafoline A, a potential bis-carbazole alkaloid: 'biomimetic' synthesis, atropisomer separation, and antimalarial activity" *Heterocycles*, **1995**, *40*, 293-300.
44. Konkol, L. C.; Guo, F.; Sarjeant, A. A.; Thomson, R. J. "Enantioselective total synthesis and studies into the configurational stability of bismurrayaquinone A" *Angew. Chem. Int. Ed.*, **2011**, *50*, 9931-9934.
45. Park, Y. S.; Grove, C. I.; González-López, M.; Urgaonkar, S.; Fetting, J. C.; Shaw, J. T. "Synthesis of (-)-viriditoxin: a 6,6'-binaphthopyran-2-one that targets bacterial cell division protein FtsZ" *Angew. Chem. Int. Ed.*, **2011**, *50*, 3730-3733.
46. Stack, M. E.; Mazzola, E. P.; Eppley, R. M. "Structures of xanthoviridicatin D and xanthoviridicatin G, metabolites of penicillium viridicatum: application of proton and carbon-13 NMR spectroscopy" *Tet. Lett.*, **1979**, 4989-4992.
47. Fukuyama, Y.; Kiriya, Y.; Okino, J.; Kodama, M. "Belamcandaquinones A and B, novel dimeric 1,4-benzoquinone derivatives possessing cyclooxygenase inhibitory activity" *Tet. Lett.*, **1993**, *34*, 7633-7636.
48. Baker, R. W.; Liu, S.; Sargent, M. V. "Synthesis and absolute configuration of axially chiral binaphthoquinones" *Aust. J. Chem.*, **1998**, *51*, 255-266.
49. Maharoof, U. S. M.; Sulikowski, G. A. "Investigations into arylquinone atropisomers: synthesis and evaluation" *Tet. Lett.*, **2003**, *44*, 9021-9023.

50. Narayan, S.; Roush, W. R. "Studies toward the total synthesis of angelmicin B (hibarimicin B): synthesis of a model CD-D' aryl naphthoquinone" *Org. Lett.*, **2004**, *6*, 3789-3792.
51. Romaine, I. M.; Hempel, J. E.; Shanmugam, G.; Hori, H.; Igarashi, Y.; Polavarapu, P. L.; Sulikowski, G. A. "Assignment and stereocontrol of hibarimicin atropoisomers" *Org. Lett.*, **2011**, *13*, 4538-4541.

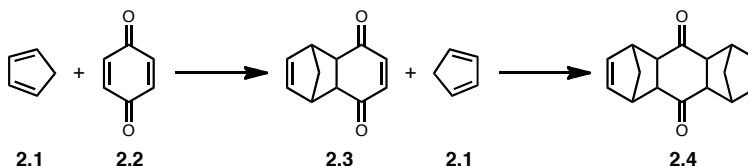
## CHAPTER II

### THE DIELS-ALDER REACTION IN NATURAL PRODUCT TOTAL SYNTHESIS

#### Origin and History of the Diels-Alder Reaction

Nearly a century removed from the publication of their groundbreaking research, the memories of Otto Diels and Kurt Alder live on through the widespread use of the chemical reaction that bears their names. And one of its many uses includes enabling the assembly of complex natural products such as aromatic polyketides.

Beginning with Zincke in 1892, as well as Lebedev, von Euler, Josephson, and Albrecht through the beginning of the new century, numerous studies began to track down the now famous cycloaddition reaction; however, not until 1928 did Diels and Alder publish their successful identification of the products of what at the time was referred to as the diene synthesis.<sup>1</sup> Thus, it was noted that mixing of cyclopentadiene (**2.1**) and quinone (**2.2**) formed a 1:1 and a 2:1 adduct, which were identified as the bridged cyclic structures **2.3** and **2.4**, respectively.<sup>2</sup> And although the products were correctly identified, much mechanistic investigation remained.



**Scheme 2.1.** The original Diels-Alder reaction.

The importance of their findings was apparently not lost on Diels and Alder, as they made several illuminating concluding statements. On the potential scope of the diene synthesis, “Thus it appears to us that the possibility of synthesis of complex compounds related to or identical with natural products such as terpenes, sesquiterpenes, perhaps also alkaloids, has been moved to the near prospect.”<sup>2</sup> And in a curious move to claim their territory, “We explicitly reserve for ourselves the application of the reaction discovered by us to the solution of such problems.”<sup>2</sup> Thus, the Diels-Alder era of synthetic chemistry opened, and due to the impact of their research, they received the 1950 Nobel Prize in chemistry.

### **Diels-Alder Mechanistic Details**

Numerous guidelines have been identified that govern current understanding and analysis of the Diels-Alder reaction. The canonical example utilizes a diene, which contains a conjugated system of 4  $\pi$  electrons, that reacts in an intermolecular fashion with a dienophile, a minimal 2  $\pi$  system, in a pericyclic, concerted manner.<sup>3</sup> If carbon atoms in the diene or dienophile are substituted for alternative atoms, the reaction is termed a hetero-Diels-Alder. The reaction constitutes the height of atom economy, in which full conservation exists from starting materials to product, and complex molecular architecture can be arrived at with the formation of a six-membered ring with up to four new stereocenters.<sup>4</sup>

Reactivity in the Diels-Alder [4+2]-cycloaddition follows frontier molecular orbital (FMO) patterns. The Diels-Alder reaction operates by the interaction between

filled and unfilled orbitals in the two reactants, where the closest energy highest occupied molecular orbital (HOMO) and the lowest unoccupied molecular orbital (LUMO) in the diene and dienophile interact to determine the nature of the resultant product.<sup>3</sup> Electron releasing substituents increase the energy level of the HOMO, while electron withdrawing substituents lower the LUMO energy level; therefore, in the normal electron demand Diels-Alder, an electron rich diene reacts with an electron poor dienophile to form a six-membered ring. Conversely, an inverse demand Diels-Alder utilizes an electron deficient diene and an electron rich dienophile. And the energy gap between these interacting molecular orbitals determines the activation energy required to drive the reaction forward.

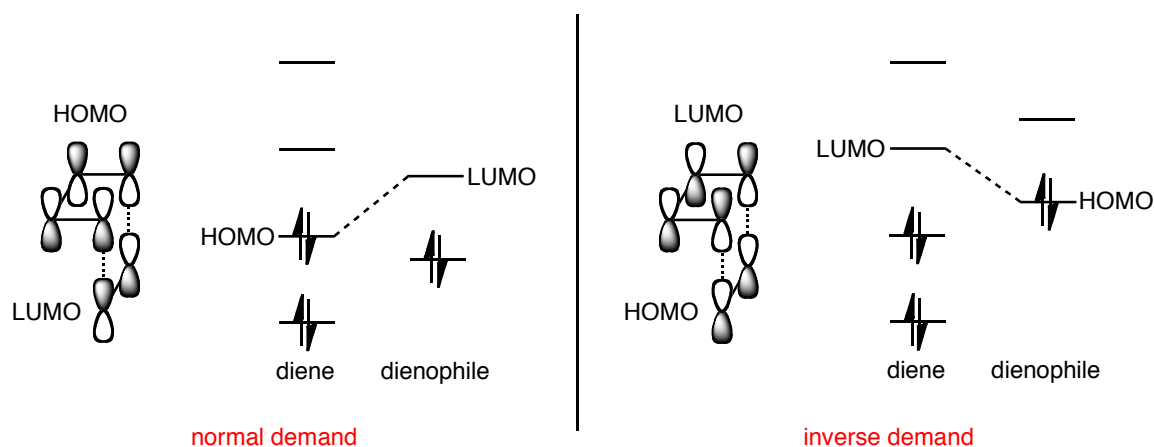
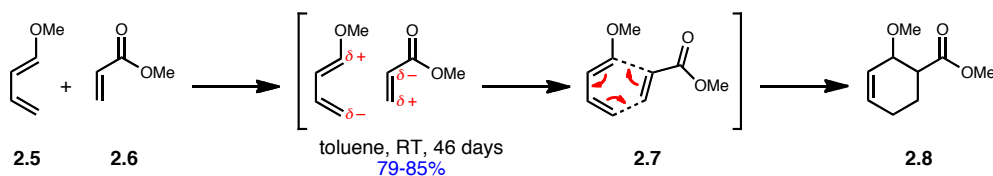


**Figure 2.1.** Frontier molecular orbital analysis of Diels-Alder electronics.

Beginning with Alder's follow-up investigations, factors that govern the regio- and stereoselectivity of the reaction have been proposed. Specifically, unsymmetrical dienes and dienophiles react with preference for formation of the ortho and para adducts

over the meta regioisomer in a manner consistent with the requisite partial charges, and this mnemonic is consistent with an FMO analysis utilizing orbital coefficients.<sup>3</sup> Scheme 2.2 demonstrates the so-called “ortho rule” where partial charges can be used to rationalize the preference for this effect with the example of methoxybutadiene **2.5** reacting with methyl acrylate (**2.6**) to form the ortho-substituted cyclohexene **2.8**.<sup>5</sup> Intermediate **2.7** importantly indicates that although symmetrical dienes and dienophiles react in a synchronous concerted manner, where sigma bond formation occurs equally, polar unsymmetrical partners undergo asynchronous bond formation, and all points along the continuum between concerted and fully stepwise can be accessed based on the nature of the reactants. The reaction shown in Scheme 2.2 shows formation of the ortho-adduct **2.8**, and in this example, no meta-product formation occurs.

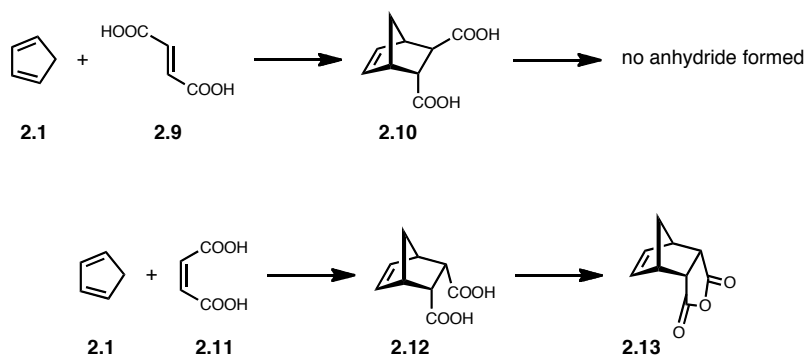


**Scheme 2.2.** Regiochemical preferences in the intermolecular Diels-Alder.

Alder’s subsequent research culminated with a stereochemical analysis of the reaction. Specifically, the Alder-Stein rule indicates that olefin geometry in the starting materials relays in a stereospecific manner to the stereochemistry observed in the product. This principle was demonstrated by the reaction of cyclopentadiene (**2.1**) with maleic acid (*cis*-1,4-butenedioic acid, **2.11**) and fumaric acid (*trans*-1,4-butenedioic acid, **2.9**).<sup>6</sup> While both reactions yield the bridged products **2.12** and **2.10**, the fumaric acid



product was found to not undergo anhydride formation, which is consistent with a *trans* orientation of the requisite diacid. Conversely, the maleic acid product successfully formed the anhydride **2.13**, which indicated a *cis* relationship between the vicinal acid functionalities. In this way, the correlation could be made that the olefin geometry of the dienophile directly affected the relative stereochemistry found in the product. Similarly, olefin geometry of substituted dienes also relays into the product's relative stereochemistry.

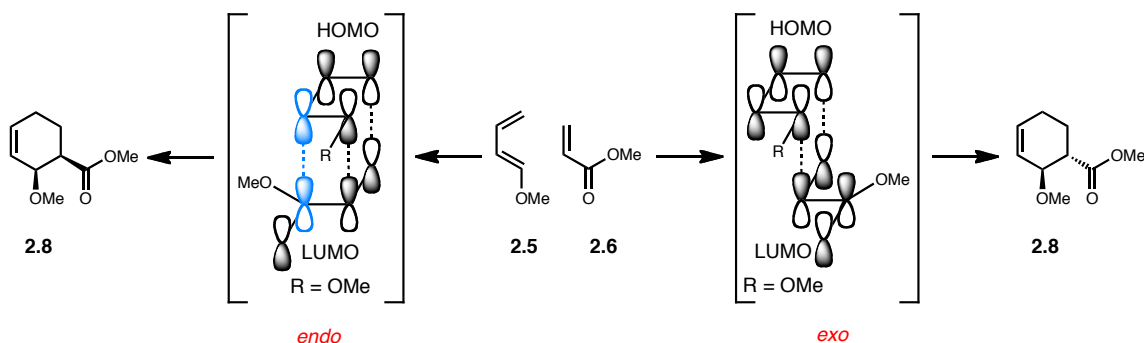


**Scheme 2.3.** Alder and Stein's *cis* principle.

One of the more important features of the Diels-Alder reaction that exerts a profound effect on product stereochemistry is the Alder *endo* rule. Because the diene and dienophile do not approach each other head on due to the lack of orbital overlap, the spatial interaction of reactants within the transition state can be described by the orientation of their requisite appendages. Therefore, for example, as the dienophile approaches the diene from below, the dienophile substituents can align either directly under the conjugated diene system forming the *endo* transition state, or they can orient away from the diene to form the *exo* transition state. While the *exo* approach can logically

be assumed the favored orientation based on a steric argument, Alder and co-workers determined that the *endo* transition state is preferred in many Diels-Alder reactions.<sup>7</sup> The basis for this seemingly counterintuitive result has been determined to arise from stabilization of the *endo* transition state by secondary non-bonding orbital interactions that overcome the perceived destabilizing steric effect.

Using the example from Scheme 2.2, the reaction of methoxybutadiene (**2.5**) with methyl acrylate (**2.6**) can provide two distinct relative stereochemical outcomes, namely *cis*-**2.8** or *trans*-**2.8**. Steric repulsion of the reactant appendages can account for the *exo* transition state leading to the *trans* product; however, the secondary orbital interaction between the blue orbitals in Scheme 2.4 stabilizes the transition state energy and leads to the Diels-Alder favoring the *endo* approach that leads to *cis*-**2.8** in many cases. It is noteworthy that the *endo* transition state represents formation of the kinetic product, and with appropriately high temperatures, retro Diels-Alder can ultimately favor the thermodynamic *exo* product over longer reaction times.<sup>3</sup>



**Scheme 2.4.** Stereochemical outcomes due to the Alder *endo* rule.

In the years since its discovery, the Diels-Alder has enjoyed widely successful application, and ever more variations on its original form continue to be investigated. As mentioned previously, the hetero-Diels-Alder has added a new dimension to the possibility of ring products. Additionally, modern Diels-Alder research continues to push the boundaries of the reaction's versatility, and the applications of Lewis acids can greatly impact its successful implementation into synthetic applications. However, two other forms of the Diels-Alder require further discussion, namely the intramolecular (IMDA) and transannular (TADA) versions.

The intermolecular version of the Diels-Alder utilizes a diene and dienophile that can incorporate substituents at all carbon locations. The intramolecular Diels-Alder reaction links the diene and dienophile through a covalent tether, and various attachment points lead to differing product structures. With the increasing complexity of the Diels-Alder starting material, significant complexity can be added to the resulting product: in addition to the four stereocenters created, two new rings are formed, where the second ring derives from the length of the covalent tether.

The most traditional application of the IMDA is shown as the type I motif in Figure 2.2, where the diene attachment point occurs at the 4-position and the dienophile orients itself in the lowest energy linear conformation shown as **2.14**.<sup>8</sup> In special cases, which necessarily require a longer linker unit, the type I system can form bridged products that arise from an oppositely oriented dienophile (**2.15**). The type II IMDA is the more energetically favorable method for formation of bridged products, where the dienophile approaches in the linear fashion of **2.14** but the linkage point to the diene occurs at the 3-position. Again, shorter tether lengths may preclude the necessary

transition state, but many successful examples of the type II IMDA have emerged in the literature in the past two decades. Finally, as a further extension of the molecular complexity produced by the IMDA, the transannular Diels-Alder (TADA) increases the number of rings produced to three by tethering the diene and dienophile at both ends to produce a macrocyclic precursor **2.17**.<sup>9</sup> Due to macrocyclic strain energy, mode **2.17** predominates in the chemical literature; however, a handful of type II TADA reactions, such as Shair's total synthesis of (–)-longithorone A, have confirmed the possibility of its success.<sup>10</sup> And while the TADA offers one of the most extensive ring formation patterns available in one single transformation, synthesis of the requisite macrocycles has limited its widespread and practical application in total synthesis.

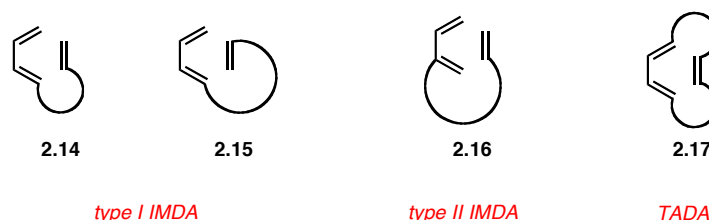
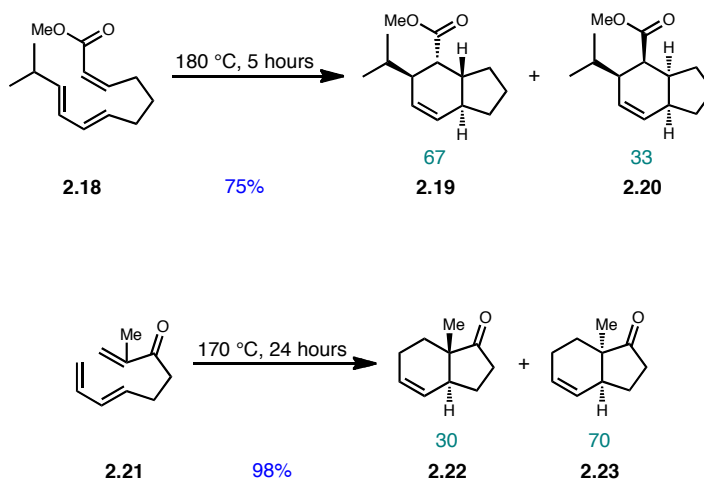


**Figure 2.2.** Diels-Alder motifs of increasing molecular complexity.

The early years following the first IMDA reports in the early 1950s focused on evaluation of simplistic substrates for general parameters and stereochemical outcomes which were nicely reviewed by Fallis in 1983.<sup>4</sup> Of note from these studies is the stereoselectivity of the resulting products, where two similar IMDA reactions are shown in Scheme 2.5. Although the 6-5 ring structure between the two reactions remains conserved, the *trans*-fused product **2.19** is favored in the first reaction, while the second

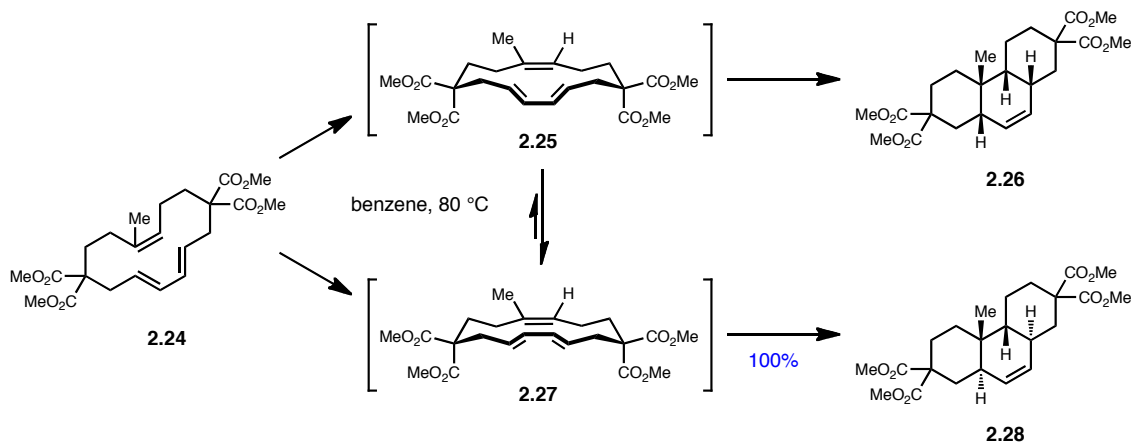
reaction favors the *cis*-fused product **2.23** by a similar margin. As previously mentioned, the *trans* products arise from an *exo* transition state, which interestingly indicates that other factors, mainly sterics within the transition state and olefin geometry, affect the stereochemical outcome of the IMDA.



**Scheme 2.5.** Early IMDA example substrates.

Initial work by Deslongchamps indicated similar stereochemical effects within the TADA manifold relying heavily on the olefin geometry to relay into relative orientation of substituents in the resulting products.<sup>9</sup> For example, the *trans-trans-cis* geometry (TTC) macrocycle **2.24** could be predicted to have access to two possible transition states, **2.25** and **2.27**. Upon heating in refluxing benzene, however, only the tricycle **2.28** with *trans-syn-trans* ring juncture orientation was isolated. This result can be rationalized through likely 1,3-diaxial interactions in the transition state **2.25** between the two pseudo-axial methyl ester substituents and 1,4-diene hydrogens. Therefore, the example shown in Scheme 2.6 highlights various stereochemical considerations necessary for TADA

analysis, and steric factors and inherent olefin geometries play integral roles in the formation of relative stereochemistry. Related work by Jacobsen takes TADA stereochemistry to a new level with application of asymmetric catalysis to the system allowing for stereocontrol and even altering inherent macrocyclic stereochemical bias.<sup>11</sup>

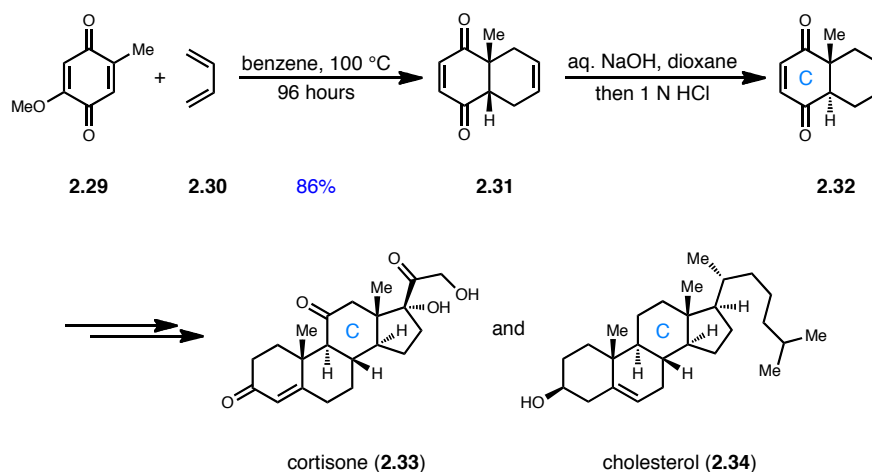


**Scheme 2.6.** Stereochemical outcome of a representative TADA.

## Applications of the Diels-Alder to Total Synthesis

In the two decades between Diels and Alder's initial publication of their reaction and their receipt of the Nobel Prize in 1950, the reaction struggled to take hold in the synthetic community. However, almost coinciding with their international recognition, the Diels-Alder reaction finally began featuring in prominent total syntheses of the 1950s, which included the first synthesis of morphine and Stork's synthesis of cantharidin.<sup>12</sup> But its truly enlightening incorporation into complex molecule total synthesis did not appear until R. B. Woodward harnessed the Diels-Alder's potential in his syntheses of cortisone

(**2.33**) and cholesterol (**2.34**) which were reported in 1952.<sup>13</sup> Utilizing the disubstituted quinone **2.29** as the dienophile and butadiene (**2.30**), the cycloaddition was effected by heating in benzene for four days which produced the *endo* product in high yield. Two features of this reaction remain impressive even today: Woodward recognized that the differing electronics of the two quinone olefins could direct the regioselectivity of the reaction, and considering that the C-ring exists in a *trans* orientation with the appended cyclopentane, that the *cis* product **2.31** arising from the *endo* transition state was the kinetic product that could be equilibrated to the thermodynamic *trans* product **2.32** by treatment with base.<sup>12</sup> This product was then elaborated into both cortisone (**2.33**) and cholesterol (**2.34**), a truly monumental feat in the history of organic total synthesis.



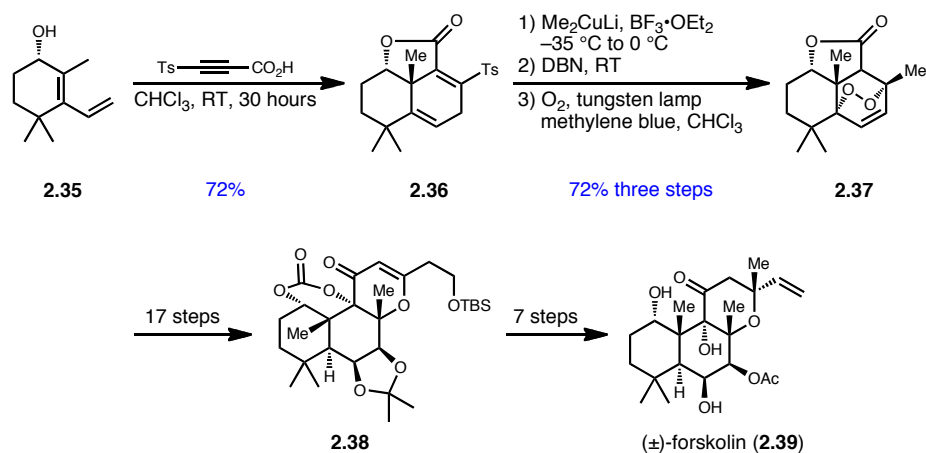
**Scheme 2.7.** Woodward's total syntheses of cortisone and cholesterol.

The historical examples of intermolecular Diels-Alder reactions in total synthesis serve to illustrate the enabling nature of a reaction that reliably produces fused bicyclic systems. However, with time, the intramolecular Diels-Alder has greatly increased the

array of potential ring systems and has opened new doors to various stereochemical motifs. This fact is highlighted by Corey's synthesis of forskolin (**2.39**), which was reported in 1988 and utilized a tethered IMDA to quickly form the 6,6-core ring system.<sup>14</sup>

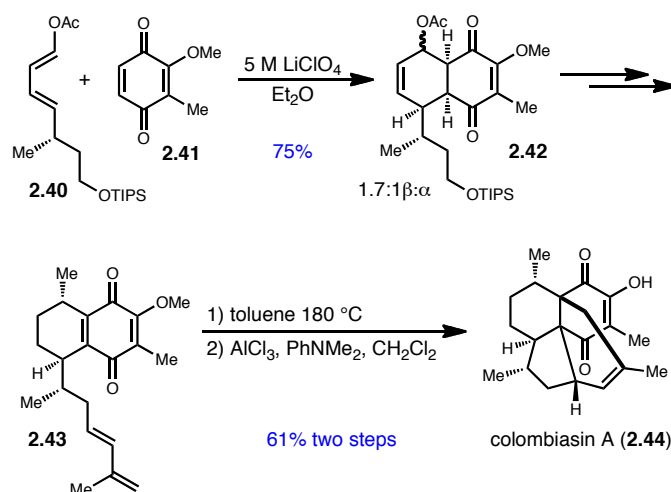
Forskolin (**2.39**), which was isolated from *Coleus forskohlii*, is an activator of adenylyl cyclase which catalyzes the conversion of ATP to cAMP causing a variety of important physiological responses. Corey strategically positioned his IMDA strategy toward the beginning of the synthesis, and in setting the key *trans* ring juncture of the first two rings, he was able to utilize substrate control to direct the formation of many of the remaining chiral centers. Central to the synthetic strategy was the selective formation of the methyl-substituted quaternary ring juncture carbon, and for this approach, the IMDA proved well-suited. The stereochemically defined **2.35** was directly esterified with the propargylic acid, and the intermediate ester underwent spontaneous Diels-Alder reaction to form the tricyclic lactone **2.36**. Thus, the secondary alcohol stereocenter in **2.35** directed the dienophile from the  $\alpha$ -face of the diene and provided the correct quaternary methyl stereochemistry found in **2.39**. In this total synthesis, Corey successfully demonstrated the power of the IMDA at the beginning of a synthesis which relayed into the subsequent necessary stereochemistry-forming reactions.





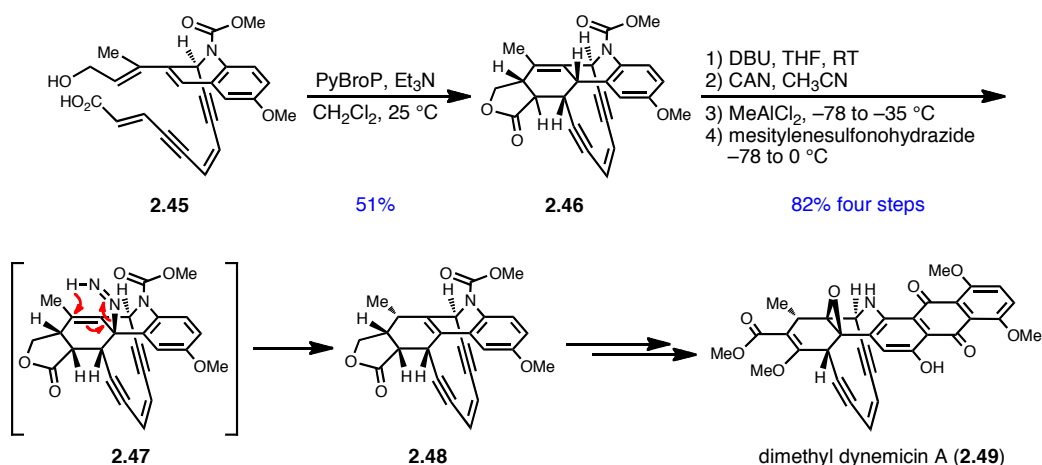
**Scheme 2.8.** Corey's IMDA-enabled total synthesis of forskolin.

In contrast to Corey's strategy of an early-stage IMDA, the reaction can also provide much benefit when utilized at the end of a synthesis. In this mode, depending on the specific structure, a central core with appendages can simplify the early transformations, and with a well-planned strategy, the natural product structure can be rapidly assembled through a single intramolecular step such as in Rychnovsky's synthesis of (–)-colombiasin A (**2.44**).<sup>15</sup> Synthesis of the IMDA precursor **2.43** notably proceeded through the synthesis of decalin **2.42** which was assembled by an intermolecular Diels-Alder between chiral diene **2.40** and quinone dienophile **2.41**. As noted in previously in Corey's synthesis of forskolin, the IMDA benefits the relay of existing stereochemistry into the stereochemical outcome of the cycloaddition, and in the case of colombiasin A, the tethered diene approached the internal quinone dienophile from the  $\beta$ -face due to the chirality of its decalin attachment point. In this way, the complex ring structure of colombiasin A (**2.44**) arose from the much simpler precursor **2.43**, which was synthesized in fifteen linear steps. Final demethylation with  $\text{AlCl}_3$  provided the natural product.



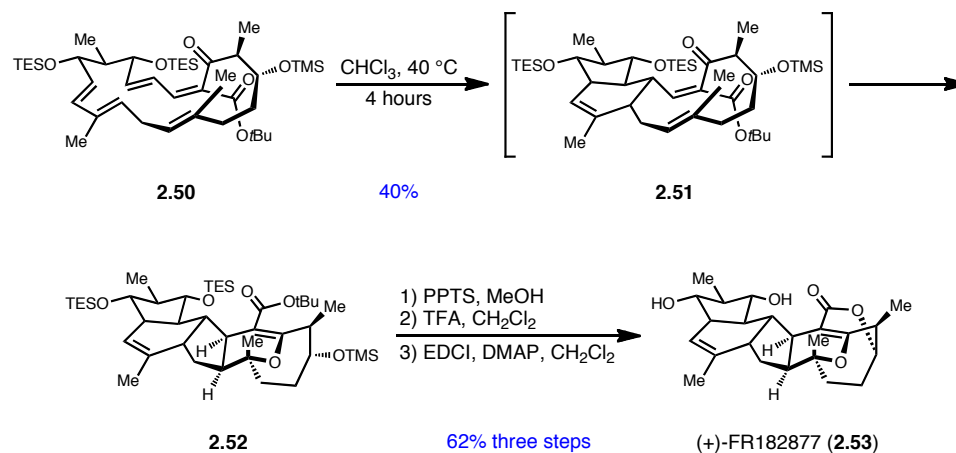
**Scheme 2.9.** Rychnovsky's late-stage IMDA toward colombiasin A.

In much the same way as the IMDA can efficiently form complicated ring structures, as seen in Scheme 2.9, the transannular Diels-Alder strategy can render difficult triene systems labile to cycloaddition due in part to the proximity effect.<sup>16</sup> Schreiber's synthesis of dimethyl dynemicin A (**2.49**) exemplified this principle, in which the advanced intermediate acid **2.45** was macrocyclized using PyBroP in  $\text{CH}_2\text{Cl}_2$ , and after 13 hours at room temperature, the TADA product **2.46** was directly isolated in good yield.<sup>17</sup> In comparison, the related IMDA of a protected form of **2.45** resulted in slow decomposition at or above 180 °C, thus lending support to the proximity effect mentioned above.<sup>18</sup> Following lactone epimerization and benzylic oxidation, an interesting sequence of hydroxyl ionization and hyrazide trapping led to the intermediate diazene **2.47** which underwent stereospecific sigmatropic rearrangement to **2.48**, the core of the dynemicins. Final appending of the remaining two rings led to dimethyl dynemicin A (**2.49**).<sup>19</sup>



**Scheme 2.10.** Schreiber's TADA toward dimethyl dynamycin A.

Reported in 2002, Sorensen's synthesis of (+)-FR182877 (**2.53**) stands near the pinnacle of complexity-driven Diels-Alder capability.<sup>20</sup> The 19-membered macrocycle **2.50** was assembled in seven steps from advanced convergent building blocks, and miraculously, by gentle heating in chloroform, **2.50** underwent a double TADA, first forming the cyclohexene intermediate **2.51** then a hetero-TADA with the remaining enone to form five new rings with seven new contiguous stereocenters. Completion of the target molecule required simple deprotection steps followed by lactonization to provide (+)-FR182877 (**2.53**). Sorensen's use of the TADA perfectly showcases the power of a reaction that only requires shrewd synthetic planning and execution of macrocycle formation.



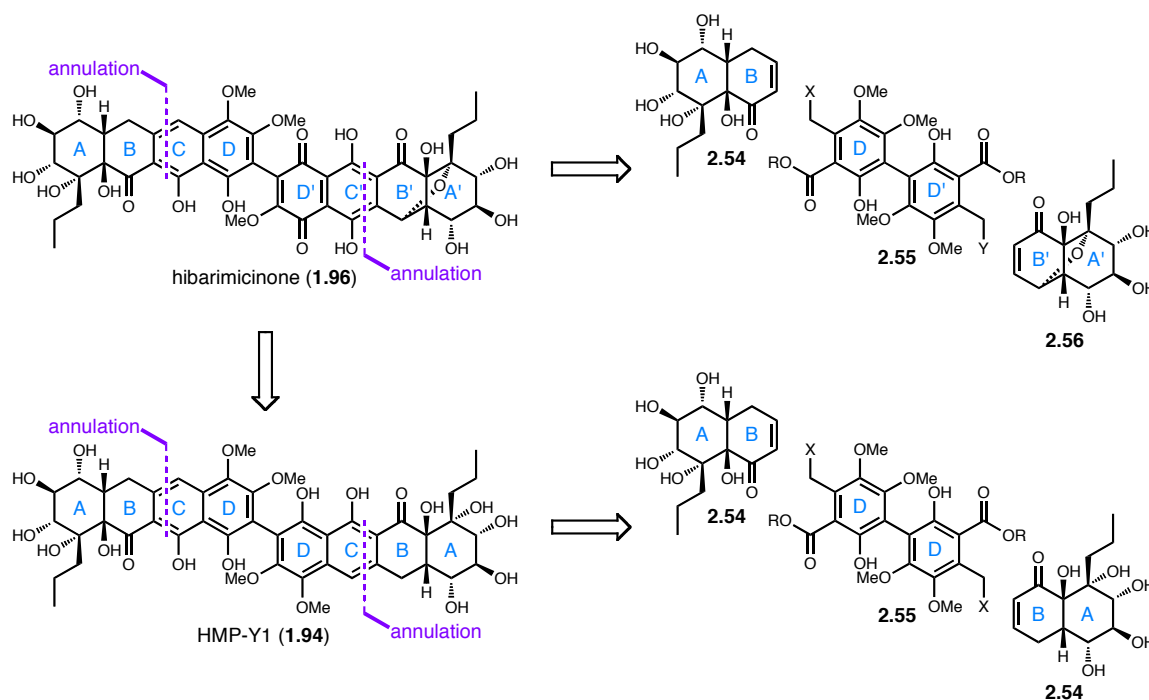
**Scheme 2.11.** Sorensen's double TADA toward (+)-FR182877.

The highlighted examples of the Diels-Alder reaction in total synthesis serve to illustrate not only the history and breadth of its application but also its importance as an enabling step toward complicated molecular structures. The focus on IMDA and TADA approaches above is also meant to provide context for a discussion of synthetic routes toward the hibarimicins, of which all but one has incorporated in some capacity the Diels-Alder reaction.

### Previous Synthetic Studies Toward the Hibarimicins

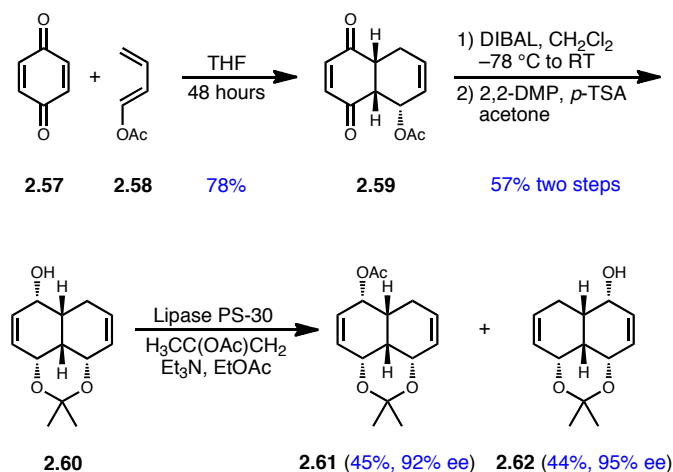
Several research laboratories have reported efforts toward the hibarimicin natural products, beginning in 2002, and although they have targeted differing members of the family, the common linking bond is the general consensus for a two-directional synthetic approach. The retrosyntheses initially targeted hibarimicinone (**1.96**), and keeping in mind Scheme 1.9, further dissection to the previously identified biosynthetic

intermediate HMP-Y1 (**1.94**) could provide a biomimetic intermediate target. From either the semi- $C_2$ -symmetric hibarimicinone (**1.96**) or  $C_2$ -symmetric HMP-Y1 (**1.94**), based on the principle championed by Schreiber of double processing from the center of a molecule outward, a biaryl **2.55** could be annulated with appropriately functionalized enones **2.54** and **2.56** toward hibariminone or in a symmetrical fashion with two equivalents of enone **2.54** toward HMP-Y1.<sup>21</sup> Varying functionalities at X and Y in **2.55** were proposed to allow differential functionalization toward the semi-symmetric hibarimicinone. Thus much of the early work toward the hibarimicins focused on the synthesis of the A'B'-decalinic ring system (**2.56**).



**Scheme 2.12.** Retrosynthetic consensus for early work toward hibarimicinone.

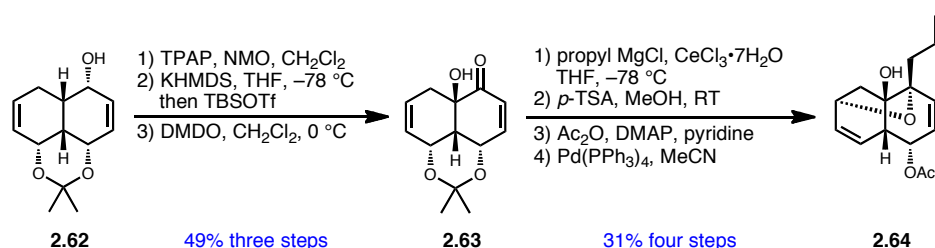
The first synthetic report toward the synthesis of hibarimicinone came from our laboratory in 2002, in which routes were proposed from a single intermediate for synthesis of **2.54** and **2.56** toward hibarimicinone.<sup>22</sup> This approach relied on the elaboration of enantiomeric decalins into the AB- and A'B'-ring systems, and thus racemic Diels-Alder cyclization of quinone (**2.57**) and 1-acetoxybutadiene (**2.58**) provided the *cis*-decalin **2.59**. Complete reduction and 1,3-diol protection provided racemic **2.60**. Lipase resolution enabled separation of the mixture in high enantiomeric excess for both **2.61** and **2.62**, where the free alcohol **2.62** was to become the A'B' hibarimicin decalin **2.56**, while the acetate **2.61** was to be elaborated to the AB decalin **2.54**.



**Scheme 2.13.** Sulikowski's route to divergent hibarimicinone precursors.

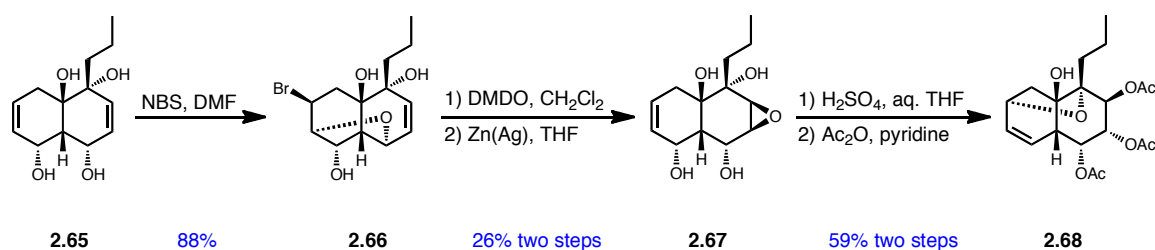
In an effort to transform **2.62** into the A'B' decalin **2.56**, Ley oxidation was followed by silyl enol ether formation and Rubottom oxidation with DMDO to give a single diastereomer of **2.63**. Installation of the propyl group by nucleophilic addition of

the cerium reagent led to the tertiary alcohol in a 5:1 diastereomeric ratio, and *p*-toluenesulfonic acid then removed the acetonide protecting group. Acetylation led to an intermediate ripe for cycloetherification which was attempted with palladium tetrakis(triphenylphosphine); however, cyclization unexpectedly occurred through an  $S_N2'$ -type addition to the C-16 carbon with olefin migration and acetyl ejection yielding **2.64**.



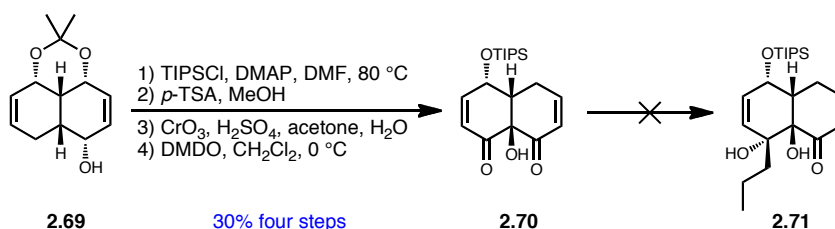
**Scheme 2.14.** Cycloetherification toward the A'B'-decalin system.

Reasoning that the *trans* diol at C-11/12 in **2.56** may affect the cycloetherification outcome, the C-7/16 olefin was masked by bromoetherification with the C-10 secondary alcohol to provide **2.66** followed by epoxidation and retro-bromoetherification and acidic solvolysis for diol installation. The three secondary alcohols were acetylated to **2.68** for the purpose of obtaining an X-ray crystal structure, and ultimately not only did the resulting triol exist as the incorrect relative stereochemistry but a presumed cyclodehydration occurred yielding the same undesired furan product as previously observed in **2.64**.



**Scheme 2.15.** *Trans* diol installation and attempted cycloetherification.

A final attempt was made toward the AB-ring system **2.54** based upon the logic of installing the C-15 ketone earlier in the sequence, which involved using the opposite enantiomer: the free alcohol version of **2.61**. TIPS protection of the secondary alcohol was thus followed by acetonide deprotection, bis-Jones oxidation and tertiary alcohol installation to yield **2.70**. Unfortunately, all attempts at regioselective alkylation toward **2.71** were unsuccessful.

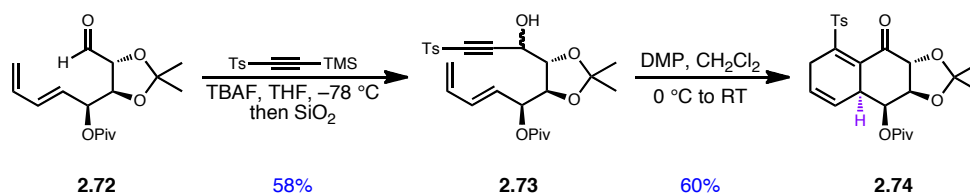


**Scheme 2.16.** Attempted synthesis of the AB-decalin system.

Just one year later, our group's strategy had been modified to focus on synthesis of the  $C_2$ -symmetric biosynthetic intermediate HMP-Y1 (**1.94**) which could follow the retrosynthesis laid out in Scheme 2.12. Additionally, the synthetic approach sought to utilize the intramolecular Diels-Alder reaction as a linchpin toward the AB-decalin



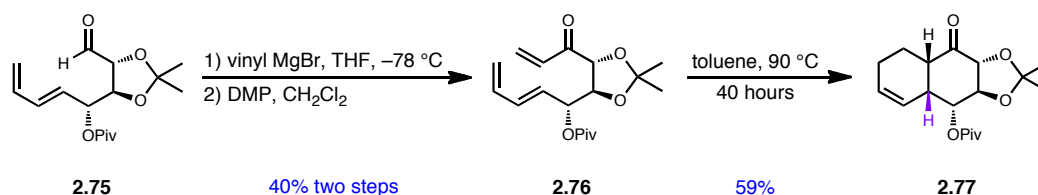
system **2.54**. Therefore, based on literature precedent, it was reasoned that the  $\beta$ -OPiv group in **2.73** would direct formation of the C-9 stereochemistry and thus compound **2.73** was the first to be investigated.<sup>23</sup> While the lithiated form of ethynyl *p*-tolylsulfone was ineffective in the addition to aldehyde **2.72**, Kuwajima's conditions effected reasonable conversion to the diastereomeric mixture of secondary alcohols **2.73**. Oxidation with Dess-Martin periodinane then led to the intermediate alkynone, which underwent spontaneous IMDA to the bicycle **2.74** with formation of the undesired C-9 stereochemistry. Carrying the opposing  $\alpha$ -OPiv series (not shown) through the same sequence again led to the undesired C-9 stereochemistry and thus required altering of the synthetic plan.



**Scheme 2.17.** Sulikowski's alkynyl IMDA toward the AB-decalin system.

In hopes of switching the Diels-Alder selectivity, a simple enone dienophile **2.76** was prepared utilizing the  $\alpha$ -OPiv series in which vinyl Grignard addition to the aldehyde **2.75** and subsequent Dess-Martin oxidation led to the Diels-Alder precursor **2.76**. Indeed, when heated at 90 °C for 40 hours, the desired ring junction stereochemistry emerged in **2.77** leading to an interesting comparison between the cycloadditions of **2.73** and **2.76** which vary only in the structure of the dienophile. Further studies by our laboratory

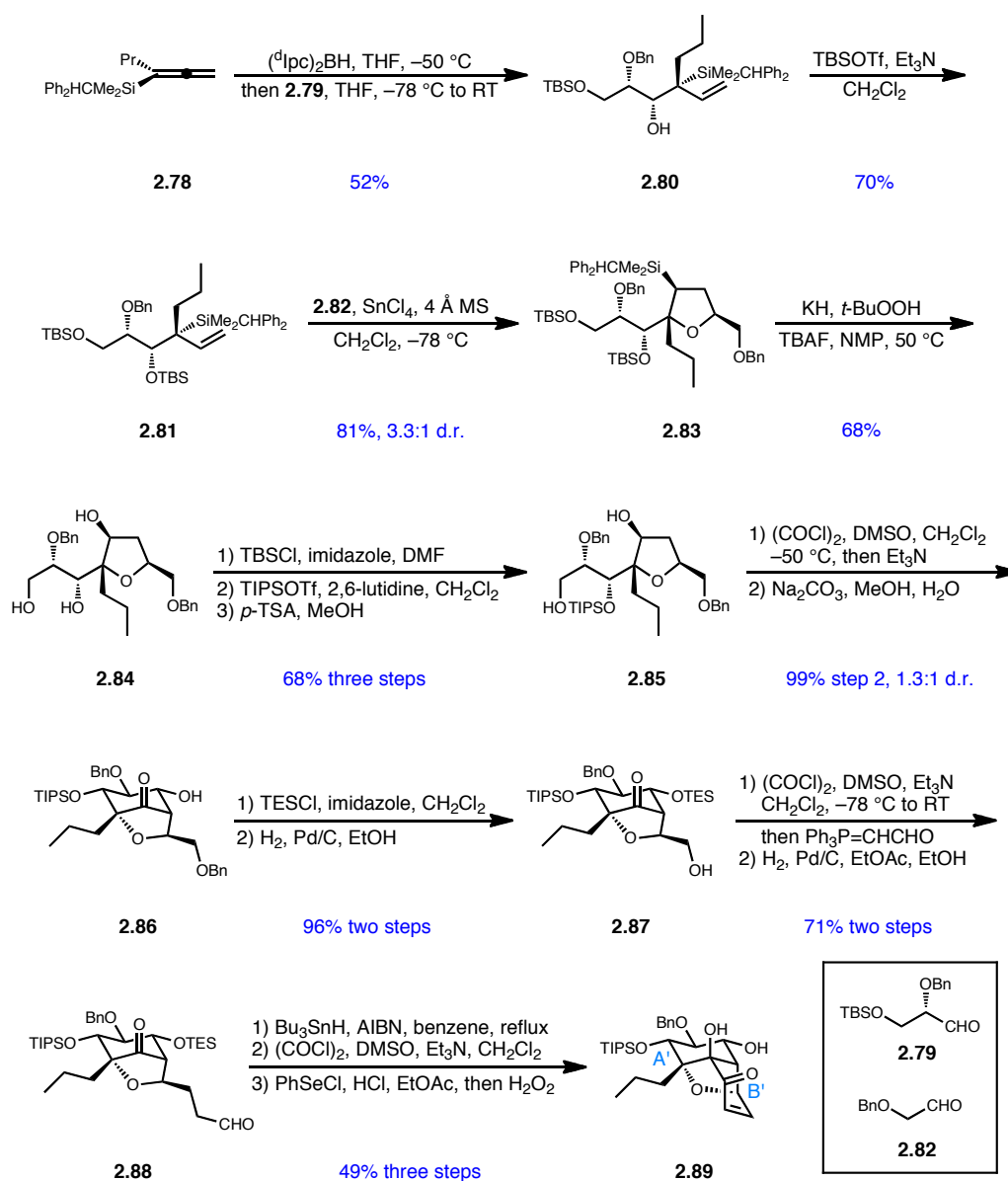
suggest that altering the nature of alcohol protecting groups within the IMDA linking chain influence precursor orientation and thus stereoselectivity observed in the product.<sup>24</sup>



**Scheme 2.18.** Altering dienophile structure leads to different stereochemistry.

Roush and co-workers reported the first successful synthesis of the A'B'-decalin of hibarimicinone in 2005.<sup>25</sup> Their strategy involved assembling the two six-membered rings from a pre-formed furan. The furan was derived from their previously developed three component coupling of  $\gamma$ -silylallylboranes through hydroboration of allene **2.78** and subsequent addition to the aldehyde **2.79**. Following silylation, the furan **2.83** was formed through a [3+2] cycloaddition with aldehyde **2.82**. A modified Tamao-Fleming oxidation yielded the desired alcohol diastereomer **2.84** which was subjected to a series of protection and deprotection to arrive at the selectively TIPS-protected diol **2.85**. Swern oxidation led to the keto-aldehyde intermediate that when treated under basic conditions effected aldol cyclization to the bicyclic system **2.86** in a 1.3:1 diastereomeric ratio, where the undesired diastereomer could be converted under the same reaction conditions to the 1.3:1 ratio favoring the desired diastereomer. Protection of the newly present alcohol was followed by regioselective debenzoylation to yield the primary alcohol **2.87**. A sequence of Swern oxidation, Wittig olefination, and olefin hydrogenation led to **2.88** which set up for the final ring forming reaction. Thus, pinacol-enabled ring closure by

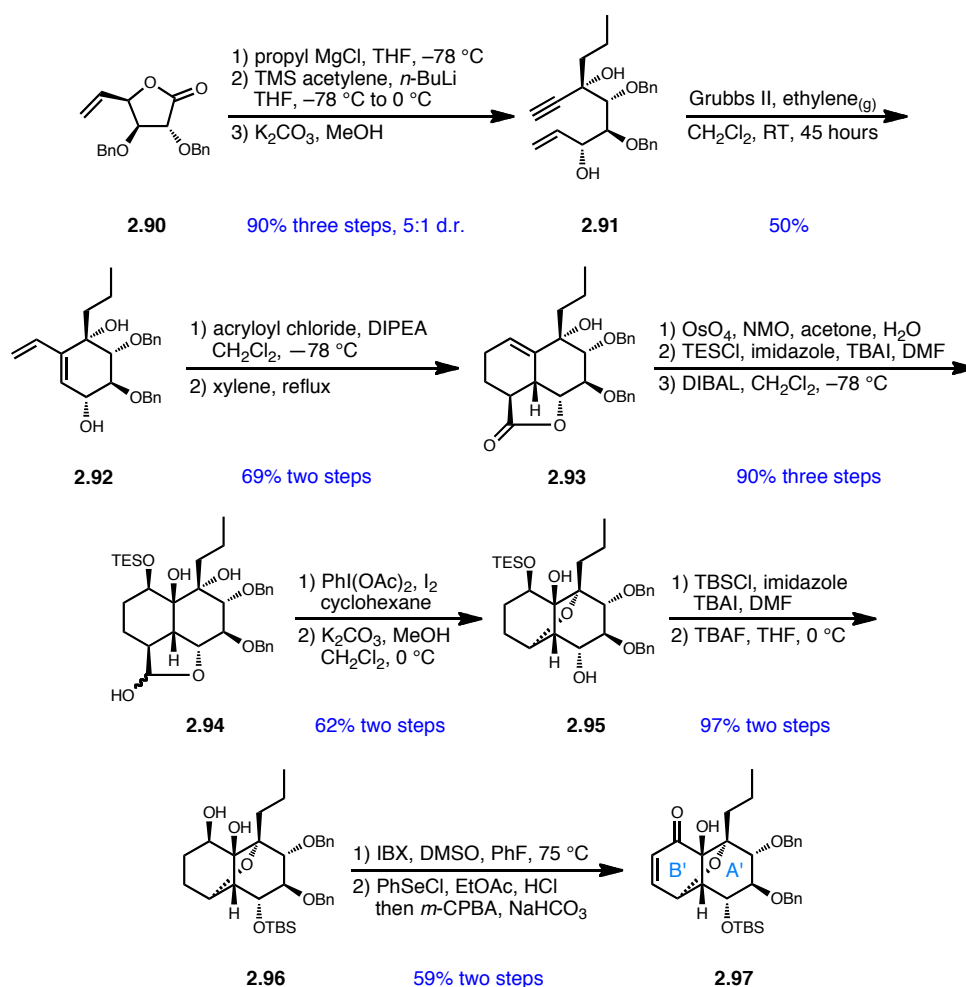
treatment with  $\text{Bu}_3\text{SnH}$  and AIBN in refluxing benzene successfully effected formation of the A'B'-decalinic ring system found in hibarimicinone. The remaining steps to the fully functionalized A'B'-system involved Swern oxidation of the secondary alcohol and enone installation through  $\alpha$ -phenylselenation and oxidation with hydrogen peroxide to arrive at **2.89**. Roush's synthesis of the A'B'-decalin of hibarimicinone required 16 linear steps and utilized the unique approach of forming the furan ring system first as a scaffold for decalin formation.



**Scheme 2.19.** Roush's synthesis of the A'B'-decalin system.

In contrast to Roush's strategy through the furan moiety, Mootoo and co-workers reported the synthesis of the A'B'-decalin unit in 2008 that focused on formation of the decalin functionality followed by installation of the bridging furan.<sup>26</sup> This approach centered on a key IMDA to quickly provide the functionalized decalin structure. Thus,

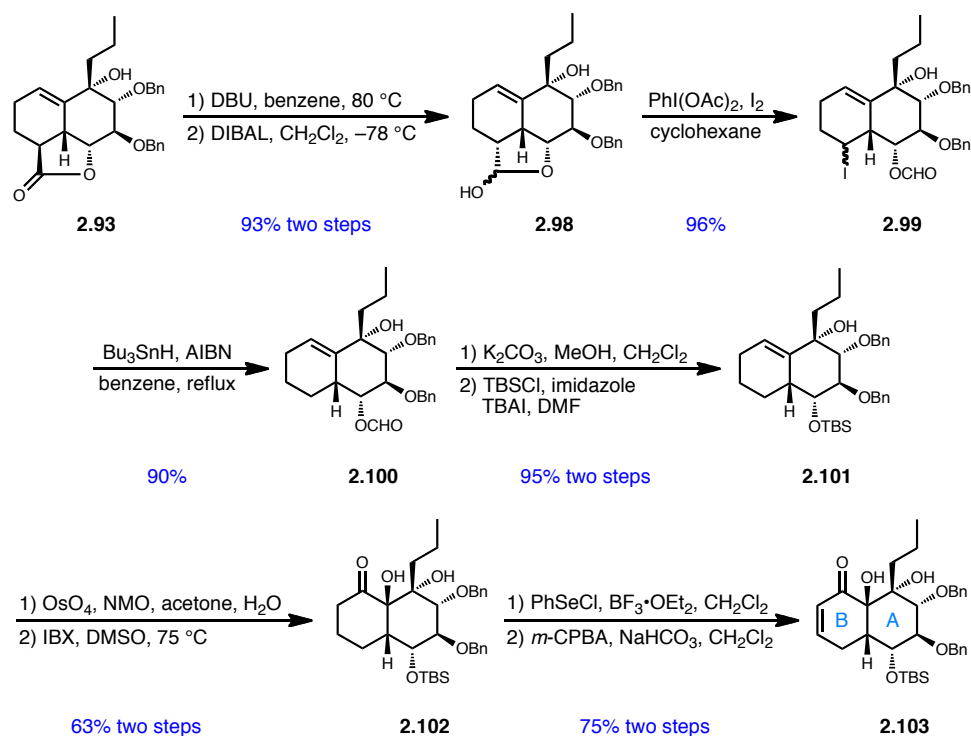
the lactone **2.90**, which derived from methyl- $\alpha$ -D-glucopyranoside, was bis-alkylated, first with propylmagnesium chloride then with the lithium salt of TMS acetylene in a 5:1 diastereomeric ratio favoring the desired  $\alpha$ -tertiary alcohol. TMS alkyne deprotection provided the key intermediate **2.91** which was subjected to Grubbs second generation catalyst under an atmosphere of ethylene to effect a ring closing enyne metathesis, smoothly arriving at the highly functionalized A'-ring precursor **2.92**. Installation of the dienophile by esterification with acryloyl chloride provided the proposed IMDA substrate which was successfully cyclized in refluxing xylene to form the decalin **2.93**. Mootoo and co-workers then shrewdly exploited the decalin conformation for stereoselective dihydroxylation on the convex face of the trisubstituted olefin followed by silyl protection. For the dual purpose of removing the extra lactone carbon and furan formation, the lactone was reduced to the lactol **2.94** with DIBAL, and under radical-mediated conditions with phenyliodonium diacetate (PIDA) and iodine, carbon-carbon bond fragmentation and intramolecular capture with the tertiary alcohol resulted in formation of the furan ring. The resulting formate was removed with potassium carbonate in methanol to yield the free secondary alcohol **2.95**. The final steps necessary for formation of the A'B'-ring system required a regioselective protection/deprotection sequence, and **2.96** was converted to the enone through IBX oxidation to the ketone followed by phenylselenation/oxidation to arrive at the A'B'-decalin **2.97**. Mootoo's route to this key building block toward hibarimicinone established two important precedents for future synthetic approaches, namely the use of an IMDA rapidly form the decalinic structure and a method for removing the unwanted lactone carbon while concomitantly forming the key ethereal linkage found in the A'B'-ring structure.



**Scheme 2.20.** Mootoo's synthesis of the A'B'-decalin toward hibarimicinone.

Considering Roush's and Mootoo's syntheses of the A'B'-ring system toward hibarimicinone, these approaches also require the assembly of the AB-decalin **2.54** for differential bis-annulation with the biaryl core **2.55**. Toward this end, two separate publications have addressed this need, first by Mootoo and co-workers utilizing the same manifold employed in their synthesis of the A'B'-system.<sup>27</sup> Thus, from the previously synthesized IMDA product **2.93**, slight modification of the previously published route led to the AB-ring system.

While attempting direct radical fragmentation of the lactol form of **2.93**, it was determined that the ring strain of the *trans* lactol negatively affected the success of the reaction. Therefore, DBU-mediated epimerization to the *cis* lactone and reduction to the lactol yielded **2.98**, which proved to be a superb substrate for the fragmentation reaction. And unlike in their synthesis of the A'B' subunit, intramolecular oxygen capture did not occur, with the substrate striking a balance between reactivity and conformation necessary for cycloetherification. With the epimeric mixture of iodides **2.99**, tributyltin hydride-mediated dehalogenation provided **2.100** which was subjected to formate removal and TBS protection to provide the key intermediate **2.101**. In a four step sequence similar to their previously utilized strategy, dihydroxylation and IBX oxidation were followed by phenylselenation/oxidation to provide the target enone **2.103** in good yield. In this work, Mootoo and co-workers effectively diverged from their previously successful approach to synthesize the remaining outer core partner for the two-directional bis-annulation sequence outlined in Scheme 2.12. To date, no further reports from the Mootoo laboratories have appeared describing their work toward the central biaryl core.



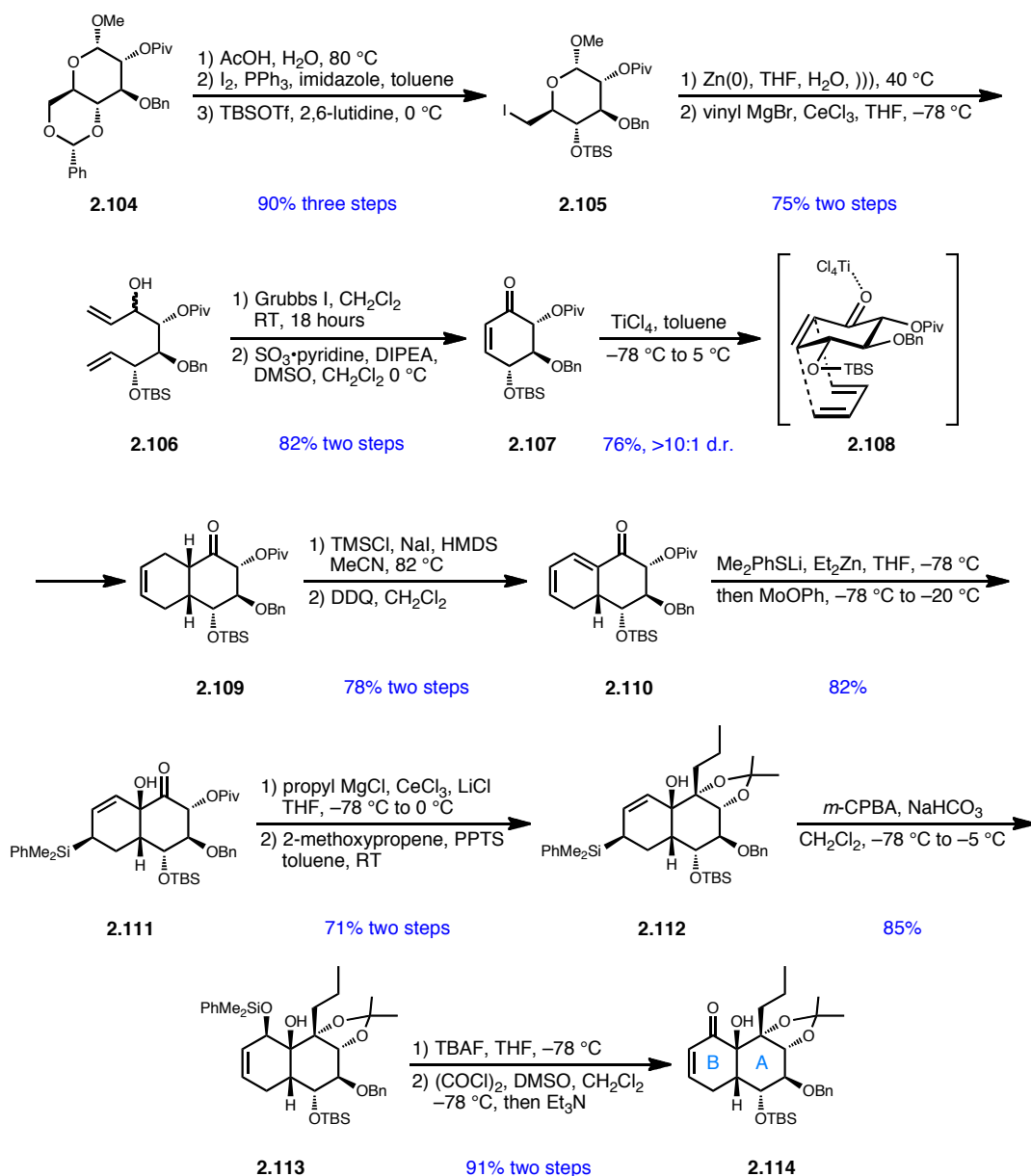
**Scheme 2.21.** Mootoo's modified route to the AB-decalin system.

Shortly following Mootoo's report of their unified strategy toward the AB-ring system of hibarimicinone, Shair and co-workers published the gram-scale synthesis of a variably protected AB-decalin with the same key functionalities as synthesized by Mootoo.<sup>28</sup> Key to their strategy was an intermolecular Diels-Alder reaction to form the decalin system and a silyl-zincate conjugate addition/oxidation sequence to install functionality for further oxidation.

Like Mootoo, starting from methyl- $\alpha$ -D-glucopyranoside, an overall six-step procedure arrived at the appropriately functionalized pyranoside **2.104**, which was subjected to sonication with activated zinc dust to effect fragmentation to the intermediate aldehyde, which was alkylated with vinylmagnesium bromide in the



presence of cerium trichloride to yield the inconsequential mixture of diastereomeric alcohols **2.106**. Ring closing metathesis with Grubbs first generation catalyst and Parikh-Doering oxidation led to the Diels-Alder precursor **2.107**. By Lewis-acid complexation, the desired intermolecular Diels-Alder with butadiene occurred with high diastereoselectivity through transition state **2.108**, where a purely steric analysis would suggest its unfavorable interactions with the OTBS and OPiv groups; however, rationalization by Cieplak theory would suggest stabilization of forming  $\sigma^*$ -orbital adjacent to the OTBS group by electron donation from the axial hydrogen. Thus, the *cis* decalin **2.109** was carried forward through silyl-enol ether formation and oxidation to the dienone **2.110**, which when subjected to the silyl zincate, underwent 1,6-conjugate addition and the resulting zinc enolate was oxidized with MoOPh to provide the  $\alpha$ -hydroxyketone **2.111** as a single diastereomer. Due to the favorable conformation of the *cis* decalin, nucleophilic addition of the propyl unit afforded a single diastereomer of the tertiary alcohol while concomitantly removing the pivaloyl protecting group. Acetonide formation between the free secondary and tertiary alcohols led to **2.112**, and *m*-CPBA epoxidation of the disubstituted olefin led to 1,5-silyl migration forming the allylic silyl ether **2.113**. Finally, TBAF-mediated silyl deprotection followed by Swern oxidation led to the protected AB-subunit **2.114** containing the same key functionalities targeted by the Mootoo group. Importantly, the Shair group's approach was carried out completely on gram scale allowing for synthesis of large quantities of material for further studies toward HMP-Y1 and hibarimicinone. Their intermolecular Diels-Alder strategy highlights the versatility of various forms of the Diels-Alder reaction toward synthesis of hibarimicinone intermediates.



**Scheme 2.22.** Shair's synthesis of the AB-decalin unit.

The absolute stereochemistry of the hibarimicins remained unknown through the publication of Roush, Mootoo, and Shair's work, and the arbitrarily-depicted absolute orientation shown in Figure 1.6 continued as the general consensus through 2011. Ultimately, two studies finally established the absolute configuration of hibarimicinone,

beginning with a little-noticed abstract in the Japanese abstracting service *Tennen Yuki Kagobutsu Toronkai Koen Yoshishu* reported in 2004.<sup>29</sup> Our laboratory obtained a copy of the abstract through our ongoing collaboration with Professors Hori and Igarashi in Japan, which outlined the determination of the absolute stereochemistry of the hibarimicins through Mosher ester analysis and sugar moiety synthesis.

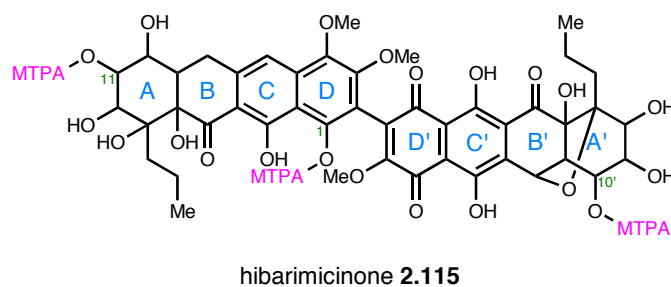


**Figure 2.3.** Determination of hibarimicinone absolute stereochemistry.

Specifically, Mosher ester analysis was performed at the C-1, C-11, and C-10' hydroxyl groups shown in Figure 2.3, although details and experimental methods for these studies were not included. Additionally, the circular dichroism spectrum for hibarimicinone was used for postulation of the absolute atropisomerism about the highly congested aryl-quinone bond. Taken in concert with data determined by the model system synthesis by our laboratory shown in Figure 1.9, the absolute stereochemistry of hibarimicin B was determined to be opposite of the stereochemistry reported in previous synthetic efforts and is shown in Figure 2.4. This information proved vital in the two total syntheses of hibarimicinone that were reported in 2012.

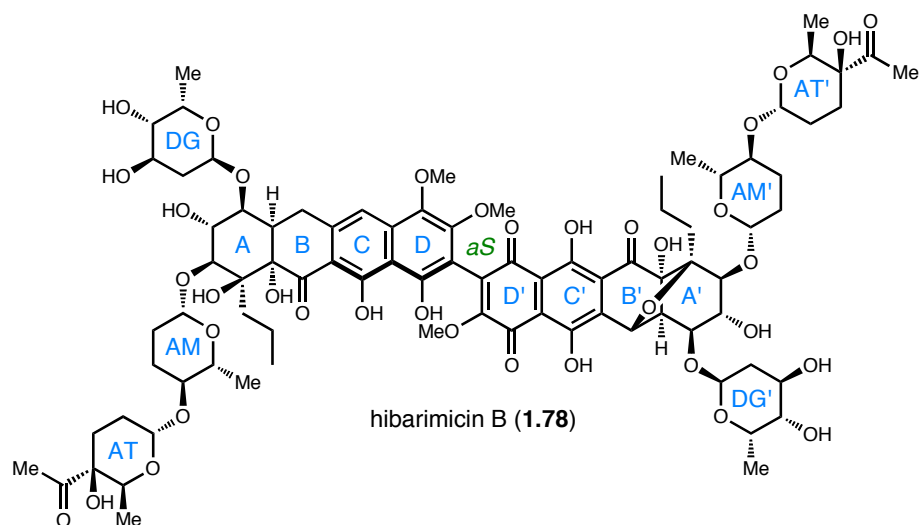


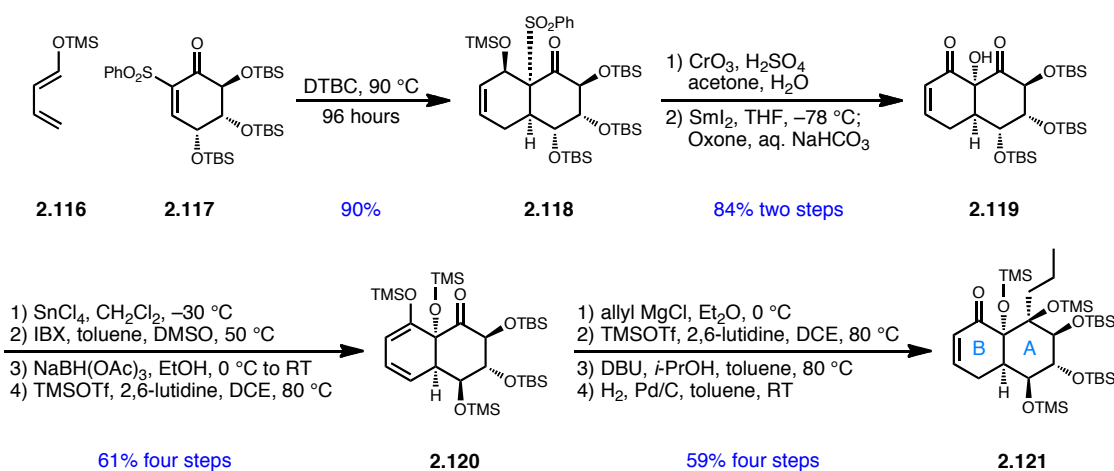
**Figure 2.4.** Absolute stereochemistry of hibarimicin B.

### Total Syntheses of HMP-Y1 and Hibarimicinone

The determination of the absolute stereochemistry of the hibarimicins proved to be a turning point in the history of the hibarimicins: Hosokawa and co-workers reported the first total synthesis of hibarimicinone with the correct absolute stereochemistry early in 2012.<sup>30</sup> Their route resembled a combination of the retrosyntheses presented in Scheme 2.12, in which a differentially functionalized biaryl core was elaborated through a two-directional bis-annulation sequence with two equivalents of a decalinic enone in a manner similar to the retrosynthetic disconnection of HMP-Y1. The approach relied upon formation of a single atropisomer of the biaryl core, differential functionalization of the bis-tetracycle, and formation of the furan linkage through an *ortho*-quinone methide.

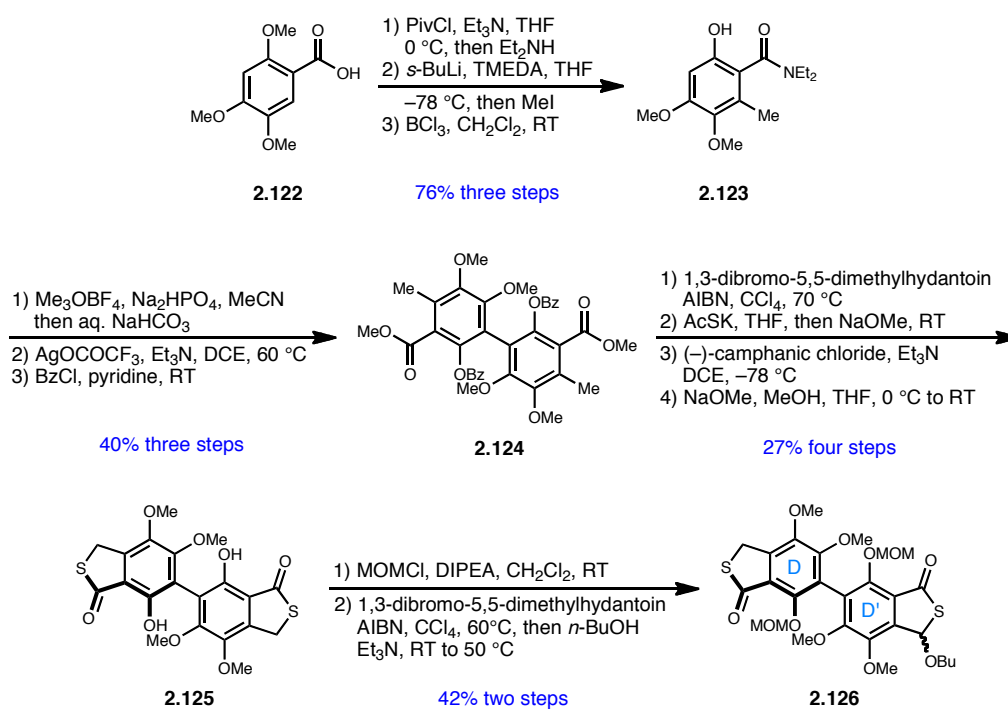
Hosokawa's synthesis of the AB-decalin enone began with an intermolecular Diels-Alder reaction between the highly elaborated  $\alpha$ -phenylsulfonyl enone **2.117** and 1-

trimethylsiloxybutadiene (**2.116**) in the presence of di-*t*-butylcatechol (DTBC) which arrived at the desired *cis*-decalin **2.118** regio- and stereoselectively. Jones oxidation provided the enone, and reductive samarium enolate formation with SmI<sub>2</sub> was followed by enolate oxidation with Oxone to provide the tertiary alcohol **2.119**. Regioselective desilylation with SnCl<sub>4</sub> removed only the C-10 TBS-ether, and the resulting alcohol was oxidized with IBX. The triketone was regio- and stereoselectively reduced with NaBH(OAc)<sub>3</sub> to provide the correct regiochemistry of the triol system, and the remaining secondary and tertiary alcohols were protected as TMS ethers while concomitantly forming the extended silyl enol ether **2.120**. The remaining steps toward the AB-ring system involved stereoselective allylation with allyl Grignard, tertiary alcohol protection, reformation of the enone with DBU, and regioselective hydrogenation of the allyl functionality provided the protected AB-decalin **2.121**.



**Scheme 2.23.** Hosokawa's synthesis of the AB-decalin system.

For the two-directional strategy toward hibarimicinone, a biaryl ring system was needed that contained varying functionalities on either end for regioselective manipulation later in the synthesis. Thus, the acid **2.122** was transformed to the amide followed by regioselective lithiation and reaction with methyl iodide. Boron trichloride-mediated regioselective demethylation provided the phenol **2.123** which was converted to the methyl ester. The key step involved oxidative dimerization with silver triflate to form the racemic bis-phenol which was protected as the bis-benzoate **2.124**. Radical bis-bromination was followed by displacement with potassium thioacetate, thiolactone formation, and concomitant benzoate cleavage. By forming the mono-camphanic ester, the diastereomeric mixture became separable, and the desired *aR* atropisomer could be carried forward through ester removal to arrive at the atropisomerically enriched bis-phenol **2.125**. Bis-MOM protection was followed by breaking of the biaryl core symmetry through mono-bromination and displacement with *n*-butanol to provide the unsymmetrical diastereomeric mixture **2.126** which was properly functionalized for the proposed bis-annulation sequence with the previously synthesized AB-ring system **2.121**.

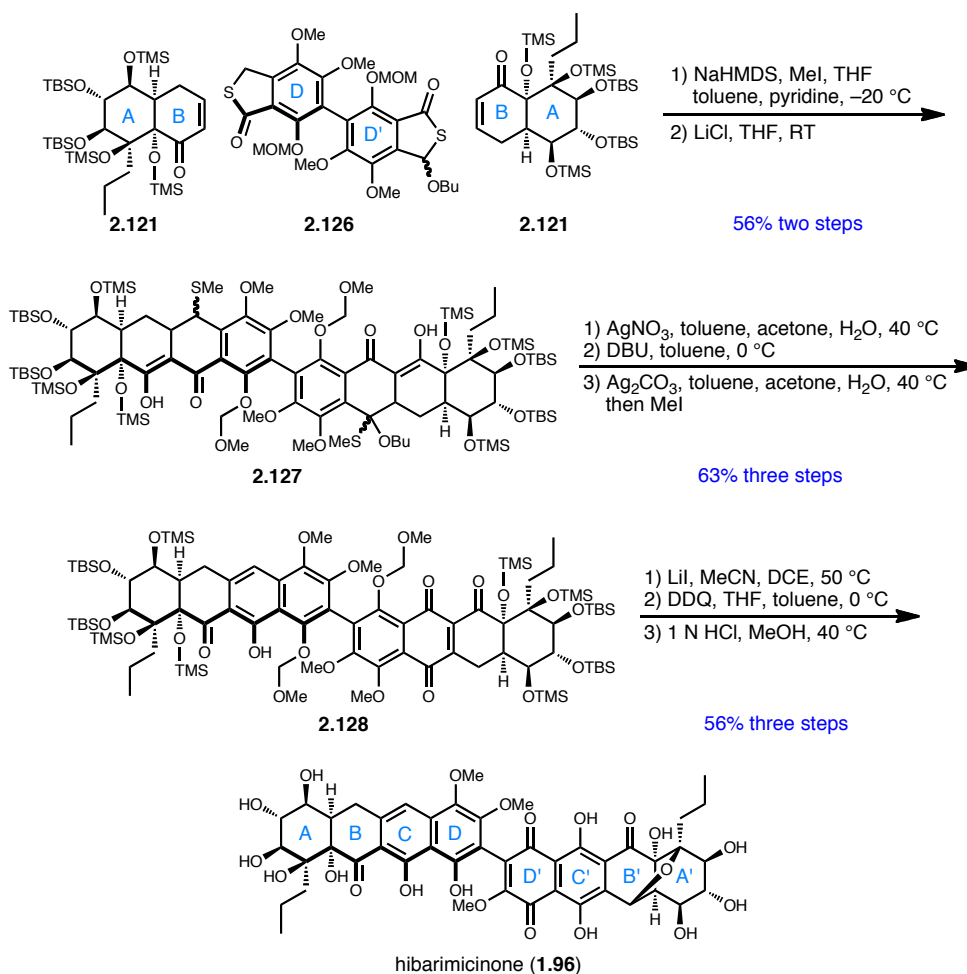


**Scheme 2.24.** Synthesis of the unsymmetrical biaryl D-D' moiety.

The remaining steps necessary for synthesis of hibarimicinone involved the linchpin bis-Michael-Dieckmann condensation between the biaryl **2.126** and the enone **2.121**, which was effected with NaHMDS and followed by methylation of the thiolate intermediate to form the basic bis-tetracyclic core of the target. Interestingly, the annulation sequence was favored for the unsubstituted thiolactone in THF while the Michael-Dieckmann condensation with the substituted thiolactone was most effective in toluene, and thus the two-directional annulation was performed in the mixture of solvents. Enolization of the resulting bis- $\beta$ -diketone formed bis-enol **2.127**, and hydrolysis of the semithioacetal and formation of the hydroquinone was effected by a sequence of silver nitrate then DBU. By treating the hydroquinone with silver carbonate, the C'-ring was oxidized to the quinone with concomitant aromatization of the C-ring to

provide the quinone **2.128**. The important furan linkage was then installed by formation of the quinone methide with lithium iodide which allowed for Michael addition of the C-13' tertiary alcohol, and MOM ether deprotection also occurred. Treatment with DDQ oxidized the resulting hydroquinone back to the quinone oxidation state, and a final step involving heating with 1 N HCl in methanol led to global silyl deprotection and tautomerization of the C'-D' ring system to afford hibarimicinone (**1.96**). Hosokawa's first total synthesis not only confirmed the absolute stereochemistry of hibarimicinone but also validated the two-directional annulation sequence that had been the cornerstone of all synthetic efforts to that point. Additionally, Hosokawa's synthesis proved the validity of a biomimetic ether linkage formation through an *ortho*-quinone methide intermediate.

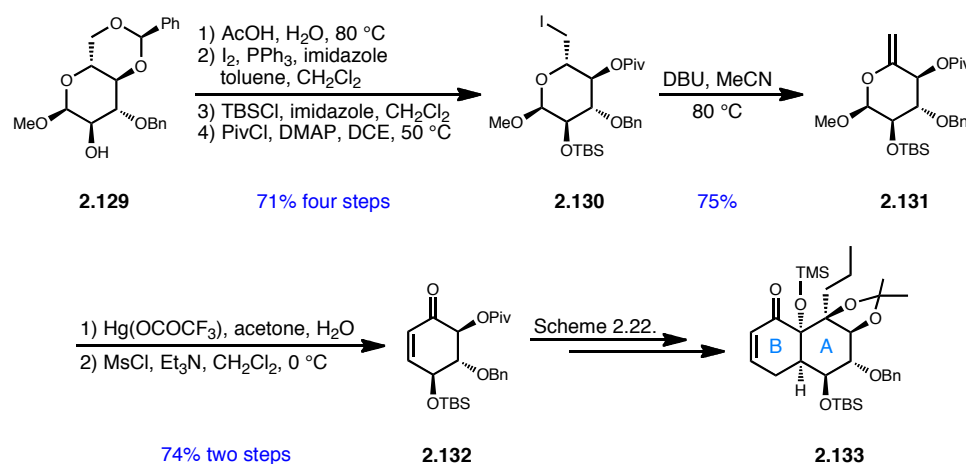




**Scheme 2.25.** Hosokawa's first total synthesis of hibarimicinone.

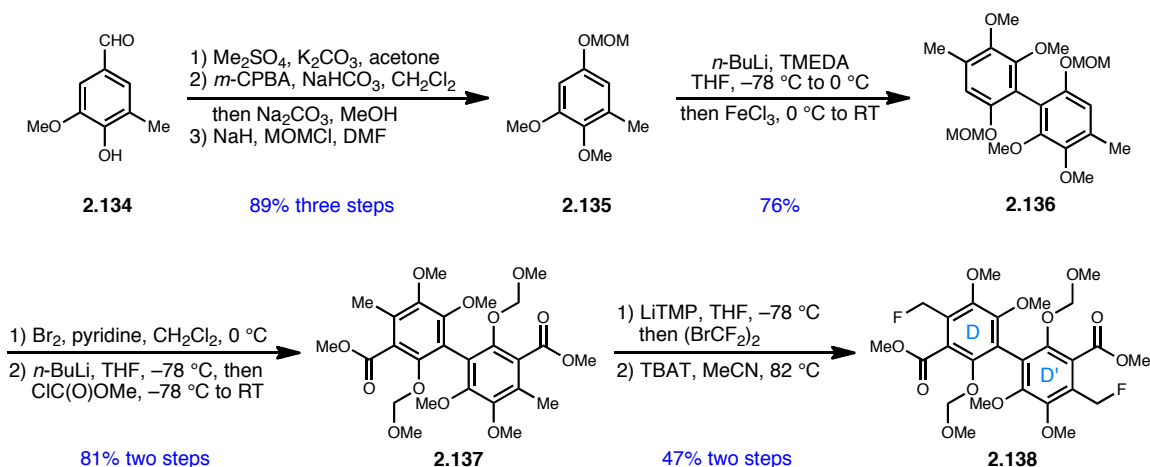
A second total synthesis of hibarimicinone, as well as the synthesis of the biosynthetic intermediate HMP-Y1, appeared from the Shair laboratory during the writing of this document.<sup>31</sup> Drawing on the previously determined hibarimicinone absolute stereochemistry and utilizing a similar two-directional approach to Hosokawa, Shair and co-workers also reported extensive studies regarding the atropisomerism of HMP-Y1 and hibarimicinone.

Following the publication of the Shair laboratory's gram-scale synthesis of the AB-decalin unit **2.114** shown in Scheme 2.22, it became apparent that the absolute configuration of **2.114** corresponded to the unnatural enantiomer of hibarimicinone, and thus for their total synthesis, Shair and co-workers modified their initial assembly of the AB-decalin to arrive at the desired enantiomer. Derived from the same starting material as in their synthesis of **2.114**, methyl- $\alpha$ -D-glucopyranoside, **2.129** was subjected to a series of functional group interconversions and protection steps to form the primary iodide **2.130**. To switch the absolute stereochemistry of the AB-subunit previously synthesized through a Vasella fragmentation, the primary iodide was eliminated to form the exocyclic olefin **2.131** which was subjected to a type-II Ferrier rearrangement with  $\text{Hg}(\text{OCOCF}_3)_3$  and converted to the enone **2.132**. The enone **2.132** corresponds to the enantiomer of **2.107** synthesized in the Shair group's previous report and thus was elaborated to the AB-decalin **2.133** using the same sequence as shown in Scheme 2.22.



**Scheme 2.26.** Shair's synthesis of the natural AB-decalin enantiomer.

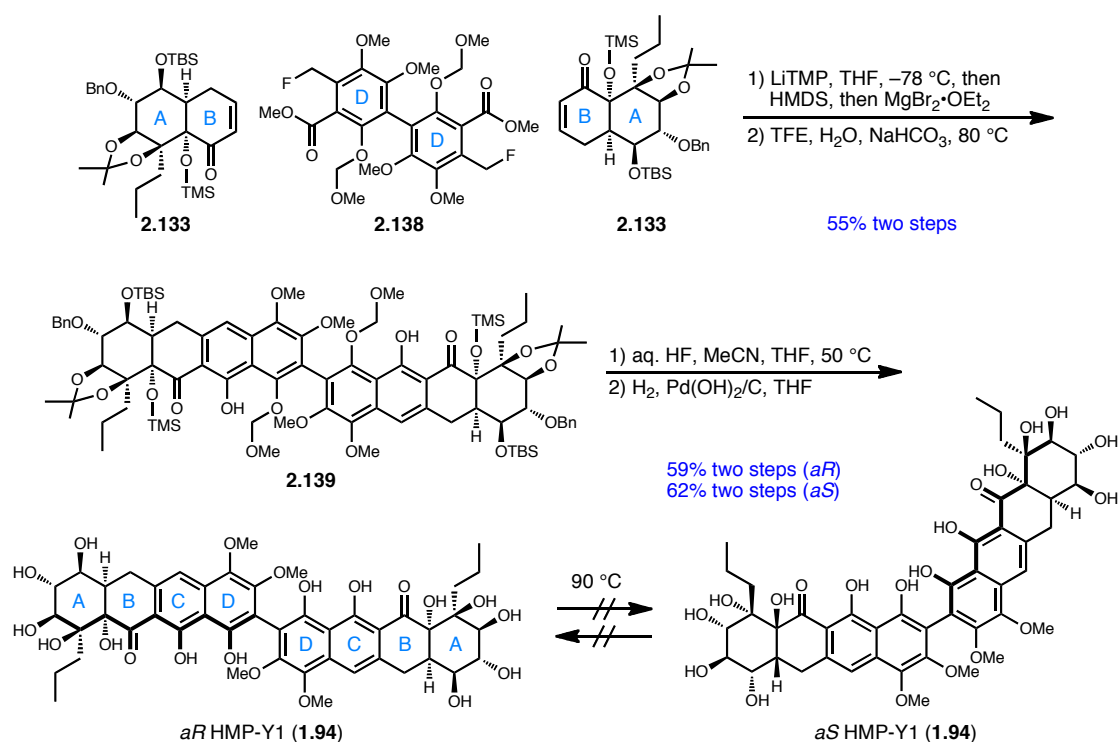
Shair's proposed two-directional synthesis of the bis-tetracyclic ring system of HMP-Y1 and hibarimicinone hinged upon an improved benzylic fluoride-mediated Michael-Dieckmann cyclization, and therefore an appropriately functionalized D-D' biaryl core required assembly. Starting from 5-methylvanillin (**2.134**), a three step sequence involving phenol methylation, Baeyer-Villiger oxidation, and MOM protection led to the toluene derivative **2.135**. Regioselective aryl lithiation and treatment with iron trichloride effected homodimerization to the racemic biaryl **2.136**. Installation of a bis-methyl ester required bis-bromination, lithiation, and addition to methyl chloroformate leading to **2.137**. Finally, bis-benzylic fluoride incorporation for the upcoming bis-Michael-Dieckmann cyclization occurred through bis-benzylic bromination followed by fluoride displacement with TBAT to yield the symmetrical D-D' biaryl core **2.138**.



**Scheme 2.27.** Synthesis of a symmetrical D-D' biaryl core for bis-annulation.

With the key building blocks in hand, the bis-annulation sequence toward HMP-Y1 occurred smoothly by deprotonation of the benzylic fluoride methylene positions of

**2.138** with LiTMP (lithium tetramethylpiperidine) followed by Michael addition into enone **2.133** and subsequent Dieckmann condensation to form the C-rings. Notably, addition of  $\text{MgBr}_2 \cdot \text{OEt}_2$  was essential to the Dieckmann condensation's completion. In a novel method, treatment of the bis-cyclic benzylic fluorides with trifluoroethanol (TFE) effected C-ring aromatization, likely through hydrolysis of a hydrogen-bound fluorine-TFE complex which provided the protected HMP-Y1 **2.139**. At this point, the racemic mixture of atropisomers became chromatographically separable, and each atropisomer was carried forward separately. Acetonide, MOM, and silyl ether deprotection with aqueous HF was finally followed by hydrogenolysis of the benzyl ethers to provide both atropisomers of HMP-Y1 (**1.94**). Attempted thermal interconversion failed when heated at 90 °C, and thus confirmation was provided for the proposal that atropostereochemistry is retained during the biological conversion of HMP-Y1 to hibarimicinone. Therefore, the *aR* atropisomer was validated as the correct axial stereochemistry for HMP-Y1, and its conversion to hibarimicinone with retention of axial chirality confirms the absolute biaryl stereochemistry of *aS* for hibarimicinone, which was synthetically validated by Hosokawa's total synthesis.

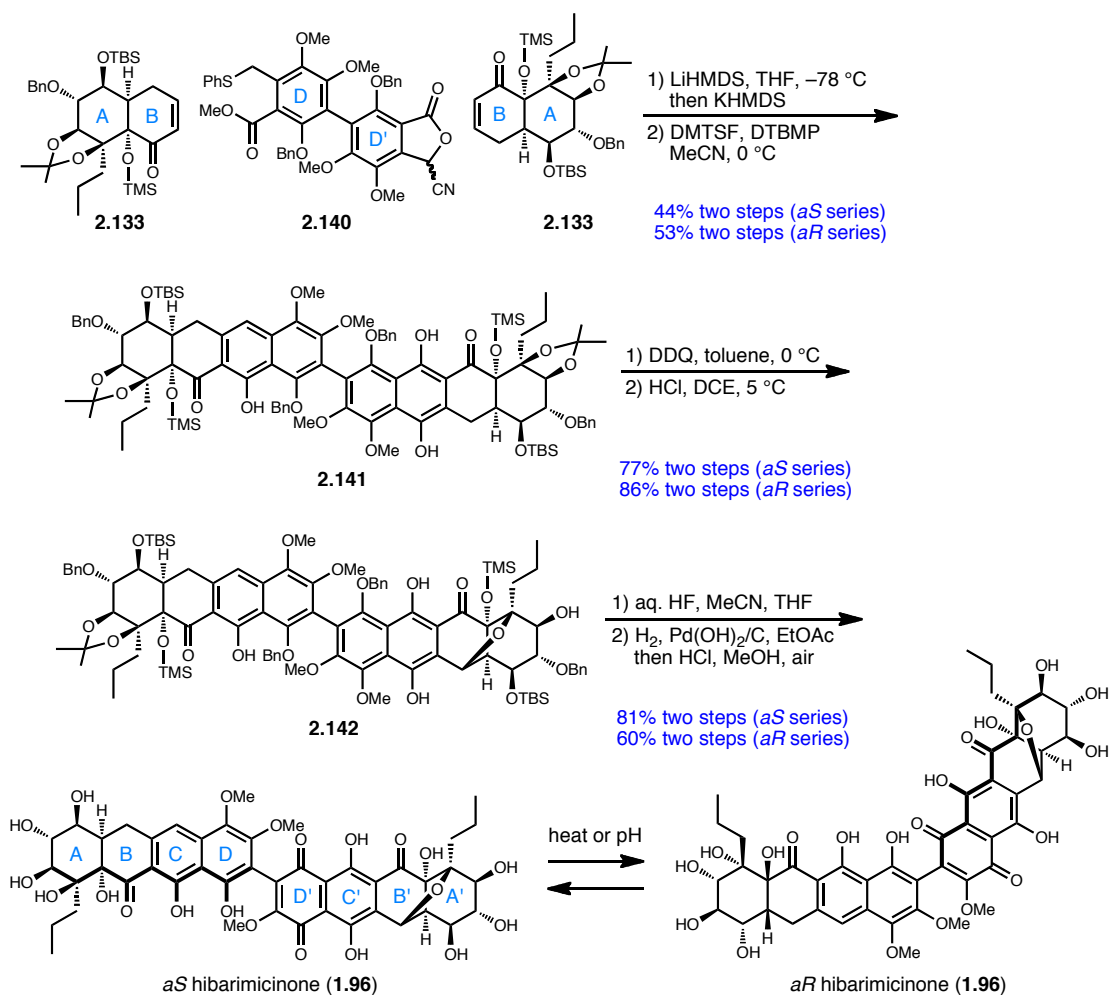


**Scheme 2.28.** The first total synthesis of HMP-Y1.

Shair and co-workers originally intended for a biomimetic synthesis of hibarimicinone that utilized the biosynthetic intermediate HMP-Y1 as a key precursor. In this line of reasoning, they attempted mono-oxidation of HMP-Y1 with CAN in a mixture of acetonitrile, THF, and water and arrived at the mono-quinone C'-ring product in only 15% yield. Although this approach lends credit to the possibility of the originally proposed synthetic analysis, attempts at improving the yield remained fruitless, and therefore a more robust strategy was employed with a differentially functionalized D-D' ring system **2.140** which was arrived at from **2.137** in seven steps.

With the unsymmetrical **2.140**, bis-annulation with **2.133** occurred by sequential treatment with LiHMDS then KHMDS. Separation of atropisomers became possible at

this point, and each was carried through the remaining steps separately. Phenyl sulfide elimination led to aromatization of the C-ring affording **2.141**, which was oxidized to the C'-ring mono-quinone. In the key furan linkage forming step, addition of anhydrous HCl led to ether **2.142** through a presumed quinone methide intermediate with tertiary alcohol Michael addition and reformation of the hydroquinone. The final deprotection steps simply required aqueous HF-mediated removal of the silyl ether and acetonide protecting groups and was followed by hydrogenolysis of the remaining benzyl ethers to provide the natural (*aS* **1.96**) and unnatural (*aR* **1.96**) forms of hibarimicinone. Interestingly, an axial interconversion pathway was identified based on treatment with either pH 7.5 buffer at room temperature or with 1 N HCl in methanol at 60 °C. Considering these results, a proposed mechanism for interconversion relies upon the same proposal set forth in Scheme 1.16 in which formation of a planar conjugated tautomer allows for transition between the two atropisomers with a lower barrier to rotation. Ultimately, the Shair laboratory's total synthesis of hibarimicinone has provided important information regarding the nature of hibarimicin atropisomers and along the way has demonstrated novel methods for performing bis-annulation sequences, either to form symmetrical or unsymmetrical products.



**Scheme 2.29.** Shair's completion of the total synthesis of hibarimicinone.

## Conclusion

The Diels-Alder reaction holds a rich history of enabling complex natural product total synthesis, either in the form of the inter-, intra-, or transannular-modes. Previous work toward HMP-Y1 and hibarimicinone has revealed the importance of the Diels-Alder reaction in assembly of components for their synthesis, and important details have emerged regarding considerations for further synthetic investigations including the nature

of the HMP-Y1 and hibarimicinone axial chirality. With this knowledge, the remaining chapters highlight the studies toward total synthesis of HMP-Y1 and hibarimicinone that have occurred in our laboratories in the recent past.

The remaining chapters of this dissertation detail the application of the intramolecular Diels-Alder reaction in the development of two differing approaches to the natural product hibarimicin B and its biosynthetic intermediates HMP-Y1 and hibarimicinone.

## References

1. Berson, J. A. "Discoveries missed, discoveries made: creativity, influence, and fame in chemistry" *Tetrahedron*, **1992**, 48, 3-17.
2. Diels, O.; Alder, K. "Synthesen in der hydroaromatischen reihe" *Justus Liebigs Ann. Chem.*, **1928**, 460, 98-122.
3. Fringuelli, F.; Taticchi, A. "The Diels-Alder reaction: selected practical methods" **2002**, New York: John Wiley & Sons, Ltd.
4. Fallis, A. G. "The intramolecular Diels-Alder reaction: recent advances and synthetic applications" *Can. J. Chem.*, **1984**, 62, 183-234.
5. Sustmann, R.; Tappanchai, S.; Bandmann, H. "a(E)-1-methoxy-1,3-butadiene and 1,1-dimethoxy-1,3-butadiene in (4+2) cycloadditions. A mechanistic comparison" *J. Am. Chem. Soc.*, **1996**, 118, 12555-12561.
6. Alder, K.; Stein, G. "Untersuchungen über den verlauf der diensynthese" *Angew. Chem.*, **1937**, 50, 510-519.
7. Alder, K.; Stein, G.; Freiherr von Buddenbrock, R.; Eckardt, W.; Frercks, W.; Schneider, S. "Über den sterischen verlauf von additions- und substitutionsreaktionen. I. Zur stereochemie der dien-synthese" *Justus Leibigs Ann. Chem.*, **1934**, 514, 1-33.



8. Taber, D. F. "Intramolecular Diels-Alder and Alder ene reactions" **1983**, Heidelberg: Springer-Verlag.
9. Deslongchamps, P. "Transannular Diels-Alder reaction on macrocycles. A general strategy for the synthesis of polycyclic compounds" *Pure & Appl. Chem.*, **1992**, *64*, 1831-1847.
10. Layton, M. E., Morales, C. A., Shair, M. D. "Biomimetic synthesis of (-)-longithorone A" *J. Am. Chem. Soc.*, **2002**, *124*, 773-775.
11. Balskus, E. P.; Jacobsen, E. N. "Asymmetric catalysis of the transannular Diels-Alder reaction" *Science*, **2007**, *317*, 1736-1740.
12. Nicolaou, K. C.; Snyder, S. A.; Montagnon, T.; Vassilikogiannakis, G. "The Diels-Alder reaction in total synthesis" *Angew. Chem. Int. Ed.*, **2002**, *41*, 1668-1698.
13. Woodward, R. B.; Sondheimer, F.; Taub, D.; Heusler, K.; McLamore, W. M. "The total synthesis of steroids" *J. Am. Chem. Soc.*, **1952**, *74*, 4223-4251.
14. Corey, E. J.; Da Silva Jardine, P.; Rohloff, J. D. "Total synthesis of (±)-forskolin" *J. Am. Chem. Soc.*, **1988**, *110*, 3673-3674.
15. Kim, A. I.; Rychnovsky, S. D. "Unified strategy for the synthesis of (-)-elisapterosin B and (-)-colombiasin A" *Angew. Chem. Int. Ed.*, **2003**, *42*, 1267-1270.
16. Krenske, E. H.; Perry, E. W.; Jerome, S. V.; Maimone, T. J.; Baran, P. S.; Houk, K. N. "Why a proximity-induced Diels-Alder reaction is so fast" *Org. Lett.*, **2012**, *14*, 3016-3019.
17. Wood, J. L.; Porco, Jr., J. A.; Taunton, J.; Lee, A. Y.; Clardy, J.; Schreiber, S. L. "Application of the allylic diazene rearrangement: synthesis of the enediyne-bridged tricyclic core of dynemicin A" *J. Am. Chem. Soc.*, **1992**, *114*, 5898-5900.
18. Porco, Jr., J. A.; Schoenen, F. J.; Stout, T. J.; Clardy, J.; Schreiber, S. L. "Transannular Diels-Alder route to systems related to dynemicin A" *J. Am. Chem. Soc.*, **1990**, *112*, 7410-7411.
19. Taunton, J.; Wood, J. L.; Schreiber, S. L. "Total syntheses of di- and tri-*O*-methyl dynemicin A methyl esters" *J. Am. Chem. Soc.*, **1993**, *115*, 10378-10379.

20. Vosburg, D. A.; Vanderwal, C. D.; Sorensen, E. J. "A synthesis of (+)-FR182877, featuring tandem transannular Diels-Alder reactions inspired by a postulated biogenesis" *J. Am. Chem. Soc.*, **2002**, *124*, 4552-4553.
21. Poss, C. S.; Schreiber, S. L. "Two-directional chain synthesis and terminus differentiation" *Acc. Chem. Res.*, **1994**, *27*, 9-17.
22. Lee, C.-S.; Audelo, M. Q.; Reibenpies, J.; Sulikowski, G. A. "Studies toward the total synthesis of hibarimicinone. Progress on the assembly of the AB- and GH-ring systems" *Tetrahedron*, **2002**, *58*, 4403-4409.
23. Kim, K.; Maharroof, U. S. M.; Raushel, J.; Sulikowski, G. A. "Diverging stereochemical pathways in an intramolecular Diels-Alder reaction determined by dienophile structure" *Org. Lett.*, **2003**, *5*, 2777-2780.
24. Lee, W.-D.; Kim, K.; Sulikowski, G. A. "Studies into the stereoselectivity of tartrate-derived dienophiles" *Org. Lett.*, **2005**, *7*, 1687-1689.
25. Lambert, W. T.; Roush, W. R. "Synthesis of the A-B subunit of angelmicin B" *Org. Lett.*, **2005**, *7*, 5501-5504.
26. Li, J.; Todaro, L. J.; Mootoo, D. R. "Synthesis of the AB subunit of angelmicin B through a tandem alkoxy radical fragmentation-etherification sequence" *Org. Lett.*, **2008**, *10*, 1337-1340.
27. Li, J.; Todaro, L.; Mootoo, D. R. "Synthesis of an A'B' precursor to angelmicin B: Product diversification in the Suárez lactol fragmentation" *Eur. J. Org. Chem.*, **2011**, 6281-6287.
28. Milgram, B. C.; Liao, B. B.; Shair, M. D. "Gram-scale synthesis of the A'B'-subunit of Angelmicin B" *Org. Lett.*, **2011**, *13*, 6436-6439.
29. Hori, H.; Igarashi, Y.; Kajiura, T.; Sato, S.; Furumai, T.; Higashi, K.; Ishiyama, T.; Uehara, Y.; Oki, T. "Structure, biosynthesis and biological activities of v-Src tyrosine specific protein kinase inhibitor, hibarimicins" *Tennen Yuki Kagobutsu Toronkai Koen Yoshishu*, **2004**, *46*, 49-54.
30. Tatsuta, K.; Fukuda, T.; Ishimori, T.; Yachi, R.; Yoshida, S.; Hashimoto, H.; Hosokawa, S. "The first total synthesis of hibarimicinone, a potent v-Src tyrosine kinase inhibitor" *Tet. Lett.*, **2012**, *53*, 422-425.
31. Liao, B. B.; Milgram, B. C.; Shair, M. D. "Total syntheses of HMP-Y1, hibarimicinone, and HMP-P1" *J. Am. Chem. Soc.*, **2012**, *134*, 16765-16772.

## CHAPTER III

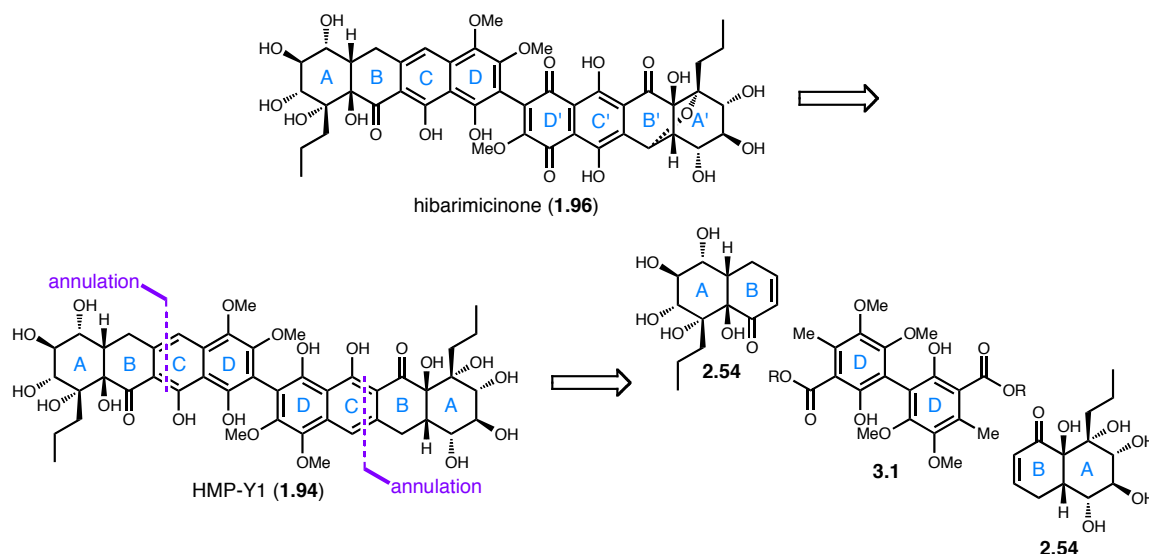
### A TWO DIRECTIONAL SYNTHETIC APPROACH

#### **Synthetic Analysis Toward HMP-Y1 and Hibarimicinone**

From the beginning of our group's interest in the hibarimicins, our synthetic strategy hinged upon the use of a two-directional bis-annulation sequence. Numerous benefits existed with this aim, beginning with a plan to derive the complex semi- $C_2$ -symmetric hibarimicinone (**1.96**) through a biomimetic conversion of HMP-Y1 (**1.94**). Because HMP-Y1 exhibits  $C_2$ -symmetry, we reasoned that the two-directional bis-annulation could occur between two equivalents of an appropriately functionalized enone by way of a Michael-Dieckmann condensation cascade, and thus our plan would only require synthesis of two key coupling partners. Additionally, much benefit existed in targeting a highly functionalized biaryl core.

At the outset of our studies toward the hibarimicins, the absolute stereochemistry of the AB- and A'B'-ring systems remained unresolved, and questions still remained regarding the existence and nature of atropisomerism in HMP-Y1 and the aryl-quinone in hibarimicinone. With this in mind, our two-directional strategy sought to identify the natural atropisomer of both of our synthetic targets by elaboration of the *aR* and *aS* biaryl cores to the natural product for spectroscopic correlation. Thus, we reasoned that a rapid synthesis and evaluation of optically pure biaryls **3.1** would benefit the overall strategy of assigning hibarimicinone axial chirality. These principles become apparent with the

general synthetic approach outlined in Scheme 3.1, and for the sake of clarity, the AB- and A'B'-absolute stereochemistry are denoted as historically accurate for our work.

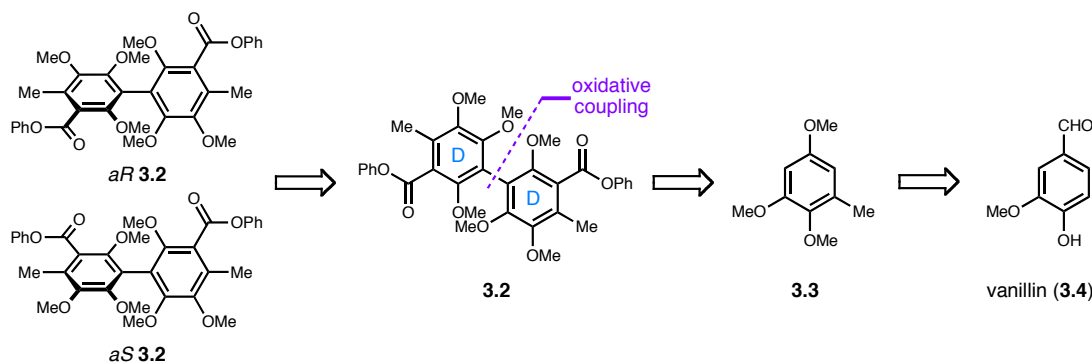


**Scheme 3.1.** Two-directional synthetic analysis toward HMP-Y1.

### Romaine's Work Toward the Biaryl Core

Two former members of our laboratory played key roles in initiating our hibarimicin studies. Ian Romaine's pioneering work toward the biaryl core, which no other research groups had previously given focus despite their interest in the AB and A'B' subunits, proved the feasibility of the two-directional approach, and his efforts require summarizing for contextual purposes. We thus proposed arrival at both *aR*-**3.2** and *aS*-**3.2** which would derive from a racemic mixture of a biaryl intermediate through chromatographic separation. Oxidative coupling of a properly suited aryl ring **3.3** would

provide access to the symmetric biaryl, and **3.3** was proposed to derive from vanillin (**3.4**).

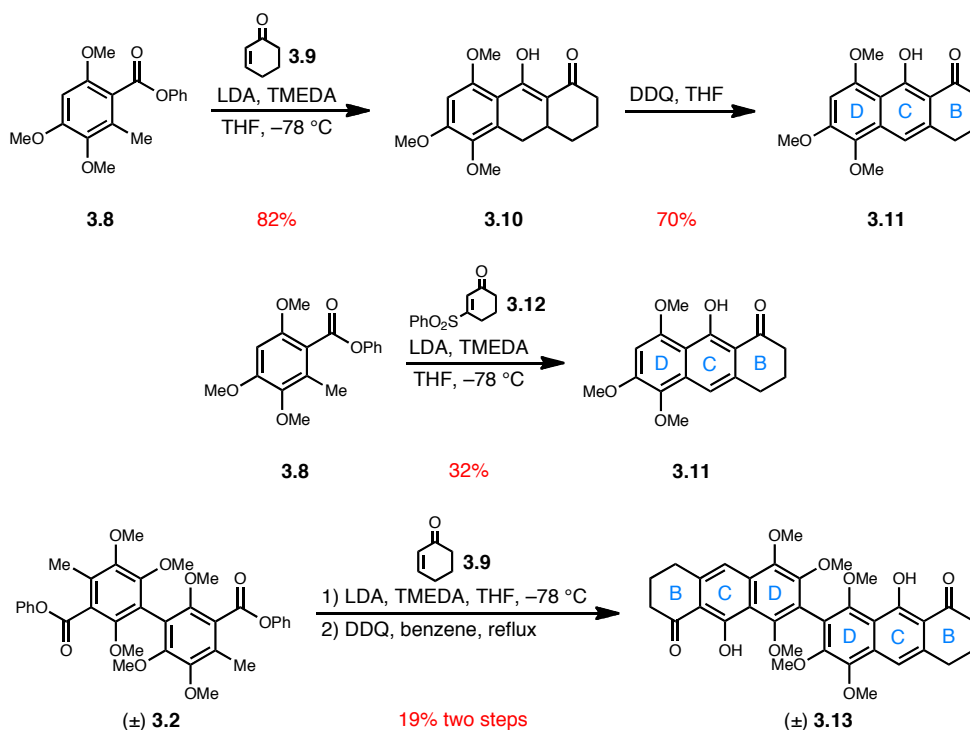


**Scheme 3.2.** Biaryl core retrosynthetic analysis.

Synthesis of the biaryl core began from vanillin (**3.4**) by regioselective aromatic bromination followed by Baeyer-Villiger oxidation to hydroquinone **3.5**.<sup>1</sup> Bis-methyl ether formation was followed by lithium-halogen exchange and methylation with methyl iodide to provide the desired toluene derivative **3.3** as a key precursor for oxidative dimerization. Using Spring's oxidative homodimerization procedure, by aryl deprotonation with *n*-BuLi and cuprate formation followed by addition of the oxidant **3.6**, racemic biaryl **3.7** was formed in reasonable yield.<sup>2</sup> Bis-bromination was then followed by lithium-halogen exchange and addition to phenyl chloroformate to provide a racemic mixture of the biaryl bis-phenyl ester **3.2**. For the purpose of ultimately determining the hibarimicinone axial chirality, chromatographic separation of the racemic atropisomers was attempted on each of the biaryl intermediates, and finally the bis-phenyl ester **3.2** succumbed to separation on chiral HPLC to arrive at atropopure samples. Axial chirality



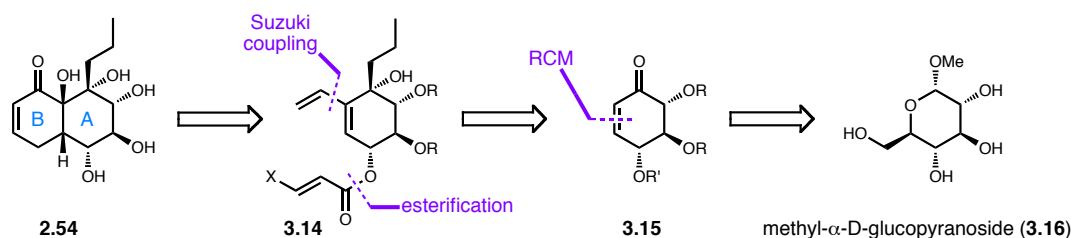
tricycle **3.10** was treated with DDQ in refluxing benzene to arrive at the model BCD-ring system **3.11** in good yield. Similarly, performing the Michael-Dieckmann sequence with the  $\beta$ -phenylsulfonylone **3.12** led directly to the desired naphthalene product **3.11** but in lower yield than the two step procedure.<sup>4</sup> With conditions worked out for mono-annulation, we moved to perform a bis-annulation with the related biaryl bis-phenyl ester **3.2** and cyclohexenone (**3.9**). After extensive experimentation, we were unable to improve the yield of bis-tricycle beyond 32%. These results, while confirmatory, loomed large over the big picture approach to HMP-Y1 and hibarimicinone by way of a bis-annulation sequence. Subsequent bis-oxidation with DDQ led to the racemic bis-tricycle **3.13** which constituted the BCD-BCD ring system found in HMP-Y1; however, again, the yield of this sequence remained concerning.



**Scheme 3.4.** Annulation model systems with cyclohexenone.

## Engers' Work Toward the AB-Decalin

With both pure biaryl atropisomers in hand, a route to the AB-decalinic enone **2.54** was designed based on our laboratory's previous experiences highlighted in Chapter II. Thus, a key intramolecular Diels-Alder reaction was posed as a stereochemistry-defining step for the C-9 bridgehead hydrogen that would direct formation by tethering with the adjacent chiral secondary alcohol at C-10 from an IMDA precursor **3.14**. In this manner, the dienophile would be installed through an esterification reaction, and the terminal diene would arise from a palladium-mediated Suzuki cross coupling to arrive at enone **3.15**. The A-ring subunit **3.15** was proposed to derive from a linear precursor through a ring closing metathesis reaction, and the three stereochemically defined secondary alcohols would be available directly from the chiral feedstock methyl- $\alpha$ -D-glucopyranoside (**3.16**).

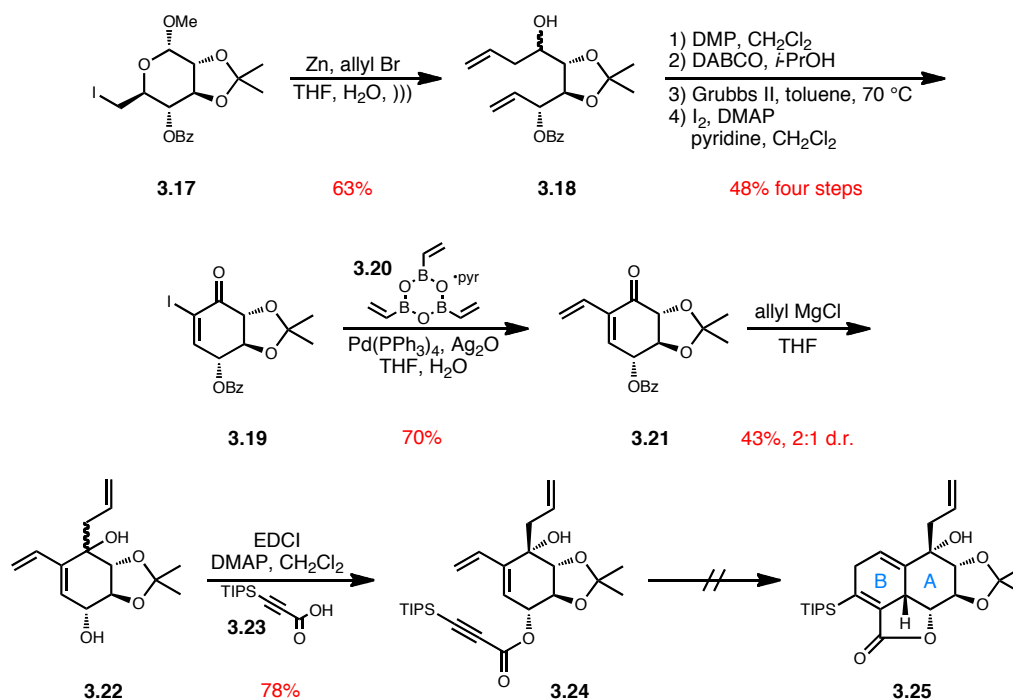


**Scheme 3.5.** Retrosynthetic analysis toward the AB-ring system subunit.

A previous postdoctoral fellow in our laboratory, Dr. Darren Engers, led the initial expedition through this proposed synthetic plan, and much of his effort laid the groundwork for the research that was to come. In five steps from methyl- $\alpha$ -D-

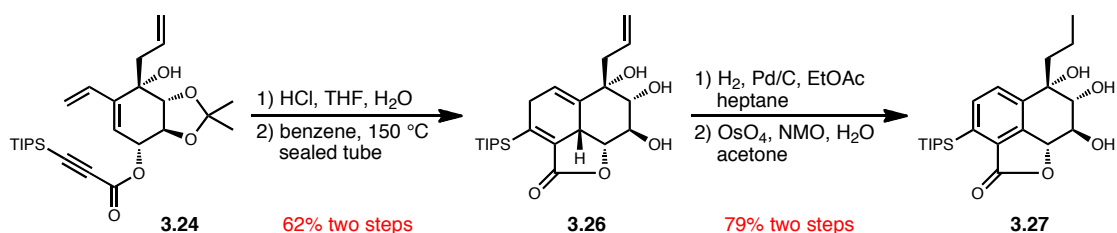


glucopyranoside (**3.16**), we arrived at the primary iodide **3.17** which was treated with zinc dust with sonication to effect Vasella fragmentation to the intermediate aldehyde. The aldehyde reacted in situ with allylzinc bromide to afford the homoallylic alcohol **3.18** in good yield.<sup>5</sup> The four step sequence of alcohol oxidation, terminal olefin isomerization, ring closing metathesis, and enone  $\alpha$ -iodination arrived at the iodo-enone **3.19**.<sup>6</sup> Installation of the diene through a Suzuki cross coupling reaction then led to a key substrate **3.21** for three-carbon unit addition. Unfortunately, our best results came with allyl Grignard with concomitant benzoate deprotection to provide the tertiary alcohol **3.22** as a 2:1 mixture of inseparable diastereomers in relatively low yield. Despite this disappointing result, the mixture of diastereomers was subjected to esterification with the propargylic acid **3.23** which led to separable diastereomers of **3.24**, of which the desired was carried forward. Again, we encountered only disappointment when all attempts at IMDA cyclization failed to afford the decalin **3.25**. It was reasoned that the locked conformation of **3.24** imparted by the acetonide protecting group led to poor orbital overlap, and thus the free diol was targeted as a potential solution to the problem.



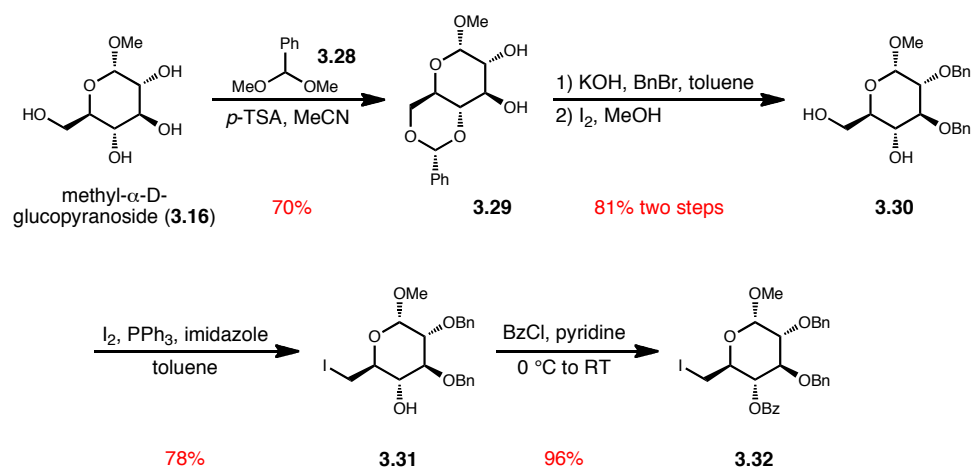
**Scheme 3.6.** Engers' early approach toward the AB-decalin.

To test the potential adverse conformational effects of the acetonide in the IMDA, the acetonide group was removed with aqueous acid, and gratifyingly, Diels-Alder cyclization occurred smoothly at 150 °C in a sealed tube to provide the bicyclic product **3.26**. Next, we needed to install the necessary hydroxy-ketone functionality at the trisubstituted olefin; however, first, regioselective terminal olefin hydrogenation was effected in 30 minutes with an atmosphere of hydrogen and palladium on carbon. Finally, attempted trisubstituted olefin dihydroxylation was met with unexpected results, favoring the aromatized product **3.27** over the desired diol. Therefore, we were forced to rethink our approach to the AB-decalin **2.54**, centering on protecting group strategy and the nature of our dienophile, which as an alkyne led to a delicate product ripe for aromatization.



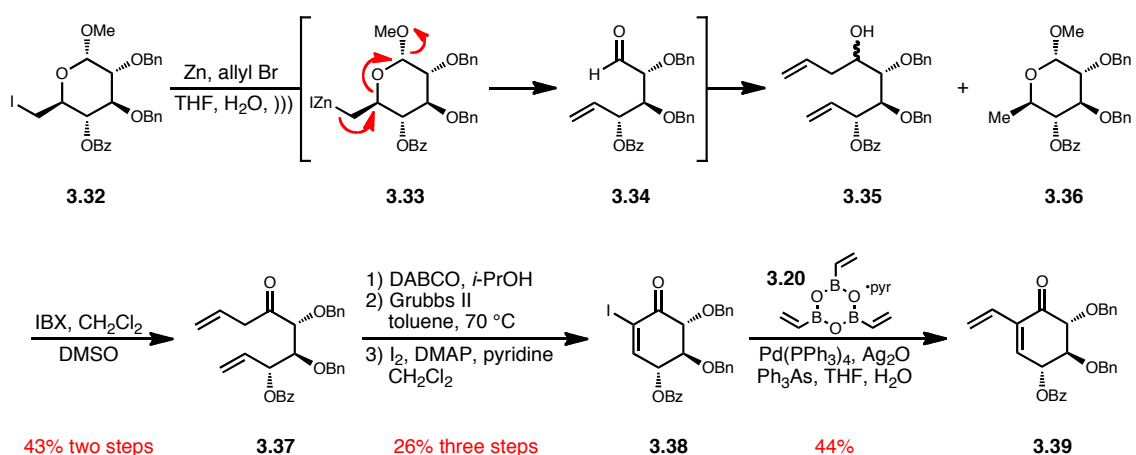
**Scheme 3.7.** IMDA followed by attempted hydroxy-ketone installation.

Toward the end of his tenure, Dr. Engers contributed a highly effective route to large quantities of the benzyl-protected glucose derivative **3.32**, which was available in five steps from methyl- $\alpha$ -D-glucopyranoside (**3.16**) as reported by Liotta and co-workers.<sup>7</sup> Thus, regioselective benzylidene acetal formation was followed by benzylation of the remaining secondary alcohols and in situ HI formation effected acetal removal to provide **3.30**. Primary alcohol iodination was finally followed by benzoate protection of the remaining secondary alcohol yielding **3.32** in high yields throughout the entire sequence. This route reliably provided greater than 60 grams per single batch; however, the necessity for flash column chromatographic purification of each step on large scale proved highly cumbersome. Nevertheless, access to stockpiles of advanced material allowed for effective large scale throughput to later synthetic stages.



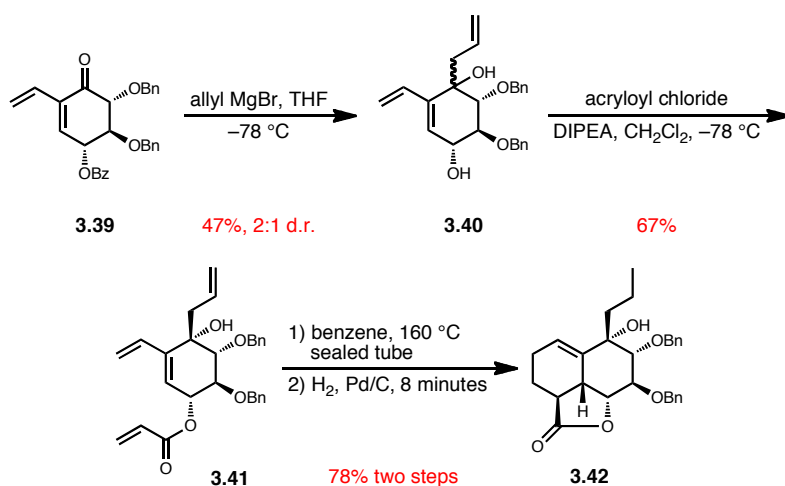
**Scheme 3.8.** Synthesis of the benzyl-glucopyranoside series.

Following precedent set with the acetonide series, Vasella fragmentation and in situ addition of allylzinc bromide to the intermediate aldehyde **3.34** led to the homoallylic alcohol **3.35** with quantities of the protonated methyl byproduct **3.36** detected by NMR as an inseparable mixture with the desired product. Oxidation of the inconsequential mixture of diastereomers provided the ketone **3.37**, and although a yield was not determined for the formation of the impurity **3.36**, it likely significantly contributed to the low two-step yield of **3.37**. The previously developed three-step sequence to iodo-enone **3.19** involving olefin transposition, ring closing metathesis, and  $\alpha$ -iodination was utilized to arrive at **3.38** in low yield. Suzuki cross coupling with the cyclic vinyl-boronate **3.20** again occurred in less than desirable yield to nevertheless arrive at the dienone **3.39**.



**Scheme 3.9.** Engers' route to the benzyl-protected dienone.

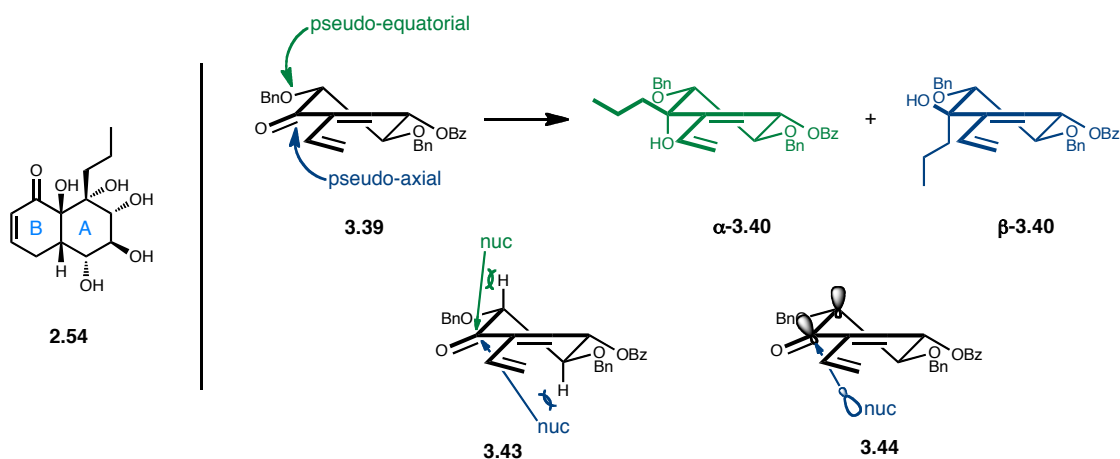
Despite low yields leading to the dienone **3.39**, we forged ahead with the previously established allyl Grignard addition to form the C-13 tertiary alcohol with concomitant benzoate deprotection to arrive at the inseparable mixture of diastereomers of **3.40**. Esterification with acryloyl chloride afforded the IMDA precursor **3.41** at which point the undesired diastereomer became chromatographically separable. We were pleased to observe clean cycloaddition to the decalin product upon heating in benzene at 160 °C in a sealed tube, and regioselective terminal olefin hydrogenation led to **3.42** in high yields. This application of the IMDA perfectly highlights the enabling nature of such a simple transformation, where the key C-9 ring juncture stereochemistry was set in a predictable and specific manner.



**Scheme 3.10.** Engers' acrylate IMDA toward the decalinic enone.

An analysis of the key tertiary alcohol-forming step with allyl Grignard, which remained the weak point in our sequence toward Diels-Alder product **3.42**, indicated the delicate balance of steric and electronic effects at play and the overriding substrate control in the diastereoselectivity. First, based on the relative stereochemistry found in **2.54** and considering the conformation of the dienone **3.39**, a pseudo-equatorial attack on the ketone is necessary. When analyzing the facial addition based on the Burgi-Dunitz angle, the pseudo-axial attack suffers from a detrimental 1,3-diaxial interaction with the axial hydrogen, whereas the pseudo-equatorial addition encounters an unfavorable Gauche interaction, both shown in **3.43**. These effects manifest in varying levels based on the size of the nucleophile. Additionally, while axial attack to cyclohexanones is favored, this preference increases when compared to cyclohexenones because of a large change in internal dihedral angle, from  $51^\circ$  to  $22^\circ$ , that exacerbates the aforementioned Gauche interaction.<sup>8</sup> One other stereoselecting factor involves the Cieplak effect, shown in **3.44** which exhibits a stabilizing effect on the forming  $\sigma^*$ -orbital from the adjacent C-H  $\sigma$ -

orbital through hyperconjugation.<sup>9</sup> Ultimately, the equatorial versus axial orientation of the nucleophilic unit in the products  **$\alpha$ -3.40** and  **$\beta$ -3.40** respectively also play into the final stereoselectivity of the reaction, and all of these factors affect the observed low diastereoselectivity of the allyl addition to **3.39** slightly favoring the desired pseudo-equatorial addition. Finally, further evidence for strong substrate control included attempted Schaus allylation with an allyl borane-BINOL complex that led to high yields but exclusively the undesired diastereomer.<sup>10</sup>

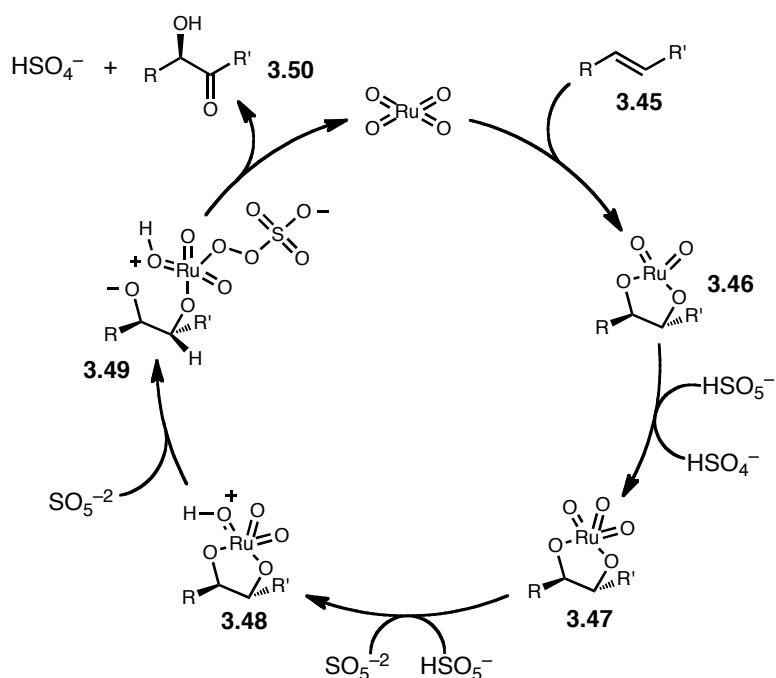


**Scheme 3.11.** Stereochemical effects in the nucleophilic addition.

With the trisubstituted olefin in **3.42**, significant experimentation was required to determine the best conditions for hydroxy-ketone installation. It was proposed that the stereochemistry of the resulting tertiary alcohol should be set by substrate control, where oxidation of the olefin would occur from the convex face of the molecule. Attempts included dihydroxylation, as in Scheme 3.7, as well as epoxidation; however, our most successful results came by treatment with in situ generated  $\text{RuO}_4$  in the presence of

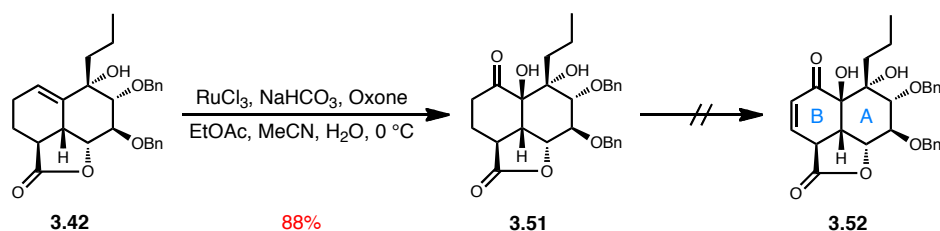
excess Oxone. Initially reported by Plietker, the method takes advantage of the mechanistic pathway innate to OsO<sub>4</sub> dihydroxylation.<sup>11</sup> In the same manner that OsO<sub>4</sub> undergoes a [3+2]-addition to olefins to form an osmate ester, RuO<sub>4</sub> forms the ruthenate ester **3.46**. With excess Oxone present, the ruthenate ester is oxidized by Oxone to Ru(VIII)-complex **3.47**. At this point in the OsO<sub>4</sub>-mediated dihydroxylation mechanism, water serves to break down the osmate ester to the requisite diol; however, with excess Oxone and a low volume of water present, the Ru(VIII)-ester preferentially reacts with the oxidant following protonation to reach the intermediate **3.49**, which effects substrate oxidation to the hydroxy-ketone **3.50** and regenerating RuO<sub>4</sub>. With symmetrical olefinic substrates, regioselectivity does not present an issue, but when R and R' are not equal, regioselectivity is at least partly governed by substituent electronics, in which the hydroxyl-functionality is directed toward electron withdrawing groups.<sup>12</sup>





**Scheme 3.12.** Mechanism of RuO<sub>4</sub>-mediated ketohydroxylation.

Thus, ketohydroxylation of the trisubstituted olefin **3.42** successfully installed the necessary α-hydroxy-ketone to provide **3.51** with complete stereoselectivity for the convex-face addition. In addition, keeping in mind the regioselectivity observed for ruthenate ester opening by Oxone as shown in Scheme 3.12, formation of the tertiary alcohol is favored at lower temperatures. This method proved highly successful in providing rapid generation of two functionalities present in hibarimicinone with stereoselectivity for the bridgehead tertiary alcohol. Unfortunately, all attempts at installing the necessary enone failed, likely due to the small reaction scales resulting from difficulties with material throughput. Therefore, we returned to our synthetic strategy in hopes of improving our ability to arrive at a related enone precursor to **3.51** in higher overall yield.



**Scheme 3.13.** Failed enone installation approach.

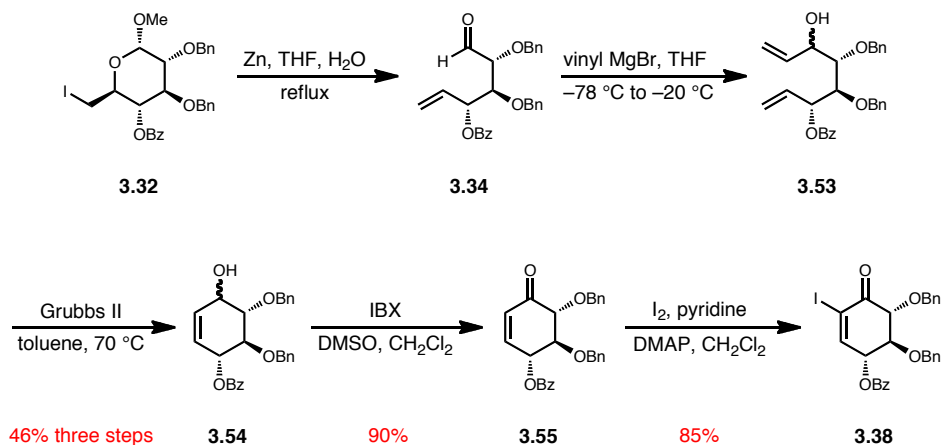
### An Improved Route to the AB-Enone Precursor

We originally identified four major points of necessary improvement in our approach to the AB-decalin **2.54**. The five-step sequence from the functionalized glucose **3.32** to iodo-enone **3.38** proved problematic in yield and the formation of inseparable impurities. Next, the Suzuki cross coupling to install the required diene functionality remained low yielding and appeared ripe for optimization. Although the limiting step in our sequence remained the C-13 tertiary alcohol formation, we saw few options left following Engers' extensive investigation, and we thus settled for moving quantities of material through this step, where we could reliably isolate and functionalize the resulting product. Finally, while keeping in mind difficulties encountered with enone formation from **3.51**, we sought to incorporate functionality that would facilitate enone installation outside of the realm of traditional enone-generating reactions.

Therefore, inspired by reports of direct vinyl additions to Vasella products, we moved to modify this procedure to allow large-scale transformation.<sup>13</sup> The previously developed in situ allylzincation was hampered by scale limitations with sonication, and thus we developed a procedure that utilized refluxing the primary iodide **3.32** in the

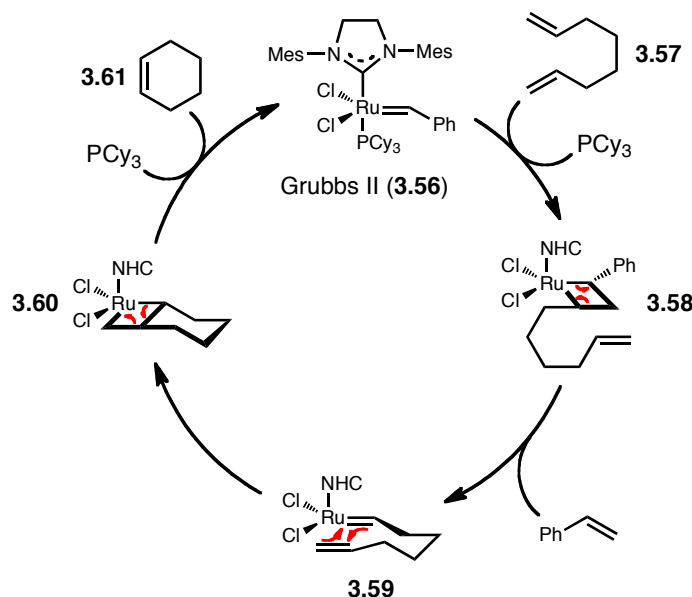
presence of zinc dust to effect Vasella fragmentation to the linear aldehyde **3.34**. Instead of utilizing in situ nucleophilic addition to the intermediate aldehyde, we elected for quick isolation and immediate reaction with vinylmagnesium bromide at  $-78\text{ }^{\circ}\text{C}$  to arrive at the inconsequential mixture of allylic alcohol diastereomers **3.53**, and satisfactorily, minimal formation of the methyl impurity **3.36** was observed.

Ring closing metathesis of **3.53** occurred readily with both diastereomers to provide the cyclic allylic alcohol **3.54**, and it became apparent that the allylic alcohol was a superior substrate for the necessary reaction when compared to the  $\alpha,\beta$ -unsaturated ketone in Scheme 3.9. This effect should not be surprising when considering work by Hoyer and co-workers that showed preferential reaction of allylic alcohols in the ring closing metathesis manifold by presumed pre-association or ligand exchange of the catalyst with the alcohol substituent.<sup>14</sup> Therefore, the two lowest yielding steps in the previous sequence, Vasella fragmentation/nucleophilic addition and ring closing metathesis, were improved to an overall three step yield of 46%. Subsequent IBX oxidation and  $\alpha$ -iodination provided the desired iodo-enone **3.38** in high yield.



**Scheme 3.14.** Improved route to the iodo-enone.

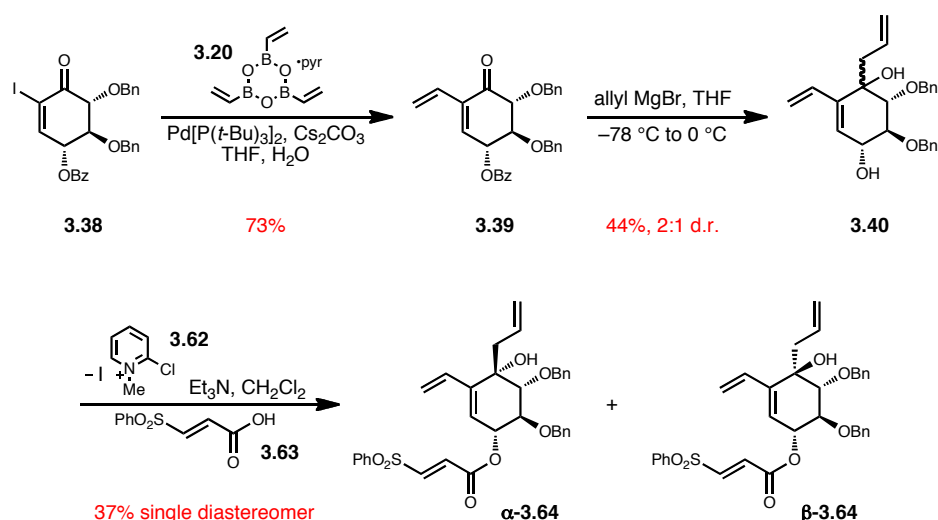
Ring closing metathesis has revolutionized organic chemistry in the past two decades, and the three major players in its development, Schrock, Grubbs, and Chauvin were awarded the Nobel Prize in Chemistry for 2005. For synthetic chemists, it has enabled ring formation where few robust methods existed previously, and mechanistically it draws on the electronic properties of the transition metal catalysts molybdenum and most commonly ruthenium. While the molybdenum catalysts suffer from high sensitivity to air and water, Grubbs' first generation catalyst,  $(\text{PCy}_3)_2\text{RuCl}_2\text{CHPh}$ , exhibits excellent stability, and the incorporation of an imidazole-derived N-heterocyclic carbene in Grubbs' second generation catalyst (**3.56**) further improved the reactivity.<sup>15</sup> The cycle shown in Scheme 3.15 illustrates the ring closing metathesis of the ideal 1,7-octadiene substrate (**3.57**), which first undergoes a [2+2]-cyclization with the ruthenium alkylidene to form the four-membered ruthenium intermediate **3.58** which decomposes through a pericyclic process to the substrate-derived ruthenium alkylidene **3.59**. Association and cycloaddition with the remaining terminal olefin provides the bicyclic intermediate **3.60**, which finally undergoes pericyclic decomposition and ligand exchange to regenerate a form of the catalyst and provide the cyclohexene (**3.61**). The efficiency, high compatibility with many functional groups, and versatility makes the ring closing metathesis reaction a highly important reaction in the repertoire of the synthetic organic chemist.



**Scheme 3.15.** Catalytic cycle for ring closing metathesis.

With the newly improved synthesis of iodo-enone **3.38**, we set forth to optimize reaction conditions for installation of the terminal diene for the IMDA reaction. Original conditions developed by Engers involved the use of tetrakis(triphenylphosphine) palladium(0) with triphenylarsine and silver(I) oxide in a mixture of THF and water. Additionally, the cyclic boronate-pyridine complex **3.20** provided a stable source of three equivalents of vinyl boronic acid.<sup>16</sup> The modest 44% yield of **3.39** was gratifyingly improved to 73% when changing to Fu's catalyst, palladium bis(tri-*t*-butylphosphine), with cesium carbonate in a mixture of THF and water, and this procedure could be effectively scaled to multi-gram reactions with only minor drop in yield.<sup>17,18</sup> From **3.39**, we decided to move forward through the allyl addition step to form **3.40**, which occurred in 44% yield as a 2:1 mixture of inseparable diastereomers.

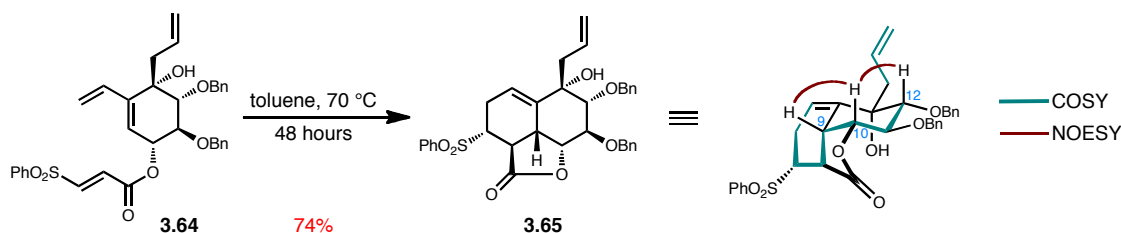
At this point, in contrast to the acrylate dienophile utilized previously by Engers, we elected to utilize the 3-phenylsulfonylacrylic ester, in which the phenylsulfone substituent would provide a leaving group for easy enone formation. Therefore, esterification with 3-phenylsulfonylacrylic acid (**3.63**) under Mukaiyama's conditions effectively formed the desired IMDA precursor  **$\alpha$ -3.64**, at which point the undesired diastereomer  **$\beta$ -3.64** became chromatographically separable.<sup>19,20</sup>



**Scheme 3.16.** Improved synthesis of a modified IMDA substrate.

We finally arrived at the proposed IMDA precursor **3.64** as a single diastereomer in an improved 8 steps from iodide **3.32**, and we reasoned that not only would the phenylsulfone functionality play an important role in enone formation but also in the IMDA reaction. As described in Figure 2.1, addition of an electron withdrawing group to the dienophile has the effect of lowering the dienophile LUMO and thus should improve the reactivity. And we were excited to observe clean cycloaddition to the desired decalin

**3.65** by heating in toluene at 70 °C for 2 days. Extensive 1D and 2D NMR spectroscopy allowed structure assignment, and two key NOESY correlations between C-9/C-10 and C-10/C-12 confirmed the desired stereochemistry at the bridgehead C-9 hydrogen. Importantly, the correct C-9 stereochemistry validated the IMDA approach toward the decalin, and we next targeted enone **3.52**.

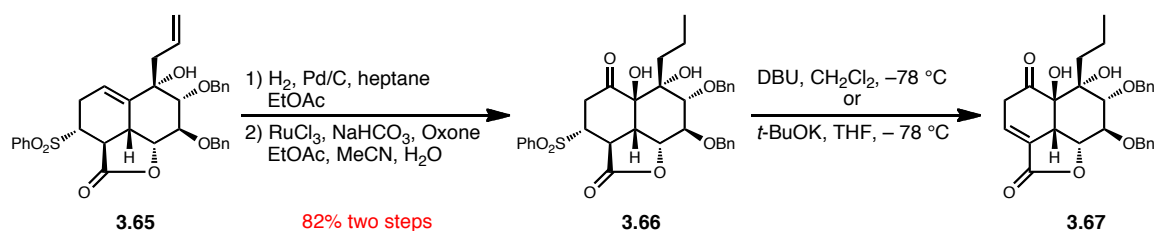


**Scheme 3.17.** Key IMDA toward the AB-decalin.

Analogous to Engers' approach to the enone, we first performed regioselective hydrogenation on the terminal olefin which required only 30 minutes before over-reduction began to occur at the trisubstituted olefin. Subsequent ketohydroxylation successfully provided the key substrate **3.66**; however, attempts at purification with a variety of solid phases led only to decomposition. Despite this fact, the reaction proceeded cleanly enough to compare  $^1\text{H}$  NMR spectra with the previously synthesized acrylate IMDA analog **3.51** to confirm that the reaction had again occurred with complete stereoselectivity for the correct C-14 orientation.

Finally, we had arrived at an enone precursor that only required base-mediated elimination of the sulfone. Unfortunately, treatment of **3.66** initially with DBU and later with varying bases such as potassium *tert*-butoxide at low temperature led exclusively to

the undesired olefin regioisomer **3.67**. This product was easily assigned by  $^1\text{H}$  NMR due to the difference in the number and splitting patterns of olefinic protons of the two possible products. We reasoned that the undesired product formation may be a result of altered  $\text{pK}_\text{a}$ 's arising from ring strain in the lactone, and retrospectively, this regioisomer could be expected to be the thermodynamic product as effected by the *cis*-ring fusion and observed by Ziegler and co-workers in their efforts toward forskolin.<sup>21</sup> We thus moved to relieve this ring strain by opening the lactone functionality.

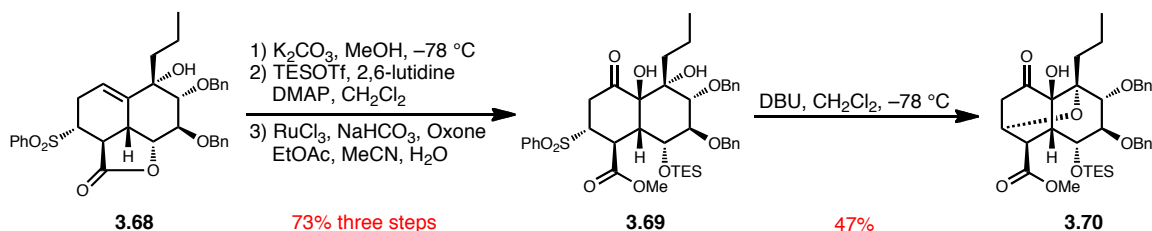


**Scheme 3.18.** Failed sulfone elimination to the AB-enone.

Through a straightforward sequence, lactone opening with  $\text{K}_2\text{CO}_3$  in methanol led to the methyl ester and free secondary alcohol which was silyl protected and subjected to ketohydroxylation conditions to arrive at the fully functionalized enone precursor **3.69**. Again, because of the sensitivity of the sulfone moiety, this product was unstable to chromatographic purification; however, we utilized the relatively clean crude material for base-mediate enone formation. Treatment of **3.69** with DBU at low temperature formed a highly unexpected product, which we ultimately identified as the caged ether **3.70**. This compound presumably arose by enone formation and subsequent Michael addition of the C-13 tertiary alcohol. We were unable to suppress this secondary reaction, and because

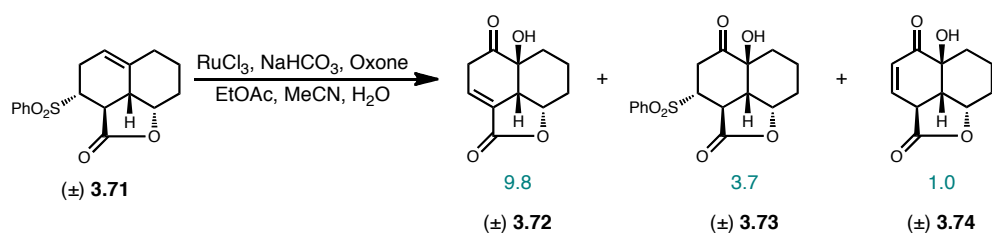


**3.70** was isolated as a single diastereomer, no absolute determination regarding the regioselectivity of elimination could be made.



**Scheme 3.19.** An unexpected etherification of an enone intermediate.

Due to our difficulty arriving at meaningful quantities of enone precursors **3.66** and **3.69** but considering our interest in probing the elimination regioselectivity, we quickly synthesized the reported IMDA product **3.71** which perfectly suited our needs for an elimination model system.<sup>22</sup> The racemic **3.71** contained all of our necessary functionality without the extraneous oxygenation, and we attempted ketohydroxylation with the intent of studying the subsequent base-mediated elimination regioselectivity. Interestingly, based on analysis of a  $^1H$  NMR mixture of products, we determined that our desired product **3.73** was highly labile to the ketohydroxylation conditions and provided a mixture of predominantly the undesired olefin regioisomer **3.72**. When taken in consideration with results leading to the formation of **3.67**, this lends further support the concept that the  $\alpha,\beta$ -unsaturated lactone is the thermodynamic product. Ultimately because we were unable to isolate pure **3.73** without in situ elimination, this system was of little use for our purposes.

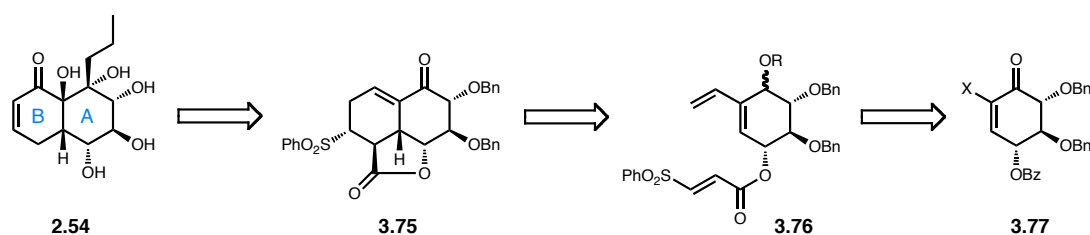


**Scheme 3.20.** A sulfone elimination model system.

These three major results proved disconcerting and caused a complete rethinking of our synthetic strategy. However, we were also concurrently attempting a tangential reworking of a substrate for C-13 tertiary alcohol formation that we hoped would impress strong substrate control toward the desired stereochemical orientation and improve the remaining limiting step in material throughput for our synthetic route.

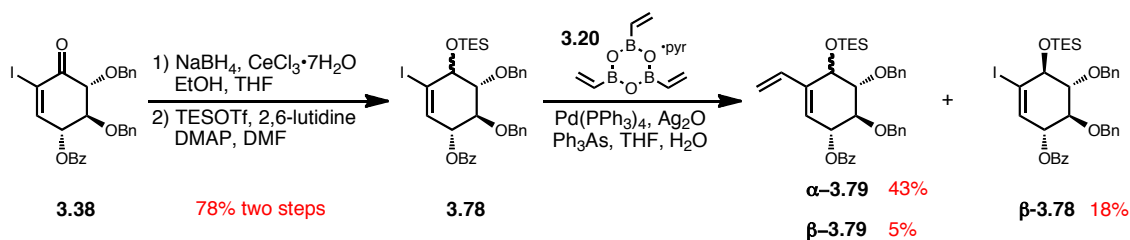
### Toward a Substrate-Controlled Tertiary Alcohol Formation

In our work toward the enone **3.52**, tertiary alcohol formation presented the remaining complication for producing quantities of an enone precursor for extensive enone formation studies. Therefore, we devised a synthetic route that would diverge from a previously synthesized intermediate and would install the C-13 propyl unit in high yield and stereoselectivity. This approach hinged upon using the *cis*-decalin substrate conformation to direct the face of nucleophilic addition to a decalinic ketone **3.75**, which would be assembled in analogy to our previous work and would diverge from **3.77**, where X could equal H, I, or vinyl as previously synthesized.



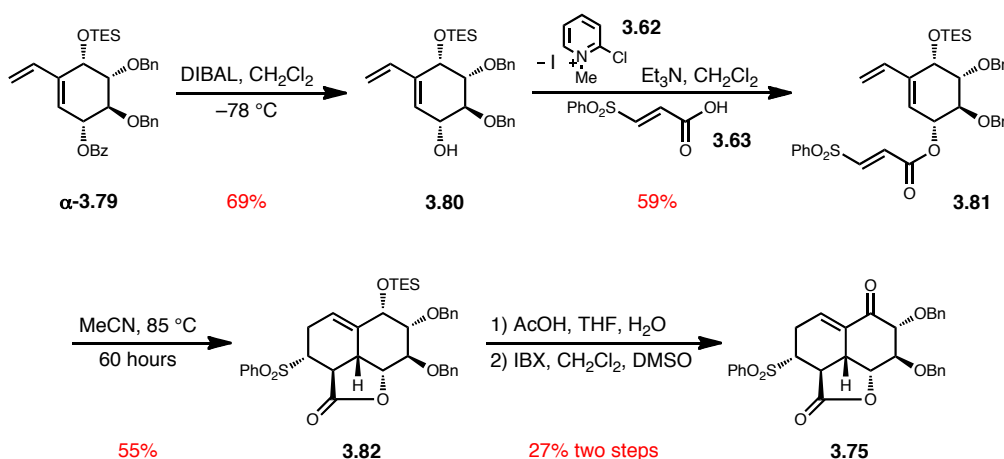
**Scheme 3.21.** Synthetic strategy for a substrate controlled propyl addition.

We believed that the C-13 ketone in **3.38** would require masking for the sequence of reactions necessary to arrive at **3.75**, and thus we targeted the series of enones previously synthesized as substrates for reduction and protection. We initially attempted Luche reduction on our most advanced amenable intermediate, dienone **3.39**, however primary attempts with  $\text{NaBH}_4$ ,  $\text{CeCl}_3 \cdot 7\text{H}_2\text{O}$ , and MeOH failed to deliver the desired allylic alcohol likely caused by the starting material's insolubility in methanol.<sup>23</sup> Changing the reaction solvent to a 1:1 mixture of ethanol and THF provided the desired product, albeit in low yield. Finally, we met success when taking a step back and utilizing Luche conditions on the iodo-enone **3.38**, where we arrived at a diastereomeric mixture of allylic alcohols in 86% yield.<sup>24</sup>



**Scheme 3.22.** Encountered difficulties with a modified Suzuki coupling substrate.

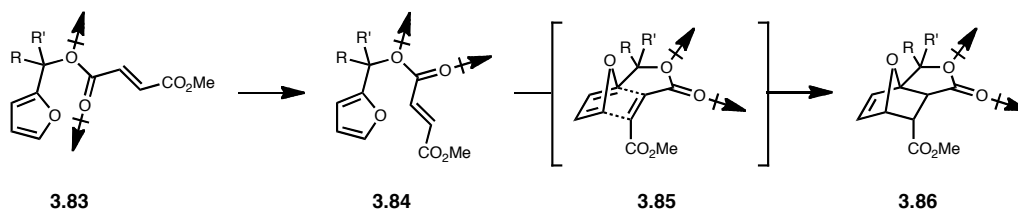
Silyl protection of the allylic alcohol mixture cleanly provided **3.78** which we subjected to our standard Suzuki cross coupling conditions. Interestingly, the two diastereomers exhibited differential reactivity, and we isolated primarily the  $\alpha$ -OTES product **3.79** with larger amounts of unreacted  $\beta$ -OTES starting material **3.78**. Despite attempts to improve this reactivity with other conditions, we resorted to carrying forward only  $\alpha$ -**3.79**, and even resubjection of  $\beta$ -**3.78** to the reaction conditions never provided greater than 50% conversion to product. Unfortunately, our ability to reliably produce large amounts of vinyl iodide **3.78** became overshadowed by the unexpected problems encountered with relying on a mixture of diastereomers through our proposed sequence of reactions.



**Scheme 3.23.** Synthesis of the proposed decalinic enone **3.75**.

Moving forward with the single diastereomer **3.79** in spite of our Suzuki cross coupling complications, the benzoate protecting group was effectively removed with DIBAL at low temperature and was followed by esterification as previously developed to

arrive at the desired IMDA precursor **3.81**. When considering the optimal solvent for this cycloaddition, we turned to work by Jung and Gervay regarding the reactive rotamer effect as seen in the IMDA in Scheme 3.24.<sup>25</sup>



**Scheme 3.24.** The reactive rotamer effect in the IMDA.

For the prototype IMDA of the furan diene with the methyl fumarate dienophile **3.83**, various substitutions at the R and R' locations failed to produce a significant effect on the rate of the IMDA reaction, as was proposed based on the *gem*-dialkyl effect. The original postulate involving the *gem*-dialkyl effect relied upon Thorpe-Ingold bond angle compression and a resultant lower entropy of activation. However, ultimately the reactive rotamer effect and activation enthalpy lowering explained the observed results. Thus, the most stable *s-trans* conformation **3.83** is expected to be the predominant conformation in solution, whereas the higher energy *s-cis* conformation **3.84** must be accessible for the IMDA to occur. This conformation results in a highly polar transition state **3.85** as shown with the indicated dipole moments, and thus the reactive rotamer effect for IMDAs involving an ester-linked diene and dienophile can be exploited by stabilization of the transition state with polar solvents. Indeed, in the system shown in Scheme 3.24, a significant rate enhancement was observed when changing from toluene to acetonitrile and even greater with DMSO. Therefore, we chose acetonitrile as an optimal solvent for

the desired IMDA, and we successfully arrived at the decalin **3.82** in reasonable yield by heating **3.81** in refluxing acetonitrile for 60 hours.

We had finally arrived at our proposed Diels-Alder product **3.82** as shown in Scheme 3.23; however, serious complications remained regarding material throughput with the Suzuki cross coupling reaction. We successfully found deprotection conditions for the TES-ether involving treatment with acetic acid and THF and water, and the allylic alcohol was oxidized in mediocre yield with IBX. Ultimately, the limited amounts of material past the IMDA reaction never allowed for full characterization of the free allylic alcohol or ketone **3.75**, and we never produced enough **3.75** to reasonably probe its reactivity and the resulting stereoselectivity of a 1,2-nucleophilic addition. We had effectively managed to trade one significant problem for another, as is often too much of a reality in complex molecule total synthesis, and we again had to reimagine our synthetic strategy to account for our previous results.

## Conclusion

Our proposed two-directional annulation strategy toward HMP-Y1 and hibarimicinone aimed to allow straightforward manipulation of each biaryl atropisomer for ultimate assignment of the natural product axial chirality. While we could reliably produce the racemic biaryl core **3.2** and perform chiral chromatographic separation, preliminary studies indicated low yielding bis-annulation reactions. Additionally, multiple routes were devised to arrive at the proposed decalinic enone **2.54**; however, we consistently encountered problems at varying points in the synthetic sequences. First,

traditional enone installation attempts with the hydroxy-ketone **3.51** failed, and two substrates with a sulfone leaving group led only to unexpected and undesired products. Finally, our attempt to improve the limiting propyl unit-appending step led to problems earlier in the route which rendered the sequence useless. These results taken together pointed to the need for a complete overhaul of our approach to HMP-Y1 and hibarimicinone that would subvert issues encountered in the crux of the two-directional strategy.

## Experimental Methods

**General Procedure.** All non-aqueous reactions were performed under an argon atmosphere in flame-dried glassware. Stainless steel syringes or cannula were used to transfer air- and moisture-sensitive liquids. Reaction temperatures were controlled using a thermocouple thermometer and analog hotplate stirrer. Reactions were conducted at room temperature (RT, approximately 23 °C) unless otherwise noted. Analytical thin-layer chromatography was performed on E. Merck pre-coated silica gel 60 F254 plates and visualized using UV, ceric ammonium molybdate (CAM) and potassium permanganate (KMnO<sub>4</sub>) stains. Flash column chromatography was conducted as described by Still *et. al.* using indicated solvents and Dynamic Adsorbents silica gel 60 (230-240 mesh).<sup>26</sup> Where necessary, silica gel was neutralized by treatment of the silica gel prior to chromatography with the eluent containing 1% triethylamine (Et<sub>3</sub>N). Where necessary, silica gel was treated prior to chromatography with the eluent containing 1%

glacial acetic acid (AcOH). Yields were reported as isolated, spectroscopically pure compounds.

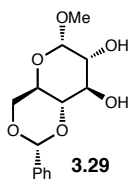
**Materials.** Reagents were purchased at the highest commercial quality and used without further purification unless otherwise stated. When necessary, intermediates were dried by azeotropic removal of water by evaporation from benzene (three iterations) and further dried on high-vacuum for the indicated amount of time. Toluene and dichloromethane ( $\text{CH}_2\text{Cl}_2$ ) were obtained by passing commercially available solvents through activated alumina columns (MBraun MB-SPS solvent system). Tetrahydrofuran (THF) was purified by distillation from sodium metal with benzophenone indicator, and when necessary, was further dried over activated 4 Å molecular sieves under an atmosphere of argon. Triethylamine ( $\text{Et}_3\text{N}$ ) was distilled from calcium hydride and stored over sodium hydroxide. The molarity of commercial *n*-butyllithium solutions was determined by titration using diphenylacetic acid as an indicator (average of three determinations).

**Instrumentation.** Optical rotations were obtained using a Perkin Elmer 341 polarimeter and zeroed with the pure solvent, spectrophotometric-grade chloroform.  $^1\text{H}$  NMR spectra were recorded on Bruker 300, 400, 500, or 600 MHz spectrometers and are reported relative to deuterated solvent signals ( $\text{CDCl}_3$ : 7.26;  $\text{C}_6\text{D}_6$ : 7.16). Data for  $^1\text{H}$  NMR spectra are reported as follows: chemical shift ( $\delta$  ppm), multiplicity (s = singlet, d = doublet, t = triplet, q = quartet, p = pentet, sept. = septet, m = multiplet, br = broad, app = apparent), coupling constants (Hz), and integration.  $^{13}\text{C}$  NMR spectra were recorded at 100, 125, or 150 MHz and are reported relative to deuterated solvent signals ( $\text{CDCl}_3$ :

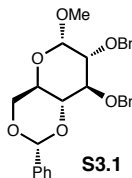


77.0; C<sub>6</sub>D<sub>6</sub>: 128.1). Infrared spectra were obtained as thin films on NaCl plates using a Thermo Electron IR100 series instrument and are reported in terms of frequency of absorption (cm<sup>-1</sup>). High-resolution mass spectra were obtained from the Department of Chemistry and Biochemistry, University of Notre Dame using either a JEOL AX505HA or JEOL LMS-GCmate mass spectrometer.

### Preparative Procedures

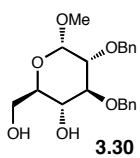


Methyl- $\alpha$ ,D-glucopyranoside (40.0 g, 206 mmol, 1.0 eq) was dissolved in acetonitrile (1.00 L), and to the solution was added benzaldehyde dimethyl acetal (40.2 mL, 268 mmol, 1.3 eq) and camphorsulphonic acid (1.91 g, 8.24 mmol, 0.04 eq) and the reaction was stirred at RT for 18 h. Triethylamine (20.0 mL) was added and stirred for one hour, and the reaction mixture was concentrated to a slurry and purified by flash column chromatography (25% then 90% EtOAc/hexanes) yielded **3.29** as a white solid (40.5 g, 143 mmol, 70%). Spectral data were consistent with reported literature values.<sup>27</sup>

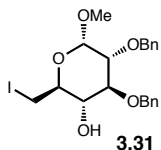


A solution of **3.29** (36.9 g, 131 mmol, 1 eq), KOH (50.6 g, 902 mmol, 6.9 eq), and benzyl bromide (108 mL, 902 mmol, 6.9 eq) in toluene (470 mL) was heated at reflux for 2.5 h. At RT toluene (750 mL) was added and the mixture was washed with H<sub>2</sub>O (2 x 750 mL) and evaporated to an oil. The oil was twice dissolved in toluene (300 mL) and evaporated to dryness. Purification by flash column

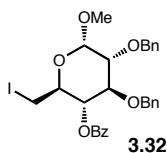
chromatography (11:1, 10:1, and 9:1 hexanes/acetone) yielded **S3.1** as a white solid (50.8 g, 110 mmol, 84%). Spectral data were consistent with reported literature values.<sup>7</sup>



A solution of **S3.1** (68.2 g, 147 mmol, 1 eq) and I<sub>2</sub> (13.9 g, 54.6 mmol, 0.37 eq) in methanol (1.50 L) was heated at reflux for 6 h. At RT, 10% aqueous Na<sub>2</sub>S<sub>2</sub>O<sub>3</sub> was added (400 mL) and the mixture was evaporated to an oil. The oil was dissolved in water (500 mL) and extracted with CH<sub>2</sub>Cl<sub>2</sub> (3 x 600 mL), and the organic layers were combined, dried (MgSO<sub>4</sub>), filtered and concentrated. Purification by flash column chromatography (20%, 40% and 60% acetone/hexanes) provided **3.30** as a white solid (46.1 g, 123 mmol, 83%). Spectral data were consistent with reported literature values.<sup>7</sup>

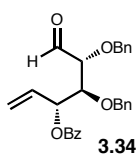


To a solution of **3.30** (43.6 g, 116 mmol, 1.0 eq) in toluene (1.19 L), I<sub>2</sub> (44.3 g, 175 mmol, 1.5 eq), triphenylphosphine (42.8 g, 163 mmol, 1.4 eq), and imidazole (23.8 g, 349 mmol, 3.0 eq) were added and the reaction was heated at 50 °C for 2.5 h. At RT methanol (900 mL) was added and the mixture was concentrated to an oil. The mixture was diluted with 10% aqueous Na<sub>2</sub>S<sub>2</sub>O<sub>3</sub> (350 mL) and extracted with CH<sub>2</sub>Cl<sub>2</sub> (3 x 350 mL). The organic layers were combined, dried (MgSO<sub>4</sub>), filtered and concentrated to a yellow oil. Purification by flash column chromatography (5%, 8% and 11% acetone/hexanes) resulted in **3.31** as a clear oil (54.7 g, 129 mmol, 97%). Spectral data were consistent with reported literature values.<sup>7</sup>



To a solution of **3.31** (54.1 g, 112 mmol, 1.0 eq) in pyridine (1.12 L) at 0 °C was added benzoyl chloride (30.8 mL, 265 mmol, 2.4 eq) dropwise, followed by removal of the ice bath after 30 min and the reaction was

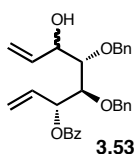
stirred at RT for 18 h. The reaction was poured over ice (2000 mL) and extracted with CH<sub>2</sub>Cl<sub>2</sub> (3 x 1.0 L). The combined organic layers were washed with ice cold 6 M aqueous HCl (4 x 1.0 L), saturated aqueous NaHCO<sub>3</sub> (1 x 1.0 L) and water (4 x 1.2 L). The organic layer was dried (MgSO<sub>4</sub>), filtered and concentrated. The crude material was purified by flash chromatography (5-15% acetone/hexanes) to yield **3.32** as a white solid (63.3 g, 108 mmol, 96%). Spectral data were consistent with reported literature values.<sup>7</sup>



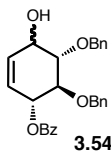
A solution of **3.32** (15.0 g, 25.5 mmol, 1.0 eq) and zinc dust (33.3 g, 510 mmol, 20 eq) in THF/H<sub>2</sub>O (4:1, 1.02 L) was heated at reflux. After 2 h the reaction was removed from heating, and once at RT the mixture was filtered

through a plug of celite and THF was removed in vacuo. The remaining aqueous solution was diluted with EtOAc/H<sub>2</sub>O (3:1, 400 mL), separated and the aqueous layer extracted with EtOAc (3 x 300 mL). The combined organic layers were dried (MgSO<sub>4</sub>), filtered and concentrated to provide crude **3.34** as a yellow oil. Material was immediately taken forward crude, except for characterization purposes. <sup>1</sup>H NMR (400 MHz, CDCl<sub>3</sub>): δ 9.69 (d, *J* = 1.1 Hz, 1H), 8.01 (d, *J* = 7.7 Hz, 2H), 7.57 (t, *J* = 7.7 Hz, 1H), 7.44 (t, *J* = 7.7, 2H), 7.38-7.31 (m, 5H), 7.29-7.20 (m, 5H), 5.97-5.85 (m, 2H), 5.39 (d, *J* = 16.4 Hz, 1H), 5.28 (d, *J* = 10.3 Hz, 1H), 4.74 (d, *J* = 11.8 Hz, 1H), 4.71 (d, *J* = 11.3 Hz, 1H), 4.62 (d, *J* = 11.3 Hz, 1H), 4.56 (d, *J* = 11.8 Hz, 1H), 4.05 (dd, *J* = 5.6, 4.2 Hz, 1H), 3.96 (dd, *J* = 4.1, 1.2 Hz, 1H); <sup>13</sup>C NMR (CDCl<sub>3</sub>, 100 MHz): δ 202.4, 165.1, 137.2, 136.7, 133.2,

132.6, 129.7, 128.6, 128.5, 128.4 (2C), 128.3, 128.2, 128.0, 119.3, 82.4, 80.4, 74.5, 74.2, 73.4; IR (film)  $\nu_{\text{max}}$  3064, 3032, 2870, 1724, 1268  $\text{cm}^{-1}$ ; HRMS (ESI)  $m/z$  calcd. for  $\text{C}_{27}\text{H}_{26}\text{NaO}_5$   $[\text{M}+\text{Na}]^+$  453.1672, found 453.1661.

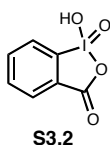


A crude solution of **3.34** in THF (644 mL) was cooled to  $-78\text{ }^{\circ}\text{C}$  and vinyl magnesium bromide (1M in THF, 80.6 mL, 80.6 mmol, 2.5 eq) was added dropwise. The  $-78\text{ }^{\circ}\text{C}$  bath was allowed to warm to  $-20\text{ }^{\circ}\text{C}$  over 3 h, and to the reaction was added saturated aqueous  $\text{NH}_4\text{Cl}$  (500 mL). The  $-20\text{ }^{\circ}\text{C}$  bath was removed and once at RT the mixture was diluted with EtOAc/ $\text{H}_2\text{O}$  (4:1, 500 mL). The aqueous layer was extracted with EtOAc (3 x 375 mL), and the combined organic layers were dried ( $\text{MgSO}_4$ ), filtered and concentrated to provide **3.53** as a yellow oil. The mixture of crude diastereomers was taken forward without further purification.

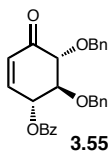


A solution of crude **3.53** (13.5 g, 29.5 mmol, 1.0 eq) and Grubbs second generation catalyst (750 mg, 0.884 mmol, 0.03 eq) in toluene (589 mL) was heated at  $70\text{ }^{\circ}\text{C}$ . After 24 h the reaction was removed from heating, and at RT the mixture was filtered through a plug of silica with EtOAc washes, and the filtrate was concentrated. The crude residue was purified by column chromatography (5-25% EtOAc/hexanes) to yield **3.54** as a light brown solid (5.09 g, 11.8 mmol, 46% three steps) as a 1.3:1 mixture of diastereomers. MP:  $75\text{--}77\text{ }^{\circ}\text{C}$ ;  $^1\text{H}$  NMR (400 MHz,  $\text{CDCl}_3$ ): major diastereomer  $\delta$  8.01-7.98 (m, 2H), 7.58 (dt,  $J = 7.2, 0.4\text{ Hz}$ , 1H), 7.43 (dt,  $J = 8.0, 0.8\text{ Hz}$ , 2H), 7.37-7.32 (m, 5H), 7.25-7.23 (m, 2H), 7.22-7.19 (m, 3H), 5.84-5.80 (m, 2H), 5.72-5.67 (m, 1H), 5.00 (d,  $J = 11.6\text{ Hz}$ , 1H), 4.85 (d,  $J = 11.2\text{ Hz}$ , 1H), 4.78 (d,  $J = 11.2\text{ Hz}$ , 1H).

1H), 4.73 (dd,  $J = 12.0, 2.8$  Hz, 1H), 4.40-4.36 (m, 1H), 3.97 (dd,  $J = 9.6, 7.2$  Hz, 1H), 3.73-3.67 (m, 1H), 2.29 (d,  $J = 4.8$  Hz, 1H); minor diastereomer  $\delta$  8.01-7.98 (m, 2H), 7.58 (dt,  $J = 7.2, 0.4$  Hz, 1H), 7.43 (dt,  $J = 8.0, 0.8$  Hz, 2H), 7.37-7.32 (m, 5H), 7.25-7.23 (m, 2H), 7.22-7.19 (m, 3H), 5.96 (ddd,  $J = 10.0, 4.4, 1.6$  Hz, 1H), 5.84-5.80 (m, 1H), 5.72-5.67 (m, 1H), 4.85 (d,  $J = 11.2$  Hz, 2H), 4.78 (d,  $J = 11.2$  Hz, 1H), 4.73 (dd,  $J = 12.0, 2.8$  Hz, 1H), 4.40-4.36 (m, 1H), 4.15 (dd,  $J = 9.6, 7.2$  Hz, 1H), 3.73-3.67 (m, 1H), 2.78 (d,  $J = 3.6$  Hz, 1H); IR (film)  $\nu_{\max}$  3451, 3063, 3032, 2880, 1717  $\text{cm}^{-1}$ ; HRMS (ESI)  $m/z$  calcd. for  $\text{C}_{27}\text{H}_{26}\text{NaO}_5$   $[\text{M}+\text{Na}]^+$  453.1672, found 453.1635.

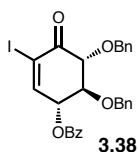


To a 1 L 3-necked flask with a mechanical stirrer attached open to the air was added 2-iodobenzoic acid (25.0 g, 101 mmol, 1.0 eq) and tap water (325 mL). The suspension was slowly stirred and Oxone (89.9 g, 146 mmol, 1.5 eq) was added. The reaction was heated in an oil bath to 89 °C (internal temperature 70-73 °C) then heated for 3 h with vigorous stirring. Stirring was stopped and the reaction was removed from heating. At RT, the reaction was cooled to 0 °C and allowed to sit for 1 h. The reaction precipitated a white solid, which was collected by filtration, and the solid was washed with  $\text{H}_2\text{O}$  (6 x 50 mL) and acetone (3 x 50 mL). The reaction yielded 2-iodoxybenzoic acid (**S3.2**) as a free-flowing white crystalline solid (22.0 g, 78.5 mmol, 78%). Spectral data were consistent with reported literature values.<sup>28</sup>



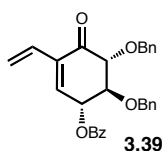
A solution of **3.54** (4.26 g, 9.90 mmol, 1.0 eq) in  $\text{CH}_2\text{Cl}_2/\text{DMSO}$  (98.0 mL, 1:1) was cooled to 0 °C, at which point 2-iodoxybenzoic acid (4.16 g, 14.8 mmol, 1.5 eq) was added and stirred for 15 min followed by removal of the ice

bath and stirring at RT. After 12 h, the mixture was diluted with CH<sub>2</sub>Cl<sub>2</sub>/H<sub>2</sub>O (500 mL, 1:1). The aqueous layer was extracted with CH<sub>2</sub>Cl<sub>2</sub> (3 x 250 mL), and the combined organic layers were washed with H<sub>2</sub>O (2 x 300 mL). The organic layer was dried (MgSO<sub>4</sub>), filtered and concentrated to a clear oil. Purification by flash column chromatography (5-20% EtOAc/hexanes) gave **3.55** as a white solid (3.69 g, 8.61 mmol, 87%). MP: 63-66 °C;  $[\alpha]_D^{20}$  -198 (*c* 0.36, CHCl<sub>3</sub>); <sup>1</sup>H NMR (400 MHz, CDCl<sub>3</sub>): δ 7.97 (dd, *J* = 8.4, 1.6 Hz, 2H), 7.60 (dt, *J* = 7.2, 1.2 Hz, 1H), 7.47-7.43 (m, 4H), 7.37-7.30 (m, 3H), 7.18-7.14 (m, 5H), 6.78 (dd, *J* = 10.4, 2.4 Hz, 1H), 6.15 (dd, *J* = 10.4, 2.4 Hz, 1H), 6.00 (dt, *J* = 8.4, 2.4 Hz, 1H), 5.12 (d, *J* = 11.2 Hz, 1H), 4.89 (d, *J* = 11.2 Hz, 1H), 4.80 (d, *J* = 11.2 Hz, 1H), 4.74 (d, *J* = 11.2 Hz, 1H), 4.21 (d, *J* = 10.4 Hz, 1H), 4.14 (dd, *J* = 10.8, 8.4 Hz, 1H); <sup>13</sup>C NMR (CDCl<sub>3</sub>, 100 MHz): δ 196.8, 165.6, 145.5, 137.5 (2C), 133.5, 129.8, 129.2, 129.1, 128.5, 128.4, 128.3, 128.2 (2C), 127.9, 127.7, 83.7, 81.8, 75.2, 74.6, 73.0; IR (film) ν<sub>max</sub> 3088, 3063, 3032, 2916, 2873, 1723, 1699 cm<sup>-1</sup>; HRMS (FAB+) *m/z* calcd. for C<sub>27</sub>H<sub>23</sub>O<sub>5</sub> [M+H]<sup>+</sup> 427.1545, found 427.1534.



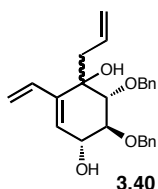
To a solution of **3.55** (4.29 g, 10.0 mmol, 1.0 eq) in CH<sub>2</sub>Cl<sub>2</sub> (92.4 mL) was added pyridine (46.2 mL) and DMAP (4.00 mg, 0.033 mmol, 0.0033 eq) and the solution was cooled to 0 °C. To the cooled solution was added I<sub>2</sub> (6.35 g, 25.0 mmol, 2.5 eq) in CH<sub>2</sub>Cl<sub>2</sub>/pyridine (61.6 mL, 1:1) slowly by cannula. The reaction was stirred at 0 °C for 30 min and the ice bath was removed. After 18 h stirring at RT, the solution was added to 1:1 Et<sub>2</sub>O/H<sub>2</sub>O (600 mL) and the organic layer was washed with 10% aqueous HCl (3 x 250 mL), H<sub>2</sub>O (1 x 250 mL), 10% aqueous Na<sub>2</sub>S<sub>2</sub>O<sub>3</sub> (3 x 250 mL) and brine (2 x 250 mL), then dried (MgSO<sub>4</sub>), filtered and concentrated. Purification by

flash column chromatography (5-30% EtOAc/hexanes) provided **3.38** as a yellow solid (4.70 g, 8.48 mmol, 85%). MP: 120-122 °C;  $[\alpha]_D^{20}$  -108 (*c* 0.19, CHCl<sub>3</sub>); <sup>1</sup>H NMR (400 MHz, CDCl<sub>3</sub>): δ 7.95 (dd, *J* = 8.4, 1.2 Hz, 2H), 7.61 (dt, *J* = 7.2, 0.8 Hz, 1H), 7.54 (d, *J* = 2.4 Hz, 1H), 7.47-7.43 (m, 4H), 7.37-7.32 (m, 3H), 7.19-7.14 (m, 5H), 5.89 (dd, *J* = 8.4, 2.4 Hz, 1H), 5.12 (d, *J* = 11.2 Hz, 1H), 4.88 (d, *J* = 11.6 Hz, 1H), 4.77 (d, *J* = 11.2 Hz, 1H), 4.73 (d, *J* = 11.6 Hz, 1H), 4.27 (d, *J* = 10.4 Hz, 1H), 4.14 (dd, *J* = 10.8, 8.4 Hz, 1H); <sup>13</sup>C NMR (100 MHz, CDCl<sub>3</sub>): δ 191.4, 165.5, 153.3, 137.3, 137.1, 133.7, 129.9, 128.8, 128.5 (2C), 128.4, 128.3, 128.2, 128.1, 127.9, 103.5, 82.1, 80.9, 75.2, 75.7, 74.0; IR (film)  $\nu_{\max}$  2929, 1726, 1707, 1450, 1313, 1251 cm<sup>-1</sup>; HRMS (ESI) *m/z* calcd. for C<sub>27</sub>H<sub>24</sub>IO<sub>5</sub> [M+H]<sup>+</sup> 555.0663, found 555.0638.

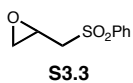


To a solution of **3.38** (4.00 g, 7.22 mmol, 1.0 eq) in THF/H<sub>2</sub>O (144 mL, 2:1) was added Cs<sub>2</sub>CO<sub>3</sub> (3.53 g, 10.8 mmol, 1.5 eq) and 2,4,6-trivinyl-1,3,5,2,4,6-trioxatriborinane•pyridine (**3.20**, 1.31 g, 5.41 mmol, 0.75 eq), and the mixture was degassed (3x) with liquid N<sub>2</sub>. To the flask was added Pd[P(*t*-Bu)<sub>3</sub>]<sub>2</sub> (369 mg, 0.722 mmol, 0.10 eq) and the reaction was stirred at RT. After 4 h, the mixture was diluted with EtOAc (500 mL) and washed with brine (2 x 500 mL). The combined aqueous layers were extracted with EtOAc (1 x 500 mL), and the combined organic layers were dried (MgSO<sub>4</sub>), filtered and concentrated to a brown oil. Immediate purification by flash column chromatography (5% and 10% EtOAc/hexanes) gave **3.39** as a white solid (1.90 g, 4.18 mmol, 58%). MP: 52-56 °C;  $[\alpha]_D^{20}$  -54.4 (*c* 0.31, CHCl<sub>3</sub>); <sup>1</sup>H NMR (500 MHz, CDCl<sub>3</sub>): δ 7.98 (dd, *J* = 8.0, 1.0 Hz, 2H), 7.61 (app. t, *J* = 7.0 Hz, 1H), 7.48-7.44 (m, 4H), 7.39-7.30 (m, 3H), 7.20-7.14 (m, 5H), 6.73 (d, *J* = 2.5 Hz, 1H), 6.50

(dd,  $J = 17.5, 11$  Hz, 1H), 6.04 (dd,  $J = 8.5, 2.0$  Hz, 1H), 5.83 (d,  $J = 18.0$  Hz, 1H), 5.35 (d,  $J = 11.5$  Hz, 1H), 5.12 (d,  $J = 11.5$  Hz, 1H), 4.91 (d, 11.5 Hz, 1H), 4.79 (d,  $J = 11.5$  Hz, 1H), 4.75 (d,  $J = 11.5$  Hz, 1H), 4.23 (d,  $J = 10.5$  Hz, 1H), 4.13 (dd,  $J = 10.5, 8.0$  Hz, 1H);  $^{13}\text{C}$  NMR (125 MHz,  $\text{CDCl}_3$ ):  $\delta$  195.7, 165.7, 139.0, 137.6, 136.0, 133.5, 129.9, 129.3, 129.1, 128.5, 128.4, 128.3, 128.2 (2C), 127.9, 127.7, 119.3, 84.1, 81.3, 75.1, 74.5, 72.9; IR (film)  $\nu_{\text{max}}$  3063, 3031, 2911, 1721, 1697  $\text{cm}^{-1}$ ; HRMS (ESI)  $m/z$  calcd. for  $\text{C}_{29}\text{H}_{26}\text{NaO}_5$   $[\text{M}+\text{Na}]^+$  477.1672, found 477.1645.



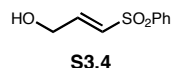
To a solution of **3.39** (1.90 g, 4.18 mmol, 1.0 eq) in THF (209 mL) at  $-78$   $^{\circ}\text{C}$  was added allyl magnesium chloride (2 M in THF, 6.27 mL, 12.5 mmol, 3.0 eq) dropwise. The  $-78$   $^{\circ}\text{C}$  bath was replaced after 3 h with an ice bath, and the reaction was stirred at  $0$   $^{\circ}\text{C}$  for 1.5 h. To the mixture was added saturated aqueous  $\text{NH}_4\text{Cl}$  (200 mL) and the ice bath was removed. At RT the mixture was extracted with EtOAc (3 x 400 mL), and the combined organic layers were dried ( $\text{MgSO}_4$ ), filtered and concentrated. Purification by flash column chromatography (5-30% EtOAc/hexanes) yielded **3.40** as a clear oil (727.0 mg, 1.852 mmol, 44%) in a 2:1 mixture of inseparable diastereomers. IR (film)  $\nu_{\text{max}}$  3400, 3064, 3030, 2910, 1110  $\text{cm}^{-1}$ ; HRMS (ESI)  $m/z$  calcd. for  $\text{C}_{25}\text{H}_{29}\text{O}_4$   $[\text{M}+\text{H}]^+$  393.2060, found 393.2069.



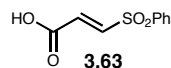
To a solution of allyl phenyl sulfone (5.00 mL, 32.6 mmol, 1.0 eq) in DCE (25 mL) was added *m*-CPBA (11.3 g, 65.3 mmol, 2.0 eq) and the reaction was heated at reflux for 2.5 h. At  $0$   $^{\circ}\text{C}$ , which caused the reaction to solidify, 10% aqueous  $\text{Na}_2\text{S}_2\text{O}_3$  (100 mL) and  $\text{CH}_2\text{Cl}_2$  were added and the mixture was extracted with



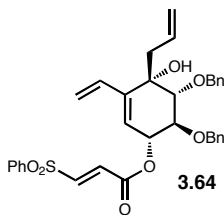
CH<sub>2</sub>Cl<sub>2</sub> (3 x 75 mL). The combined organic layers were washed with saturated aqueous NaHCO<sub>3</sub> (1 x 50 mL), and the aqueous layer was extracted with CH<sub>2</sub>Cl<sub>2</sub> (3 x 50 mL). The combined organic layers were dried (MgSO<sub>4</sub>), filtered, and concentrated. Purification by flash column chromatography (33% EtOAc/hexanes) provided **S3.3** as a clear oil (5.78 g, 29.2 mmol, 89%). Spectral data were consistent with reported literature values.<sup>19</sup>



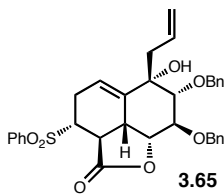
To a solution of **S3.3** (5.78 g, 29.2 mmol, 1.0 eq) in CH<sub>2</sub>Cl<sub>2</sub> (35 mL) at –10 °C was added a solution of DBU (4.44 g, 29.2 mmol, 1.0 eq) in CH<sub>2</sub>Cl<sub>2</sub> (18 mL) via syringe pump over 3 h while remaining at –10 °C. The reaction became a thick solid slurry, and at 0 °C, 20% aqueous HCl (50 mL) was added and the thick mixture was extracted with CHCl<sub>3</sub> (5 x 25 mL). The combined organic layers were dried (MgSO<sub>4</sub>), filtered, and concentrated. Material was taken to the next step crude.



To a solution of crude **S3.4** (4.43 g, 22.3 mmol, 1.0 eq) in acetone (175 mL) was added Jones' reagent [prepared by addition of concentrated H<sub>2</sub>SO<sub>4</sub> (3.9 mL) to CrO<sub>3</sub> (3.35 g, 33.5 mmol, 1.5 eq) then at 0 °C addition of H<sub>2</sub>O (11 mL)] dropwise until the reaction remained orange/brown for 15 min. To the reaction was added *i*-PrOH until the reaction turned green, and the mixture was filtered through a plug of celite with EtOAc washes. The filtrate was concentrated, and the white solid (containing green liquid) was recrystallized from toluene (green liquid was removed by pipette once all material solubilized) to yield **3.63** as a white solid (2.40 g, 11.3 mmol, 51%). Spectral data were consistent with reported literature values.<sup>19</sup>

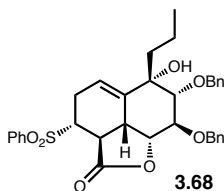


To a solution of **3.40** (727 mg, 1.85 mmol, 1.0 eq) in CH<sub>2</sub>Cl<sub>2</sub> (41.0 mL) was added (*E*)-3-(phenylsulfonyl)acrylic acid (**3.63**, 393 mg, 1.85 mmol, 1.0 eq) and 2-chloro-1-methylpyridinium iodide (**3.62**, 710 mg, 2.78 mmol, 1.5 eq) and the mixture was heated to reflux. To the reaction was added Et<sub>3</sub>N (774 μL, 5.56 mmol, 3.0 eq) by syringe pump over 1 h followed by refluxing for an additional 30 min. The flask was removed from heating, and at RT the mixture was added to saturated aqueous NaHCO<sub>3</sub> (200 mL) and the biphasic mixture was extracted with CH<sub>2</sub>Cl<sub>2</sub> (3 x 200 mL). The organic layers were washed with saturated aqueous NH<sub>4</sub>Cl (2 x 200 mL), dried (MgSO<sub>4</sub>), filtered and concentrated. Purification by flash column chromatography (5-30% EtOAc/hexanes) yielded **3.64** as a clear oil (400 mg, 0.682 mmol, 37%), the undesired diastereomer was separated and discarded.  $[\alpha]_{\text{D}}^{20}$  -63.8 (*c* 0.16, CHCl<sub>3</sub>); <sup>1</sup>H NMR (400 MHz, CDCl<sub>3</sub>): δ 7.91 (dd, *J* = 8.4, 1.2 Hz, 2H), 7.70 (app. t, *J* = 7.6 Hz, 1H), 7.59 (app. t, *J* = 8.0 Hz, 2H), 7.40-7.32 (m, 7H), 7.22-7.19 (m, 3H), 6.66 (d, *J* = 15.2 Hz, 1H), 6.36 (dd, *J* = 17.6, 11.2 Hz, 1H), 5.61 (d, *J* = 1.6 Hz, 1H), 5.54-5.47 (m, 2H), 5.46-5.38 (m, 1H), 5.19 (d, *J* = 11.2 Hz, 1H), 5.07-4.95 (m, 4H), 4.81 (d, *J* = 11.6 Hz, 1H), 4.70 (d, *J* = 10.8 Hz, 1H), 4.61 (d, *J* = 11.6 Hz, 1H), 3.97 (dd, *J* = 9.6, 8.0 Hz, 1H), 3.65 (d, *J* = 10.0, 1H), 2.94 (s, 1H), 2.60 (dd, *J* = 14.0, 5.2 Hz, 1H), 2.47 (dd, *J* = 14.0, 9.2 Hz, 1H); <sup>13</sup>C NMR (125 MHz, CDCl<sub>3</sub>): δ 163.0, 143.6, 140.8, 138.4, 137.9, 137.7, 134.4, 133.3, 132.8, 130.4, 129.6, 128.6, 128.5, 128.3, 128.1, 128.0 (2C), 123.2, 119.3, 117.8, 78.4, 78.3, 75.6, 74.9 (3C), 41.5, 29.7; IR (film) ν<sub>max</sub> 3529, 3064, 3032, 2922, 2853, 1729 cm<sup>-1</sup>; HRMS (ESI) *m/z* calcd. for C<sub>34</sub>H<sub>35</sub>O<sub>7</sub>S [M+H]<sup>+</sup> 587.2098, found 587.2072.



A solution of **3.64** (400 mg, 0.682 mmol, 1.0 eq) in toluene (40 mL) was heated at 70 °C. After 46 h, the solution was removed from heating, and at RT was concentrated. Purification by flash column

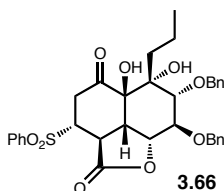
chromatography (10-50% EtOAc/hexanes) gave **3.65** as a clear oil (298 mg, 0.508 mmol, 74%).  $[\alpha]_D^{20}$  -14.7 (*c* 0.27, CHCl<sub>3</sub>); <sup>1</sup>H NMR (400 MHz, CDCl<sub>3</sub>): δ 7.79 (dd, *J* = 8.4, 1.2 Hz, 2H), 7.63 (app. t, *J* = 7.2 Hz, 1H), 7.49 (app. t, *J* = 8.0 Hz, 2H), 7.40-7.28 (m, 10H), 5.88 (m, 1H), 5.74 (dddd, *J* = 17.2, 10.4, 7.2, 7.2 Hz, 1H), 5.09-5.01 (m, 2H), 4.78 (d, *J* = 11.6 Hz, 1H), 4.75 (dd, *J* = 7.6, 1.2 Hz, 1H), 4.61 (d, *J* = 10.2 Hz, 1H), 4.59 (d, *J* = 10.6 Hz, 1H), 4.55 (d, *J* = 11.6 Hz, 1H), 3.86 (dd, *J* = 6.4, 2.8 Hz, 1H), 3.73 (dt, *J* = 9.6, 3.2 Hz, 1H), 3.59 (d, *J* = 3.2 Hz, 1H), 3.03 (ddd, *J* = 17.6, 6.4, 3.2 Hz, 1H), 2.90-2.78 (m, 3H), 2.41 (dddd, *J* = 17.6, 9.2, 2.8, 1.2 Hz, 1H), 2.34 (dd, *J* = 14.4, 7.6 Hz, 1H), 2.24 (dd, *J* = 14.4, 7.2 Hz, 1H); <sup>13</sup>C NMR (100 MHz, CDCl<sub>3</sub>): δ 171.1, 141.3, 137.8, 137.1, 136.8, 133.9, 132.2, 129.1, 128.7, 128.5, 128.2, 128.0, 127.9 (2C), 120.6, 118.5, 84.4, 80.9, 79.9, 74.7, 73.8, 72.5, 58.6, 43.3, 41.4, 40.2, 29.6, 25.1; IR (film)  $\nu_{\max}$  3519, 3064, 3030, 2921, 1790 cm<sup>-1</sup>; HRMS (ESI) *m/z* calcd. for C<sub>34</sub>H<sub>34</sub>NaO<sub>7</sub>S [M+Na]<sup>+</sup> 609.1917, found 609.1935.



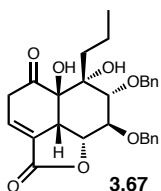
To a solution of **3.65** (298 mg, 0.508 mmol, 1.0 eq) in heptane/EtOAc (36.3 mL, 3:2) under argon atmosphere was added 5% Pd/C (70 mg, 0.14 g/mmol SM) and the reaction mixture was placed

under H<sub>2</sub> atmosphere (balloon). After 20 min, the reaction was filtered through Celite with EtOAc, and the filtrate was concentrated to provide **3.68** as a clear oil requiring no further purification (256 mg, 0.435 mmol, 86%).  $[\alpha]_D^{20}$  -23.3 (*c* 0.27, CHCl<sub>3</sub>); <sup>1</sup>H NMR

(400 MHz, CDCl<sub>3</sub>):  $\delta$  7.78 (dd,  $J$  = 8.4, 1.2 Hz, 2H), 7.63 (app. t,  $J$  = 7.6 Hz, 1H), 7.48 (app. t,  $J$  = 8.0 Hz, 2H), 7.40-7.27 (m, 10H), 5.85 (m, 1H), 4.77 (m, 2H), 4.58 (d,  $J$  = 11.6 Hz, 1H), 4.57 (d,  $J$  = 11.6 Hz, 1H), 4.51 (d,  $J$  = 11.6 Hz, 1H), 3.84 (dd,  $J$  = 6.0, 2.0 Hz, 1H), 3.72 (dt,  $J$  = 9.2, 2.8 Hz, 1H), 3.54 (d,  $J$  = 2.0 Hz, 1H), 3.04 (ddd,  $J$  = 17.6, 6.4, 2.8 Hz, 1H), 2.90-2.78 (m, 2H), 2.75 (s, 1H), 2.40 (dddd, 17.8, 9.7, 2.6, 1.7 Hz, 1H), 1.46-1.40 (m, 2H), 1.27-1.18 (m, 2H), 0.88-0.85 (m, 3H); <sup>13</sup>C NMR (100 MHz, CDCl<sub>3</sub>):  $\delta$  171.3, 141.8, 137.8, 137.2, 136.8, 134.0, 129.1, 128.7, 128.5, 128.3, 128.1, 127.9 (2C), 120.0, 85.3, 81.0, 80.2, 77.2, 75.0, 73.5, 72.2, 58.7, 43.4, 40.4, 38.6, 25.0, 16.6, 14.3; IR (film)  $\nu_{\text{max}}$  3584, 2959, 2360, 1789, 1447, 1306 cm<sup>-1</sup>; HRMS (ESI)  $m/z$  calcd. for C<sub>34</sub>H<sub>36</sub>NaO<sub>7</sub>S [M+Na]<sup>+</sup> 611.2074, found 611.2095.

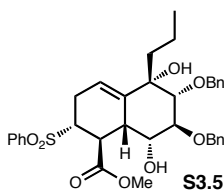


To a solution of EtOAc/CH<sub>3</sub>CN/H<sub>2</sub>O (3.25 mL, 6:6:1) was added NaHCO<sub>3</sub> (2.50 mg, 0.0297 mmol, 2.5 eq), RuCl<sub>3</sub> (0.1 M in H<sub>2</sub>O, 1.19  $\mu$ L, 0.119  $\mu$ mol, 0.01 eq) and Oxone (37.0 mg, 0.0595 mmol, 5.0 eq) and the solution turned yellow. At 0 °C, **3.68** (7.0 mg, 0.0119 mmol, 1.0 eq) was added, and after 10 min, the reaction was filtered through Celite with EtOAc, and the filtrate was washed with 10% aqueous Na<sub>2</sub>S<sub>2</sub>O<sub>3</sub> (2 x 15 mL). The combined organic layers were dried (MgSO<sub>4</sub>), filtered and concentrated to yield crude **3.66** as a clear oil (7.00 mg, 0.0119 mmol, 95%). Attempts at purification resulted in decomposition.



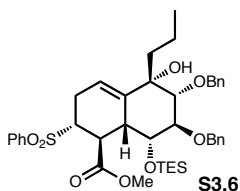
To a solution of **3.66** (7.0 mg, 0.0113 mmol, 1.0 eq) in CH<sub>2</sub>Cl<sub>2</sub> (1.10 mL) at 0 °C was added DBU (1.70  $\mu$ L, 0.0113 mmol, 1.0 eq). After 20 min, the reaction mixture was added to saturated aqueous NH<sub>4</sub>Cl (15 mL) and

extracted with CH<sub>2</sub>Cl<sub>2</sub> (3 x 10 mL). The combined organic layers were washed with saturated aqueous NH<sub>4</sub>Cl (1 x 10 mL), dried (MgSO<sub>4</sub>), filtered and concentrated. Purification by flash column chromatography (5-25% EtOAc/hexanes) provided **3.67**. [ $\alpha$ ]<sub>D</sub><sup>20</sup> -126 (*c* 0.09, CHCl<sub>3</sub>); <sup>1</sup>H NMR (600 MHz, CDCl<sub>3</sub>):  $\delta$  7.40-7.21 (m, 10H), 6.81 (dd, *J* = 7.3, 3.7 Hz, 1H), 5.00 (d, *J* = 10.7 Hz, 1H), 4.97 (d, *J* = 10.9 Hz, 1H), 4.93 (dd, *J* = 8.6, 8.0 Hz, 1H), 4.73 (d, *J* = 11.1 Hz, 1H), 4.59 (d, *J* = 10.5 Hz, 1H), 4.26 (s, 1H), 3.99 (dd, *J* = 9.7, 7.7 Hz, 1H), 3.71 (d, *J* = 9.8 Hz, 1H), 3.59 (ddd, *J* = 22.3, 4.0, 4.0 Hz, 1H), 3.44 (ddd, *J* = 12.3, 3.5, 3.5 Hz, 1H), 3.26 (ddd, *J* = 22.3, 3.2, 3.1 Hz, 1H), 2.10 (s, 1H), 1.66-1.49 (m, 2H), 1.39-1.29 (m, 1H), 1.16-1.06 (m, 1H), 0.80 (dd, *J* = 7.3, 7.3 Hz, 3H); <sup>13</sup>C NMR (150 MHz, CDCl<sub>3</sub>):  $\delta$  208.7, 167.5, 138.0, 137.7, 132.7, 128.5, 128.4, 128.1, 128.0 (2C), 127.7, 127.0, 82.7, 81.7, 81.1, 79.5, 77.9, 76.3, 74.8, 48.6, 41.2, 37.1, 16.8, 14.9; IR (film)  $\nu_{\max}$  3460, 2925, 1766, 1714, 1369, 1086 cm<sup>-1</sup>; HRMS (ESI) *m/z* calcd. for C<sub>28</sub>H<sub>30</sub>NaO<sub>7</sub> [M+Na]<sup>+</sup> 501.1884, found 501.1882.



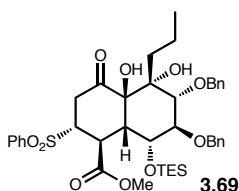
A solution of **3.68** (128 mg, 0.217 mmol, 1.0 eq) in MeOH (22.0 mL) was cooled to -78 °C. To the solution was added K<sub>2</sub>CO<sub>3</sub> (35.0 mg, 0.250 mmol, 1.2 eq) and the reaction was stirred at -78 °C for 15 h. The mixture was added saturated aqueous NaHCO<sub>3</sub> (20 mL), followed by removal from the -78 °C bath. At RT the mixture was diluted with H<sub>2</sub>O (20 mL) and extracted with CH<sub>2</sub>Cl<sub>2</sub> (4 x 30 mL), and the combined organic layers were dried (MgSO<sub>4</sub>), filtered and concentrated to yield **S3.5** as a clear oil (123 mg, 0.197 mmol, 91%) requiring no further purification. [ $\alpha$ ]<sub>D</sub><sup>20</sup> -4.0 (*c* 1.0, CHCl<sub>3</sub>); <sup>1</sup>H NMR (400 MHz, CDCl<sub>3</sub>):  $\delta$  7.78 (dd, *J* = 8.4, 1.2 Hz, 2H), 7.66 (app. t, *J* = 7.6 Hz, 1H), 7.57 (app. t, *J* = 7.6 Hz, 2H), 7.38-7.30 (m,

7H), 7.26-7.19 (m, 3H), 5.97 (d,  $J = 6.4$  Hz, 1H), 4.54 (d,  $J = 12.0$  Hz, 1H), 4.54 (d,  $J = 10.4$ , 1H), 4.49 (d,  $J = 12.0$  Hz, 1H), 4.38 (d,  $J = 10.8$  Hz, 1H), 3.91 (app. t,  $J = 2.8$  Hz, 1H), 3.78 (s, 3H), 3.74 (d,  $J = 11.6$  Hz, 1H), 3.57 (dt,  $J = 12.4$ , 4.8 Hz, 1H), 3.52 (s, 1H), 3.28 (dd,  $J = 12.4$ , 9.6 Hz, 1H), 2.97 (d,  $J = 11.6$  Hz, 1H), 2.87 (d,  $J = 9.2$  Hz, 1H), 2.59 (s, 1H), 2.36 (dt,  $J = 17.2$ , 5.2 Hz, 1H), 2.17 (dt,  $J = 14.0$ , 2.4 Hz, 1H), 1.84 (dt,  $J = 17.2$ , 4.8 Hz, 1H), 1.50 (dt,  $J = 12.0$ , 4.6 Hz, 1H), 1.32-1.23 (m, 1H), 1.21-1.08 (m, 1H), 0.83 (t,  $J = 7.2$  Hz, 3H);  $^{13}\text{C}$  NMR (100 MHz,  $\text{CDCl}_3$ ):  $\delta$  174.2, 137.3, 136.9, 136.3, 135.9, 133.9, 129.2, 129.1, 128.8, 128.7, 128.6, 128.5, 128.0, 127.6, 121.3, 82.5, 74.8, 74.3, 74.0, 72.4, 69.7, 61.6, 52.5, 41.9, 41.2, 38.9, 24.9, 16.2, 14.2; IR (film)  $\nu_{\text{max}}$  3491, 2928, 1737, 1447  $\text{cm}^{-1}$ ; HRMS (ESI)  $m/z$  calcd. for  $\text{C}_{35}\text{H}_{41}\text{O}_8\text{S}$   $[\text{M}+\text{H}]^+$  621.2517, found 621.2480.

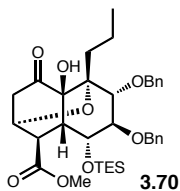


To a solution of **S3.5** (15.0 mg, 0.0242 mmol, 1.0 eq) in DMF (100  $\mu\text{L}$ ) at 0  $^\circ\text{C}$  was added 2,6-lutidine (17.0  $\mu\text{L}$ , 0.145 mmol, 6.0 eq), DMAP (2 mg, catalytic), and TESOTf (22.0  $\mu\text{L}$ , 0.0967 mmol, 4.0 eq), and the reaction was removed from the 0  $^\circ\text{C}$  bath after 1 h. After 18 h at RT, saturated aqueous  $\text{NH}_4\text{Cl}$  (10 mL) was added and the mixture was extracted with  $\text{CH}_2\text{Cl}_2$  (3 x 15 mL). The combined organic layers were washed with  $\text{H}_2\text{O}$  (4 x 20 mL) and brine (1 x 25 mL), then dried ( $\text{MgSO}_4$ ), filtered and concentrated. Purification by flash column chromatography (10-20% EtOAc/hexanes) provided **S3.6** as a light yellow oil (16.0 mg, 0.0218 mmol, 90%).  $[\alpha]_{\text{D}}^{20}$   $-4.4$  (c 0.09,  $\text{CHCl}_3$ );  $^1\text{H}$  NMR (400 MHz,  $\text{CDCl}_3$ ):  $\delta$  7.93 (app. d,  $J = 7.6$  Hz, 2H), 7.66 (app. t,  $J = 7.6$  Hz, 1H), 7.57 (app. t,  $J = 7.6$  Hz, 2H), 7.39-7.22 (m, 10H), 5.93 (d,  $J = 6.8$  Hz, 1H), 4.62 (d,  $J = 11.6$  Hz, 1H), 4.53 (d,  $J = 11.6$  Hz,

1H), 4.49 (d,  $J = 12.0$  Hz, 1H), 4.40 (d,  $J = 12.0$  Hz, 1H), 3.86 (br. s, 1H), 3.78 (s, 3H), 3.68 (t,  $J = 2.8$  Hz, 1H), 3.58 (dt,  $J = 12.0, 4.4$  Hz, 1H), 3.40 (d,  $J = 3.2$  Hz, 1H), 3.18 (s, 1H), 2.92 (dd,  $J = 12.4, 9.2$  Hz, 1H), 2.77 (app. d,  $J = 8.8$  Hz, 1H), 2.42 (dt,  $J = 16.8, 5.2$  Hz, 1H), 2.13 (app. t,  $J = 14.0$  Hz, 1H), 1.94 (dt,  $J = 17.6, 4.4$  Hz, 1H), 1.46 (dt,  $J = 12.0, 4.0$  Hz, 1H), 1.18-0.92 (m, 2H), 0.85-0.79 (m, 12H), 0.53-0.46 (m, 6H);  $^{13}\text{C}$  NMR (100 MHz,  $\text{CDCl}_3$ ):  $\delta$  173.9, 137.6 (2C), 137.1, 136.8, 133.9, 129.5, 129.1, 128.5, 128.3, 128.0 (2C), 127.8, 119.9, 81.0, 79.4, 77.9, 74.4, 73.2, 72.0, 70.8, 61.9, 52.4, 41.8, 41.7, 38.9, 24.8, 16.8, 14.4, 6.8, 4.8; IR (film)  $\nu_{\text{max}}$  3534, 2954, 2912, 2874, 1739, 1455  $\text{cm}^{-1}$ ; HRMS (ESI)  $m/z$  calcd. for  $\text{C}_{41}\text{H}_{54}\text{O}_8\text{NaSSi} [\text{M}+\text{Na}]^+$  757.3206, found 757.3253.

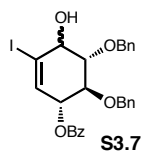


To a solution of EtOAc/ $\text{CH}_3\text{CN}/\text{H}_2\text{O}$  (3.25 mL, 6:6:1) was added  $\text{NaHCO}_3$  (4.00 mg, 0.0476 mmol, 2.5 eq),  $\text{RuCl}_3$  (0.1 M in  $\text{H}_2\text{O}$ , 1.91  $\mu\text{L}$ , 0.191  $\mu\text{mol}$ , 0.01 eq) and Oxone (59.0 mg, 0.0952 mmol, 5.0 eq) and the solution turned yellow. At  $0^\circ\text{C}$ , **S3.6** (14.0 mg, 0.0190 mmol, 1.0 eq) was added. After 10 min the reaction was filtered through Celite with EtOAc, and the filtrate was washed with 10% aqueous  $\text{Na}_2\text{S}_2\text{O}_3$  (2 x 15 mL). The combined organic layers were dried ( $\text{MgSO}_4$ ), filtered and concentrated to yield crude **3.69** as a clear oil (13.0 mg, 0.0170 mmol, 89%). Attempts at purification resulted in decomposition.



To a solution of crude **3.69** (13.0 mg, 0.0170 mmol, 1.0 eq) in  $\text{CH}_2\text{Cl}_2$  (1.7 mL) at RT was added DBU (3.00  $\mu\text{L}$ , 0.0186 mmol, 1.1 eq) and the reaction immediately turned yellow. After 40 min, saturated aqueous  $\text{NH}_4\text{Cl}$  (5 mL) was added and the mixture was extracted with  $\text{CH}_2\text{Cl}_2$  (4 x 10 mL). The

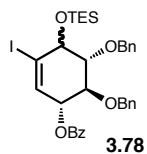
combined organic layers were washed with saturated aqueous  $\text{NH}_4\text{Cl}$  (1 x 25 mL), dried ( $\text{MgSO}_4$ ), filtered and concentrated. Purification by flash column chromatography (5-10% EtOAc/hexanes) provided **3.70** as a clear oil (5.00 mg, 0.00800 mmol, 47%).  $[\alpha]_{\text{D}}^{20}$  -15.3 (*c* 0.15,  $\text{CHCl}_3$ );  $^1\text{H}$  NMR (500 MHz,  $\text{CDCl}_3$ ):  $\delta$  7.36 (app. d,  $J = 7.0$  Hz, 2H), 7.32 (app. t,  $J = 7.0$  Hz, 2H), 7.27-7.18 (m, 6H), 4.97 (d,  $J = 11.5$  Hz, 1H), 4.92 (d,  $J = 11.0$  Hz, 1H), 4.83 (d,  $J = 11.5$  Hz, 1H), 4.60-4.56 (m, 1H), 4.57 (d,  $J = 11.0$  Hz, 1H), 4.30 (dd,  $J = 9.5, 5.0$  Hz, 1H), 3.88 (t,  $J = 9.0$  Hz, 1H), 3.74 (d,  $J = 9.0$  Hz, 1H), 3.69 (s, 3H), 3.61 (s, 1H), 3.59-3.58 (m, 1H), 2.73 (ddd,  $J = 20.0, 3.5, 2.0$  Hz, 1H), 2.58 (dd,  $J = 4.5, 4.0$  Hz, 1H), 2.43 (dd,  $J = 19.5, 1.5$  Hz, 1H), 1.68 (dt,  $J = 14.0, 3.5$  Hz, 1H), 1.50-1.42 (m, 1H), 1.30-1.23 (m, 2H), 0.90 (t,  $J = 8.0$  Hz, 9H), 0.72 (t,  $J = 7.5$  Hz, 3H), 0.59 (q,  $J = 8.0$  Hz, 6H);  $^{13}\text{C}$  NMR (100 MHz,  $\text{CDCl}_3$ ):  $\delta$  208.4, 172.1, 139.0, 138.2, 128.3, 128.2, 128.1, 127.6, 127.2, 127.1, 84.3, 81.3, 79.0, 77.6, 76.2, 75.7, 71.4, 67.6, 52.4, 44.9, 43.0, 40.0, 39.3, 17.9, 14.9, 6.8, 4.8; IR (film)  $\nu_{\text{max}}$  3473, 2955, 2876, 1741, 1455  $\text{cm}^{-1}$ ; HRMS (ESI)  $m/z$  calcd. for  $\text{C}_{35}\text{H}_{48}\text{NaO}_8\text{Si}$   $[\text{M}+\text{Na}]^+$  647.3011, found 647.3032.



To a solution of **3.38** (250 mg, 0.451 mmol, 1.0 eq) in EtOH/THF (9.0 mL, 1:1) was added  $\text{CeCl}_3 \cdot 7\text{H}_2\text{O}$  (336 mg, 0.902 mmol, 2.0 eq) and stirred at RT for 20 min. To the mixture was added  $\text{NaBH}_4$  (17.0 mg, 0.456 mmol, 1.0 eq) and the reaction was stirred at RT. After 45 min saturated aqueous  $\text{NH}_4\text{Cl}$  (100 mL) and  $\text{H}_2\text{O}$  (50 mL) were added and the mixture was extracted with EtOAc (4 x 100 mL). The combined organic layers were dried ( $\text{MgSO}_4$ ), filtered and concentrated. Purification by flash column chromatography (5-15% EtOAc/hexanes) gave **S3.7** as a crystalline white solid (217 mg, 0.390 mmol, 86%) as a 3.8:1 inseparable mixture of diastereomers. MP: 150-

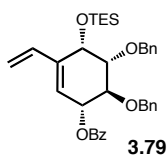


154 °C;  $^1\text{H}$  NMR (400 MHz,  $\text{CDCl}_3$ ): major diastereomer  $\delta$  7.97 (app. dd,  $J = 7.2, 1.2$  Hz, 2H), 7.59 (ddt,  $J = 7.6, 2.8, 1.2$  Hz, 1H), 7.45-7.40 (m, 2H), 7.35-7.32 (m, 5H), 7.26-7.20 (m, 5H), 6.45 (d,  $J = 3.2$  Hz, 1H), 5.53 (ddd,  $J = 6.8, 2.8, 0.4$  Hz, 1H), 4.83 (d,  $J = 11.2$  Hz, 1H), 4.82-4.77 (m, 1H), 4.76 (d,  $J = 11.2$  Hz, 1H), 4.70 (d,  $J = 11.2$  Hz, 1H), 4.44 (t,  $J = 3.6$  Hz, 1H), 4.14 (dd,  $J = 9.2, 6.8$  Hz, 1H), 3.81 (dd,  $J = 9.2, 4.0$  Hz, 1H), 2.90 (d,  $J = 3.6$  Hz, 1H); minor diastereomer  $\delta$  7.97 (app. dd,  $J = 7.2, 1.2$  Hz, 2H), 7.59 (ddt,  $J = 7.6, 2.8, 1.2$  Hz, 1H), 7.45-7.40 (m, 2H), 7.35-7.32 (m, 5H), 7.26-7.20 (m, 5H), 6.46 (dd,  $J = 3.2, 1.6$  Hz, 1H), 5.62 (ddd, 6.4, 3.2, 2.4 Hz, 1H), 4.85 (d,  $J = 7.2$  Hz, 1H), 4.83 (d,  $J = 7.2$  Hz, 1H), 4.82 (d,  $J = 11.6$  Hz, 1H), 4.78 (d,  $J = 11.6$  Hz, 1H), 4.30 (tt,  $J = 6.4, 2.0$  Hz, 1H), 4.01 (dd,  $J = 8.4, 6.0$  Hz, 1H), 3.85 (dd,  $J = 8.4, 6.0$  Hz, 1H), 2.69 (d,  $J = 6.4$  Hz, 1H); IR (film)  $\nu_{\text{max}}$  3543, 3062, 3031, 2924, 2872, 1716, 1452  $\text{cm}^{-1}$ ; HRMS (ESI)  $m/z$  calcd. for  $\text{C}_{27}\text{H}_{25}\text{INaO}_5$   $[\text{M}+\text{Na}]^+$  579.0639, found 579.0649.



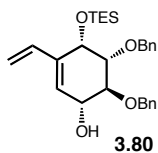
To a solution of **S3.7** (217 mg, 0.390 mmol, 1.0 eq) in DMF (780  $\mu\text{L}$ ) at 0 °C was added DMAP (2 mg, catalytic), 2,6-lutidine (136  $\mu\text{L}$ , 1.17 mmol, 3.0 eq) and TESOTf (176  $\mu\text{L}$ , 0.780 mmol, 2.0 eq) and the reaction stirred at 0 °C and at RT for 18 h. To the reaction was added saturated aqueous  $\text{NH}_4\text{Cl}$  (100 mL) and the mixture was extracted with  $\text{CH}_2\text{Cl}_2$  (3 x 150 mL). The combined organic layers were washed with  $\text{H}_2\text{O}$  (4 x 200 mL) and brine (1 x 250 mL), followed by drying ( $\text{MgSO}_4$ ), filtration and concentration. Purification by flash column chromatography (7.5% EtOAc/hexanes) provided **3.78** as a clear oil (238 mg, 0.355 mmol, 91%) as a 1.9:1 inseparable mixture of diastereomers.  $^1\text{H}$  NMR (400 MHz,  $\text{CDCl}_3$ ): major diastereomer  $\delta$  7.96 (dt,  $J = 7.2, 1.2$  Hz, 2H), 7.57 (app. t,  $J = 7.2$  Hz, 1H), 7.42 (app. dt,  $J = 8.0, 2.4$  Hz, 2H), 7.34-7.29 (m,

5H), 7.23-7.05 (m, 5H), 6.32 (d,  $J = 2.8$  Hz, 1H), 5.49 (dd,  $J = 7.2, 2.8$  Hz, 1H), 4.87-4.67 (m, 4H), 4.49 (d,  $J = 3.2$  Hz, 1H), 4.23 (dd,  $J = 10.0, 7.6$  Hz, 1H), 3.66 (dd,  $J = 10.0, 3.2$  Hz, 1H), 1.03-0.96 (m, 9H), 0.77-0.68 (m, 6H); minor diastereomer  $\delta$  7.96 (dt,  $J = 7.2, 1.2$  Hz, 2H), 7.57 (app. t,  $J = 7.2$  Hz, 1H), 7.42 (app. dt,  $J = 8.0, 2.4$  Hz, 2H), 7.34-7.29 (m, 5H), 7.23-7.05 (m, 5H), 6.40 (app. t,  $J = 2.4$  Hz, 1H), 5.67 (dt,  $J = 7.6, 2.4$  Hz, 1H), 5.07 (d,  $J = 11.6$  Hz, 1H), 4.87-4.67 (m, 3H), 4.40 (dt,  $J = 6.8, 2.4$  Hz, 1H), 3.97 (dd,  $J = 9.6, 7.6$  Hz, 1H), 3.74 (dd,  $J = 9.6, 7.2$  Hz, 1H), 1.03-0.96 (m, 9H), 0.77-0.68 (m, 6H); IR (film)  $\nu_{\text{max}}$  3063, 3031, 2953, 2916, 2875, 1723, 1453  $\text{cm}^{-1}$ ; HRMS (ESI)  $m/z$  calcd. for  $\text{C}_{33}\text{H}_{39}\text{INaO}_5\text{Si} [\text{M}+\text{Na}]^+$  693.1504, found 693.1483.



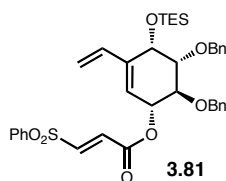
To a solution of **3.78** (690 mg, 1.03 mmol, 1.0 eq) in THF:H<sub>2</sub>O (5.17 mL, 8:1) was added Ag<sub>2</sub>O (381 mg, 1.65 mmol, 1.6 eq), Ph<sub>3</sub>As (19.0 mg, 0.0617 mmol, 0.06 eq) and 2,4,6-trivinyl-1,3,5,2,4,6-trioxatriborinane•pyridine (**3.20**, 187 mg, 0.772 mmol, 0.75 eq). The mixture was degassed with liquid N<sub>2</sub>, then tetrakis (triphenylphosphine) palladium(0) (36.0 mg, 0.0309 mmol, 0.03 eq) was added and the reaction was stirred at RT. After 20 h, the reaction was diluted with EtOAc (200 mL) and washed with brine (2 x 250 mL). The combined organic layers were dried (MgSO<sub>4</sub>), filtered and concentrated, and purification by flash column chromatography (2-15% EtOAc/hexanes) yielded the  $\alpha$ -OTES product (**3.79**, 250 mg, 0.438 mmol, 43%), the unreacted  $\beta$ -OTES SM (**3.78**, 127 mg, 0.189 mmol, 18%) and a minor amount of the  $\beta$ -OTES product (**3.79**, 28.0 mg, 0.0491 mmol, 5%). Major diastereomer ( $\alpha$ -OTES):  $[\alpha]_{\text{D}}^{20} -119$  ( $c$  0.90, CHCl<sub>3</sub>); <sup>1</sup>H NMR (400 MHz, CDCl<sub>3</sub>):  $\delta$  8.00 (dd,  $J = 7.6, 1.6$  Hz, 2H), 7.58 (tt,  $J = 7.6, 1.2$  Hz, 1H), 7.46-7.40 (m, 4H),

7.38-7.31 (m, 3H), 7.27-7.25 (m, 2H), 7.17-7.16 (m, 3H), 6.26 (dd,  $J = 17.6, 10.8$  Hz, 1H), 5.74 (dd,  $J = 7.6, 2.8$  Hz, 1H), 5.70 (d,  $J = 3.2$  Hz, 1H), 5.39 (d,  $J = 17.6$  Hz, 1H), 5.19 (d,  $J = 11.2$  Hz, 1H), 4.92 (d,  $J = 11.6$  Hz, 1H), 4.91 (d,  $J = 11.6$  Hz, 1H), 4.80 (d,  $J = 11.6$  Hz, 1H), 4.78 (d,  $J = 11.6$  Hz, 1H), 4.68 (d,  $J = 2.8$  Hz, 1H), 4.39 (dd,  $J = 10.4, 7.6$  Hz, 1H), 3.55 (dd,  $J = 10.4, 3.2$  Hz, 1H), 0.97 (t,  $J = 8.0$  Hz, 9H), 0.77-0.60 (m, 6H);  $^{13}\text{C}$  NMR (100 MHz,  $\text{CDCl}_3$ ):  $\delta$  166.2, 139.4, 138.5, 138.2, 135.7, 133.0, 130.0, 129.8, 128.3, 128.2 (3C), 128.0, 127.6, 127.4, 126.2, 115.2, 80.3, 78.0, 75.5, 74.7, 74.0, 67.0, 7.1, 5.4; IR (film)  $\nu_{\text{max}}$  3032, 2953, 2875, 1720, 1267  $\text{cm}^{-1}$ ; HRMS (ESI)  $m/z$  calcd. for  $\text{C}_{35}\text{H}_{42}\text{NaO}_5\text{Si}$   $[\text{M}+\text{Na}]^+$  593.2694, found 593.2704. Minor diastereomer ( $\beta$ -OTES):  $^1\text{H}$  NMR (400 MHz,  $\text{CDCl}_3$ ):  $\delta$  8.01 (dd,  $J = 8.4, 1.2$  Hz, 2H), 7.58 (tt,  $J = 7.6, 1.2$  Hz, 1H), 7.43 (t,  $J = 7.6$  Hz, 2H), 7.34-7.31 (m, 5H), 7.16-7.10 (m, 5H), 6.32 (dd,  $J = 17.2, 10.8$  Hz, 1H), 5.90 (app. d,  $J = 7.2$  Hz, 1H), 5.78 (d,  $J = 2.0$  Hz, 1H), 5.46 (d,  $J = 17.6$  Hz, 1H), 5.15 (d,  $J = 10.8$  Hz, 1H), 5.02 (d,  $J = 11.6$  Hz, 1H), 4.76-4.68 (m, 3H), 4.57 (app. d,  $J = 6.4$  Hz, 1H), 3.92 (app. t,  $J = 8.8$  Hz, 1H), 3.77 (dd,  $J = 8.8, 6.8$  Hz, 1H), 0.96 (t,  $J = 7.6$  Hz, 9H), 0.66 (q,  $J = 8.0$  Hz, 6H).



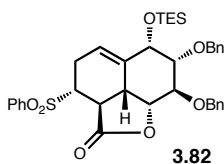
To a solution of **3.79** (54.0 mg, 0.0946 mmol, 1.0 eq) in  $\text{CH}_2\text{Cl}_2$  (946  $\mu\text{L}$ ) at  $-78^\circ\text{C}$  was added DIBAL (1.0 M in heptane, 189  $\mu\text{L}$ , 0.189 mmol, 2.0 eq). After 3 h, MeOH (1 mL) was added, and the  $-78^\circ\text{C}$  bath was removed. The reaction was stirred at RT in a saturated solution of Rochelle's salt (sodium potassium tartrate, 20 mL) and  $\text{CH}_2\text{Cl}_2$  (20 mL) for 1 h, and the biphasic mixture was separated and the aqueous layer was extracted with  $\text{CH}_2\text{Cl}_2$  (3 x 20 mL). The combined organic layers were dried ( $\text{MgSO}_4$ ), filtered and concentrated, and purification by flash column

chromatography (10% EtOAc/hexanes) gave **3.80** as a clear oil (35.0 mg, 0.0750 mmol, 79%).  $[\alpha]_D^{20} +21.0$  ( $c$  0.19,  $\text{CHCl}_3$ );  $^1\text{H}$  NMR (400 MHz,  $\text{CDCl}_3$ ):  $\delta$  7.39-7.27 (m, 10H), 6.27 (dd,  $J = 17.6, 11.2$  Hz, 1H), 5.68 (d,  $J = 3.2$  Hz, 1H), 5.34 (d,  $J = 17.6$  Hz, 1H), 5.14 (d,  $J = 10.8$  Hz, 1H), 4.98 (d,  $J = 11.6$  Hz, 1H), 4.83 (d,  $J = 11.2$  Hz, 1H), 4.77 (d,  $J = 11.6$  Hz, 1H), 4.76 (d,  $J = 11.6$  Hz, 1H), 4.62 (d,  $J = 3.2$  Hz, 1H), 4.20 (dd,  $J = 8.8, 6.0$  Hz, 1H), 4.01 (dd,  $J = 10.0, 6.8$  Hz, 1H), 3.40 (dd,  $J = 9.6, 2.8$  Hz, 1H), 2.18 (d,  $J = 5.6$  Hz, 1H), 0.93 (t,  $J = 8.0$  Hz, 9H), 0.71-0.56 (m, 6H);  $^{13}\text{C}$  NMR (100 MHz,  $\text{CDCl}_3$ ):  $\delta$  138.8, 138.3, 138.1, 136.0, 129.1, 128.5, 128.2, 128.0 (2C), 127.7, 127.6, 114.5, 81.4, 80.5, 74.4, 73.6, 72.6, 66.9, 7.0, 5.3; IR (film)  $\nu_{\text{max}}$  3413, 3031, 2953, 2875, 1129  $\text{cm}^{-1}$ ; HRMS (ESI)  $m/z$  calcd. for  $\text{C}_{28}\text{H}_{39}\text{O}_4\text{Si}$   $[\text{M}+\text{H}]^+$  467.2618, found 467.2612.



To a solution of **3.80** (18.0 mg, 0.0386 mmol, 1.0 eq) in  $\text{CH}_2\text{Cl}_2$  (1.0 mL) was added (*E*)-3-(phenylsulfonyl)acrylic acid (**3.63**, 8.20 mg, 0.0386 mmol, 1.0 eq) and 2-chloro-1-methylpyridinium iodide (**3.62**, 15.0 mg, 0.0579 mmol, 1.5 eq) and the mixture was heated at reflux. At 40 °C,  $\text{Et}_3\text{N}$  (20.0  $\mu\text{L}$ , 0.116 mmol, 3.0 eq) was added in 4 portions over 1 h, followed by refluxing for 20 min. The reaction mixture was removed from heating and at RT, saturated aqueous  $\text{NaHCO}_3$  (20 mL) was added and the mixture was extracted with  $\text{CH}_2\text{Cl}_2$  (3 x 20 mL). The combined organic phases were washed with saturated aqueous  $\text{NH}_4\text{Cl}$  (25 mL), dried ( $\text{MgSO}_4$ ), filtered and concentrated. Purification by flash column chromatography (5% and 10% EtOAc/hexanes) yielded **3.81** as a clear oil (17.0 mg, 0.0257 mmol, 67%).  $[\alpha]_D^{20} -37.1$  ( $c$  0.32,  $\text{CHCl}_3$ );  $^1\text{H}$  NMR (400 MHz,  $\text{CDCl}_3$ ):  $\delta$  7.93 (dd,  $J = 7.2, 1.6$  Hz, 2H), 7.70 (dt,  $J = 7.2, 1.2$  Hz, 1H), 7.60 (app. t,  $J = 7.6$  Hz, 2H), 7.39-7.30 (m, 6H), 7.27-7.24

(m, 4H), 7.21 (d,  $J = 15.2$  Hz, 1H), 6.65 (d,  $J = 15.2$  Hz, 1H), 6.18 (dd,  $J = 17.6, 11.2$  Hz, 1H), 5.48 (dd,  $J = 10.0, 3.2$  Hz, 1H), 5.47 (s, 1H), 5.35 (d,  $J = 17.6$  Hz, 1H), 5.18 (d,  $J = 11.2$  Hz, 1H), 4.89 (d,  $J = 12.0$  Hz, 1H), 4.87 (d,  $J = 11.2$  Hz, 1H), 4.76 (d,  $J = 11.6$  Hz, 1H), 4.64 (d,  $J = 12.0$  Hz, 1H), 4.60 (d,  $J = 2.8$  Hz, 1H), 4.21 (dd,  $J = 10.4, 7.2$  Hz, 1H), 3.44 (dd,  $J = 10.0, 2.8$  Hz, 1H), 0.93 (t,  $J = 8.0$  Hz, 9H), 0.72-0.56 (m, 6H);  $^{13}\text{C}$  NMR (100 MHz,  $\text{CDCl}_3$ ):  $\delta$  163.1, 143.3, 140.3, 138.5, 138.3, 138.0, 135.4, 134.4, 130.7, 129.6, 128.4 (2C), 128.3, 128.2 (2C), 127.9, 127.7, 124.6, 115.8, 80.3, 77.2, 76.4, 74.6, 74.0, 66.7, 7.0, 5.4; IR (film)  $\nu_{\text{max}}$  3064, 3032, 2953, 2911, 2875, 1729, 1455  $\text{cm}^{-1}$ ; HRMS (ESI)  $m/z$  calcd. for  $\text{C}_{37}\text{H}_{45}\text{O}_7\text{SSi} [\text{M}+\text{H}]^+$  661.2656, found 661.2650.



A solution of **3.81** (11.0 mg, 0.0166 mmol, 1.0 eq) in  $\text{CH}_3\text{CN}$  (10 mL) was heated at reflux for 48 h then removed from heating and concentrated. Purification by flash column chromatography (20% and 25% EtOAc/hexanes) yielded **3.82** as a clear oil (6.0 mg, 9.09  $\mu\text{mol}$ , 55%).  $[\alpha]_{\text{D}}^{20} +20.4$  ( $c$  0.22,  $\text{CHCl}_3$ );  $^1\text{H}$  NMR (400 MHz,  $\text{CDCl}_3$ ):  $\delta$  7.62 (dd,  $J = 7.4, 1.0$  Hz, 2H), 7.57 (app. t,  $J = 7.6$  Hz, 1H), 7.41 (app. t,  $J = 7.8$  Hz, 2H), 7.38-7.26 (m, 10H), 6.00 (ddd,  $J = 9.0, 5.2, 2.4$  Hz, 1H), 4.87 (d,  $J = 12.2$  Hz, 1H), 4.69-4.62 (m, 3H), 4.62 (d,  $J = 12.2$  Hz, 1H), 4.53 (d,  $J = 11.7$  Hz, 1H), 3.84 (dd,  $J = 4.4, 1.8$  Hz, 2H), 3.70 (dt,  $J = 10.0, 1.5$  Hz, 1H), 3.28 (dd,  $J = 13.8, 10.2$  Hz, 1H), 3.20 (ddd,  $J = 17.3, 6.9, 1.4$  Hz, 1H), 2.90 (dd,  $J = 12.2, 10.1$  Hz, 1H), 2.42 (app. dt,  $J = 13.4, 9.5, 4.8$  Hz, 1H), 0.98 (t,  $J = 8.0$  Hz, 9H), 0.64 (q,  $J = 7.8$  Hz, 6H);  $^{13}\text{C}$  NMR (100 MHz,  $\text{CDCl}_3$ ):  $\delta$  171.8, 139.2, 138.4, 137.6, 137.2, 133.8, 129.2, 129.0, 128.5, 128.3, 127.9, 127.7, 127.6, 119.2, 82.3, 81.2, 79.4, 73.6, 71.9, 71.3, 59.2,

43.0, 41.0, 29.7, 24.4, 6.9, 4.7; IR (film)  $\nu_{\text{max}}$  3063, 2919, 1789, 1452  $\text{cm}^{-1}$ ; HRMS (ESI)  $m/z$  calcd. for  $\text{C}_{37}\text{H}_{44}\text{NaO}_7\text{SSi}$   $[\text{M}+\text{Na}]^+$  683.2469, found 683.2484.

## References

1. Romaine, I. M.; Hempel, J. E.; Shanmugam, G.; Hori, H.; Igarashi, Y.; Polavarapu, P. L.; Sulikowski, G. A. "Assignment and stereocontrol of hibarimicin atropoisomers" *Org. Lett.*, **2011**, *13*, 4538-4541.
2. Surry, D. S.; Fox, D. J.; Macdonald, S. J. F.; Spring, D. R. "Aryl-aryl coupling via directed lithiation and oxidation" *Chem. Comm.*, **2005**, 2589-2590.
3. Leeper, F. J.; Staunton, J. "Biomimetic syntheses of polyketide aromatics from reaction of an orsellinate anion with pyrones and a pyrylium salt" *J. Chem. Soc. Perkin Trans. 1*, **1984**, 1053-1059.
4. Dodd, J. H.; Starrett, Jr., J. E.; Weinreb, S. M. "Total synthesis of tri-O-methylolivivin" *J. Am. Chem. Soc.*, **1984**, *106*, 1811-1812.
5. Hanna, I.; Ricard, L. "From galactose to highly functionalized seven- and eight-membered carbocyclic rings by ring-closing metathesis" *Org. Lett.*, **2000**, *2*, 2651-2654.
6. Johnson, C. R.; Adams, J. P.; Braun, M. P.; Senanayake, C. B. W. "Direct  $\alpha$ -iodination of cycloalkenones" *Tet. Lett.*, **1992**, *33*, 917-918.
7. Sletten, E. M.; Liotta, L. J. "A flexible stereospecific synthesis of polyhydroxylated pyrrolizidines from commercially available pyranosides" *J. Org. Chem.*, **2006**, *71*, 1335-1343.
8. Wu, Y.-D.; Houk, K. N.; Trost, B. M. "Origin of enhanced axial attack by sterically undemanding nucleophiles on cyclohexenones" *J. Am. Chem. Soc.*, **1987**, *109*, 5560-5561.
9. Cieplak, A. S. "Stereochemistry of nucleophilic addition to cyclohexanone. The importance of two-electron stabilizing interactions" *J. Am. Chem. Soc.*, **1981**, *103*, 4540-4552.
10. Lou, S.; Moquist, P. N.; Schaus, S. E. "Asymmetric allylboration of ketones catalyzed by chiral diols" *J. Am. Chem. Soc.*, **2006**, *128*, 12660-12661.

11. Plietker, B. "The RuO<sub>4</sub>-catalyzed ketohydroxylation. Part I. Development, scope, and limitation" *J. Org. Chem.*, **2004**, *69*, 8287-8296.
12. Plietker, B. "The RuO<sub>4</sub>-catalyzed ketohydroxylation. Part II: A regio-, chemo- and stereoselectivity study" *Eur. J. Org. Chem.*, **2005**, 1919-1929.
13. Hyldtoft, L.; Madsen, R. "Carbohydrate carbocyclization by a novel zinc-mediated domino reaction and ring-closing olefin metathesis" *J. Am. Chem. Soc.*, **2000**, *122*, 8444-8452.
14. Hoye, T. R.; Zhao, H. "Some allylic substituent effects in ring closing metathesis reactions: allylic alcohol activation" *Org. Lett.*, **1999**, *1*, 1123-1125.
15. Scholl, M.; Ding, S.; Lee, C. W.; Grubbs, R. H. "Synthesis and activity of a new generation of ruthenium-based olefin metathesis catalysts coordinated with 1,3-dimesityl-4,5-dihydroimidazol-2-ylidene ligands" *Org. Lett.*, **1999**, *1*, 953-956.
16. Kerins, F.; O'Shea, D. F. "Generation of substituted styrenes via Suzuki cross-coupling of aryl halides with 2,4,6-trivinylcyclotriboroxane" *J. Org. Chem.*, **2002**, *67*, 4968-4971.
17. Esteban, J.; Costa, A. M.; Vilarrasa, J. "Synthesis of amphidinolide E C10—C26 fragment" *Org. Lett.*, **2008**, *10*, 4843-4846.
18. Dai, C.; Fu, G. C. "The first general method for palladium-catalyzed Negishi cross-coupling of aryl and vinyl chlorides: use of commercially available Pd(P(*t*-Bu)<sub>3</sub>)<sub>2</sub> as a catalyst" *J. Am. Chem. Soc.*, **2001**, *123*, 2719-2724.
19. Buser, S.; Vasella, A. "7-Oxaborane and norbornane mimics of a distorted β-D-mannopyranoside: synthesis and evaluation as β-mannosidase inhibitors" *Helv. Chim. Acta*, **2005**, *88*, 3151-3173.
20. Mukaiyama, T.; Usui, M.; Shimada, E.; Saigo, K. "A convenient method for the synthesis of carboxylic esters" *Chem. Lett.*, **1975**, 1045-1048.
21. Ziegler, F. E.; Jaynes, B. H.; Saindane, M. T. "A C<sub>6</sub>, C<sub>7</sub> oxygen functionalized intermediate for the synthesis of forskolin: stereochemical control in an intramolecular Diels-Alder reaction" *Tet. Lett.*, **1985**, *26*, 3307-3310.
22. Streckowski, L.; Kong, S.; Battiste, M. A. "Intermolecular Diels-Alder reactions of 3-vinylcyclohex-2-en-1-ol and a silyl ether derivative" *J. Org. Chem.*, **1988**, *53*, 901-904.

23. Luche, J.-L. "Lanthanides in organic chemistry. 1. Selective 1,2-reductions of conjugated ketones" *J. Am. Chem. Soc.*, **1978**, *100*, 2226-2227.
24. Gaddam, S.; Khilevich, A.; Filer, C.; Rizzo, J. D.; Giltner, J.; Flavin, M. T.; Xu, Z.-Q. "Synthesis of dual  $^{14}\text{C}$ -labeled (+)-calanolide A, a naturally occurring anti-HIV agent" *J. Label. Compd. Radiopharm*, **1997**, *39*, 901-906.
25. Jung, M. E.; Gervay, J. "*Gem*-dialkyl effect in the intramolecular Diels-Alder reaction of 2-furfuryl methyl fumarates: the reactive rotamer effect, enthalpic basis for acceleration, and evidence for a polar transition state" *J. Am. Chem. Soc.*, **1991**, *113*, 224-232.
26. Still, W. C.; Kahn, M.; Mitra, A. "Rapid chromatographic technique for preparative separations with moderate resolution" *J. Org. Chem.*, **1978**, *43*, 2923-2925.
27. Tatina, M.; Yousuf, S. K.; Mukherjee, D. "2,4,6-Trichloro-1,3,5-triazine (TCT) mediated one-pot sequential functionalisation of glycosides for the generation of orthogonally protected monosaccharide building blocks" *Org. Biomol. Chem.*, **2012**, *10*, 5357-5360.
28. Frigerio, M.; Santagostino, M.; Sputore, S. "A user-friendly entry to 2-iodoxybenzoic acid (IBX)" *J. Org. Chem.*, **1999**, *64*, 4537-4538.



## **Appendix A1:**

**Spectra relevant to Chapter III.**

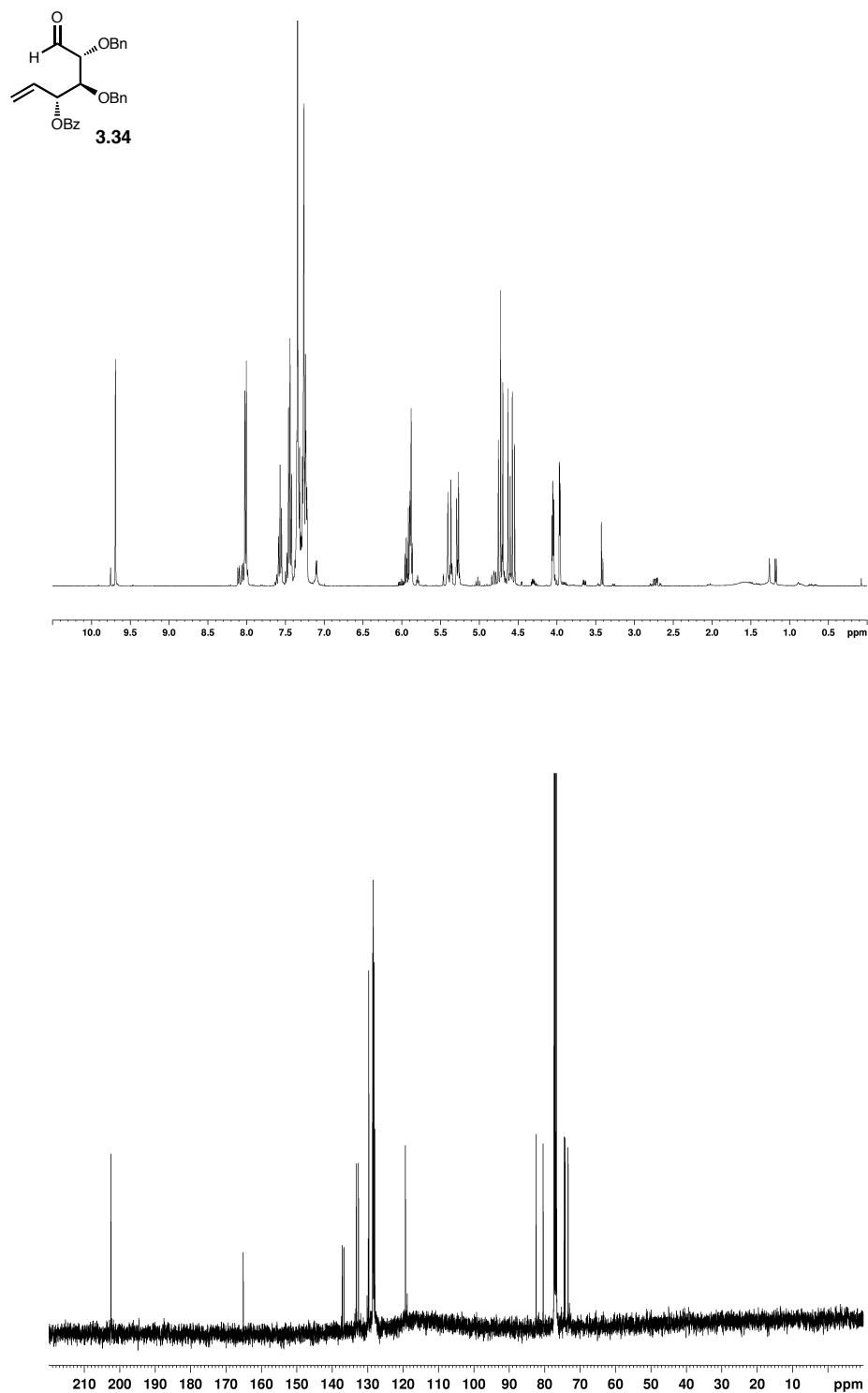


**Figure A1.1.**  $^1\text{H}$  NMR spectrum (400 MHz,  $\text{CDCl}_3$ ) and  $^{13}\text{C}$  NMR spectrum (100 MHz,  $\text{CDCl}_3$ ) of compound **3.34**.

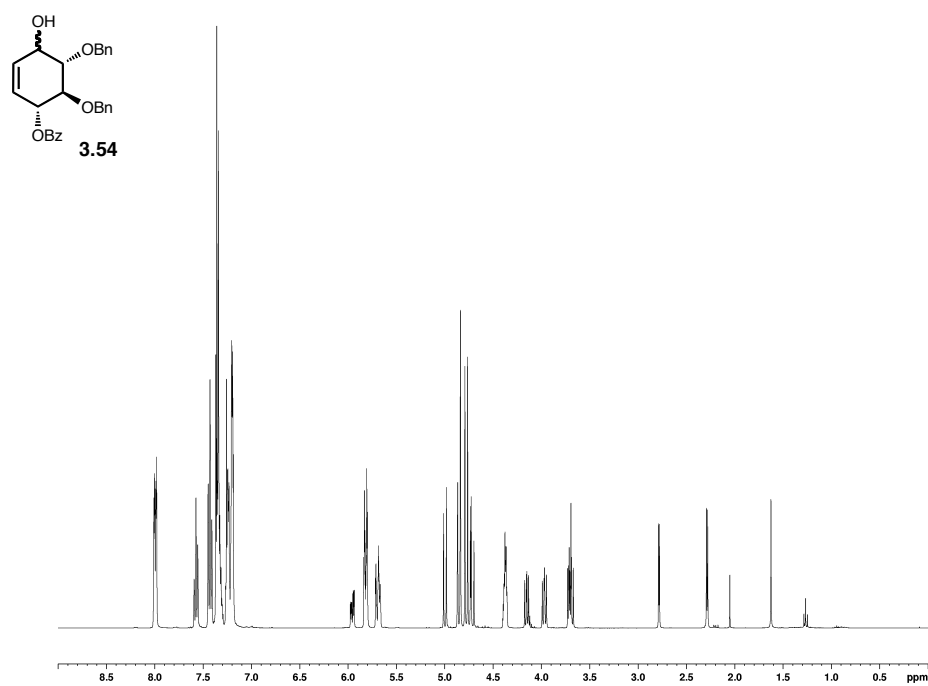


**Figure A1.2.**  $^1\text{H}$  NMR spectrum (400 MHz,  $\text{CDCl}_3$ ) of compound **3.54**.

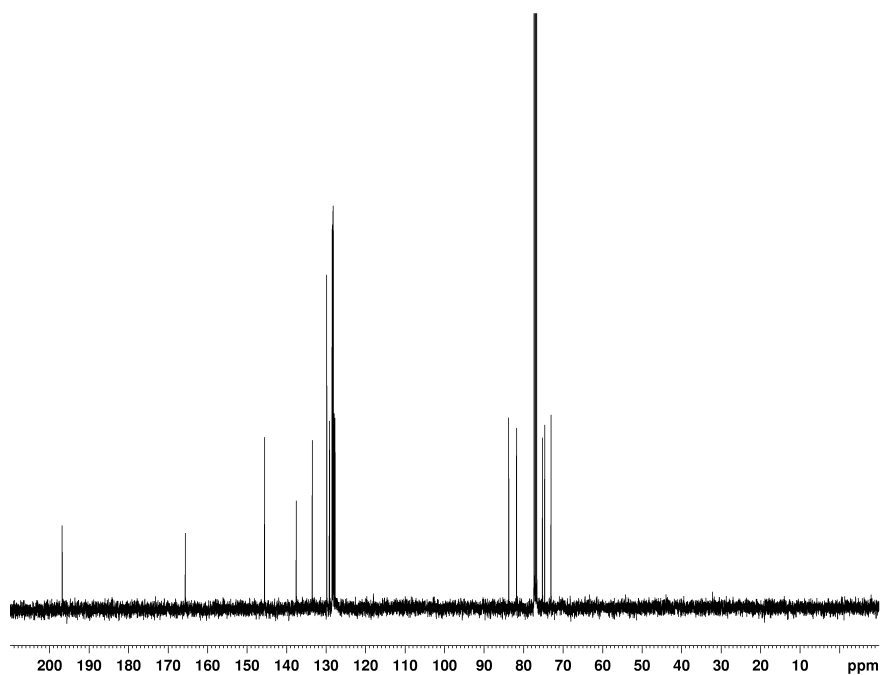
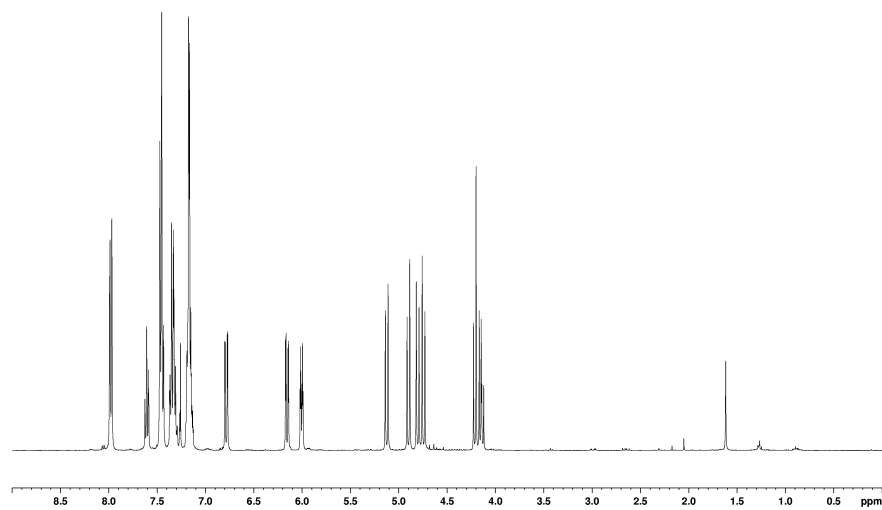
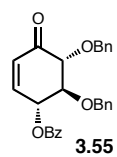


**Figure A1.3.**  $^1\text{H}$  NMR spectrum (400 MHz,  $\text{CDCl}_3$ ) and  $^{13}\text{C}$  NMR spectrum (100 MHz,  $\text{CDCl}_3$ ) of compound **3.55**.

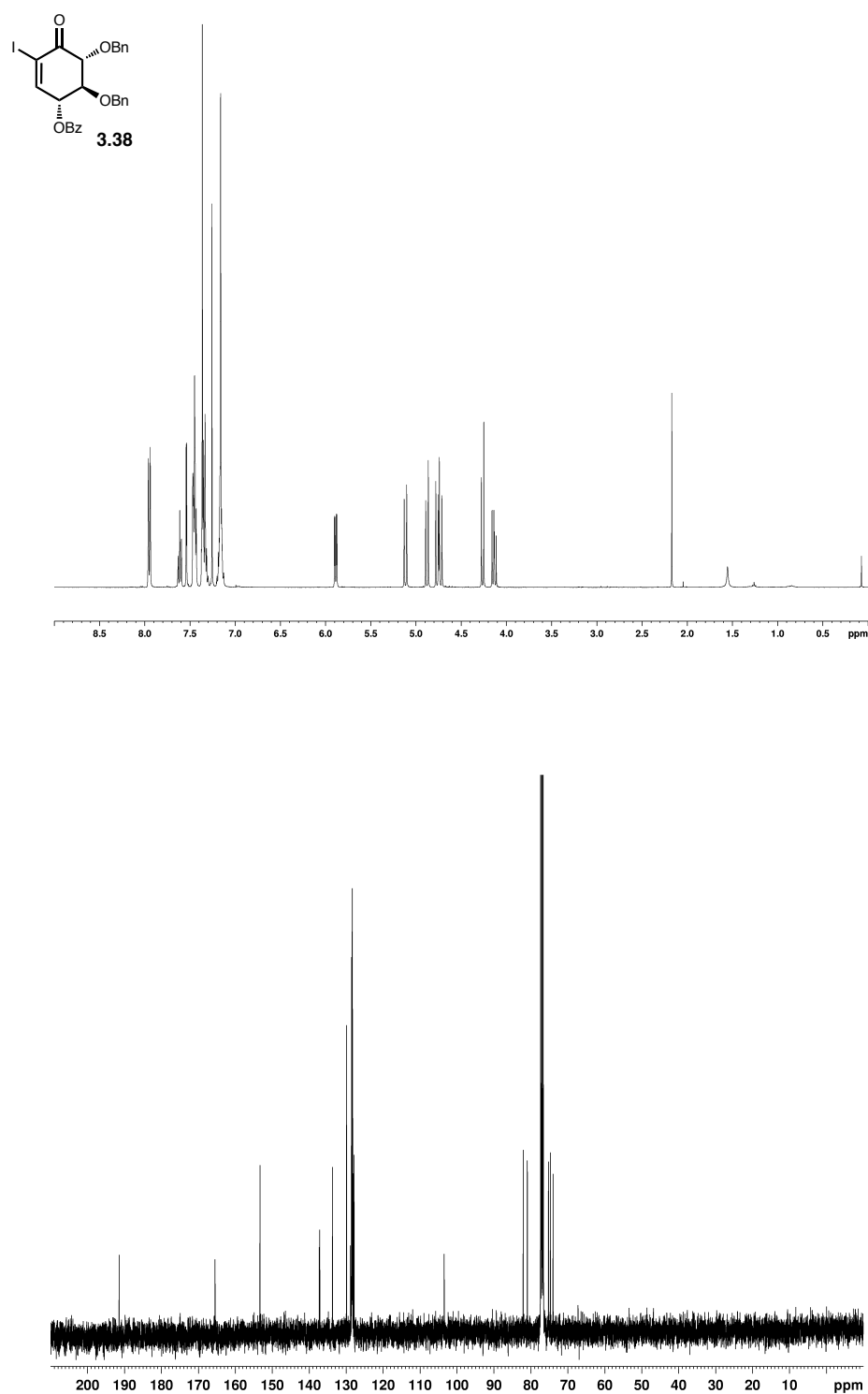


**Figure A1.4.**  $^1\text{H}$  NMR spectrum (400 MHz,  $\text{CDCl}_3$ ) and  $^{13}\text{C}$  NMR spectrum (100 MHz,  $\text{CDCl}_3$ ) of compound **3.38**.

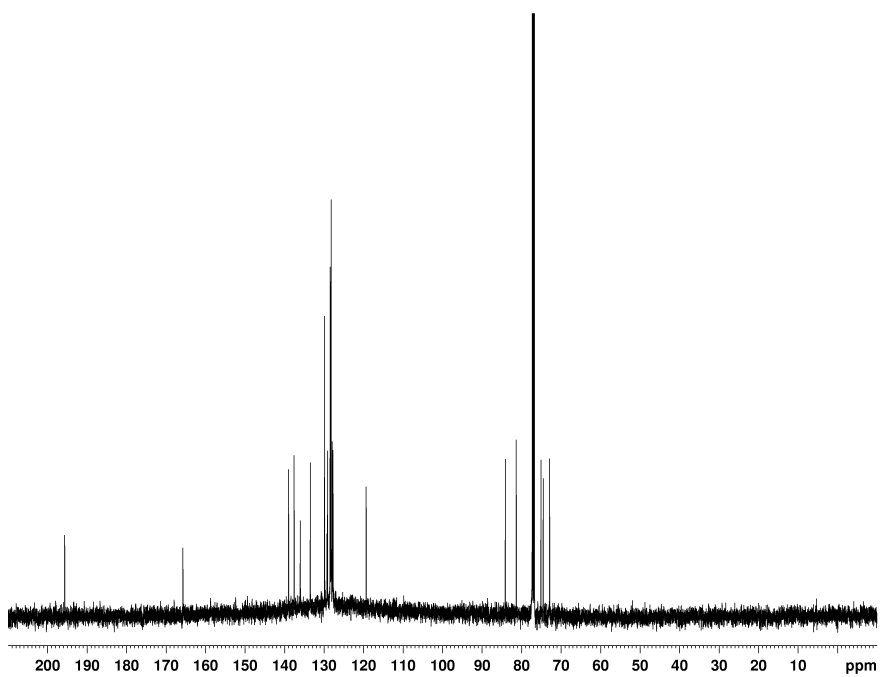
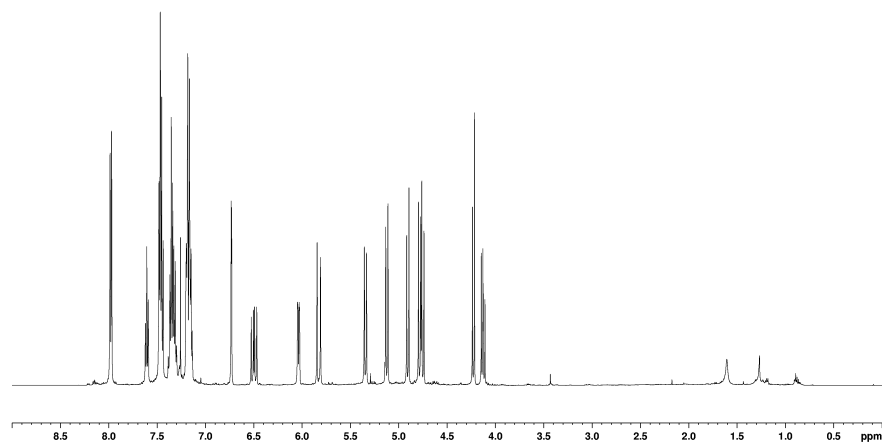
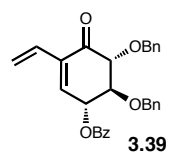


**Figure A1.5.**  $^1\text{H}$  NMR spectrum (500 MHz,  $\text{CDCl}_3$ ) and  $^{13}\text{C}$  NMR spectrum (125 MHz,  $\text{CDCl}_3$ ) of compound **3.39**.

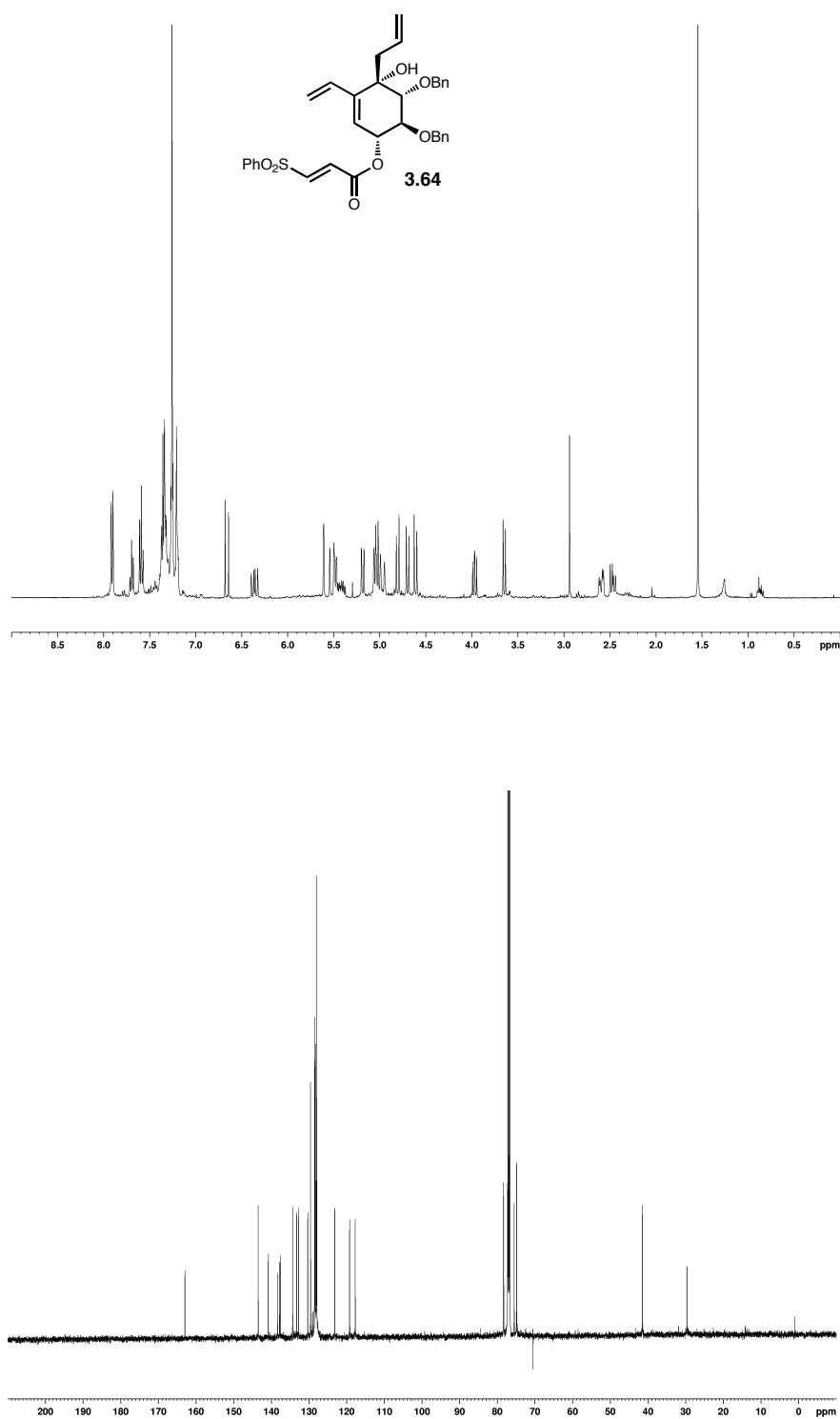


**Figure A1.6.**  $^1\text{H}$  NMR spectrum (500 MHz,  $\text{CDCl}_3$ ) and  $^{13}\text{C}$  NMR spectrum (125 MHz,  $\text{CDCl}_3$ ) of compound **3.64**.

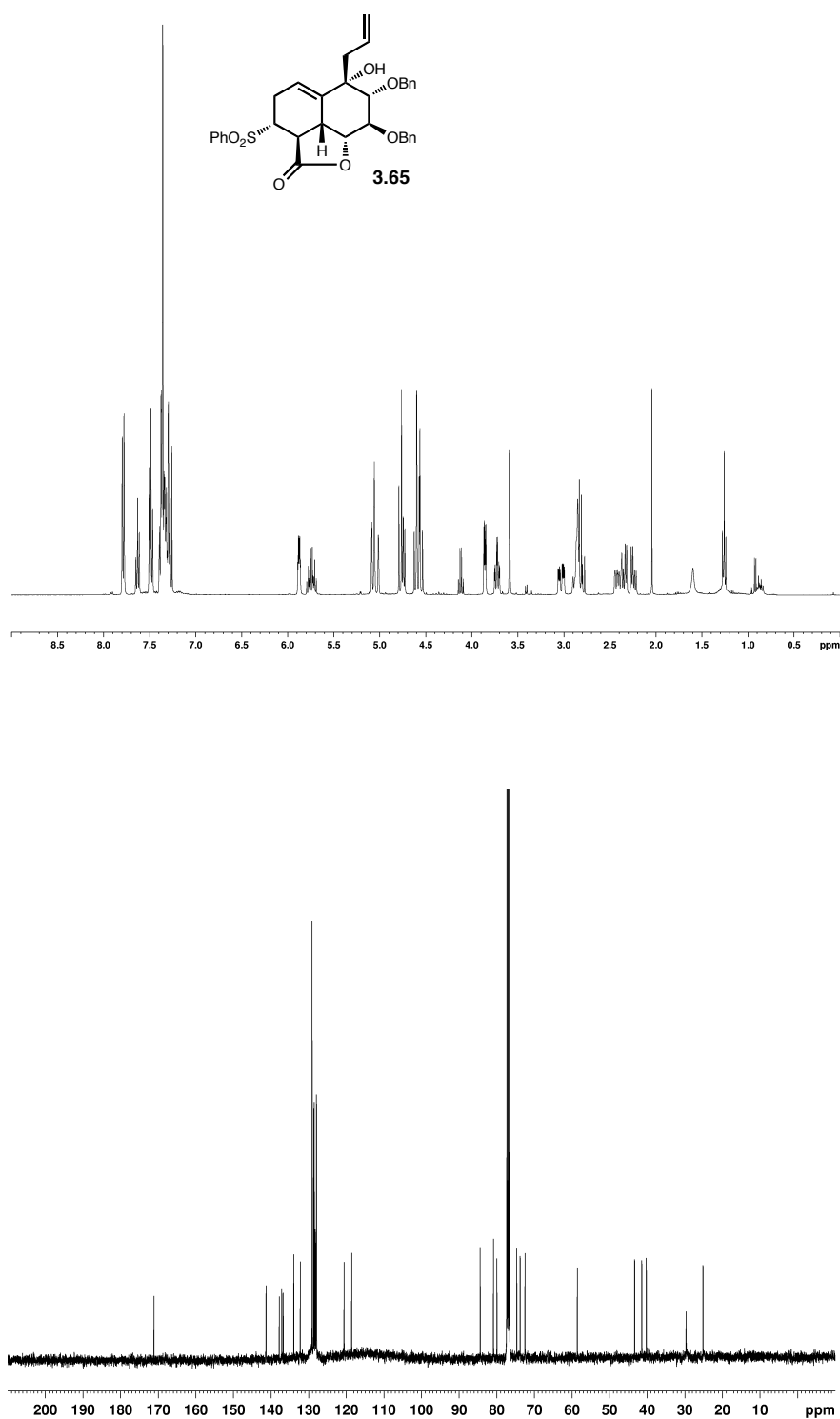


**Figure A1.7.**  $^1\text{H}$  NMR spectrum (400 MHz,  $\text{CDCl}_3$ ) and  $^{13}\text{C}$  NMR spectrum (100 MHz,  $\text{CDCl}_3$ ) of compound **3.65**.



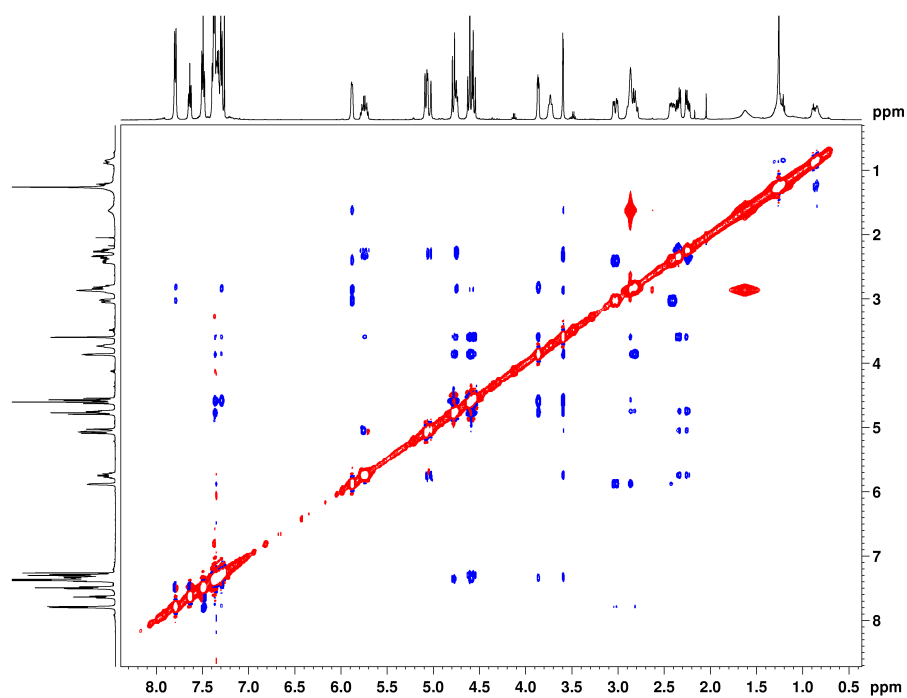
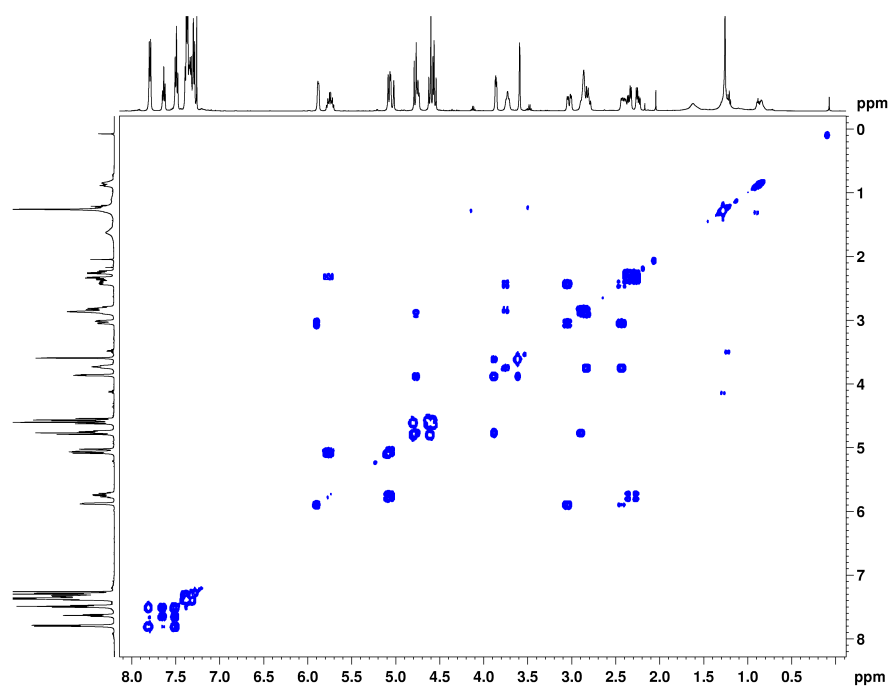


**Figure A1.8.** COSY spectrum (500 MHz, CDCl<sub>3</sub>) and NOESY spectrum (500 MHz, CDCl<sub>3</sub>) of compound **3.65**.

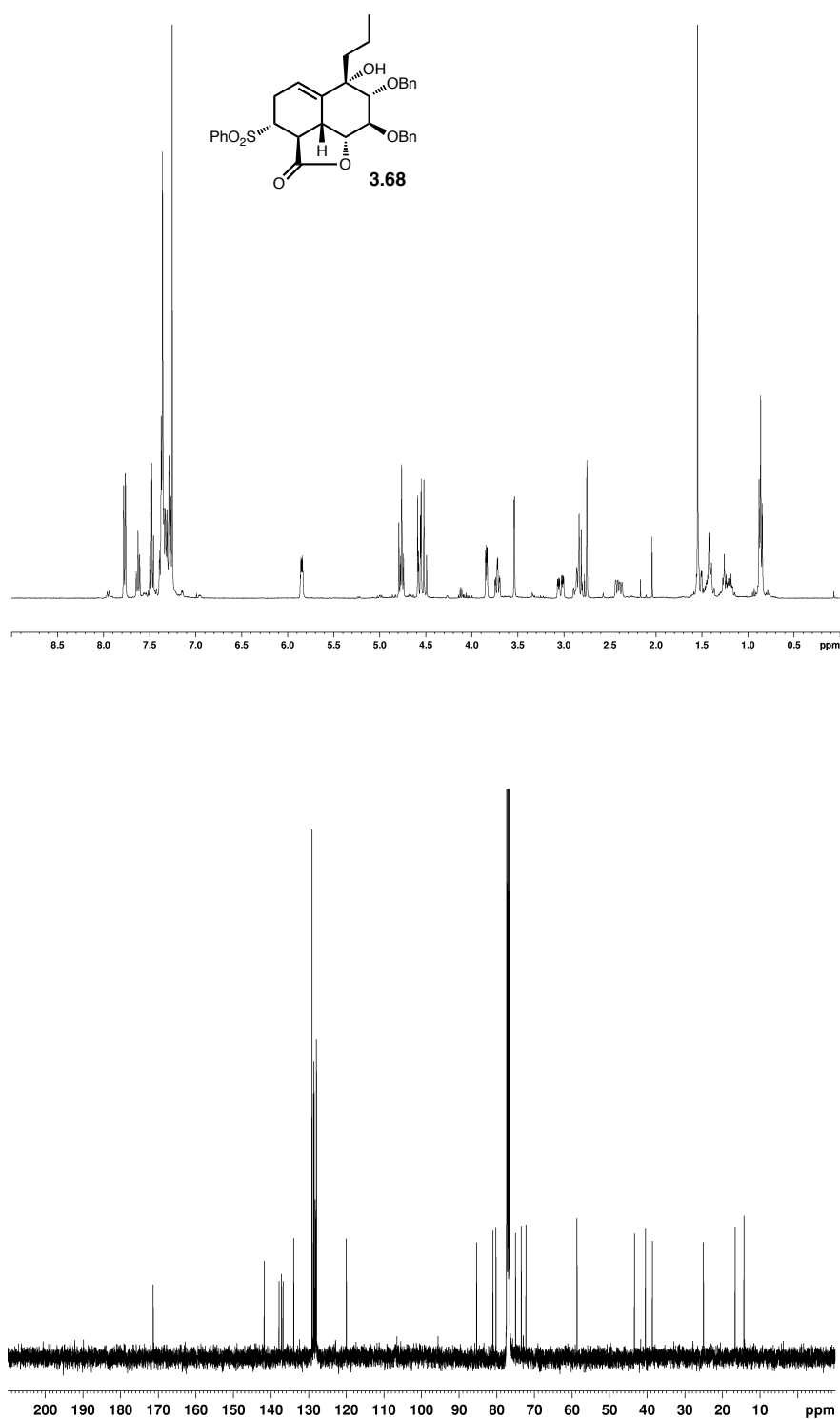


**Figure A1.9.**  $^1\text{H}$  NMR spectrum (400 MHz,  $\text{CDCl}_3$ ) and  $^{13}\text{C}$  NMR spectrum (100 MHz,  $\text{CDCl}_3$ ) of compound **3.68**.

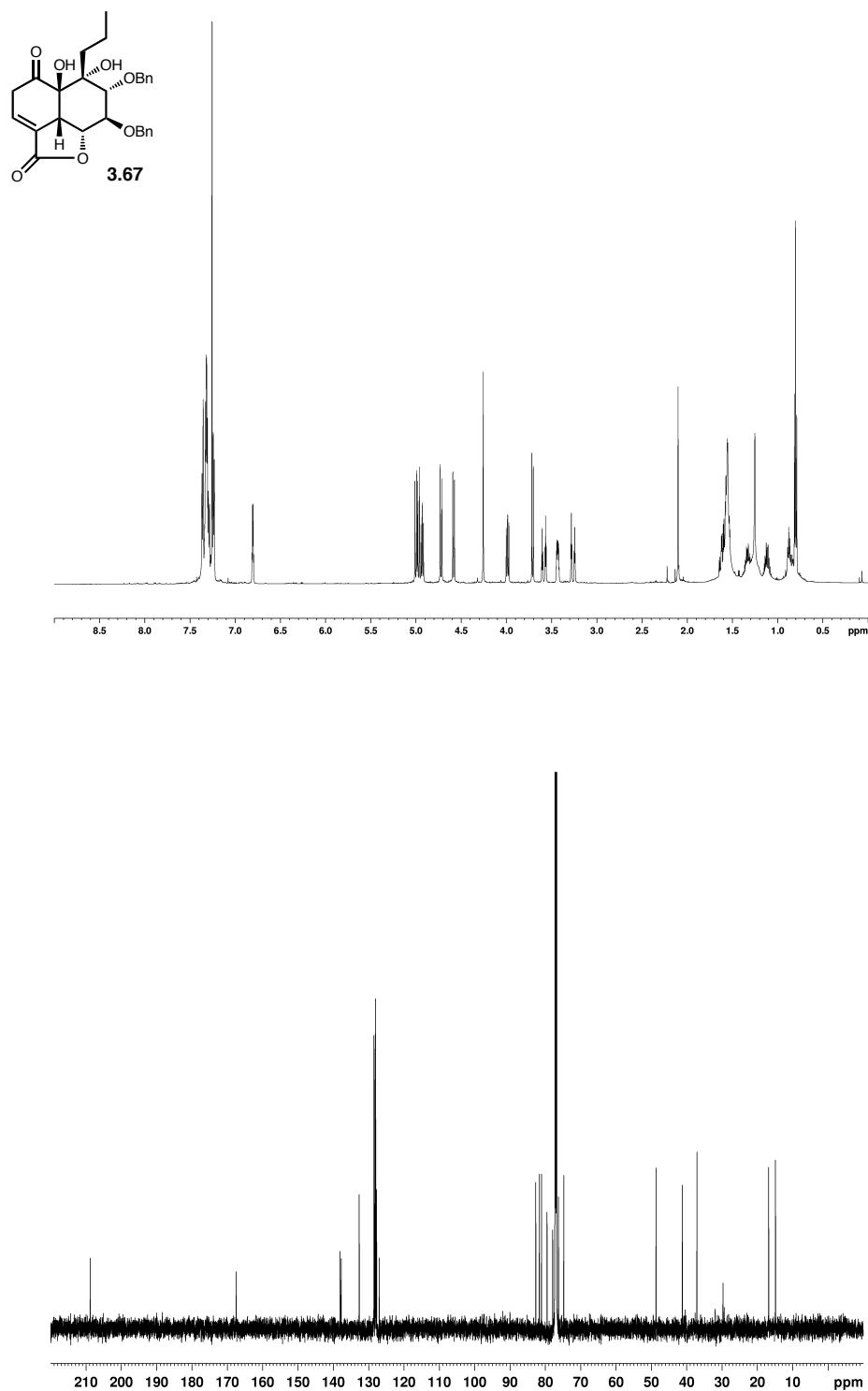


**Figure A1.10.**  $^1\text{H}$  NMR spectrum (600 MHz,  $\text{CDCl}_3$ ) and  $^{13}\text{C}$  NMR spectrum (150 MHz,  $\text{CDCl}_3$ ) of compound **3.67**.

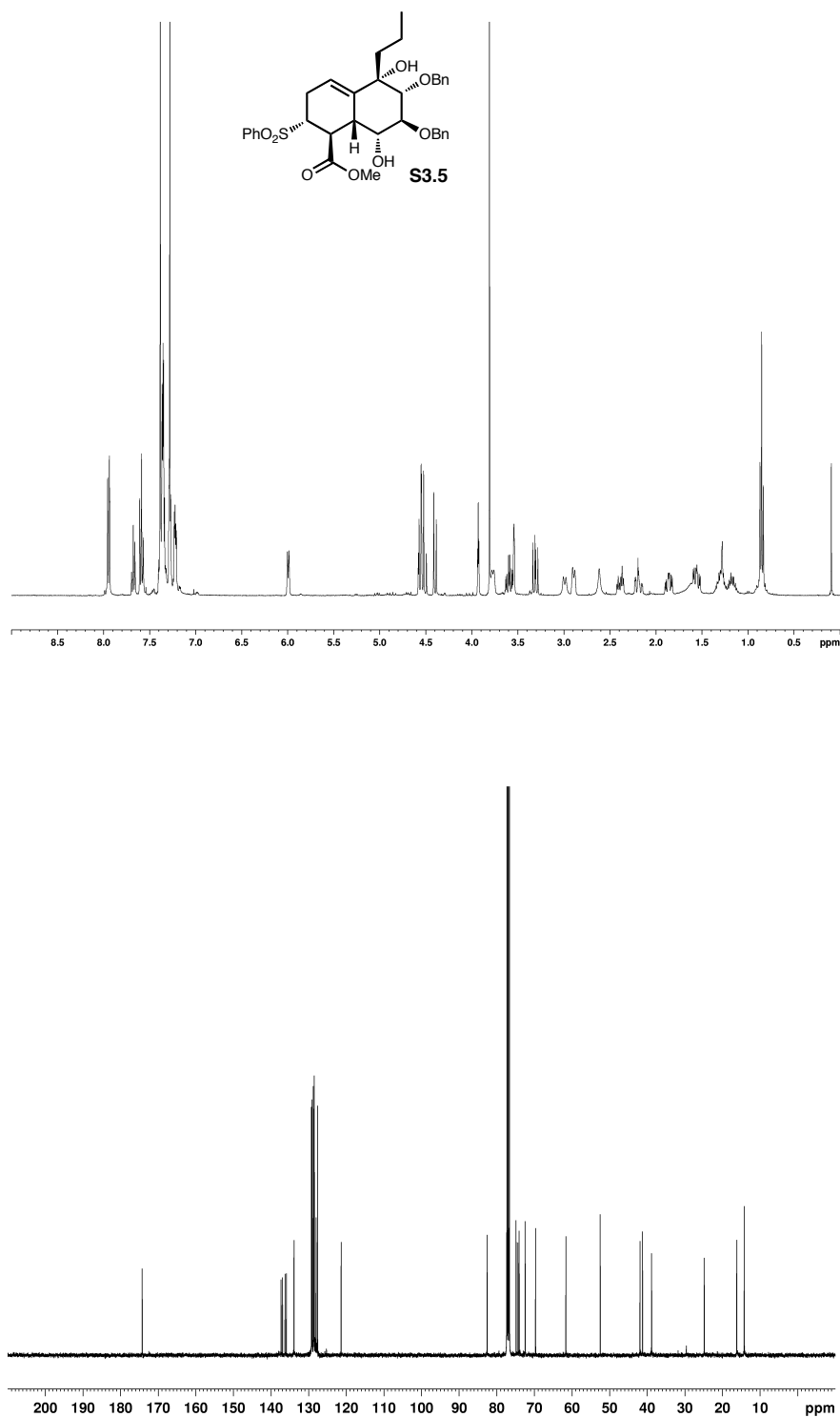


**Figure A1.11.**  $^1\text{H}$  NMR spectrum (400 MHz,  $\text{CDCl}_3$ ) and  $^{13}\text{C}$  NMR spectrum (100 MHz,  $\text{CDCl}_3$ ) of compound S3.5.

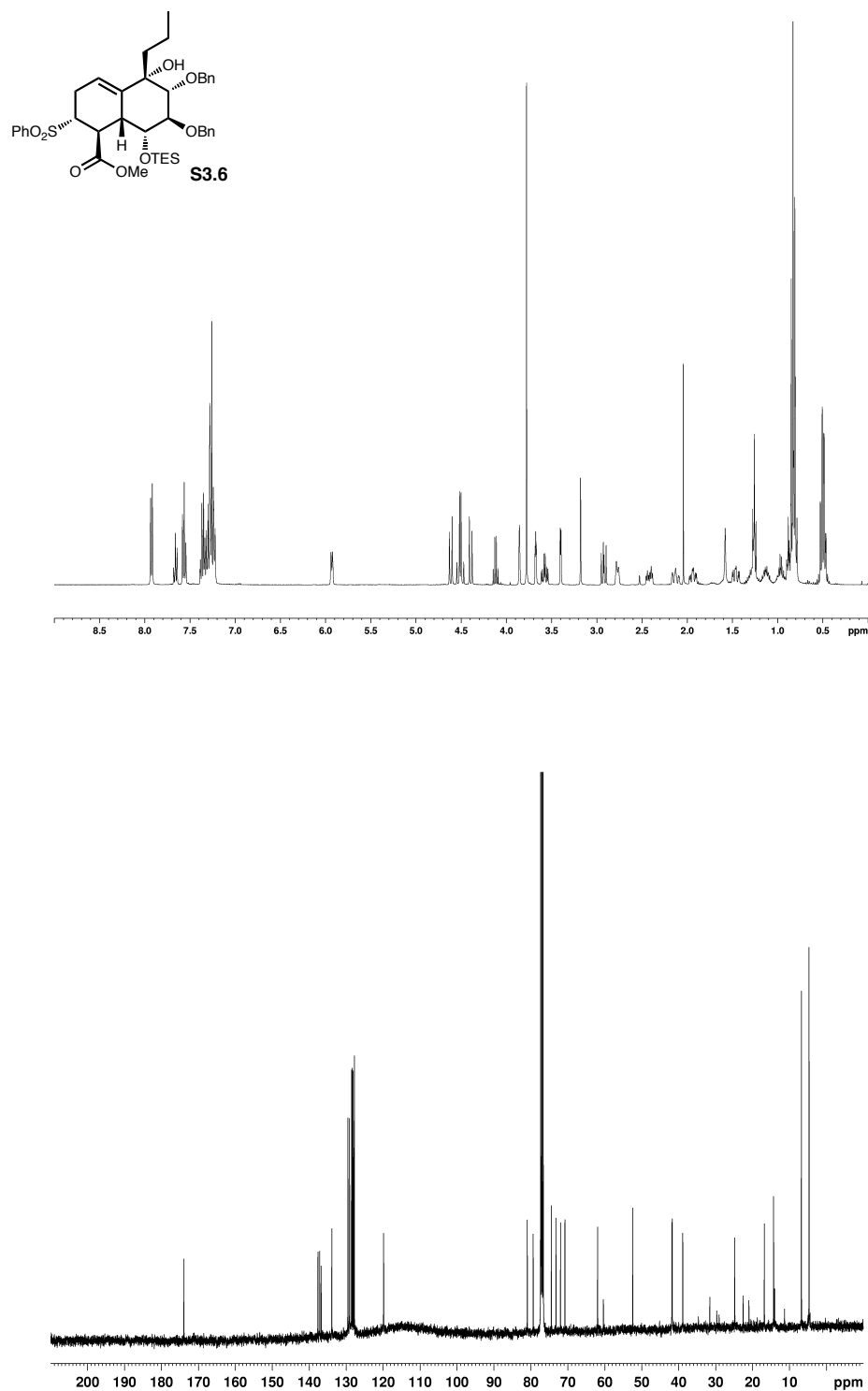


**Figure A1.12.**  $^1\text{H}$  NMR spectrum (400 MHz,  $\text{CDCl}_3$ ) and  $^{13}\text{C}$  NMR spectrum (100 MHz,  $\text{CDCl}_3$ ) of compound **S3.6**.

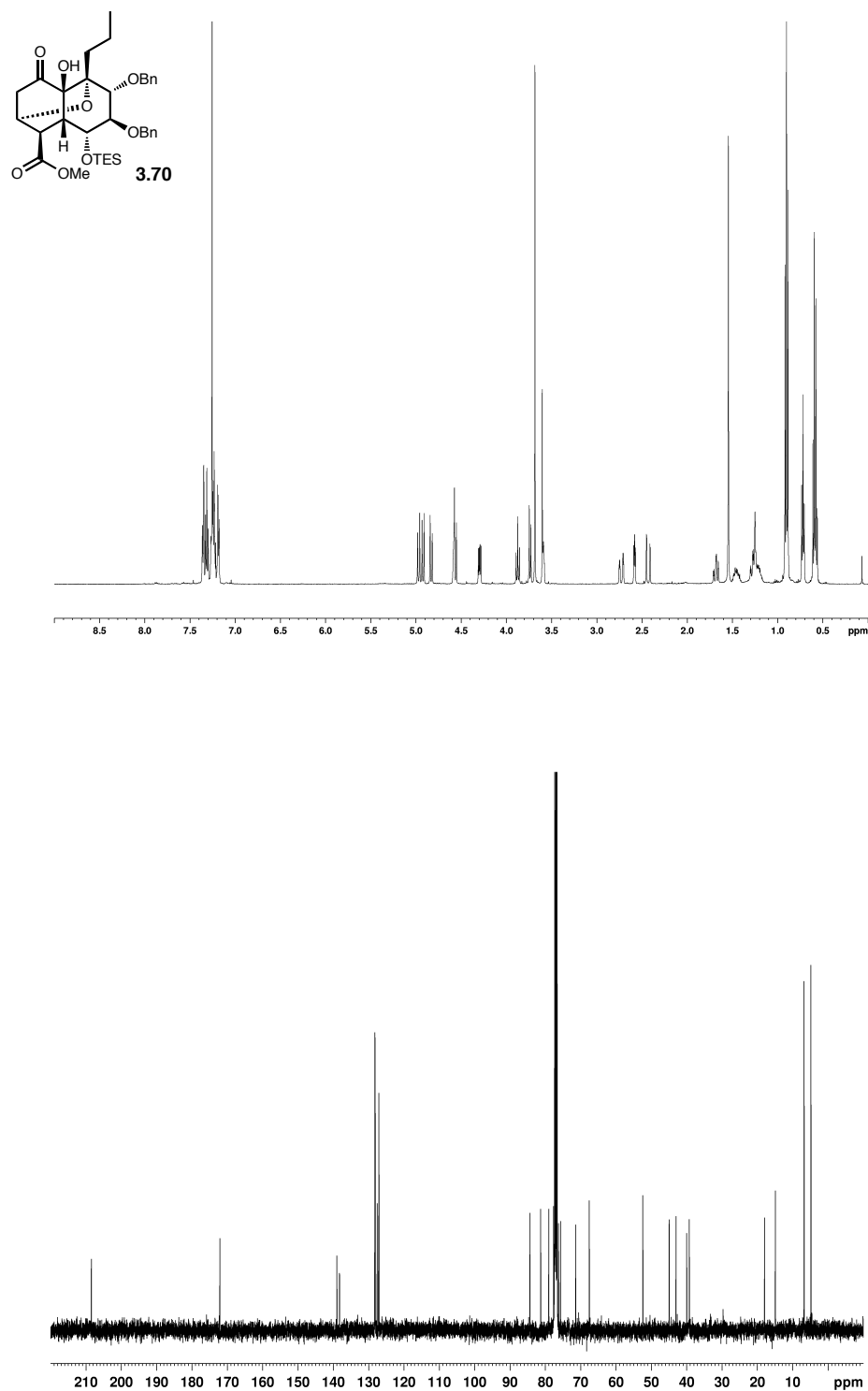


**Figure A1.13.**  $^1\text{H}$  NMR spectrum (500 MHz,  $\text{CDCl}_3$ ) and  $^{13}\text{C}$  NMR spectrum (100 MHz,  $\text{CDCl}_3$ ) of compound **3.70**.

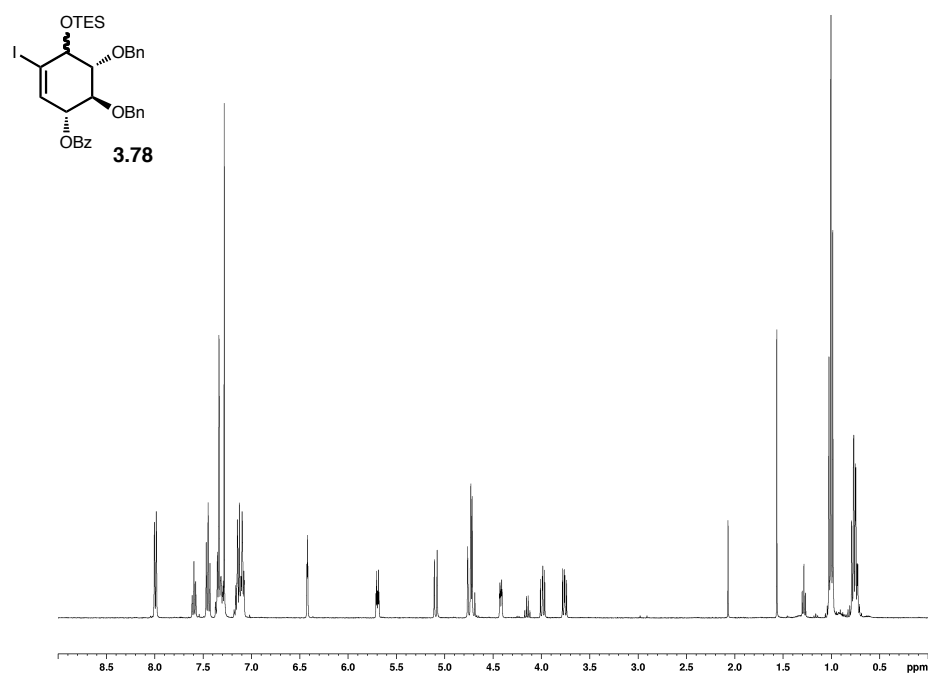
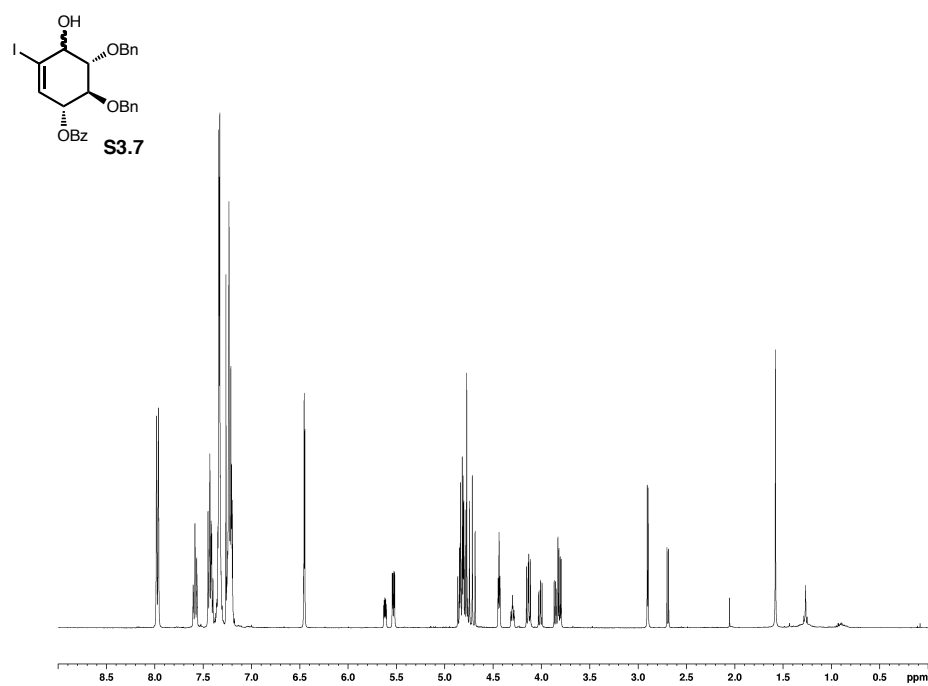


**Figure A1.14.**  $^1\text{H}$  NMR spectrum (400 MHz,  $\text{CDCl}_3$ ) of compound **S3.7** and  $^1\text{H}$  NMR spectrum (400 MHz,  $\text{CDCl}_3$ ) of compound **3.78**.

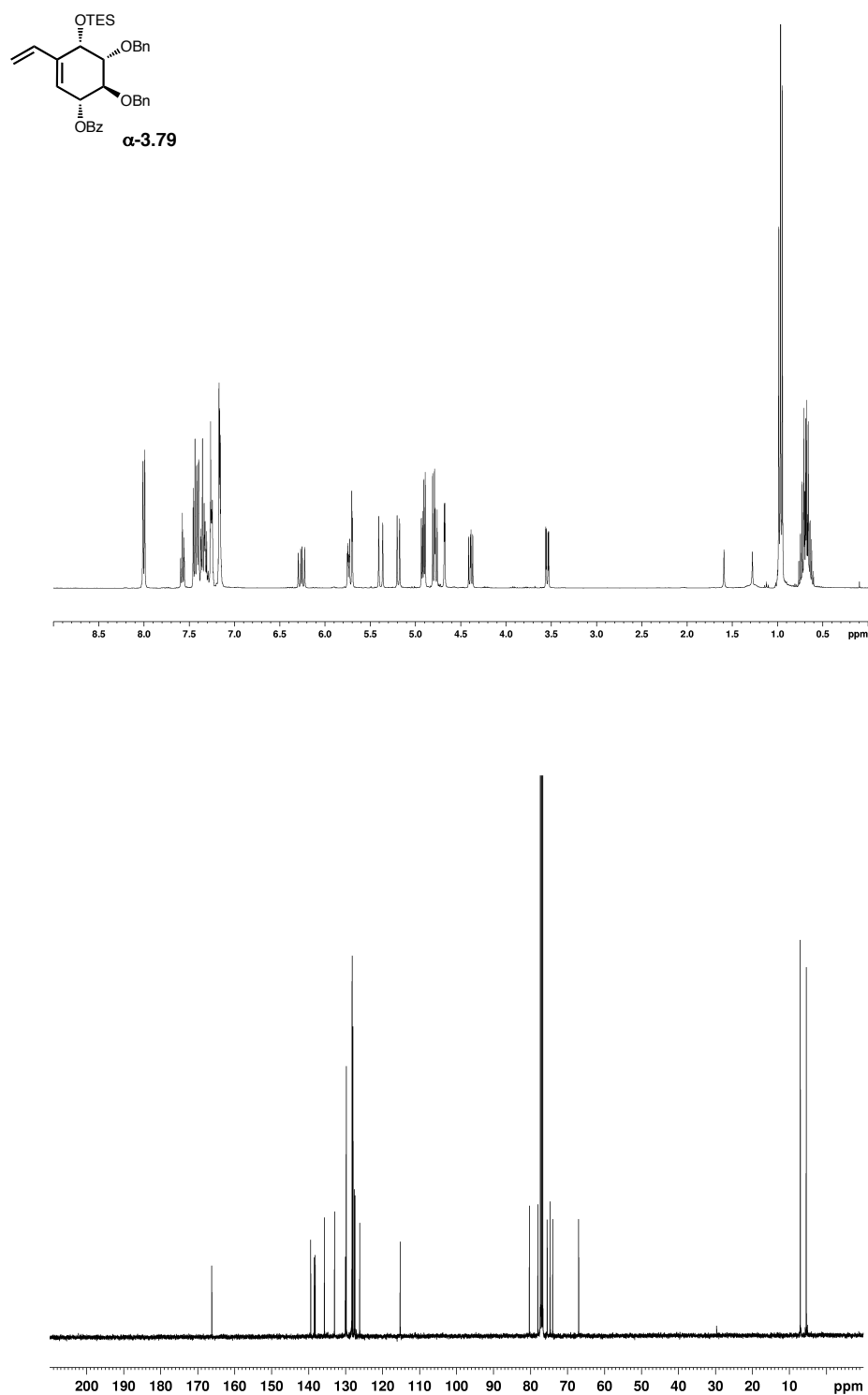


**Figure A1.15.**  $^1\text{H}$  NMR spectrum (400 MHz,  $\text{CDCl}_3$ ) and  $^{13}\text{C}$  NMR spectrum (100 MHz,  $\text{CDCl}_3$ ) of compound  **$\alpha$ -3.79**.



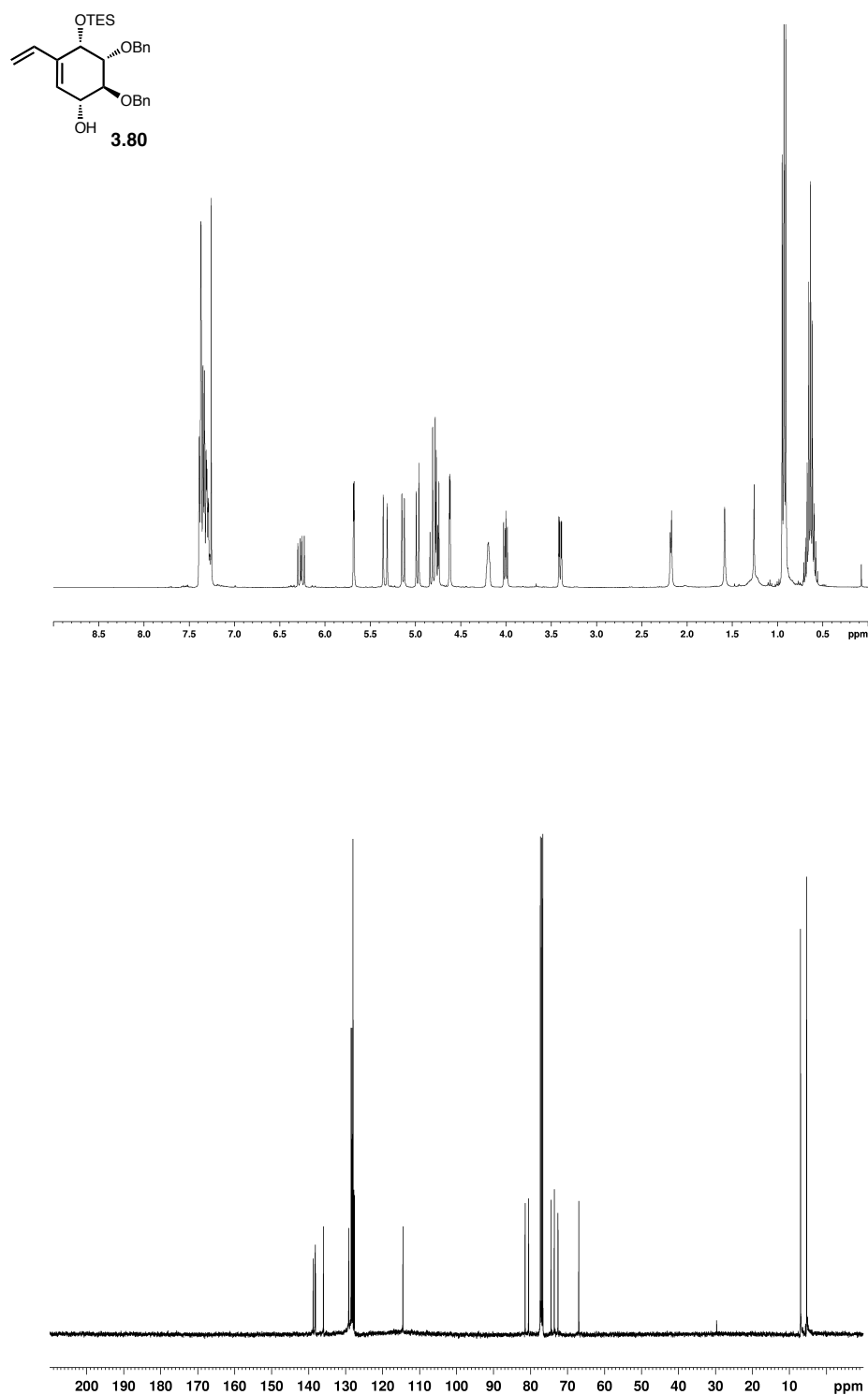


**Figure A1.16.**  $^1\text{H}$  NMR spectrum (400 MHz,  $\text{CDCl}_3$ ) and  $^{13}\text{C}$  NMR spectrum (100 MHz,  $\text{CDCl}_3$ ) of compound **3.80**.

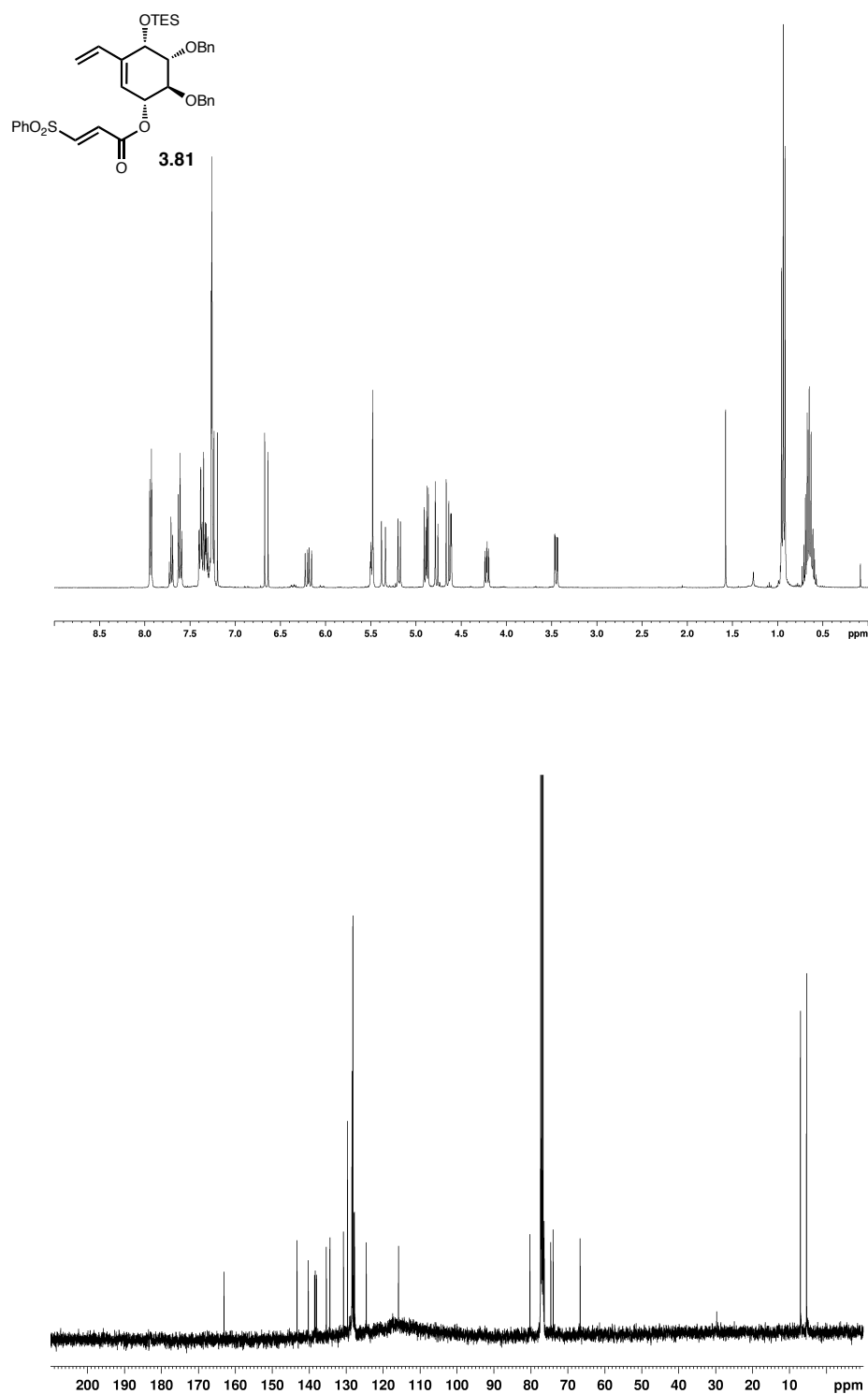


**Figure A1.17.**  $^1\text{H}$  NMR spectrum (400 MHz,  $\text{CDCl}_3$ ) and  $^{13}\text{C}$  NMR spectrum (100 MHz,  $\text{CDCl}_3$ ) of compound **3.81**.

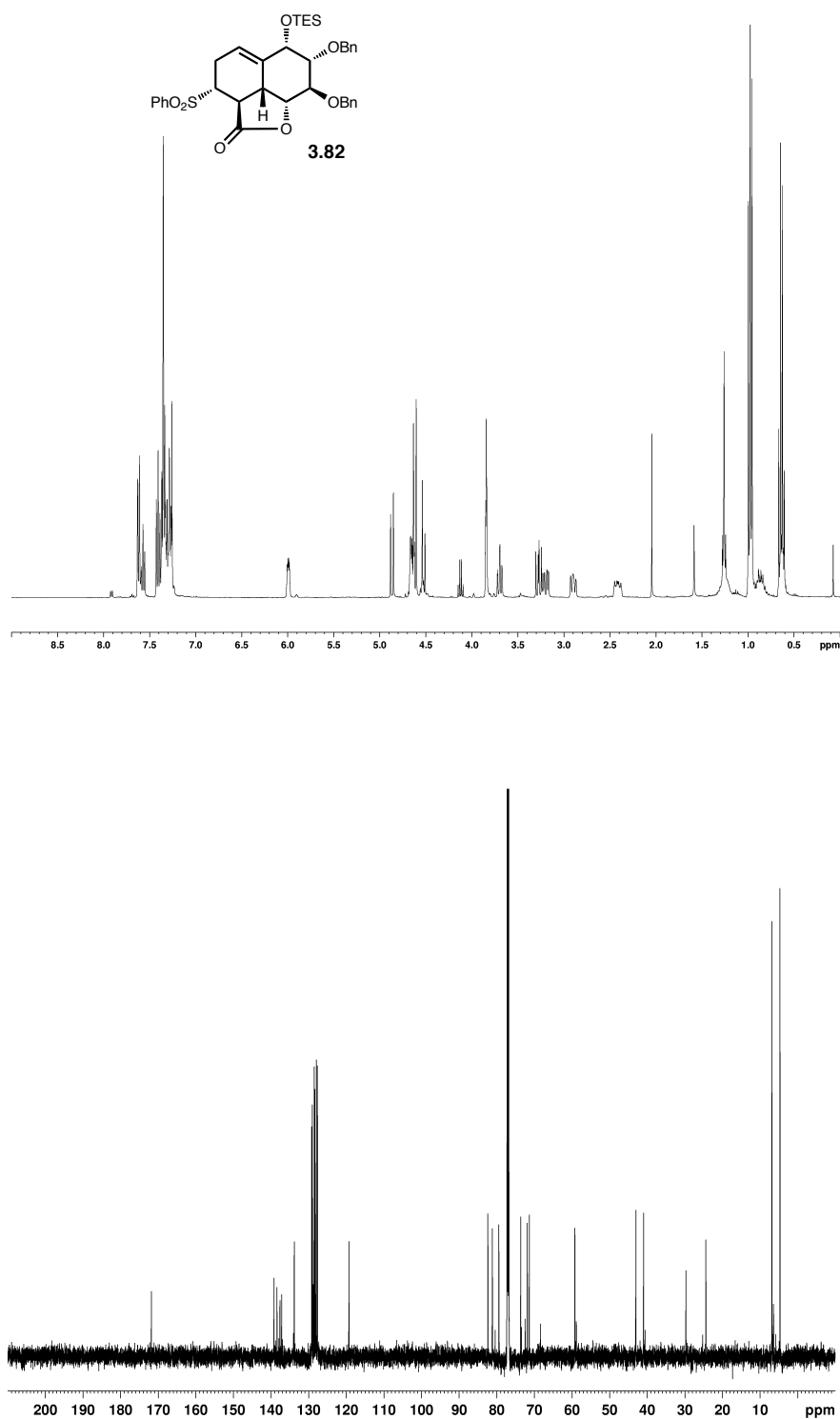


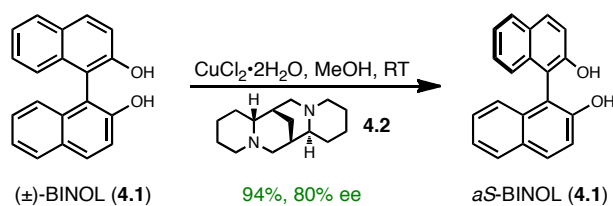
**Figure A1.18.**  $^1\text{H}$  NMR spectrum (400 MHz,  $\text{CDCl}_3$ ) and  $^{13}\text{C}$  NMR spectrum (100 MHz,  $\text{CDCl}_3$ ) of compound **3.82**.

## CHAPTER IV

### A TRANSANNULAR DIELS-ALDER-ENABLED BIOMIMETIC DIMERIZATION APPROACH

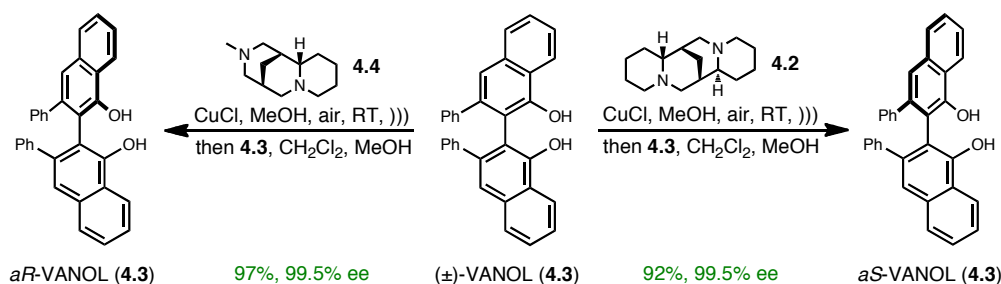
#### Access to Single Biaryl Atropisomers

At this point in our research, the nature and identity of hibarimicin axial chirality was still unknown, and thus a total synthesis of HMP-Y1 (**1.94**) and hibarimicinone (**1.96**) would require access to both atropisomers; however, our initial efforts involving a two-directional synthesis had failed to produce the necessary AB-enone for these purposes. We therefore needed to radically rethink our synthetic strategy while keeping in mind the atropisomerism limitation, and we became interested in the possibility of accessing single atropisomeric products without the need for chromatographic separation of a racemic mixture. To this end, we took notice of work developed by Brussee and applied by Wulff and co-workers involving the deracemization of BINOL and other related biaryl phenol ligands. Brussee and co-workers initially introduced the concept of racemic BINOL (**4.1**) resolution by treatment with a mixture of  $\text{CuCl}_2 \cdot 2\text{H}_2\text{O}$  and (–)-sparteine (**4.2**) in methanol.<sup>1</sup> This method produced *aS*-BINOL (**4.1**) in 94% isolated yield and 80% ee.



**Scheme 4.1.** Brussee's deracemization of BINOL.

Decades later, Wulff and co-workers reported an improved procedure utilizing in situ air oxidation of Cu(I) which was effectively applied to the resolution of vaulted biaryls such as VANOL (**4.3**).<sup>2,3</sup> Thus, with the racemic ligand VANOL (**4.3**), the *aS*-isomer could be isolated in 92% yield and 99.5% ee by deracemization with the Cu(II) complex generated from CuCl and (–)-sparteine (**4.2**). Additionally, by employing the (+)-sparteine surrogate O'Brien's diamine (**4.4**), the *aR*-isomer was isolated in similarly impressive yield and enantiomeric excess.<sup>4</sup>

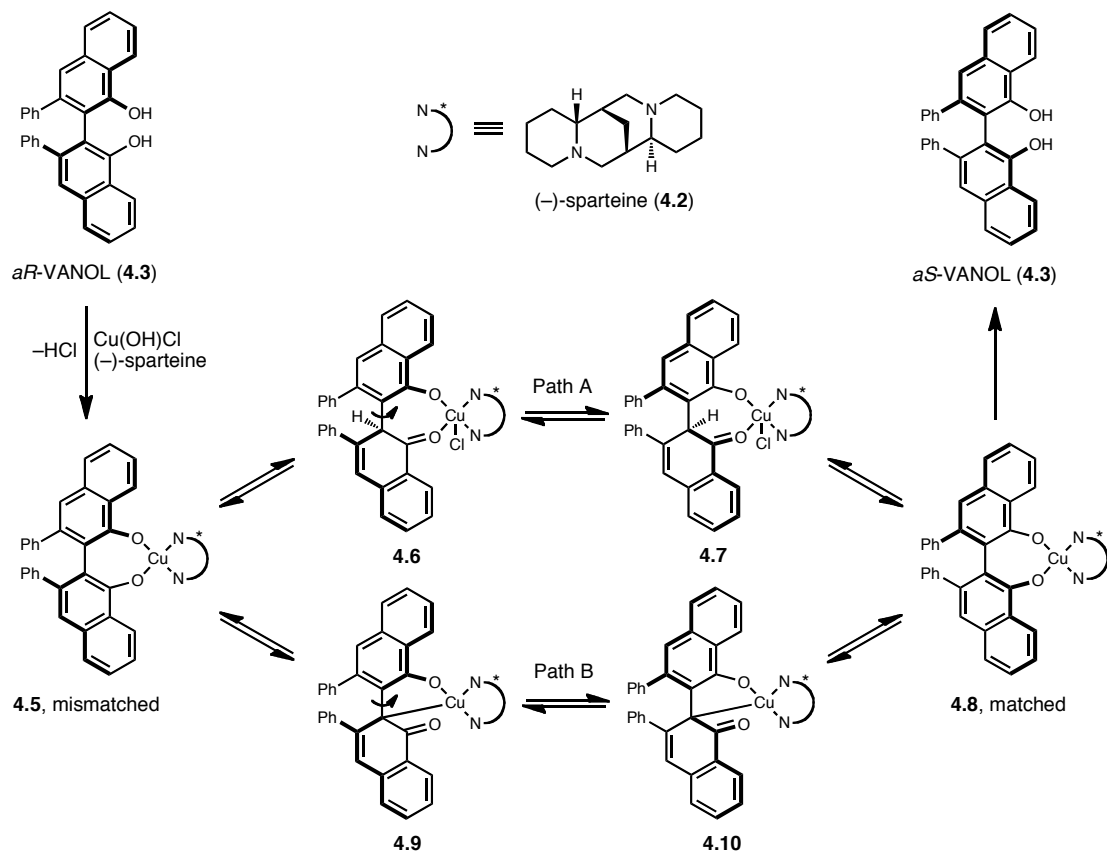


**Scheme 4.2.** Access to pure *aR*- and *aS*-VANOL from a racemic mixture.

As proposed by Wulff, the mechanism of this deracemization is believed to follow the concept of dynamic thermodynamic resolution and relies upon an  $sp^3$ -hybridized intermediate.<sup>5</sup> Kinetic resolution exploits reactivity rates of diastereomeric

intermediates formed from racemic mixtures based on effective differences in  $\Delta G_{\text{activation}}$  and results in only one enantiomer preferentially reacting. Conversely, thermodynamic resolution involves a mechanism for equilibration between two populations of diastereomeric intermediates, which allows almost complete conversion to the thermodynamically favored product based on a matched or mismatched diastereomeric relationship.

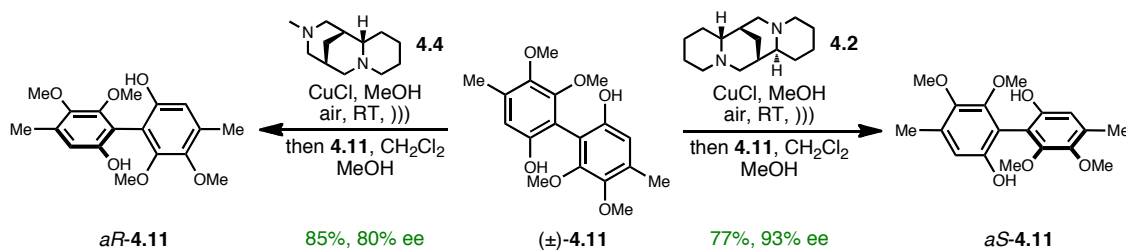
For the specific case of *aR*-VANOL (**4.3**), association with the pre-formed Cu(II)-sparteine complex results in the mismatched intermediate **4.5**. Two paths for interconversion have been proposed based on previously reported analogous systems, and likely both paths contribute under differing conditions. In path A, **4.5** undergoes phenol tautomerization with the addition of HCl which forms an C-sp<sup>3</sup> center that can freely rotate into the more thermodynamically stable conformer **4.7**. Retautomerization arrives at the matched case **4.8**, which dissociates from the Cu(II)-sparteine complex and liberates *aS*-VANOL (**4.3**). Path B alternatively does not require the action of HCl and directly forms a C-Cu quaternary center through phenol tautomerization which similarly to path A undergoes bond rotation to the more thermodynamically stable **4.10**. Retautomerization by C-Cu bond cleavage leads to the matched system **4.8**. And by switching the chiral environment imposed by the ligand, the matched and mismatched cases reverse and thus the *aR*-isomer becomes the thermodynamically favored product.



**Scheme 4.3.** Mechanism of VANOL dynamic thermodynamic resolution.

We believed that the biaryl bis-phenol present in HMP-Y1 provided a perfect substrate for exploitation of this methodology. In this way, a diastereomeric mixture of HMP-Y1 atropisomers or an adequate precursor could be converted to either the *aS*- or the *aR*-atropisomer without the need to utilize chromatographic separation or stereoselective oxidative dimerization. Therefore, to probe the feasibility of this approach, we applied this method to our previously synthesized biaryl bis-phenol **4.11**.<sup>6</sup> When racemic **4.11** was treated under deracemization conditions with (–)-sparteine, we reliably isolated *aS*-**4.11** in good yield and high enantiomeric excess. Similarly, applying

O'Brien's diamine (**4.4**) led to *aR*-**4.11** in high yield and slightly lower ee; however, we were pleased with these results.



**Scheme 4.4.** Dynamic thermodynamic resolution of our model substrate.

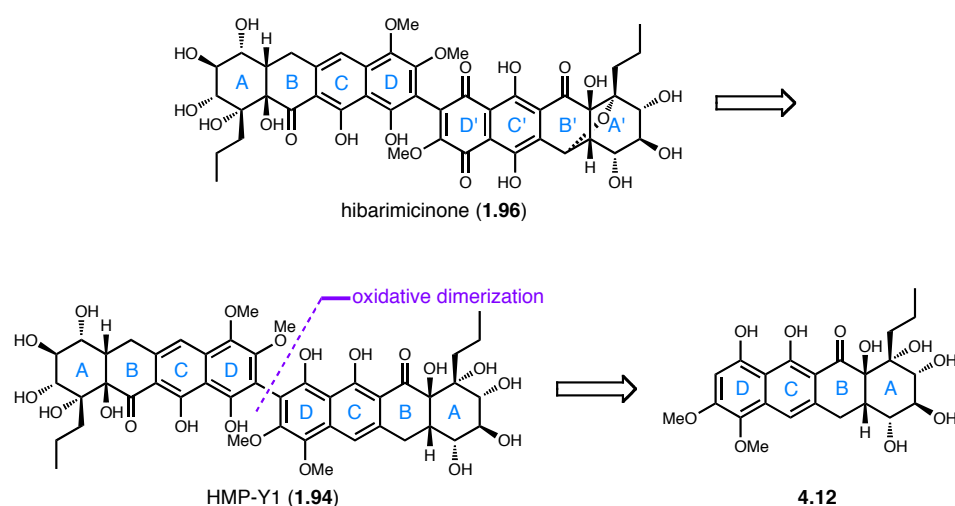
### Biomimetic Dimerization Synthetic Analysis

The results shown in Scheme 4.4 proved significant in developing a synthetic strategy toward HMP-Y1 and hibarimicinone. Our previous difficulties with a two-directional approach now required a novel method of single atropisomer synthesis; however, we still required access to both hibarimicinone atropisomers. Thus, with the developed deracemization protocol, we became free to propose a fresh synthetic scheme that followed nature's lead: a biomimetic oxidative dimerization.

Still targeting the  $C_2$ -symmetric biosynthetic intermediate HMP-Y1 (**1.94**), we proposed the monomeric tetracycle **4.12**, which constitutes each half of HMP-Y1, as a key intermediate target. We believed this tetracycle could significantly improve the efficiency of an ultimate total synthesis of hibarimicinone for a number of reasons. An approach to **4.12** would set up a straightforward route with few transformations to HMP-Y1, in theory only involving oxidative homodimerization. And in order to avoid the



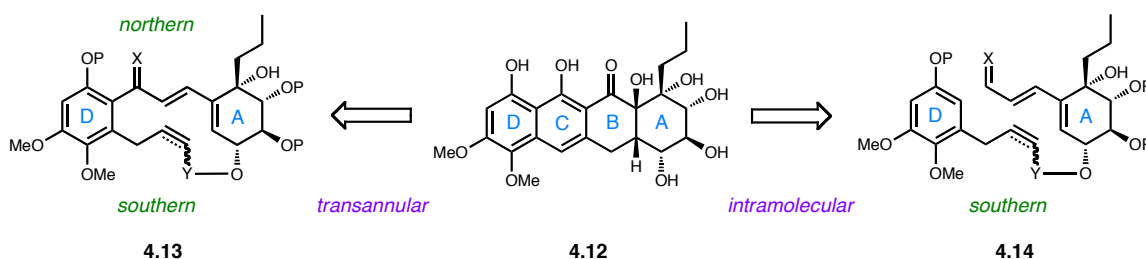
necessity of AB-enone **2.54** synthesis, an alternate two-directional strategy from the central core biaryl dimer would require a large number of doubly processed reactions. Most importantly, our newly developed application of the dynamic thermodynamic resolution negated the need for chromatographic separation and opened the door to perform an unselective dimerization which we predicted would occur in the absence of external chirality, followed by deracemization to both atropisomeric forms.



**Scheme 4.5.** A biomimetic dimerization toward HMP-Y1 and hibarimicinone.

Tetracycle **4.12** provided an array of new options for synthetic schemes, but we chose to remain wedded to our cornerstone Diels-Alder strategy to form the key C-9 stereocenter. We believed this approach would provide rapid access to the tetracyclic monomer considering much of the molecular complexity exists in the A- and D-rings. Additionally, the two key *cis*-decalin stereocenters would then arise from our tethered Diels-Alder and a subsequent substrate controlled ketohydroxylation. Thus, the only constraint necessary for correct C-9 stereocontrol remained tethering to the adjacent  $\alpha$ -

secondary alcohol. This Diels-Alder could then be performed in two distinct modes: transannular (**4.13**), or intramolecular (**4.14**), where the fully functionalized A- and D-rings were tethered with a northern and southern carbon linker or just with a southern linker, respectively. And we proposed the possibility of varying oxidation states at the X variable as well as carbon and non-carbon linkers at the Y position for southern tethering.

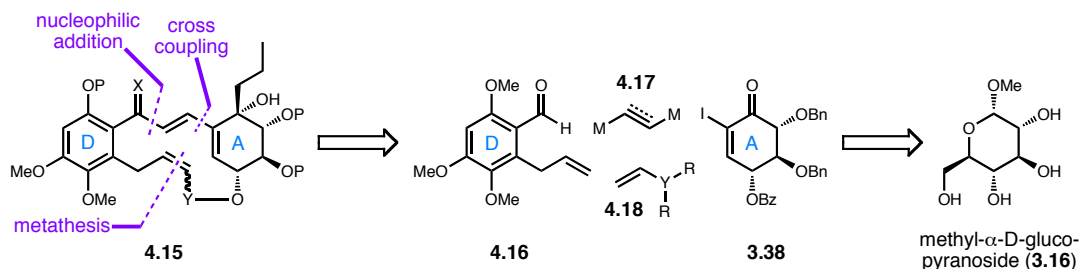


**Scheme 4.6.** A Diels-Alder-enabled strategy to tetracycline **4.12**.

### First Generation TADA Approach

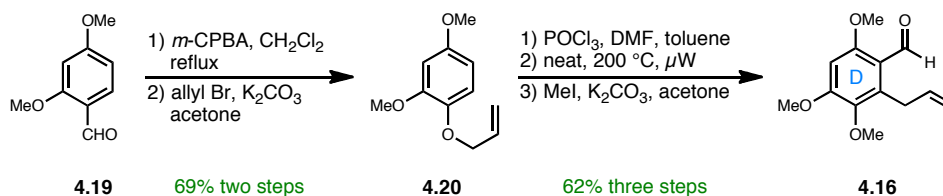
We were drawn initially to the transannular disconnection, not only for its novelty and single-step formation of the tetracyclic framework but also due to the perceived differences in complexity of northern and southern tether formation. Therefore, we targeted formation of the northern bridge first, and we proposed various two and three carbon linker units for this purpose; however, we ultimately settled on a bifunctional reagent that could participate in cross coupling with the vinyl iodide **3.38** and nucleophilic addition to the aryl aldehyde **4.16**, where the order of operations remained flexible. The southern tether was proposed to be formed through metathesis (ring closing

or cross) of a suitably functionalized olefin **4.18** and attachment with the C-10 secondary alcohol.



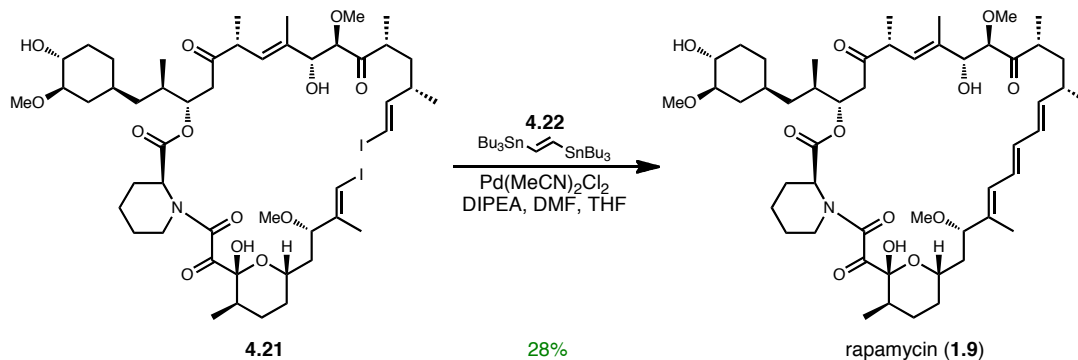
**Scheme 4.7.** Synthetic analysis for assembly of a TADA precursor.

To synthesize the functionalized D-ring **4.16**, a straightforward five step sequence from 2,4-dimethoxybenzaldehyde (**4.19**) was employed that resembled our previous work with the two-directional strategy. Baeyer-Villiger oxidation with *m*-CPBA with a hydrolytic workup provided the phenol which was allylated to provide **4.20**.<sup>7</sup> We found that regioselective Vilsmeier-Haack formylation occurred readily on the allyl ether **4.20**, and the aryl aldehyde proved stable to high temperatures necessary for inducing a Claisen rearrangement.<sup>8</sup> Finally, the resulting phenol was methylated to provide the fully functionalized D-ring **4.16** in high yield on decagram scale.



**Scheme 4.8.** Synthesis of the D-ring aryl aldehyde.

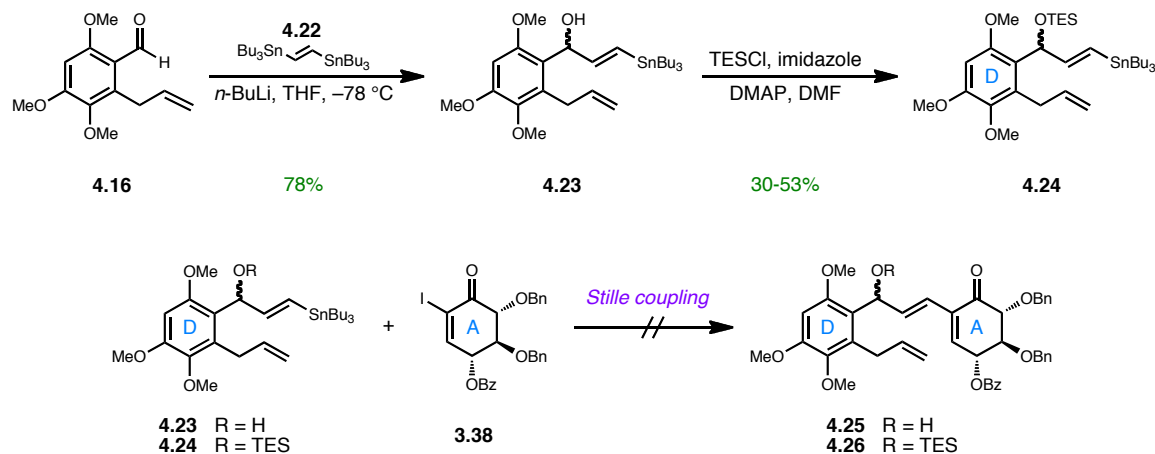
With the aryl aldehyde **4.16** in hand, we sought out the use of a bifunctional ethylene reagent for connecting the aldehyde and vinyl iodide **3.38**. And two specific pieces of work led us to our first northern tether candidate. In Nicolaou and co-workers' synthesis of rapamycin (**1.9**), they utilized a highly unique method for macrocyclic ring closure, specifically through a "stitching" reaction with *trans*-1,2-bis(tributylstannyl) ethylene (**4.22**).<sup>9</sup> And while our approach did not directly map onto Nicolaou's precedent, we consequently considered Corey's demonstration that **4.22** could be reliably mono-lithiated with *n*-BuLi.<sup>10,11</sup> Thus, the homo-disubstituted ethylene reagent suited both of our needs for a nucleophilic reagent also capable of undergoing cross coupling.



**Scheme 4.9.** Nicolaou's "stitching-cyclization" method for rapamycin.

We quickly optimized conditions for mono-lithiation of **4.22** and its addition into the aldehyde **4.16** which provided the secondary alcohol **4.23** as an inconsequential mixture of diastereomers. The resultant secondary alcohol was protected as its TES ether **4.24**, but unfortunately the reaction suffered in yield largely due to proto-destannylation to form the terminal olefin. Nevertheless, we attempted Stille coupling with both the free

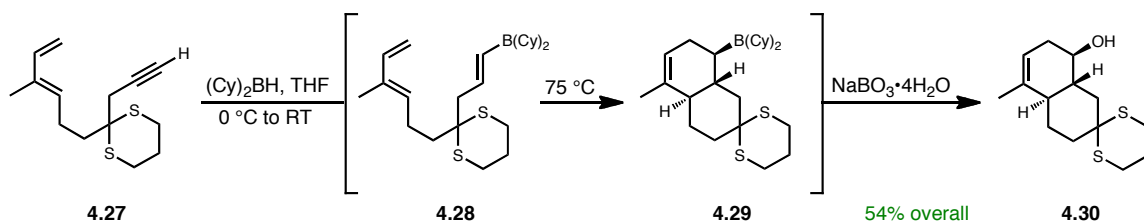
and protected alcohols **4.23** and **4.24**, however, no cross coupling of either substrate was observed. While this approach ultimately failed, necessary large quantities of the high molecular weight bis(tributylstannyl)ethylene **4.22** made the sequence less than desirable for long-term application.



**Scheme 4.10.** Unsuccessful Stille coupling toward the northern tether.

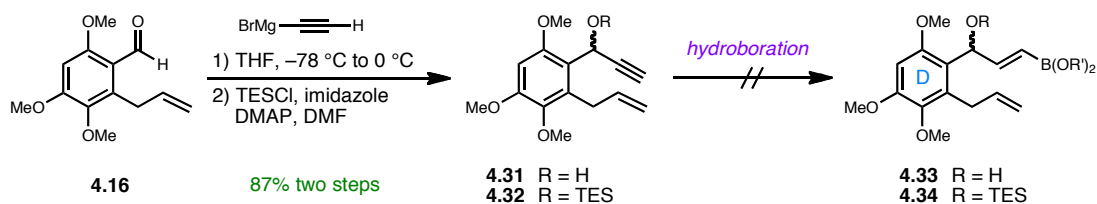
We next turned to an alternative two carbon nucleophile that would require elaboration prior to reaction with the vinyl iodide **3.38**. Reasoning that an alkyne unit could undergo hydroboration for ultimate Suzuki coupling, we considered a publication by Singleton and co-workers that demonstrated chemoselective hydroboration of a terminal alkyne without reaction with a terminal olefin.<sup>12</sup> In this example, hydroboration of **4.27** with dicyclohexylborane led to the *trans*-vinylborane **4.28** which was characterized in situ and subsequently heated to effect an IMDA reaction to arrive at the *trans*-decalin **4.29**. Finally, oxidation with sodium perborate yielded the secondary

alcohol **4.30** in 54% overall yield. We believed a similar approach to an intermediate aryl enyne derivative would enable Suzuki coupling with vinyl iodide **3.38**.



**Scheme 4.11.** Singleton's chemoselective hydroboration.

Following Singleton's precedent, nucleophilic addition of ethynyl Grignard to aldehyde **4.16** yielded the propargylic alcohol **4.31** as an inconsequential mixture of diastereomers in excellent yield, and the secondary alcohol was protected as its TES ether **4.32** in analogy to the previous sequence. We then investigated various hydroboration conditions with both the free (**4.31**) and TES-protected (**4.32**) alcohols hoping to find chemoselectivity for the alkyne over the alkene but to no avail.



**Scheme 4.12.** Failed alkyne hydroboration for Suzuki coupling.

Our progress with a “D-ring-first” approach was ultimately limited by intermediate instability and chemoselectivity issues, and in light of our previous

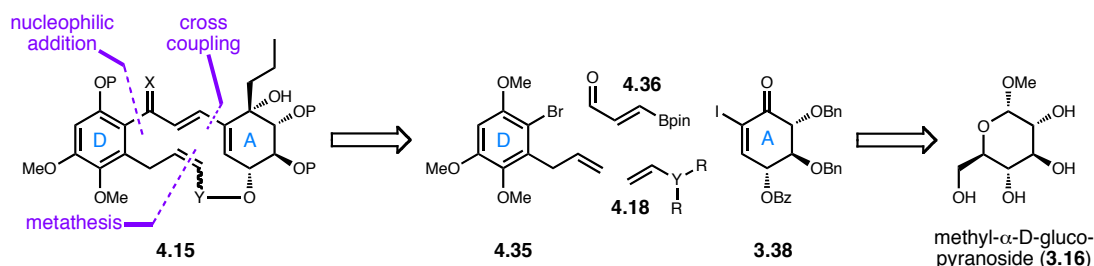
successes with vinyl iodide cross coupling, we decided to pursue an “A-ring-first” strategy where the aryl ring would be appended last. This design, however, would require an alternative linker unit if we specifically intended to implement a Suzuki cross coupling reaction.

### Second Generation TADA Approach

Previous studies had shown robust capability for vinyl iodide **3.38** to undergo Suzuki cross coupling reaction with vinyl boronic acid. In analogy to our failed alkyne hydroboration approach, a functionalized vinyl boronate could be utilized in a Suzuki cross coupling followed by unification with a suitable aryl moiety. We decided to revert back to boron as our metal of choice and discounted bis(tributylstannyl)ethylene **4.22** for several key reasons. While “stitching” reactions enjoyed various successes, we did not believe that a mono-Stille coupling was feasible and would likely result in quantities of dimerized products. Additionally, tin-lithium exchange of a more highly functionalized vinyl tin substrate with multiple electrophilic centers posed serious challenges. Therefore, we targeted 3-boronoacrolein (**4.36**) and its intermediates as 3-carbon donors for unification of the A- and D-rings.

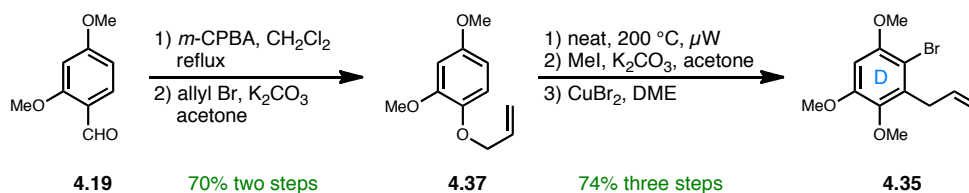
This strategy required slight modification of our aryl ring substrate to reflect switching of the electrophilic and nucleophilic components, and aryl bromide **4.35** was proposed. Again, analogous to our first attempts at the TADA precursor **4.15**, the order of reaction remained flexible and the approach to the southern tether remained unchanged. And our confidence with the proposed Suzuki cross coupling meant that our final

northern tether hurdle would involve appending the aryl ring **4.35** to the functionalized A-ring moiety.



**Scheme 4.13.** Second generation TADA synthetic analysis.

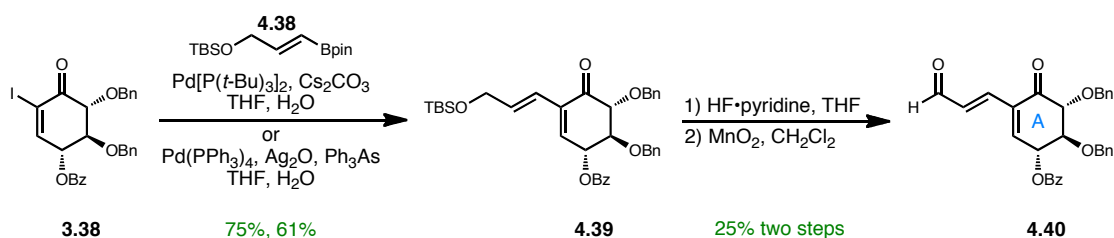
Synthesis of the modified D-ring closely followed our previous assembly of the aryl aldehyde **4.16** starting with 2,4-dimethoxybenzaldehyde (**4.19**). Baeyer-Villiger oxidation provided the phenol which was transformed to the allyl ether **4.37** through standard conditions. Heating the neat allyl ether **4.37** at 200 °C via microwave irradiation cleanly provided the Claisen-rearranged product, and the resulting phenol was methylated. Finally, regioselective bromination with  $\text{CuBr}_2$  in DME at room temperature for 48 hours provided the functionalized D-ring **4.35** with handles for both northern and southern tether formation.



**Scheme 4.14.** Synthesis of the aryl bromide.



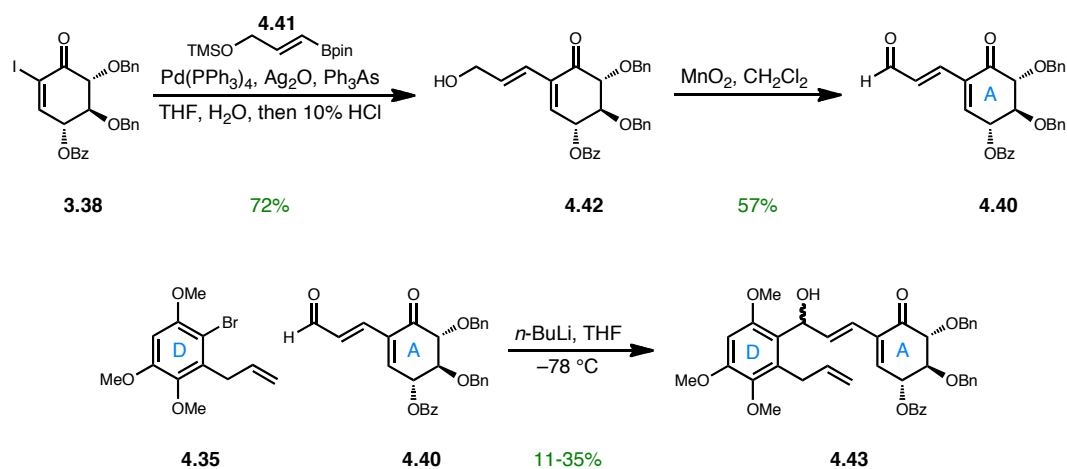
We now had in hand our proposed A- and D-rings, and we moved to determine effective conditions for unification with 3-boronoacrolein (**4.36**). Thus, Suzuki cross coupling with the bifunctional linker **4.38** was effected under two differing sets of conditions previously optimized for earlier substrates.<sup>13</sup> Ultimately, although Pd(PPh<sub>3</sub>)<sub>4</sub> provided dienone **4.39** in slightly lower yield, we elected to proceed with these conditions due to complications with removal of Pd[P(*t*-Bu)<sub>3</sub>]<sub>2</sub> and presumed long-term product stability in its presence. Surprisingly, we met complications with silyl ether deprotection which with either TBAF or HF•pyridine provided the free alcohol in highly variable yields. Nevertheless, allylic oxidation with MnO<sub>2</sub> arrived at the desired three-carbon functionalized aldehyde **4.40** in reasonable yield. This compound contained important functionality for upcoming steps, namely the electrophilic aldehyde for aryl ring attachment and the diene necessary for our cornerstone transannular Diels-Alder reaction.



**Scheme 4.15.** Synthesis of the tethered A-ring.

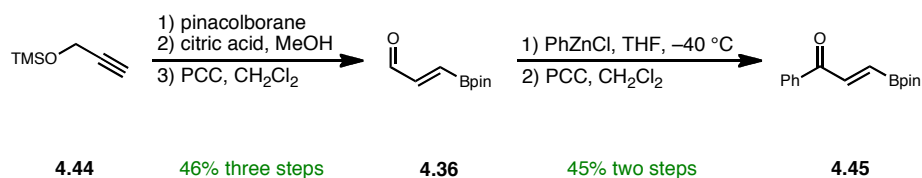
Although we had successfully assembled the desired A-ring **4.40** with three-carbon linker, material throughput remained low due to problematic silyl ether deprotection. Therefore, we devised an improved Suzuki cross coupling partner in which the TBS ether was substituted for a more highly labile TMS ether. Synthesis of the TMS

ether **4.41** required slight modification from literature procedures which traditionally utilized immediate TMS-deprotection following hydroboration of the requisite TMS-propargylic alcohol; however, we found that concentration and direct distillation of the reaction mixture provided the desired TMS reagent **4.41** in reasonable reproducibility.<sup>14,15</sup> And with a simple acidic workup following Suzuki coupling, the allylic alcohol **4.42** was isolated in good yield for the two steps. In this way, we removed the necessary additional deprotection step, and allylic oxidation again arrived at the functionalized aldehyde **4.40** for coupling. Finally, with both building blocks in hand, we attempted nucleophilic addition of an aryl-lithiate of **4.35** to the aldehyde **4.40** and were met with disappointing yield for formation of the northern-tethered product **4.43**. However, retrospectively, we should not have been surprised by this result, as the aldehyde **4.40** contained numerous other electrophilic centers that likely contributed to other undesired products.



**Scheme 4.16.** Improved synthesis of the A-ring aldehyde and tethering.

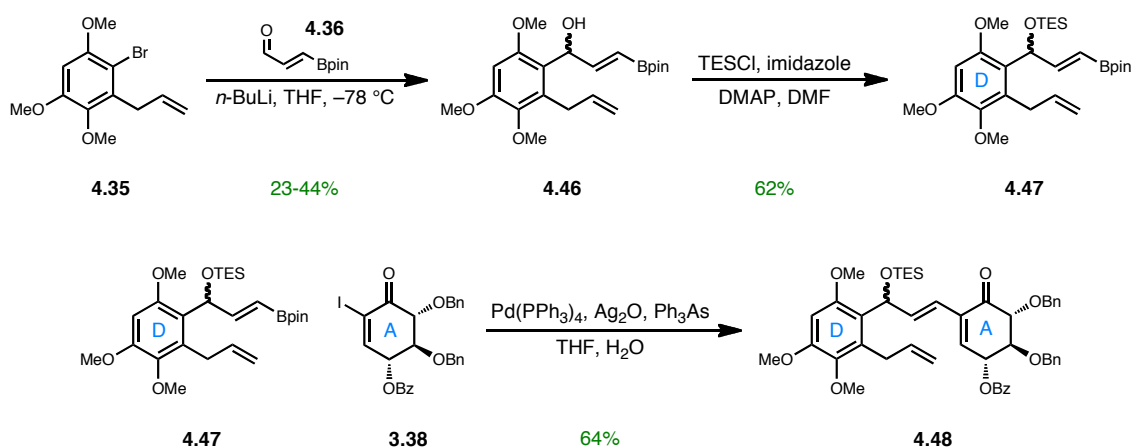
With the results of Scheme 4.16 in mind, we sought to reverse the order of tether formation in hopes of improving nucleophilic aryl addition regioselectivity. Aldehyde **4.36** has a relatively limited scope when considering nucleophilic additions but has been more highly utilized in aldol and Diels-Alder chemistry.<sup>14,16</sup> However, Vaultier and co-workers reported on zinc nucleophile addition to aldehyde **4.36**, which was synthesized in three steps from TMS-propargylic alcohol **4.44** by hydroboration, TMS deprotection, and PCC oxidation.<sup>17</sup> Addition of phenylzinc chloride provided an intermediate benzylic alcohol which was finally oxidized with PCC to the ketone **4.45** in good overall yield. Notably, lithium and magnesium nucleophiles suffered poor yields in the addition to **4.36** presumably due to competitive addition to the electrophilic boronate center.



**Scheme 4.17.** Vaultier's arylzinc addition to aldehyde **4.36**.

Our synthesis of the aldehyde linker **4.36** was modified slightly from that of Vaultier, namely in oxidation to the aldehyde in which we utilized DMP instead of PCC. Use of the aldehyde posed numerous technical problems including instability, difficulty with drying due to its low molecular weight, and complications with residual acid removal from the use of DMP. These issues manifested themselves in an unfortunately low yield of the aryl lithiate addition to provide the secondary alcohol **4.46**, ranging from 23 to 44%. Attempts at alcohol oxidation as shown in Scheme 4.17 were ultimately

unsuccessful, and we therefore elected for silyl ether protection to provide **4.47** in reasonable yield. We were pleased to finally observe synthesis of the northern-tethered product **4.48** through Suzuki reaction of the two coupling partners **4.47** and **3.38** in good yield. A big picture view of Scheme 4.18, however, showed problems with aryl addition to the aldehyde linker, and we recognized the limitations that this route would impose on large scale synthesis of **4.48**. Regrettably, we failed to investigate the exact conditions laid out by Vaultier for smooth aryl zinc addition to aldehyde **4.36** or their use of PCC for pre- and post-nucleophilic addition oxidation.



**Scheme 4.18.** Alternate order for northern tethering.

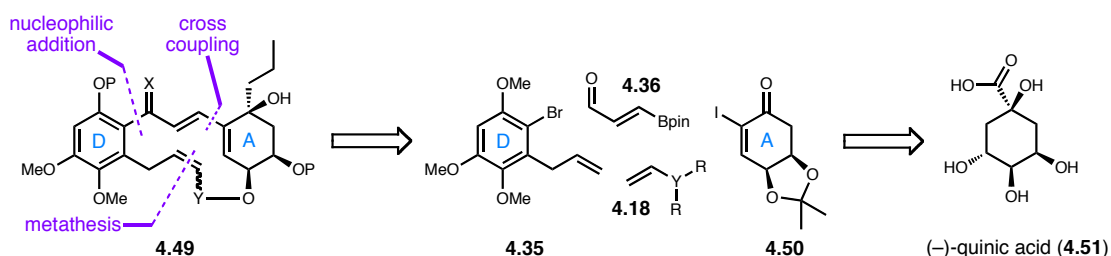
The roadblocks presented in both northern tether routes in Scheme 4.16 and Scheme 4.18 appeared difficult to overcome without a major redesign of our synthetic strategy. We hoped to move away from aryl addition to the aldehyde linker **4.36**, but aryl addition to the functionalized A-ring aldehyde suffered from lack of chemoselectivity. We had in hand two different D-ring surrogates appended with both electrophilic and

nucleophilic functionalities, but at this point, we had not considered modifications to a vinyl iodide A-ring. Thus, we set out to simplify functionalities present in the A-ring to facilitate unification with the D-ring for an ultimate transannular Diels-Alder reaction.

### A New A-Ring Surrogate from Quinic Acid

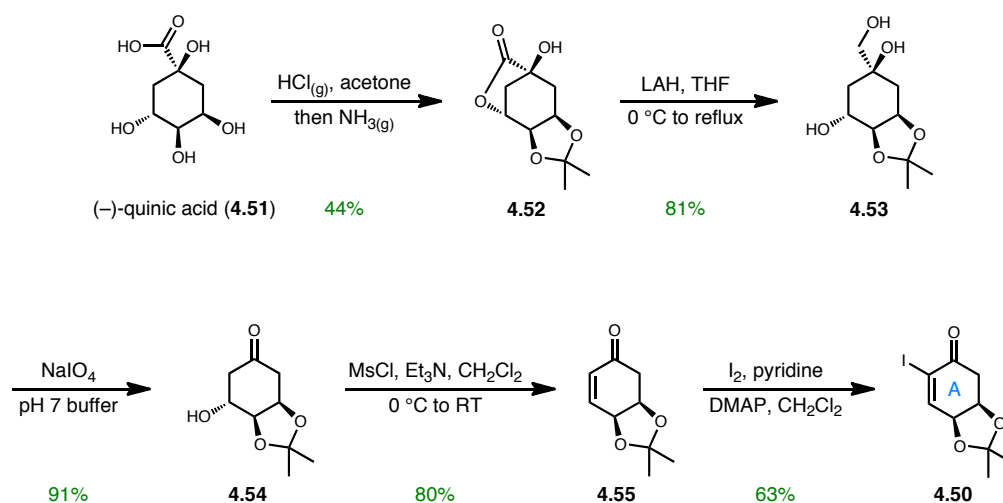
Iodo enone **3.38** contained three of the six contiguous stereocenters found in HMP-Y1; however, we believed our forward progress toward the macrocyclic TADA precursor was hampered by the extensive functionality present including multiple electrophilic centers. Additionally, the absolute stereochemistry of HMP-Y1 and hibarimicinone remained unknown at this point, and we saw no reason to remain wedded to a single final enantiomer when no data existed to suggest one over the other. Therefore, we saw numerous advantages to completely reimagining a route to a similar vinyl iodide for cross coupling. First, we were eager to shed the five-step sequence from methyl- $\alpha$ -D-glucopyranoside to the Vasella precursor **3.32** in which each step required large-scale chromatography. Also, we hoped to identify a readily-available starting material that contained fewer reactive functional groups and could foreseeably be transformed into the desired A-ring. Finally, we sought out a starting material that had previously been utilized for synthesis of a similar vinyl iodide to **3.38**, and fortunately, our laboratory had experience with utilizing (–)-quinic acid in a similar sequence to synthesize a highly analogous iodo-enone **4.50**.<sup>18</sup> Notably, the C-10 stereocenter (hibarimicin numbering) necessitated synthesis of the opposite hibarimicinone enantiomer compared to the methyl- $\alpha$ -D-glucopyranoside route, but again at this point in

our research, this change was of no consequence considering our lack of absolute stereochemical knowledge. Thus, our retrosynthetic analysis toward the macrocyclic TADA precursor **4.49** remained largely the same, but several key features were modified. We had removed the C-12 secondary alcohol stereocenter, and the C-11 alcohol would require inversion to the correct hibarimicinone relative stereochemistry, but most importantly, iodo-enone **4.50** contained only minimal necessary functionality for speeding our progress toward the macrocycle **4.49**.



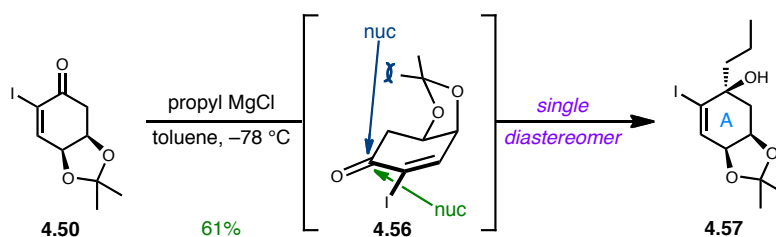
**Scheme 4.19.** TADA synthetic analysis from (–)-quinic acid.

Following literature precedent, (–)-quinic acid was subjected to acetonide-forming conditions on large scale to arrive at the acetonide-lactone **4.52** which was followed by global reduction with LAH forming triol **4.53**.<sup>19</sup> Oxidative cleavage of the 1,2-diol in **4.53** led to  $\beta$ -hydroxy ketone **4.54**, and mesylation/elimination readily occurred to form enone **4.55**.<sup>20</sup> Finally, similar conditions to those utilized in our previous approaches installed the  $\alpha$ -iodo enone in good yield. Importantly, the five-step sequence shown in Scheme 4.20 required only two chromatographic purifications, for the final two steps, and we reliably produced decagram quantities of **4.50** for each batch.



**Scheme 4.20.** Synthesis of a (-)-quinic acid-derived iodo-enone.

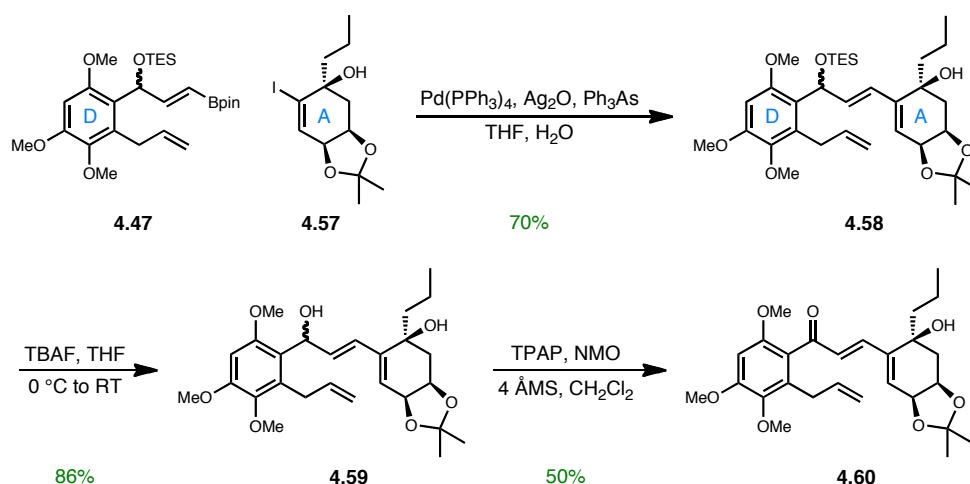
Iodo-enone **4.50** highly resembled the previously utilized iodo-enone **3.38** derived from methyl- $\alpha$ -D-glucopyranoside, and we were curious about installation of the C-13 tertiary alcohol present in hibarimicinone. Because we hoped to functionalize the ketone in **4.50** prior to northern tether formation, we targeted the iodo-enone for three-carbon unit nucleophilic addition. We began with the necessary functionality by using propylmagnesium chloride in THF at  $-78\text{ }^{\circ}\text{C}$ , and interestingly, we observed 1,4-addition as the major product. Seeking modifications, we employed Baran's use of toluene as a solvent for Grignard addition, and we were ecstatic to not only observe primarily 1,2-addition to **4.50** but also essential formation of a single desired diastereomer.<sup>21</sup> This result can be easily rationalized due to severe steric interactions with the acetonide moiety in the pseudo-equatorial transition state **4.56** for  $\beta$ -face addition.<sup>22</sup> Thus, we had overcome the major hurdle present in our two-directional strategies and contrastingly directly installed the necessary propyl unit in high yield and with complete stereoselectivity.



**Scheme 4.21.** Selective C-13 stereocenter formation.

Now that we had access to quantities of the (–)-quinic acid-derived A-ring **4.57**, we elected to attempt northern tether formation with our previously synthesized vinyl boronate **4.47** under our standard Suzuki coupling conditions. We were pleased to observe high yield for this cross coupling reaction to form the A-D linked product **4.58**, and we pushed this material forward through silyl ether deprotection and benzylic alcohol oxidation to the  $\alpha,\beta$ -unsaturated ketone **4.60**. With this northern tethered compound **4.60**, we envisioned multiple possibilities for macrocyclic closure by southern tether formation; however, our major hurdle remained producing quantities of the vinyl boronate **4.47** which suffered from low yields in the aryl addition to the aldehyde linker **4.36**. Thus, we reasoned that reversing the order of operations, analogous to Scheme 4.16, could improve these problems as long as the route from vinyl iodide **4.57** to an  $\alpha,\beta$ -unsaturated aldehyde occurred with good yields.



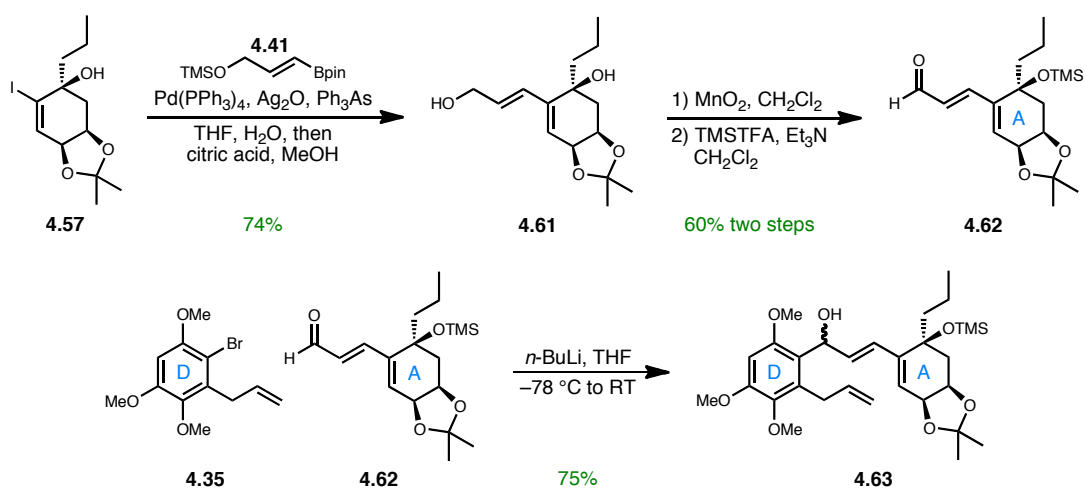


**Scheme 4.22.** Northern tether formation with the (–)-quinic acid-derived A-ring.

To reverse operation order, we reverted to Suzuki cross coupling between the vinyl iodide **4.57** and the vinyl boronate linker **4.41** which occurred smoothly, and under the reaction conditions, some of the TMS ether was deprotected. Therefore, the crude reaction mixture was stirred with citric acid in methanol to effect the remainder of TMS removal, and the allylic alcohol **4.61** was isolated in high yield. A two step sequence of allylic oxidation and tertiary alcohol protection as the TMS ether with TMSTFA worked well to arrive at the linker-installed A-ring **4.62** for northern tether formation with the aryl bromide **4.35**.<sup>23</sup> In this way, we now had optimized routes for large scale production of both A- and D-ring surrogates in decagram quantities with no severely limiting steps, and we were hopeful about our chances to effect tethering with the new minimally functionalized A-ring **4.62**.

After significant experimentation, we successfully united **4.35** and **4.62** to provide the northern-tethered allylic alcohol **4.63** as a mixture of diastereomers in excellent yield. For the success of the reaction, both starting materials and solvent required rigorous

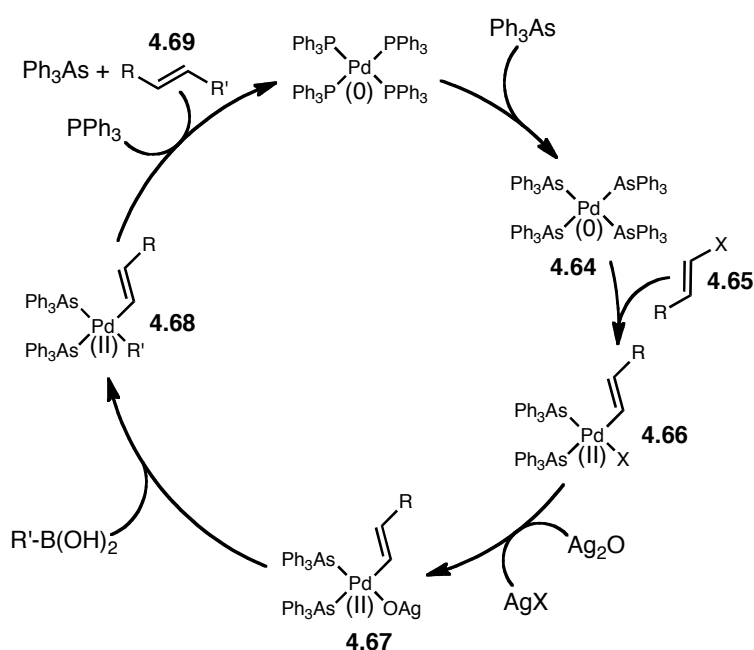
drying, and the reaction proceeded slowly enough to require stirring overnight at room temperature before full starting material consumption. We were elated by this result, as we had finally synthesized an A-D linked intermediate in high yield, and this reaction was easily increased to multi-gram scale. We could then foresee numerous paths forward for southern tether linking, with the terminal olefin and *cis*-diol functionalities as key handles for macrocycle formation.



**Scheme 4.23.** Improved synthesis of the A-ring aldehyde and tethering.

Our most successful Suzuki cross coupling conditions utilize two reagents less common to the reaction in triphenylarsine and silver(I) oxide. Triphenylarsine has been shown to be advantageous in the transmetallation step due to its lower coordinating strength to palladium as compared with triphenylphosphine.<sup>24</sup> Silver oxide has also been reported to improve the reactivity of boronic acids in Suzuki couplings, and thus the likely mechanism is shown in Scheme 4.24.<sup>25</sup> Beginning with tetrakis (triphenylphosphine)-palladium(0), ligand exchange with triphenylarsine provides the

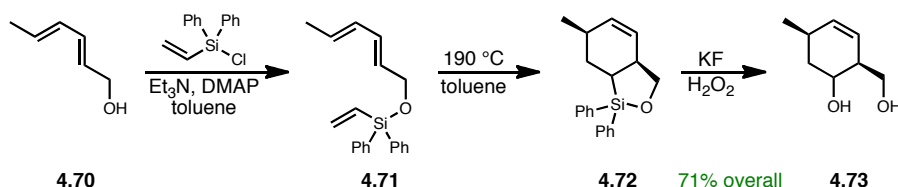
activated  $\text{Pd}(\text{Ph}_3\text{As})_4$  catalyst (**4.64**) which undergoes oxidative insertion with the vinyl halide **4.65**. The palladium(II) intermediate **4.66** undergoes anion exchange, and the intermediate **4.67** is set up for transmetalation with the boronic acid. The di-alkylpalladium(II) intermediate **4.68** then undergoes reductive elimination to provide the disubstituted olefin **4.69**, completing the catalytic cycle, and regenerating the palladium(0) catalyst.



**Scheme 4.24.** Mechanism of Suzuki cross coupling of vinyl halides.

Our southern tether strategy stemmed from precedent shown for previous IMDA reactions involving a silicon linker, where the silicon group could be easily removed following ring closure. In the case of work by Sieburth and co-workers, primary alcohol **4.70** was silylated with vinyl diphenylchlorosilane, and the resulting triene **4.71** was heated in toluene to effect IMDA reaction.<sup>26</sup> The bicyclic product **4.72** was then

subjected to Tamao-Fleming oxidation conditions to provide the diol **4.73** in a 1:1 mixture of diastereomers. And although our strategy would require C-Si bond reduction, we hoped to follow this general approach.



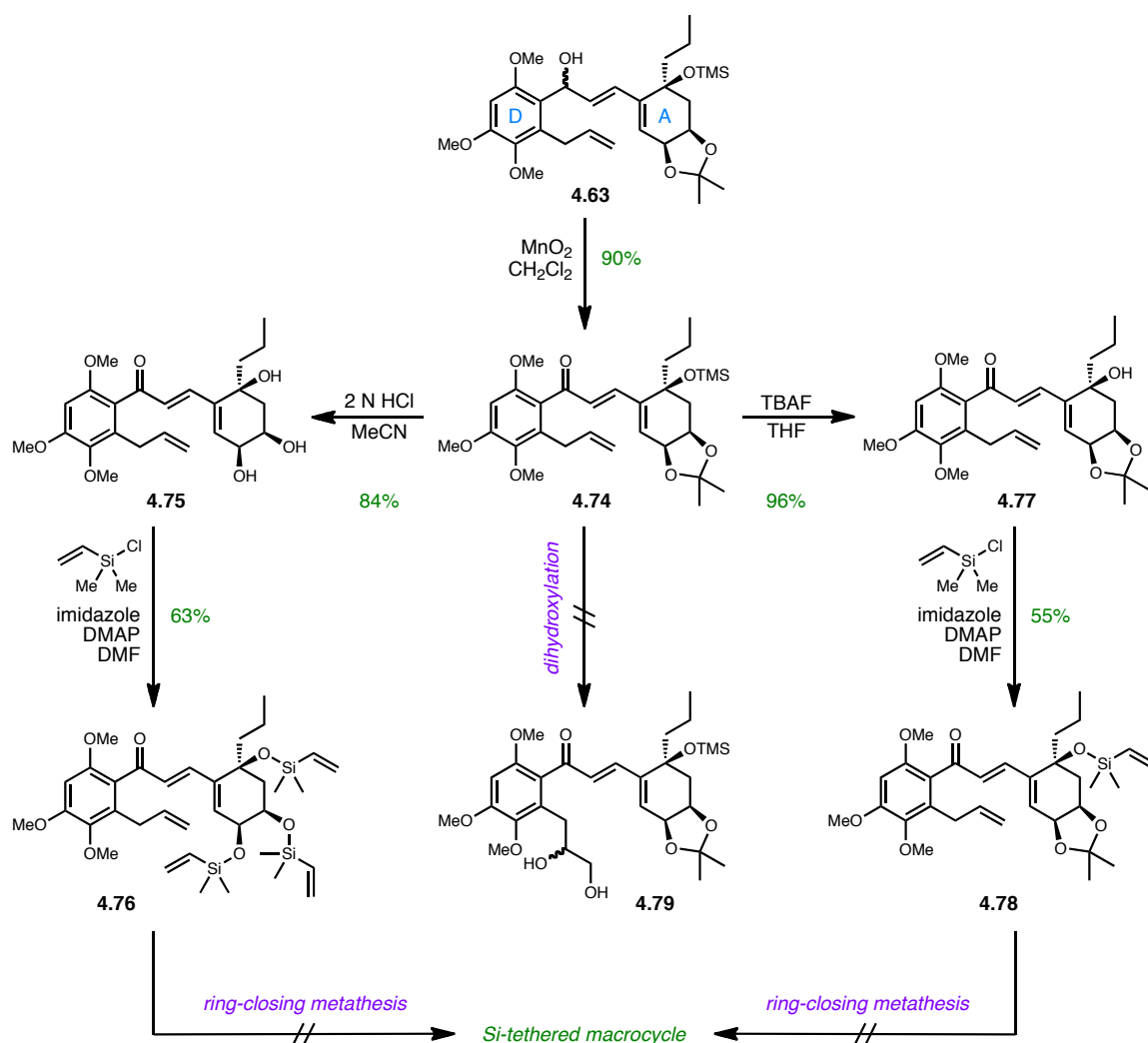
**Scheme 4.25.** Sieburth's silyl-tethered IMDA/Tamao-Fleming sequence.

We first elected to oxidize the resultant mixture of diastereomers through allylic oxidation with  $\text{MnO}_2$  so as to more easily operate with a single diastereomer, and we arrived at the  $\alpha,\beta$ -unsaturated ketone **4.74** in high yield. From ketone **4.74**, we hoped to unmask the *cis*-diol functionality through acetonide deprotection, and treatment of **4.74** with 2 N HCl in acetonitrile effectively led to triol **4.75**. From this intermediate, we hoped to regioselectively install a vinyl moiety for macrocyclic ring closing metathesis. A vinyl silicon linker was chosen for its ease of removal following the proposed transannular Diels-Alder reaction. Unfortunately, even after sequential investigation of the number of silyl chloride equivalents necessary, we observed only formation of the tri-siloxane **4.76**. Undeterred, we reasoned that the two extra vinyl-silane functionalities posed minimal threat to a potential ring closing metathesis reaction; however, under various tested conditions we never observed an indication of macrocycle formation.

Considering that all three alcohols present on the A-ring possessed the correct orientation necessary to direct facial selectivity in the TADA, we made a slight leap by

forming the tertiary vinyl-silane **4.77** in hopes of effecting formation of a bridged macrocycle. Again, we were met with disappointment, and under numerous conditions for ring closing metathesis, no macrocycle ever formed.

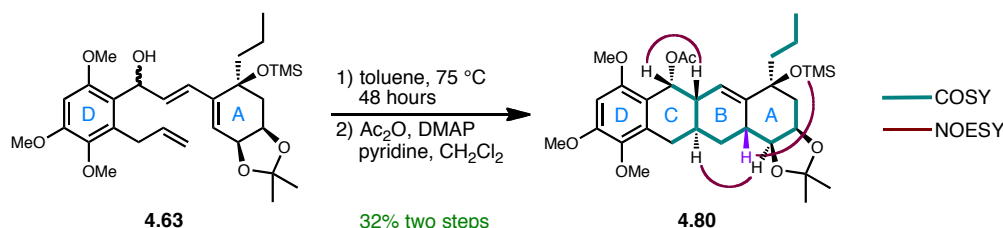
At this point, we acknowledged the difficulty of relying on regioselective vinyl-moiety attachment on the requisite *cis*-diol, and we began to investigate terminal olefin functionalization. We reasoned that an alkyne would open numerous doors to modification due to its ability to undergo deprotonation, and thus we screened dihydroxylation conditions including classic Upjohn and Sharpless conditions but to no avail. Although the terminal olefin would be predicted to be most reactive on electronic and steric rationales, we believe that cross reactivity with the other two olefins in **4.74** led to complex mixtures of products. Additionally, attempted cross metathesis with vinylchlorosilanes ultimately failed as well.<sup>27,28</sup> With these disappointing results, we elected to take a step back and focus on a simpler substrate for dihydroxylation which we reasoned could ultimately be converted to the desired terminal alkyne to which **4.79** would ultimately lead.



**Scheme 4.26.** Failed attempts toward southern tether formation.

Before we abandoned the northern-tethered terminal olefin substrate **4.63**, we became intrigued to determine the innate stereoselectivity of an intramolecular Diels-Alder reaction to either confirm or contradict our predictions for the C-9 bridgehead center. After some experimentation, we began to observe cyclization of the allylic alcohol substrate **4.63** when heated in toluene at 75 °C, and full starting material consumption had occurred within 48 hours. The major product of the reaction was isolated in 34%

yield (we believe the remainder of the mass balance underwent cyclization followed by dehydration of the free secondary alcohol based on crude NMR), and the product was acetylated to facilitate characterization. Ultimately, we had formed the ABCD tetracycle **4.80** with the undesired C-9 stereochemistry which was confirmed by extensive 2-D NMR and readily apparent through a NOESY correlation of the C-9 hydrogen with the TMS group. Additionally, NOESY correlations and coupling constants were used to assign the remaining stereocenters, and noting that **4.80** was isolated as a single diastereomer, the  $\beta$ -secondary alcohol presumably made up a portion of the dehydrated material. This result confirmed our suspicions regarding facial approach of the olefin dienophile in which the acetonide strongly directs the olefin to the  $\alpha$ -face of the diene and provided further support for the southern tether as imperative to Diels-Alder stereochemistry.



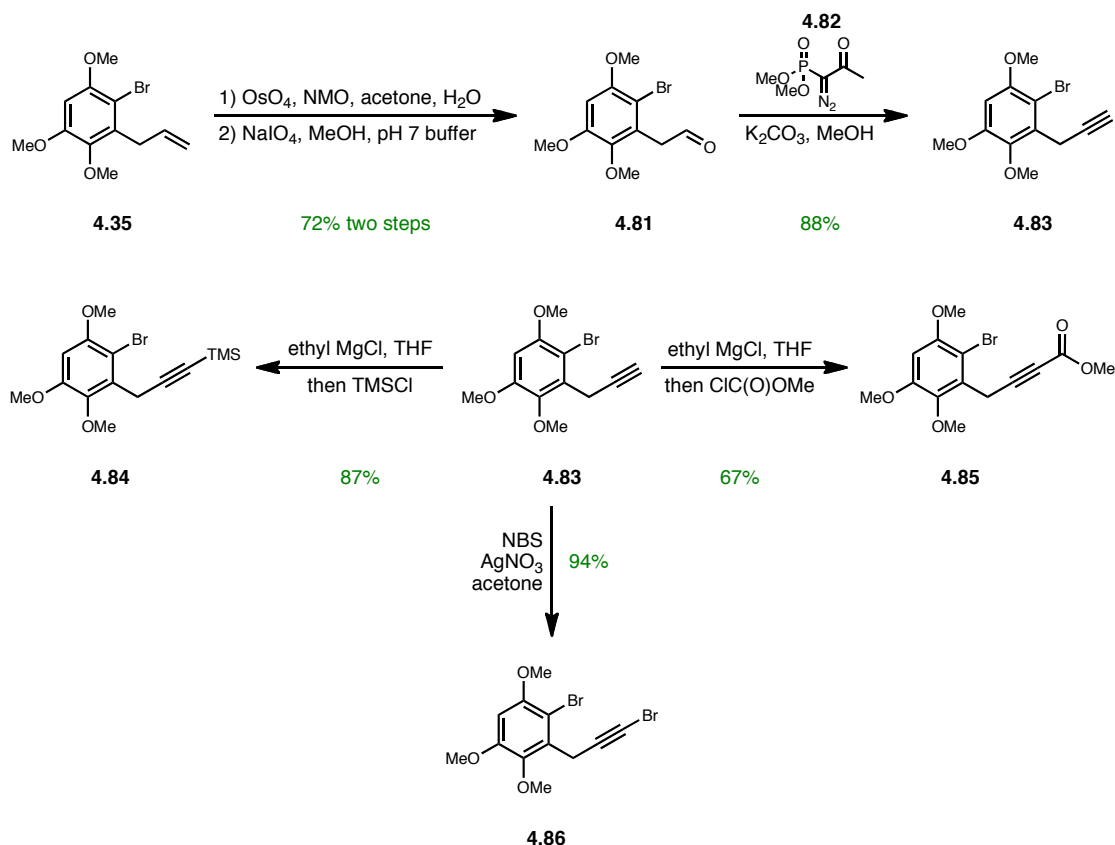
**Scheme 4.27.** Incorrect C-9 stereochemistry from a northern-tethered IMDA.

### The Terminal Alkyne Series for Southern Tethering

We set out to convert aryl olefin **4.35** to a terminal alkyne through an intermediate aldehyde for which we imagined multiple possibilities. We first attempted olefin

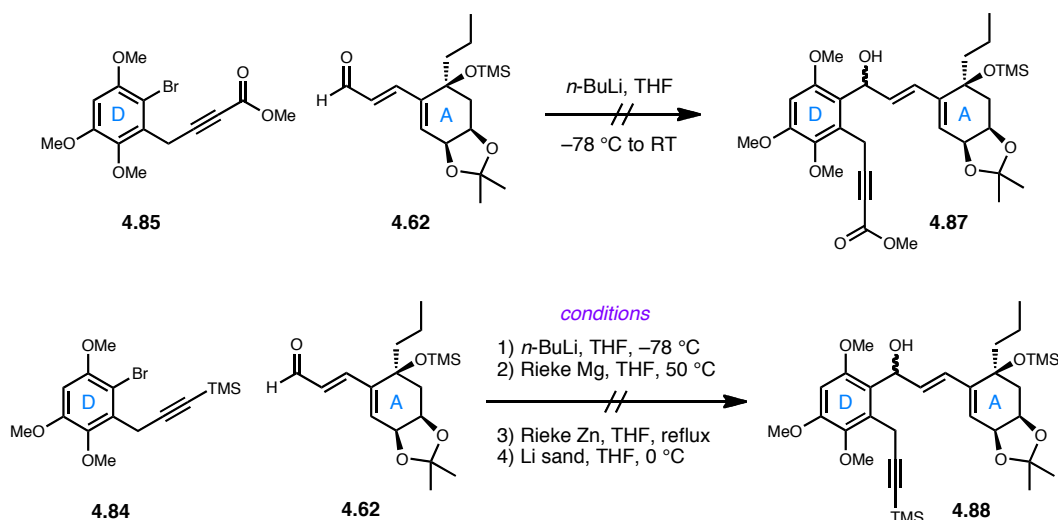
dibromination; however, this reaction resulted in concomitant aryl ring halogenation. Ozonolysis did effect conversion to the desired aldehyde but also resulted in an unknown reaction with the aryl ring as well. Finally, simple dihydroxylation and oxidative cleavage with NaIO<sub>4</sub> cleanly formed the necessary aldehyde **4.81**, and we then converted the aldehyde with the Bestmann-Ohira reagent (**4.82**) to the terminal alkyne **4.83** in high yield.<sup>29</sup> Notably, single step oxidative cleavage with OsO<sub>4</sub> and NaIO<sub>4</sub> in one pot resulted in lower yield, and thus we elected for a two step procedure without purification of the intermediate diol. With the terminal alkyne, we installed various functionality that we hoped would allow southern tether formation. Thus, deprotonation of the alkyne with ethylmagnesium chloride produced the intermediate alkynyl Grignard which could be reacted with either TMSCl or methyl chloroformate to yield **4.84** and **4.85** respectively. Additionally, we were able to form the alkynyl bromide **4.86** in excellent yield.





**Scheme 4.28.** Aryl alkyne synthesis and functionalization.

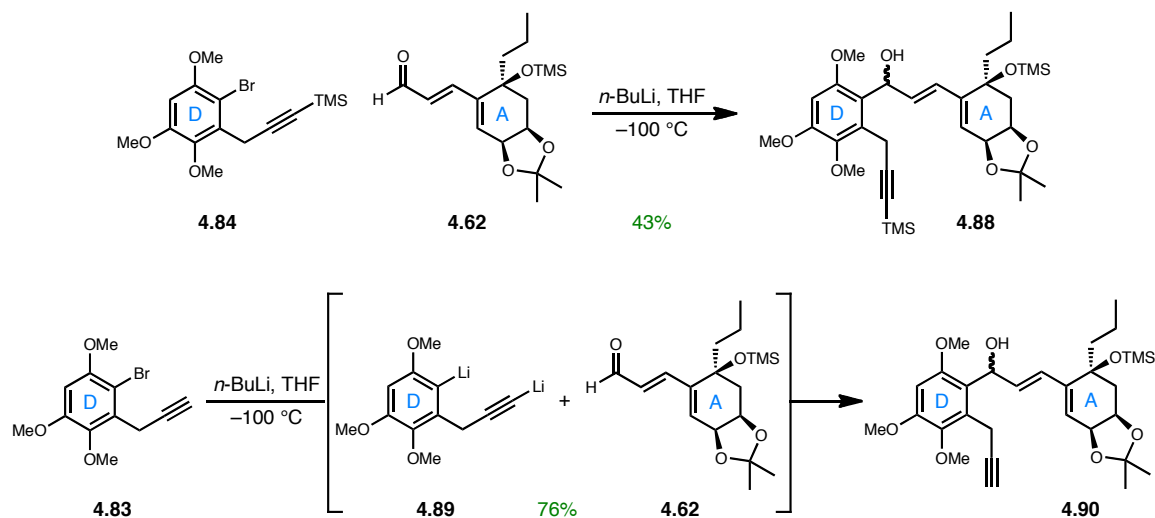
Alkynyl ester **4.85** was initially our preferred functionality for eventual southern tethering as it would only require hydrolysis to provide an acid for macrolactonization. Unfortunately, we were unable to effect northern tether formation between aryl bromide **4.85** and the A-ring aldehyde **4.62** as the methyl ester was likely an incompatible functionality with *n*-BuLi. We then turned our attention to the TMS-alkyne **4.84** which we reasoned could be deprotected and functionalized post-tethering. We screened a large number of conditions with various metals but disappointingly never observed formation of the desired product **4.88**.



**Scheme 4.29.** Attempted northern tether formation with functionalized alkynes.

Despite our difficulties at uniting an alkyne-functionalized aryl ring with our A-ring aldehyde **4.62**, we remained convinced that slight modification of our standard *n*-BuLi conditions, which reliably underwent deuterium incorporation in test reactions, would lead to the desired product. TMS alkyne **4.84** remained our primary aryl bromide as we believed that the alkyne would require masking to allow for chemoselectivity upon treatment with *n*-BuLi. We finally glimpsed success when allylic alcohol **4.88** was isolated in 43% yield by simply running the reaction at  $-100\text{ }^{\circ}\text{C}$  instead of  $-78\text{ }^{\circ}\text{C}$ , but the reaction resisted improvement. Faced with these results, we became less convinced that a TMS-alkyne functionality truly provided benefit over the free alkyne, and we thus attempted formation of the di-lithiate intermediate **4.89** at  $-100\text{ }^{\circ}\text{C}$  and addition to the aldehyde **4.62**. Gratifyingly, we isolated the desired product **4.90** as a mixture of diastereomers in high yield with complete chemoselectivity for aryl-lithiate addition. In this way, we viewed formation of the alkynyl lithiate as a form of in situ protection which

was ultimately reprotonated during the workup step. This reaction proved highly scalable, and we could produce multiple grams of the allylic alcohol **4.90** in a single reaction.

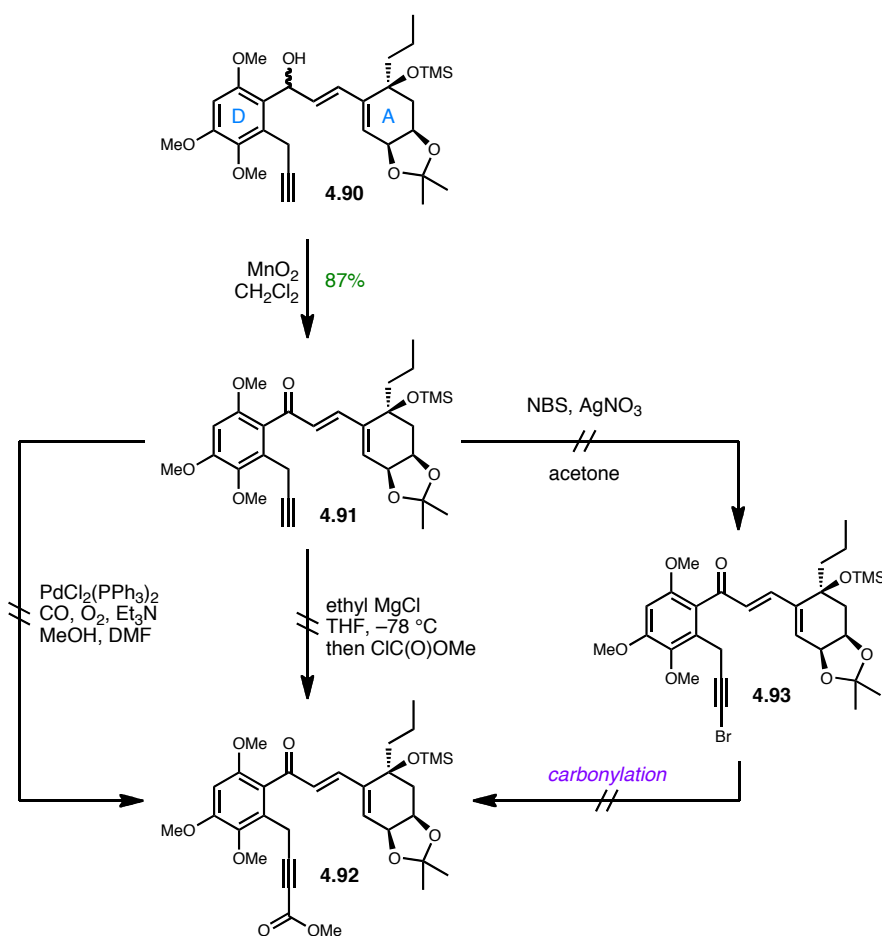


**Scheme 4.30.** Successful northern tethering with terminal alkyne functionality.

We immediately converted the diastereomeric mixture of allylic alcohols **4.90** to the  $\alpha,\beta$ -unsaturated ketone **4.91** for ease of characterization of further reaction products. But this strategy ultimately led to other complications. Our original plans for the terminal alkyne involved deprotonation and addition to methyl chloroformate to provide the alkynyl ester **4.92**. Unfortunately but not surprisingly, we were unable to chemoselectively deprotonate the alkyne as our standard bases preferentially underwent nucleophilic addition to the ketone moiety.

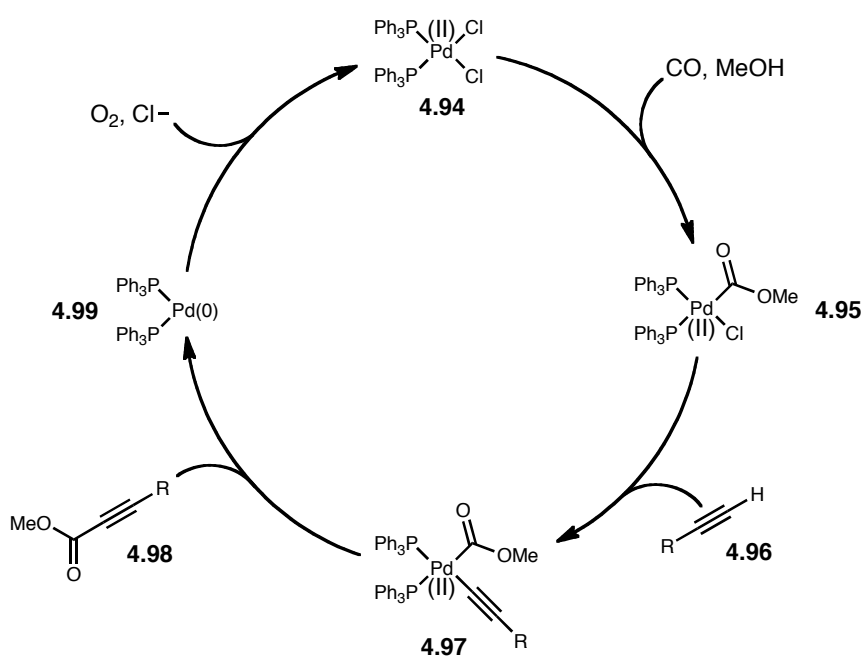
An alternate route to the alkynyl ester **4.92** involved carbonylative cross coupling of either the terminal alkyne **4.91** or the halo-alkyne **4.93**. While reports of these types of transformations remain limited in scope and application and their mechanisms are not

well understood, we hoped that a palladium-catalyzed method would overcome inherent difficulties of alkynyl nucleophile formation in the presence the ketone functionality. Thus, we screened various systems reported by Yamamoto, Tsuji, and Temkin but unfortunately failed to observe product formation.<sup>30,31,32</sup> When we attempted to optimize conditions on the simpler aryl alkyne **4.83**, we observed mixtures of desired product with the isomerized allenic ester. In light of these results, we resorted to less traditional methods for ester installation.



**Scheme 4.31.** Failed attempts at alkyne functionalization.

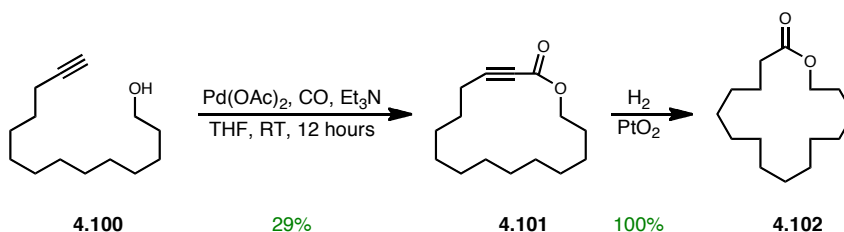
Yamamoto and co-workers probed the details of the carbonylation of a terminal alkyne and proposed a mechanism based on their studies. Starting with a palladium(II) catalyst **4.94**, formation of the palladium-methoxycarbonyl species **4.95** is followed by addition of the terminal alkyne **4.96** to form intermediate **4.97**. Reductive elimination of the alkynyl ester **4.98** generates a palladium(0) species **4.99** which is oxidized by molecular oxygen to complete the catalytic cycle.



**Scheme 4.32.** Proposed mechanism of alkyne carbonylation.

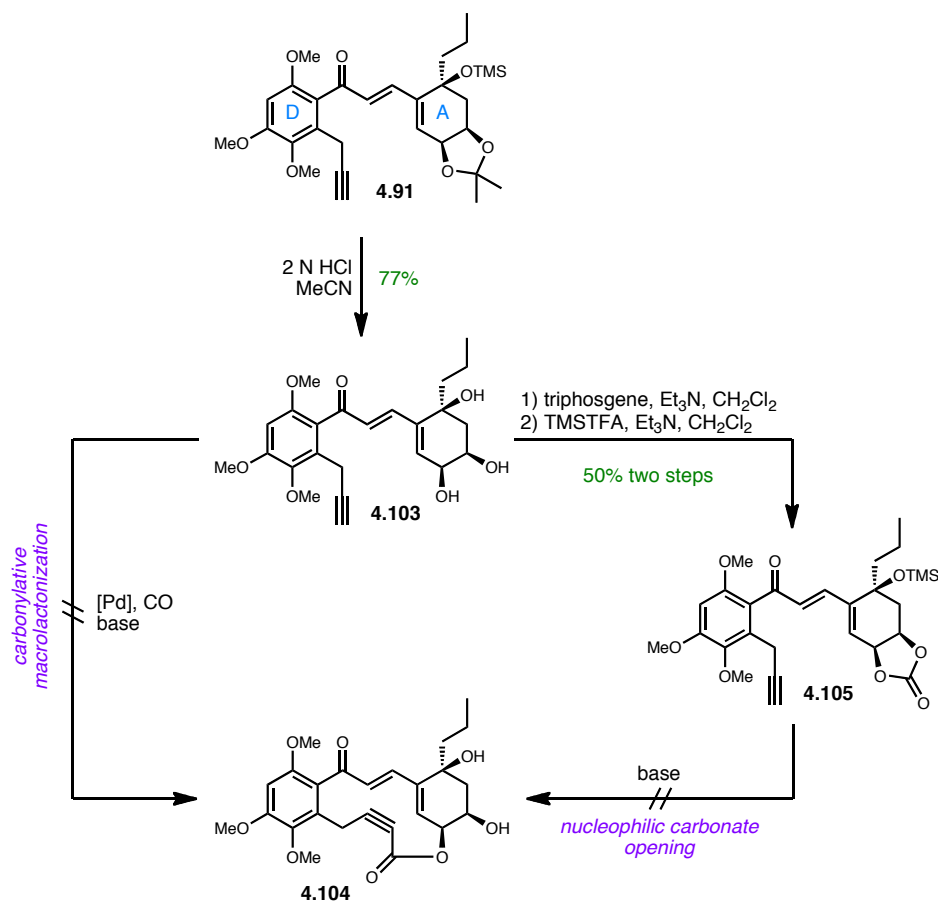
Despite failure with carbonylative methyl ester formation, we were intrigued by Ogasawara's report of a carbonylative macrolactonization of the alkynol **4.100** with common ester-forming conditions.<sup>33</sup> This method did not come without limitations: in order to achieve 29% yield for the alkynyl lactone **4.101**, two molar equivalents of Pd(OAc)<sub>2</sub> were required, and large amounts of starting material were isolated following

the reaction. Nevertheless, we reasoned that with an acetonide-protected alkyne compound, we could at very least hope for confirmation that our proposed alkynyl lactone could indeed be formed.



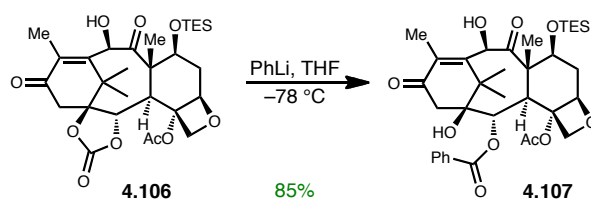
**Scheme 4.33.** Ogasawara's carbonylative macrolactonization.

Treatment of alkynyl ketone **4.91** with 2 N HCl in acetonitrile cleanly effected acetonide and TMS ether deprotection to the triol **4.103**. From this intermediate, we saw two possible, albeit unlikely, routes to forming macrolactone **4.104**. In analogy to Ogasawara's carbonylative macrolactonization, we treated alkynyl triol **4.103** with palladium-mediated carbonylation conditions with the hope that the alkynyl palladium intermediate would be intercepted by the adjacent secondary alcohol; however, we never observed any conversion to desired product.



**Scheme 4.34.** Alternate macrolactonization attempts.

Alternatively, we viewed a cyclic carbonate formed from the *cis*-diol functionality of **4.103** as a potential intramolecular electrophilic acceptor of an alkynyl nucleophile. This approach stemmed from precedent set by Nicolaou and co-workers in their synthesis of taxol in which a cyclic carbonate moiety in **4.106** was opened with phenyllithium to install the innate benzoate functionality and arrive at **4.107**.<sup>34</sup> This example did not clearly map onto our substrate, as Nicolaou's work utilized an intermolecular delivery of a nucleophile that was used in large molar excess.



**Scheme 4.35.** Nicolaou's nucleophilic opening of a cyclic carbonate.

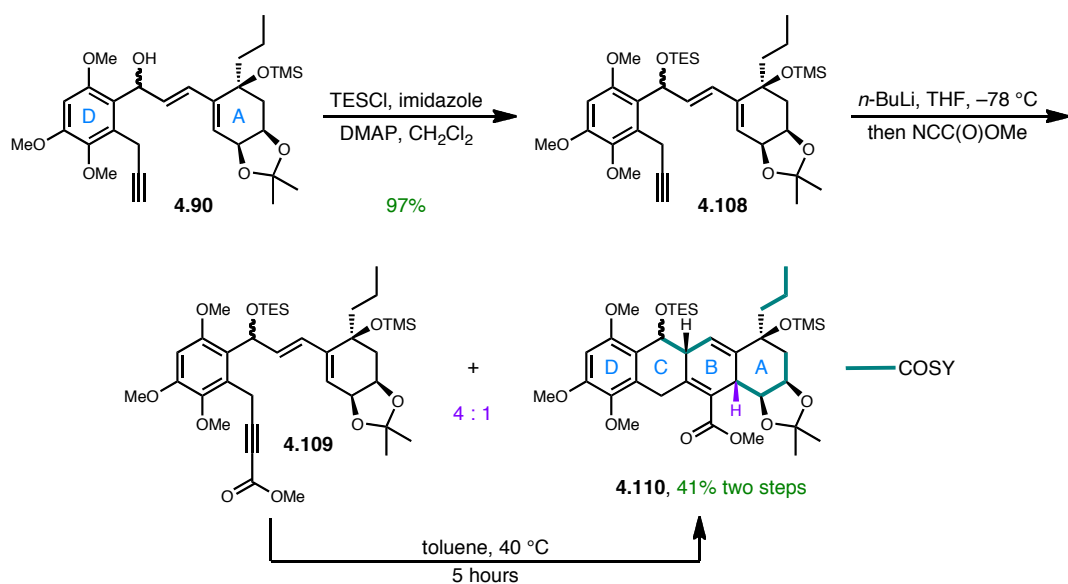
Despite the obvious differences with Scheme 4.35, conversion to the necessary cyclic carbonate **4.105** proved straightforward, but again, we were met with failure as all conditions utilized to effect cyclization did not lead to the desired macrocycle.<sup>35</sup> These results were not surprising considering our lack of success with carbonylative methyl ester formation and the necessary conformation for alkyne attack of the cyclic carbonate. However, we recognized the need to employ a protected version of the allylic alcohol **4.90** to allow for alkyne deprotonation for functionalization.

To see this plan through, silyl ether protection of the mixture of secondary alcohols yielded **4.108**, and we then explored alkyne functionalization. By removing the electrophilic center in **4.91**, we were pleased to observe chemoselective deprotonation, and we optimized conditions to install the desired methyl ester with Manders' reagent.<sup>36</sup> And despite the mixture of diastereomers, we curiously observed a mixture of the uncyclized ester **4.109** and the IMDA product **4.110** by <sup>1</sup>H NMR following standard workup and purification. To confirm the identity of this new compound, we heated the mixture in toluene at 40 °C to effect conversion of the remainder of the uncyclized product. Indeed, after 5 hours, the alkynyl ester **4.109** had fully converted to the IMDA product **4.110**. Tetracycle **4.110** proved difficult to assign by 2-D NMR methods due to the unsaturation found in the B-ring. No major NOESY correlations indicated



stereochemistry, but the C-9 stereocenter was assigned to be the undesired  $\beta$ -hydrogen based on coupling constants with the adjacent  $\alpha$ -face hydrogen. This facial selectivity came as no surprise based on precedent within the terminal olefin series as well as modeling logic with the presence of the acetonide moiety. This result provided even further evidence for the necessity of southern tethering to effect formation of the correct C-9 stereocenter. However, we were surprised to observe room temperature IMDA of **4.109**.

An electronic analysis of the alkynyl ester **4.109** reveals a highly activated Diels-Alder substrate within a normal electron demand paradigm. In contrast to the  $\alpha,\beta$ -unsaturated ketone **4.91**, the allylic-OTES diene serves as a highly electron rich diene system. Logically, the terminal alkyne starting material **4.108** does not undergo cyclization due to the unfavorable Diels-Alder dienophile electronics; however, installation of the methyl ester to arrive at **4.109** significantly lowers the LUMO of the dienophile, and the energy necessary to bridge the energy gap is available at room temperature. Regrettably, we never investigated the rate of conversion between **4.109** and **4.110** by simply allowing the mixture to sit at room temperature for an extended period of time.

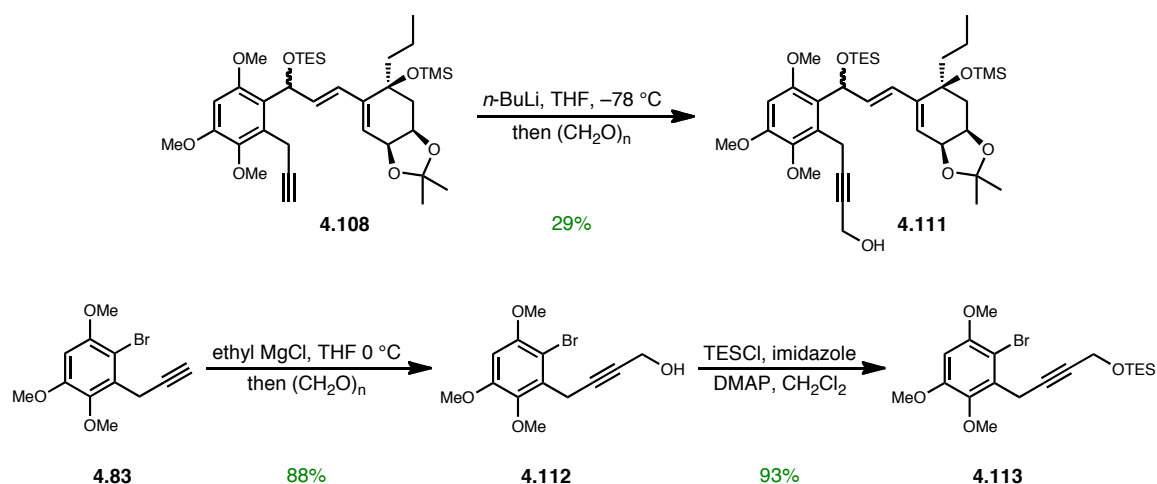


**Scheme 4.36.** Alkyne functionalization and an unexpected IMDA.

We had planned to attempt macrocyclization of **4.109** to form the southern tether which we had now shown as essential for correct stereoselectivity in the Diels-Alder. However, room temperature Diels-Alder cyclization provided no reasonable window in which to perform the necessary steps for macrocyclization first. Therefore, we were forced to redesign our synthetic route once again to account for these results. We reasoned that although northern tether formation did not occur with an aryl alkynyl ester **4.85**, we might be able to functionalize the aryl-alkyne with a lower oxidation state group so as to allow fine-tuning of Diels-Alder electronics and avoid unwanted cyclization.

## The Propargylic Alcohol Series for Macrocycle Formation

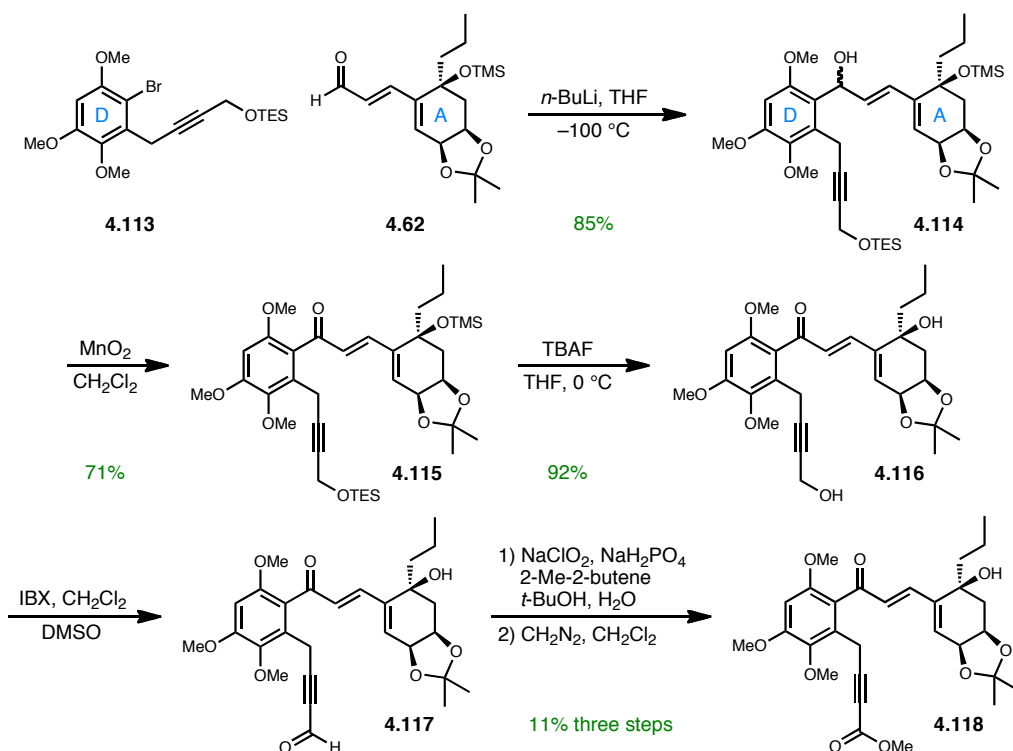
Drawing on our experience with alkyne functionalization in Scheme 4.36, we believed that we could effectively substitute the electrophile to produce a lower oxidation state product. We were familiar with the use of paraformaldehyde as an electrophilic reagent for carbon elongation, and we succeeded, albeit in very low yield, to produce the propargylic alcohol **4.111**. Ultimately, if we were to apply this route to a total synthesis of hibarimicinone, we would require a much more robust synthetic route. With this in mind, we turned back to the aryl alkyne **4.83** which we reasoned could be transformed to the propargylic alcohol, and its protected form could be used in northern tethering with aldehyde **4.62**. Deprotonation of the aryl alkyne **4.83** under our standard conditions was followed by the addition of rigorously dry paraformaldehyde, and after 22 hours, propargylic alcohol **4.112** was isolated in excellent yield. In preparation for lithium-halogen exchange, we elected to protect the secondary alcohol as a silyl ether which proceeded with similar success to provide the TES-ether **4.113**.



**Scheme 4.37.** Synthesis of an aryl propargylic alcohol.

Aryl bromide **4.113** was treated with *n*-BuLi at  $-100\text{ }^{\circ}\text{C}$  in analogy to Scheme 4.30 followed by addition of the aldehyde **4.62**, and again we arrived at the northern-tethered compound **4.114** in exceptional yield. With the lessons of the undesired IMDA reaction in Scheme 4.36, we hoped to modulate the Diels-Alder electronics of **4.114** so as to effect cyclization only once the southern tether had been formed. Therefore, allylic alcohol **4.114** was oxidized with  $\text{MnO}_2$  serving to deactivate the dienophile toward cyclization, and the propargyl ether also represented a deactivated dienophile in the normal electron demand paradigm. In this way, we had deactivated the diene and could then oxidize the propargylic alcohol without fear of an undesired IMDA. Deprotection of the primary silyl ether occurred readily to provide **4.116**, and we then screened numerous oxidation conditions to arrive at the intermediate aldehyde **4.117**. Initially, DMP and pyridine in  $\text{CH}_2\text{Cl}_2$  provided the aldehyde in 40% yield; however, we ultimately settled on IBX as our oxidant of choice. Unfortunately, propargylic aldehyde **4.117** proved highly unstable, and this fact loomed large in the following steps. Because of the

instability of **4.117**, we moved material directly to the next oxidation step, and for the sake of characterization, we treated the intermediate acid with diazomethane to produce the methyl ester **4.118**. The three step sequence from the propargylic alcohol **4.116** to methyl ester **4.118** occurred in 11% overall yield, which we viewed as unsustainable for our purposes considering the remaining steps necessary for southern tether formation.



**Scheme 4.38.** Synthesis of a deactivated alkynyl ester.

Our remaining forays relied on far flung approaches to tethering such as bifunctional silyl linkers with various polyol substrate derivatives of propargylic alcohol **4.116**. While we successfully produced various intermediates, these strategies never

gained any traction, and we were again forced to confront the serious issues presented by functionalization of the A-ring *cis*-diol and southern tethering.

## Conclusion

Despite our lack of success with a two-directional strategy toward HMP-Y1 and hibarimicinone, we demonstrated the power of a deracemization protocol that opened the door to a biomimetic approach. We identified a monomeric tetracycle that we planned would ultimately undergo oxidative dimerization and deracemization, and we evaluated numerous synthetic strategies for its synthesis. Formation of the northern tether could occur from either direction by building onto either the A- or D-ring, and tethering with the methyl- $\alpha$ -D-glucopyranoside-derived A-ring was ultimately met with limitations for both synthetic options. Therefore, we identified a (–)-quinic acid-derived A-ring that greatly improved the requisite tethering reactions. With various northern-tethered substrates at our disposal, we attempted macrocycle formation to no avail, and two demonstrations of IMDA reactions confirmed the necessity of the southern tether for correct C-9 stereochemistry. As we failed to achieve southern tethering toward the proposed tetracycle, we finally recognized the need to directly tackle the difficult task of functionalizing the A-ring *cis*-diol toward a southern-tethered intermediate. These experiments are detailed in the following chapter.

## Experimental Methods

**General Procedure.** All non-aqueous reactions were performed under an argon atmosphere in flame-dried glassware. Stainless steel syringes or cannula were used to transfer air- and moisture-sensitive liquids. Reaction temperatures were controlled using a thermocouple thermometer and analog hotplate stirrer. Reactions were conducted at room temperature (RT, approximately 23 °C) unless otherwise noted. Analytical thin-layer chromatography was performed on E. Merck pre-coated silica gel 60 F254 plates and visualized using UV, ceric ammonium molybdate (CAM) and potassium permanganate (KMnO<sub>4</sub>) stains. Flash column chromatography was conducted as described by Still *et. al.* using indicated solvents and Dynamic Adsorbents silica gel 60 (230-240 mesh).<sup>37</sup> Where necessary, silica gel was neutralized by treatment of the silica gel prior to chromatography with the eluent containing 1% triethylamine (Et<sub>3</sub>N). Where necessary, silica gel was treated prior to chromatography with the eluent containing 1% glacial acetic acid (AcOH). Yields were reported as isolated, spectroscopically pure compounds.

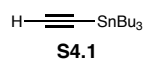
**Materials.** Reagents were purchased at the highest commercial quality and used without further purification unless otherwise stated. When necessary, intermediates were dried by azeotropic removal of water by evaporation from benzene (three iterations) and further dried on high-vacuum for the indicated amount of time. Toluene and dichloromethane (CH<sub>2</sub>Cl<sub>2</sub>) were obtained by passing commercially available solvents through activated alumina columns (MBraun MB-SPS solvent system). Tetrahydrofuran (THF) was

purified by distillation from sodium metal with benzophenone indicator, and when necessary, was further dried over activated 4 Å molecular sieves under an atmosphere of argon. Triethylamine (Et<sub>3</sub>N) was distilled from calcium hydride and stored over sodium hydroxide. The molarity of commercial *n*-butyllithium solutions was determined by titration using diphenylacetic acid as an indicator (average of three determinations).

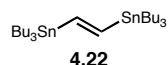
**Instrumentation.** Optical rotations were obtained using a Perkin Elmer 341 polarimeter and zeroed with the pure solvent, spectrophotometric-grade chloroform. <sup>1</sup>H NMR spectra were recorded on Bruker 300, 400, 500, or 600 MHz spectrometers and are reported relative to deuterated solvent signals (CDCl<sub>3</sub>: 7.26; C<sub>6</sub>D<sub>6</sub>: 7.16). Data for <sup>1</sup>H NMR spectra are reported as follows: chemical shift (δ ppm), multiplicity (s = singlet, d = doublet, t = triplet, q = quartet, p = pentet, sept. = septet, m = multiplet, br = broad, app = apparent), coupling constants (Hz), and integration. <sup>13</sup>C NMR spectra were recorded at 100, 125, or 150 MHz and are reported relative to deuterated solvent signals (CDCl<sub>3</sub>: 77.0; C<sub>6</sub>D<sub>6</sub>: 128.1). Infrared spectra were obtained as thin films on NaCl plates using a Thermo Electron IR100 series instrument and are reported in terms of frequency of absorption (cm<sup>-1</sup>). High-resolution mass spectra were obtained from the Department of Chemistry and Biochemistry, University of Notre Dame using either a JEOL AX505HA or JEOL LMS-GCmate mass spectrometer.



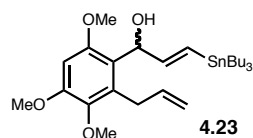
## Preparative Procedures



To a solution of lithium acetylide ethylene diamine complex (90%, 12.0 g, 117 mmol, 1.1 eq) in THF (400 mL) at 0 °C was added Bu<sub>3</sub>SnCl (29.5 mL, 110 mmol, 1.0 eq) via dropping funnel with vigorous stirring over 45 min then stirred at RT for 22 h. The reaction was cooled to 0 °C and H<sub>2</sub>O (10 mL) was added then the mixture was concentrated. The residue was diluted with H<sub>2</sub>O (75 mL) and extracted with hexanes (4 x 30 mL), and the combined organic layers were dried (MgSO<sub>4</sub>), filtered and concentrated. Distillation (0.1 mm Hg, 92-95 °C) provided **S4.1** as a clear liquid (9.37 g, 29.7 mmol, 25%). Spectral data were consistent with reported literature values.<sup>38</sup>

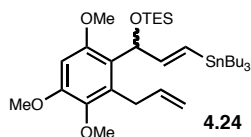


To **S4.1** (9.37 g, 29.7 mmol, 1.0 eq) was added AIBN (122 mg, 0.743 mmol, 0.025 eq) and Bu<sub>3</sub>SnH (9.60 mL, 35.7 mmol, 1.2 eq) and the reaction was heated at 90 °C for 6 h. At RT, distillation (0.1 mm Hg, 190-200 °C) required constant heating of the shortpath column and yielded **4.22** as a cloudy white liquid (17.7 g, 29.1 mmol, 98%). Spectral data were consistent with reported literature values.<sup>38</sup>



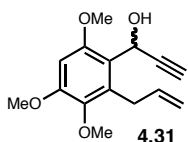
To a solution of **4.22** (1.83 g, 3.02 mmol, 3.0 eq) in THF (9.0 mL) at -78 °C was added *n*-BuLi (2.2 M in hexanes, 1.52 mL, 3.32 mmol, 3.3 eq) and the reaction was stirred at -40 °C for 30 min. At -78 °C, a solution of **4.16** (238 mg, 1.01 mmol, 1.0 eq) in THF (1.1 mL) was added dropwise and the reaction was stirred at -78 °C for 3 h. To the reaction was added saturated aqueous NH<sub>4</sub>Cl (20 mL) and the mixture was extracted with Et<sub>2</sub>O (3 x 20 mL). The combined organic layers

were dried (MgSO<sub>4</sub>), filtered and concentrated. Purification by flash column chromatography (5-15% EtOAc/hexanes) containing 1% Et<sub>3</sub>N provided **4.23** as a light yellow oil (336 mg, 0.607 mmol, 60%). <sup>1</sup>H NMR (400 MHz, CDCl<sub>3</sub>): δ 6.45 (s, 1H), 6.27 (dd, *J* = 19.1, 4.4 Hz, 1H), 6.03 (dd, *J* = 19.0, 1.6 Hz, 1H), 5.95 (ddt, *J* = 17.1, 10.2, 5.7 Hz, 1H), 5.24 (ddd, *J* = 10.8, 4.5, 1.5 Hz, 1H), 5.03 (app. dd, *J* = 10.2, 1.6 Hz, 1H), 4.96 (app. dd, *J* = 17.1, 1.7 Hz, 1H), 3.87 (s, 3H), 3.80 (s, 3H), 3.77 (d, *J* = 10.9 Hz, 1H), 3.74 (s, 3H), 3.55 (ddt, *J* = 15.8, 5.7, 1.6 Hz, 1H), 3.43 (ddt, *J* = 15.8, 5.5, 1.8 Hz, 1H), 1.55-1.37 (m, 6H), 1.27 (sex, *J* = 7.3 Hz, 6H), 0.95-0.75 (m, 15H); <sup>13</sup>C NMR (100 MHz, CDCl<sub>3</sub>): δ 154.2, 152.2, 149.6, 141.4, 136.9, 132.1, 126.3, 122.1, 115.6, 96.4, 73.2, 61.0, 55.9, 55.8, 30.4, 29.1, 27.2, 13.7, 9.4; IR (film) ν<sub>max</sub> 3555, 2924, 2871, 1598, 1485 cm<sup>-1</sup>; HRMS (ESI) *m/z* calcd. for C<sub>27</sub>H<sub>46</sub>NaO<sub>4</sub>Sn [M+Na]<sup>+</sup> 577.2315, found 577.2293.

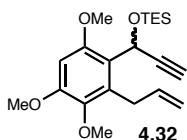


To a solution of **4.23** (65 mg, 0.117 mmol, 1.0 eq), imidazole (24 mg, 0.352 mmol, 3.0 eq), and DMAP (2 mg, catalytic) in DMF (150 μL) at 0 °C was added TESCl (39 μL, 0.235 mmol, 2.0 eq) and the reaction was stirred at 0 °C for 1 h and at RT for 20 hours. To the reaction was added saturated aqueous NH<sub>4</sub>Cl (10 mL) and the mixture was extracted with CH<sub>2</sub>Cl<sub>2</sub> (3 x 10 mL). The combined organic layers were washed with H<sub>2</sub>O (1 x 10 mL) and brine (1 x 10 mL) then dried (MgSO<sub>4</sub>), filtered and concentrated. Purification by flash column chromatography (0-1.5% EtOAc/hexanes) containing 1% Et<sub>3</sub>N yielded **4.24** as a light yellow oil (67 mg, 0.100 mmol, 85%). <sup>1</sup>H NMR (600 MHz, CDCl<sub>3</sub>): δ 6.40 (s, 1H), 6.24-6.07 (m, 2H), 5.92 (ddt, *J* = 16.9, 10.2, 6.1 Hz, 1H), 5.87 (app. d., *J* = 1.7 Hz, 1H), 4.94 (dd, *J* = 17.2, 1.9 Hz, 1H), 4.91 (dd, *J* = 10.2, 1.8 Hz, 1H), 3.86 (s, 3H), 3.81 (s, 3H), 3.73 (s, 3H), 3.67 (app. dd, *J* =

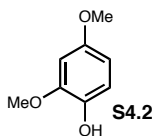
14.8, 6.3 Hz, 1H), 3.54 (app. dd,  $J = 14.7, 5.8$  Hz, 1H), 1.54-1.39 (m, 6H), 1.28 (sex, 6H), 0.94-0.78 (m, 24H), 0.59-0.50 (m, 6H);  $^{13}\text{C}$  NMR (150 MHz,  $\text{CDCl}_3$ ):  $\delta$  152.9, 152.0, 150.7, 142.6, 138.7, 134.9, 124.9, 123.0, 114.1, 95.6, 69.7, 60.5, 56.4, 55.7, 31.4, 29.1, 27.3, 13.7, 9.4, 6.8, 4.8; IR (film)  $\nu_{\text{max}}$  2955, 2929, 1596, 1464, 1326, 1235  $\text{cm}^{-1}$ ; HRMS (ESI)  $m/z$  calcd. for  $\text{C}_{33}\text{H}_{60}\text{NaO}_4\text{SiSn} [\text{M}+\text{Na}]^+$  691.3181, found 691.3188.



To a solution of **4.16** (500 mg, 2.12 mmol, 1.0 eq) in THF (21 mL) at  $-78^\circ\text{C}$  was added ethynyl magnesium bromide (0.5 M in THF, 8.5 mL, 4.23 mmol, 2.0 eq) dropwise and the reaction was stirred at  $-78^\circ\text{C}$  for 30 min and at  $0^\circ\text{C}$  for 1 h. To the reaction was added saturated aqueous  $\text{NH}_4\text{Cl}$  (50 mL) and the mixture was extracted with  $\text{CH}_2\text{Cl}_2$  (3 x 50 mL). The combined organic layers were dried ( $\text{MgSO}_4$ ), filtered and concentrated. Purification by flash column chromatography (20% and 30% EtOAc/hexanes) provided **4.31** as a light yellow oil (498 mg, 1.90 mmol, 90%).  $^1\text{H}$  NMR (400 MHz,  $\text{CDCl}_3$ ):  $\delta$  6.48 (s, 1H), 5.97 (ddt,  $J = 17.1, 10.3, 5.5$  Hz, 1H), 5.50 (dd,  $J = 10.7, 2.3$  Hz, 1H), 5.05 (ddd,  $J = 10.2, 3.1, 1.5$  Hz, 1H), 4.97 (ddd,  $J = 17.1, 3.3, 1.6$  Hz, 1H), 3.94 (d,  $J = 10.7$  Hz, 1H), 3.91 (s, 3H), 3.86 (s, 3H), 3.72 (s, 3H), 3.57 (ddt,  $J = 16.1, 5.7, 1.8$  Hz, 1H), 3.50 (ddt,  $J = 16.1, 5.7, 1.7$  Hz, 1H), 2.44 (d,  $J = 2.4$  Hz, 1H);  $^{13}\text{C}$  NMR (100 MHz,  $\text{CDCl}_3$ ):  $\delta$  154.2, 152.9, 141.3, 136.3, 131.4, 120.2, 115.8, 96.5, 84.6, 71.5, 60.9, 59.2, 56.2, 55.8, 30.1; IR (film)  $\nu_{\text{max}}$  3530, 3285, 2940, 2840, 1597  $\text{cm}^{-1}$ ; HRMS (ESI)  $m/z$  calcd. for  $\text{C}_{15}\text{H}_{18}\text{NaO}_4 [\text{M}+\text{Na}]^+$  285.1097, found 285.1090.

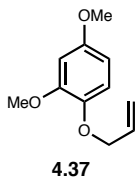


To a solution of **4.31** (217 mg, 8.27 mmol, 1.0 eq), imidazole (282 mg, 4.14 mmol, 5.0 eq), and DMAP (2 mg, catalytic) in DMF (827  $\mu$ L) at 0  $^{\circ}$ C was added TESCl (417  $\mu$ L, 2.48 mmol, 3.0 eq) and the reaction was stirred at 0  $^{\circ}$ C for 30 min and at RT for 22 h. To the reaction was added saturated aqueous  $\text{NH}_4\text{Cl}$  (25 mL) and the mixture was extracted with  $\text{CH}_2\text{Cl}_2$  (3 x 25 mL). The combined organic layers were washed with  $\text{H}_2\text{O}$  (1 x 25 mL) and brine (1 x 25 mL) then dried ( $\text{MgSO}_4$ ), filtered and concentrated. Purification by flash column chromatography (5% and 10% EtOAc/hexanes) yielded **4.32** as a clear oil (285 mg, 0.757 mmol, 91%).  $^1\text{H}$  NMR (400 MHz,  $\text{CDCl}_3$ ):  $\delta$  6.38 (s, 1H), 6.15 (d,  $J$  = 2.4 Hz, 1H), 6.05 (ddt,  $J$  = 17.1, 10.2, 6.2 Hz, 1H), 5.08 (app. dd,  $J$  = 17.2, 1.8 Hz, 1H), 4.97 (app. dd,  $J$  = 10.1, 1.7 Hz, 1H), 3.85 (s, 3H), 3.83-3.78 (m, 2H), 3.82 (s, 3H), 3.76 (s, 3H), 2.43 (d,  $J$  = 2.4 Hz, 1H), 0.91 (t,  $J$  = 8.0 Hz, 9H), 0.61 (ddd,  $J$  = 15.2, 7.5, 2.0 Hz, 6H);  $^{13}\text{C}$  NMR (100 MHz,  $\text{CDCl}_3$ ):  $\delta$  152.9, 152.2, 142.7, 138.1, 135.1, 120.7, 114.5, 95.5, 85.6, 72.1, 60.6, 56.4, 56.3, 55.7, 31.8, 6.6, 4.6; IR (film)  $\nu_{\text{max}}$  3287, 2956, 2877, 1596  $\text{cm}^{-1}$ ; HRMS (ESI)  $m/z$  calcd. for  $\text{C}_{21}\text{H}_{32}\text{NaO}_4\text{Si} [\text{M}+\text{Na}]^+$  399.1962, found 399.1951.

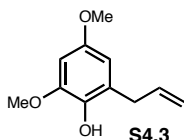


To a solution of 2,4-dimethoxybenzaldehyde (**4.19**, 20.0 g, 120 mmol, 1.0 eq) in  $\text{CH}_2\text{Cl}_2$  (401 mL) was added *m*-CPBA (40.5 g, 181 mmol, 1.5 eq) and the reaction was heated at reflux for 17 h. At RT the mixture was concentrated to an orange solid that was dissolved in EtOAc (400 mL) and washed with saturated aqueous  $\text{NaHCO}_3$  (2 x 400 mL) and brine (1 x 400 mL). The organic layer was concentrated to an orange oil that was dissolved in MeOH (266 mL), and to the solution was added 2 N aqueous KOH (132 mL) and the mixture was stirred at RT for 1 h. The mixture was

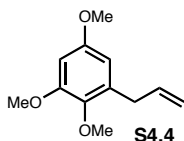
neutralized with 1 N aqueous HCl (300 mL) and extracted with EtOAc (4 x 200 mL), and the combined organic layers were washed with brine (1 x 400 mL), dried (MgSO<sub>4</sub>), filtered, and concentrated to provide **S4.2** as a brown oil (17.5 g, 114 mmol, 95% crude). The material was taken directly to the next step without purification.



To a solution of **S4.2** (17.5 g crude, 114 mmol, 1.0 eq) in acetone (568 mL) was added K<sub>2</sub>CO<sub>3</sub> (39.2 g, 284 mmol, 2.5 eq) and allyl bromide (24.0 mL, 284 mmol, 2.5 eq) and the reaction was heated at reflux for 18 h. At RT, the solid was removed by filtration with acetone washes, and the filtrate was concentrated to a brown oil. Purification by flash column chromatography (5-10% EtOAc/hexanes) yielded **4.37** as a yellow oil (16.4 g, 84.4 mmol, 70% two steps). Spectral data were consistent with reported literature values.<sup>7</sup>

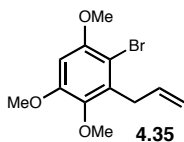


**4.37** (16.4 g, 84.4 mmol, 1.0 eq) was added in one-gram portions to microwave vials which were capped and heated via microwave irradiation at 200 °C for 1.25 h each. The brown oils were combined to provide **S4.3** (15.5 g, 79.7 mmol, 94%). Spectral data were consistent with reported literature values.<sup>39</sup>

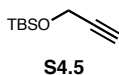


To a solution of **S4.3** (15.5 g, 79.7 mmol, 1.0 eq) in acetone (797 mL) was added K<sub>2</sub>CO<sub>3</sub> (110 g, 797 mmol, 10 eq) and MeI (49.6 mL, 797 mmol, 10 eq) and the mixture was heated at reflux for 20 h. At RT, the solid was removed by filtration through a plug of Celite with acetone washes, and the filtrate was concentrated to a brown oil. Purification by flash column chromatography (5-10%

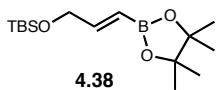
EtOAc/hexanes) yielded **S4.4** as a yellow oil (14.1 g, 67.5 mmol, 85%). Spectral data were consistent with reported literature values.<sup>39</sup>



To a solution of **S4.4** (14.1 g, 67.5 mmol, 1.0 eq) in DME (225 mL) was added CuBr<sub>2</sub> (30.1 g, 135 mmol, 2.0 eq) and the reaction was stirred at RT for 48 h. The green reaction was diluted with EtOAc (100 mL) and filtered through a plug of Celite with a layer of silica gel above with EtOAc washes. The filtrate was washed with 15% aqueous NH<sub>4</sub>OH (3 x 300 mL), and the aqueous layer was dried (MgSO<sub>4</sub>), filtered, and concentrated to a brown oil. Purification by flash column chromatography (5% EtOAc/hexanes) provided **4.35** as a yellow oil (17.7 g, 61.8 mmol, 92%). Spectral data were consistent with reported literature values.<sup>40</sup>

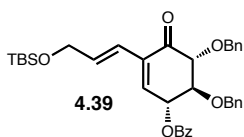


Freshly distilled propargyl alcohol (4.00 mL, 69.4 mmol, 1.0 eq) was added to DMF (8.3 mL) followed by TBSCl (12.5 g, 83.2 mmol, 1.2 eq) and imidazole (11.8 g, 173 mmol, 2.5 eq) and the reaction was stirred at RT for 20 h. Pentane (80 mL) was added and the mixture was washed with H<sub>2</sub>O (4 x 60 mL). The organic layer was dried (MgSO<sub>4</sub>), filtered and concentrated. Distillation (0.1 mm Hg, 24-26 °C) provided TBS-propargyl alcohol (**S4.5**) as a clear liquid (5.16 g, 30.3 mmol, 44%). Spectral data were consistent with reported literature values.<sup>41</sup>



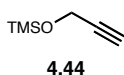
To a solution of pinacol (1.25 g, 10.6 mmol, 2.0 eq) in CH<sub>2</sub>Cl<sub>2</sub> (1.0 mL) at 0 °C was added BH<sub>3</sub>•SMe<sub>2</sub> (10 M, 1.05 mL, 10.6 mmol, 2.0 eq) and the mixture was stirred at 0 °C for 1 h and at RT for 3 h. To the mixture was

added a solution of TBS-propargyl alcohol (**S4.5**, 900 mg, 5.28 mmol, 1.0 eq) in CH<sub>2</sub>Cl<sub>2</sub> (500  $\mu$ L) via cannula, and the reaction was sealed in a pressure tube and heated at 50 °C for 96 h. At RT, H<sub>2</sub>O (20 mL) was slowly and carefully added, and the mixture was extracted with Et<sub>2</sub>O (3 x 50 mL). The combined organic layers were dried (MgSO<sub>4</sub>), filtered and concentrated. Purification by flash column chromatography (2.5% and 5% Et<sub>2</sub>O/hexanes) yielded **4.38** as a clear oil (1.02 g, 3.42 mmol, 65%). Spectral data were consistent with reported literature values.<sup>13</sup>

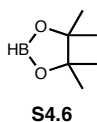


To a solution of **3.38** (500 mg, 9.02 mmol, 1.0 eq) and **4.38** (538 mg, 1.80 mmol, 2.0 eq) in THF/H<sub>2</sub>O (9.0 mL, 8:1) was added Ag<sub>2</sub>O (334 mg, 1.44 mmol, 1.6 eq) and Ph<sub>3</sub>As (28.0 mg, 0.0902 mmol, 0.1 eq). The mixture was degassed (3x) with liquid N<sub>2</sub>, then Pd(PPh<sub>3</sub>)<sub>4</sub> (52.0 mg, 0.0451 mmol, 0.05 eq) was added and the reaction was stirred at RT for 24 h. The reaction was diluted with EtOAc (100 mL) and washed with brine (1 x 100 mL), and the combined aqueous layers were extracted with EtOAc (1 x 100 mL). The combined organic layers were dried (MgSO<sub>4</sub>), filtered and concentrated. Purification by flash column chromatography (2.5%, 5%, 7.5% and 10% EtOAc/hexanes) provided **4.39** as a clear oil (356 mg, 0.595 mmol, 66%). <sup>1</sup>H NMR (400 MHz, CDCl<sub>3</sub>):  $\delta$  7.98 (app. d,  $J$  = 7.4 Hz, 2H), 7.60 (app. t,  $J$  = 7.2 Hz, 1H), 7.51-7.41 (m, 4H), 7.39-7.28 (m, 3H), 7.23-7.10 (m, 5H), 6.67 (dd,  $J$  = 11.3, 2.6 Hz, 1H), 6.48 (dt,  $J$  = 16.1, 4.5 Hz, 1H), 6.37 (app. d,  $J$  = 15.8 Hz, 1H), 6.03 (app. d,  $J$  = 8.1 Hz, 1H), 5.12 (d,  $J$  = 11.5 Hz, 1H), 4.90 (d,  $J$  = 11.5 Hz, 1H), 4.77 (d,  $J$  = 11.6 Hz, 1H), 4.74 (d,  $J$  = 11.8 Hz, 1H), 4.27 (m, 2H), 4.22 (d,  $J$  = 10.6 Hz, 1H), 4.11 (dd,  $J$  = 10.5, 8.2 Hz, 1H), 0.92 (s, 9H), 0.08 (s, 6H); <sup>13</sup>C NMR (100 MHz, CDCl<sub>3</sub>):  $\delta$  195.8, 165.8, 138.6,

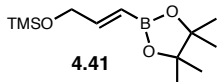
137.6, 135.4, 134.9, 133.4, 129.8, 129.3, 128.4 (2C), 128.3, 128.2 (2C), 127.9, 127.7, 121.1, 84.2, 81.4, 75.0, 74.5, 73.0, 63.4, 25.9, 25.8, 18.4, -5.3; IR (film)  $\nu_{\text{max}}$  2954, 2928, 2856, 1723, 1701  $\text{cm}^{-1}$ ; HRMS (ESI)  $m/z$  calcd. for  $\text{C}_{36}\text{H}_{42}\text{NaO}_6\text{Si} [\text{M}+\text{Na}]^+$  621.2643, found 621.2633.



To a solution of propargyl alcohol (9.61 mL, 165 mmol, 1.0 eq) in  $\text{CH}_2\text{Cl}_2$  (100 mL) at 0 °C was added imidazole (14.6 g, 215 mmol, 1.3 eq) and TMSCl (23.2 mL, 182 mmol, 1.1 eq) and a white solid precipitated from the reaction. The reaction was stirred at 0 °C for 1 h and at RT for 2 h, then cooled to 0 °C and saturated aqueous  $\text{NH}_4\text{Cl}$  (50 mL) was added. The mixture was diluted with  $\text{CH}_2\text{Cl}_2$  (100 mL) and washed with  $\text{H}_2\text{O}$  (3 x 100 mL), and the organic layer was dried ( $\text{MgSO}_4$ ), filtered and concentrated. Distillation (185 mm Hg, 64-66 °C) provided OTMS-propargyl alcohol (**4.44**) as a clear liquid (13.8 g, 107 mmol, 65%). Spectral data were consistent with reported literature values.<sup>15</sup>



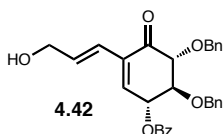
To a solution of pinacol (25.0 g, 212 mmol, 1.0 eq) in  $\text{CH}_2\text{Cl}_2$  (24.9 mL) at 0 °C was added  $\text{BH}_3\cdot\text{SMe}_2$  (22.0 mL, 220 mmol, 1.0 eq) slowly. The reaction was stirred at 0 °C for 30 min and at RT for 3.5 h. Distillation (185 mm Hg,  $\text{CH}_2\text{Cl}_2$  at 22-24 °C, product at 50-60 °C) yielded pinacolborane (**S4.6**) as a clear liquid (15.6 g, 122 mmol, 58%). Spectral data were consistent with reported literature values.<sup>15</sup>



To a solution of OTMS-propargyl alcohol (**4.44**, 11.7 mL, 76.4 mmol, 1.0 eq) in  $\text{CH}_2\text{Cl}_2$  (38.2 mL) at 0 °C was added pinacolborane (**S4.7**,



15.6 g, 122 mmol, 1.6 eq) slowly, and the reaction was stirred at 0 °C for 2 h and at RT for 22 h. The reaction was concentrated to an off-white oil, and distillation (0.1 mm Hg, 67-73 °C) provided **4.41** as a clear liquid/oil (9.94 g, 38.8 mmol, 51%). <sup>1</sup>H NMR (400 MHz, CDCl<sub>3</sub>): δ 6.67 (ddd, *J* = 17.9, 4.0, 3.9 Hz, 1H), 5.72 (ddd, *J* = 18.0, 2.0, 1.9 Hz, 1H), 4.21 (dd, *J* = 3.9, 2.0 Hz, 2H), 1.26 (s, 12H), 0.12 (s, 9H).

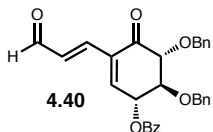


Method A: To a solution of **4.39** (330 mg, 0.551 mmol, 1.0 eq) in THF (11 mL) at 0 °C was added HF•pyridine (70%, 143 μL, 5.51 mmol, 10 eq) and the ice bath was allowed to melt over 4 h. Additional HF•pyridine (70%, 40.0 μL, 1.54 mmol, 2.8 eq) was added and the reaction was stirred at RT overnight. To the reaction was added H<sub>2</sub>O (10 mL) and the mixture was extracted with CH<sub>2</sub>Cl<sub>2</sub> (3 x 20 mL). The combined organic layers were washed with saturated aqueous NaHCO<sub>3</sub> (1 x 20 mL) then dried (MgSO<sub>4</sub>), filtered and concentrated. Purification by flash column chromatography (25-55% EtOAc/hexanes) yielded **4.42** as a yellow oil (115 mg, 0.237 mmol, 43%).

Method B: To a solution of **3.38** (300 mg, 0.541 mmol, 1.0 eq) and **4.41** (277 mg, 1.08 mmol, 2.0 eq) in THF/H<sub>2</sub>O (5.4 mL, 8:1) was added Ag<sub>2</sub>O (201 mg, 0.866 mmol, 1.6 eq) and Ph<sub>3</sub>As (17.0 mg, 0.0541 mmol, 0.1 eq). The mixture was degassed (3x) with liquid N<sub>2</sub>, then Pd(PPh<sub>3</sub>)<sub>4</sub> (31.0 mg, 0.0271 mmol, 0.05 eq) was added and the reaction was stirred at RT for 24 h. The reaction was diluted with EtOAc (40 mL) and washed with 1 N aqueous HCl (3 x 25 mL), and the combined aqueous layers were extracted with EtOAc (1 x 40 mL). The combined organic layers were dried (MgSO<sub>4</sub>), filtered and

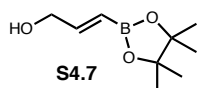
concentrated. Purification by flash column chromatography (10-50% EtOAc/hexanes) provided **4.42** as a clear oil (188 mg, 0.388 mmol, 72%).

$[\alpha]_{\text{D}}^{20}$  -166 (*c* 0.17, CHCl<sub>3</sub>); <sup>1</sup>H NMR (400 MHz, CDCl<sub>3</sub>): δ 7.97 (dd, *J* = 8.3, 1.2 Hz, 2H), 7.60 (app. t, *J* = 7.5 Hz, 1H), 7.49-7.41 (m, 4H), 7.39-7.27 (m, 3H), 7.21-7.11 (m, 5H), 6.70 (d, *J* = 2.5 Hz, 1H), 6.49 (dt, *J* = 16.0, 5.0 Hz, 1H), 6.38 (d, *J* = 16.0 Hz, 1H), 6.02 (dd, *J* = 8.3, 1.9 Hz, 1H), 5.10 (d, *J* = 11.2 Hz, 1H), 4.90 (d, *J* = 11.4 Hz, 1H), 4.77 (d, *J* = 11.4 Hz, 1H), 4.74 (d, *J* = 11.4 Hz, 1H), 4.24 (app. d, *J* = 4.8 Hz, 2H), 4.22 (d, *J* = 10.6 Hz, 1H), 4.11 (dd, *J* = 10.6, 8.3 Hz, 1H); <sup>13</sup>C NMR (100 MHz, CDCl<sub>3</sub>): δ 195.8, 165.8, 139.1, 137.6, 137.5, 135.3, 134.3, 133.5, 129.8, 129.3, 128.5, 128.4, 128.3, 128.2 (2C), 127.9, 127.7, 122.5, 84.1, 81.3, 75.1, 74.5, 72.9, 63.3; IR (film)  $\nu_{\text{max}}$  3442, 3063, 3032, 2921, 1721, 1698 cm<sup>-1</sup>; HRMS (ESI) *m/z* calcd. for C<sub>30</sub>H<sub>28</sub>NaO<sub>6</sub> [M+Na]<sup>+</sup> 507.1778, found 507.1763.

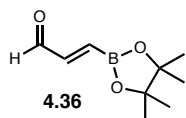


To a solution of **4.42** (115 mg, 0.237 mmol, 1.0 eq) in CH<sub>2</sub>Cl<sub>2</sub> (20 mL) was added MnO<sub>2</sub> (310 mg, 3.56 mmol, 15 eq) and the slurry was stirred at RT for 18 h. The reaction was diluted with CH<sub>2</sub>Cl<sub>2</sub> (20 mL) and filtered through a plug of Celite with CH<sub>2</sub>Cl<sub>2</sub> washes (3 x 20 mL). The filtrate was concentrated, and purification by flash column chromatography (10-50% EtOAc/hexanes) gave **4.40** as a white solid (63.0 mg, 0.131 mmol, 55%). MP: 131-134 °C;  $[\alpha]_{\text{D}}^{20}$  -162 (*c* 0.21, CHCl<sub>3</sub>); <sup>1</sup>H NMR (400 MHz, CDCl<sub>3</sub>): δ 9.61 (d, *J* = 7.6 Hz, 1H), 7.97 (app. d, *J* = 7.2 Hz, 2H), 7.62 (app. t, *J* = 7.2 Hz, 1H), 7.50-7.42 (m, 4H), 7.40-7.29 (m, 4H), 7.23-7.12 (m, 5H), 7.05 (d, *J* = 2.5 Hz, 1H), 6.82 (dd, *J* = 16.3, 7.7 Hz, 1H), 6.09 (dd, *J* = 8.4, 2.4 Hz, 1H), 5.11 (d, *J* = 11.4 Hz, 1H), 4.91 (d, *J* = 11.4 Hz, 1H), 4.81 (d, *J* = 11.4 Hz, 1H), 4.76 (d, *J*

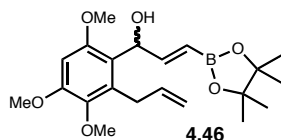
= 11.5 Hz, 1H), 4.27 (d,  $J$  = 10.6 Hz, 1H), 4.18 (dd,  $J$  = 10.4, 8.3 Hz, 1H);  $^{13}\text{C}$  NMR (100 MHz,  $\text{CDCl}_3$ ):  $\delta$  194.5, 193.5, 165.6, 145.6, 143.3, 137.3, 137.2, 133.7, 133.6, 132.8, 129.9, 128.9, 128.5 (2C), 128.3, 128.2 (2C), 128.1, 127.8, 83.9, 80.8, 75.2, 74.6, 72.5; IR (film)  $\nu_{\text{max}}$  3063, 3032, 2918, 1722, 1686, 1453  $\text{cm}^{-1}$ ; HRMS (ESI)  $m/z$  calcd. for  $\text{C}_{30}\text{H}_{26}\text{NaO}_6$   $[\text{M}+\text{Na}]^+$  505.1622, found 505.1615.



To a solution of **4.41** (2.48 g, 9.66 mmol, 1.0 eq) in THF (48 mL) was added  $\text{H}_2\text{O}$  (4.8 mL) and AcOH (9.7 mL) and the reaction was stirred at RT for 22 h. The solvents were removed in vacuo followed by distillation (0.1 mm Hg, 78-83  $^{\circ}\text{C}$ ) yielded **S4.7** as a clear oil (1.22 g, 6.60 mmol, 68%). Spectral data were consistent with reported literature values.<sup>15</sup>

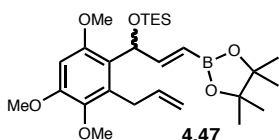


To a solution of **S4.7** (50 mg, 0.272 mmol, 1.0 eq) in  $\text{CH}_2\text{Cl}_2$  (750  $\mu\text{L}$ ) at 0  $^{\circ}\text{C}$  was added DMP (138 mg, 0.326 mmol, 1.2 eq) and the reaction was stirred at RT with exclusion of light for 2 h. The reaction was concentrated, dissolved in petroleum ether/ $\text{Et}_2\text{O}$  (55 mL, 10:1) and the solid was removed by filtration to yield **4.36** as a light yellow oil (39 mg, 0.214 mmol, 79%). Spectral data were consistent with reported literature values.<sup>14</sup>



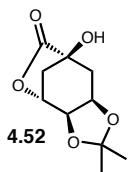
To a solution of **4.35** (158 mg, 0.549 mmol, 2.0 eq) in THF (1.5 mL) at  $-78^{\circ}\text{C}$  was added  $n\text{-BuLi}$  (2.2 M in hexanes, 262  $\mu\text{L}$ , 0.577 mmol, 2.1 eq) and the yellow mixture was stirred at  $-78^{\circ}\text{C}$  for 30 min. To the mixture at  $-78^{\circ}\text{C}$  was added a solution of **4.36** (50 mg, 0.275 mmol, 1.0 eq) in THF (1.2

mL) and the reaction was stirred at  $-78\text{ }^{\circ}\text{C}$  for 30 min, at  $0\text{ }^{\circ}\text{C}$  for 30 min and at RT for 24 h. To the reaction was added saturated aqueous  $\text{NH}_4\text{Cl}$  and the mixture was extracted with  $\text{CH}_2\text{Cl}_2$  (3 x 20 mL). The combined organic layers were dried ( $\text{MgSO}_4$ ), filtered and concentrated. Purification by flash column chromatography (15-45% EtOAc/hexanes) yielded **4.46** as a light yellow oil (47 mg, 0.120 mmol, 44%).  $^1\text{H}$  NMR (400 MHz,  $\text{CDCl}_3$ ):  $\delta$  6.83 (dd,  $J = 18.1, 4.7$  Hz, 1H), 6.42 (s, 1H), 5.94 (ddt, 17.1, 10.2, 5.7 Hz, 1H), 5.52 (dd,  $J = 18.1, 1.8$  Hz, 1H), 5.29 (ddd,  $J = 10.7, 4.6, 1.5$  Hz, 1H), 5.04 (ddd,  $J = 10.2, 3.3, 1.7$  Hz, 1H), 4.97 (ddd,  $J = 17.1, 3.4, 1.7$  Hz, 1H), 3.85 (s, 3H), 3.85-3.81 (m, 1H), 3.80 (s, 3H), 3.72 (s, 3H), 3.57 (ddt, 15.9, 5.7, 1.8 Hz, 1H), 3.34 (ddt,  $J = 15.9, 5.7, 1.8$  Hz, 1H), 1.24 (s, 12H);  $^{13}\text{C}$  NMR (100 MHz,  $\text{CDCl}_3$ ):  $\delta$  154.3, 154.2, 152.4, 141.4, 136.6, 132.0, 121.0, 115.8, 96.3, 83.2, 72.1, 61.0, 55.9, 55.8, 30.3, 24.7; IR (film)  $\nu_{\text{max}}$  3533, 2977, 2937, 1637, 1597, 1485  $\text{cm}^{-1}$ ; HRMS (ESI)  $m/z$  calcd. for  $\text{C}_{21}\text{H}_{31}\text{BNaO}_6$   $[\text{M}+\text{Na}]^+$  413.2110, found 413.2090.

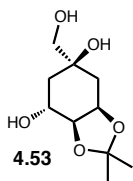


To a solution of **4.46** (132 mg, 0.338 mmol, 1.0 eq) in DMF (676  $\mu\text{L}$ ) was added imidazole (115 mg, 1.69 mmol, 5.0 eq) and DMAP (2 mg, catalytic) and the mixture was cooled to  $0\text{ }^{\circ}\text{C}$ . TESCl (170  $\mu\text{L}$ , 1.01 mmol, 3.0 eq) was added and the reaction was stirred at RT for 3 h. To the reaction was added saturated aqueous  $\text{NH}_4\text{Cl}$  (10 mL) and the mixture was extracted with  $\text{CH}_2\text{Cl}_2$  (3 x 10 mL). The combined organic layers were dried ( $\text{MgSO}_4$ ), filtered and concentrated. Purification by flash column chromatography (5-20% EtOAc/hexanes containing 1%  $\text{Et}_3\text{N}$ ) yielded **4.47** as a clear oil (78 mg, 0.155 mmol, 46%).  $^1\text{H}$  NMR (400 MHz,  $\text{CDCl}_3$ ):  $\delta$  6.72 (dd,  $J = 17.9, 3.2$  Hz, 1H), 6.35 (s, 1H), 5.98 (app. t,  $J = 2.5$  Hz, 1H),

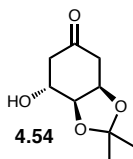
5.87 (ddt,  $J = 16.9, 10.3, 6.1$  Hz, 1H), 5.71 (dd,  $J = 17.9, 2.1$  Hz, 1H), 4.95-4.84 (m, 2H), 3.84 (s, 3H), 3.77 (s, 3H), 3.71 (s, 3H), 3.63 (ddt,  $J = 14.7, 6.4, 1.5$  Hz, 1H), 3.44 (ddt,  $J = 14.7, 5.8, 1.5$  Hz, 1H), 1.23 (br. s, 12H), 0.83 (t,  $J = 7.9$  Hz, 9H), 0.50 (q,  $J = 7.9$  Hz, 6H);  $^{13}\text{C}$  NMR (100 MHz,  $\text{CDCl}_3$ ):  $\delta$  156.2, 152.6, 152.2, 142.5, 138.4, 135.2, 121.8, 114.2, 95.3, 82.9, 68.0, 60.4, 56.2, 55.7, 31.3, 24.7 (2C), 6.7, 4.6; IR (film)  $\nu_{\text{max}}$  2956, 2877, 1637, 1595  $\text{cm}^{-1}$ ; HRMS (ESI)  $m/z$  calcd. for  $\text{C}_{27}\text{H}_{45}\text{BNaO}_6\text{Si} [\text{M}+\text{Na}]^+$  527.2976, found 527.2956.



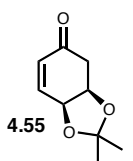
$\text{HCl}_{(\text{g})}$  was bubbled through acetone (867 mL) in a 2 L 3-necked flask for 1 min at a medium rate then (–)-quinic acid (**4.51**, 50.0 g, 260 mmol, 1.0 eq) was added and the white slurry was stirred at RT for 22 h. The clear yellow reaction was cooled to 0 °C and  $\text{NH}_{3(\text{g})}$  was bubbled through the solution until neutralization. The precipitated  $\text{NH}_4\text{Cl}$  was removed by filtration and the filtrate was concentrated to a volume of ~200 mL. To the solution was added hexanes (~200 mL) until crystallization initiated, and the material was stored overnight at –20 °C. The solid was collected by filtration with cold hexanes, and the filtrate was concentrated and dried on high-vac until solid. The solids were recrystallized from 1:1  $\text{CHCl}_3$ /hexanes (450 mL) and the insoluble solids were removed by hot filtration. The precipitated solid was collected by filtration to yield **4.52** as a white solid (31.8 g, 149 mmol, 57%). Spectral data were consistent with reported literature values.<sup>19</sup>



To a slurry of LAH (8.00 g, 211 mmol, 1.3 eq) in THF (448 mL) in a 2 L 3-necked flask at 0 °C was added a solution of **4.52** (36.1 g, 169 mmol, 1.0 eq) in THF (181 mL) via syringe pump over 4 h with vigorous stirring while remaining at 0 °C. The gray slurry was heated at reflux for 22 h then cooled to 0 °C and H<sub>2</sub>O (8.1 mL) was carefully added dropwise, then 15% aqueous NaOH (8.1 mL) and H<sub>2</sub>O (24 mL). To the mixture was added Celite (90.3 g) and the slurry was stirred at RT for 3 h. The slurry was filtered through a plug of Celite with hot CHCl<sub>3</sub>/EtOH (95:5, 1.0 L), and the filtrate was concentrated to ~100 mL, crystallized with hexanes (~100 mL), and stored at -20 °C overnight. Collection of the white crystalline solid by filtration yielded **4.53** (20.6 g, 94.4 mmol, 56%). Spectral data were consistent with reported literature values.<sup>19</sup>

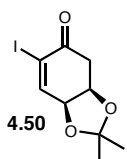


To a solution of **4.53** (20.6 g, 94.4 mmol, 1.0 eq) in pH 7 buffer (248 mL) at 0 °C was added NaIO<sub>4</sub> (26.0 g, 122 mmol, 1.3 eq) slowly and the white slurry was stirred at RT for 1 h. The reaction mixture was extracted with CH<sub>2</sub>Cl<sub>2</sub> (12 x 250 mL), and the combined organic layers were dried (MgSO<sub>4</sub>), filtered, and concentrated to provide **4.54** as a yellow oil (15.9 g, 85.5 mmol, 91%). Spectral data were consistent with reported literature values.<sup>20</sup>

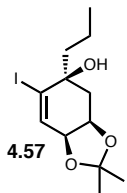


To a solution of **4.54** (15.9 g, 85.5 mmol, 1.0 eq) in CH<sub>2</sub>Cl<sub>2</sub> (259 mL) at 0 °C was added Et<sub>3</sub>N (35.7 mL, 256 mmol, 3.0 eq) slowly then a solution of methanesulfonyl chloride (7.94 mL, 103 mmol, 1.2 eq) in CH<sub>2</sub>Cl<sub>2</sub> (31 mL) via syringe pump over 2 h while remaining at 0 °C. The reaction was stirred at RT for 2 h

then washed with H<sub>2</sub>O (3 x 150 mL). The combined aqueous layers were extracted with Et<sub>2</sub>O (2 x 150 mL), and the combined organic layers were washed with saturated aqueous NaHCO<sub>3</sub> (1 x 150 mL) and brine (1 x 150 mL) then dried (MgSO<sub>4</sub>), filtered, and concentrated. Immediate purification by flash column chromatography (17% and 20% EtOAc/hexanes) provided **4.55** as a maroon oil that solidified at 0 °C (8.37 g, 49.8 mmol, 58%). Spectral data were consistent with reported literature values.<sup>20</sup>

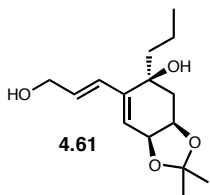


To a solution of **4.55** (8.37 g, 49.8 mmol, 1.0 eq) in CH<sub>2</sub>Cl<sub>2</sub> (101 mL) at 0 °C was added DMAP (1.22 g, 9.95 mmol, 0.2 eq) and pyridine (50.3 mL) slowly. To the mixture was added a solution of I<sub>2</sub> (31.6 g, 124 mmol, 2.5 eq) in CH<sub>2</sub>Cl<sub>2</sub> (51 mL) and pyridine (51 mL) via syringe pump over 3 h while remaining at 0 °C. The reaction was stirred at RT for 2 h, diluted with Et<sub>2</sub>O (500 mL) and washed with H<sub>2</sub>O (2 x 400 mL). The combined aqueous layers were extracted with Et<sub>2</sub>O (2 x 250 mL), and the combined organic layers were washed with 1 N aqueous HCl (4 x 400 mL), H<sub>2</sub>O (2 x 400 mL), 10% aqueous Na<sub>2</sub>S<sub>2</sub>O<sub>3</sub> (2 x 400 mL), and brine (1 x 400 mL), then dried (MgSO<sub>4</sub>), filtered, and concentrated. Immediate purification by flash column chromatography (18% EtOAc/hexanes) yielded **4.50** as an orange solid (9.49 g, 32.3 mmol, 65%). Spectral data were consistent with reported literature values.<sup>42</sup>



To a solution of **4.50** (9.49 g, 32.3 mmol, 1.0 eq) in toluene (323 mL) at -78 °C was added propyl magnesium chloride (2 M in Et<sub>2</sub>O, 48.4 mL, 96.8 mmol, 3.0 eq) over 5 seconds and the reaction turned green then yellow/brown and was stirred at -78 °C for 1.5 h. To the reaction at -78 °C was added saturated aqueous

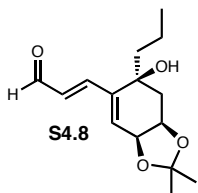
NH<sub>4</sub>Cl (100 mL) and at RT the mixture was added to saturated aqueous NH<sub>4</sub>Cl (500 mL) and H<sub>2</sub>O (200 mL) and extracted with CH<sub>2</sub>Cl<sub>2</sub> (4 x 300 mL). The combined organic layers were washed with brine (1 x 250 mL), dried (MgSO<sub>4</sub>), filtered, and concentrated. Purification by flash column chromatography (10% EtOAc/hexanes) yielded **4.57** as an orange solid (7.23 g, 21.4 mmol, 66%). MP: 56-59 °C; [ $\alpha$ ]<sub>D</sub><sup>20</sup> -127 (*c* 0.25, CHCl<sub>3</sub>); <sup>1</sup>H NMR (400 MHz, CDCl<sub>3</sub>):  $\delta$  6.40 (dd, *J* = 2.6, 0.8 Hz, 1H), 4.55-4.50 (m, 1H), 4.39 (dd, *J* = 5.0, 2.8 Hz, 1H), 3.59 (s, 1H), 2.43 (dd, *J* = 15.1, 4.1 Hz, 1H), 2.14 (dd, *J* = 15.1, 2.1 Hz, 1H), 1.61-1.54 (m, 2H), 1.47 (s, 3H), 1.36 (s, 3H), 1.23 (ddt, *J* = 16.3, 7.4, 7.2 Hz, 2H), 0.96 (t, *J* = 7.2 Hz, 3H); <sup>13</sup>C NMR (100 MHz, CDCl<sub>3</sub>):  $\delta$  138.1, 114.7, 110.3, 74.4, 73.3, 72.0, 45.5, 32.6, 28.0, 26.6, 17.1, 14.3; IR (film)  $\nu_{\text{max}}$  3518, 2984, 2959, 2933, 2873, 1620, 1381 cm<sup>-1</sup>; HRMS (ESI) *m/z* calcd. for C<sub>12</sub>H<sub>19</sub>INaO<sub>3</sub> [M+Na]<sup>+</sup> 361.0271, found 361.0270.



To a solution of **4.57** (4.00 g, 11.8 mmol, 1.0 eq) in THF (210 mL) and H<sub>2</sub>O (26 mL) was added **4.41** (4.55 g, 17.7 mmol, 1.5 eq), Ag<sub>2</sub>O (4.39 g, 18.9 mmol, 1.6 eq), and Ph<sub>3</sub>As (543 mg, 1.77 mmol, 0.15 eq), and the mixture was degassed (3x) with liquid N<sub>2</sub>, then Pd(PPh<sub>3</sub>)<sub>4</sub> (1.03 g, 0.887 mmol, 0.075 eq) was added and the reaction was stirred at RT for 20 h. The reaction was diluted with EtOAc (350 mL) and washed with brine (2 x 250 mL). The combined aqueous layers were extracted with EtOAc (2 x 150 mL), and the combined organic layers were dried (MgSO<sub>4</sub>), filtered, and concentrated. The orange oil was dissolved in MeOH (118 mL) and citric acid (1.13 g, 5.90 mmol, 0.5 eq) was added and the mixture was stirred at RT for 30 min. The mixture was concentrated, dissolved in Et<sub>2</sub>O (300 mL) and washed with

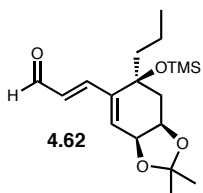


saturated aqueous NaHCO<sub>3</sub> (4 x 175 mL). The combined aqueous layers were extracted with Et<sub>2</sub>O (2 x 150 mL), and the combined organic layers were dried (MgSO<sub>4</sub>), filtered, and concentrated. Purification by flash column chromatography (40-80% EtOAc/hexanes) yielded **4.61** as an orange oil (2.24 g, 8.35 mmol, 71%).  $[\alpha]_{\text{D}}^{20}$  -50.0 (*c* 0.30, CHCl<sub>3</sub>); <sup>1</sup>H NMR (400 MHz, CDCl<sub>3</sub>): δ 6.33 (app. d, *J* = 15.6 Hz, 1H), 6.08 (dt, *J* = 15.6, 5.7 Hz, 1H), 5.66 (app. d, *J* = 2.6 Hz, 1H), 4.54 (dd, *J* = 5.3, 2.9 Hz, 1H), 4.50-4.43 (m, 1H), 4.21 (br. s, 2H), 3.41 (s, 1H), 2.19 (dd, *J* = 15.0, 4.4 Hz, 1H), 1.99 (dd, *J* = 14.9, 2.5 Hz, 1H), 1.62-1.53 (m, 2H), 1.41 (s, 3H), 1.36 (s, 3H), 1.32-1.10 (m, 2H), 0.90 (t, *J* = 7.3 Hz, 3H); <sup>13</sup>C NMR (100 MHz, CDCl<sub>3</sub>): δ 141.8, 130.6, 128.6, 122.7, 109.6, 73.1, 72.9, 70.3, 63.6, 41.4, 34.9, 28.3, 26.6, 17.0, 14.5; IR (film) ν<sub>max</sub> 3412, 2960, 2934, 2873, 1372, 1218 cm<sup>-1</sup>; HRMS (ESI) *m/z* calcd. for C<sub>15</sub>H<sub>24</sub>NaO<sub>4</sub> [M+Na]<sup>+</sup> 291.1567, found 291.1558.

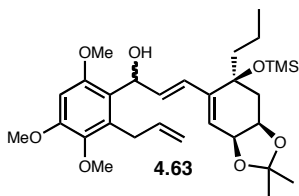


To a solution of **4.61** (2.24 g, 8.35 mmol, 1.0 eq) in CH<sub>2</sub>Cl<sub>2</sub> (167 mL) at RT was added MnO<sub>2</sub> (10.9 g, 125 mmol, 15 eq) and the reaction was stirred shielded from light for 2 h. The reaction was diluted with CH<sub>2</sub>Cl<sub>2</sub> (100 mL) and filtered through a plug of Celite with extensive CH<sub>2</sub>Cl<sub>2</sub> washes and the filtrate was concentrated to yield **S4.8** as a white solid requiring no further purification (1.93 g, 7.23 mmol, 87%).  $[\alpha]_{\text{D}}^{20}$  -56.6 (*c* 0.33, CHCl<sub>3</sub>); <sup>1</sup>H NMR (400 MHz, CDCl<sub>3</sub>): δ 9.58 (d, *J* = 7.8 Hz, 1H), 7.26 (d, *J* = 15.9 Hz, 1H), 6.50 (dd, *J* = 15.8, 7.8 Hz, 1H), 5.96 (app. s, 1H), 4.58 (app. s, 1H), 4.52 (app. s, 1H), 3.49 (s, 1H), 2.26 (dd, *J* = 15.1, 4.2 Hz, 1H), 2.03 (dd, *J* = 15.1, 1.6 Hz, 1H), 1.60 (ddt, *J* = 14.0, 12.3, 5.1 Hz, 2H), 1.38 (s, 3H), 1.37 (s, 3H), 1.33-1.19 (m, 1H), 1.18-1.04 (m, 1H), 0.89 (t, *J* = 7.3 Hz, 3H); <sup>13</sup>C NMR

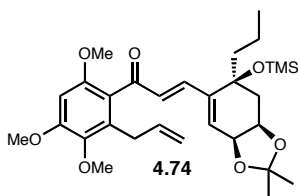
(100 MHz, CDCl<sub>3</sub>):  $\delta$  193.9, 151.4, 140.4, 131.1, 129.0, 110.0, 72.8, 72.5, 70.0, 41.6, 34.5, 28.2, 26.4, 17.0, 14.4; IR (film)  $\nu_{\max}$  3477, 2961, 2933, 2360, 1681, 1381 cm<sup>-1</sup>; HRMS (ESI)  $m/z$  calcd. for C<sub>15</sub>H<sub>22</sub>NaO<sub>4</sub> [M+Na]<sup>+</sup> 289.1410, found 289.1396.



To a solution of **S4.8** (1.93 g, 7.23 mmol, 1.0 eq) in CH<sub>2</sub>Cl<sub>2</sub> (15 mL) at 0 °C was added Et<sub>3</sub>N (8.05 mL, 57.8 mmol, 8.0 eq) then TMSTFA (6.77 mL, 43.4 mmol, 6.0 eq) which caused gas evolution and the reaction was stirred at 0 °C for 5 min then at RT. The reaction turned dark red, and after 4 h, was cooled to 0 °C and brine (75 mL) was carefully added. The mixture was added to brine (100 mL) and extracted with CH<sub>2</sub>Cl<sub>2</sub> (4 x 75 mL). The combined organic layers were dried (MgSO<sub>4</sub>), filtered, and concentrated. Immediate purification by flash column chromatography (5-10% EtOAc/hexanes containing 1% Et<sub>3</sub>N) provided **4.62** as a yellow solid (1.93 g, 5.69 mmol, 79%). MP: 85-87 °C; [ $\alpha$ ]<sub>D</sub><sup>20</sup> +47.8 (*c* 0.28, CHCl<sub>3</sub>); <sup>1</sup>H NMR (400 MHz, C<sub>6</sub>D<sub>6</sub>):  $\delta$  9.40 (d, *J* = 7.5 Hz, 1H), 6.74 (d, *J* = 16.1 Hz, 1H), 6.61 (dd, *J* = 16.1, 7.5 Hz, 1H), 5.82 (d, *J* = 3.8 Hz, 1H), 4.11 (dd, *J* = 6.5, 4.0 Hz, 1H), 4.00 (ddd, *J* = 11.4, 5.8, 5.8 Hz, 1H), 2.23 (dd, *J* = 11.9, 5.6 Hz, 1H), 1.89 (app. t, *J* = 11.4 Hz, 1H), 1.48 (s, 3H), 1.42 (dt, *J* = 13.0, 4.4 Hz, 1H), 1.37-1.26 (m, 1H), 1.29 (s, 3H), 1.25-1.10 (m, 1H), 1.01 (dt, *J* = 13.2, 4.6 Hz, 1H), 0.77 (t, *J* = 7.3 Hz, 3H), 0.07 (s, 9H); <sup>13</sup>C NMR (100 MHz, C<sub>6</sub>D<sub>6</sub>):  $\delta$  193.0, 149.7, 146.5, 131.9, 109.7, 77.0, 72.1, 71.2, 43.3, 39.9, 28.4, 25.8, 17.2, 14.6, 2.1; IR (film)  $\nu_{\max}$  2960, 2874, 2721, 1687, 1622, 1373, 1253 cm<sup>-1</sup>; HRMS (ESI)  $m/z$  calcd. for C<sub>18</sub>H<sub>31</sub>O<sub>4</sub>Si [M+H]<sup>+</sup> 339.1986, found 339.1982.

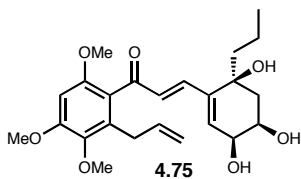


To a solution of **4.35** (600 mg, 2.09 mmol, 1.0 eq, dried by azeotropic removal of H<sub>2</sub>O with benzene 2x and on high-vac for 2 h) in THF (15 mL, dried over activated 4 Å MS for 2 h) at –78 °C was added *n*-BuLi (2.2 M in hexanes, 1.04 mL, 2.30 mmol, 1.1 eq) dropwise and the yellow mixture was stirred at –78 °C for 30 min. To the mixture at –78 °C was added a solution of **4.62** (778 mg, 2.30 mmol, 1.1 eq, dried by azeotropic removal of H<sub>2</sub>O with benzene 2x and on high-vac for 1 h) in THF (5.9 mL, dried over activated 4 Å MS for 2 h) via cannula and the reaction was stirred at –78 °C for 30 min and at RT for 22 h. To the reaction was added saturated aqueous NH<sub>4</sub>Cl and the mixture was extracted with CH<sub>2</sub>Cl<sub>2</sub> (4 x 40 mL). The combined organic layers were dried (MgSO<sub>4</sub>), filtered, and concentrated. Purification by flash column chromatography (10-50% EtOAc/hexanes containing 1% Et<sub>3</sub>N) provided **4.63** as an inseparable mixture of diastereomers as a yellow oil (820 mg, 1.50 mmol, 72%). IR (film)  $\nu_{\text{max}}$  3546, 2959, 2873, 2839, 1597, 1485, 1326, 1250 cm<sup>-1</sup>; HRMS (ESI)  $m/z$  calcd. for C<sub>30</sub>H<sub>47</sub>O<sub>7</sub>Si [M+H]<sup>+</sup> 547.3092, found 547.3086.



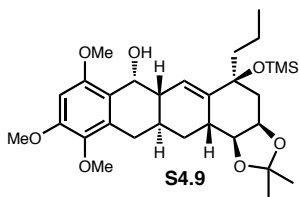
To a solution of **4.63** (267 mg, 0.488 mmol, 1.0 eq) in CH<sub>2</sub>Cl<sub>2</sub> (9.8 mL) was added MnO<sub>2</sub> (1.06 g, 12.2 mmol, 25 eq) and the black slurry was stirred at RT for 5 h. The reaction was diluted with CH<sub>2</sub>Cl<sub>2</sub> (25 mL) and filtered through a plug of Celite with CH<sub>2</sub>Cl<sub>2</sub> washes (3 x 25 mL). The filtrate was concentrated, and purification by flash column chromatography (10-40% EtOAc/hexanes) yielded **4.74** as an orange oil (252 mg, 0.463 mmol, 95%). [ $\alpha$ ]<sub>D</sub><sup>20</sup> +67.6 (*c* 0.71, CHCl<sub>3</sub>); <sup>1</sup>H NMR (400 MHz, C<sub>6</sub>D<sub>6</sub>):  $\delta$  7.34 (d, *J* = 16.2 Hz, 1H), 7.04

(d,  $J = 16.2$  Hz, 1H), 6.15 (dddd,  $J = 17.0, 10.2, 6.4, 6.4$  Hz, 1H), 6.09 (s, 1H), 5.99 (d,  $J = 3.8$  Hz, 1H), 5.17 (dd,  $J = 17.1, 1.7$  Hz, 1H), 5.01 (dd,  $J = 10.0, 1.3$  Hz, 1H), 4.13 (dd,  $J = 6.5, 3.9$  Hz, 1H), 4.05 (ddd,  $J = 17.0, 11.4, 5.8$  Hz, 1H), 3.76-3.62 (m, 2H), 3.71 (s, 3H), 3.33 (s, 3H), 3.26 (s, 3H), 2.25 (dd,  $J = 11.9, 5.5$  Hz, 1H), 1.95 (dd,  $J = 11.4, 11.4$  Hz, 1H), 1.58-1.44 (m, 1H), 1.49 (s, 3H), 1.33-1.18 (m, 1H), 1.29-1.18 (m, 1H), 1.28 (s, 3H), 1.10 (ddd,  $J = 13.2, 13.2, 4.5$  Hz, 1H), 0.79 (t,  $J = 7.3$  Hz, 3H), 0.09 (s, 9H);  $^{13}\text{C}$  NMR (100 MHz,  $\text{C}_6\text{D}_6$ ):  $\delta$  195.6, 154.3, 153.6, 146.9, 142.5, 141.9, 137.5, 133.2, 131.9, 125.3, 123.5, 115.8, 109.5, 96.3, 77.0, 72.2, 71.4, 60.5, 55.8, 55.5, 43.6, 40.2, 31.8, 28.4, 25.8, 17.2, 14.6, 2.0; IR (film)  $\nu_{\text{max}}$  2959, 2937, 1650, 1595, 1332, 1253  $\text{cm}^{-1}$ ; HRMS (ESI)  $m/z$  calcd. for  $\text{C}_{30}\text{H}_{45}\text{O}_7\text{Si}$   $[\text{M}+\text{H}]^+$  545.2929, found 545.2929.

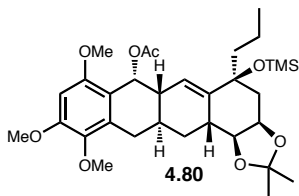


To a solution of **4.74** (113 mg, 0.207 mmol, 1.0 eq) in  $\text{CH}_3\text{CN}$  (830  $\mu\text{L}$ ) was added 2 N aqueous HCl (830  $\mu\text{L}$ ) and the dark red reaction mixture was stirred at RT for 4 h. To the reaction was added saturated aqueous  $\text{NaHCO}_3$  (10 mL) and the mixture was extracted with EtOAc (3 x 10 mL). The combined organic layers were dried ( $\text{MgSO}_4$ ), filtered, and concentrated. Purification by flash column chromatography (5% MeOH/ $\text{CH}_2\text{Cl}_2$ ) yielded **4.75** as a yellow oil (75 mg, 0.173 mmol, 84%).  $[\alpha]_{\text{D}}^{20} +64.2$  ( $c$  2.5,  $\text{CHCl}_3$ );  $^1\text{H}$  NMR (400 MHz,  $\text{CDCl}_3$ ):  $\delta$  7.03 (d,  $J = 16.0$  Hz, 1H), 6.72 (d,  $J = 16.0$  Hz, 1H), 6.41 (s, 1H), 5.90 (s, 1H), 5.83 (dddd,  $J = 15.7, 6.4, 6.4, 3.2$  Hz, 1H), 4.95 (ddd,  $J = 6.9, 1.6, 1.6$  Hz, 1H), 4.92 (dd,  $J = 1.4, 1.4$  Hz, 1H), 4.25 (br. m, 1H), 4.18 (br. m, 1H), 3.90 (s, 3H), 3.76 (s, 3H), 3.75 (s, 3H), 3.40 (br. s, 1H), 3.35 (dd,  $J = 1.4, 1.4$  Hz, 1H), 3.33 (dd,  $J = 1.4, 1.4$  Hz, 1H), 2.96 (br. s, 1H), 2.46 (br. s, 1H), 2.14 (dd,  $J = 14.5, 4.9$  Hz, 1H), 1.83 (dd,  $J =$

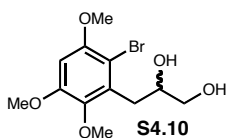
14.8, 1.7 Hz, 1H), 1.64-1.48 (m, 2H), 1.25-1.05 (m, 2H), 0.87 (t,  $J = 7.2$  Hz, 3H);  $^{13}\text{C}$  NMR (100 MHz,  $\text{CDCl}_3$ ):  $\delta$  196.7, 154.1, 153.4, 143.3, 141.4, 141.1, 136.7, 132.4, 131.3, 130.3, 121.9, 115.6, 95.4, 71.1, 69.1, 68.1, 60.9, 56.2, 55.9, 42.1, 37.4, 31.1, 17.1, 14.4; IR (film)  $\nu_{\text{max}}$  3410, 2959, 2929, 1640, 1594, 1332, 1083  $\text{cm}^{-1}$ ; HRMS (ESI)  $m/z$  calcd. for  $\text{C}_{24}\text{H}_{33}\text{O}_7$   $[\text{M}+\text{H}]^+$  433.2221, found 433.2218.



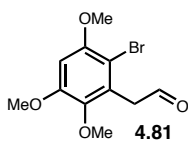
A solution of **4.63** (113 mg, 0.207 mmol, 1.0 eq) in toluene (40 mL) was heated at 75 °C for 48 h. At RT, the reaction was concentrated, and purification by flash column chromatography (25-45% EtOAc/hexanes) containing 1%  $\text{Et}_3\text{N}$  provided **S4.9** as a yellow oil (32 mg, 0.0585 mmol, 28%).  $[\alpha]_{\text{D}}^{20} +57.0$  ( $c$  0.48,  $\text{CHCl}_3$ );  $^1\text{H}$  NMR (600 MHz,  $\text{C}_6\text{D}_6$ ):  $\delta$  6.13 (s, 1H), 6.05 (s, 1H), 5.10 (d,  $J = 3.7$  Hz, 1H), 4.13 (dd,  $J = 9.7, 6.4$  Hz, 1H), 4.05 (ddd,  $J = 13.4, 5.6, 2.1$  Hz, 1H), 3.71 (s, 3H), 3.44 (s, 3H), 3.29 (s, 3H), 3.18 (dd,  $J = 16.4, 3.6$  Hz, 1H), 2.98 (dd,  $J = 7.9, 6.9$  Hz, 1H), 2.47 (dd,  $J = 12.9, 2.3$  Hz, 1H), 2.38 (14.0, 8.0 Hz, 1H), 2.26 (m, 1H), 2.21 (dd,  $J = 16.5, 11.9$  Hz, 1H), 2.04 (dd,  $J = 14.1, 5.3$  Hz, 1H), 1.89 (ddd,  $J = 13.2, 13.2, 4.0$  Hz, 1H), 1.84 (ddd,  $J = 10.5, 1.6, 1.6$  Hz, 1H), 1.72 (ddd,  $J = 12.3, 12.3, 4.6$  Hz, 1H), 1.65-1.58 (m, 1H), 1.59 (s, 3H), 1.55 (ddd,  $J = 12.8, 12.8, 5.9$  Hz, 1H), 1.51-1.43 (m, 1H), 1.29 (s, 3H), 0.98 (t,  $J = 7.3$  Hz, 3H), 0.19 (s, 9H);  $^{13}\text{C}$  NMR (150 MHz,  $\text{C}_6\text{D}_6$ ):  $\delta$  154.5, 152.8, 141.4, 141.0, 132.8, 126.9, 121.4, 108.3, 95.4, 78.8, 75.4, 73.2, 65.3, 59.8, 55.9, 55.2, 43.3 (2C), 40.7, 36.4, 32.0, 31.2, 28.5, 25.5, 24.0, 17.6, 15.0, 2.5; IR (film)  $\nu_{\text{max}}$  3485, 2958, 2280, 1601, 1489, 1466, 1330  $\text{cm}^{-1}$ ; HRMS (ESI)  $m/z$  calcd. for  $\text{C}_{30}\text{H}_{46}\text{NaO}_7\text{Si}$   $[\text{M}+\text{Na}]^+$  569.2905, found 569.2930.



To a solution of **S4.9** (20 mg, 0.0366 mmol, 1.0 eq) in CH<sub>2</sub>Cl<sub>2</sub> (732  $\mu$ L) at 0 °C was added DMAP (2 mg, catalytic), pyridine (15  $\mu$ L, 0.183 mmol, 5.0 eq), and Ac<sub>2</sub>O (17  $\mu$ L, 0.183 mmol, 5.0 eq) and the reaction was stirred at 0 °C for 1 h and at RT for 21 h. To the reaction was added saturated aqueous NH<sub>4</sub>Cl and the mixture was extracted with CH<sub>2</sub>Cl<sub>2</sub> (3 x 10 mL). The combined organic layers were dried (MgSO<sub>4</sub>), filtered, and concentrated. Purification by flash column chromatography (20% EtOAc/hexanes containing 1% Et<sub>3</sub>N) yielded **4.80** as a clear oil (15 mg, 0.0255 mmol, 70%).  $[\alpha]_D^{20}$  +88.1 (*c* 0.60, CHCl<sub>3</sub>); <sup>1</sup>H NMR (600 MHz, C<sub>6</sub>D<sub>6</sub>):  $\delta$  6.79 (d, *J* = 3.3 Hz, 1H), 6.23 (s, 1H), 6.11 (s, 1H), 4.10 (ddd, *J* = 7.9, 6.3, 5.6 Hz, 1H), 4.04 (dd, *J* = 9.7, 6.6 Hz, 1H), 3.71 (s, 3H), 3.37 (s, 3H), 3.37 (s, 3H), 3.17 (dd, *J* = 16.8, 4.0 Hz, 1H), 2.94 (dd, *J* = 7.6, 7.1 Hz, 1H), 2.40 (dd, *J* = 14.1, 8.2 Hz, 1H), 2.38 (dd, *J* = 13.3, 2.7 Hz, 1H), 2.18 (dd, *J* = 16.8, 11.9 Hz, 1H), 2.14-2.06 (m, 1H), 2.11 (dd, *J* = 13.8, 5.2 Hz, 1H), 1.91 (ddd, *J* = 11.0, 4.3, 2.0 Hz, 1H), 1.86 (ddd, *J* = 13.2, 13.2, 3.7 Hz, 1H), 1.79 (s, 3H), 1.64 (ddd, *J* = 12.4, 12.4, 4.2 Hz, 1H), 1.61-1.54 (m, 1H), 1.59 (s, 3H), 1.47 (ddd, *J* = 13.0, 13.0, 6.0 Hz, 1H), 1.35-1.27 (m, 1H), 1.31 (s, 3H), 0.97 (dd, *J* = 7.3, 7.0 Hz, 3H), 0.17 (s, 9H); <sup>13</sup>C NMR (150 MHz, C<sub>6</sub>D<sub>6</sub>):  $\delta$  169.4, 155.2, 153.5, 142.6, 141.0, 133.6, 125.7, 117.0, 108.5, 95.4, 78.8, 75.2, 73.3, 66.8, 59.8, 55.6, 55.5, 43.7, 43.2, 40.8, 36.4, 31.5, 30.8, 28.4, 25.4, 24.9, 21.1, 17.8, 14.8, 2.5; IR (film)  $\nu_{\max}$  3436, 2959, 2102, 1734, 1644, 1233 cm<sup>-1</sup>; HRMS (ESI) *m/z* calcd. for C<sub>32</sub>H<sub>48</sub>NaO<sub>8</sub>Si [M+Na]<sup>+</sup> 611.3011, found 611.3013.

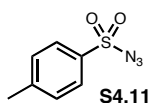


To a solution of **4.35** (3.60 g, 12.5 mmol, 1.0 eq) in acetone (12.5 mL) and H<sub>2</sub>O (12.5 mL) was added NMO (1.84 g, 15.7 mmol, 1.25 eq) and OsO<sub>4</sub> (1 mg, catalytic) and the reaction was vigorously stirred at RT for 20 h. The thick slurry was diluted with EtOAc (50 mL), added to 20% aqueous Na<sub>2</sub>SO<sub>3</sub> (250 mL) and extracted with EtOAc (3 x 100 mL). The combined organic layers were dried (MgSO<sub>4</sub>), filtered and concentrated. The white solid (**S4.10**) was taken forward crude, except for characterization, in which recrystallization (EtOAc) provided **S4.10** as a crystalline white solid. MP: 116-120 °C; <sup>1</sup>H NMR (400 MHz, CDCl<sub>3</sub>): δ 6.47 (s, 1H), 4.01-3.91 (m, 1H), 3.87 (s, 3H), 3.86 (s, 3H), 3.79 (s, 3H), 3.61 (ddd, *J* = 11.5, 8.0, 3.1 Hz, 1H), 3.47 (dt, *J* = 11.4, 5.0 Hz, 1H), 3.09 (dd, *J* = 13.2, 7.2 Hz, 1H), 3.02 (dd, *J* = 13.2, 6.4 Hz, 1H), 2.79 (d, *J* = 5.9 Hz, 1H), 2.56 (dd, *J* = 8.0, 5.1 Hz, 1H); <sup>13</sup>C NMR (100 MHz, CDCl<sub>3</sub>): δ 153.0, 152.2, 141.6, 132.4, 104.8, 96.7, 71.4, 65.6, 61.0, 56.7, 56.0, 34.1; IR (film) ν<sub>max</sub> 3301, 2965, 2361, 2341, 1579 cm<sup>-1</sup>; HRMS (ESI) *m/z* calcd. for C<sub>12</sub>H<sub>18</sub>BrO<sub>5</sub> [M+H]<sup>+</sup> 321.0332, found 321.0345.

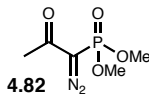


To a solution of crude **S4.10** (3.90 g, 12.1 mmol, 1.0 eq) in MeOH (121 mL) and pH 7 buffer (60.7 mL) was added NaIO<sub>4</sub> (3.35 g, 15.7 mmol, 1.3 eq) and the reaction was stirred at RT for 45 min. The thick white slurry was diluted with H<sub>2</sub>O (250 mL) and extracted with CH<sub>2</sub>Cl<sub>2</sub> (4 x 175 mL), and the combined organic layers were washed with brine (1 x 175 mL), dried (MgSO<sub>4</sub>), filtered and concentrated. Purification by flash column chromatography (20-40% EtOAc/hexanes) provided **4.81** as a white solid (2.91 g, 10.1 mmol, 81% two steps). MP: 83-85 °C; <sup>1</sup>H NMR (400 MHz, CDCl<sub>3</sub>): δ 9.70 (s, 1H), 6.53 (s, 1H), 3.94 (d, *J* = 1.3 Hz, 2H), 3.87 (s, 3H), 3.85 (s, 3H),

3.70 (s, 3H);  $^{13}\text{C}$  NMR (100 MHz,  $\text{CDCl}_3$ ):  $\delta$  198.4, 152.7, 152.3, 142.1, 128.2, 104.5, 97.4, 60.9, 56.6, 56.0, 44.9; IR (film)  $\nu_{\text{max}}$  2969, 2939, 1714, 1348  $\text{cm}^{-1}$ ; HRMS (ESI)  $m/z$  calcd. for  $\text{C}_{11}\text{H}_{14}\text{BrO}_4$   $[\text{M}+\text{H}]^+$  289.0070, found 289.0068.

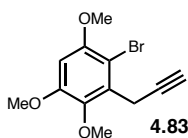


To a solution of sodium azide (11.3 g, 173 mmol, 1.1 eq) in EtOH (64 mL) and  $\text{H}_2\text{O}$  (32 mL) was added a hot solution ( $\sim 45^\circ\text{C}$ ) of toluenesulfonyl chloride (30.0 g, 157 mmol, 1.0 eq) in EtOH (160 mL), and the reaction precipitated NaCl and became slightly orange. After 3 h at RT, EtOH was removed in vacuo and the residue was added to  $\text{H}_2\text{O}$  (190 mL) and separated. The oil was washed with  $\text{H}_2\text{O}$  (2 x 20 mL), dried ( $\text{MgSO}_4$ ), and filtered to yield **S4.11** as a clear oil (19.5 g, 99.1 mmol, 63%). Spectral data were consistent with reported literature values.<sup>43</sup>

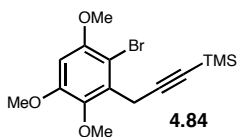


To a slurry of NaH (60% in mineral oil, 1.32 g, 33.1 mmol, 1.1 eq) in THF (53 mL) and toluene (40 mL) at  $0^\circ\text{C}$  was added neat dimethyl 2-oxopropylphosphonate (5.00 g, 30.1 mmol, 1.0 eq) which caused gas evolution. After 5 min, a solution of **S4.11** (6.53 g, 33.1 mmol, 1.1 eq) in THF (18 mL) was added via cannula and the reaction was stirred at RT for 22 h. The orange slurry was diluted with petroleum ether (500 mL) and filtered through a plug of celite with extensive petroleum ether washes. Concentration of the opaque filtrate was followed by purification by flash column chromatography (1:1 EtOAc/petroleum ether (1000 mL) and 1:1:0.1 EtOAc/petroleum ether/MeOH (600 mL)) to yield the Bestmann-Ohira reagent (**4.82**) as a yellow oil (4.10 g, 21.3 mmol, 71%). Spectral data were consistent with reported literature values.<sup>29</sup>



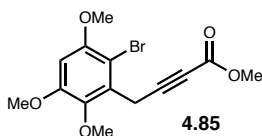


To a solution of **4.81** (2.91 g, 10.1 mmol, 1.0 eq) in MeOH (101 mL) was added  $\text{K}_2\text{CO}_3$  (4.17 g, 30.2 mmol, 3.0 eq) and a solution of the Bestmann-Ohira reagent (**4.82**, 2.90 g, 15.1 mmol, 1.5 eq) in MeOH (20 mL) via cannula and the reaction was stirred at RT for 4 h. The reaction was diluted with  $\text{H}_2\text{O}$  (275 mL) and extracted with EtOAc (3 x 200 mL). The combined organic layers were washed with brine (1 x 200 mL), dried ( $\text{MgSO}_4$ ), filtered, and concentrated. Purification by flash column chromatography (10-30% EtOAc/hexanes) provided **4.83** as a white solid (2.76 g, 9.68 mmol, 96%). MP: 91-94 °C;  $^1\text{H}$  NMR (400 MHz,  $\text{CDCl}_3$ ):  $\delta$  6.51 (s, 1H), 3.88 (s, 3H), 3.88 (s, 3H), 3.86 (s, 3H), 3.77 (d,  $J = 2.7$  Hz, 2H), 2.02 (t,  $J = 2.7$  Hz, 1H);  $^{13}\text{C}$  NMR (100 MHz,  $\text{CDCl}_3$ ):  $\delta$  152.8, 152.5, 141.5, 131.7, 104.2, 97.1, 81.5, 68.4, 61.3, 56.7, 56.1, 20.0; IR (film)  $\nu_{\text{max}}$  3302, 2966, 2939, 2840, 2361, 2341, 1580, 1341  $\text{cm}^{-1}$ ; HRMS (ESI)  $m/z$  calcd. for  $\text{C}_{12}\text{H}_{14}\text{BrO}_3$   $[\text{M}+\text{H}]^+$  285.0121, found 285.0104.

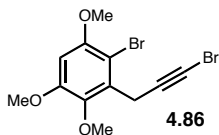


To a solution of **4.83** (300 mg, 1.05 mmol, 1.0 eq) in THF (4.2 mL) at 0 °C was added ethyl magnesium chloride (2.0 M in THF, 3.16 mL, 6.31 mmol, 6.0 eq) dropwise and the mixture was stirred at 0 °C for 50 min. To the mixture at 0 °C was added  $\text{TMSCl}$  (1.34 mL, 10.5 mmol, 10 eq) dropwise and the reaction was stirred at 0 °C for 1 h and at RT for 22 h. To the reaction was added saturated aqueous  $\text{NH}_4\text{Cl}$  (15 mL) and the mixture was extracted with  $\text{CH}_2\text{Cl}_2$  (4 x 15 mL). The combined organic layers were dried ( $\text{MgSO}_4$ ), filtered, and concentrated. Purification by flash column chromatography (20% EtOAc/hexanes) yielded **4.84** as a white solid (326 mg, 0.912 mmol, 87%). MP: 68-71 °C;  $^1\text{H}$  NMR (400 MHz,  $\text{CDCl}_3$ ):  $\delta$  6.49 (s, 1H), 3.88 (s, 3H), 3.88 (s, 3H), 3.85 (s, 3H), 3.79 (s, 2H), 0.1 (s, 9H);  $^{13}\text{C}$  NMR

(100 MHz, CDCl<sub>3</sub>):  $\delta$  152.7, 152.4, 141.6, 132.2, 104.4, 103.8, 96.9, 84.6, 61.4, 56.7, 56.0, 21.5, 0.0; IR (film)  $\nu_{\max}$  2959, 2840, 2175, 1581, 1480, 1341 cm<sup>-1</sup>; HRMS (ESI)  $m/z$  calcd. for C<sub>15</sub>H<sub>22</sub>BrO<sub>3</sub>Si [M+H]<sup>+</sup> 357.0516, found 357.0520.

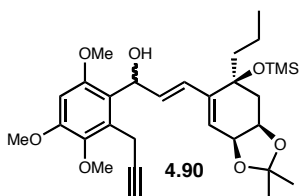


To a solution of **4.83** (62 mg, 0.217 mmol, 1.0 eq) in THF (2.17 mL) at 0 °C was added ethyl magnesium chloride (2.0 M in THF, 761  $\mu$ L, 1.52 mmol, 7.0 eq) and the mixture was stirred at 0 °C for 50 min. To the mixture at 0 °C was added methyl chloroformate (151  $\mu$ L, 1.96 mmol, 9.0 eq) and the reaction was stirred at 0 °C for 1.25 h. Saturated aqueous NH<sub>4</sub>Cl (15 mL) was added and the mixture was extracted with CH<sub>2</sub>Cl<sub>2</sub> (3 x 15 mL). The combined organic layers were dried (MgSO<sub>4</sub>), filtered, and concentrated. Purification by flash column chromatography (20-25% EtOAc/hexanes) provided **4.85** as a white solid (50 mg, 0.146 mmol, 67%). MP: 98-101 °C; <sup>1</sup>H NMR (600 MHz, CDCl<sub>3</sub>):  $\delta$  6.51 (s, 1H), 3.91 (s, 2H), 3.88 (s, 3H), 3.87 (s, 3H), 3.84 (s, 3H), 3.71 (s, 3H); <sup>13</sup>C NMR (150 MHz, CDCl<sub>3</sub>):  $\delta$  154.1, 152.9, 152.5, 141.7, 129.6, 104.2, 97.5, 86.4, 72.5, 61.4, 56.8, 56.1, 52.5, 20.3; IR (film)  $\nu_{\max}$  2944, 2843, 2238, 1713, 1583, 1479 cm<sup>-1</sup>; HRMS (ESI)  $m/z$  calcd. for C<sub>14</sub>H<sub>15</sub>BrNaO<sub>5</sub> [M+Na]<sup>+</sup> 364.9995, found 365.0012.

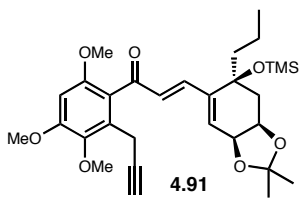


To a solution of **4.83** (75 mg, 0.263 mmol, 1.0 eq) in acetone (2.6 mL) was added NBS (56 mg, 0.316 mmol, 1.2 eq) and AgNO<sub>3</sub> (4.5 mg, 0.0263 mmol, 0.10 eq) and the reaction was stirred at RT for 3 h. The reaction was diluted with CH<sub>2</sub>Cl<sub>2</sub> (10 mL) and filtered through a plug of Celite with CH<sub>2</sub>Cl<sub>2</sub> washes (4 x 10 mL) and the filtrate was concentrated. Purification by flash column chromatography

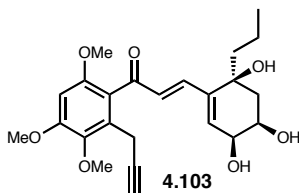
(20% EtOAc/hexanes) yielded **4.86** as an off-white solid (90 mg, 0.247 mmol, 94%). MP: 96-98 °C;  $^1\text{H}$  NMR (400 MHz,  $\text{CDCl}_3$ ):  $\delta$  6.49 (s, 1H), 3.87 (s, 3H), 3.86 (s, 3H), 3.83 (s, 3H), 3.76 (s, 2H);  $^{13}\text{C}$  NMR (100 MHz,  $\text{CDCl}_3$ ):  $\delta$  152.7, 152.4, 141.5, 131.2, 104.1, 97.0, 77.1, 61.3, 56.7, 56.0, 38.5, 21.1; IR (film)  $\nu_{\text{max}}$  2938, 2841, 2361, 2341, 1581, 1475, 1343  $\text{cm}^{-1}$ ; HRMS (ESI)  $m/z$  calcd. for  $\text{C}_{12}\text{H}_{13}\text{Br}_2\text{O}_3$   $[\text{M}+\text{H}]^+$  362.9226, found 362.9231.



To a solution of **4.83** (2.27 g, 7.95 mmol, 1.3 eq, dried by azeotropic removal of  $\text{H}_2\text{O}$  with benzene 2x and on high-vac for 2 h) in THF (32 mL, dried over activated 4 Å MS for 2 h) at  $-100$  °C was added *n*-BuLi (6.52 mL, 15.9 mmol, 2.5 eq) slowly, and the mixture was stirred at  $-100$  °C. After 8 min, a solution of **4.62** (2.15 g, 6.36 mmol, 1.0 eq, dried by azeotropic removal of  $\text{H}_2\text{O}$  with benzene 2x and on high-vac for 2 h) in THF (32 mL) was added quickly via syringe, and the red/orange reaction was stirred at  $-100$  °C. After 20 min, saturated aqueous  $\text{NH}_4\text{Cl}$  (50 mL) was added, and at RT, the mixture was diluted with saturated aqueous  $\text{NH}_4\text{Cl}$  (100 mL) and extracted with  $\text{CH}_2\text{Cl}_2$  (3 x 75 mL). The combined organic layers were washed with brine (1 x 75 mL), dried ( $\text{MgSO}_4$ ), filtered, and concentrated. Purification by flash column chromatography (30% EtOAc/hexanes containing 1%  $\text{Et}_3\text{N}$ ) provided **4.90** as a yellow solid in an inconsequential 1.5:1 mixture of inseparable diastereomers (2.62 g, 4.81 mmol, 76%). IR (film)  $\nu_{\text{max}}$  3539, 3308, 2959, 2872, 2118, 1599, 1251  $\text{cm}^{-1}$ ; HRMS (ESI)  $m/z$  calcd. for  $\text{C}_{30}\text{H}_{44}\text{NaO}_7\text{Si}$   $[\text{M}+\text{Na}]^+$  567.2749, found 567.2748.

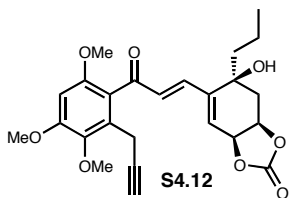


To a solution of **4.90** (100 mg, 0.184 mmol, 1.0 eq) in CH<sub>2</sub>Cl<sub>2</sub> (9.2 mL) was added MnO<sub>2</sub> (399 mg, 4.59 mmol, 25 eq) and the black slurry was stirred at RT for 5.5 h. The mixture was diluted with CH<sub>2</sub>Cl<sub>2</sub> and filtered through a plug of Celite with CH<sub>2</sub>Cl<sub>2</sub> washes. The filtrate was concentrated to provide **4.91** as a light yellow oil which required no purification (93 mg, 0.171 mmol, 93%). [ $\alpha$ ]<sub>D</sub><sup>20</sup> +80.0 (*c* 0.25, C<sub>6</sub>D<sub>6</sub>); <sup>1</sup>H NMR (400 MHz, CDCl<sub>3</sub>):  $\delta$  7.43 (d, *J* = 16.2 Hz, 1H), 7.13 (d, *J* = 16.2 Hz, 1H), 6.05 (s, 1H), 6.01 (d, *J* = 3.9 Hz, 1H), 4.15 (dd, *J* = 6.4, 4.0 Hz, 1H), 4.06 (ddd, *J* = 11.3, 11.3, 5.8 Hz, 1H), 3.84 (dd, *J* = 16.7, 2.7 Hz, 1H), 3.78 (dd, *J* = 16.7, 2.8 Hz, 1H), 3.78 (s, 3H), 3.29 (s, 3H), 3.23 (s, 3H), 2.27 (dd, *J* = 11.8, 5.5 Hz, 1H), 1.97 (dd, *J* = 11.5, 11.5 Hz, 1H), 1.77 (dd, *J* = 2.7, 2.7 Hz, 1H), 1.57 (ddd, *J* = 14.2, 14.2, 4.1 Hz, 1H), 1.49 (s, 3H), 1.47-1.34 (m, 1H), 1.28 (s, 3H), 1.26-1.17 (m, 1H), 1.11 (ddd, *J* = 13.1, 13.1, 4.5 Hz, 1H), 0.78 (dd, *J* = 7.3, 7.3 Hz, 3H), 0.12 (s, 9H); <sup>13</sup>C NMR (100 MHz, C<sub>6</sub>D<sub>6</sub>):  $\delta$  195.6, 155.1, 154.5, 147.7, 142.7, 142.5, 132.4, 131.0, 126.0, 123.7, 110.1, 97.4, 83.6, 77.7, 72.9, 72.0, 69.7, 61.3, 56.4, 56.1, 44.1, 40.7, 29.0, 26.4, 17.7, 16.9, 15.2, 2.7; IR (film)  $\nu_{\max}$  3311, 2959, 2360, 2341, 1650, 1597, 1334, 1252 cm<sup>-1</sup>; HRMS (ESI) *m/z* calcd. for C<sub>30</sub>H<sub>43</sub>O<sub>7</sub>Si [M+H]<sup>+</sup> 543.2773, found 543.2774.



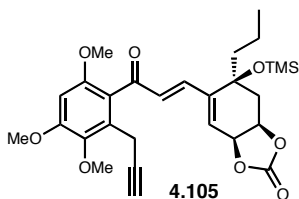
To a solution of **4.91** (146 mg, 0.269 mmol, 1.0 eq) in CH<sub>3</sub>CN (2.7 mL) was added aqueous 2 N HCl (2.7 mL) at RT and the orange reaction was stirred at RT for 3 h. To the mixture was added saturated aqueous NaHCO<sub>3</sub> (10 mL) and the mixture was extracted with EtOAc (3 x 10 mL). The combined organic layers were dried (MgSO<sub>4</sub>), filtered, and concentrated.

Purification by flash column chromatography (5% MeOH/CH<sub>2</sub>Cl<sub>2</sub>) yielded **4.103** as an orange oil (106 mg, 0.246 mmol, 92%). [ $\alpha$ ]<sub>D</sub><sup>20</sup> +113 (*c* 1.47, CHCl<sub>3</sub>); <sup>1</sup>H NMR (400 MHz, CDCl<sub>3</sub>):  $\delta$  7.11 (d, *J* = 16.0 Hz, 1H), 6.80 (d, *J* = 16.0 Hz, 1H), 6.44 (s, 1H), 5.93 (br. s, 1H), 4.20 (br. s, 1H), 4.13 (br. s, 1H), 3.90 (s, 3H), 3.83 (s, 3H), 3.75 (s, 3H), 3.68 (br. s, 1H), 3.51 (s, 1H), 3.50 (s, 1H), 3.35 (br. s, 1H), 3.15 (br. s, 1H), 2.10 (dd, *J* = 14.8, 4.9 Hz, 1H), 1.93 (dd, *J* = 2.7, 2.6 Hz, 1H), 1.80 (dd, *J* = 14.7, 1.3 Hz, 1H), 1.55 (dd, *J* = 8.7, 8.2 Hz, 2H), 1.23-1.04 (m, 2H), 0.86 (dd, *J* = 7.3, 7.1 Hz, 3H); <sup>13</sup>C NMR (100 MHz, CDCl<sub>3</sub>):  $\delta$  196.2, 154.4, 153.8, 143.6, 141.0, 140.9, 131.1, 130.8, 129.6, 121.4, 96.1, 82.4, 71.2, 69.0, 68.9, 68.0, 61.1, 56.2, 55.9, 41.9, 37.4, 17.1, 16.1, 14.4; IR (film)  $\nu_{\text{max}}$  3410, 3305, 2959, 2249, 1597, 1335 cm<sup>-1</sup>; HRMS (ESI) *m/z* calcd. for C<sub>24</sub>H<sub>31</sub>O<sub>7</sub> [M+H]<sup>+</sup> 431.2064, found 431.2063.



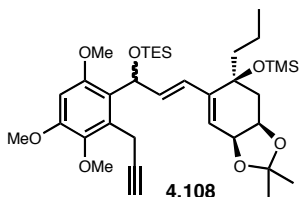
To a solution of **4.103** (67 mg, 0.156 mmol, 1.0 eq) in CH<sub>2</sub>Cl<sub>2</sub> (760  $\mu$ L) at 0 °C was added Et<sub>3</sub>N (108  $\mu$ L, 0.778 mmol, 5.0 eq) then a solution of triphosgene (51 mg, 0.171 mmol, 1.1 eq) in CH<sub>2</sub>Cl<sub>2</sub> (760  $\mu$ L) via cannula and the reaction was stirred at 0 °C for 5 min and at RT for 1.5 h. To the reaction was added saturated aqueous NH<sub>4</sub>Cl (15 mL) and the mixture was extracted with CH<sub>2</sub>Cl<sub>2</sub> (3 x 10 mL). The combined organic layers were dried (MgSO<sub>4</sub>), filtered, and concentrated. Purification by flash column chromatography (50% EtOAc/hexanes) provided **S4.12** as a yellow oil (51 mg, 0.112 mmol, 72%). <sup>1</sup>H NMR (600 MHz, C<sub>6</sub>D<sub>6</sub>):  $\delta$  7.36 (d, *J* = 16.0 Hz, 1H), 7.14 (d, *J* = 16.1 Hz, 1H), 6.06 (s, 1H), 5.53 (d, *J* = 3.5 Hz, 1H), 4.04 (dd, *J* = 7.3, 3.5 Hz, 1H), 3.92-3.84 (m, 2H), 3.85 (dd, *J* = 5.0, 2.7 Hz, 1H), 3.75 (s, 3H), 3.31 (s, 3H), 3.29 (s, 3H), 1.86 (dd, *J* = 2.6, 2.6 Hz, 1H),

1.77 (dd,  $J = 13.1, 5.4$  Hz, 1H), 1.71 (br. s, 1H), 1.34 (ddd,  $J = 13.5, 13.5, 4.1$  Hz, 1H), 1.21 (dd,  $J = 12.7, 10.5$  Hz, 1H), 1.20-1.13 (m, 1H), 0.98 (dddd,  $J = 17.5, 5.3, 5.0, 4.9$  Hz, 1H), 0.87 (ddd,  $J = 13.6, 13.6, 4.7$  Hz, 1H), 0.69 (dd,  $J = 7.3, 7.3$  Hz, 3H);  $^{13}\text{C}$  NMR (150 MHz,  $\text{C}_6\text{D}_6$ ):  $\delta$  194.5, 155.0, 154.5, 153.9, 148.7, 142.0, 139.4, 133.1, 130.7, 122.6, 121.3, 96.7, 83.2, 72.6, 71.8, 71.5, 69.2, 60.8, 56.0, 55.5, 41.8, 37.4, 16.9, 16.2, 14.5; IR (film)  $\nu_{\text{max}}$  3468, 3292, 2961, 2361, 1801, 1650, 1596, 1335  $\text{cm}^{-1}$ ; HRMS (ESI)  $m/z$  calcd. for  $\text{C}_{25}\text{H}_{29}\text{O}_8$   $[\text{M}+\text{H}]^+$  457.1857, found 457.1871.

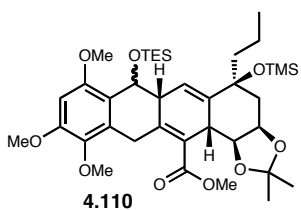


To a solution of **S4.12** (51 mg, 0.112 mmol, 1.0 eq) in  $\text{CH}_2\text{Cl}_2$  (600  $\mu\text{L}$ ) at 0  $^\circ\text{C}$  was added  $\text{Et}_3\text{N}$  (124  $\mu\text{L}$ , 0.894 mmol, 8.0 eq) then TMSTFA (105  $\mu\text{L}$ , 0.670 mmol, 6.0 eq) and the reaction was stirred at RT for 5 h. To the reaction was added brine (10 mL) and the mixture was extracted with  $\text{CH}_2\text{Cl}_2$  (3 x 10 mL). The combined organic layers were dried ( $\text{MgSO}_4$ ), filtered, and concentrated. Purification by flash column chromatography (40% EtOAc/hexanes containing 1%  $\text{Et}_3\text{N}$ ) gave **4.105** as a yellow oil (41 mg, 0.0776 mmol, 69%).  $[\alpha]_{\text{D}}^{20} +33.3$  ( $c$  1.16,  $\text{CHCl}_3$ );  $^1\text{H}$  NMR (400 MHz,  $\text{C}_6\text{D}_6$ ):  $\delta$  7.29 (d,  $J = 16.2$  Hz, 1H), 6.96 (d,  $J = 16.2$  Hz, 1H), 6.06 (s, 1H), 5.55 (d,  $J = 3.7$  Hz, 1H), 4.01 (dd,  $J = 7.7, 3.8$  Hz, 1H), 3.96-3.84 (m, 2H), 3.80 (dd,  $J = 8.0, 2.6$  Hz, 1H), 3.77 (s, 3H), 3.30 (s, 3H), 3.23 (s, 3H), 2.08 (dd,  $J = 12.2, 5.7$  Hz, 1H), 1.77 (dd,  $J = 2.6, 2.6$  Hz, 1H), 1.71 (dd,  $J = 11.6, 11.6$  Hz, 1H), 1.32-1.19 (m, 2H), 1.08-0.97 (m, 1H), 0.79 (ddd,  $J = 13.1, 13.1, 4.6$  Hz, 1H), 0.70 (dd,  $J = 7.2, 7.2$  Hz, 3H), 0.0 (s, 9H);  $^{13}\text{C}$  NMR (100 MHz,  $\text{C}_6\text{D}_6$ ):  $\delta$  194.6, 154.8, 154.1, 153.6, 149.6, 142.2, 139.7, 132.8, 130.6, 122.6, 120.1, 96.7, 83.0, 75.1, 72.3, 71.4, 69.1, 60.8, 55.8, 55.5, 43.7, 38.3, 17.0, 16.2, 14.4, 1.9; IR (film)  $\nu_{\text{max}}$  3293,

2960, 2361, 1805, 1597, 1335  $\text{cm}^{-1}$ ; HRMS (ESI)  $m/z$  calcd. for  $\text{C}_{28}\text{H}_{37}\text{O}_8\text{Si}$   $[\text{M}+\text{H}]^+$  529.2252, found 529.2255.



To a solution of **4.90** (250 mg, 0.459 mmol, 1.0 eq) in  $\text{CH}_2\text{Cl}_2$  (1.53 mL) was added imidazole (156 mg, 2.29 mmol, 5.0 eq) and DMAP (2 mg, catalytic) at 0 °C. To the solution was added TESC1 (231  $\mu\text{L}$ , 1.38 mmol, 3.0 eq) and the slurry was stirred at 0 °C for 10 min. To the reaction was added saturated aqueous  $\text{NH}_4\text{Cl}$  and the mixture was extracted with  $\text{CH}_2\text{Cl}_2$  (3 x 20 mL). The combined organic layers were dried ( $\text{MgSO}_4$ ), filtered, and concentrated. Purification by flash column chromatography (12% EtOAc/hexanes containing 1%  $\text{Et}_3\text{N}$ ) provided **4.108** as a yellow oil in an inconsequential 1.5:1 mixture of inseparable diastereomers (292 mg, 0.443 mmol, 97%). IR (film)  $\nu_{\text{max}}$  3309, 2957, 2877, 2118, 1597, 1463, 1244  $\text{cm}^{-1}$ ; HRMS (ESI)  $m/z$  calcd. for  $\text{C}_{36}\text{H}_{58}\text{NaO}_7\text{Si}_2$   $[\text{M}+\text{Na}]^+$  681.3613, found 681.3629.



To a solution of **4.108** (113 mg, 0.171 mmol, 1.0 eq) in THF (1.7 mL) at -78 °C was added *n*-BuLi (2.4 M in hexanes, 105  $\mu\text{L}$ , 0.257 mmol, 1.5 eq) and the mixture was stirred at -78 °C for 30 min. To the mixture was added Manders' reagent (41  $\mu\text{L}$ , 0.514 mmol, 3.0 eq) and the reaction was stirred at -78 °C for 2 h. To the reaction was added saturated aqueous  $\text{NH}_4\text{Cl}$  (25 mL) and at RT the mixture was extracted with  $\text{CH}_2\text{Cl}_2$  (3 x 15 mL). The combined organic layers were dried ( $\text{MgSO}_4$ ), filtered, and concentrated. Immediate purification by flash column chromatography (10% EtOAc/hexanes containing 1%  $\text{Et}_3\text{N}$ )

provided a 4:1 mixture of uncyclized to cyclized product as 1:1 mixtures of diastereomers. Material was taken to next step without characterization.

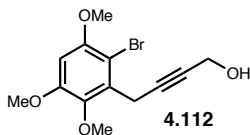
A solution of the previous products (4:1 mixture of products as 1:1 mixtures of diastereomers, 61 mg, 0.0851 mmol, 1.0 eq) in toluene (20 mL) was heated at 40 °C for 6 h then at RT concentrated. Purification by flash column chromatography (10-20% EtOAc/hexanes containing 1% Et<sub>3</sub>N) provided **4.110** as a separable mixture of two diastereomers.

$\beta$ -OTES: (27 mg, 0.0377 mmol, 22% two steps).  $[\alpha]_{\text{D}}^{20} +57.9$  (*c* 0.19, CHCl<sub>3</sub>); <sup>1</sup>H NMR (600 MHz, C<sub>6</sub>D<sub>6</sub>):  $\delta$  6.44 (d, *J* = 3.5 Hz, 1H), 6.08 (s, 1H), 5.13 (d, *J* = 7.0 Hz, 1H), 4.69 (d, *J* = 16.0 Hz, 1H), 4.12 (dd, *J* = 7.8, 7.6 Hz, 1H), 3.91 (dd, *J* = 12.1, 6.1 Hz, 1H), 3.88 (s, 3H), 3.59 (dd, *J* = 9.7, 6.1 Hz, 1H), 3.55 (s, 3H), 3.44 (ddd, *J* = 15.1, 11.2, 4.9 Hz, 1H), 3.36 (s, 3H), 3.32 (s, 3H), 3.09 (d, *J* = 15.5 Hz, 1H), 2.41 (dd, *J* = 14.3, 6.3 Hz, 1H), 1.87 (dd, *J* = 14.1, 5.8 Hz, 1H), 1.88-1.82 (m, 1H), 1.71-1.63 (m, 1H), 1.56 (ddd, *J* = 13.3, 13.3, 4.5 Hz, 1H), 1.55 (s, 3H), 1.42-1.33 (m, 1H), 1.15 (s, 3H), 1.12 (dd, *J* = 8.1, 7.9 Hz, 9H), 0.96 (dd, *J* = 7.3, 7.2 Hz, 3H), 0.81 (q, *J* = 8.0 Hz, 6H), 0.25 (s, 9H); <sup>13</sup>C NMR (150 MHz, C<sub>6</sub>D<sub>6</sub>):  $\delta$  169.1, 154.8, 153.3, 140.3, 140.2, 137.9, 133.6, 126.2, 122.9, 119.7, 108.8, 95.3, 82.1, 75.8, 74.8, 73.0, 60.3, 55.7, 54.3, 51.2, 48.7, 44.1, 40.3, 39.6, 29.6, 27.9, 25.4, 17.2, 14.9, 7.6, 6.3, 2.3; IR (film)  $\nu_{\text{max}}$  2956, 2877, 2279, 1726, 1599, 1462, 1246 cm<sup>-1</sup>; HRMS (ESI) *m/z* calcd. for C<sub>38</sub>H<sub>61</sub>O<sub>9</sub>Si<sub>2</sub> [M+H]<sup>+</sup> 717.3849, found 717.3857.

$\alpha$ -OTES: (23 mg, 0.0321 mmol, 19% two steps).  $[\alpha]_{\text{D}}^{20} +50.7$  (*c* 0.26, CHCl<sub>3</sub>); <sup>1</sup>H NMR (600 MHz, C<sub>6</sub>D<sub>6</sub>):  $\delta$  6.13 (s, 1H), 5.64 (d, *J* = 3.4 Hz, 1H), 5.28 (d, *J* = 2.2 Hz, 1H), 4.93

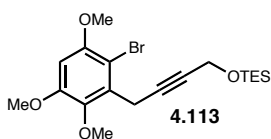


(d,  $J = 21.4$  Hz, 1H), 4.28-4.22 (m, 2H), 4.18 (dd,  $J = 6.9, 6.9$  Hz, 1H), 3.70-3.64 (m, 1H), 3.67 (s, 3H), 3.60 (s, 3H), 3.40 (s, 3H), 3.39 (s, 3H), 2.83 (ddd,  $J = 5.3, 3.5, 1.4$  Hz, 1H), 2.54 (dd,  $J = 14.2, 5.7$  Hz, 1H), 2.06 (dd,  $J = 14.2, 5.2$  Hz, 1H), 1.81 (ddd,  $J = 12.9, 12.9, 3.3$  Hz, 1H), 1.74-1.67 (m, 1H), 1.62 (s, 3H), 1.60 (ddd,  $J = 12.7, 12.7, 4.6$  Hz, 1H), 1.49-1.41 (m, 1H), 1.33 (s, 3H), 0.99 (dd,  $J = 7.3, 7.3$  Hz, 3H), 0.93 (dd,  $J = 8.0, 7.9$  Hz, 9H), 0.64 (dd, 14.8, 7.8 Hz, 2H), 0.60 (dd,  $J = 16.3, 7.9$  Hz, 2H), 0.56 (dd,  $J = 14.8, 8.0$  Hz, 2H), 0.24 (s, 9H);  $^{13}\text{C}$  NMR (150 MHz,  $\text{C}_6\text{D}_6$ ):  $\delta$  169.4, 153.3, 152.7, 141.5, 140.9, 135.1, 131.9, 122.3, 120.8, 108.7, 94.4, 82.9, 74.7, 73.2, 66.2, 59.8, 55.8, 54.5, 51.0, 45.2, 43.5, 40.0 (2C), 28.0, 27.5, 25.6, 17.2, 14.9, 7.3, 5.4, 2.4; IR (film)  $\nu_{\text{max}}$  2955, 2876, 2279, 1725, 1600, 1462, 1332, 1247  $\text{cm}^{-1}$ ; HRMS (ESI)  $m/z$  calcd. for  $\text{C}_{38}\text{H}_{61}\text{O}_9\text{Si}_2$   $[\text{M}+\text{H}]^+$  717.3849, found 717.3859.

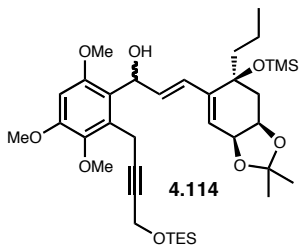


To a solution of **4.83** (1.00 g, 3.51 mmol, 1.0 eq) in THF (35.1 mL) at 0 °C was added ethyl magnesium chloride (2.0 M in THF, 10.5 mL, 21.0 mmol, 6.0 eq) and the mixture was stirred at 0 °C for 1 h. To the mixture at 0 °C was added paraformaldehyde (1.05 g, 35.1 mmol, 10 eq, dried on high-vac with  $\text{P}_2\text{O}_5$  overnight) and the reaction was stirred at RT for 22 h. To the reaction was added saturated aqueous  $\text{NH}_4\text{Cl}$  (100 mL) and the mixture was extracted with  $\text{CH}_2\text{Cl}_2$  (3 x 100 mL). The combined organic layers were washed with brine (1 x 100 mL), dried ( $\text{MgSO}_4$ ), filtered, and concentrated. Purification by flash column chromatography (40-50% EtOAc/hexanes) provided **4.112** as a white solid (970 mg, 3.08 mmol, 88%).  $^1\text{H}$  NMR (400 MHz,  $\text{CDCl}_3$ ):  $\delta$  6.49 (s, 1H), 4.19 (s, 2H), 3.87 (s, 3H), 3.86 (s, 3H), 3.83 (s, 3H), 3.77 (t,  $J = 2.1$  Hz, 2H), 1.83 (br. s, 1H);  $^{13}\text{C}$  NMR (100 MHz,  $\text{CDCl}_3$ ):  $\delta$  152.8, 152.5,

141.4, 131.9, 104.2, 97.0, 83.2, 78.5, 61.4, 56.7, 56.1, 51.3, 20.3; IR (film)  $\nu_{\max}$  3303, 2963, 1582, 1477  $\text{cm}^{-1}$ ; HRMS (ESI)  $m/z$  calcd. for  $\text{C}_{13}\text{H}_{16}\text{BrO}_4$   $[\text{M}+\text{H}]^+$  315.0226, found 315.0234.

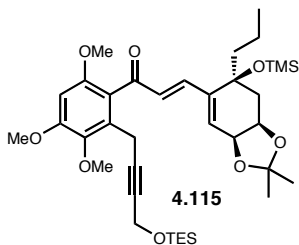


To a solution of **4.112** (970 mg, 3.08 mmol, 1.0 eq) in  $\text{CH}_2\text{Cl}_2$  (10.3 mL) at 0 °C was added imidazole (419 mg, 6.16 mmol, 2.0 eq), DMAP (2 mg, catalytic), and TESCl (775  $\mu\text{L}$ , 4.62 mmol, 1.5 eq) and the white slurry was stirred at 0 °C for 30 min. To the reaction was added saturated aqueous  $\text{NH}_4\text{Cl}$  (100 mL) and the mixture was extracted with  $\text{CH}_2\text{Cl}_2$  (3 x 100 mL). The combined organic layers were dried ( $\text{MgSO}_4$ ), filtered, and concentrated. Purification by flash column chromatography (20% EtOAc/hexanes) yielded **4.113** as a clear oil (1.23 g, 2.86 mmol, 93%).  $^1\text{H}$  NMR (400 MHz,  $\text{CDCl}_3$ ):  $\delta$  6.48 (s, 1H), 4.25 (t,  $J = 2.2$  Hz, 2H), 3.87 (s, 3H), 3.86 (s, 3H), 3.83 (s, 3H), 3.77 (t,  $J = 2.2$  Hz, 2H), 0.91 (t,  $J = 8.0$  Hz, 9H), 0.59 (q,  $J = 7.9$  Hz, 6H);  $^{13}\text{C}$  NMR (100 MHz,  $\text{CDCl}_3$ ):  $\delta$  152.7, 152.4, 141.6, 132.1, 104.4, 97.0, 82.1, 78.7, 61.4, 56.7, 56.1, 51.6, 20.4, 6.6, 4.4; IR (film)  $\nu_{\max}$  2953, 2876, 1582, 1475  $\text{cm}^{-1}$ ; HRMS (ESI)  $m/z$  calcd. for  $\text{C}_{19}\text{H}_{30}\text{BrO}_4\text{Si}$   $[\text{M}+\text{H}]^+$  429.1091, found 429.1096.



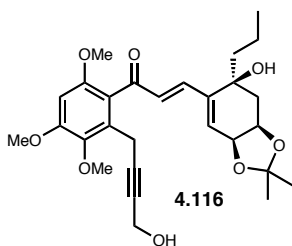
To a solution of **4.113** (1.35 g, 3.13 mmol, 1.5 eq, dried by azeotropic removal of  $\text{H}_2\text{O}$  with benzene 2x and on high-vac for 3 h) in THF (11 mL, dried over activated 4 Å MS for 3 h) at -100 °C was added  $n\text{-BuLi}$  (2.5 M in hexanes, 1.44 mL, 3.55 mmol, 1.7 eq) slowly, and the mixture was stirred at -100 °C for 12 min. To the mixture

at  $-100\text{ }^{\circ}\text{C}$  was added a solution of **4.62** (707 mg, 2.09 mmol, 1.0 eq, dried by azeotropic removal of  $\text{H}_2\text{O}$  with benzene 2x and on high-vac for 3 h) in THF (11 mL, dried over activated 4 Å MS for 3 h) via cannula quickly, and the reaction was stirred at  $-100\text{ }^{\circ}\text{C}$  for 30 min. To the reaction was added saturated aqueous  $\text{NH}_4\text{Cl}$  (25 mL) and at RT the mixture was added to saturated aqueous  $\text{NH}_4\text{Cl}$  (75 mL) and extracted with  $\text{CH}_2\text{Cl}_2$  (3 x 100 mL). The combined organic layers were dried ( $\text{MgSO}_4$ ), filtered, and concentrated. Purification by flash column chromatography (10-40% EtOAc/hexanes containing 1%  $\text{Et}_3\text{N}$ ) provided **4.114** as a yellow oil in an inseparable mixture of diastereomers (1.23 g, 1.78 mmol, 85%). IR (film)  $\nu_{\text{max}}$  3466, 2957, 2876, 1598, 1462, 1076  $\text{cm}^{-1}$ ; HRMS (ESI)  $m/z$  calcd. for  $\text{C}_{37}\text{H}_{60}\text{NaO}_8\text{Si}_2$   $[\text{M}+\text{Na}]^+$  711.3719, found 711.3729.



To a solution of **4.114** (264 mg, 0.383 mmol, 1.0 eq) in  $\text{CH}_2\text{Cl}_2$  (19 mL) was added  $\text{MnO}_2$  (833 mg, 9.58 mmol, 25 eq) and the black slurry was stirred at RT protected from light for 2 h. The reaction was diluted with  $\text{CH}_2\text{Cl}_2$  and filtered through a plug of Celite with extensive  $\text{CH}_2\text{Cl}_2$  washes, and the filtrate was concentrated. Purification by flash column chromatography (20-30% EtOAc/hexanes containing 1%  $\text{Et}_3\text{N}$ ) yielded **4.115** as a yellow oil (152 mg, 0.221 mmol, 58%).  $[\alpha]_{\text{D}}^{20} +18.6$  ( $c$  0.74,  $\text{CHCl}_3$ );  $^1\text{H}$  NMR (400 MHz,  $\text{C}_6\text{D}_6$ ):  $\delta$  7.43 (d,  $J = 16.2$  Hz, 1H), 7.15 (d,  $J = 16.2$  Hz, 1H), 6.07 (s, 1H), 6.05 (3.8 Hz, 1H), 4.27 (dd,  $J = 2.1, 2.0$  Hz, 2H), 4.19 (dd,  $J = 6.4, 4.0$  Hz, 1H), 4.07 (ddd,  $J = 11.4, 11.4, 5.8$  Hz, 1H), 3.88-3.84 (m, 2H), 3.85 (s, 3H), 3.30 (s, 3H), 3.24 (s, 3H), 2.28 (dd,  $J = 11.8, 5.5$  Hz, 1H), 1.97 (dd,  $J = 11.5, 11.4$  Hz, 1H), 1.58 (ddd,  $J = 12.6, 12.6, 4.1$  Hz, 1H), 1.50 (s, 3H), 1.48-1.38 (m, 1H), 1.34-1.22 (m, 1H), 1.29 (s, 3H),

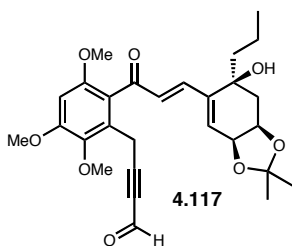
1.13 (ddd,  $J = 13.3, 13.3, 4.5$  Hz, 1H), 1.01 (dd,  $J = 8.0, 7.9$  Hz, 9H), 0.81 (dd,  $J = 7.4, 7.2$  Hz, 3H), 0.65 (dd,  $J = 15.8, 7.8$  Hz, 6H), 0.14 (s, 9H);  $^{13}\text{C}$  NMR (100 MHz,  $\text{C}_6\text{D}_6$ ):  $\delta$  195.0, 154.5, 153.9, 147.3, 142.2, 142.0, 131.9, 130.8, 125.5, 123.2, 109.5, 96.8, 83.8, 79.7, 77.1, 72.3, 71.4, 60.8, 55.9, 55.5, 52.0, 43.6, 40.2, 28.5, 25.8, 17.2, 16.9, 14.6, 7.1, 5.0, 2.1; IR (film)  $\nu_{\text{max}}$  2957, 2877, 1651, 1597, 1334, 1078  $\text{cm}^{-1}$ ; HRMS (ESI)  $m/z$  calcd. for  $\text{C}_{37}\text{H}_{59}\text{O}_8\text{Si}_2$   $[\text{M}+\text{H}]^+$  687.3743, found 687.3739.



To a solution of **4.115** (186 mg, 0.271 mmol, 1.0 eq) in THF (2.7 mL) at 0 °C was added TBAF (1 M in THF, 1.35 mL, 1.35 mmol, 5.0 eq) and the reaction was stirred at 0 °C. After 1 h, saturated aqueous  $\text{NH}_4\text{Cl}$  (25 mL) was added and the mixture

was extracted with  $\text{CH}_2\text{Cl}_2$  (3 x 25 mL), and the combined organic layers were dried ( $\text{MgSO}_4$ ), filtered, and concentrated. Purification by flash column chromatography (70-90% EtOAc/hexanes) provided **4.116** as an orange oil (125 mg, 0.250 mmol, 92%).  $^1\text{H}$  NMR (400 MHz,  $\text{CDCl}_3$ ):  $\delta$  7.14 (d,  $J = 16.0$  Hz, 1H), 6.81 (d,  $J = 16.0$  Hz, 1H), 6.42 (s, 1H), 5.99 (d,  $J = 2.8$  Hz, 1H), 4.58 (dd,  $J = 5.2, 3.1$  Hz, 1H), 4.48 (dd,  $J = 7.1, 4.6$  Hz, 1H), 4.07 (dd,  $J = 1.9, 1.8$  Hz, 2H), 3.89 (s, 3H), 3.82 (s, 3H), 3.74 (s, 3H), 3.74-3.67 (m, 1H), 3.59 (ddd,  $J = 16.9, 2.1, 2.0$  Hz, 1H), 3.50 (ddd,  $J = 16.9, 2.0, 2.0$  Hz, 1H), 2.60 (br. s, 1H), 2.16 (dd,  $J = 14.9, 4.7$  Hz, 1H), 2.02 (dd,  $J = 15.0, 2.7$  Hz, 1H), 1.64-1.53 (m, 2H), 1.39 (s, 3H), 1.35 (s, 3H), 1.31-1.19 (m, 2H), 0.87 (dd,  $J = 7.3, 7.2$  Hz, 3H);  $^{13}\text{C}$  NMR (100 MHz,  $\text{CDCl}_3$ ):  $\delta$  196.1, 154.2, 153.6, 142.8, 141.2, 140.9, 131.4, 130.0, 127.8, 121.6, 109.8, 95.9, 83.8, 79.5, 72.7, 72.4, 70.7, 61.1, 56.1, 55.9, 50.8, 41.3, 35.2, 28.1,

26.3, 17.0, 16.3, 14.4; IR (film)  $\nu_{\max}$  3433, 2934, 2871, 2246, 1645, 1596, 1334, 1076  $\text{cm}^{-1}$ ; HRMS (ESI)  $m/z$  calcd. for  $\text{C}_{28}\text{H}_{36}\text{NaO}_8$   $[\text{M}+\text{Na}]^+$  523.2302, found 523.2280.



To a solution of **4.116** (20 mg, 0.0400 mmol, 1.0 eq) in  $\text{CH}_2\text{Cl}_2$  (500  $\mu\text{L}$ ) at 0  $^\circ\text{C}$  was added pyridine (16  $\mu\text{L}$ , 0.200 mmol, 5.0 eq) then DMP (0.3 M in  $\text{CH}_2\text{Cl}_2$ , 266  $\mu\text{L}$ , 0.0800 mmol, 2.0 eq) and the reaction was stirred at 0  $^\circ\text{C}$  for 2 h and at RT for 30 min.

To the reaction was added a 1:1 mixture of saturated aqueous  $\text{NaHCO}_3$  and saturated aqueous  $\text{Na}_2\text{S}_2\text{O}_3$  (10 mL) and the mixture was extracted with  $\text{CH}_2\text{Cl}_2$  (3 x 10 mL). The combined organic layers were washed with 10% aqueous  $\text{CuSO}_4$  (2 x 10 mL), then dried ( $\text{MgSO}_4$ ), filtered, and concentrated. Immediate purification by flash column chromatography (50% EtOAc/hexanes) provided **4.117** as a yellow oil (8.0 mg, 0.0160 mmol, 40%).  $^1\text{H}$  NMR (400 MHz,  $\text{CDCl}_3$ ):  $\delta$  9.07 (s, 1H), 7.18 (d,  $J$  = 16.0 Hz, 1H), 6.83 (d,  $J$  = 16.0 Hz, 1H), 6.47 (s, 1H), 5.95 (d,  $J$  = 2.8 Hz, 1H), 4.57 (dd,  $J$  = 5.3, 2.8 Hz, 1H), 4.49 (ddd,  $J$  = 6.9, 4.5, 1.8 Hz, 1H), 3.92 (s, 3H), 3.84 (s, 3H), 3.80-3.76 (m, 2H), 3.77 (s, 3H), 3.44 (s, 1H), 2.19 (dd,  $J$  = 14.9, 4.8 Hz, 1H), 2.02 (dd,  $J$  = 14.9, 2.6 Hz, 1H), 1.61-1.52 (m, 2H), 1.38 (s, 3H), 1.36 (s, 3H), 1.29-1.11 (m, 2H), 0.89 (dd,  $J$  = 7.3, 7.3 Hz, 3H);  $^{13}\text{C}$  NMR (100 MHz,  $\text{CDCl}_3$ ):  $\delta$  195.3, 177.0, 154.5, 154.1, 143.3, 141.4, 141.2, 130.9, 128.2, 127.6, 121.5, 109.9, 96.8, 96.4, 81.2, 72.8, 72.6, 70.4, 61.2, 56.2, 56.0, 41.5, 35.2, 28.1, 26.4, 17.0, 16.9, 14.5; IR (film)  $\nu_{\max}$  3509, 2934, 2196, 1660, 1596, 1335, 1233  $\text{cm}^{-1}$ ; HRMS (ESI)  $m/z$  calcd. for  $\text{C}_{28}\text{H}_{34}\text{NaO}_8$   $[\text{M}+\text{Na}]^+$  521.2146, found 521.2152.

## References

1. Brussee, J.; Groenendijk, J. L. G.; te Koppele, J. M.; Jansen, A. C. A. "On the mechanism of the formation of S(-)-(1,1'-binaphthalene)-2,2'-diol via copper(II) amine complexes" *Tetrahedron*, **1985**, *41*, 3313-3319.
2. Zhang, Y.; Yeung, S-M.; Wu, H.; Heller, D. P.; Wu, C.; Wulff, W. D. "Highly enantioselective deracemization of linear and vaulted biaryl ligands" *Org. Lett.*, **2003**, *5*, 1813-1816.
3. Hu, G.; Holmes, D.; Gendhar, B. F.; Wulff, W. D. "Optically active (*aR*)- and (*aS*)-linear and vaulted biaryl ligands: deracemization versus oxidative dimerization" *J. Am. Chem. Soc.*, **2009**, *131*, 14355-14364.
4. Dearden, M. J.; Firkin, C. R.; Hermet, J.-P. R.; O'Brien, P. "A readily accessible (+)-sparteine surrogate" *J. Am. Chem. Soc.*, **2002**, *124*, 11870-11871.
5. Lee, W. K.; Park, Y. S.; Beak, P. "Dynamic thermodynamic resolution: advantage by separation of equilibrium and resolution" *Acc. Chem. Res.*, **2009**, *42*, 224-234.
6. Romaine, I. M.; Hempel, J. E.; Shanmugam, G.; Hori, H.; Igarashi, Y.; Polavarapu, P. L.; Sulikowski, G. A. "Assignment and stereocontrol of hibarimicin atropoisomers" *Org. Lett.*, **2011**, *13*, 4538-4541.
7. de Koning, C. B.; Michael, J. P.; van Otterlo, W. A. L. "Syntheses of isochromane analogues of the michellamines and korupensamines" *J. Chem. Soc. Perkin Trans. I*, **2000**, 799-811.
8. de Koning, C. B.; Green, I. R.; Michael, J. P.; Oliveira, J. R. "The synthesis of isochroman-4-ols and isochroman-3-ols: models for naturally occurring benzo[*g*]isochromanols" *Tetrahedron*, **2001**, *57*, 9623-9634.
9. Nicolaou, K. C.; Chakraborty, T. K.; Piscopio, A. D.; Minowa, N.; Bertinato, P. "Total synthesis of rapamycin" *J. Am. Chem. Soc.*, **1993**, *115*, 4419-4420.
10. Corey, E. J.; Wollenberg, R. H. "A nucleophilic ethynyl group equivalent and its use in conjugate addition to  $\alpha,\beta$ -enones" *J. Am. Chem. Soc.*, **1974**, *96*, 5581-5583.
11. Xu, Y.; Hao, W.; Wang, D.; Cai, M. "A novel stereoselective synthesis of (2*Z*)-arylsulfanylallylic alcohols by tin-lithium exchange of (*E*)- $\alpha$ -stannylvinyl sulfides" *Heteroatom Chem.*, **2008**, *19*, 639-643.

12. Singleton, D. A.; Lee, Y.-K. "Intramolecular Diels-Alder reactions of vinylboranes. A highly stereoselective two-step decalin synthesis" *Tet. Lett.*, **1995**, *36*, 3473-3476.
13. Fürstner, A.; Ackerstaff, J. "Formal total synthesis of (–)-haouamine A" *Chem. Commun.*, **2008**, 2870-2872.
14. Jin, B.; Liu, Q.; Sulikowski, G. A. "Development of an end-game strategy towards apoptolidin: a sequential Suzuki coupling approach" *Tetrahedron*, **2005**, *61*, 401-408.
15. Chalker, J. M.; Wood, C. S. C.; Davis, B. G. "A convenient catalyst for aqueous and protein Suzuki-Miyaura cross-coupling" *J. Am. Chem. Soc.*, **2009**, *131*, 16346-16347.
16. Gao, X.; Hall, D. G. "3-Boronoacrolein as an exceptional heterodiene in the highly enantio- and diastereoselective Cr(III)-catalyzed three-component [4+2]/allylboration" *J. Am. Chem. Soc.*, **2003**, *125*, 9308-9309.
17. Jehanno, E.; Vaultier, M. "An easy access to vinylboronates  $\beta$ -substituted by a keto group" *Tet. Lett.*, **1995**, *36*, 4439-4442.
18. Zhang, W.; Baranczak, A.; Sulikowski, G. A. "Stereocontrolled assembly of the C3/C3' dideoxy core of lomaiviticin A/B and congeners" *Org. Lett.*, **2008**, *10*, 1939-1941.
19. Trost, B. M.; Romero, A. G. "Synthesis of optically active isoquinuclidines utilizing a diastereoselectivity control element" *J. Org. Chem.*, **1986**, *51*, 2332-2342.
20. Audia, J. E.; Boisvert, L.; Patten, A. D.; Villalobos, A.; Danishefsky, S. J. "Synthesis of two useful, enantiomerically pure derivatives of (S)-4-hydroxy-2-cyclohexenone" *J. Org. Chem.*, **1989**, *54*, 3738-3740.
21. Chen, K.; Baran, P. S. "Total synthesis of eudesmane terpenes by site-selective C-H oxidations" *Nature*, **2009**, *459*, 824-828.
22. Altemöller, M.; Podlech, J.; Fenske, D. "Total synthesis of altenuene and isoaltenuene" *Eur. J. Org. Chem.*, **2006**, 1678-1684.
23. Danishefsky, S. J.; Mantlo, N. B.; Yamashita, D. S. "A concise route to the calicheamicin-esperamicin series: the crystal structure of a core subunit" *J. Am. Chem. Soc.*, **1988**, *110*, 6890-6891.

24. Casado, A. L.; Espinet, P. "Mechanism of the Stille reaction. 1. The transmetalation step. Coupling of  $R^1I$  and  $R^2SnBu_3$  catalyzed by *trans*-[PdR<sup>1</sup>IL<sub>2</sub>] ( $R^1 = C_6Cl_2F_3$ ;  $R^2 = \text{vinyl, 4-methoxyphenyl}$ ;  $L = AsPh_3$ )" *J. Am. Chem. Soc.*, **1998**, *120*, 8978-8985.
25. Hirabayashi, K.; Mori, A.; Kawashima, J.; Suguro, M.; Nishihara, Y.; Hiyama, T. "Palladium-catalyzed cross-coupling of silanols, silanediols, and silanetriols promoted by silver(I) oxide" *J. Org. Chem.*, **2000**, *65*, 5342-5349.
26. Sieburth, S. M.; Fensterbank, L. "An intramolecular Diels-Alder reaction of vinylsilanes" *J. Org. Chem.*, **1992**, *57*, 5279-5281.
27. Pietraszuk, C.; Fischer, H.; Kujawa, M.; Marciniak, B. "Cross-metathesis of vinylsilanes with olefins in the presence of Grubbs' catalyst" *Tet. Lett.*, **2001**, *42*, 1175-1178.
28. Pietraszuk, C.; Fischer, H.; Rogalski, S.; Marciniak, B. "The effect of substituents at silicon on the cross-metathesis of trisubstituted vinylsilanes with olefins" *J. Organometallic Chem.*, **2005**, *690*, 5912-5921.
29. Müller, S.; Liepold, B.; Roth, G. J.; Bestmann, H. J. "An improved one-pot procedure for the synthesis of alkynes from aldehydes" *Syn. Lett.*, **1996**, 521-522.
30. Izawa, Y.; Shimizu, I.; Yamamoto, A. "Palladium-catalyzed oxidative carbonylation of 1-alkynes into 2-alkynoates with molecular oxygen as oxidant" *Bull. Chem. Soc. Jpn.*, **2004**, *77*, 2033-2045.
31. Tsuji, J.; Takahashi, M.; Takahashi, T. "Facile synthesis of acetylenecarboxylates by the oxidative carbonylation of terminal acetylenes catalyzed by PdCl<sub>2</sub> under mild conditions" *Tet. Lett.*, **1980**, *21*, 849-850.
32. Zung, T. T.; Bruk, L. G.; Temkin, O. N.; Malashkevich, K. V. "Palladium-catalysed carbonylation of halogenoalkynes to alkynylcarboxylic acid esters under mild conditions" *Mendeleev Commun.*, **1995**, *5*, 3-4.
33. Setoh, M.; Yamada, O.; Ogasawara, K. "Palladium-mediated carbomacrolactonization of terminal hydroxyacetylenes and its utilization for a synthesis of exaltolide" *Heterocycles*, **1995**, *40*, 539-542.
34. Nicolaou, K. C.; Renaud, J.; Nantermet, P. G.; Couladouros, E. A.; Guy, R. K.; Wrasidlo, W. "Chemical synthesis and biological evaluation of C-2 taxoids" *J. Am. Chem. Soc.*, **1995**, *117*, 2409-2420.



35. Burk, R. M.; Roof, M. B. "A safe and efficient method for conversion 1,2- and 1,3-diols to cyclic carbonates using triphosgene" *Tet. Lett.*, **1993**, 34, 395-398.
36. Abad, A.; Agulló, C.; Cuñat, A. C.; García, A. B.; Giménez-Saiz, C. "Synthetic studies on the preparation of oxygenated sponiane diterpenes from carvone" *Tetrahedron*, **2003**, 59, 9523-9536.
37. Still, W. C.; Kahn, M.; Mitra, A. "Rapid chromatographic technique for preparative separations with moderate resolution" *J. Org. Chem.*, **1978**, 43, 2923-2925.
38. Renaldo, A. F.; Labadie, J. W.; Stille, J. K. "Palladium-catalyzed coupling of acid chlorides with organotin reagents: ethyl (*E*)-4-(4-nitrophenyl)-4-oxo-2-butenolate" *Org. Synth.*, **1989**, 67, 86.
39. Hartmann, C. E.; Gross, P. J.; Nieger, M.; Bräse, F. "Towards an asymmetric synthesis of the bacterial peptide deformylase (PDF) inhibitor fumimycin" *Org. Biomol. Chem.*, **2009**, 7, 5059-5062.
40. Romaine, I. M. "Progress toward the total synthesis of HMP-Y1 and hibarimicinone" **2010**, Doctoral dissertation, Vanderbilt University.
41. Logue, M. W.; Teng, K. "Palladium-catalyzed reactions of acyl chlorides with (1-alkynyl)tributylstannanes. A convenient synthesis for 1-alkynyl ketones" *J. Org. Chem.*, **1982**, 47, 2549-2553.
42. Barros, M. T.; Matias, P. M.; Maycock, C. D.; Ventura, M. R. "Aziridines as a protecting and directing group. Stereoselective synthesis of (+)-bromoxone" *Org. Lett.*, **2003**, 5, 4321-4323.
43. Regitz, M.; Hocker, J.; Liedhegener, A. "*t*-Butyl diazoacetate" *Org. Syn.*, **1968**, 48, 36.

## **Appendix A2:**

### **Spectra Relevant to Chapter IV.**

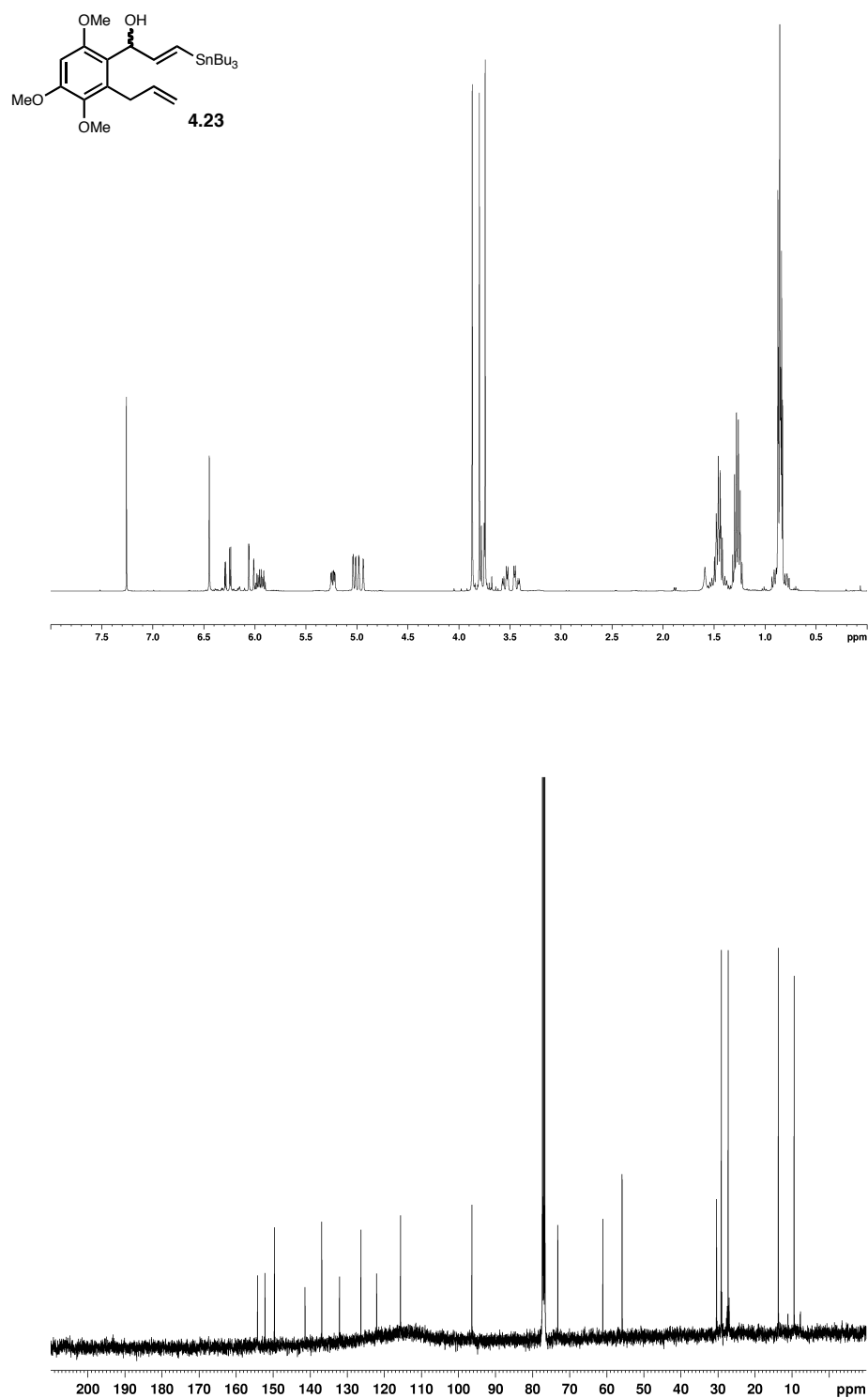


**Figure A2.1.**  $^1\text{H}$  NMR spectrum (400 MHz,  $\text{CDCl}_3$ ) and  $^{13}\text{C}$  NMR spectrum (100 MHz,  $\text{CDCl}_3$ ) of compound **4.23**.

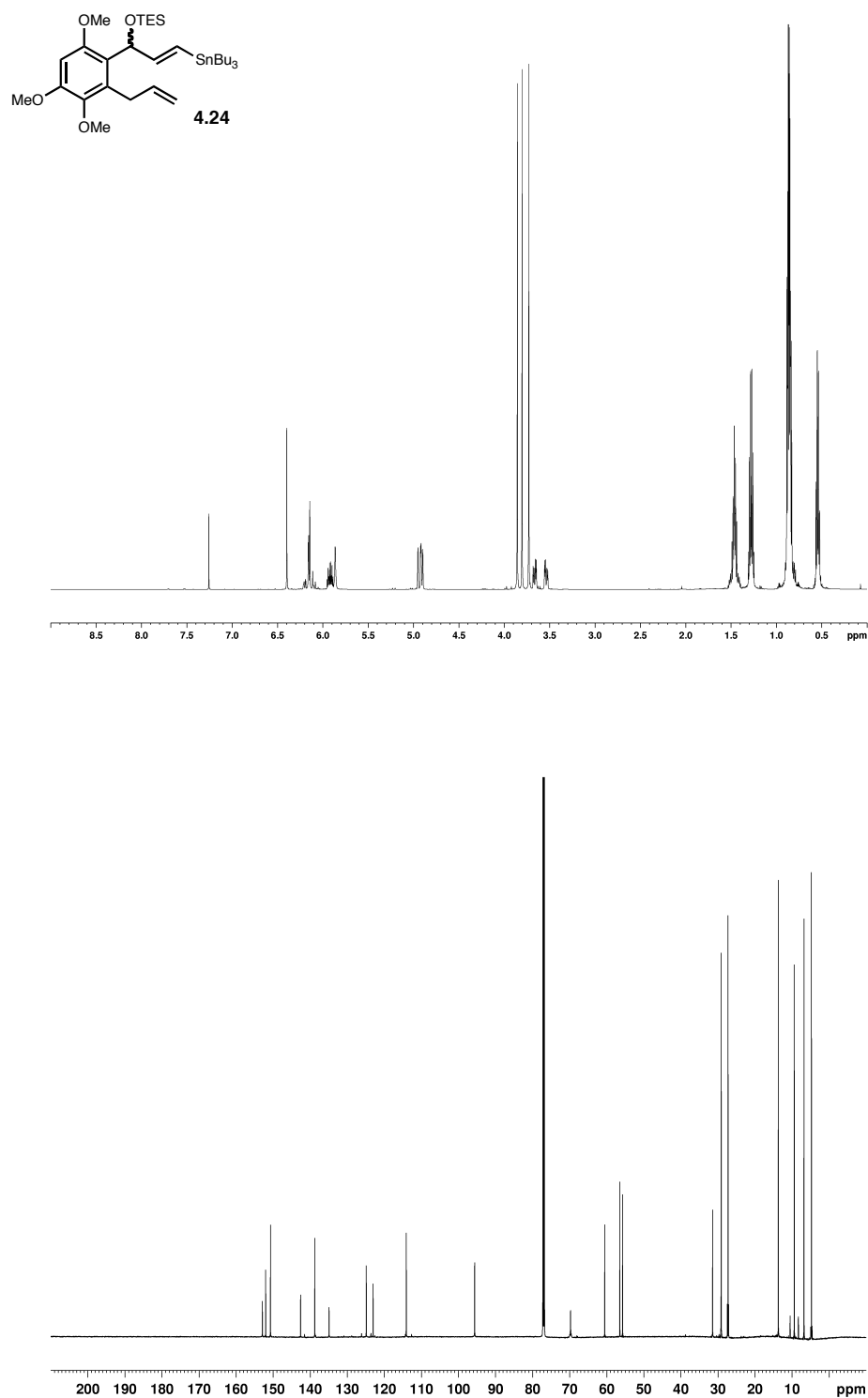


**Figure A2.2.**  $^1\text{H}$  NMR spectrum (600 MHz,  $\text{CDCl}_3$ ) and  $^{13}\text{C}$  NMR spectrum (150 MHz,  $\text{CDCl}_3$ ) of compound **4.24**.

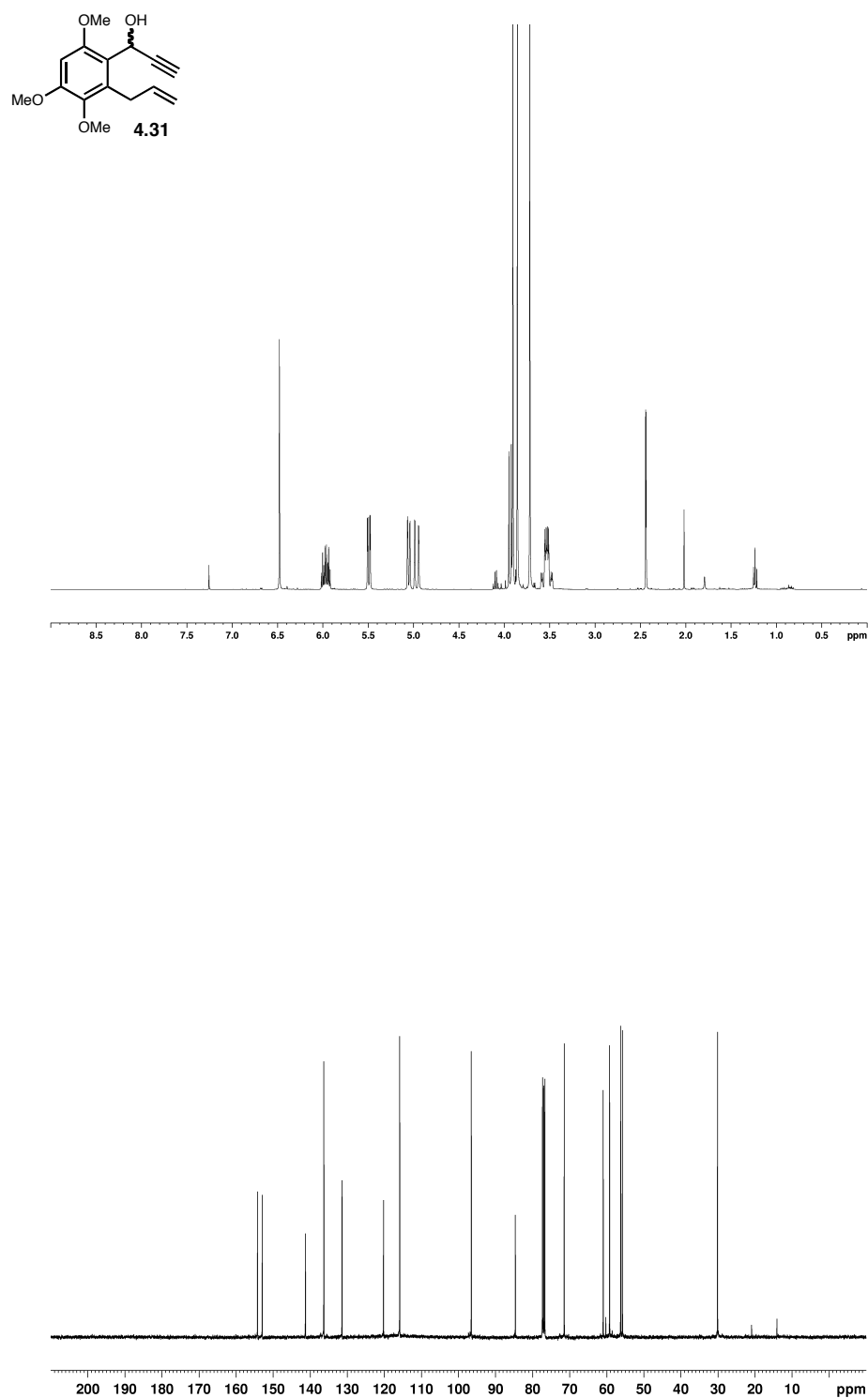


**Figure A2.3.**  $^1\text{H}$  NMR spectrum (400 MHz,  $\text{CDCl}_3$ ) and  $^{13}\text{C}$  NMR spectrum (100 MHz,  $\text{CDCl}_3$ ) of compound **4.31**.

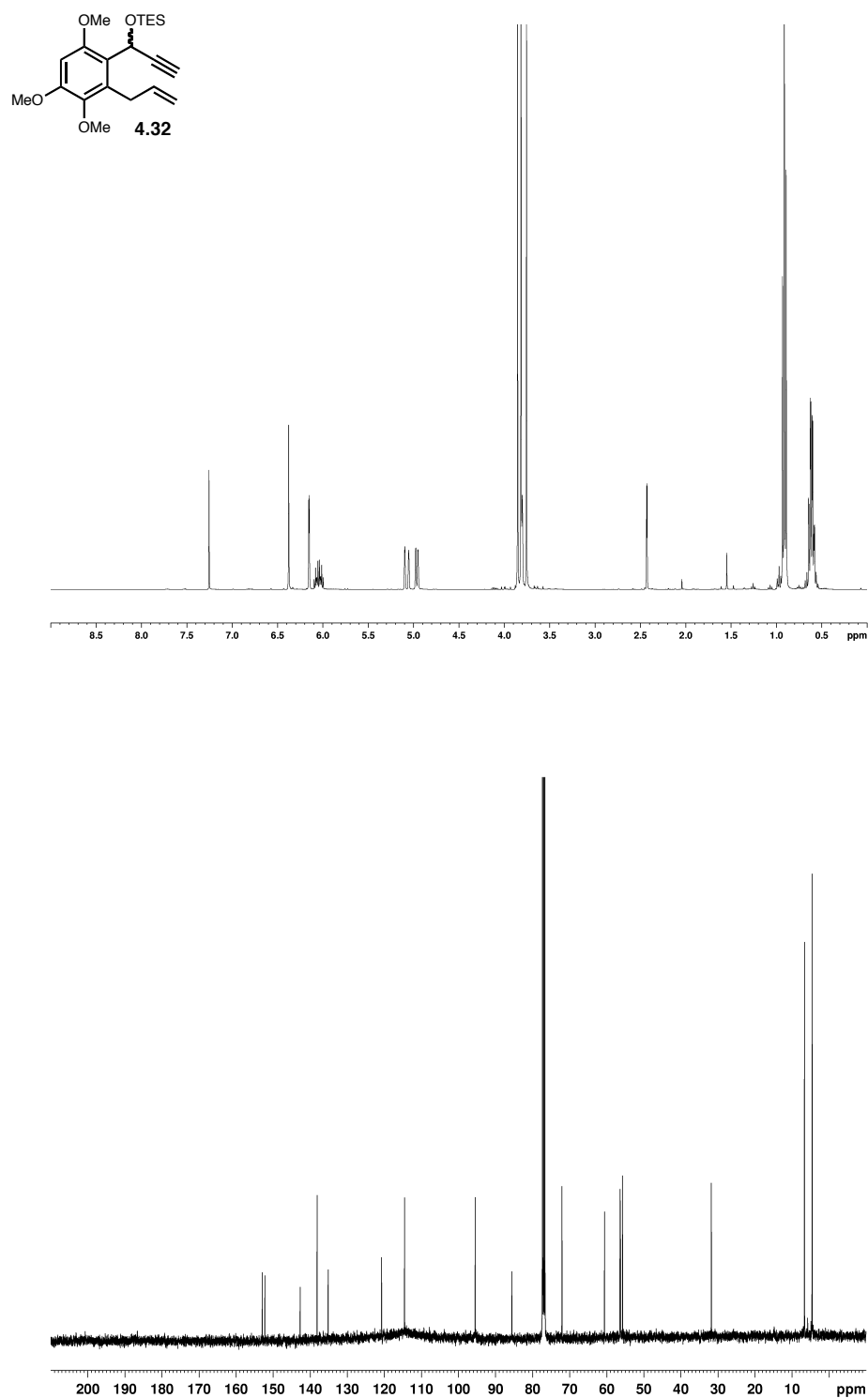


**Figure A2.4.**  $^1\text{H}$  NMR spectrum (400 MHz,  $\text{CDCl}_3$ ) and  $^{13}\text{C}$  NMR spectrum (100 MHz,  $\text{CDCl}_3$ ) of compound **4.32**.

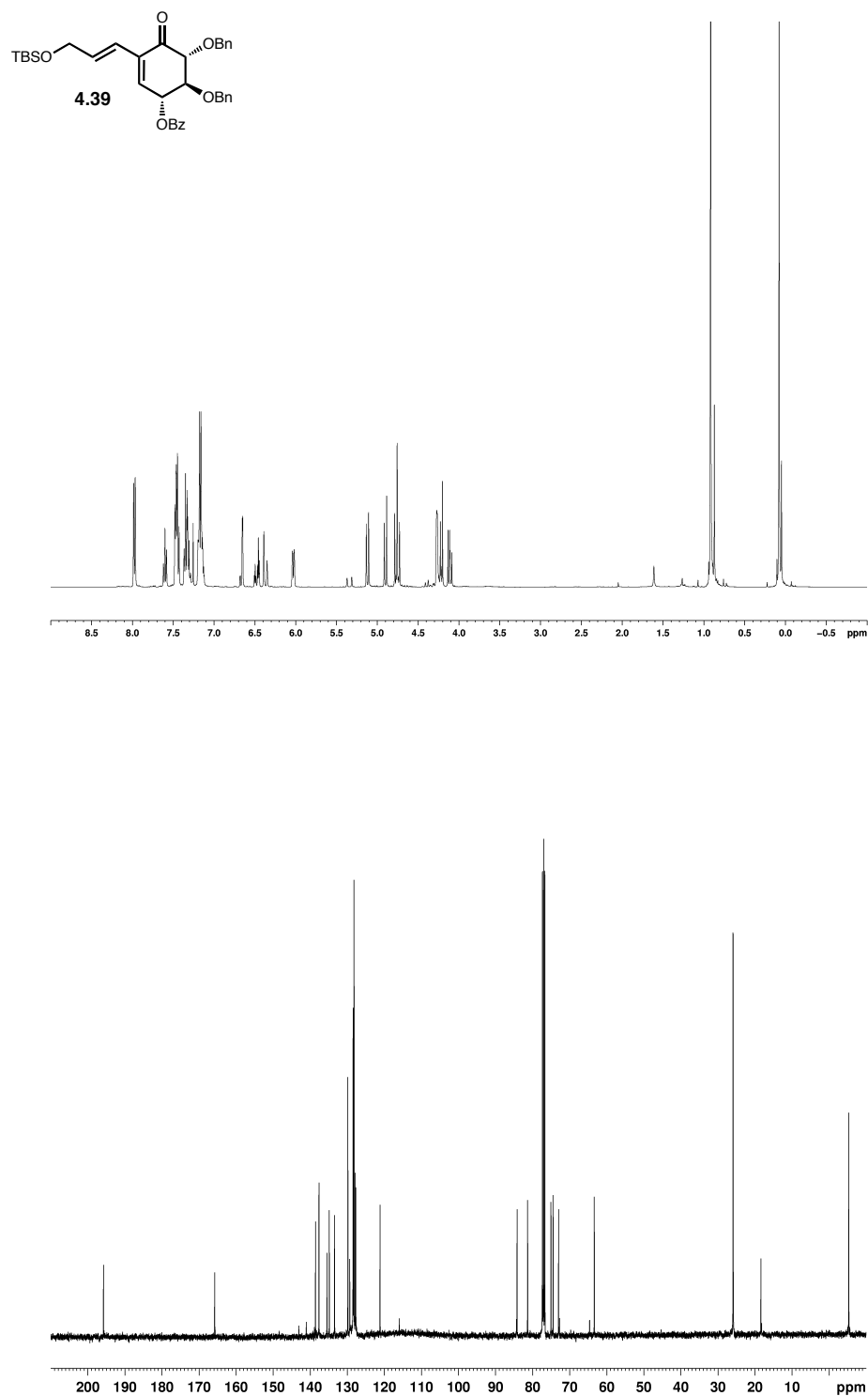


**Figure A2.5.**  $^1\text{H}$  NMR spectrum (400 MHz,  $\text{CDCl}_3$ ) and  $^{13}\text{C}$  NMR spectrum (100 MHz,  $\text{CDCl}_3$ ) of compound **4.39**.

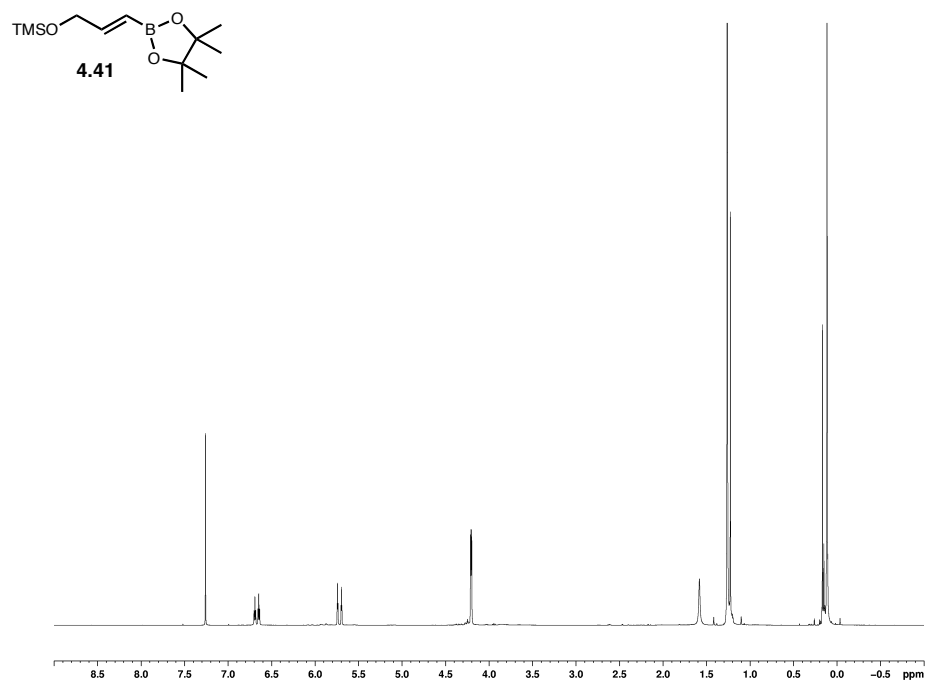


**Figure A2.6.**  $^1\text{H}$  NMR spectrum (400 MHz,  $\text{CDCl}_3$ ) of compound **4.41**.



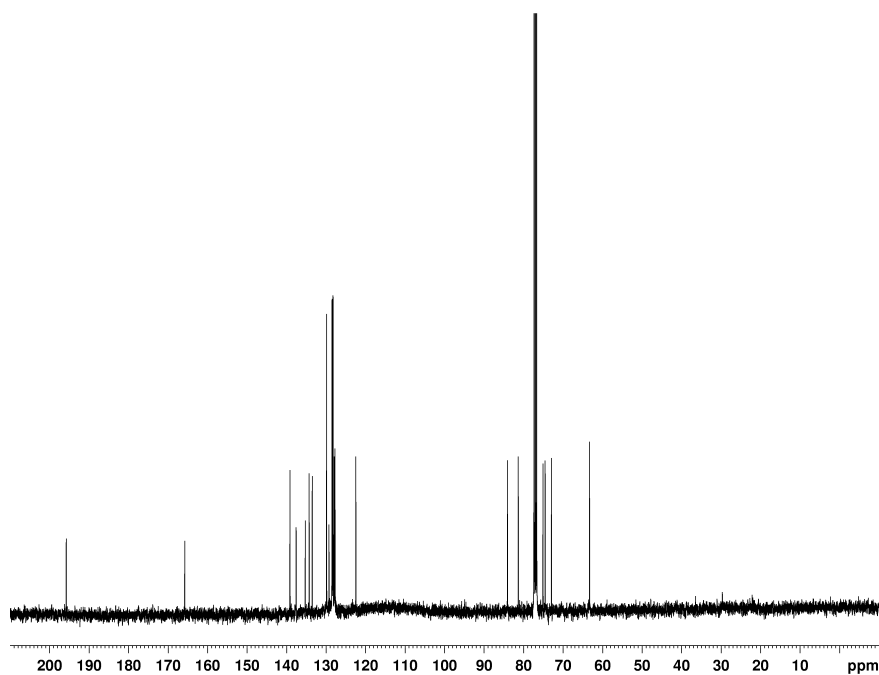
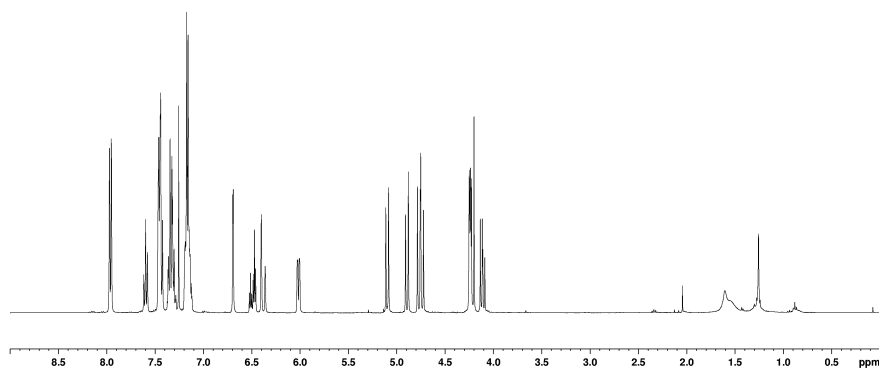
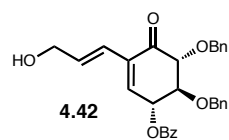


**Figure A2.7.**  $^1\text{H}$  NMR spectrum (400 MHz,  $\text{CDCl}_3$ ) and  $^{13}\text{C}$  NMR spectrum (100 MHz,  $\text{CDCl}_3$ ) of compound **4.42**.

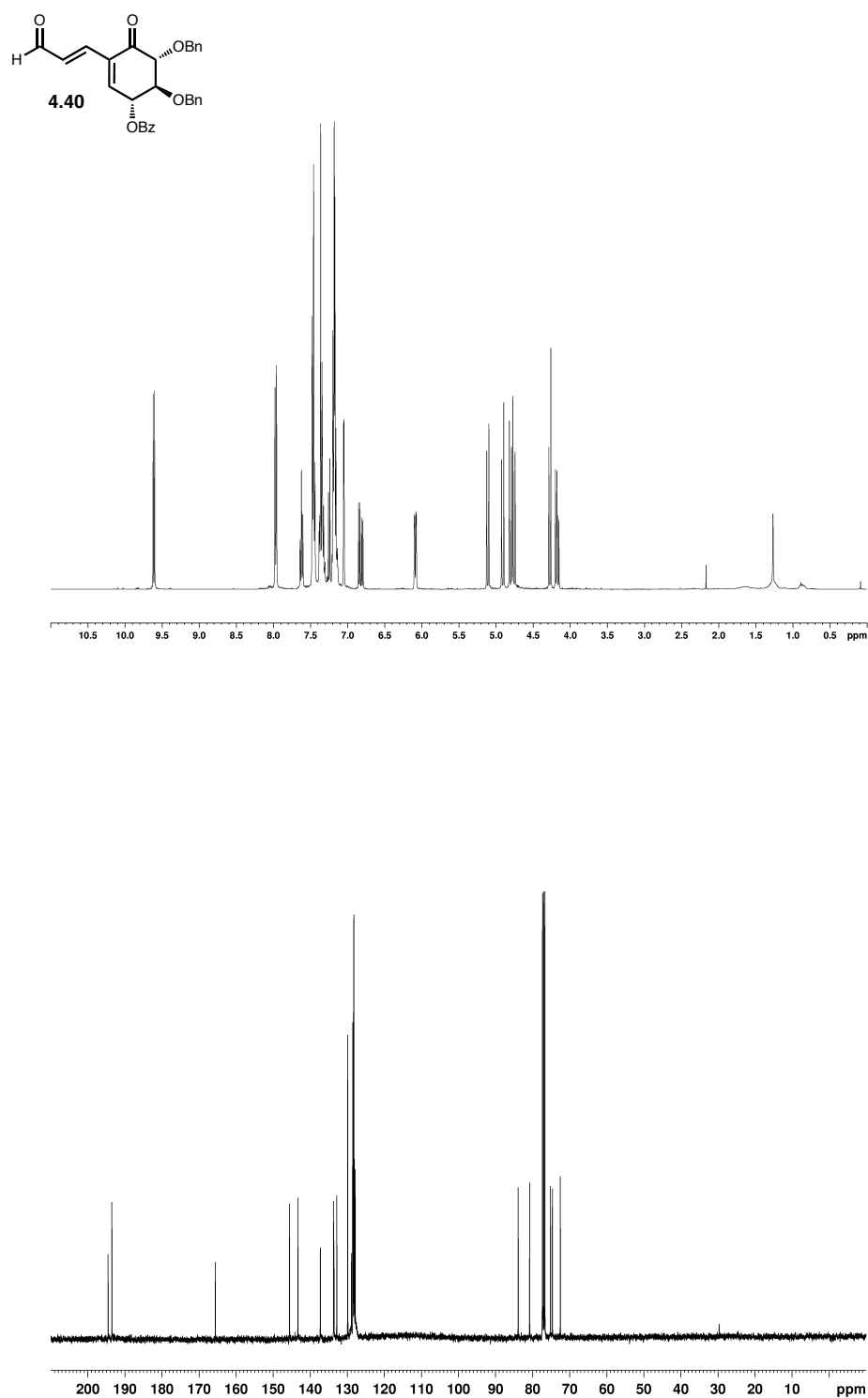


**Figure A2.8.**  $^1\text{H}$  NMR spectrum (400 MHz,  $\text{CDCl}_3$ ) and  $^{13}\text{C}$  NMR spectrum (100 MHz,  $\text{CDCl}_3$ ) of compound **4.40**.

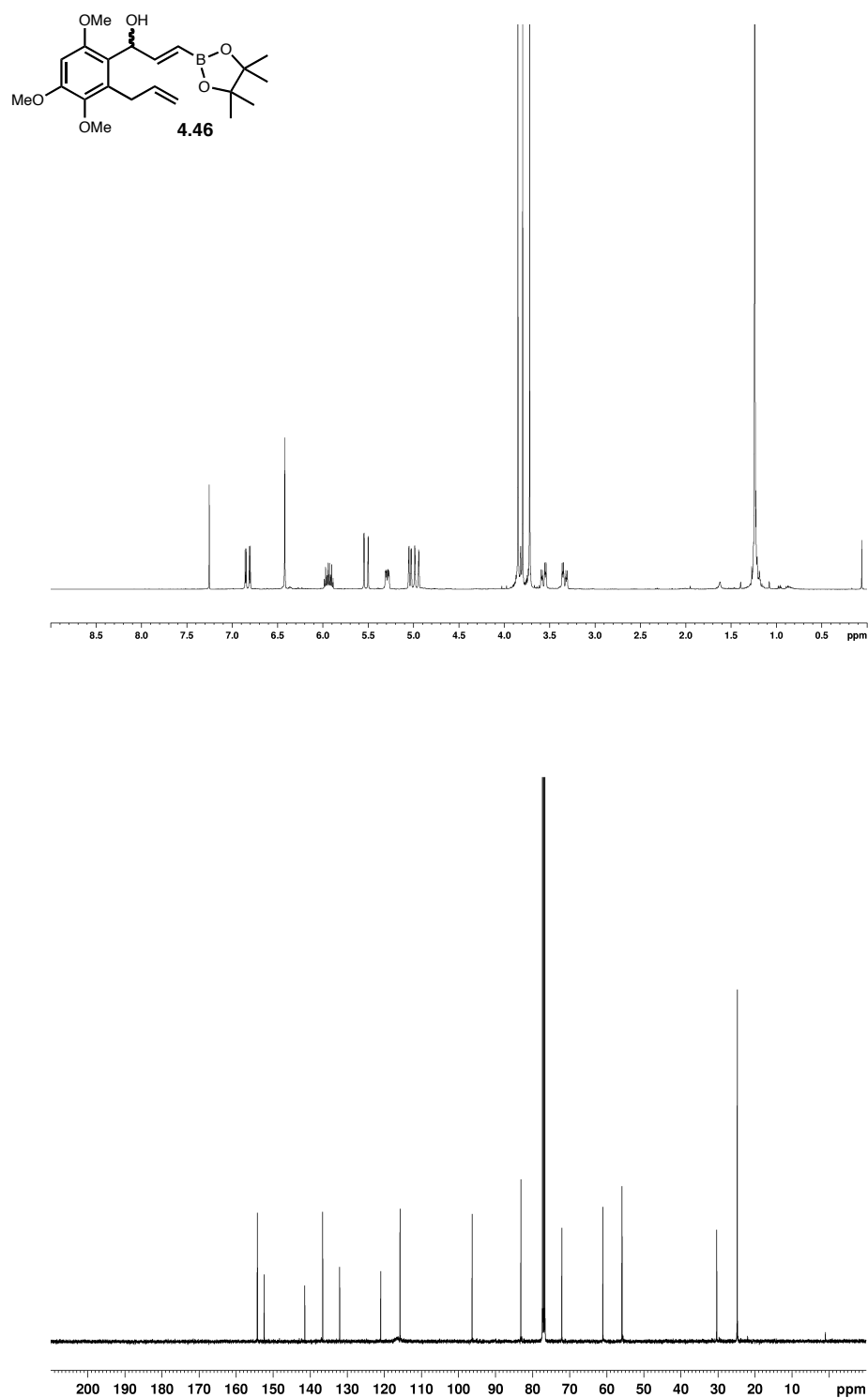


**Figure A2.9.**  $^1\text{H}$  NMR spectrum (400 MHz,  $\text{CDCl}_3$ ) and  $^{13}\text{C}$  NMR spectrum (100 MHz,  $\text{CDCl}_3$ ) of compound **4.46**.

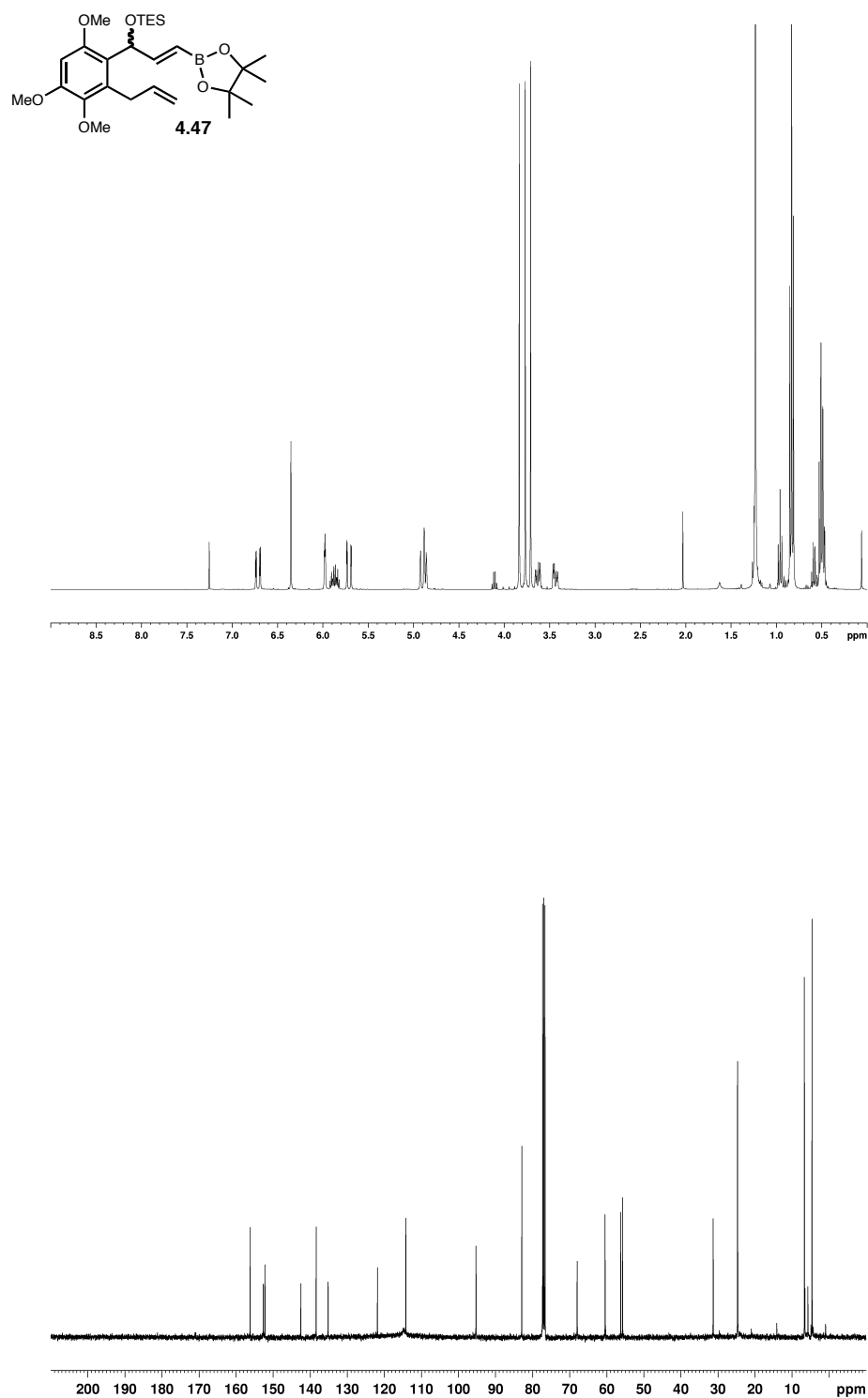


**Figure A2.10.**  $^1\text{H}$  NMR spectrum (400 MHz,  $\text{CDCl}_3$ ) and  $^{13}\text{C}$  NMR spectrum (100 MHz,  $\text{CDCl}_3$ ) of compound **4.47**.

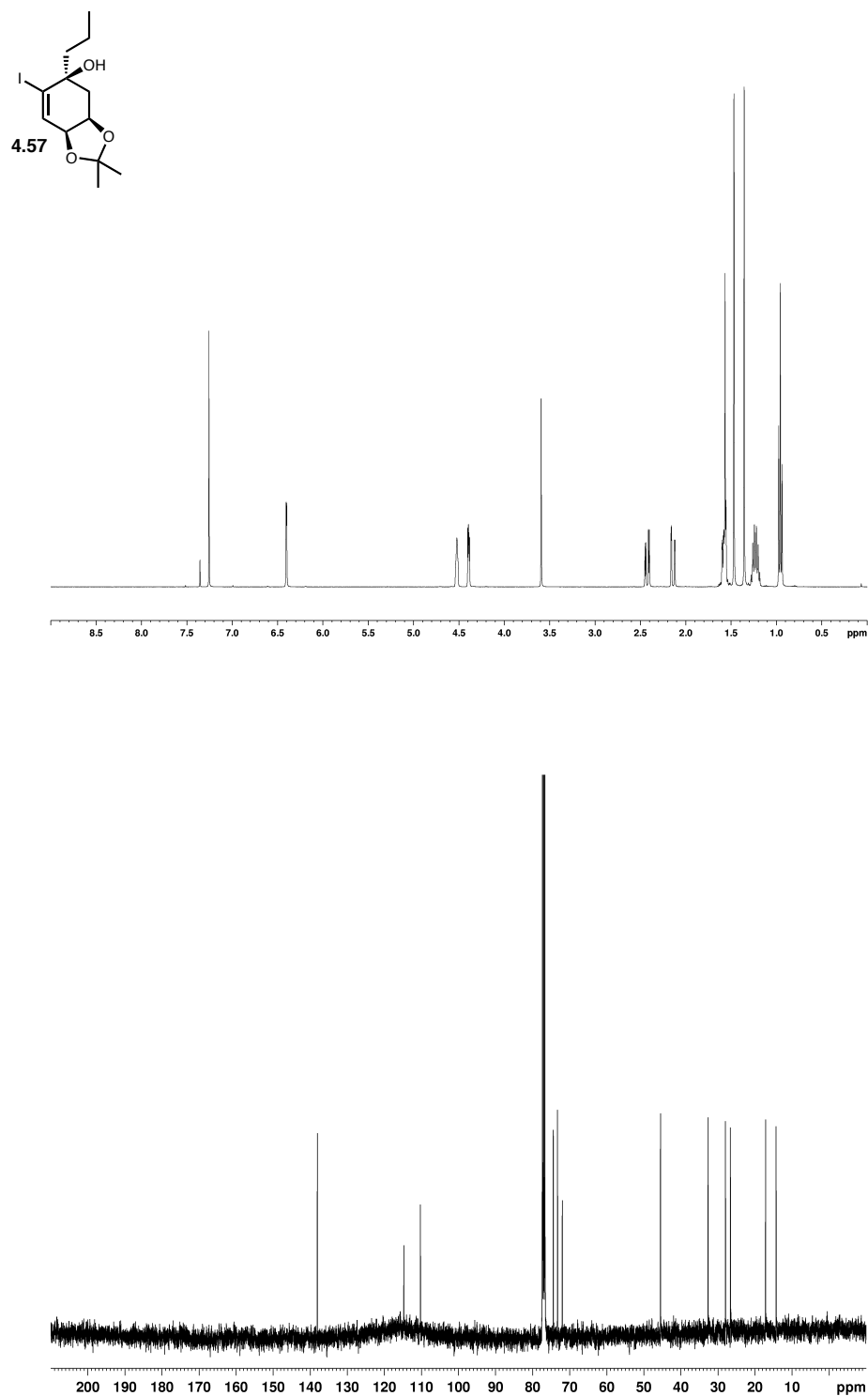


**Figure A2.11.**  $^1\text{H}$  NMR spectrum (400 MHz,  $\text{CDCl}_3$ ) and  $^{13}\text{C}$  NMR spectrum (100 MHz,  $\text{CDCl}_3$ ) of compound 4.57.

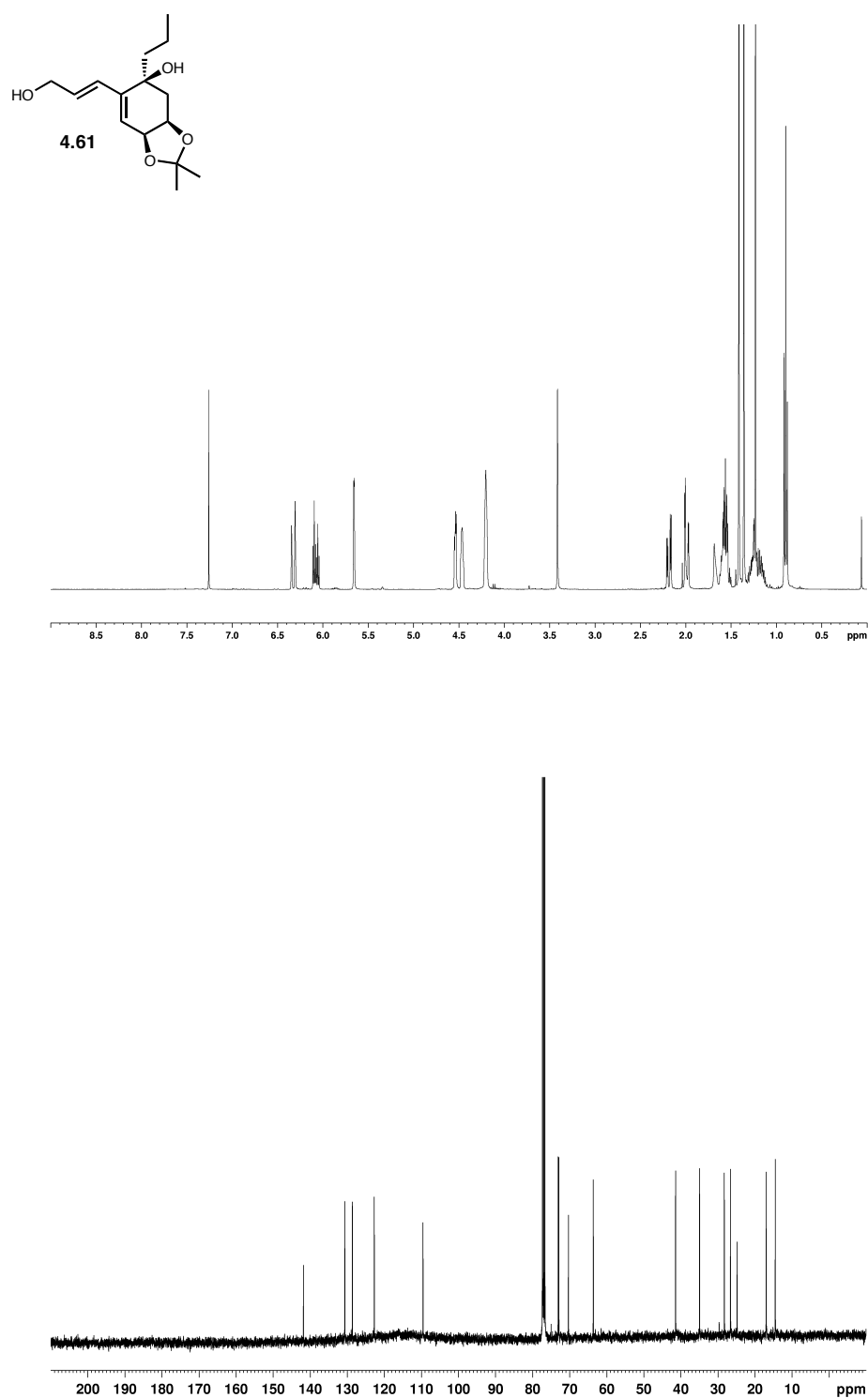


**Figure A2.12.**  $^1\text{H}$  NMR spectrum (400 MHz,  $\text{CDCl}_3$ ) and  $^{13}\text{C}$  NMR spectrum (100 MHz,  $\text{CDCl}_3$ ) of compound **4.61**.

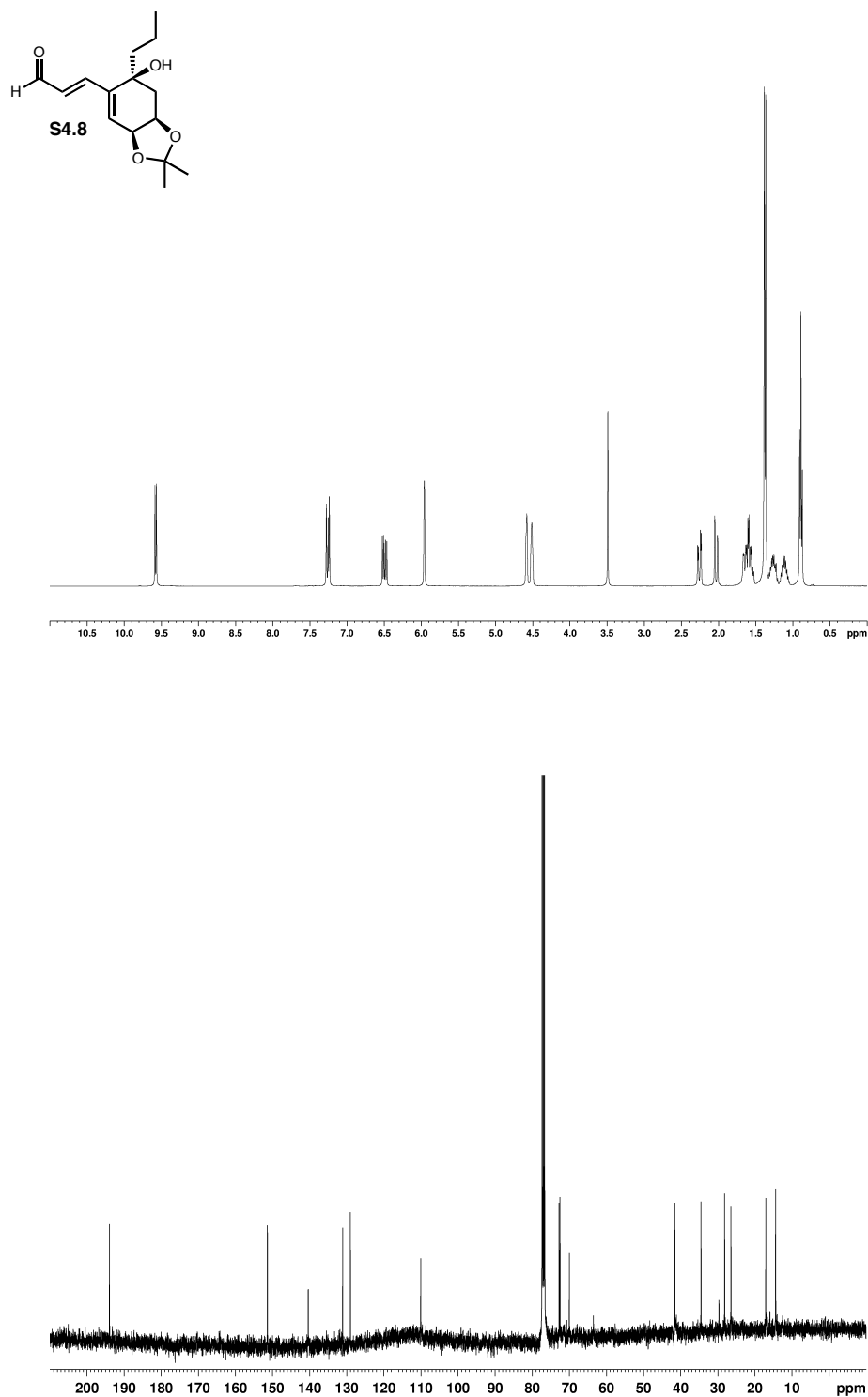


**Figure A2.13.**  $^1\text{H}$  NMR spectrum (400 MHz,  $\text{CDCl}_3$ ) and  $^{13}\text{C}$  NMR spectrum (100 MHz,  $\text{CDCl}_3$ ) of compound S4.8.

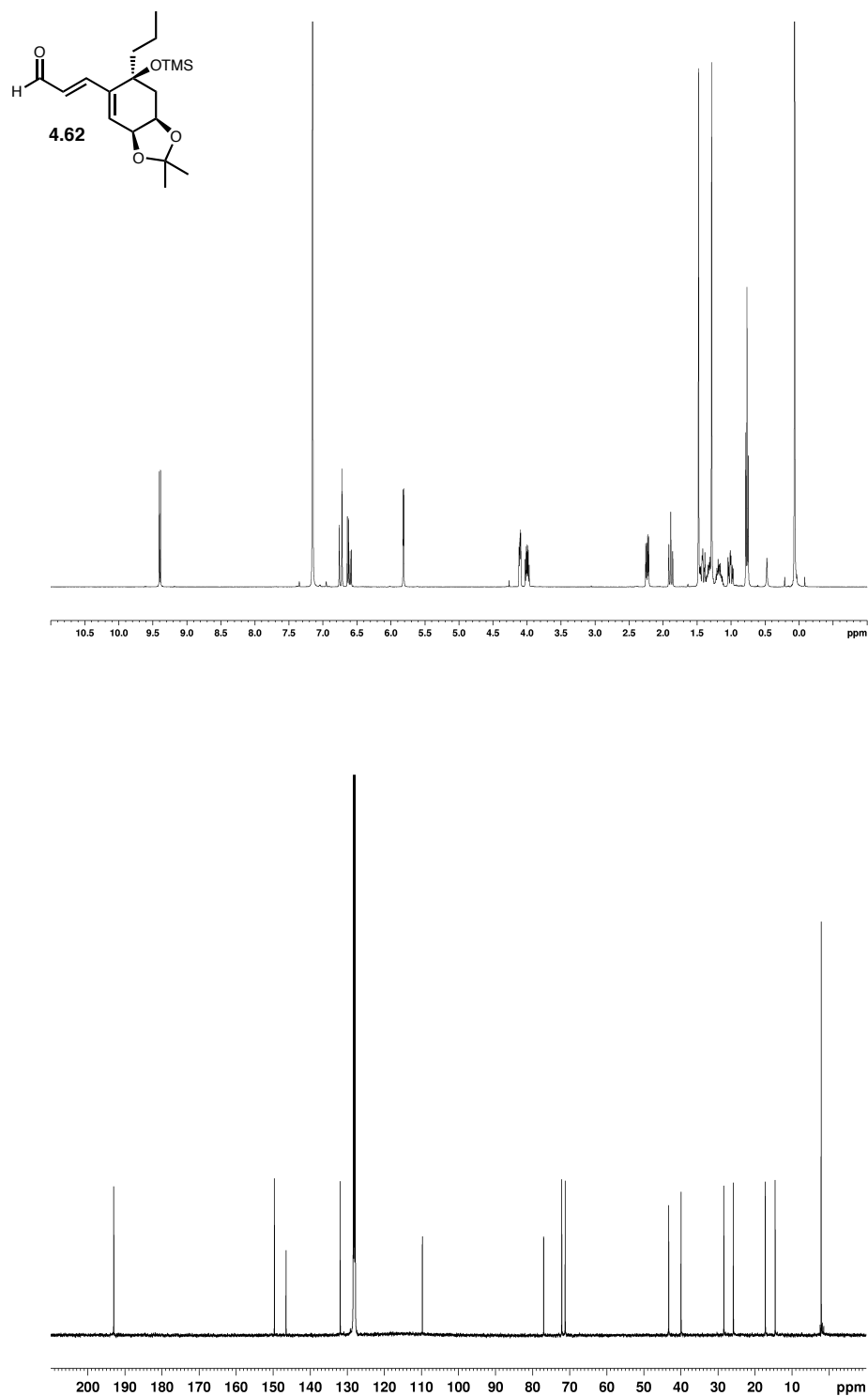


**Figure A2.14.**  $^1\text{H}$  NMR spectrum (400 MHz,  $\text{C}_6\text{D}_6$ ) and  $^{13}\text{C}$  NMR spectrum (100 MHz,  $\text{C}_6\text{D}_6$ ) of compound **4.62**.



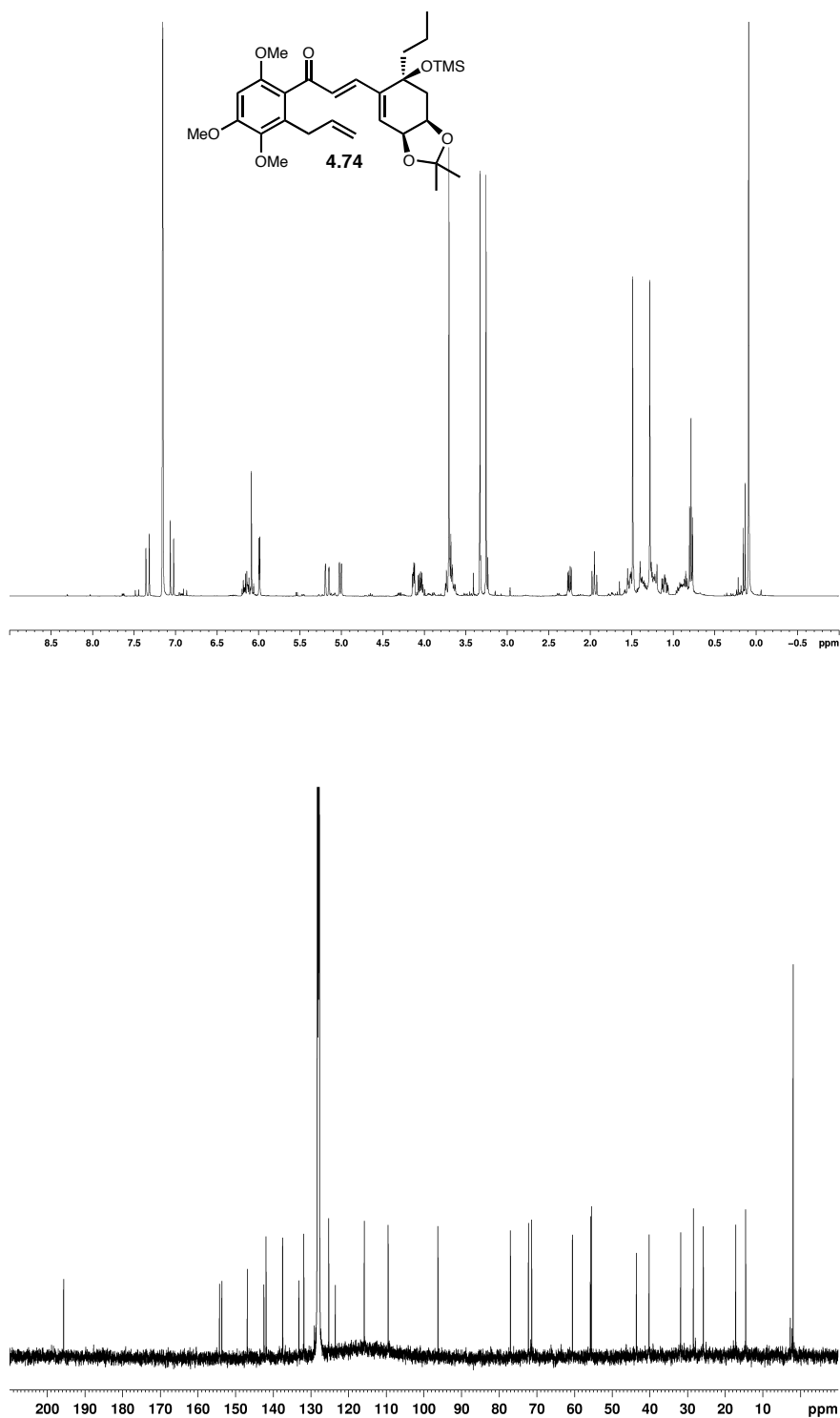


**Figure A2.15.**  $^1\text{H}$  NMR spectrum (400 MHz,  $\text{C}_6\text{D}_6$ ) and  $^{13}\text{C}$  NMR spectrum (100 MHz,  $\text{C}_6\text{D}_6$ ) of compound 4.74.

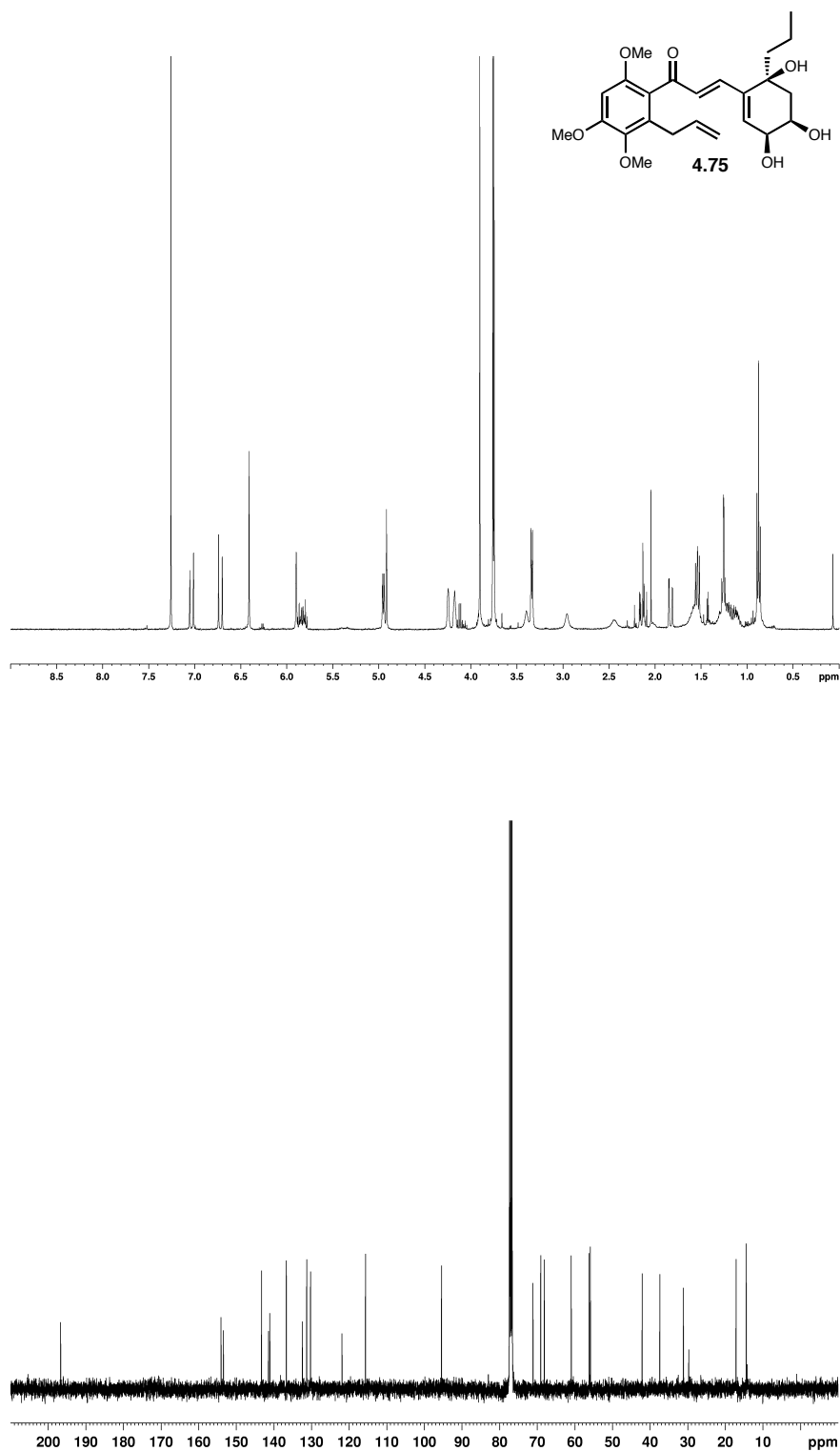


**Figure A2.16.**  $^1\text{H}$  NMR spectrum (400 MHz,  $\text{CDCl}_3$ ) and  $^{13}\text{C}$  NMR spectrum (100 MHz,  $\text{CDCl}_3$ ) of compound 4.75.

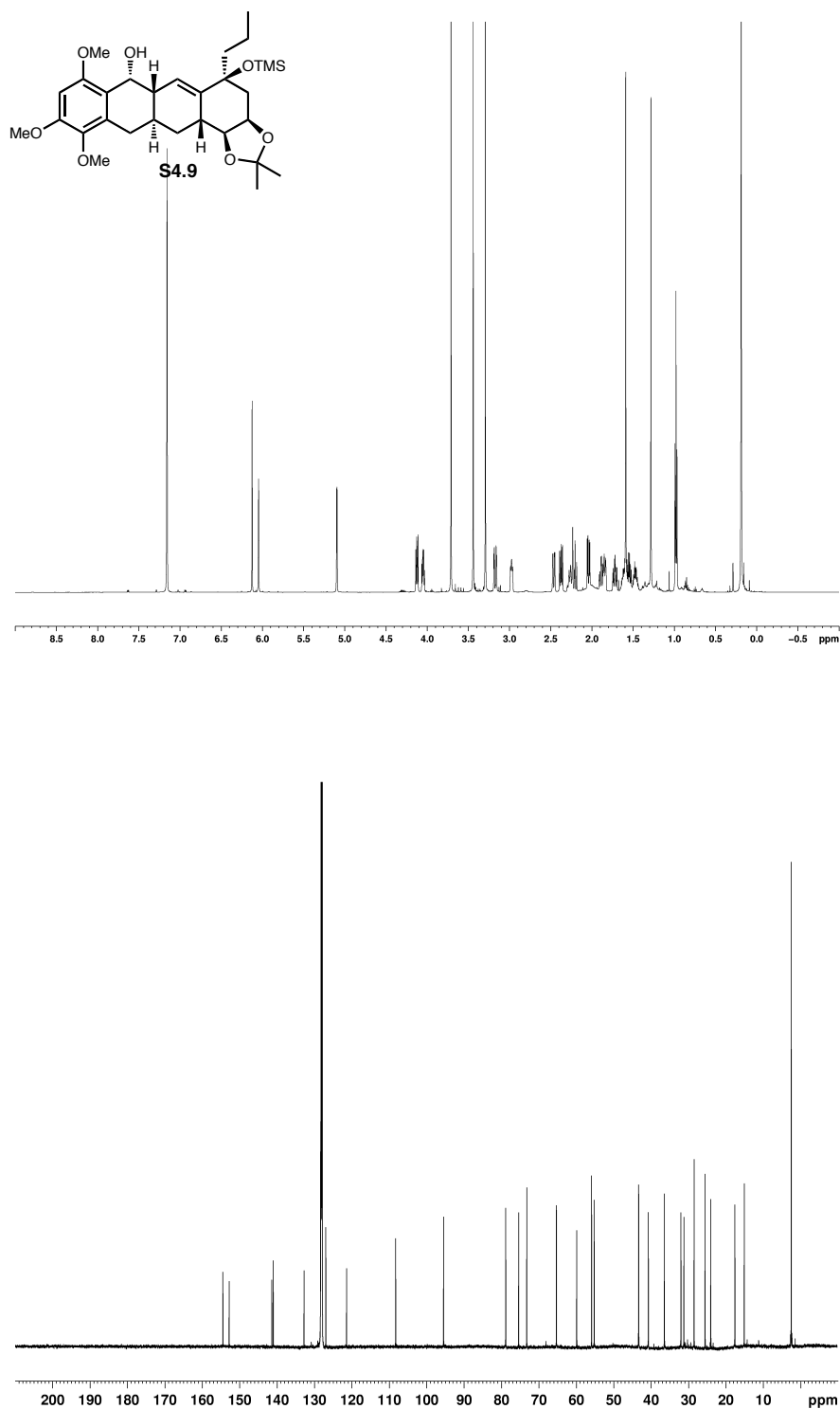


**Figure A2.17.**  $^1\text{H}$  NMR spectrum (600 MHz,  $\text{C}_6\text{D}_6$ ) and  $^{13}\text{C}$  NMR spectrum (150 MHz,  $\text{C}_6\text{D}_6$ ) of compound **S4.9**.

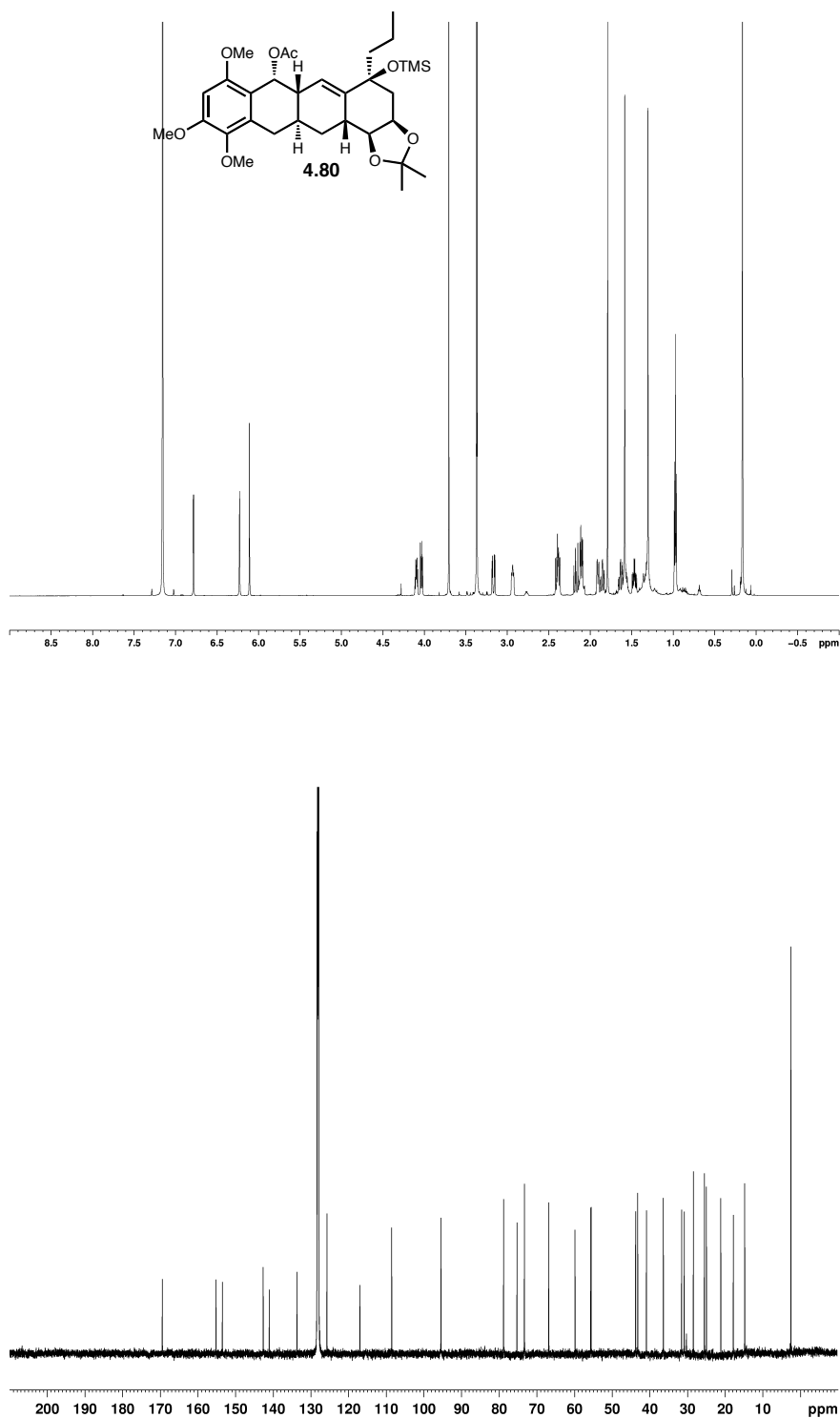


**Figure A2.18.**  $^1\text{H}$  NMR spectrum (600 MHz,  $\text{C}_6\text{D}_6$ ) and  $^{13}\text{C}$  NMR spectrum (150 MHz,  $\text{C}_6\text{D}_6$ ) of compound **4.80**.

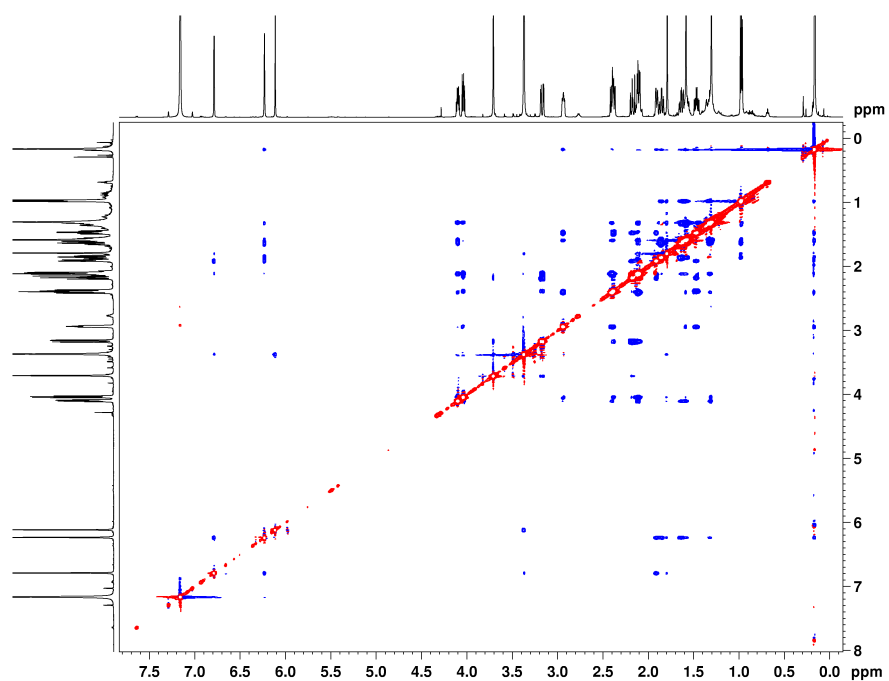
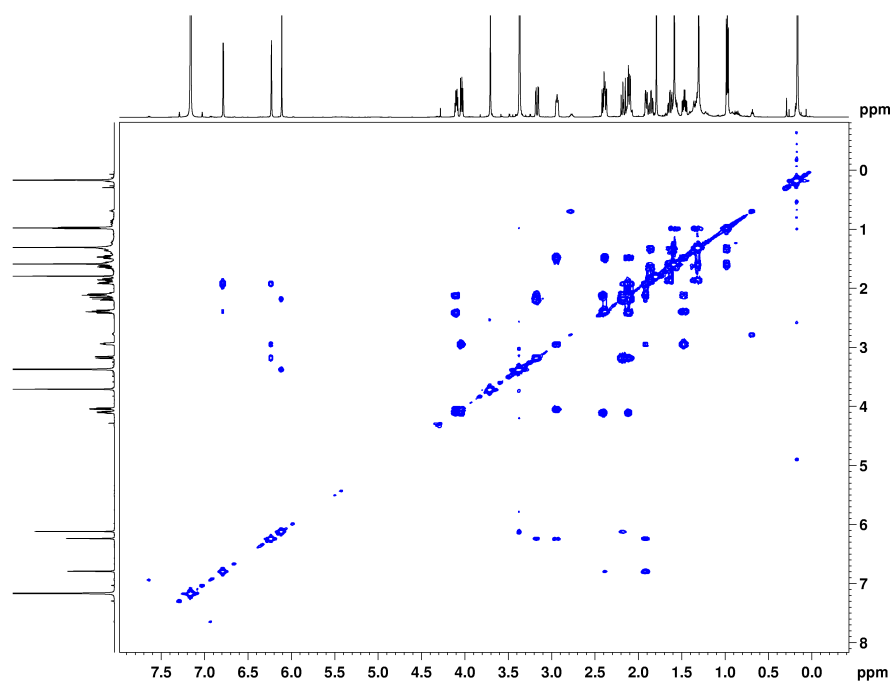


**Figure A2.19.** COSY spectrum (600 MHz,  $\text{C}_6\text{D}_6$ ) and NOESY spectrum (600 MHz,  $\text{C}_6\text{D}_6$ ) of compound **4.80**.

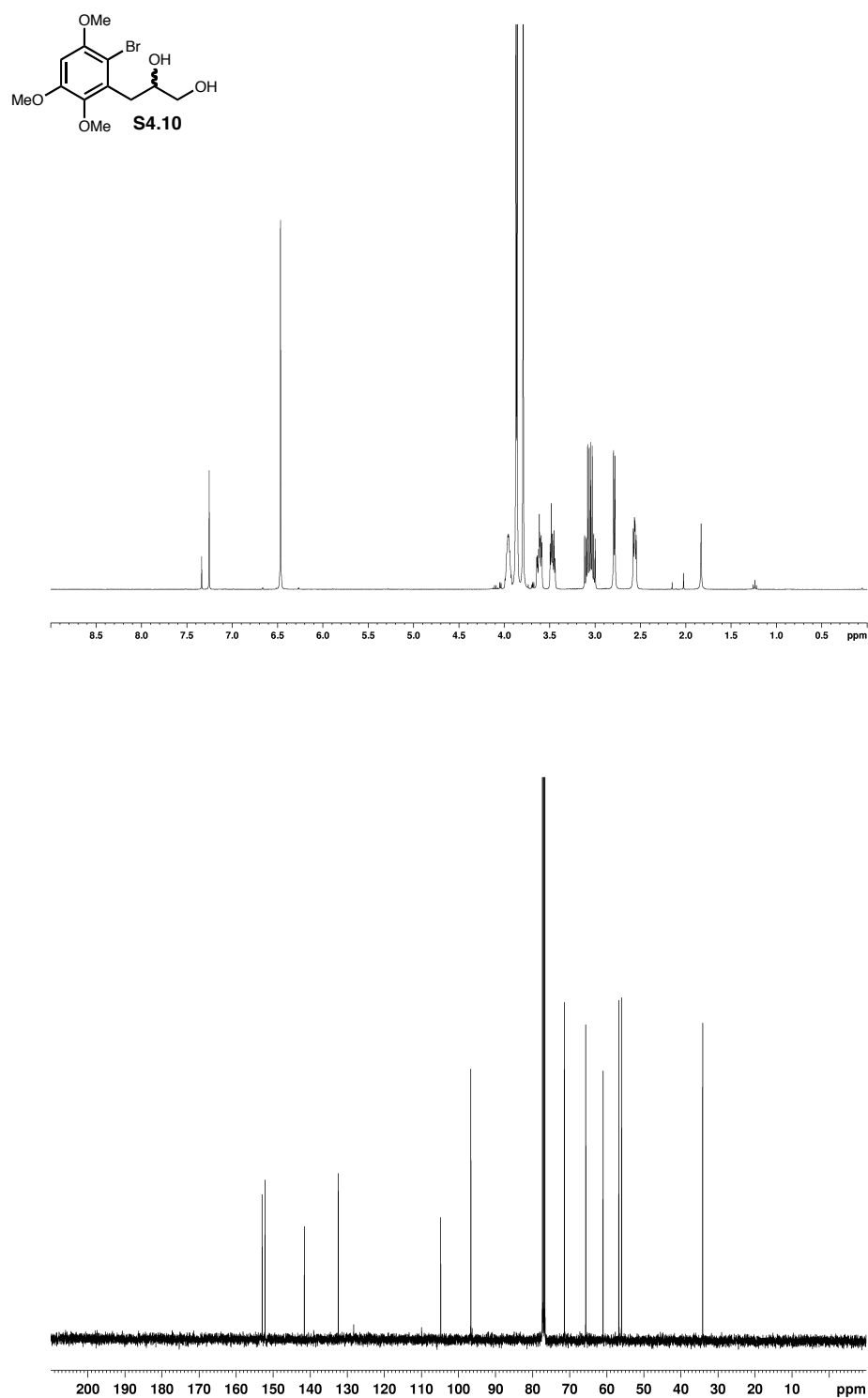


**Figure A2.20.**  $^1\text{H}$  NMR spectrum (400 MHz, CDCl<sub>3</sub>) and  $^{13}\text{C}$  NMR spectrum (100 MHz, CDCl<sub>3</sub>) of compound **S4.10**.

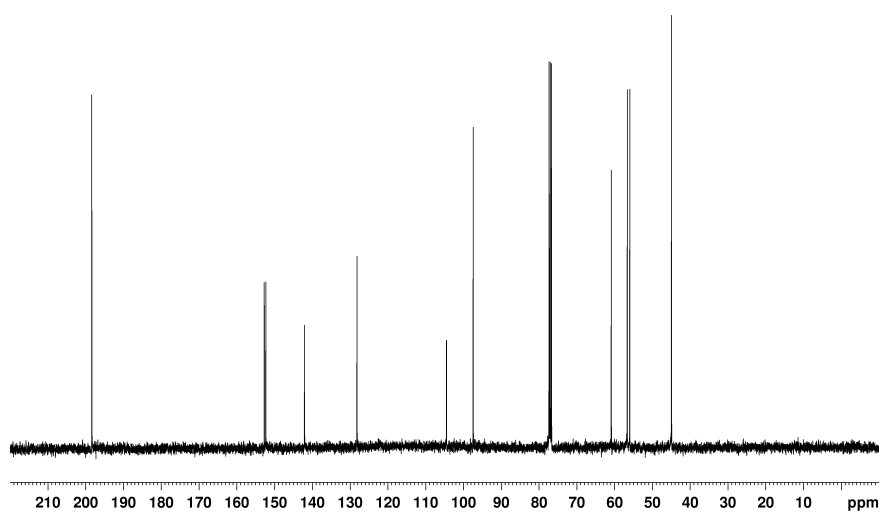
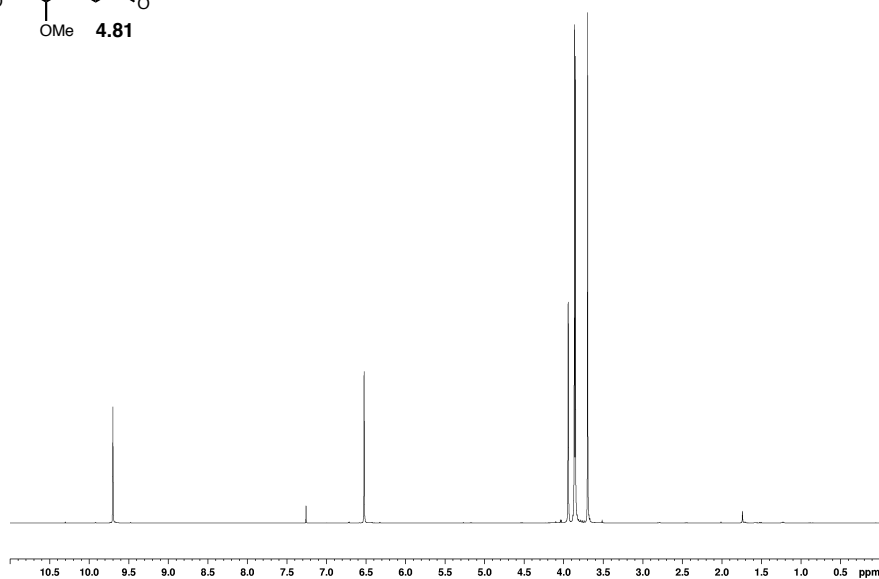
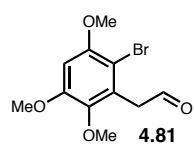


**Figure A2.21.** <sup>1</sup>H NMR spectrum (400 MHz, CDCl<sub>3</sub>) and <sup>13</sup>C NMR spectrum (100 MHz, CDCl<sub>3</sub>) of compound **4.81**.

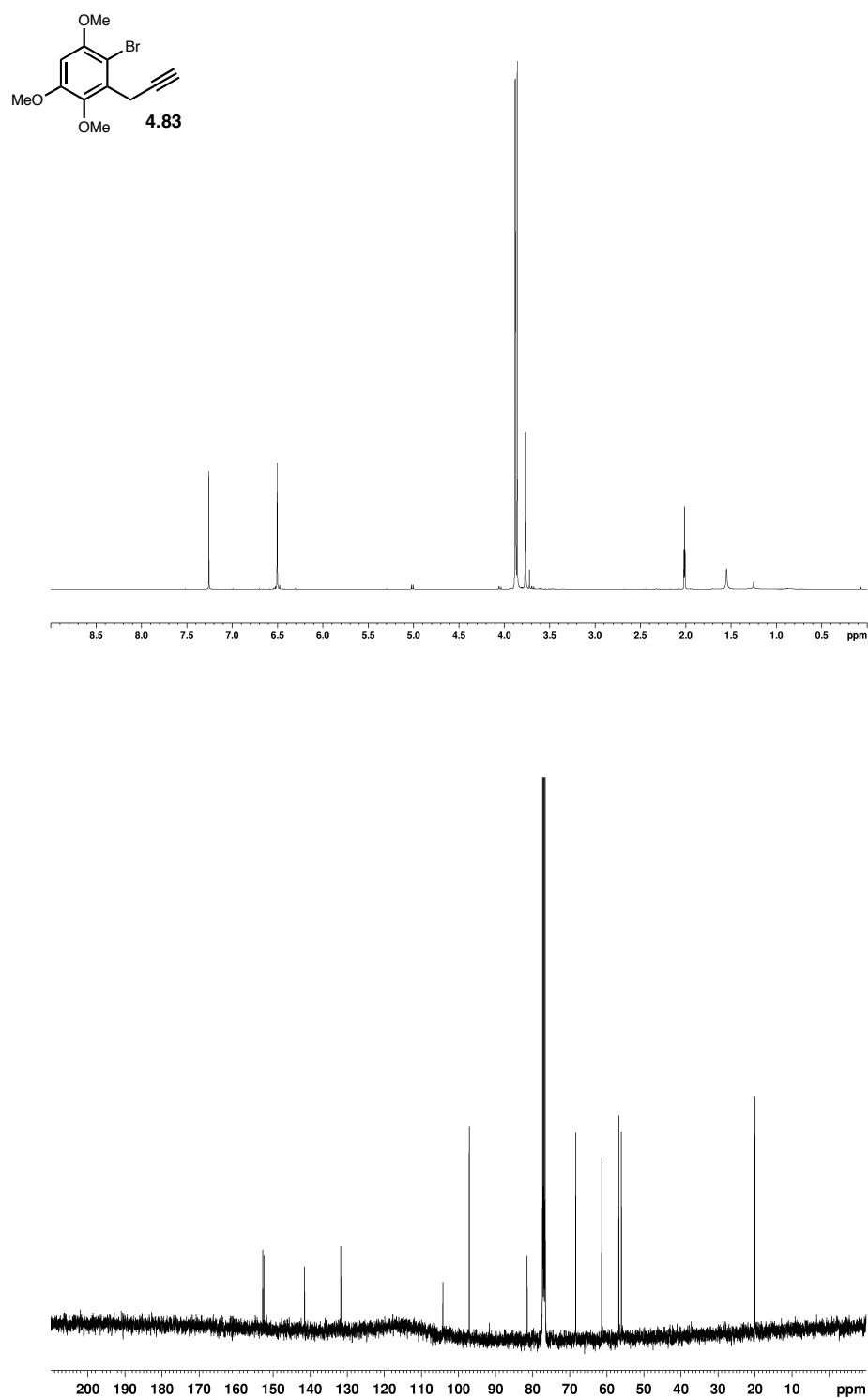


**Figure A2.22.**  $^1\text{H}$  NMR spectrum (400 MHz,  $\text{CDCl}_3$ ) and  $^{13}\text{C}$  NMR spectrum (100 MHz,  $\text{CDCl}_3$ ) of compound **4.83**.



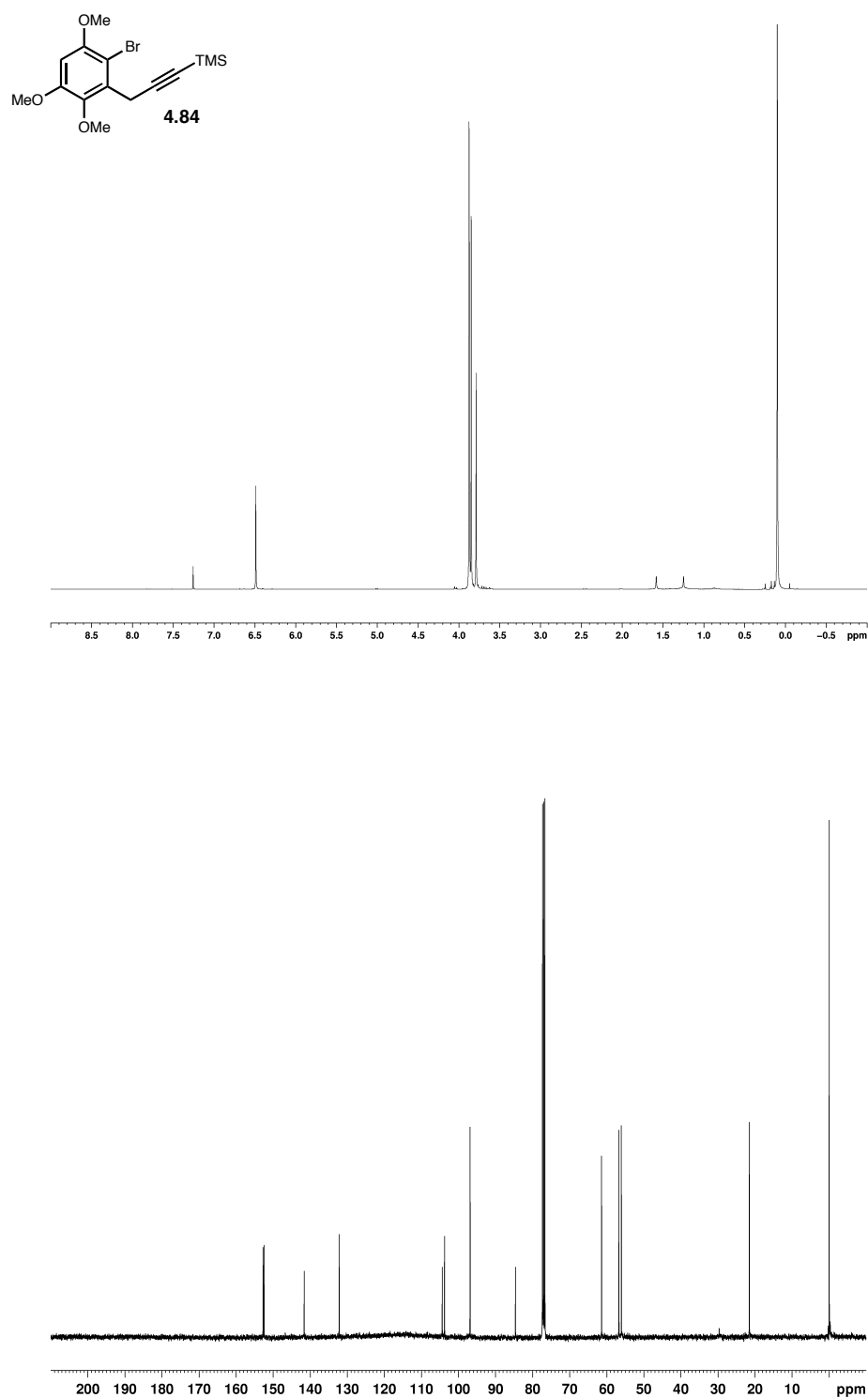


**Figure A2.23.**  $^1\text{H}$  NMR spectrum (400 MHz,  $\text{CDCl}_3$ ) and  $^{13}\text{C}$  NMR spectrum (100 MHz,  $\text{CDCl}_3$ ) of compound **4.84**.

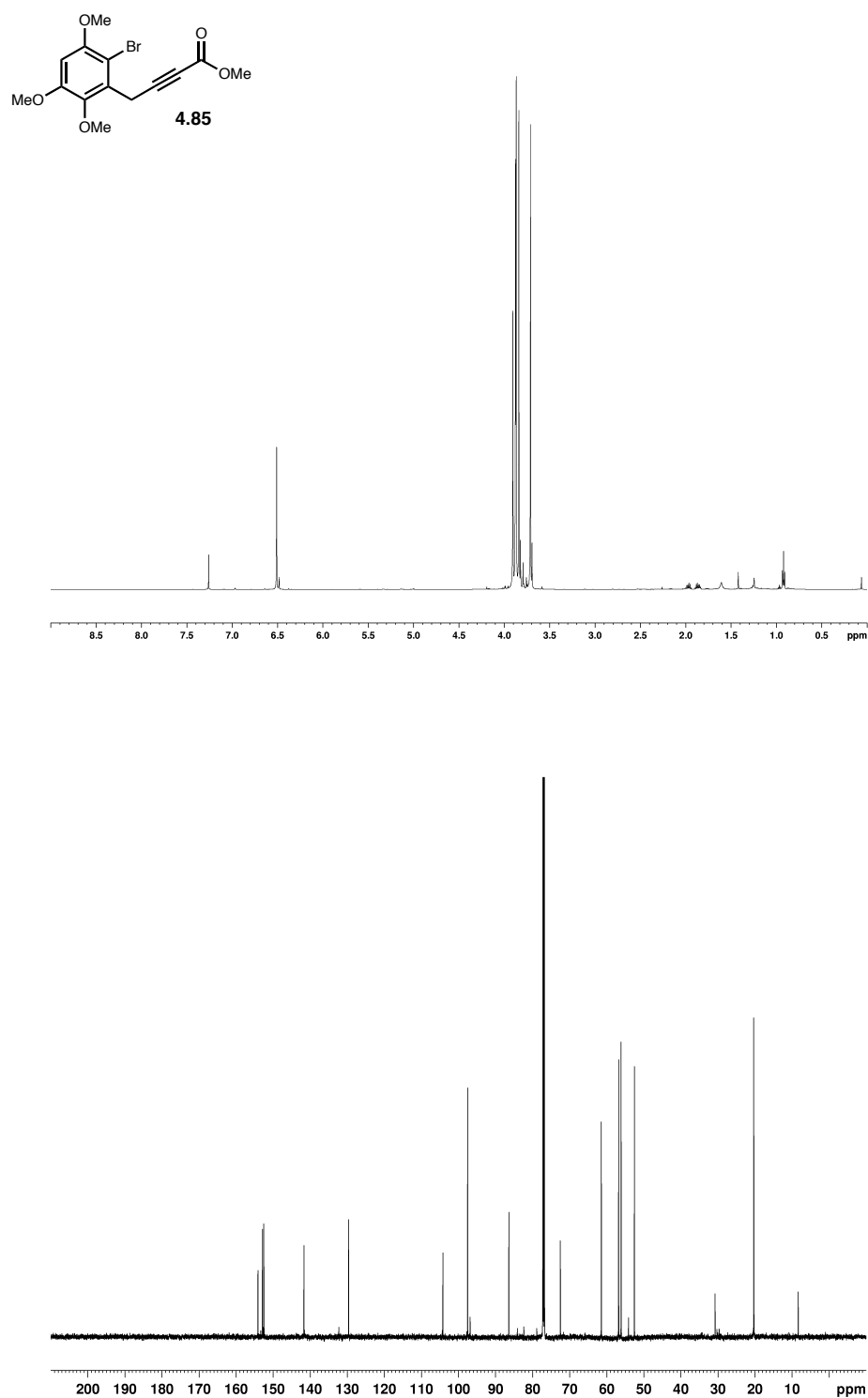


**Figure A2.24.**  $^1\text{H}$  NMR spectrum (600 MHz,  $\text{CDCl}_3$ ) and  $^{13}\text{C}$  NMR spectrum (150 MHz,  $\text{CDCl}_3$ ) of compound **4.85**.

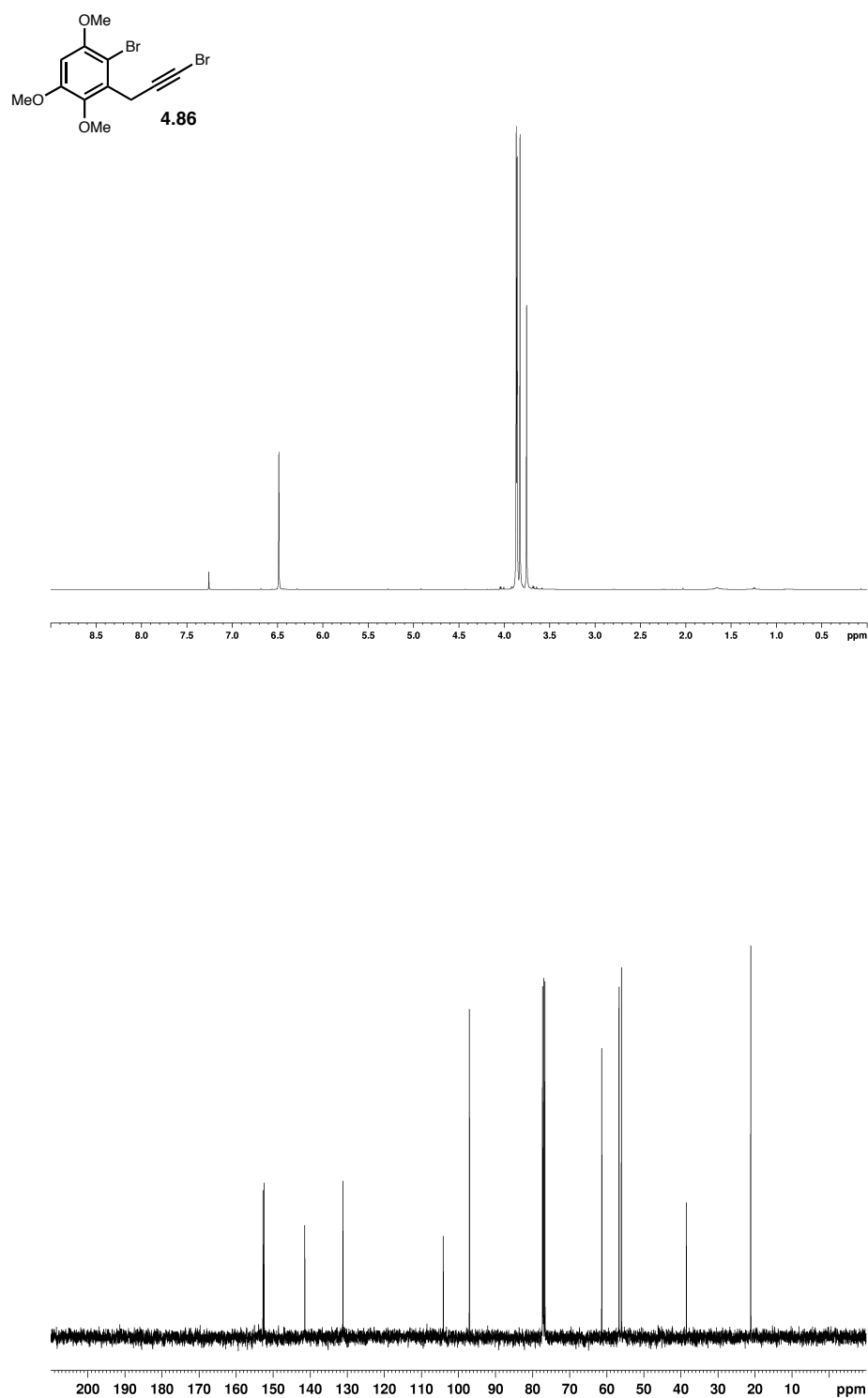


**Figure A2.25.**  $^1\text{H}$  NMR spectrum (400 MHz,  $\text{CDCl}_3$ ) and  $^{13}\text{C}$  NMR spectrum (100 MHz,  $\text{CDCl}_3$ ) of compound **4.86**.

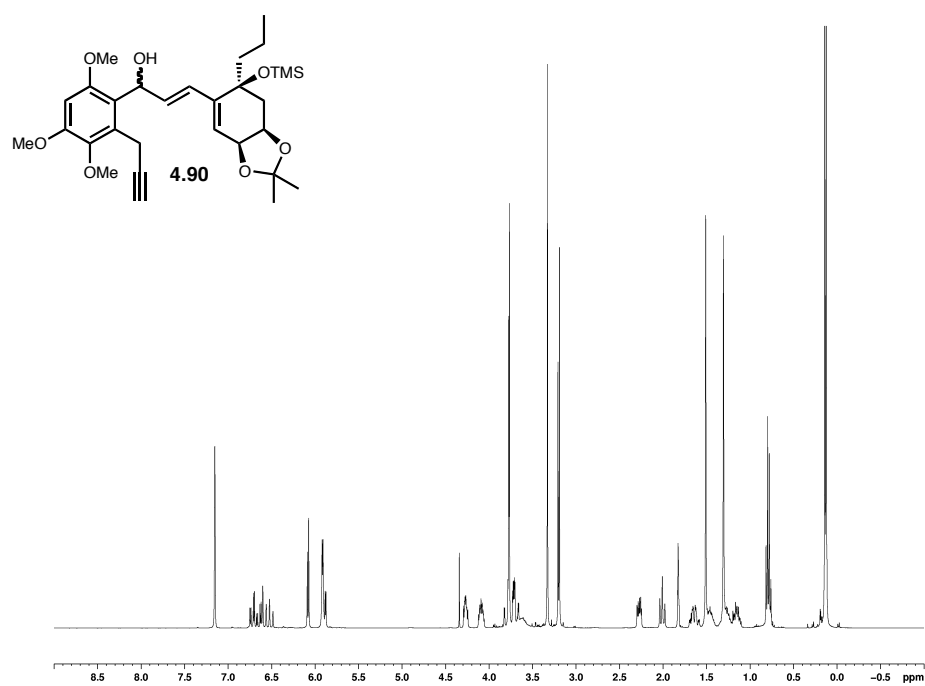


**Figure A2.26.**  $^1\text{H}$  NMR spectrum (400 MHz,  $\text{C}_6\text{D}_6$ ) of compound **4.90**.

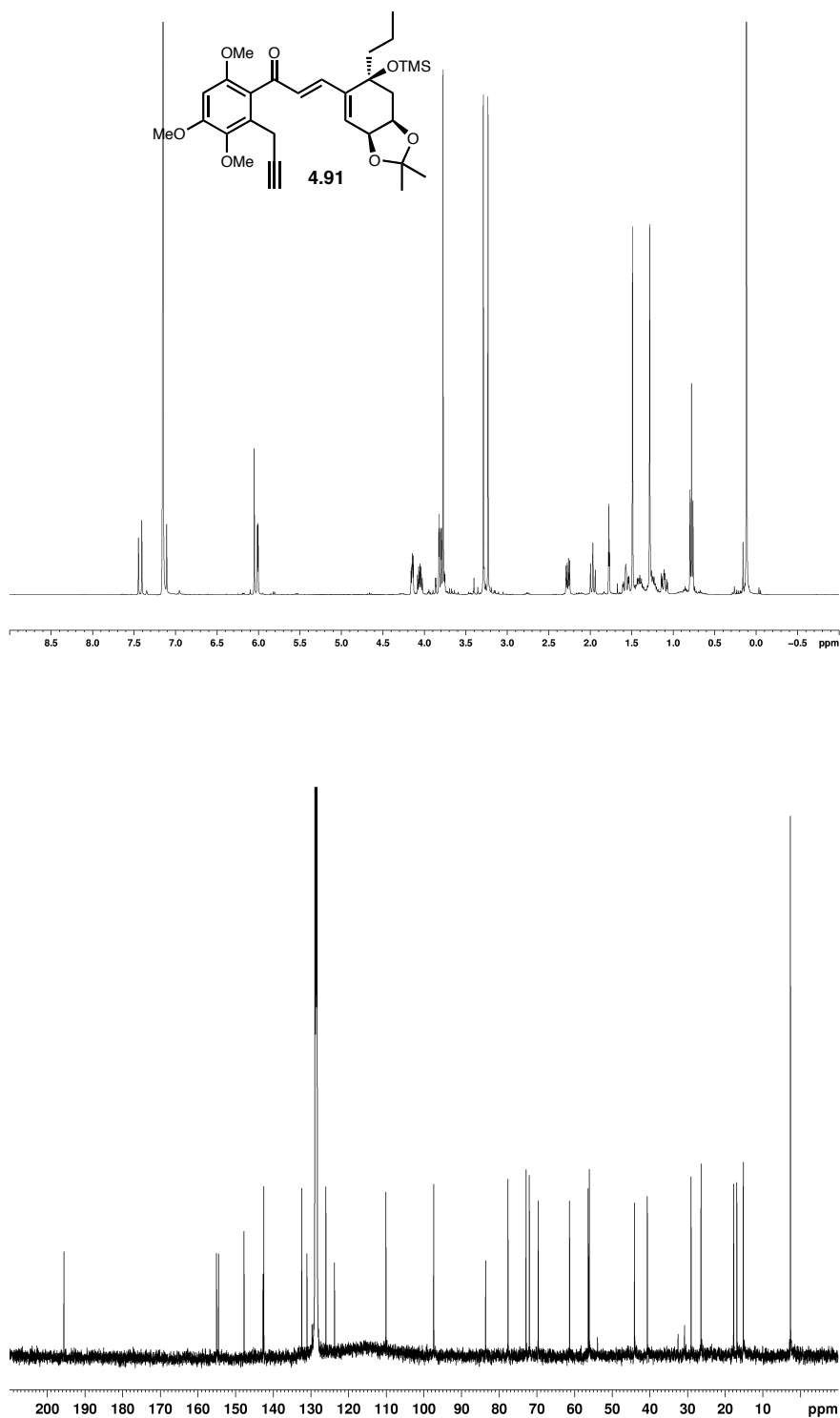


**Figure A2.27.**  $^1\text{H}$  NMR spectrum (400 MHz,  $\text{C}_6\text{D}_6$ ) and  $^{13}\text{C}$  NMR spectrum (100 MHz,  $\text{C}_6\text{D}_6$ ) of compound 4.91.

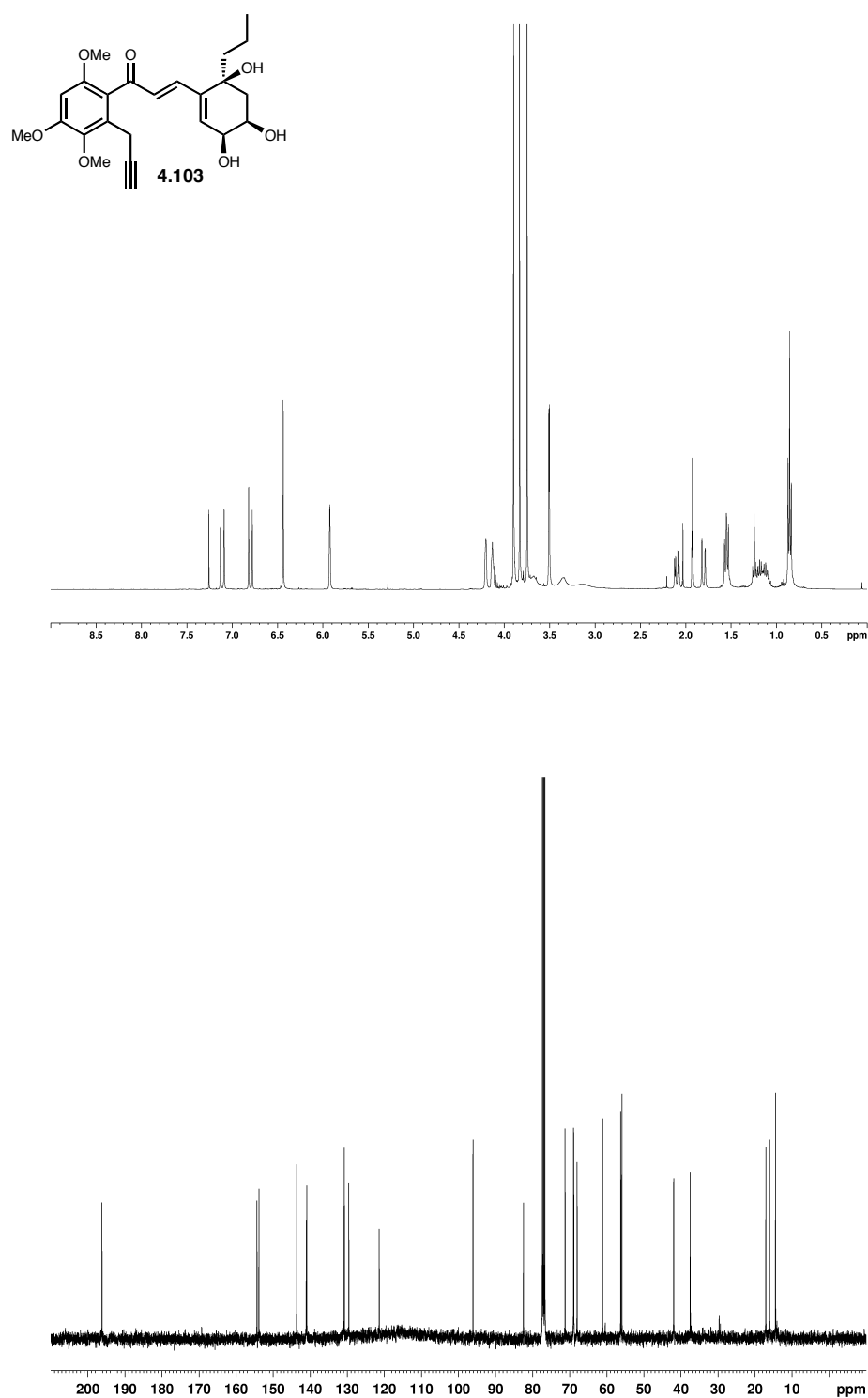


**Figure A2.28.**  $^1\text{H}$  NMR spectrum (400 MHz,  $\text{CDCl}_3$ ) and  $^{13}\text{C}$  NMR spectrum (100 MHz,  $\text{CDCl}_3$ ) of compound **4.103**.

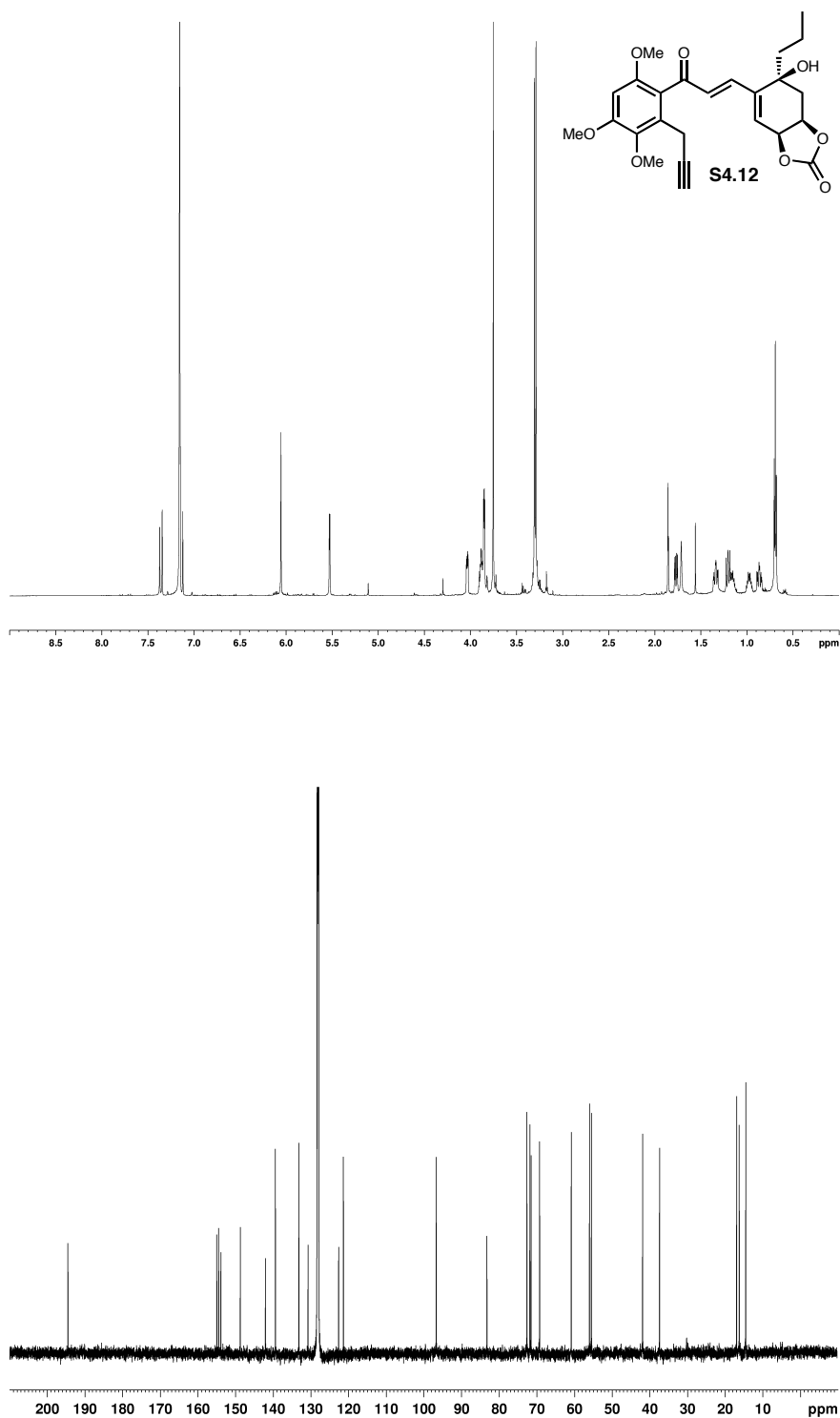


**Figure A2.29.**  $^1\text{H}$  NMR spectrum (600 MHz,  $\text{C}_6\text{D}_6$ ) and  $^{13}\text{C}$  NMR spectrum (150 MHz,  $\text{C}_6\text{D}_6$ ) of compound S4.12.

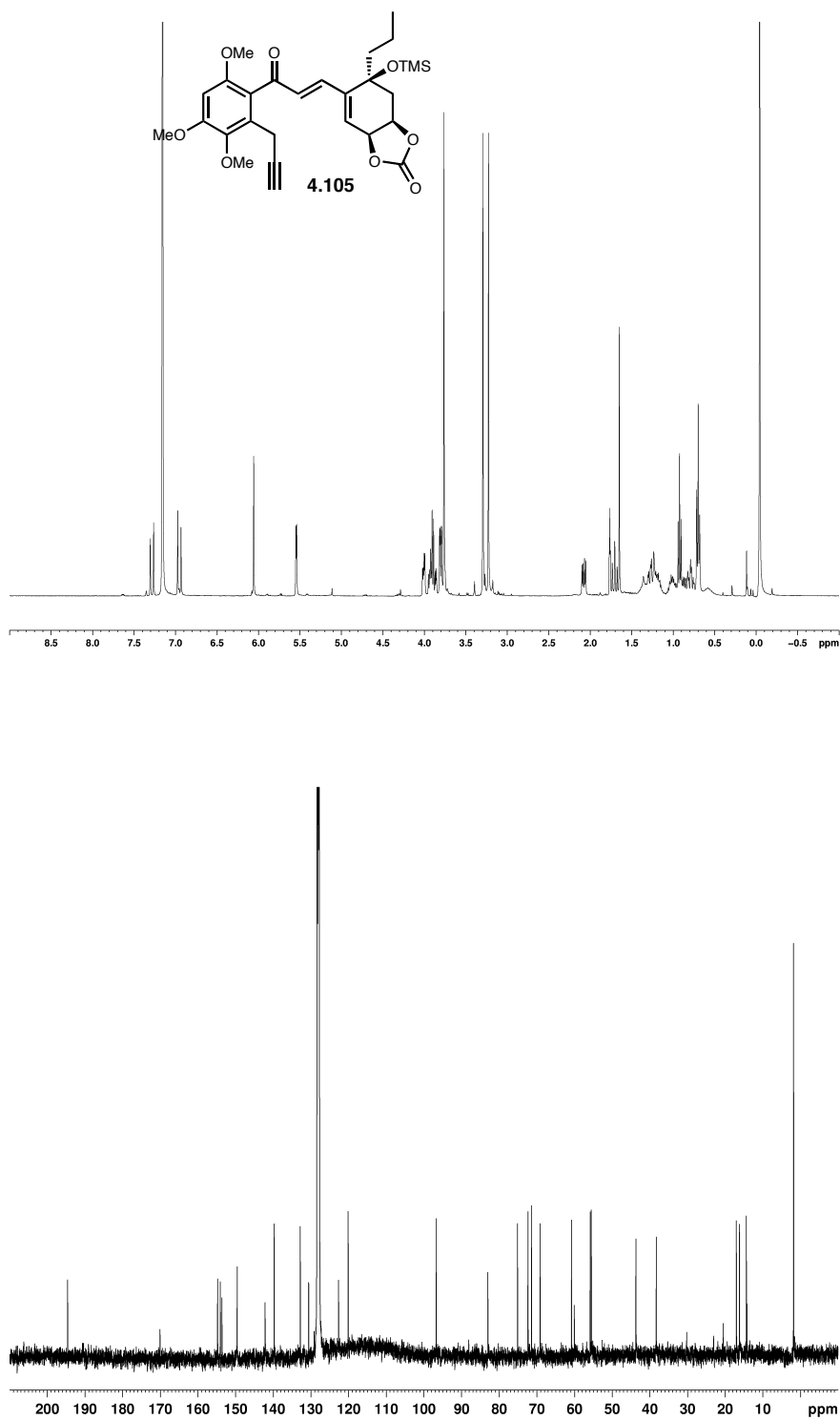


**Figure A2.30.**  $^1\text{H}$  NMR spectrum (400 MHz,  $\text{C}_6\text{D}_6$ ) and  $^{13}\text{C}$  NMR spectrum (100 MHz,  $\text{C}_6\text{D}_6$ ) of compound **4.105**.



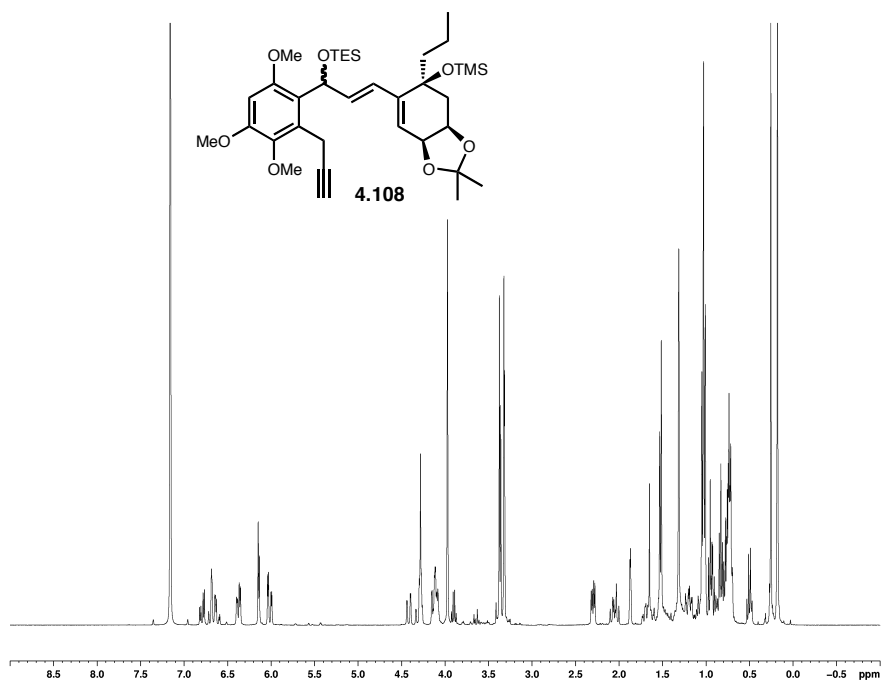


**Figure A2.31.**  $^1\text{H}$  NMR spectrum (400 MHz,  $\text{C}_6\text{D}_6$ ) of compound **4.108**.

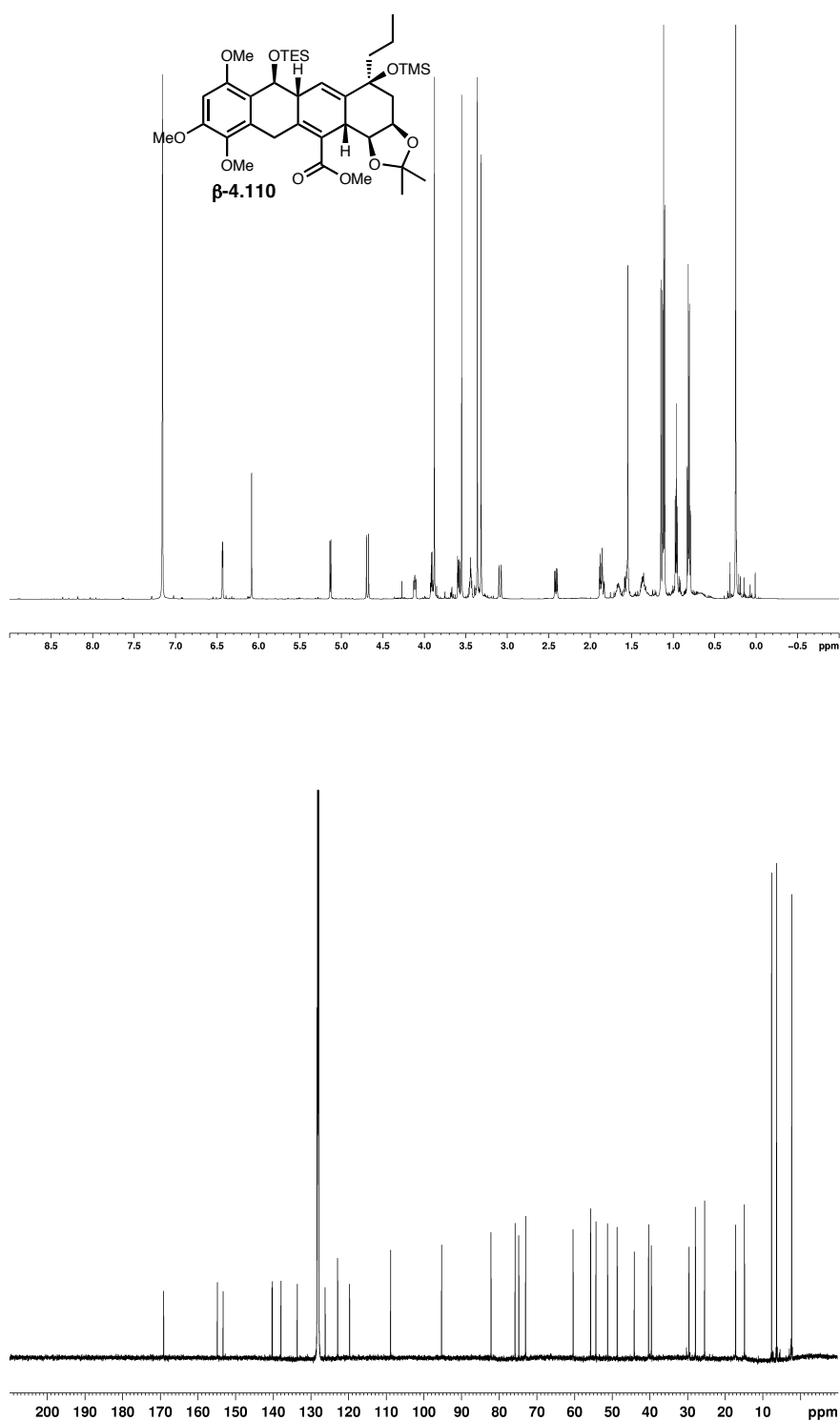


**Figure A2.32.** <sup>1</sup>H NMR spectrum (600 MHz, C<sub>6</sub>D<sub>6</sub>) and <sup>13</sup>C NMR spectrum (150 MHz, C<sub>6</sub>D<sub>6</sub>) of compound **β-4.110**.

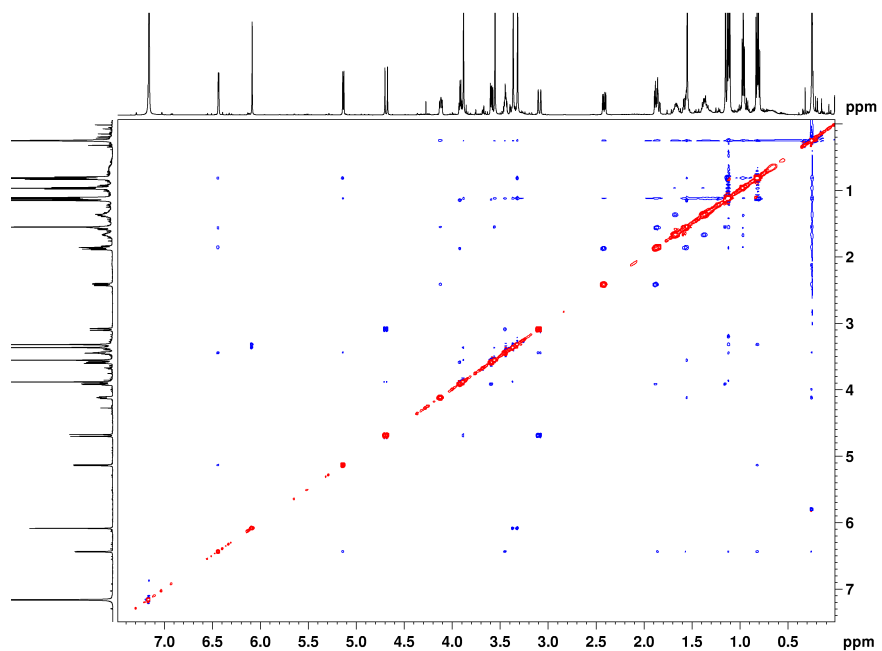
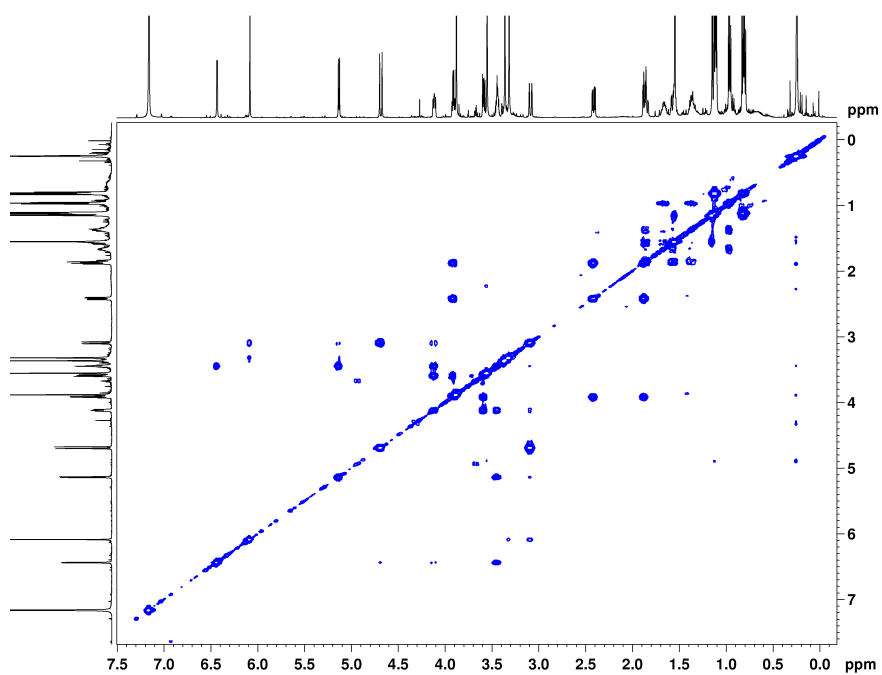


**Figure A2.33.** COSY spectrum (600 MHz,  $C_6D_6$ ) and NOESY spectrum (600 MHz,  $C_6D_6$ ) of compound  $\beta$ -4.110.





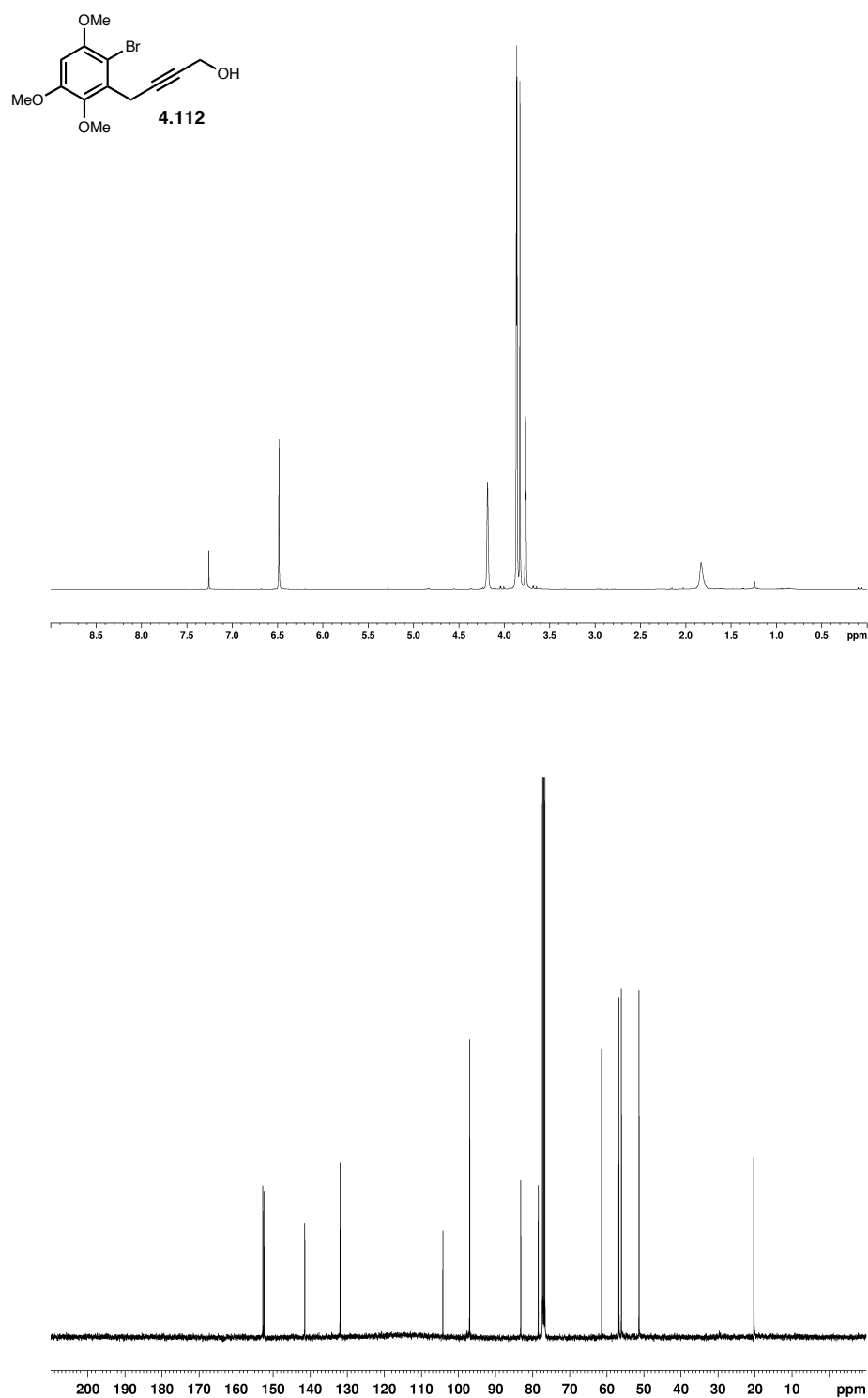


**Figure A2.36.**  $^1\text{H}$  NMR spectrum (400 MHz,  $\text{CDCl}_3$ ) and  $^{13}\text{C}$  NMR spectrum (100 MHz,  $\text{CDCl}_3$ ) of compound **4.112**.

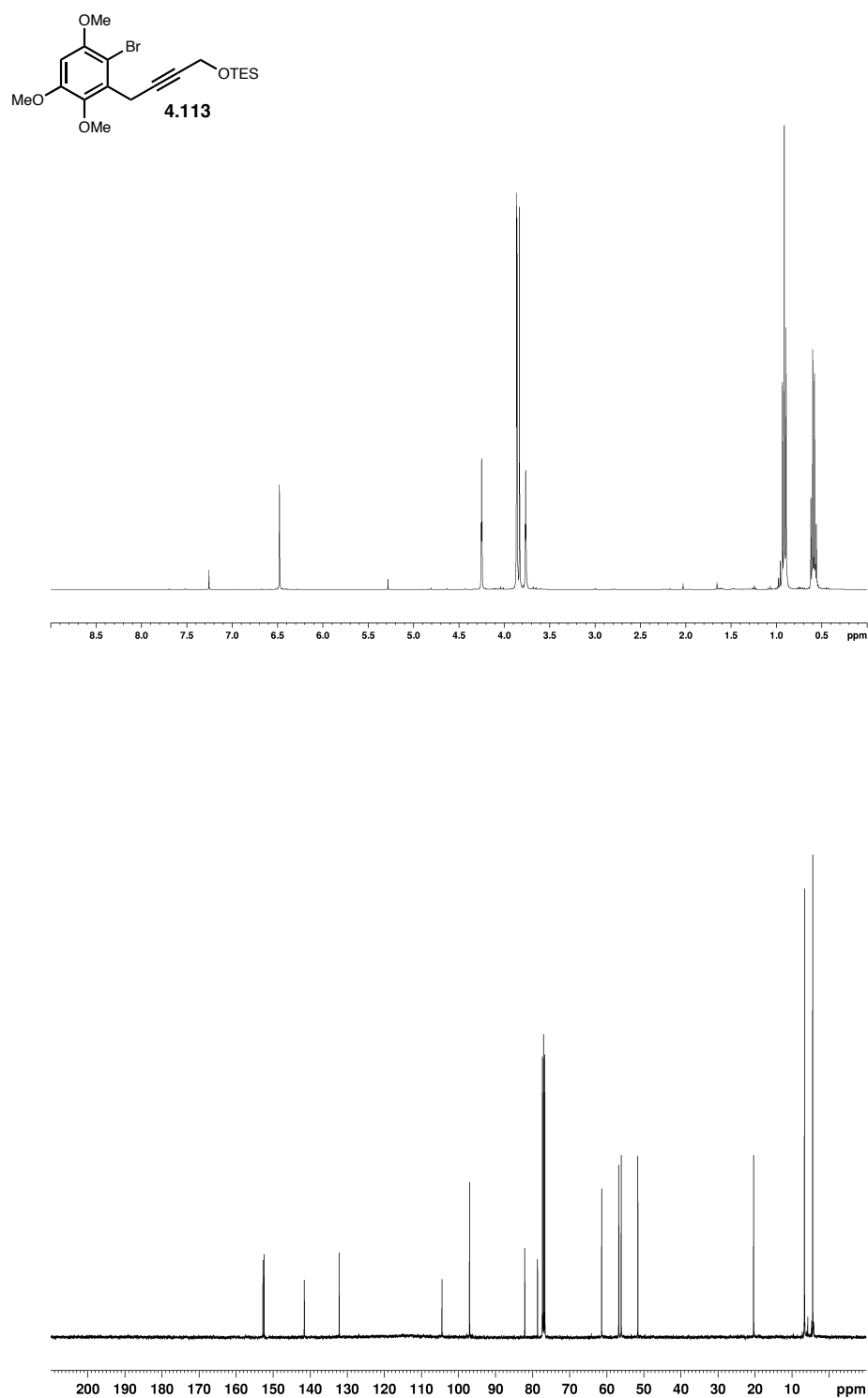


**Figure A2.37.**  $^1\text{H}$  NMR spectrum (400 MHz,  $\text{CDCl}_3$ ) and  $^{13}\text{C}$  NMR spectrum (100 MHz,  $\text{CDCl}_3$ ) of compound **4.113**.

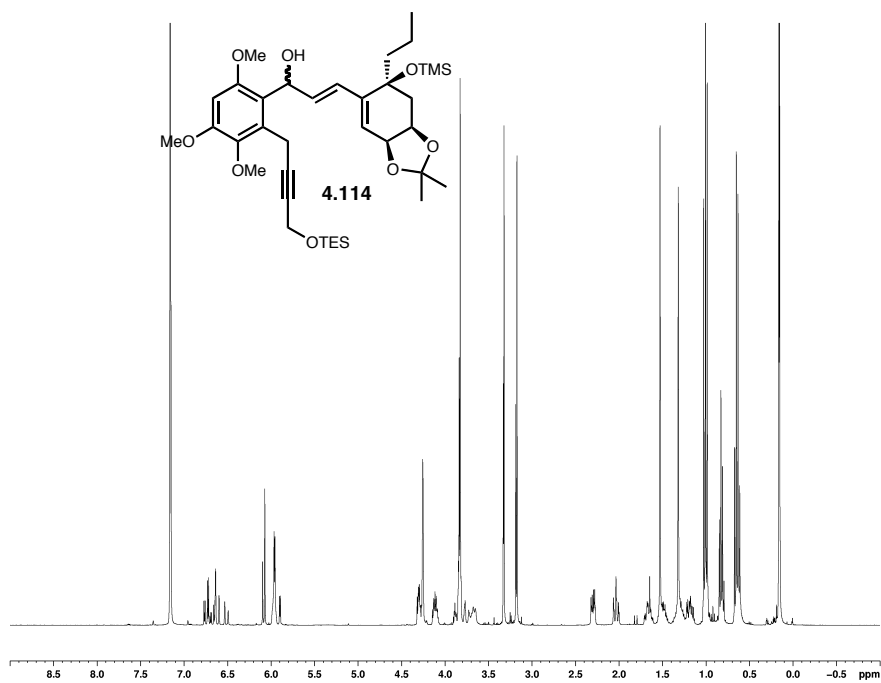


**Figure A2.38.**  $^1\text{H}$  NMR spectrum (400 MHz,  $\text{C}_6\text{D}_6$ ) of compound **4.114**.



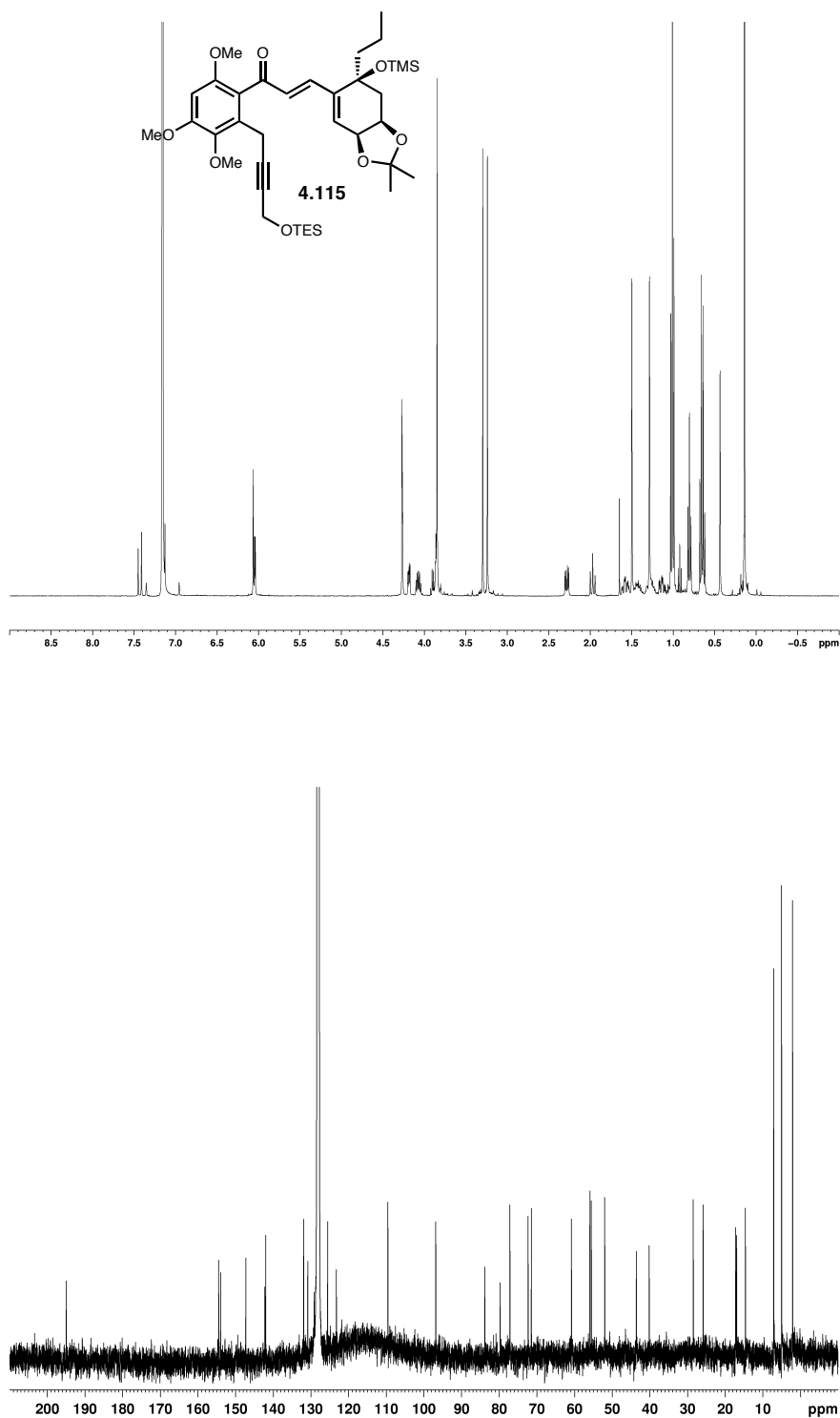


**Figure A2.39.**  $^1\text{H}$  NMR spectrum (400 MHz, C<sub>6</sub>D<sub>6</sub>) and  $^{13}\text{C}$  NMR spectrum (100 MHz, C<sub>6</sub>D<sub>6</sub>) of compound **4.115**.

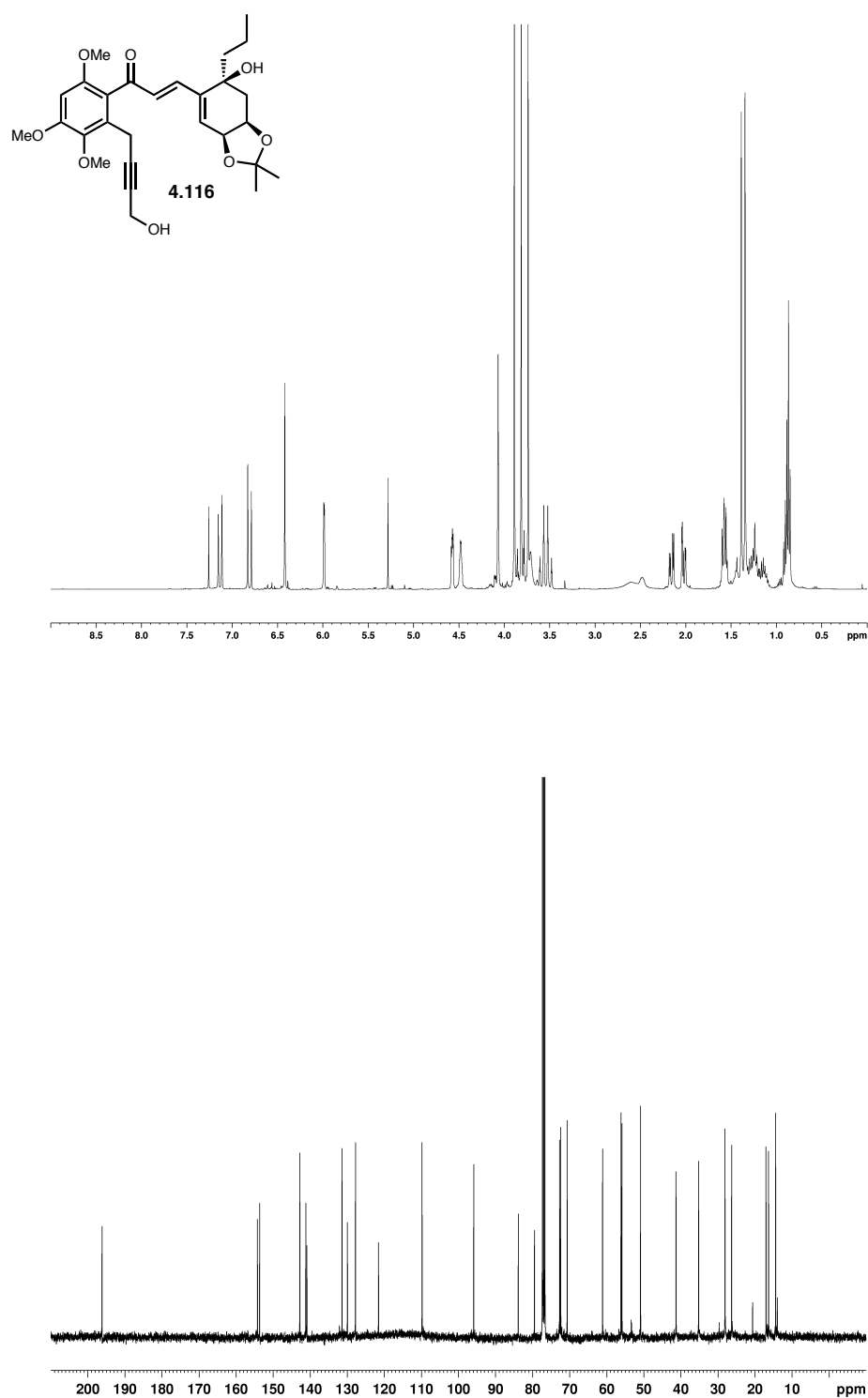


**Figure A2.40.**  $^1\text{H}$  NMR spectrum (400 MHz,  $\text{CDCl}_3$ ) and  $^{13}\text{C}$  NMR spectrum (100 MHz,  $\text{CDCl}_3$ ) of compound **4.116**.

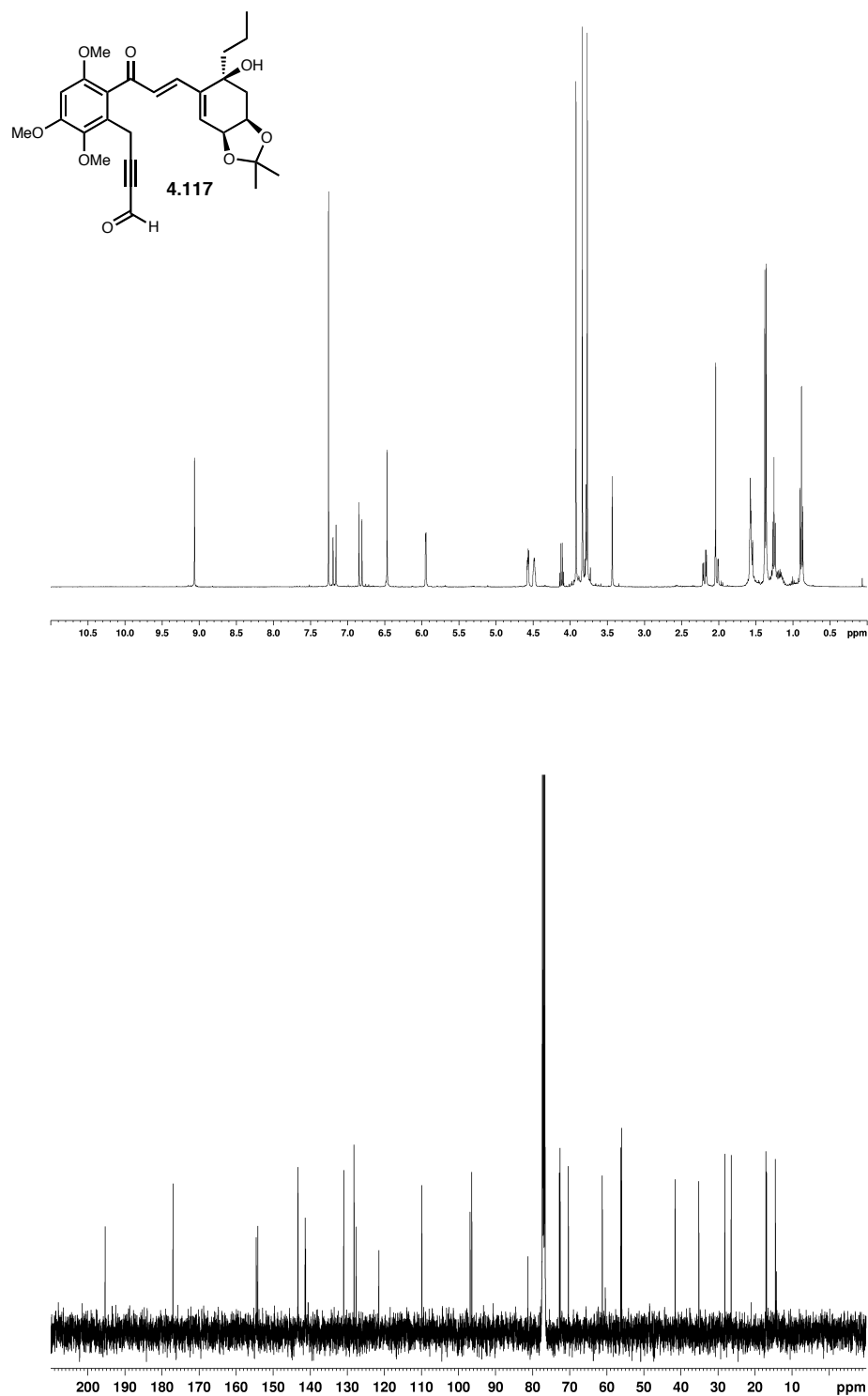


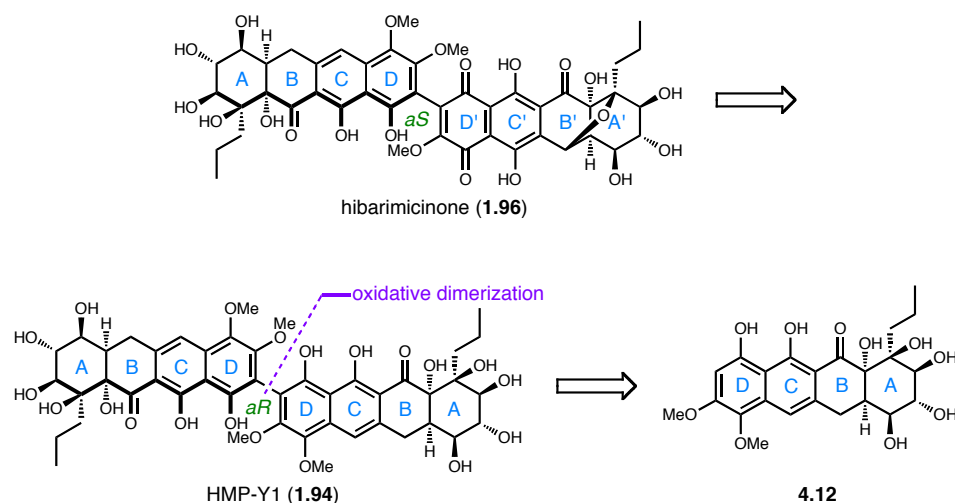
**Figure A2.41.**  $^1\text{H}$  NMR spectrum (400 MHz,  $\text{CDCl}_3$ ) and  $^{13}\text{C}$  NMR spectrum (100 MHz,  $\text{CDCl}_3$ ) of compound **4.117**.

## CHAPTER V

### AN INTRAMOLECULAR DIELS-ALDER-ENABLED DIMERIZATION APPROACH AND BEYOND

#### **A Modified D-Ring Protecting Group and Synthetic Analysis**

Several important pieces of information began to surface regarding the absolute stereochemistry of hibarimicin B (**1.78**) through the course of our studies. We had recently identified the absolute atropisomerism of HMP-Y6 (**1.93**) and thus hibarimicinone (**1.96**), and along with Hori and co-workers' Mosher ester analysis of hibarimicinone, the first total synthesis of hibarimicinone was reported in January 2012 in *Tetrahedron Letters* confirming the absolute stereochemistry.<sup>1,2,3</sup> When considered with our synthetic studies, these data showed that we had serendipitously chosen to work toward the natural enantiomer of hibarimicinone when we changed to (–)-quinic acid as our starting material. To reflect this knowledge, Scheme 5.1 displays the confirmed absolute stereochemistry of HMP-Y1 and hibarimicinone.

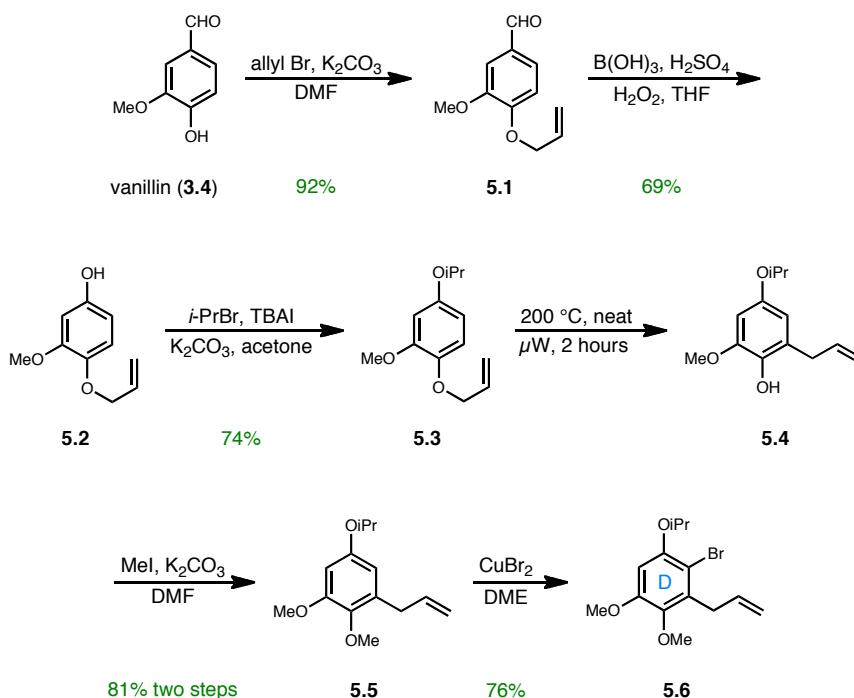


**Scheme 5.1.** Retrosynthesis reflecting new stereochemical knowledge.

In light of our disappointments with synthesis of a transannular Diels-Alder substrate, we attempted to view our efforts in a new light and realign the necessary pieces to achieve our goal. We first reevaluated the tetracyclic substrate **4.12** which we still planned to dimerize through an oxidative homocoupling relying on the free phenol at C-1. However, our previous work had proposed a difficult demethylation of the C-1 phenol in the presence of the innate C-3 and C-4 methoxy groups. Therefore, we sought to simplify a late-stage phenol deprotection by installing an orthogonal protecting group, and Shaw and co-workers' use of an isopropyl phenol protecting group in their synthesis of (–)-viriditoxin, which has been shown to undergo deprotection in the presence of aryl methyl ethers, inspired our resynthesis of our functionalized D-ring intermediate.<sup>4</sup>

Thus, our route to the isopropyl-protected D-ring **5.6** was developed by Marta Wenzler and began by allyl ether formation with vanillin (**3.4**).<sup>5</sup> Key to our route was implementation of a Baeyer-Villiger protocol that did not undergo competing olefin epoxidation, and we thus became aware of a method utilizing a simple mixture of boric

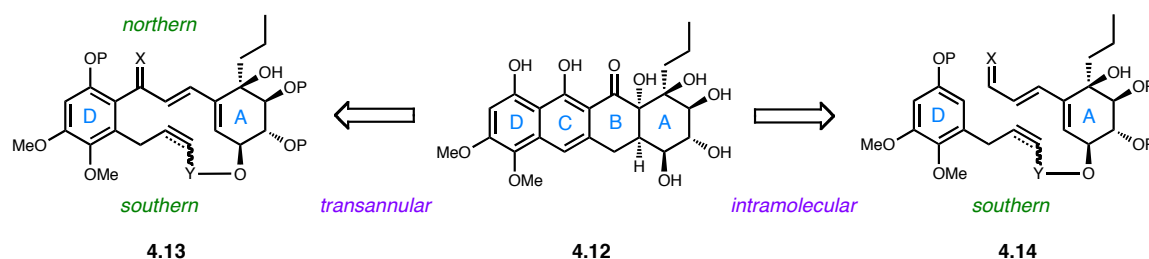
acid, sulfuric acid, and hydrogen peroxide which presumably involves the intermediacy of an aldehyde-coordinated boric acid/hydrogen peroxide complex.<sup>6</sup> Thus, Baeyer-Villiger oxidation of aldehyde **5.1** provided phenol **5.2** which was protected as its isopropyl ether **5.3**. Claisen rearrangement of the allyl ether **5.3** provided the phenol **5.4** which was methylated under standard conditions. Finally, regioselective bromination with CuBr<sub>2</sub> provided **5.6** in overall good yield. The intermediates **5.5** and **5.6** could then serve as building blocks for our future efforts.



**Scheme 5.2.** Synthesis of an orthogonally-protected D-ring.

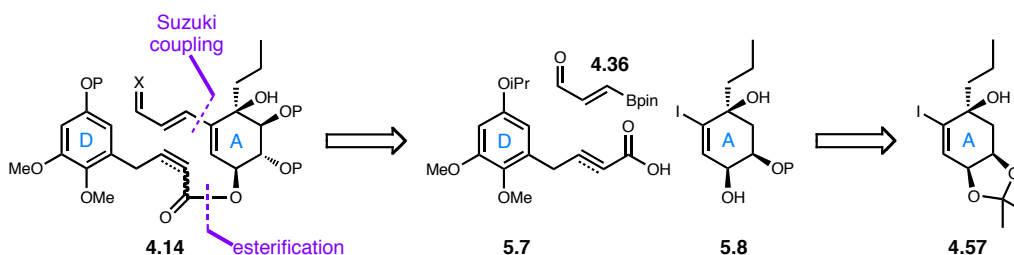
With our improved D-ring in hand, we revisited the crux of our approach to the tetracycle **4.12**, a tethered Diels-Alder reaction. Chapter IV discussed our efforts toward the macrocyclic intermediate **4.13** for TADA cyclization and reinforced the importance

of the southern tether for correct C-9 stereocenter formation. But ultimately all of our routes utilizing initial northern tether formation failed to lead to the desired southern tether formation. With this in mind, we acknowledged that a southern-tethered IMDA approach through an intermediate such as **4.14** should correctly form the necessary C-9 stereocenter, and a functionalized diene would allow for final C-ring closure.



**Scheme 5.3.** Revisiting possible Diels-Alder-enabled routes to tetracycle **4.12**.

The key to this southern-tethered IMDA route would lay in our ability to differentiate the (–)-quinic acid-derived *cis*-diol for tether formation. We hoped that the requisite triol could be regioselectively protected to provide an intermediate such as **5.8** which would allow for esterification with a suitably functionalized  $\alpha,\beta$ -unsaturated- or alkynyl-acid **5.7**.



**Scheme 5.4.** Synthetic analysis of an IMDA approach.

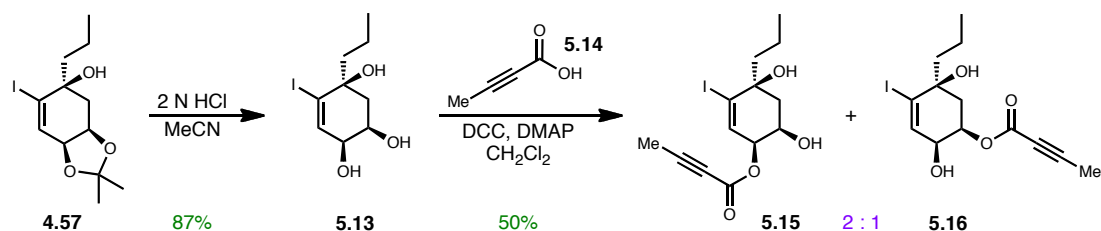
While formation of the differentially protected A-ring **5.8** would present difficulties, we were confident that the remaining esterification and Suzuki coupling steps would allow formation of an IMDA substrate toward the tetracycle **4.12**. Thus, we set out to synthesize the necessary building blocks toward IMDA precursor **4.14**.

### **Building Block Synthesis Toward an Alkynyl IMDA Precursor**

We identified our first target as an alkynyl acid containing no halide functionality for multiple reasons. As compared to the olefin, we decided that a terminal alkyne functionality would provide the largest number of options for routes to an acid for esterification. We also reasoned that an intramolecular C-ring closure would likely be difficult outside of a Nozaki-Hiyama-Kishi-type manifold, and a Friedel-Crafts-type closure might be more likely. Therefore, we set out to convert the terminal olefin of **5.5** to alkyne **5.10** based on our previous three step procedure which occurred in excellent yield. To install the acid functionality, we first employed a standard sequence of addition of the methyl ester followed by saponification arriving at **5.12**. However, both steps suffered from low yields, and we believe the hydrolysis step produced quantities of the undesired allene product as the remaining mass balance. Due to the low yielding two-step procedure, we alternately arrived at the desired alkynyl acid **5.12** in almost quantitative yield by alkyne deprotonation and bubbling of CO<sub>2(g)</sub> into the reaction mixture for 45 minutes. This approach led to large quantities of the acid, and now we needed to determine a synthetic scheme to produce the proposed vinyl iodide **5.8** shown in Scheme 5.4.

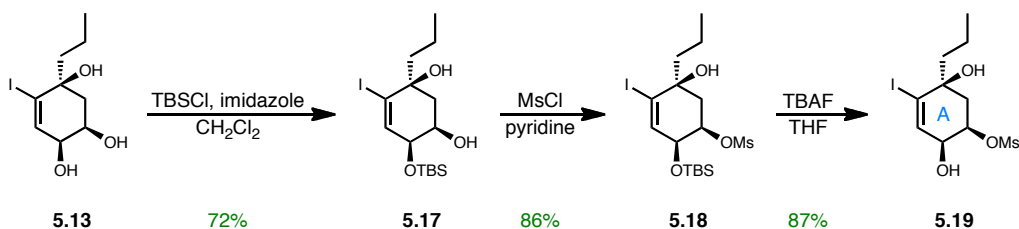






**Scheme 5.6.** Regioselectivity evaluation of a model esterification.

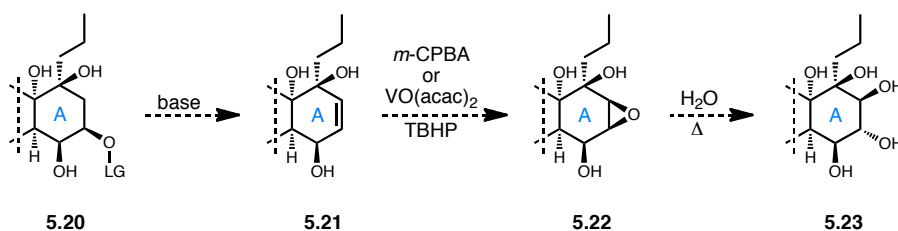
After much experimentation, we arrived at a sequence that, although more steps than desired, provided large quantities of a substrate similar to **5.8** with a free C-10 alcohol and a functionalized C-11 alcohol in good yield. The triol **5.13** was treated with TBSCl which selectively silylated the allylic alcohol, and the remaining alcohol was easily mesylated.<sup>8</sup> TBAF-mediated silyl ether removal finally formed our targeted A-ring substrate **5.19**, which we believed would allow straightforward southern tether formation.



**Scheme 5.7.** Synthesis of a differentially functionalized A-ring.

Our reasoning for installation of a mesylate group stemmed from our long term plan for formation of the necessary *trans-trans* triol system found in HMP-Y1 and hibarimicinone. Because the C-11 alcohol derived from (–)-quinic acid possessed the opposite stereochemistry to our targets, we believed that its elimination to an olefin

substrate such as **5.21** would allow for hydroxyl-directed epoxidation.<sup>9</sup> From the epoxide **5.22**, we proposed, based on literature precedent, nucleophilic opening with water to arrive at the *trans-trans* triol system **5.23**.<sup>10,11</sup> Although we were unable to predict the regioselectivity of epoxide opening, we were hopeful that a steric argument could be utilized to provide the desired regioselectivity by opening at the C-11 carbon.

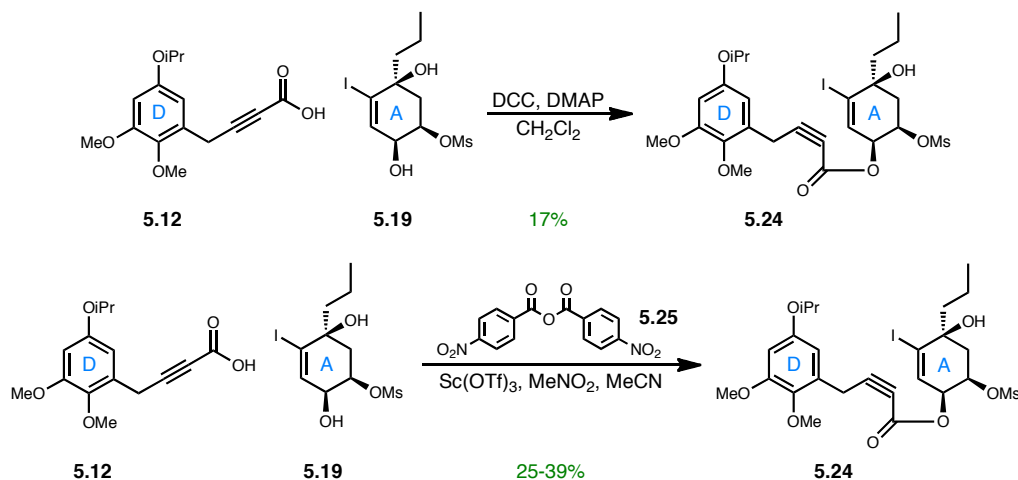


**Scheme 5.8.** Proposed installation of *trans-trans* triol functionality.

### A Southern-Tethered Alkynyl IMDA

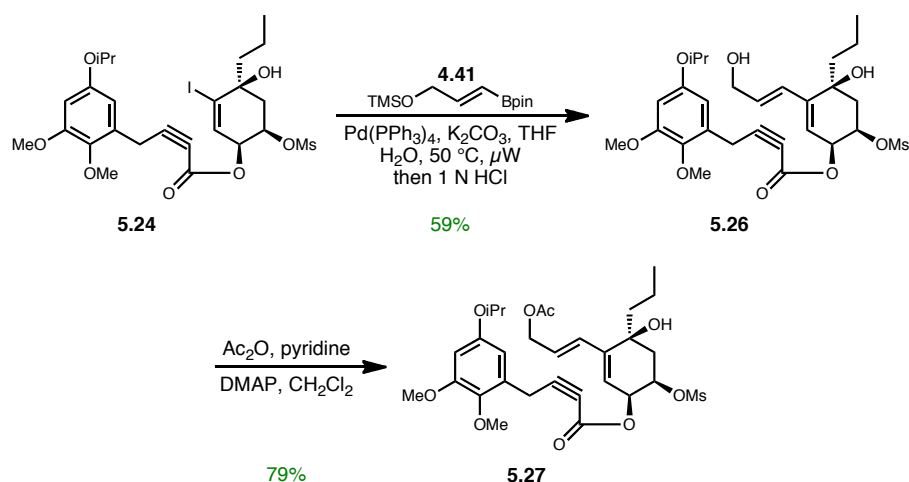
We now had in hand our three proposed building blocks for southern tethering, and we simply needed to identify proper conditions for esterification of the alkynyl acid **5.12** with the allylic alcohol **5.19**. Despite our precedent with the model system in Scheme 5.6, DCC provided the southern tether substrate **5.24** in very low yield.<sup>12</sup> Thus we continued to search for improved conditions, and after attempting couplings with EDCI, Ghosez's reagent, and others, we happened upon a procedure by Yamamoto involving the formation of a mixed anhydride in the presence of  $\text{Sc}(\text{OTf})_3$  and were surprised to isolate desired product **5.24**.<sup>13</sup> Unfortunately, yields for this reaction provided only small improvement over the more standard DCC conditions, but we were

excited to be only steps away from a southern-tethered IMDA substrate and we pressed on using the Yamamoto conditions.



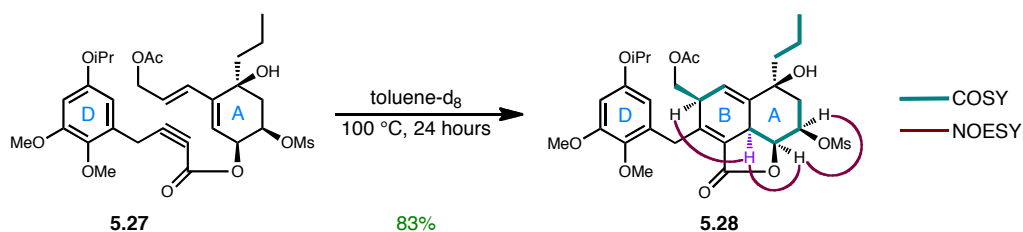
**Scheme 5.9.** Formation of a southern-tethered alkynyl ester.

Once we had successfully synthesized the southern-tethered ester **5.24**, we quickly identified conditions to arrive at an IMDA precursor. Thus, modification of our standard Suzuki coupling conditions involved heating a mixture of the vinyl iodide **5.24** and the vinyl boronate **4.41** in the presence of  $\text{Pd}(\text{PPh}_3)_4$  and potassium carbonate via microwave irradiation at 50 °C for 30 minutes which, following acidic workup, provided the allylic alcohol **5.26** in moderate yield.<sup>14</sup> Finally, we arbitrarily installed an acetate protecting group for the purposes of the cycloaddition, and we were ecstatic to arrive at our long-awaited precursor **5.27** for a southern-tethered Diels-Alder.



**Scheme 5.10.** Arrival at a southern-tethered IMDA precursor.

The crux of our synthetic plans relied on a southern-tethered Diels-Alder to set the correct C-9 stereochemistry, and we had finally produced a substrate that met these criteria. For ease of reaction monitoring, the diene-yne **5.27** was heated in deuterated toluene in an NMR tube, and at 100 °C for 24 hours, we observed conversion to a new product. Extensive 1-D and 2-D NMR studies confirmed our suspicions: we had successfully performed an intramolecular Diels-Alder to arrive at an ABD ring system with the correct C-9 bridgehead stereochemistry. This proof-of-concept reaction became the pinnacle of our efforts, and our future work would rely on this important data.

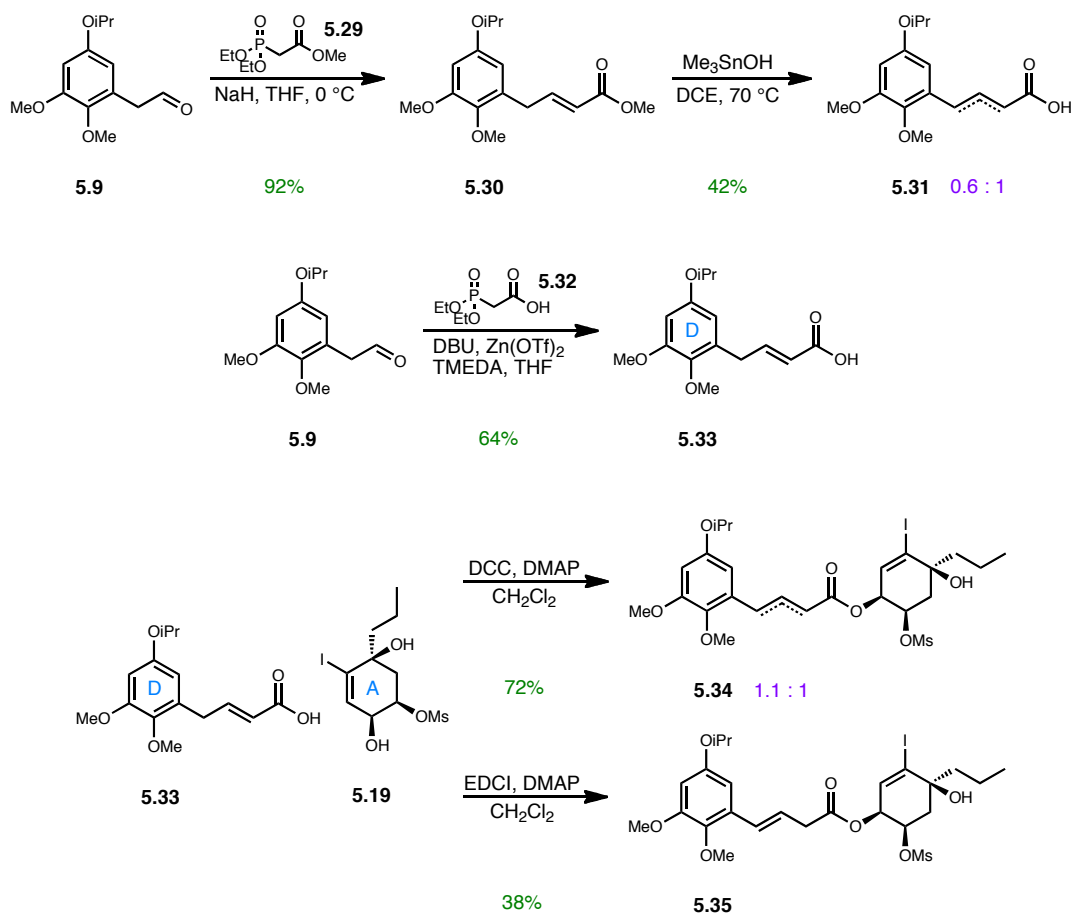


**Scheme 5.11.** A southern-tethered IMDA leads to desired C-9 stereochemistry.

This success quickly became overshadowed by the reality of our route to **5.28**: the Sc(OTf)<sub>3</sub>-mediated esterification reaction proved intractable for production of reasonable amounts of material due to both its yield and inconsistency. Additionally, we remained uncertain how to predictably utilize the tetrasubstituted C-7/C-8 olefin toward our desired target. Considering these issues, we reasoned that an  $\alpha,\beta$ -unsaturated acid might address both concerns, and instead of refocusing our efforts on improving the alkynyl acid esterification, we turned toward synthesis of an olefinic dienophile.

### **Toward a Southern-Tethered Alkenyl IMDA Substrate**

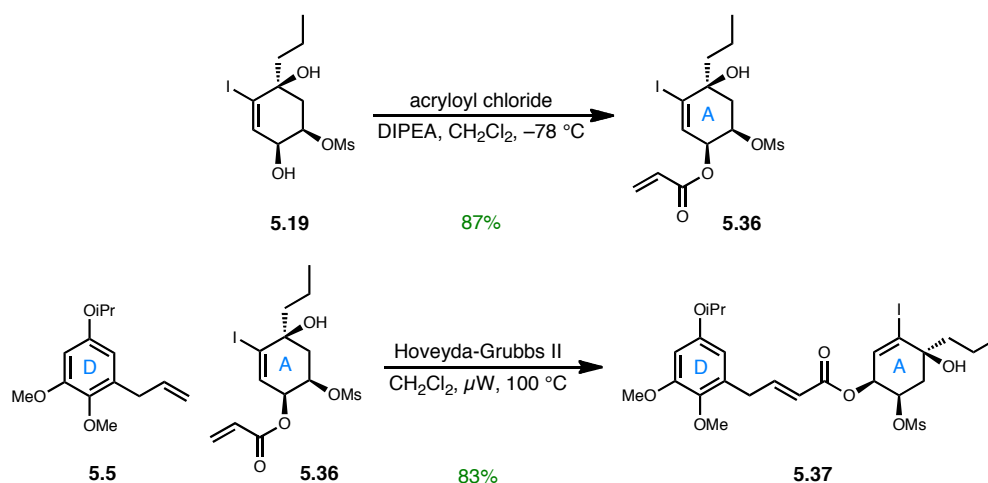
We had utilized aldehyde **5.9** previously for synthesis of the aryl alkyne **5.10**, and we hoped this intermediate would expedite synthesis of an  $\alpha,\beta$ -unsaturated acid. Horner-Wadsworth-Emmons (HWE) reaction with methyl diethylphosphonoacetate (**5.29**) easily led to the methyl ester **5.30**; however, after attempts at ester hydrolysis led to partial olefin isomerization, we became keenly aware of the tenuous nature of the olefin regiochemistry. To avoid the need for base-mediated hydrolysis, we successfully employed a procedure developed by Helquist involving HWE reaction with diethylphosphonoacetic acid (**5.32**) leading to the  $\alpha,\beta$ -unsaturated acid **5.33** in reasonable yield.<sup>15</sup> With both coupling pieces in hand, we reverted to standard esterification conditions and were disappointed to observe partial olefin isomerization when employing DCC and almost complete isomerization with EDCI. These results implied the need to avoid traditional ester-forming procedures in attempting southern tethering.



**Scheme 5.12.** Attempted southern tethering of an  $\alpha,\beta$ -unsaturated acid.

Our previous experience with acrylate esters prompted a completely novel approach to the southern tether: cross metathesis between an aryl olefin D-ring and an acrylate ester A-ring. These two metathesis partners seemed well-suited for coupling when considering Grubbs' model for cross metathesis selectivity.<sup>16</sup> Terminal olefins readily undergo homodimerization and are considered type I olefins, while acrylates undergo slow homodimerization and are type II olefins. Therefore, use of an excess of the aryl olefin with an acrylate ester A-ring should lead to the desired southern tether.

We first converted the allylic alcohol **5.19** to the acrylate ester **5.36** with ease, and we were greatly pleased when upon heating of 3 molar equivalents of the aryl olefin **5.5** and the acrylate ester **5.36** with Hoveyda-Grubbs second generation catalyst via microwave irradiation for 1.5 hours, formation of the southern-tethered  $\alpha,\beta$ -unsaturated ester **5.37** occurred in stellar yield. At this point, we saw a straightforward path to an IMDA substrate that we hoped would lead to the desired ABD-ring system toward the tetracyclic target.

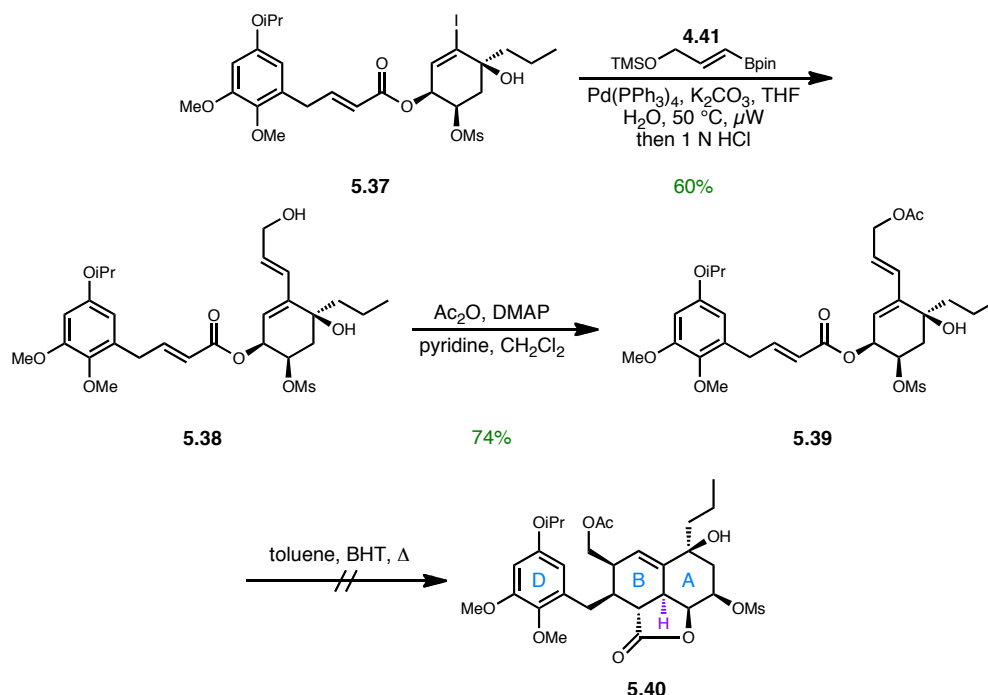


**Scheme 5.13.** Cross-metathesis route to the southern tether.

Suzuki cross coupling of the vinyl iodide **5.37** under our newest optimized microwave conditions afforded the allylic alcohol **5.38** which was acylated with acetic anhydride in good yield to quickly arrive at the proposed IMDA precursor **5.39**. Believing we had approached the tipping point in our synthesis, we were highly disappointed to observe only decomposition and no desired cyclization. This unexpected pathway began to occur at 100 °C, precisely the temperature that effected Diels-Alder



cyclization of the similar alkynyl ester **5.27**. Although we failed to unambiguously determine the nature of the decomposition products, we isolated what appeared by  $^1\text{H}$  NMR to be a fragmented form of the D-ring and tether with no indication of the presence of peaks from the A-ring. And while the topic of relative reactivity of olefin vs. alkyne dienophiles has been explored with no true consensus, we hypothesized that a combination of potentially slightly lower reactivity of the  $\alpha,\beta$ -unsaturated ester **5.39** compared to the alkynyl ester **5.27** and the presence of a possibly labile mesylate group contributed to the decomposition of **5.39** under IMDA conditions.<sup>17</sup>



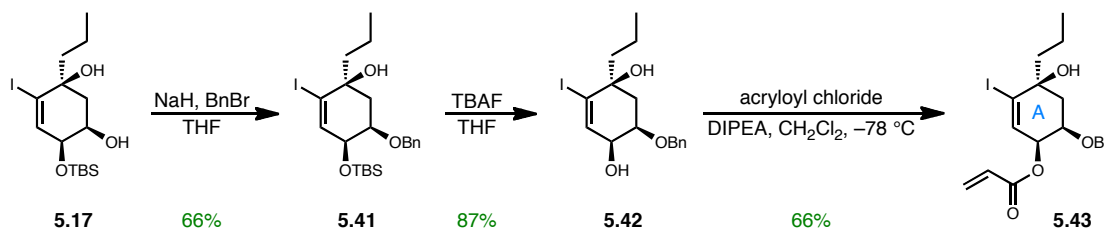
**Scheme 5.14.** Failed southern-tethered IMDA.

Several issues appeared upon the failure of the  $\alpha,\beta$ -unsaturated ester **5.39** IMDA reaction. Reconsidering the reactive rotamer effect described in Scheme 3.24, we

reasoned that an ester-linkage might hinder the necessary orientation for Diels-Alder cycloaddition and sought out other linkers with greater conformational flexibility. Additionally, despite the ultimate necessity of a leaving group on the C-11 secondary alcohol for our proposed triol installation shown in Scheme 5.8, we proposed the incorporation of a more robust orthogonal protecting group that would impart stability toward the necessary high temperatures of an IMDA reaction.

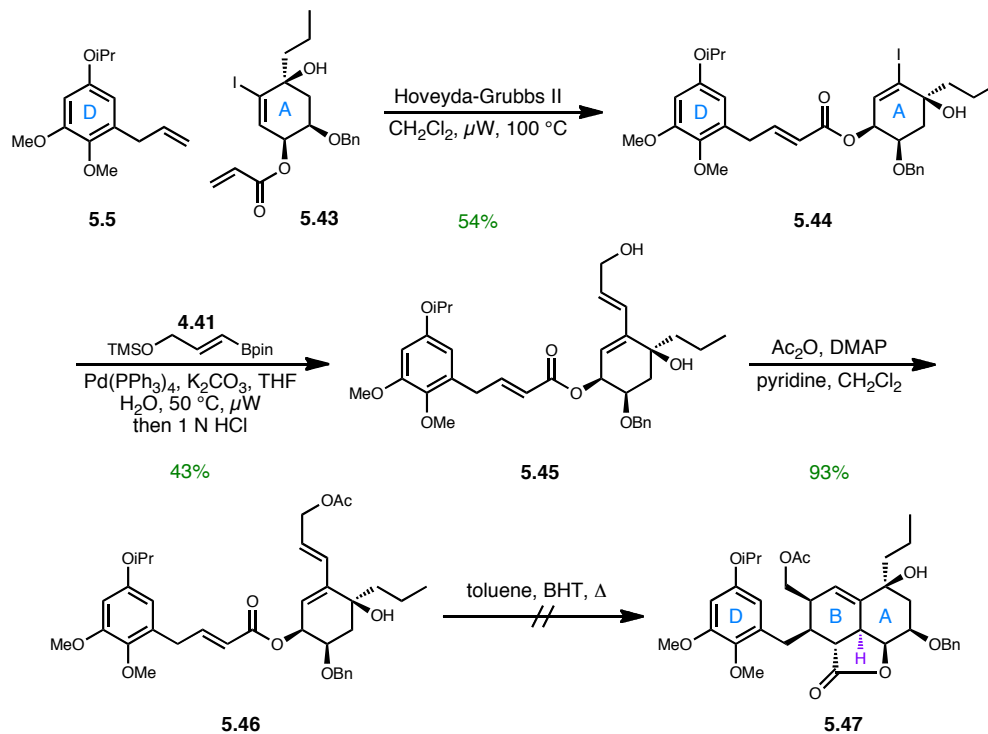
### Third Generation Southern-Tethered IMDA Approach

We first chose to investigate replacement of the mesylate group with a more robust protecting group, and a benzyl ether seemed to suit our needs. We reasoned that we could quickly evaluate an IMDA reaction with the benzyl series utilizing the same sequence previously optimized for the mesylate series. Therefore benzyl protection of the free secondary alcohol intermediate **5.17** was followed by TBAF-mediated desilylation and acrylate ester formation to provide the A-ring cross metathesis partner.



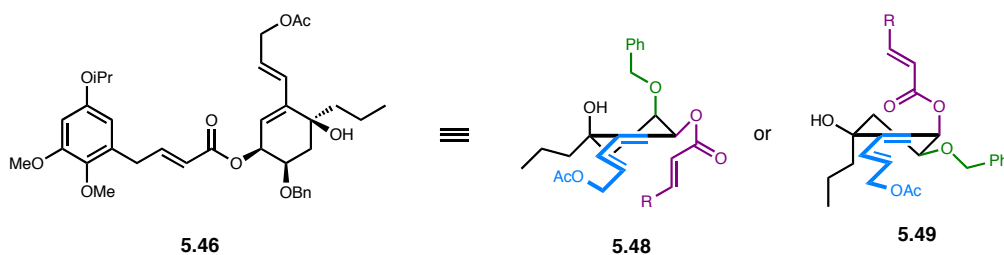
**Scheme 5.15.** Synthesis of the benzyl series acrylate ester.

Following the same route as previously developed, cross metathesis with an excess of the aryl olefin **5.5** provided the southern-tethered ester **5.44**, and the functionalized diene was installed through microwave-mediated Suzuki cross coupling. Finally, acetylation of the primary alcohol capped off our rapid generation of the benzyl series IMDA precursor **5.46**, and we were hopeful that with a more stable substrate an ABD-ring system product was close at hand. Therefore, we systematically heated the triene **5.46** in toluene with catalytic BHT, and we were severely disappointed to observe no conversion to the desired product. In fact, with heating at 200 °C for multiple days, only starting material was isolated.



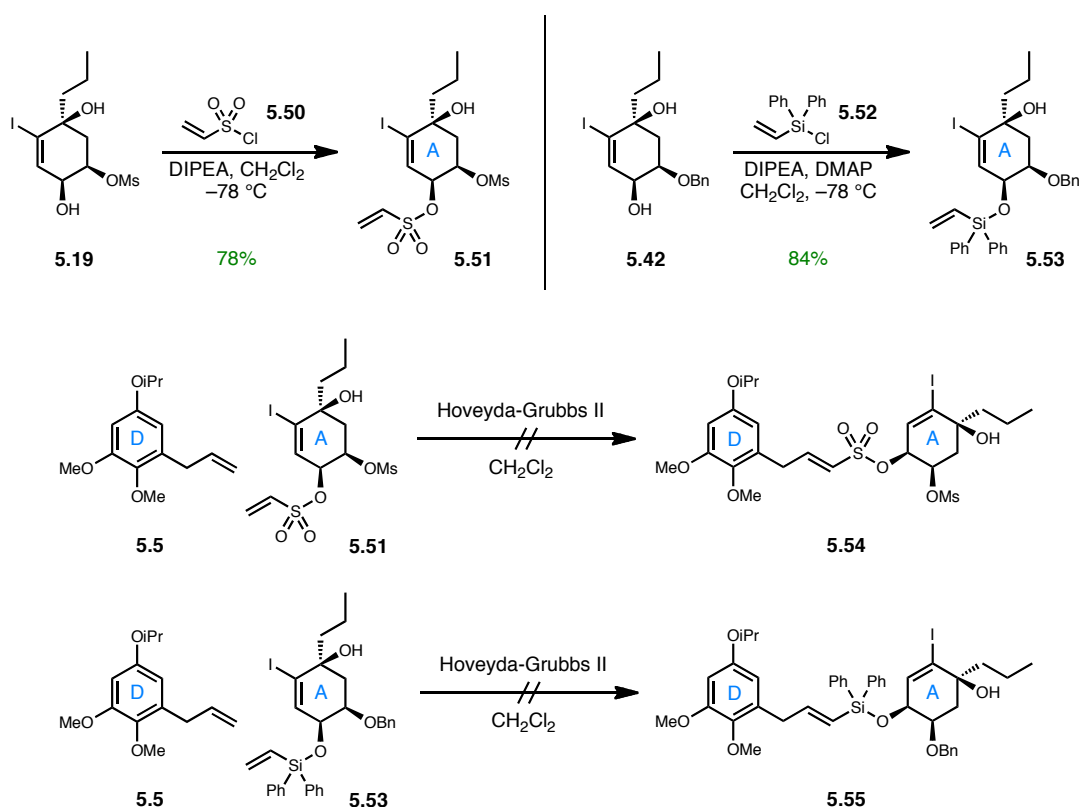
**Scheme 5.16.** Failed IMDA route with the benzyl series.

We were initially perplexed as to the lack of reactivity of the triene **5.46**; however, an analysis of possible conformations led to a reasonable explanation of our observed results. Assuming that the cyclohexene A-ring exists in a twist-boat conformation, three major functionalities compete for equatorial orientations. In conformation **5.48**, the ester dienophile inhabits the desired pseudo-equatorial orientation that appears necessary for orbital overlap in the Diels-Alder transition state and the propyl group also is shown as pseudo-equatorial. However, the adjacent O-benzyl group is then required to exist in a pseudo-axial orientation. Conversely in conformation **5.49**, the O-benzyl group is shown as pseudo-equatorial and the remaining ester and propyl groups occupy pseudo-axial orientations. We reasoned that conformation **5.49** must predominate considering the unreactivity of **5.46** where the ester dienophile points away from the diene. Thus, the large size of the benzyl protecting group apparently imparts a large effect on the solution conformation of the molecule and rendered it unreactive even upon heating at high temperatures. This information points to a situation in which the mesylate group allowed population of the necessary **5.48** orientation but was too unstable to allow cycloaddition with the inferred higher LUMO energy acrylate ester dienophile when compared to the alkynyl dienophile.



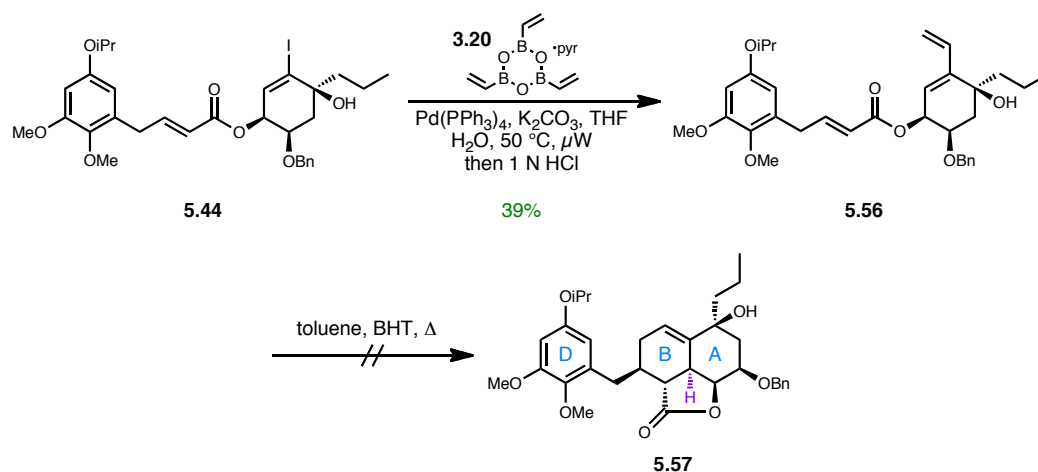
**Scheme 5.17.** Conformational analysis of the benzyl series IMDA substrate.

In light of the undesirable results with the ester dienophile, we pursued other linking elements such as sulfur and silicon which we reasoned could provide greater conformational flexibility as well as simplify their removal following cycloaddition. Therefore, formation of the vinyl sulfonate **5.51** and vinyl siloxane **5.53** proceeded smoothly, and we then attempted cross metathesis with these substrates. Grubbs' model for cross metathesis selectivity implied that both **5.51** and **5.53** should be considered type III olefins that do not undergo homodimerization; however, when applying our standard cross metathesis conditions, we observed no desired product and only homodimerization of the aryl olefin **5.5**.<sup>16</sup> These results were not completely surprising, as only few reports address the cross metathesis of vinyl siloxanes and none to our knowledge exist for the cross metathesis of vinyl sulfonates.<sup>18</sup> Nevertheless, we were disappointed considering both functional groups have been successfully applied in the IMDA framework.<sup>19,20</sup> Finally, we set out to determine whether functionality present on the diene and/or dienophile was partly responsible for the observed lack of reactivity of our synthesized IMDA substrates.



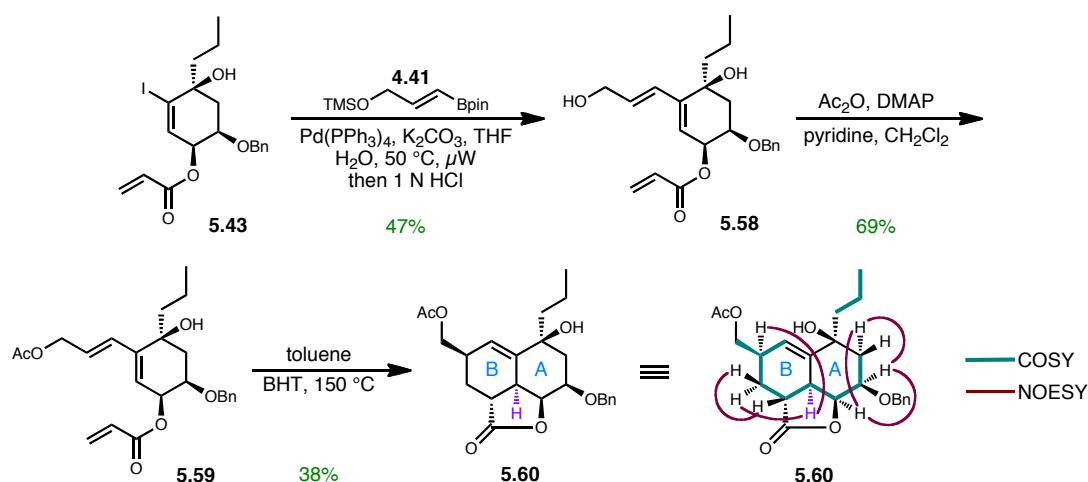
**Scheme 5.18.** Unsuccessful cross metatheses of alternate vinyl A-ring substrates.

Our unsuccessful IMDA reactions prompted a closer look as to causative factors. We reasoned that independently truncating both the diene and dienophile might provide some insight into this issue, and based on our previously synthesized substrates, access to these intermediates required a minimal number of steps. Thus, we first synthesized the diene-truncated IMDA precursor **5.56** by substituting the cyclic vinyl boronate **3.20** into our recently optimized Suzuki cross coupling conditions. Unfortunately, heating **5.56** at temperatures up to 200 °C for multiple days resulted only in isolation of starting material, and we concluded that the substitution off of the diene did not appear to directly affect the cycloaddition.



**Scheme 5.19.** An attempted diene-truncated IMDA.

Truncation of the dienophile required Suzuki cross coupling utilizing the vinyl iodide **5.43** which occurred in modest yield. Acetylation then led to the dienophile-truncated IMDA precursor **5.59** which was heated in toluene with catalytic BHT. Upon heating to  $150^\circ\text{C}$ , we began to observe conversion to a more polar product, and full conversion occurred after heating for 4 days. Isolation of the new product indicated the desired cycloadduct **5.60** with the correct C-9 stereochemistry as would be predicted by a southern-tethered Diels-Alder. With this data, we became more perplexed as to the factors involved in rendering a southern-tethered IMDA substrate reactive within the benzyl series. Clearly our conformational analysis shown in Scheme 5.17 was not the only contributor, and we reasoned that the additional dienophile functionality donated significant electron density causing raising of the dienophile LUMO energy. This logic could begin to account for the lack of reactivity observed with the fully functionalized benzyl series IMDA shown in Scheme 5.16.



**Scheme 5.20.** Successful dienophile-truncated IMDA.

We had thus answered questions regarding the reactivity of a southern-tethered IMDA motif, but we remained unsatisfied as the IMDA product **5.60** did not immediately provide a reasonable route to the proposed tetracycle **4.12**. However, we had learned much from the developed reactions for synthesis of the southern-tethered series, and we began to re-envision potential within the TADA mode that we hoped would overcome issues with Diels-Alder reactivity.

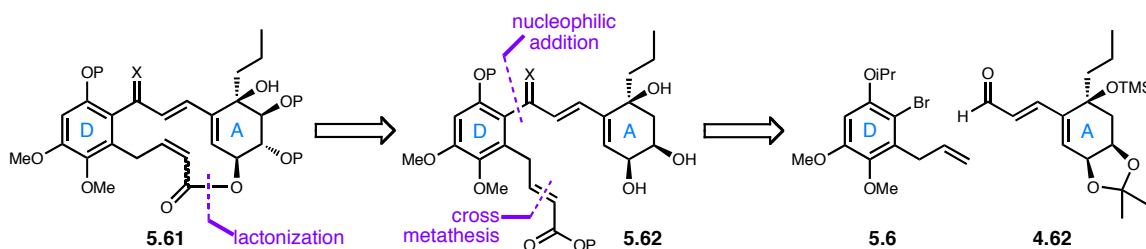
### Revisiting Synthesis of a TADA Substrate

Despite our failures with an IMDA approach, we had added an extensive array of knowledge and reactions to our toolbox, and this experience allowed a fresh viewpoint for our original TADA strategy. First, we remained concerned regarding Diels-Alder reactivity, and we believed that formation of a macrocyclic precursor could lower the transition state energy based on a Diels-Alder proximity effect.<sup>21</sup> Next, our work toward



previous TADA substrates never allowed formation of an  $\alpha,\beta$ -unsaturated acid for southern tethering; however, we had since developed conditions for cross metathesis with an aryl olefin that we were confident could deliver a desirable substrate for southern tethering. Finally, our past experience with the TADA substrates had provided a highly reliable method for northern tether formation on large scale. Therefore, we sought to combine our most successful methods toward a greatly improved route to a macrocyclic TADA precursor.

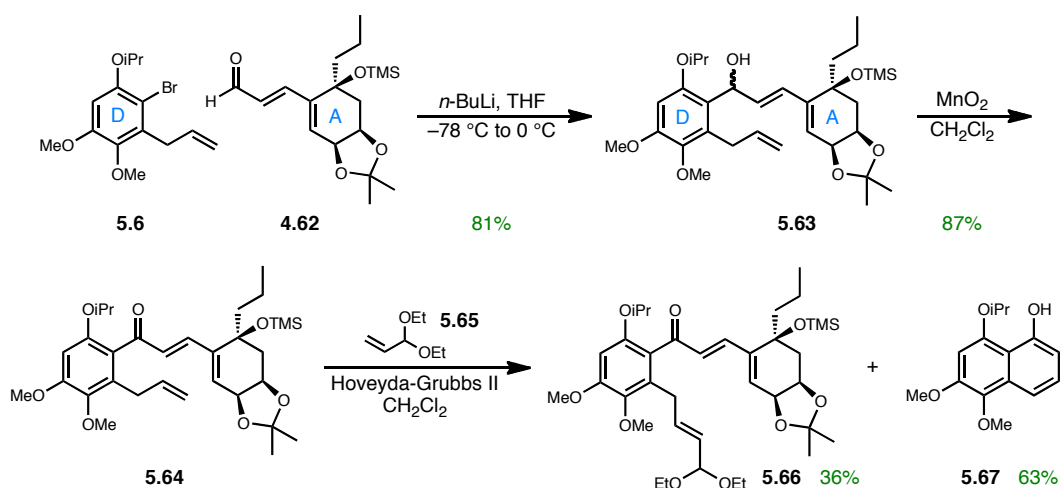
Considering this information, our newly proposed synthetic strategy involved ultimate synthesis of the macrocycle **5.61**. We proposed ring closure through a macrolactonization of a requisite acid triol such as **5.62**. We planned to arrive at the acid functionality through cross metathesis with a suitably protected acrylate ester reagent, and the northern tether would be formed through our well-established nucleophilic addition of the aryl lithiate of **5.6** with aldehyde **4.62**.



**Scheme 5.21.** An improved TADA synthetic analysis.

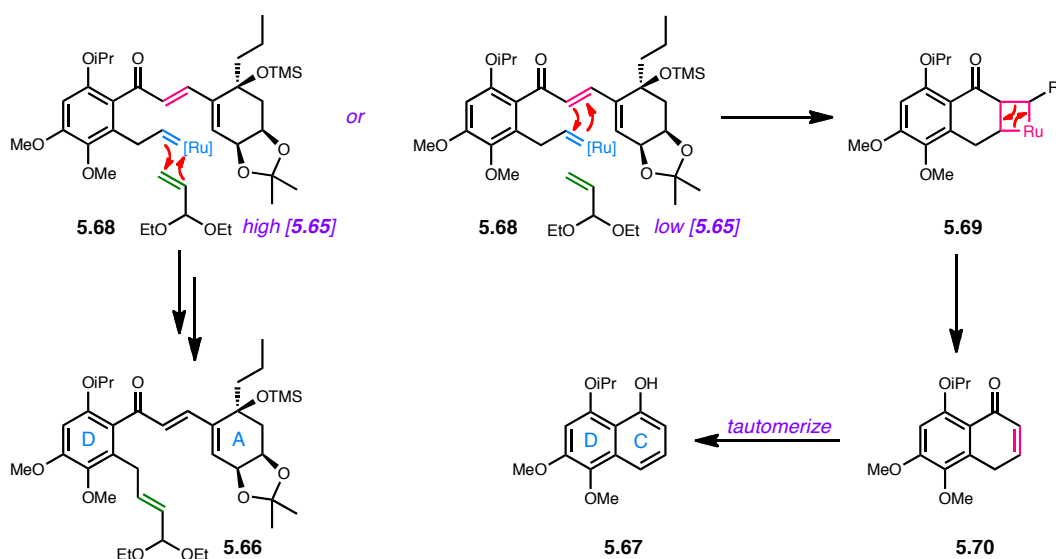
Brimming with confidence, we performed our tried and true northern tethering between the aryl bromide **5.6** and aldehyde **4.62** which provided the allylic alcohol **5.63** in excellent yield on large scale. Keeping in mind our previous issues with unwanted

cycloadditions, we then deactivated the diene by MnO<sub>2</sub>-mediated oxidation while effectively converging two diastereomers to arrive at the ketone **5.64**. With this substrate, we believed that cross metathesis would provide a functionalized olefin to be utilized in macrolactonization. Thus, we first chose acrolein diethyl acetal as our cross metathesis partner for numerous reasons. Based on our previous studies with base-mediated hydrolysis of  $\alpha,\beta$ -unsaturated methyl esters as shown in Scheme 5.12, we reasoned that incorporation of functionality at a lower oxidation state than necessary would avoid potential olefin isomerization. Additionally, we sought an acid-labile protected form of acrolein that, upon treatment with acid, would effect not only deprotection of the aldehyde functionality but also the acetonide moiety. Thus, acrolein diethyl acetal fit these parameters, and we applied it in a cross metathesis reaction with the terminal olefin substrate **5.64**. While we did isolate desired product **5.66**, we were disappointed by its mass recovery, and we quickly determined that the remaining mass balance existed in the formation of the naphthalene product **5.67**. While ultimately this undesired reaction pathway was not completely surprising, it did complicate our efforts at arriving at an acid triol substrate for macrolactonization.



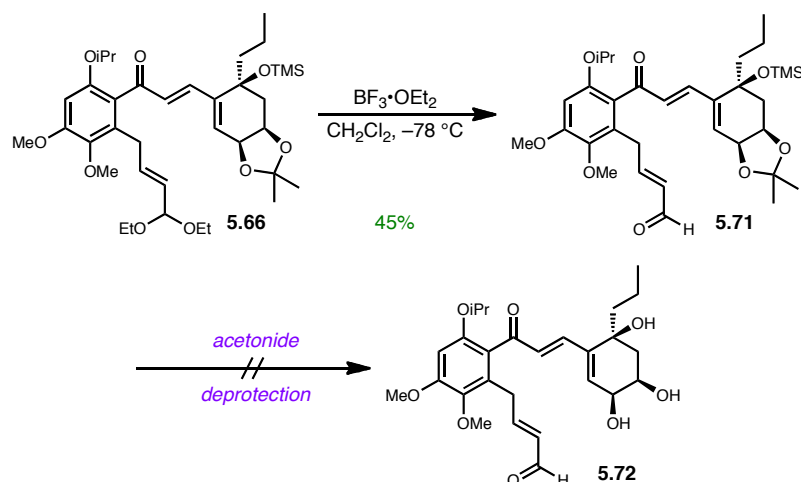
**Scheme 5.22.** Northern tethering and first generation cross metathesis.

Formation of the CD-naphthalene **5.67** is generated from the same ruthenium intermediate **5.68** that leads to the desired product **5.66**. The two pathways diverge through the differences between cross metathesis and ring closing metathesis, where cross metathesis leads to **5.66** while RCM with the enone olefin leads to the naphthalene product **5.67**. This understanding highlighted the concentration dependence of product formation where low concentration of the cross metathesis partner should favor the intramolecular RCM reaction (leading to **5.67**) over the intermolecular reaction (leading to **5.66**). However, increasing the concentration of the cross metathesis partner could improve the ratio of formed products by improving the rate of intermolecular reaction as compared to the rate of intramolecular RCM.



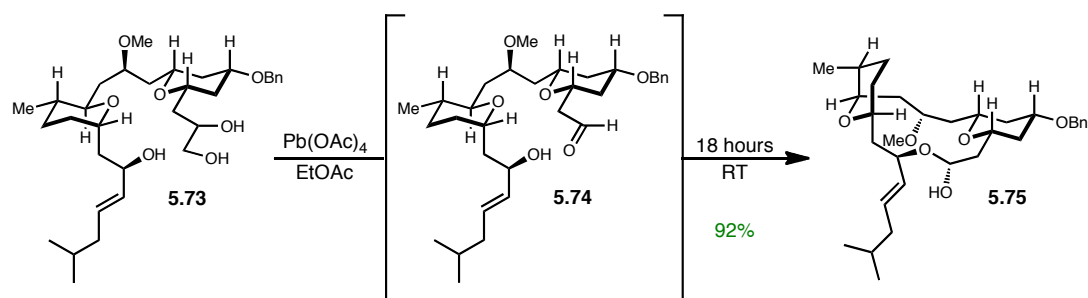
**Scheme 5.23.** Diverging metathesis pathways.

We forged ahead with the desired diethyl acetal **5.66** hoping to effect selective deprotection of both the acetonide and diethyl acetal groups. Our most successful conditions for these transformations involved removal of the diethyl acetal moiety with  $\text{BF}_3 \cdot \text{OEt}_2$  at low temperature to provide the  $\alpha,\beta$ -unsaturated aldehyde **5.71**. Unfortunately, all attempts at subsequent acetonide removal failed likely due to the instability of the aldehyde group under the acidic reaction conditions necessary.



**Scheme 5.24.** Unsuccessful deprotection to an aldehyde triol intermediate.

We had targeted the aldehyde triol **5.72** partly due to precedent set by Kozmin and co-workers in their synthesis of leucascandrolide A where a spontaneous macrolactolization reaction led to the desired macrocycle **5.75**.<sup>22</sup> As shown in Scheme 5.25, the triol **5.73** was treated with  $\text{Pb}(\text{OAc})_4$  to effect oxidative cleavage to the intermediate aldehyde **5.74** which slowly cyclized to the lactol **5.75** in high yield. Similarly, we hoped that the aldehyde triol **5.72** might spontaneously cyclize, but much higher macrocyclic strain in our system likely would preclude this type of lactol formation.

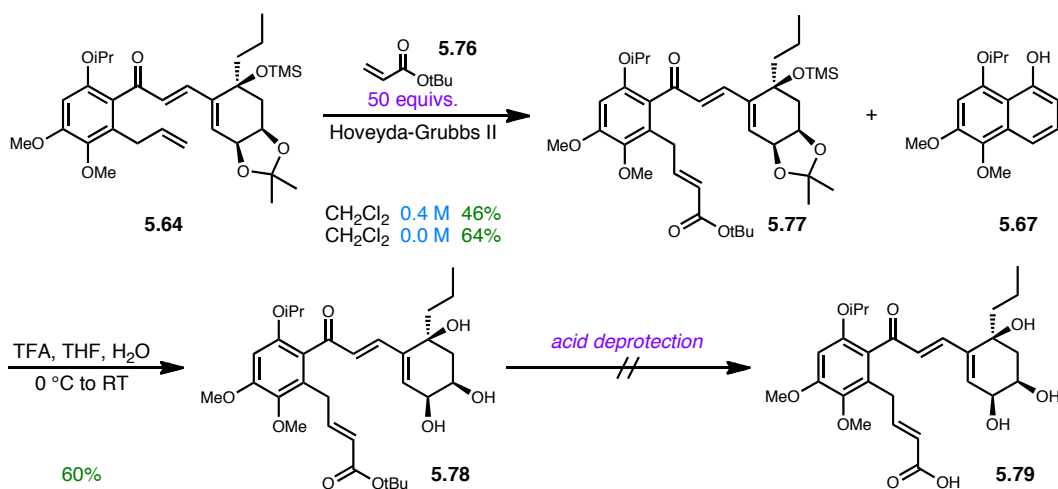


**Scheme 5.25.** Kozmin's spontaneous macrolactolization.

Instead of continuing with acrolein diethyl acetal cross metathesis, we elected to pursue a different cross metathesis partner that we hoped would simplify the two necessary deprotection steps. We still planned to avoid hydrolysis of an ester to arrive at the targeted acid triol for macrolactonization, and thus we realized that an acid-labile carboxylic acid protecting group could lead to a one-pot protocol for unmasking. Therefore, we chose *tert*-butyl acrylate (**5.76**) as our new cross metathesis partner while cognizant of the necessary concentration to favor cross metathesis over RCM (Scheme 5.23).

We first probed cross metathesis between terminal olefin **5.64** and 50 equivalents of *tert*-butyl acrylate (**5.76**), and we first began by employing  $\text{CH}_2\text{Cl}_2$  as solvent at high concentrations. On small scale, reaching concentrations higher than 0.4 M proved difficult, and we isolated desired *t*-butyl ester **5.77** in 46% yield with the remainder of the mass balance being an inseparable mixture of starting material and naphthalene **5.67**. However, we were pleased to observe improved yield when we utilized the same number of molar equivalents of *tert*-butyl acrylate (**5.76**) as the reaction solvent, we isolated **5.77** in 64% yield.. These results confirmed the schematic shown in Scheme 5.23 in which the

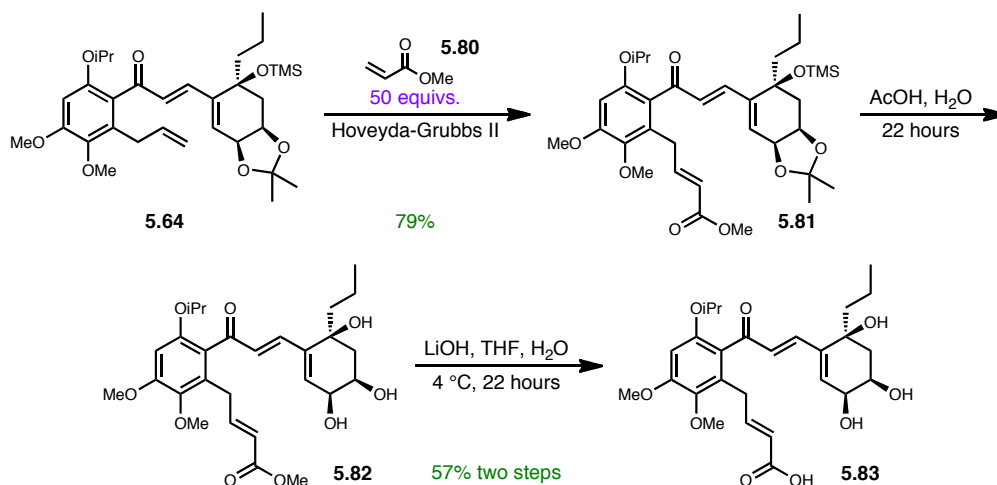
intermolecular pathway predominates under a high concentration of cross metathesis partner. From the desired product **5.77** we moved to find acidic conditions that would effect ester and acetonide deprotection. Disappointingly, our best conditions only formed the triol **5.78**, and all attempts at removing the *t*-butyl ester failed to provide the desired product.



**Scheme 5.26.** *Tert*-butyl acrylate cross metathesis and attempted deprotection.

At this point, we appeared to have limited remaining options, and our aversion to a methyl acrylate cross metathesis began to seem unfounded considering issues inherent in other ester functionalities. We reasoned that we could optimize conditions to limit olefin isomerization observed in Scheme 5.12, and ultimately the requisite cross metathesis provided the methyl ester **5.81** in pleasing yield. And finally, after extensive optimization, we arrived at the desired acid triol **5.83** through a two-step sequence involving acetonide removal and ester hydrolysis with lithium hydroxide. These conditions were the only ones that reliably produced the desired product, while others led

to varying levels of decomposition. Additionally, much of the remaining mass balance from the hydrolysis step went to olefin isomerization but was easily separable by flash column chromatography.



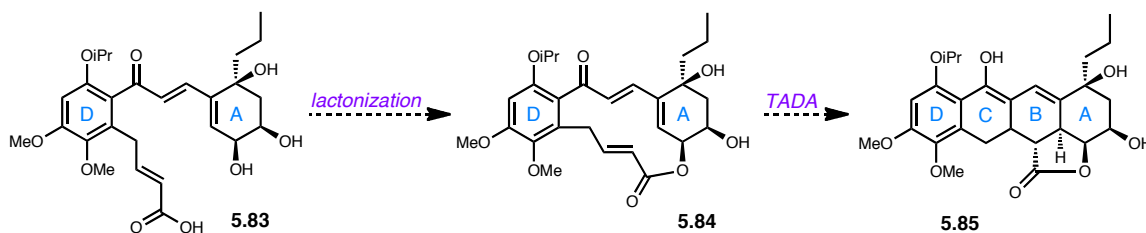
**Scheme 5.27.** Synthesis of a macrolactonization precursor.

Synthesis of the acid triol **5.83** marks the pinnacle of our studies thus far, and our current efforts involve screening macrolactonization conditions for a regioselective ring closure. Macrocyclization and subsequent transannular Diels-Alder would open a wide door toward our ultimate goal of synthesizing a tetracyclic monomer **4.12** for dimerization and elaboration to HMP-Y1 (**1.94**) and hibarimicinone (**1.96**). Our ongoing studies have continually stood on the shoulders of previous routes, and the synthetic sequence involved in arriving at **5.83** combines our most successful methods identified to date.



## Future Directions

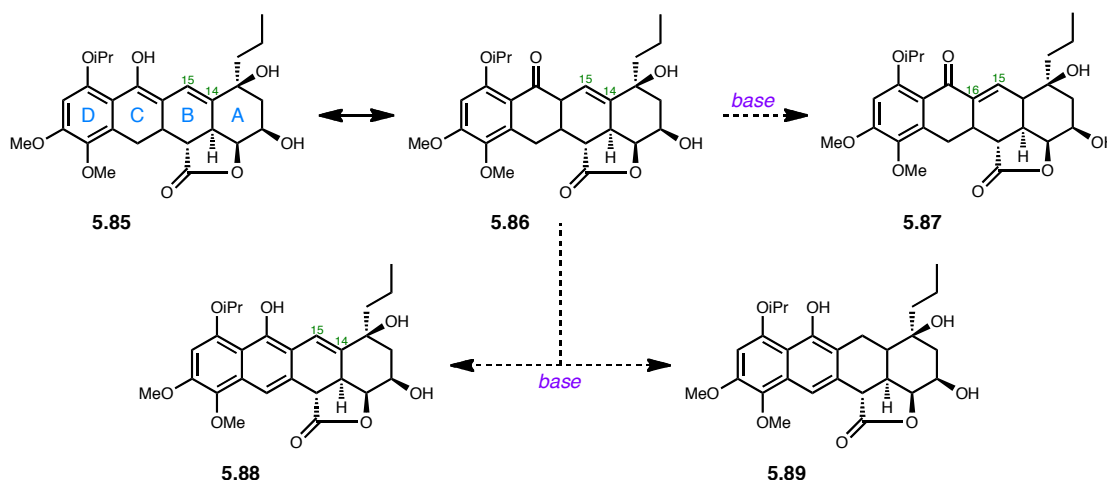
Our synthetic studies have encompassed a significant range of approaches that have all culminated in the proposed macrolactonization of acid triol **5.83** and subsequent transannular Diels-Alder. This strategy relies upon knowledge that a southern-tethered Diels-Alder reaction is necessary for correct C-9 stereocenter formation and hopes to take advantage of a proximity effect in the macrocycle for promotion of the cycloaddition. Thus, upon identification of appropriate lactonization conditions, of which we plan to investigate Yamaguchi and other well-established protocols, we hope to observe formation of the ABCD tetracycle **5.85** upon controlled heating.



**Scheme 5.28.** Remaining steps to the ABCD tetracycle.

Numerous options remain beyond this point, and although we propose one specific route, much experimentation will be necessary to determine the optimal order of operations for the major transformations remaining. One primary concern once arriving at the TADA product **5.85** is its stability under basic conditions. While the C-ring ketone is likely to exist in a conjugated enol form **5.85**, several base-promoted pathways can be imagined from the keto-tautomer **5.86**. Our biggest concern involves retaining the

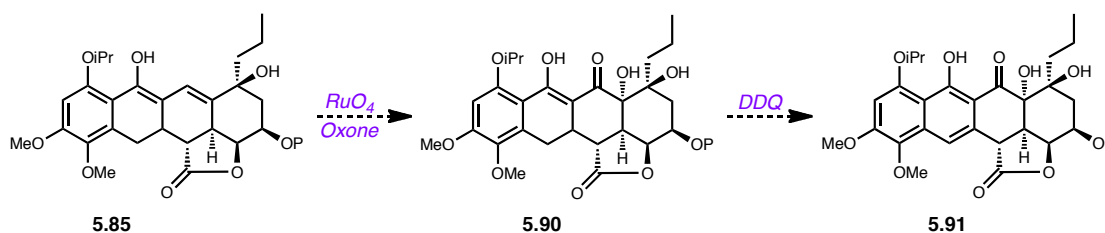
C14/C15 olefin regiochemistry as the necessary  $\alpha$ -hydroxyketone functionality will arise from the requisite olefin. Nevertheless, the enone **5.86** could be imagined to derive from isomerization into conjugation with the ketone at C-16. Additionally, if a double olefin transposition were to occur, the phenol **5.89** which is saturated at the C14/C15 carbons, could arise from tautomerization as observed in Scheme 5.26. These two possible products would ultimately thwart attempts to install the hydroxyketone functionality; however, aromatization without olefin isomerization to provide phenol **5.88** could be highly desirable.



**Scheme 5.29.** Possible base-promoted pathways for TADA product **5.85**.

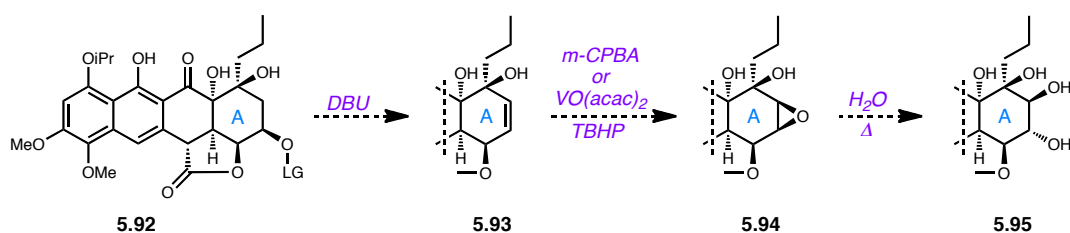
Despite these alternate pathways, we continue to operate on the presumed stability of TADA product **5.85** to ketohydroxylation conditions. Thus we plan to arrive at the hydroxyketone **5.90** as the first transformation of the newly formed tetracycle **5.85** so as to avoid issues regarding olefin isomerization. However, protection of the remaining secondary alcohol will be required, possibly prior to TADA cyclization, to avoid

unwanted oxidation. This juncture may prove to be the correct time to install the necessary leaving group in preparation for the sequence proposed in Scheme 5.8. Next on our list is C-ring oxidation to the requisite phenol. Prior work in our laboratory has demonstrated the feasibility of this transformation, and phenol **5.91** will constitute synthesis of the isopropyl-protected CD ring system.<sup>1</sup>



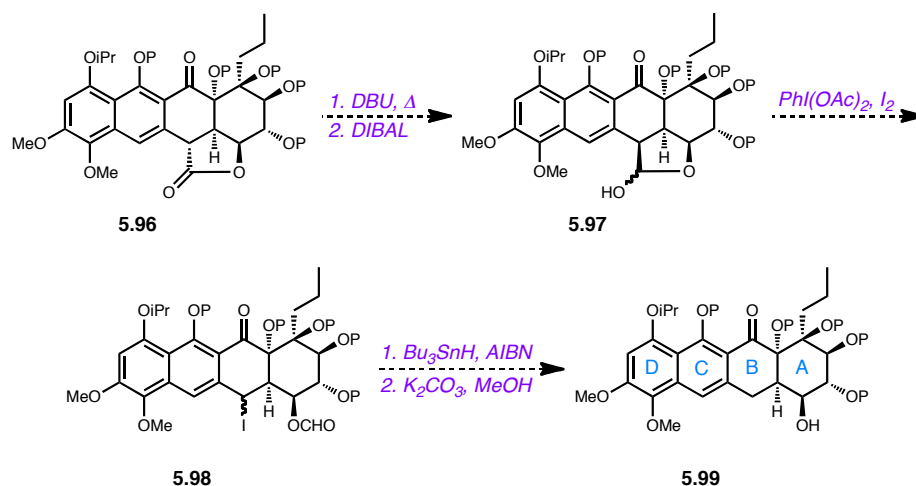
**Scheme 5.30.** Proposed B- and C-ring oxidation sequence.

Two major transformations will then remain, and as previously detailed in Scheme 5.8, we have proposed a three-step sequence for the first purpose. With a proper leaving group in place, elimination to the olefin **5.93** can be followed by hydroxyl-directed epoxidation. Water-promoted epoxide opening of **5.94** will finally install the final oxygen functionality, and the regioselectivity of epoxide opening can be predicted to occur at the less hindered site to provide **5.95**.



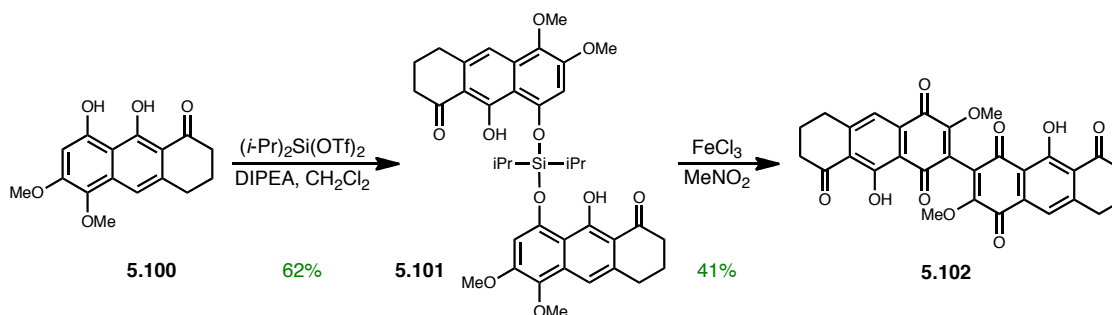
**Scheme 5.31.** Proposed installation of the A-ring *trans-trans* triol system.

Completion of the tetracyclic monomer synthesis will finally require removal of the tethering carbon utilized for TADA stereoselectivity. Mootoo and co-workers have previously addressed the issue with a highly similar AB-ring system substrate, and their approach appears to be well-suited for our needs.<sup>23</sup> Therefore, as noted in their publication, isomerization of the lactone conformation was necessary. Formation of the lactol **5.97** appears to be a tenuous step considering the presence of the C-15 ketone functionality, and if necessary, we could alter the order of operations to reflect this complication. The lactol can then be reacted with phenyliodonium diacetate to effect radical-mediated C-C bond cleavage and trapping with iodine, and the iodo-functionality **5.98** can be removed under alternate radical conditions. Finally, removal of the formate functionality should provide a fully functionalized and protected tetracyclic monomer **5.99**.



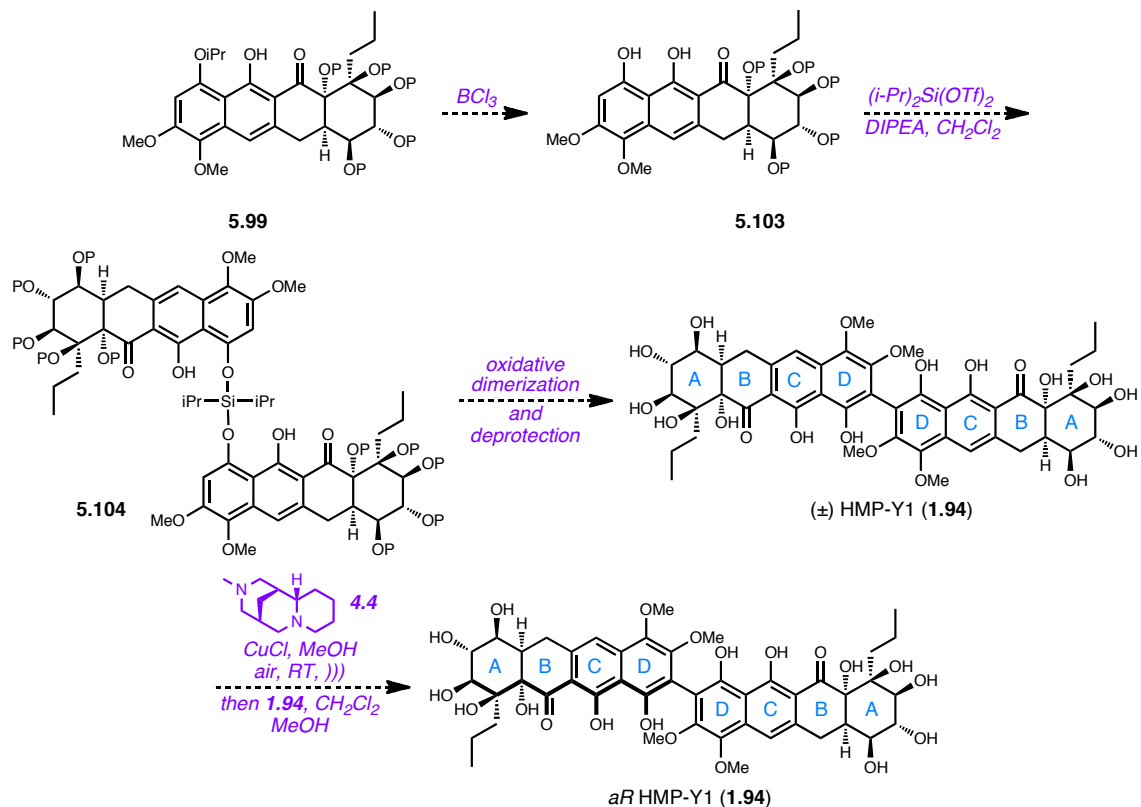
**Scheme 5.32.** Completion of the protected tetracyclic monomer **5.99**.

Fortunately, work in our laboratory has demonstrated the potential for oxidative dimerization. With the model system **5.100**, which possesses two sites of potential dimerization as well as hetero-coupling, we subverted these undesired pathways by use of a silyl linker which efficiently formed the desired symmetrical silyl-linked bi-phenol **5.101**. And although over-oxidation to the biquinone **5.102** was observed, we remain optimistic that careful optimization can lead to the dimerized bis-phenol.



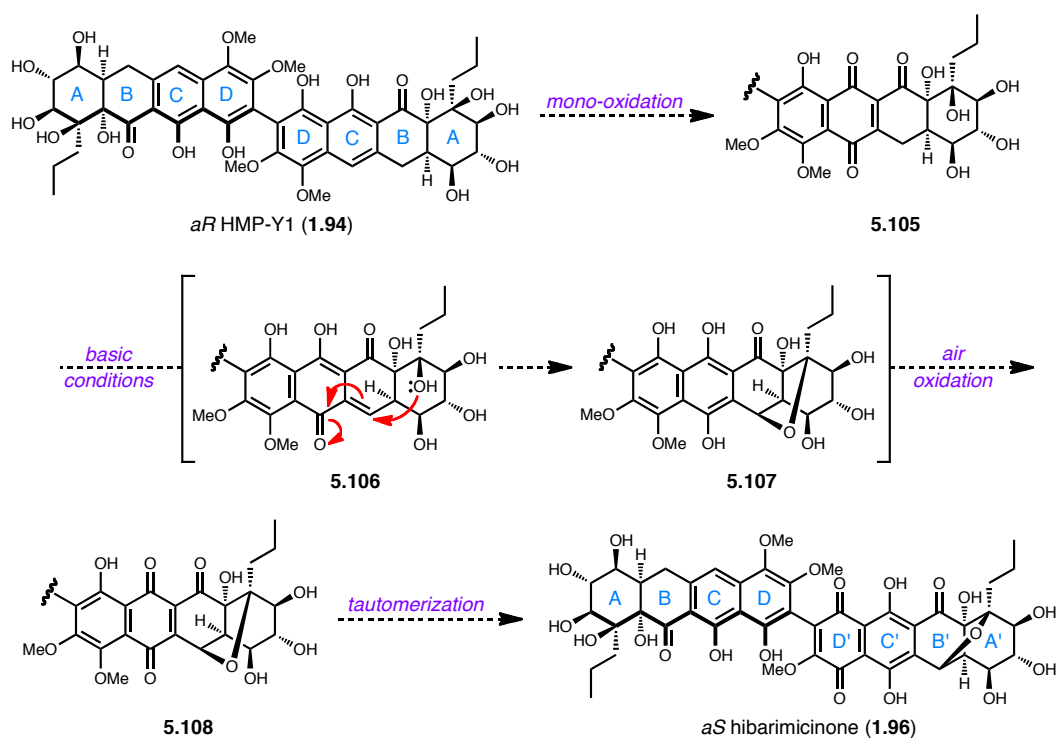
**Scheme 5.33.** Romaine's preliminary work toward oxidative dimerization.

For the purposes of oxidative dimerization, we will need to unmask the isopropyl-protected phenol at C-1 which we proposed upon its installation that mild Lewis-acidic conditions should impart selectivity for the isopropyl ether over the two other methyl ethers. In analogy to the oxidative dimerization model study shown in Scheme 5.33, the free phenolic tetracycle **5.103** contains two locations for possible oxidative dimerization which we intend to direct through formation of a bridged silaketal **5.104**. Careful determination of oxidation conditions should provide the protected racemic HMP-Y1 (**1.94**), which upon deprotection and deracemization with O'Brien's diamine will finally arrive at the biosynthetic intermediate *aR* HMP-Y1 (**1.94**).



**Scheme 5.34.** Endgame strategy for completion of *aR* HMP-Y1.

All that will remain once we have successfully employed our biomimetic route to *aR* HMP-Y1 will be conversion to hibarimicinone. Mono-oxidation of the  $C_2$ -symmetric HMP-Y1 to the quinone **5.105** will set up for a key transformation. From the beginning of our synthetic studies, we have proposed a transformative Michael addition of the C-13' tertiary alcohol into a proximate quinone methide intermediate **5.106** to form the bridging furan moiety found in hibarimicinone. We believe that the resulting intermediate hydroquinone **5.107** will undergo air oxidation to the quinone **5.108**, and upon tautomerization will provide our final target, *aS* hibarimicinone (**1.96**).



**Scheme 5.35.** Proposed completion of hibarimicinone.

## Conclusion

An IMDA approach to the proposed tetracyclic monomer was evaluated within alkyne and alkene dienophile motifs and both ultimately failed due to a low-yielding esterification step and unforeseen complications in the Diels-Alder cyclization respectively. The lessons learned in these forays were relayed into an improved approach to a TADA precursor, and we currently stand tantalizingly close to the crux of our efforts. Only two steps stand in front of formation of one of the most important intermediates originally proposed toward our total syntheses.

Overall, extensive investigations into the total synthesis of HMP-Y1 and hibarimicinone have been detailed in the preceding chapters which have encompassed both two-directional and dimerization strategies. Additionally, attempted synthesis of a tetracyclic monomer has involved evaluation of both TADA and IMDA routes, and generally, the Diels-Alder reaction has played an integral part in these studies. Despite two recent syntheses of hibarimicinone, we continue to believe that our biomimetic dimerization approach constitutes a novel and superior strategy toward these complicated natural products. Ultimately, only time will serve as the judge of these questions, and we remain confident that our efforts will not have been in vain.

## Experimental Methods

**General Procedure.** All non-aqueous reactions were performed under an argon atmosphere in flame-dried glassware. Stainless steel syringes or cannula were used to



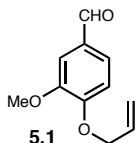
transfer air- and moisture-sensitive liquids. Reaction temperatures were controlled using a thermocouple thermometer and analog hotplate stirrer. Reactions were conducted at room temperature (RT, approximately 23 °C) unless otherwise noted. Analytical thin-layer chromatography was performed on E. Merck pre-coated silica gel 60 F254 plates and visualized using UV, ceric ammonium molybdate (CAM) and potassium permanganate (KMnO<sub>4</sub>) stains. Flash column chromatography was conducted as described by Still *et. al.* using indicated solvents and Dynamic Adsorbents silica gel 60 (230-240 mesh).<sup>24</sup> Where necessary, silica gel was neutralized by treatment of the silica gel prior to chromatography with the eluent containing 1% triethylamine (Et<sub>3</sub>N). Where necessary, silica gel was treated prior to chromatography with the eluent containing 1% glacial acetic acid (AcOH). Yields were reported as isolated, spectroscopically pure compounds.

**Materials.** Reagents were purchased at the highest commercial quality and used without further purification unless otherwise stated. When necessary, intermediates were dried by azeotropic removal of water by evaporation from benzene (three iterations) and further dried on high-vacuum for the indicated amount of time. Toluene and dichloromethane (CH<sub>2</sub>Cl<sub>2</sub>) were obtained by passing commercially available solvents through activated alumina columns (MBraun MB-SPS solvent system). Tetrahydrofuran (THF) was purified by distillation from sodium metal with benzophenone indicator, and when necessary, was further dried over activated 4 Å molecular sieves under an atmosphere of argon. Triethylamine (Et<sub>3</sub>N) was distilled from calcium hydride and stored over sodium

hydroxide. The molarity of commercial *n*-butyllithium solutions was determined by titration using diphenylacetic acid as an indicator (average of three determinations).

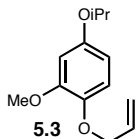
**Instrumentation.** Optical rotations were obtained using a Perkin Elmer 341 polarimeter and zeroed with the pure solvent, spectrophotometric-grade chloroform.  $^1\text{H}$  NMR spectra were recorded on Bruker 300, 400, 500, or 600 MHz spectrometers and are reported relative to deuterated solvent signals ( $\text{CDCl}_3$ : 7.26;  $\text{C}_6\text{D}_6$ : 7.16). Data for  $^1\text{H}$  NMR spectra are reported as follows: chemical shift ( $\delta$  ppm), multiplicity (s = singlet, d = doublet, t = triplet, q = quartet, p = pentet, sept. = septet, m = multiplet, br = broad, app = apparent), coupling constants (Hz), and integration.  $^{13}\text{C}$  NMR spectra were recorded at 100, 125, or 150 MHz and are reported relative to deuterated solvent signals ( $\text{CDCl}_3$ : 77.0;  $\text{C}_6\text{D}_6$ : 128.1). Infrared spectra were obtained as thin films on NaCl plates using a Thermo Electron IR100 series instrument and are reported in terms of frequency of absorption ( $\text{cm}^{-1}$ ). High-resolution mass spectra were obtained from the Department of Chemistry and Biochemistry, University of Notre Dame using either a JEOL AX505HA or JEOL LMS-GCmate mass spectrometer.

### Preparative Procedures



To a solution of vanillin (**3.4**, 10.0 g, 65.7 mmol, 1.0 eq) in DMF (33 mL) was added  $\text{K}_2\text{CO}_3$  (22.7 g, 164 mmol, 2.5 eq) then allyl bromide (11.4 mL, 131 mmol, 2.0 eq) and the thick slurry was stirred at RT for 22 h. The reaction was diluted with  $\text{H}_2\text{O}$  (100 mL) and extracted with  $\text{CH}_2\text{Cl}_2$  (3 x 100 mL). The combined

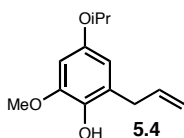
organic layers were washed with H<sub>2</sub>O (4 x 100 mL), dried (MgSO<sub>4</sub>), filtered, and concentrated. Purification by flash column chromatography (10-40% EtOAc/hexanes) provided **5.1** as a yellow oil (12.5 g, 64.8 mmol, 99%). Spectral data were consistent with reported literature values.



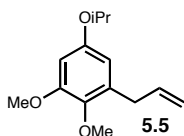
To a mixture of boric acid (19.7 g, 318 mmol, 5.0 eq) in THF (182 mL) was added H<sub>2</sub>O<sub>2</sub> (30% in H<sub>2</sub>O, 21.2 mL) then concentrated H<sub>2</sub>SO<sub>4</sub> (9.23 mL) and the mixture was stirred at RT for 30 min. A solution of **5.1** (12.2 g, 63.7 mmol, 1.0 eq) in THF (64 mL) was added via dropping funnel over 15 min, and the reaction was stirred at RT for 5 h. The orange reaction mixture was filtered through a Büchner funnel with EtOAc washes, and the filtrate was neutralized with saturated aqueous NaHCO<sub>3</sub> (4 x 100 mL) which caused vigorous bubbling and the aqueous layers turned red. The combined aqueous layers were extracted with EtOAc (3 x 100 mL), and the combined organic layers were washed with brine (1 x 100 mL), dried (MgSO<sub>4</sub>), filtered, and concentrated to provide **5.2** as a thick, dark brown oil that was immediately taken forward crude.

To a solution of crude **5.2** (11.5 g, 63.7 mmol, 1.0 eq) in acetone (64 mL) was added K<sub>2</sub>CO<sub>3</sub> (17.6 g, 127 mmol, 2.0 eq) then TBAI (1.18 mg, 3.18 mmol, 0.05 eq). To the mixture was added isopropyl bromide (20.9 mL, 223 mmol, 3.5 eq) and the reaction was heated at reflux for 24 h. At RT, the reaction was concentrated, diluted with H<sub>2</sub>O (100 mL) and extracted with CH<sub>2</sub>Cl<sub>2</sub> (4 x 100 mL). The combined organic layers were dried (MgSO<sub>4</sub>), filtered, and concentrated. Purification by flash column chromatography (10-40% EtOAc/hexanes) yielded **5.3** as a yellow oil (7.39 g, 33.3 mmol, 52% two steps). <sup>1</sup>H

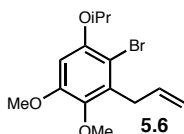
NMR (400 MHz, CDCl<sub>3</sub>):  $\delta$  6.79 (d,  $J$  = 8.7 Hz, 1H), 6.50 (d,  $J$  = 2.7 Hz, 1H), 6.37 (dd,  $J$  = 8.7, 2.7 Hz, 1H), 6.07 (dddd,  $J$  = 16.1, 10.8, 5.5, 5.5 Hz, 1H), 5.37 (dd,  $J$  = 17.3, 1.3 Hz, 1H), 5.25 (dd,  $J$  = 10.5, 0.8 Hz, 1H), 4.54 (d,  $J$  = 5.5 Hz, 2H), 4.45 (sept.,  $J$  = 6.1 Hz, 1H), 3.84 (s, 3H), 1.32 (s, 3H), 1.31 (s, 3H); <sup>13</sup>C NMR (100 MHz, CDCl<sub>3</sub>):  $\delta$  152.7, 150.6, 142.2, 133.8, 117.7, 114.8, 105.8, 102.5, 70.8, 70.5, 55.8, 22.1; IR (film)  $\nu_{\text{max}}$  2976, 2934, 1596, 1264 cm<sup>-1</sup>; HRMS (ESI)  $m/z$  calcd. for C<sub>13</sub>H<sub>19</sub>O<sub>3</sub> [M+H]<sup>+</sup> 223.1329, found 223.1339.



To three 5 mL microwave vials was added **5.3** (7.39 g, 33.3 mmol, 1.0 eq) and the vials were capped and heated via microwave irradiation at 200 °C for 2 h each. The material had turned red/orange, and the vials were combined and concentrated. Product (**5.4**) was taken forward crude, except for characterization purposes, in which purification by flash column chromatography (5-15% EtOAc/hexanes) yielded **5.4** as a light yellow oil. <sup>1</sup>H NMR (400 MHz, CDCl<sub>3</sub>):  $\delta$  6.37 (d,  $J$  = 2.7 Hz, 1H), 6.30 (d,  $J$  = 2.6 Hz, 1H), 5.98 (dddd,  $J$  = 17.0, 10.2, 6.6, 6.6 Hz, 1H), 5.28 (s, 1H), 5.12-5.02 (m, 2H), 4.41 (sept.,  $J$  = 6.1 Hz, 1H), 3.84 (s, 3H), 3.38 (br. s, 1H), 3.37 (br. s, 1H), 1.30 (s, 3H), 1.29 (s, 3H); <sup>13</sup>C NMR (100 MHz, CDCl<sub>3</sub>):  $\delta$  150.8, 146.7, 137.4, 136.5, 125.6, 115.4, 108.6, 99.4, 70.7, 55.9, 33.9, 22.0; IR (film)  $\nu_{\text{max}}$  3534, 3077, 2976, 2935, 1610, 1495, 1225 cm<sup>-1</sup>; HRMS (ESI)  $m/z$  calcd. for C<sub>13</sub>H<sub>19</sub>O<sub>3</sub> [M+H]<sup>+</sup> 223.1329, found 223.1343.

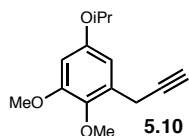


To a solution of **5.4** (7.45 g, 33.5 mmol, 1.0 eq) in DMF (52 mL) was added methyl iodide (6.26 mL, 101 mmol, 3.0 eq) then K<sub>2</sub>CO<sub>3</sub> (13.9 g, 101 mmol, 3.0 eq) and the reaction was stirred at RT for 22 h. The thick orange slurry was diluted with H<sub>2</sub>O (100 mL) and extracted with CH<sub>2</sub>Cl<sub>2</sub> (3 x 100 mL). The combined organic layers were washed with H<sub>2</sub>O (5 x 100 mL), dried (MgSO<sub>4</sub>), filtered, and concentrated. Purification by flash column chromatography (5-10% EtOAc/hexanes) provided **5.5** as a yellow oil (6.45 g, 27.3 mmol, 81% two steps). <sup>1</sup>H NMR (400 MHz, CDCl<sub>3</sub>): δ 6.36 (d, *J* = 2.8 Hz, 1H), 6.28 (d, *J* = 2.8 Hz, 1H), 5.96 (dddd, *J* = 16.9, 10.2, 6.6, 5.6 Hz, 1H), 5.08 (dd, *J* = 11.5, 1.6 Hz, 1H), 5.04 (dd, *J* = 4.1, 1.6 Hz, 1H), 4.47 (sept., *J* = 6.1 Hz, 1H), 3.82 (s, 3H), 3.75 (s, 3H), 3.38 (d, *J* = 6.5 Hz, 2H), 1.32 (s, 3H), 1.31 (s, 3H); <sup>13</sup>C NMR (100 MHz, CDCl<sub>3</sub>): δ 154.1, 153.3, 140.8, 137.2, 133.9, 115.6, 107.3, 100.0, 70.1, 60.8, 55.6, 34.1, 22.0; IR (film) ν<sub>max</sub> 2975, 2934, 1595, 1488, 1223 cm<sup>-1</sup>; HRMS (ESI) *m/z* calcd. for C<sub>14</sub>H<sub>21</sub>O<sub>3</sub> [M+H]<sup>+</sup> 237.1485, found 237.1514.



To a solution of **5.5** (1.00 g, 4.23 mmol, 1.0 eq) in DME (14 mL) was added CuBr<sub>2</sub> (1.89 g, 8.46 mmol, 2.0 eq) and the green reaction was stirred at RT for 48 h. The reaction was diluted with EtOAc (100 mL) and filtered through a plug of Celite with a layer of silica on top, and the plug was washed with EtOAc until the eluting filtrate was mostly clear. The filtrate was washed with 15% NH<sub>4</sub>OH (4 x 100 mL), and the orange organic layer was dried (MgSO<sub>4</sub>), filtered, and concentrated. Purification by flash column chromatography (5% EtOAc/hexanes) provided **5.6** as a light yellow oil (911 mg, 2.89 mmol, 68%). <sup>1</sup>H NMR (600 MHz, CDCl<sub>3</sub>): δ 6.49 (s, 1H), 5.95 (dddd, *J* = 17.1, 6.3, 6.0, 2.7 Hz, 1H), 5.03 (dd, *J* = 1.4, 1.2

Hz, 1H), 5.00 (ddd,  $J = 6.8, 3.2, 1.4$  Hz, 1H), 4.44 (sept.,  $J = 6.1$  Hz, 1H), 3.83 (s, 3H), 3.76 (s, 3H), 3.60 (ddd,  $J = 6.1, 1.4, 1.2$  Hz, 2H), 1.36 (s, 3H), 1.35 (s, 3H);  $^{13}\text{C}$  NMR (150 MHz,  $\text{CDCl}_3$ ):  $\delta$  152.1, 151.1, 142.3, 134.3, 115.5, 107.7, 100.9, 73.3, 61.1, 55.9, 34.4, 22.1; IR (film)  $\nu_{\text{max}}$  2977, 2935, 2837, 1580, 1327, 1232  $\text{cm}^{-1}$ ; HRMS (ESI)  $m/z$  calcd. for  $\text{C}_{14}\text{H}_{20}\text{BrO}_3$   $[\text{M}+\text{H}]^+$  315.0590, found 315.0576.

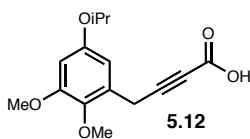


To a solution of **5.5** (3.60 g, 12.5 mmol, 1.0 eq) in acetone (13 mL) and  $\text{H}_2\text{O}$  (13 mL) was added NMO (1.84 g, 15.7 mmol, 1.3 eq) then 1 crystal of  $\text{OsO}_4$  (catalytic) and the reaction was stirred at RT for 22 h. The reaction was diluted with EtOAc (100 mL), added to 20%  $\text{Na}_2\text{SO}_3$  (250 mL), and extracted with EtOAc (3 x 100 mL). The combined organic layers were dried ( $\text{MgSO}_4$ ), filtered, and concentrated to provide **S5.1** as a light yellow solid. The material was taken forward crude.

To a solution of **S5.1** (3.80 g, 11.8 mmol, 1.0 eq) in MeOH (118 mL) open to the air was added pH 7 buffer (59 mL) then  $\text{NaIO}_4$  (3.26 g, 15.3 mmol, 1.3 eq) and the reaction was stirred at RT for 45 min. The reaction was diluted with  $\text{H}_2\text{O}$  (250 mL) and extracted with  $\text{CH}_2\text{Cl}_2$  (4 x 175 mL). The combined organic layers were washed with brine (1 x 175 mL) then dried ( $\text{MgSO}_4$ ), filtered, and concentrated to yield **5.9** as a white solid. The material was taken forward crude.

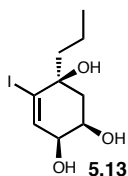
To a solution of **5.9** (3.03 g, 10.5 mmol, 1.0 eq) in MeOH (105 mL) was added  $\text{K}_2\text{CO}_3$  (4.35 g, 31.4 mmol, 3.0 eq) then a solution of the Bestmann-Ohira reagent (**4.82**, 3.02 g, 15.7 mmol, 1.5 eq) in MeOH (25 mL) via cannula and the reaction was stirred at RT for

4 h over which time the reaction turned light green. The reaction was diluted with H<sub>2</sub>O (275 mL) and extracted with EtOAc (3 x 175 mL), and the combined organic layers were washed with brine (1 x 175 mL), dried (MgSO<sub>4</sub>), filtered, and concentrated. Purification by flash column chromatography (10-35% EtOAc/hexanes) provided **5.10** as a white solid (2.84 g, 9.97 mmol, 80% three steps). <sup>1</sup>H NMR (400 MHz, CDCl<sub>3</sub>): δ 6.60 (d, *J* = 2.7 Hz, 1H), 6.38 (d, *J* = 2.7 Hz, 1H), 4.49 (sept., 6.0 Hz, 1H), 3.80 (s, 3H), 3.76 (s, 3H), 3.57 (d, *J* = 2.6 Hz, 2H), 2.13 (dd, *J* = 2.7, 2.7 Hz, 1H), 1.32 (s, 3H), 1.30 (s, 3H); <sup>13</sup>C NMR (100 MHz, CDCl<sub>3</sub>): δ 154.1, 153.1, 140.2, 130.0, 106.3, 100.6, 82.0, 70.1, 70.0, 60.4, 55.6, 21.9, 19.2; IR (film) ν<sub>max</sub> 3290, 2976, 2936, 2119, 1597, 1491, 1329 cm<sup>-1</sup>; HRMS (ESI) *m/z* calcd. for C<sub>14</sub>H<sub>19</sub>O<sub>3</sub> [M+H]<sup>+</sup> 235.1329, found 235.1332.

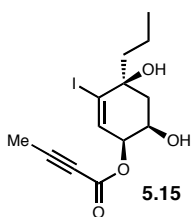


To a solution of **5.10** (589 mg, 2.51 mmol, 1.0 eq) in THF (25.1 mL) at 0 °C was added ethyl magnesium chloride (2.0 M in THF, 7.54 mL, 15.1 mmol, 6.0 eq) and the mixture was stirred at 0 °C for 1 h. CO<sub>2</sub> (g) was bubbled into the mixture at 0 °C while slowly warming to RT for 45 min, and the reaction was diluted with EtOAc (50 mL), added to 1 N HCl (50 mL), and extracted with EtOAc (3 x 50 mL). The combined organic layers were dried (MgSO<sub>4</sub>), filtered, and concentrated. Purification by flash column chromatography (30-50% EtOAc/hexanes containing 1% AcOH) yielded **5.12** as a yellow oil (671 mg, 2.41 mmol, 96%). MP: 73-76 °C; <sup>1</sup>H NMR (400 MHz, CDCl<sub>3</sub>): δ 10.63 (br. s, 1H), 6.48 (d, *J* = 2.7 Hz, 1H), 6.41 (d, *J* = 2.7 Hz, 1H), 4.49 (sept., *J* = 6.0 Hz, 1H), 3.81 (s, 3H), 3.79 (s, 3H), 3.71 (br. s, 2H), 1.33 (s, 3H), 1.31 (s, 3H); <sup>13</sup>C NMR (100 MHz, CDCl<sub>3</sub>): δ 157.6, 154.3, 153.3, 140.4, 127.8, 106.6, 101.3, 89.3, 73.8, 70.4, 60.8, 55.7, 22.0, 19.7; IR (film) ν<sub>max</sub> 3475, 2978,

2625, 2239, 1708, 1598, 1493, 1226  $\text{cm}^{-1}$ ; HRMS (ESI)  $m/z$  calcd. for  $\text{C}_{15}\text{H}_{19}\text{O}_5$   $[\text{M}+\text{H}]^+$  279.1227, found 279.1232.



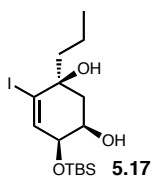
To a solution of **4.57** (2.50 g, 7.39 mmol, 1.0 eq) in  $\text{CH}_3\text{CN}$  (37.0 mL) was added 2 N aqueous HCl (37.0 mL) slowly and the reaction was stirred at RT for 2.75 h. To the reaction was carefully added saturated aqueous  $\text{NaHCO}_3$  (100 mL) and the mixture was extracted with EtOAc (3 x 75 mL). The combined organic layers were dried ( $\text{MgSO}_4$ ), filtered, and concentrated. Purification by flash column chromatography (50-70% EtOAc/hexanes) provided **5.13** as an orange oil (1.92 g, 6.44 mmol, 87%).  $[\alpha]_{\text{D}}^{20}$   $-6.9$  ( $c$  0.33,  $\text{CHCl}_3$ );  $^1\text{H}$  NMR (400 MHz,  $\text{CDCl}_3$ ):  $\delta$  6.39 (s, 1H), 4.15 (br. s, 1H), 4.09 (br. s, 1H), 4.02 (d,  $J = 3.8$  Hz, 1H), 3.85 (s, 1H), 3.83 (br. s, 1H), 2.27 (dd,  $J = 14.6, 5.1$  Hz, 1H), 1.99 (dd,  $J = 14.5, 1.5$  Hz, 1H), 1.55 (dddd,  $J = 16.9, 13.7, 6.9, 6.8, 6.2$  Hz, 2H), 1.21 (ddd,  $J = 14.4, 14.4, 7.1$  Hz, 2H), 0.94 (dd,  $J = 7.4, 7.2$  Hz, 3H);  $^{13}\text{C}$  NMR (100 MHz,  $\text{CDCl}_3$ ):  $\delta$  140.1, 113.3, 73.5, 70.5, 67.8, 45.4, 35.1, 17.0, 14.3; IR (film)  $\nu_{\text{max}}$  3371, 2958, 2932, 2872, 1620, 1396  $\text{cm}^{-1}$ ; HRMS (ESI)  $m/z$  calcd. for  $\text{C}_9\text{H}_{15}\text{IO}_3$   $[\text{M}+\text{H}]^+$  299.0145, found 299.0139.



To a solution of **5.13** (36 mg, 0.121 mmol, 1.1 eq) in  $\text{CH}_2\text{Cl}_2$  (1.1 mL) at 0  $^\circ\text{C}$  was added 2-butynoic acid (**5.14**, 9.0 mg, 0.110 mmol, 1.0 eq), DMAP (2 mg, catalytic), and DCC (23 mg, 0.110 mmol, 1.0 eq) and the reaction was stirred at 0  $^\circ\text{C}$  for 2 h and at RT for 20 h. The reaction was diluted with  $\text{H}_2\text{O}$  (10 mL) and extracted with EtOAc (3 x 10 mL). The combined organic layers were dried ( $\text{MgSO}_4$ ), filtered, and concentrated. Purification by flash column chromatography (40-

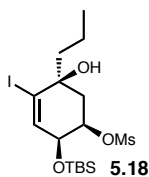


60% EtOAc/hexanes) yielded **5.15** as clear oil (20 mg, 0.0549 mmol, 50%), and the undesired regioisomer was discarded.  $^1\text{H}$  NMR (600 MHz,  $\text{CDCl}_3$ ):  $\delta$  6.28 (dd,  $J = 1.8$ , 1.7 Hz, 1H), 5.24 (dd,  $J = 3.5$ , 2.2 Hz, 1H), 4.34 (br. m, 1H), 3.54 (s, 1H), 2.64 (br. s, 1H), 2.34 (dd,  $J = 14.8$ , 5.2 Hz, 1H), 2.06-1.99 (m, 1H), 2.02 (s, 3H), 1.65-1.52 (m, 2H), 1.29-1.18 (m, 2H), 0.95 (dd,  $J = 7.4$ , 7.3 Hz, 3H);  $^{13}\text{C}$  NMR (150 MHz,  $\text{CDCl}_3$ ):  $\delta$  152.4, 134.1, 116.0, 87.8, 74.0, 73.0, 71.7, 66.4, 45.1, 34.8, 16.9, 14.3, 3.9.



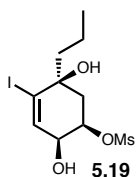
To a solution of **5.13** (1.16 g, 3.89 mmol, 1.0 eq) in  $\text{CH}_2\text{Cl}_2$  (3.3 mL) at 0 °C was added imidazole (398 mg, 5.84 mmol, 1.5 eq) then TBSCl (587 mg, 3.89 mmol, 1.0 eq) and the light yellow slurry was stirred at RT for 22 h.

To the reaction was added saturated aqueous  $\text{NH}_4\text{Cl}$  (50 mL) and the mixture was extracted with  $\text{CH}_2\text{Cl}_2$  (3 x 50 mL). The combined organic layers were dried ( $\text{MgSO}_4$ ), filtered, and concentrated. Purification by flash column chromatography (5-20% EtOAc/hexanes) yielded **5.17** as a light yellow solid (1.15 g, 2.80 mmol, 72%). MP: 32-35 °C;  $[\alpha]_D^{20} +29.8$  ( $c$  0.50,  $\text{CHCl}_3$ );  $^1\text{H}$  NMR (400 MHz,  $\text{CDCl}_3$ ):  $\delta$  6.15 (dd,  $J = 1.4$ , 1.4 Hz, 1H), 4.13 (dd,  $J = 3.8$ , 1.9 Hz, 1H), 4.07 (dd,  $J = 5.5$ , 3.7 Hz, 1H), 3.98 (s, 1H), 2.91 (d,  $J = 1.7$  Hz, 1H), 2.31 (dd,  $J = 14.7$ , 4.6 Hz, 1H), 1.90 (ddd,  $J = 14.8$ , 1.6, 1.5 Hz, 1H), 1.52 (dddd,  $J = 14.5$ , 7.8, 7.7, 5.9, 5.3, 2H), 1.21 (ddd,  $J = 15.0$ , 15.0, 7.2 Hz, 2H), 0.92 (dd,  $J = 7.4$ , 7.2 Hz, 3H), 0.89 (s, 9H), 0.11 (s, 3H), 0.09 (s, 3H);  $^{13}\text{C}$  NMR (100 MHz,  $\text{CDCl}_3$ ):  $\delta$  138.7, 114.1, 72.3, 71.2, 68.5, 45.0, 34.4, 25.6, 18.0, 16.9, 14.2, -4.8, -5.0; IR (film)  $\nu_{\text{max}}$  3501, 2933, 2860, 1620, 1395, 1256  $\text{cm}^{-1}$ ; HRMS (ESI)  $m/z$  calcd. for  $\text{C}_{15}\text{H}_{29}\text{INaO}_3\text{Si}$   $[\text{M}+\text{Na}]^+$  435.0823, found 435.0848.



To a flask under argon containing **5.17** (1.15 g, 2.80 mmol, 1.0 eq) at 0 °C was added pyridine (14 mL) then MsCl (325  $\mu$ L, 4.19 mmol, 1.5 eq) dropwise and the yellow reaction was stirred at 0 °C for 10 min and at RT

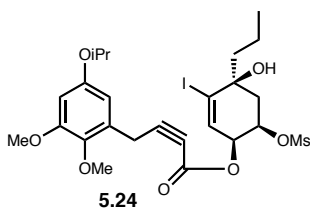
for 1 h, over which time the reaction became lighter yellow. The reaction was diluted with CH<sub>2</sub>Cl<sub>2</sub> (50 mL) and washed with 1 N aqueous HCl (4 x 50 mL), and the combined aqueous layers were extracted with CH<sub>2</sub>Cl<sub>2</sub> (3 x 50 mL). The combined organic layers were dried (MgSO<sub>4</sub>), filtered, and concentrated. Purification by flash column chromatography (10-40% EtOAc/hexanes) provided **5.18** as a clear oil (1.10 g, 2.24 mmol, 80%).  $[\alpha]_D^{20}$  +40.0 (*c* 0.85, CHCl<sub>3</sub>); <sup>1</sup>H NMR (400 MHz, CDCl<sub>3</sub>):  $\delta$  6.30 (dd, *J* = 2.9, 0.6 Hz, 1H), 4.93 (ddd, *J* = 5.3, 5.3, 1.9 Hz, 1H), 4.18 (dd, *J* = 3.2, 3.2 Hz, 1H), 3.06 (s, 3H), 2.46 (dd, *J* = 14.6, 6.8 Hz, 1H), 2.45 (br. s, 1H), 2.18 (dd, *J* = 14.6, 1.9 Hz, 1H), 1.65-1.48 (m, 2H), 1.31-1.19 (m, 2H), 0.93 (dd, *J* = 7.4, 7.2 Hz, 3H), 0.90 (s, 9H), 0.11 (s, 6H); <sup>13</sup>C NMR (125 MHz, CDCl<sub>3</sub>):  $\delta$  139.1, 114.3, 77.8, 73.0, 69.4, 44.3, 39.0, 34.7, 25.7, 18.2, 16.7, 14.2, -4.8, -4.9; IR (film)  $\nu_{\max}$  3582, 3523, 2933, 2253, 1619, 1358, 1115 cm<sup>-1</sup>; HRMS (ESI) *m/z* calcd. for C<sub>16</sub>H<sub>31</sub>INaO<sub>5</sub>SSi [M+Na]<sup>+</sup> 513.0598, found 513.0622.



To a solution of **5.18** (1.10 g, 2.24 mmol, 1.0 eq) in THF (11.2 mL) at 0 °C was added TBAF (4.49 mL, 4.49 mmol, 2.0 eq) and the reaction was stirred at 0 °C for 1 h. To the reaction was added saturated aqueous NH<sub>4</sub>Cl (50 mL)

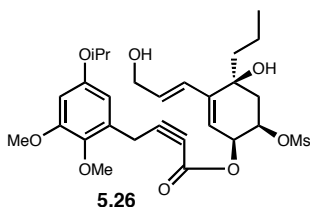
and the mixture was extracted with CH<sub>2</sub>Cl<sub>2</sub> (3 x 50 mL). The combined organic layers were dried (MgSO<sub>4</sub>), filtered, and concentrated. Purification by flash column chromatography (50-90% EtOAc/hexanes) yielded **5.19** as a white solid (739 mg, 1.96

mmol, 88%). MP: 100-103 °C;  $[\alpha]_{\text{D}}^{20} +10.7$  ( $c$  0.24,  $\text{CHCl}_3$ );  $^1\text{H}$  NMR (400 MHz,  $\text{CDCl}_3$ ):  $\delta$  6.46 (d,  $J$  = 3.1 Hz, 1H), 5.03 (ddd,  $J$  = 6.4, 6.4, 2.9 Hz, 1H), 4.27 (ddd,  $J$  = 7.2, 7.2, 3.4 Hz, 1H), 3.14 (s, 3H), 2.49 (dd,  $J$  = 14.5, 7.2 Hz, 1H), 2.41 (d,  $J$  = 7.6 Hz, 1H), 2.28 (s, 1H), 2.23 (dd,  $J$  = 14.5, 2.4 Hz, 1H), 1.70-1.50 (m, 2H), 1.35-1.22 (m, 2H), 0.96 (dd,  $J$  = 7.3, 7.3 Hz, 3H);  $^{13}\text{C}$  NMR (100 MHz,  $\text{CDCl}_3$ ):  $\delta$  138.1, 115.7, 77.5, 73.2, 68.3, 44.5, 39.1, 34.1, 16.8, 14.2; IR (film)  $\nu_{\text{max}}$  3519, 2961, 1338, 1172  $\text{cm}^{-1}$ ; HRMS (ESI)  $m/z$  calcd. for  $\text{C}_{10}\text{H}_{17}\text{INaO}_5\text{S}$   $[\text{M}+\text{Na}]^+$  398.9734, found 398.9753.



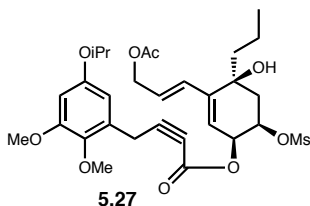
To a solution of **5.12** (70 mg, 0.253 mmol, 1.2 eq) and **5.19** (79 mg, 0.211 mmol, 1.0 eq) in a 5:1 mixture of  $\text{MeNO}_2$  and  $\text{MeCN}$  (dried over activated 4 Å MS overnight, 2.1 mL) was added *p*-nitrobenzoic anhydride (**5.25**, 100 mg, 0.316 mmol, 1.5 eq) and  $\text{Sc}(\text{OTf})_3$  (21 mg, 0.0422 mmol, 0.2 eq) and the reaction was stirred at RT for 22 h. To the reaction was added saturated aqueous  $\text{NaHCO}_3$  (25 mL) and the mixture was extracted with EtOAc (3 x 20 mL). The combined organic layers were dried ( $\text{MgSO}_4$ ), filtered, and concentrated. Purification by flash column chromatography (10-50% EtOAc/hexanes) provided **5.24** as an orange oil (35 mg, 0.0550 mmol, 26%).  $[\alpha]_{\text{D}}^{20} +13.8$  ( $c$  0.83,  $\text{CHCl}_3$ );  $^1\text{H}$  NMR (400 MHz,  $\text{CDCl}_3$ ):  $\delta$  6.44 (d,  $J$  = 2.7 Hz, 1H), 6.41 (d,  $J$  = 2.7 Hz, 1H), 6.37 (d,  $J$  = 3.1 Hz, 1H), 5.32 (dd,  $J$  = 3.4, 3.4 Hz, 1H), 5.11 (ddd,  $J$  = 6.0, 6.0, 2.2 Hz, 1H), 4.49 (sept.,  $J$  = 6.0 Hz, 1H), 3.82 (s, 3H), 3.78 (s, 3H), 3.75 (d,  $J$  = 5.2 Hz, 1H), 3.71 (s, 2H), 3.06 (s, 3H), 2.49 (dd,  $J$  = 14.7, 7.4 Hz, 1H), 2.31 (dd,  $J$  = 14.5, 2.1 Hz, 1H), 1.71-1.51 (m, 2H), 1.33 (s, 3H), 1.32 (s, 3H), 1.30-1.22 (m, 2H), 0.95 (dd,  $J$  = 7.3, 7.2 Hz, 3H);  $^{13}\text{C}$  NMR (100 MHz,  $\text{CDCl}_3$ ):  $\delta$  154.3, 153.3, 152.2, 140.4, 133.3, 127.7, 117.8, 106.7, 101.2, 89.6,

74.3, 73.2, 73.1, 70.4, 70.1, 60.8, 55.7, 44.2, 38.8, 34.8, 22.0, 19.8, 16.7, 14.2; IR (film)  $\nu_{\text{max}}$  3508, 2968, 2236, 1715, 1351, 1243  $\text{cm}^{-1}$ ; HRMS (ESI)  $m/z$  calcd. for  $\text{C}_{25}\text{H}_{33}\text{INaO}_9\text{S} [\text{M}+\text{Na}]^+$  659.0782, found 659.0788.

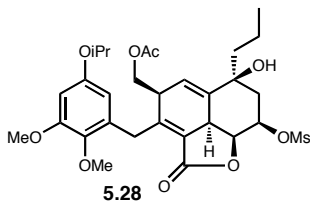


To a microwave vial was added a solution of **5.24** (21 mg, 0.0330 mmol, 1.0 eq) in THF (550  $\mu\text{L}$ ) then  $\text{H}_2\text{O}$  (110  $\mu\text{L}$ ),  $\text{K}_2\text{CO}_3$  (14 mg, 0.0990 mmol, 3.0 eq), **4.41** (17 mg, 0.0660 mmol, 2.0 eq) and  $\text{Pd}(\text{PPh}_3)_4$  (8.0 mg, 6.60  $\mu\text{mol}$ , 0.2 eq), and the reaction was heated via microwave irradiation at 50  $^\circ\text{C}$  for 30 min. The reaction was diluted with EtOAc (10 mL) and washed with 1 N HCl (3 x 10 mL). The combined aqueous layers were extracted with EtOAc (2 x 10 mL), and the combined organic layers were dried ( $\text{MgSO}_4$ ), filtered, and concentrated. Purification by flash column chromatography (30-90% EtOAc/hexanes) yielded **5.26** as an orange oil (11 mg, 0.0194 mmol, 59%).  $[\alpha]_{\text{D}}^{20} +33.5$  ( $c$  0.47,  $\text{CHCl}_3$ );  $^1\text{H}$  NMR (400 MHz,  $\text{CDCl}_3$ ):  $\delta$  6.45 (d,  $J = 2.7$  Hz, 1H), 6.41 (d,  $J = 2.7$  Hz, 1H), 6.32 (d,  $J = 15.8$  Hz, 1H), 6.20 (ddd,  $J = 15.6, 5.0, 5.0$  Hz, 1H), 5.68 (d,  $J = 2.9$  Hz, 1H), 5.48 (dd,  $J = 3.3, 3.2$  Hz, 1H), 5.10 (ddd,  $J = 5.9, 5.9, 2.3$  Hz, 1H), 4.49 (sept.,  $J = 6.1$  Hz, 1H), 4.22 (d,  $J = 4.9$  Hz, 2H), 3.83 (s, 3H), 3.79 (s, 3H), 3.75 (d,  $J = 5.8$  Hz, 1H), 3.71 (s, 2H), 3.05 (s, 3H), 2.35 (br. s, 1H), 2.33 (dd,  $J = 14.8, 7.2$  Hz, 1H), 2.17 (dd,  $J = 14.7, 2.1$  Hz, 1H), 1.66 (ddd,  $J = 13.7, 13.7, 4.8$  Hz, 1H), 1.54 (ddd,  $J = 11.9, 11.9, 5.0$  Hz, 1H), 1.33 (s, 3H), 1.33-1.29 (m, 2H), 1.32 (s, 3H), 0.91 (dd,  $J = 7.4, 7.3$  Hz, 3H);  $^{13}\text{C}$  NMR (100 MHz,  $\text{CDCl}_3$ ):  $\delta$  154.4, 153.4, 152.6, 145.1, 140.5, 132.3, 127.8, 126.7, 118.5, 106.8, 101.2, 89.1, 75.4, 73.4, 71.5, 70.4, 69.7, 63.4, 60.8, 55.8, 41.7, 38.8, 37.6, 22.1, 19.8,

16.8, 14.4; IR (film)  $\nu_{\text{max}}$  3410, 2964, 2934, 2237, 1712, 1493, 1355, 1247, 1176  $\text{cm}^{-1}$ ; HRMS (ESI)  $m/z$  calcd. for  $\text{C}_{28}\text{H}_{38}\text{NaO}_{10}\text{S}$   $[\text{M}+\text{Na}]^+$  589.2078, found 589.2057.

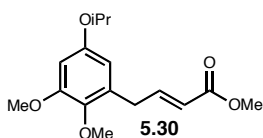


To a solution of **5.26** (10 mg, 0.0176 mmol, 1.0 eq) in  $\text{CH}_2\text{Cl}_2$  (250  $\mu\text{L}$ ) at 0  $^\circ\text{C}$  was added DMAP (catalytic, 2 mg) then  $\text{Ac}_2\text{O}$  (3  $\mu\text{L}$ , 0.0353 mmol, 2.0 eq) and pyridine (3  $\mu\text{L}$ , 0.0353 mmol, 2.0 eq) and the reaction was stirred at 0  $^\circ\text{C}$  for 1 h. To the reaction was added saturated aqueous  $\text{NH}_4\text{Cl}$  (5 mL) and the mixture was extracted with  $\text{CH}_2\text{Cl}_2$  (3 x 5 mL). The combined organic layers were dried ( $\text{MgSO}_4$ ), filtered, and concentrated. Purification by flash column chromatography (30-50% EtOAc/hexanes) provided **5.27** as a yellow oil (5.0 mg, 8.21  $\mu\text{mol}$ , 47%).  $^1\text{H}$  NMR indicated desired product which was unstable when concentrated and was taken immediately to the next step.  $^1\text{H}$  NMR (400 MHz,  $\text{CDCl}_3$ ):  $\delta$  6.45 (d,  $J = 2.7$  Hz, 1H), 6.42 (d,  $J = 2.8$  Hz, 1H), 6.35 (d,  $J = 15.7$  Hz, 1H), 6.12 (ddd,  $J = 15.8, 6.1, 6.1$  Hz, 1H), 5.69 (d,  $J = 2.5$  Hz, 1H), 5.47 (dd,  $J = 3.1, 3.0$  Hz, 1H), 5.12 (dd,  $J = 3.6, 3.2$  Hz, 1H), 4.62 (d,  $J = 6.1$  Hz, 2H), 4.49 (sept.,  $J = 6.0$  Hz, 1H), 3.83 (s, 3H), 3.79 (s, 3H), 3.71 (s, 2H), 3.05 (s, 3H), 2.33 (dd,  $J = 14.8, 6.9$  Hz, 1H), 2.17 (dd,  $J = 15.0, 2.1$  Hz, 1H), 2.10 (s, 1H), 2.08 (s, 3H), 1.70-1.48 (m, 2H), 1.34 (s, 3H), 1.32 (s, 3H), 1.30-1.15 (m, 2H), 0.91 (dd,  $J = 7.3, 7.2$  Hz, 3H).



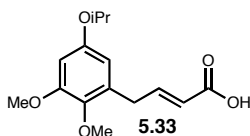
A solution of **5.27** (5.0 mg, 8.21  $\mu\text{mol}$ , 1.0 eq) in toluene (4 mL) was heated in a sealed tube at 80  $^\circ\text{C}$  for 72 h. At RT, the reaction was concentrated, and purification by flash column chromatography (40-70% EtOAc/hexanes) yielded **5.28** as a clear oil (4.0 mg, 6.57  $\mu\text{mol}$ ,

80%).  $[\alpha]_{\text{D}}^{20}$   $-10.6$  ( $c$  0.08,  $\text{CHCl}_3$ );  $^1\text{H}$  NMR (600 MHz,  $\text{CDCl}_3$ ):  $\delta$  6.37 (d,  $J = 2.8$  Hz, 1H), 6.21 (d,  $J = 2.6$  Hz, 1H), 5.86 (dd,  $J = 2.7, 1.5$  Hz, 1H), 5.15 (dd,  $J = 5.7, 2.7$  Hz, 1H), 4.85 (d,  $J = 14.9$  Hz, 1H), 4.70 (dd,  $J = 9.7, 2.9$  Hz, 1H), 4.49 (dd,  $J = 11.5, 3.9$  Hz, 1H), 4.42 (sept.,  $J = 6.0$  Hz, 1H), 4.38 (dd,  $J = 11.5, 4.9$  Hz, 1H), 3.83 (s, 3H), 3.77 (s, 3H), 3.70 (d,  $J = 15.3$  Hz, 1H), 3.52 (dd,  $J = 11.1, 10.9$  Hz, 1H), 3.12 (ddd,  $J = 12.4, 3.6, 3.6$  Hz, 1H), 2.97 (s, 3H), 2.52 (dd,  $J = 16.6, 3.8$  Hz, 1H), 2.29 (s, 1H), 2.12 (dd,  $J = 16.5, 2.2$  Hz, 1H), 2.01 (s, 3H), 1.64 (ddd,  $J = 12.1, 4.7, 4.7$  Hz, 1H), 1.51 (dd,  $J = 13.4, 4.6, 4.6$  Hz, 1H), 1.34-1.21 (m, 2H), 1.30 (d,  $J = 6.1$  Hz, 3H), 1.28 (d,  $J = 6.2$  Hz, 3H), 0.91 (dd,  $J = 7.3, 7.3$  Hz, 3H);  $^{13}\text{C}$  NMR (150 MHz,  $\text{CDCl}_3$ ):  $\delta$  171.0, 167.7, 154.3, 153.5, 151.7, 141.7, 140.9, 131.7, 128.3, 123.7, 122.6, 107.6, 100.0, 78.0, 74.1, 71.9, 70.4, 63.7, 60.8, 55.8, 46.2, 42.3, 41.3, 38.6, 29.7, 26.8, 22.1, 20.7, 16.9, 14.2; IR (film)  $\nu_{\text{max}}$  3542, 2930, 1743, 1594, 1354, 1231, 1176  $\text{cm}^{-1}$ ; HRMS (ESI)  $m/z$  calcd. for  $\text{C}_{30}\text{H}_{40}\text{NaO}_{11}\text{S}$   $[\text{M}+\text{Na}]^+$  631.2184, found 631.2188.

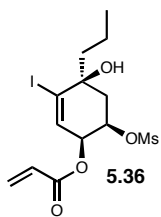


To a solution of methyl diethylphosphonoacetate (**5.29**, 77  $\mu\text{L}$ , 0.420 mmol, 2.0 eq) in THF (2.1 mL) at 0  $^{\circ}\text{C}$  was added NaH (60% in mineral oil, 16 mg, 0.399 mmol, 1.9 eq) and the mixture was stirred at 0  $^{\circ}\text{C}$  for 10 min. To the mixture was added **5.9** (50 mg, 0.210 mmol, 1.0 eq) and the reaction was stirred at RT for 3 h. To the reaction was added saturated aqueous  $\text{NH}_4\text{Cl}$  (15 mL) and the mixture was extracted with  $\text{CH}_2\text{Cl}_2$  (3 x 10 mL). The combined organic layers were dried ( $\text{MgSO}_4$ ), filtered, and concentrated. Purification by flash column chromatography (20-30% EtOAc/hexanes) provided **5.30** as a clear oil (57 mg, 0.194 mmol, 92%).  $^1\text{H}$  NMR (400 MHz,  $\text{CDCl}_3$ ):  $\delta$  7.08 (ddd,  $J = 15.5, 6.7, 6.6$  Hz, 1H), 6.38 (d,  $J = 2.7$  Hz,

1H), 6.21 (d,  $J = 2.7$  Hz, 1H), 5.80 (d,  $J = 15.6$  Hz, 1H), 4.44 (sept., 6.0 Hz, 1H), 3.81 (s, 3H), 3.73 (s, 3H), 3.69 (s, 3H), 3.49 (dd,  $J = 6.6, 1.0$  Hz, 2H), 1.31 (s, 3H), 1.29 (s, 3H);  $^{13}\text{C}$  NMR (100 MHz,  $\text{CDCl}_3$ ):  $\delta$  166.9, 154.2, 153.4, 147.6, 140.9, 131.4, 121.6, 107.4, 100.6, 70.2, 60.8, 55.6, 51.3, 32.7, 22.0; IR (film)  $\nu_{\text{max}}$  2975, 2834, 2010, 1723, 1491, 1194  $\text{cm}^{-1}$ ; HRMS (ESI)  $m/z$  calcd. for  $\text{C}_{16}\text{H}_{23}\text{O}_5$   $[\text{M}+\text{H}]^+$  295.1540, found 295.1535.

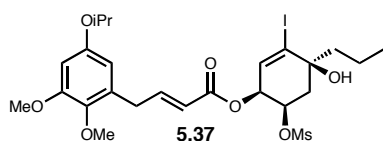


To a solution of  $\text{Zn}(\text{OTf})_2$  (306 mg, 0.840 mmol, 2.2 eq) in THF (2.0 mL) was added diethylphosphonoacetic acid (62  $\mu\text{L}$ , 0.382 mmol, 1.0 eq), TMEDA (68  $\mu\text{L}$ , 0.458 mmol, 1.2 eq), DBU (228  $\mu\text{L}$ , 1.53 mmol, 4.0 eq), and **5.9** (100 mg, 0.420 mmol, 1.1 eq) and the reaction was stirred at RT for 22 h. To the reaction was added 1 N aqueous HCl (20 mL) and the mixture was extracted with EtOAc (3 x 15 mL). The combined aqueous layers were dried ( $\text{MgSO}_4$ ), filtered, and concentrated. Purification by flash column chromatography (20-50% EtOAc/hexanes) yielded **5.33** as a brown oil (68 mg, 0.243 mmol, 64%). HRMS (ESI)  $m/z$  calcd. for  $\text{C}_{15}\text{H}_{21}\text{O}_5$   $[\text{M}+\text{H}]^+$  281.1384, found 281.1377.



To a solution of **5.19** (100 mg, 0.266 mmol, 1.0 eq) in  $\text{CH}_2\text{Cl}_2$  (1.1 mL) at  $-78$   $^\circ\text{C}$  was added DIPEA (351  $\mu\text{L}$ , 2.13 mmol, 8.0 eq) then acryloyl chloride (129  $\mu\text{L}$ , 1.59 mmol, 6.0 eq) dropwise and the reaction was stirred at  $-78$   $^\circ\text{C}$  for 30 min then at  $0$   $^\circ\text{C}$  for 1.5 h. To the reaction was added saturated aqueous  $\text{NH}_4\text{Cl}$  (20 mL) and the mixture was extracted with  $\text{CH}_2\text{Cl}_2$  (3 x 15 mL). The combined organic layers were dried ( $\text{MgSO}_4$ ), filtered, and concentrated. Purification by flash column chromatography (30-50% EtOAc/hexanes) provided **5.36** as a clear oil (100 mg,

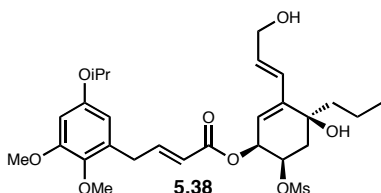
0.232 mmol, 87%).  $[\alpha]_{\text{D}}^{20} +58.9$  (*c* 0.21, CHCl<sub>3</sub>); <sup>1</sup>H NMR (400 MHz, CDCl<sub>3</sub>): δ 6.47 (dd, *J* = 17.2, 0.5 Hz, 1H), 6.37 (d, *J* = 3.2 Hz, 1H), 6.11 (dd, *J* = 17.3, 10.5 Hz, 1H), 5.91 (dd, *J* = 10.5, 0.7 Hz, 1H), 5.33 (dd, *J* = 3.5, 3.4 Hz, 1H), 5.10 (ddd, *J* = 6.5, 6.5, 2.7 Hz, 1H), 3.02 (s, 3H), 2.62 (br. s, 1H), 2.46 (dd, *J* = 14.6, 7.3 Hz, 1H), 2.32 (dd, *J* = 14.6, 2.2 Hz, 1H), 1.68-1.49 (m, 2H), 1.33-1.16 (m, 2H), 0.93 (dd, *J* = 7.4, 7.2 Hz, 3H); <sup>13</sup>C NMR (100 MHz, CDCl<sub>3</sub>): δ 164.8, 134.1, 132.6, 127.2, 117.1, 74.5, 73.1, 68.9, 44.2, 38.8, 34.7, 14.1, 14.0; IR (film)  $\nu_{\text{max}}$  3512, 2962, 2936, 1726, 1356, 1179 cm<sup>-1</sup>; HRMS (ESI) *m/z* calcd. for C<sub>13</sub>H<sub>19</sub>INaO<sub>6</sub>S [M+Na]<sup>+</sup> 452.9839, found 452.9845.



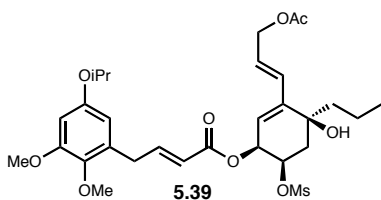
To a solution of **5.36** (100 mg, 0.232 mmol, 1.0 eq) in CH<sub>2</sub>Cl<sub>2</sub> (3.9 mL) was added **5.5** (165 mg, 0.697 mmol, 3.0 eq) then Hoveyda-Grubbs second generation catalyst (15 mg, 0.0232 mmol, 0.1 eq) and the mixture was heated via microwave irradiation at 100 °C for 1.5 h. The reaction was concentrated, and purification by flash column chromatography (30-50% EtOAc/hexanes) provided **5.37** as a yellow oil (112 mg, 0.175 mmol, 76%).  $[\alpha]_{\text{D}}^{20} +31.3$  (*c* 0.61, CHCl<sub>3</sub>); <sup>1</sup>H NMR (400 MHz, CDCl<sub>3</sub>): δ 7.15 (ddd, *J* = 15.5, 6.6, 6.6 Hz, 1H), 6.36 (d, *J* = 2.6 Hz, 1H), 6.34 (d, *J* = 3.1 Hz, 1H), 6.18 (d, *J* = 2.7 Hz, 1H), 5.77 (d, *J* = 15.7 Hz, 1H), 5.29 (dd, *J* = 3.4, 3.4 Hz, 1H), 5.07 (ddd, *J* = 9.7, 6.1, 2.5 Hz, 1H), 4.43 (sept., *J* = 6.1 Hz, 1H), 3.79 (s, 3H), 3.70 (s, 3H), 3.48 (d, *J* = 6.4 Hz, 2H), 2.97 (s, 3H), 2.54 (s, 1H), 2.44 (dd, *J* = 14.6, 7.3 Hz, 1H), 2.29 (dd, *J* = 14.5, 1.9 Hz, 1H), 1.67-1.48 (m, 2H), 1.30-1.25 (m, 2H), 1.29 (s, 3H), 1.27 (s, 3H), 0.92 (dd, *J* = 7.4, 7.1 Hz, 3H); <sup>13</sup>C NMR (100 MHz, CDCl<sub>3</sub>): δ 165.1, 154.2, 153.4, 149.8, 140.8, 134.4, 130.9, 120.6, 116.8, 107.4, 100.7, 74.7, 73.1, 70.2, 68.6, 60.7, 55.6, 44.2, 38.7, 34.8, 33.0, 22.0, 16.6, 14.1; IR



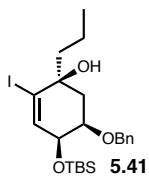
(film)  $\nu_{\max}$  3504, 2963, 2874, 2252, 1722, 1357, 1178  $\text{cm}^{-1}$ ; HRMS (ESI)  $m/z$  calcd. for  $\text{C}_{25}\text{H}_{36}\text{IO}_9\text{S} [\text{M}+\text{H}]^+$  639.1119, found 639.1106.



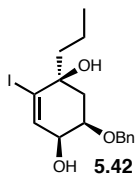
To a solution of **5.37** (112 mg, 0.175 mmol, 1.0 eq) in THF (2.9 mL) was added  $\text{H}_2\text{O}$  (585  $\mu\text{L}$ ),  $\text{K}_2\text{CO}_3 \cdot 1.5\text{H}_2\text{O}$  (87 mg, 0.526 mmol, 3.0 eq), **4.41** (90 mg, 0.351 mmol, 2.0 eq) and  $\text{Pd}(\text{PPh}_3)_4$  (41 mg, 0.0351 mmol, 0.2 eq) and the reaction was heated via microwave irradiation at 50  $^\circ\text{C}$  for 1 h. The reaction was diluted with EtOAc (10 mL), added to 1 N aqueous HCl (20 mL) and extracted with EtOAc (3 x 10 mL). The combined organic layers were dried ( $\text{MgSO}_4$ ), filtered, and concentrated. Purification by flash column chromatography (50-90% EtOAc/hexanes) yielded **5.38** as a yellow oil (60 mg, 0.106 mmol, 60%).  $[\alpha]_{\text{D}}^{20} +57.4$  ( $c$  1.89,  $\text{CHCl}_3$ );  $^1\text{H}$  NMR (400 MHz,  $\text{CDCl}_3$ ):  $\delta$  7.17 (ddd,  $J = 15.5, 6.6, 6.6$  Hz, 1H), 6.39 (d,  $J = 2.7$  Hz, 1H), 6.31 (d,  $J = 15.9$  Hz, 1H), 6.21 (d,  $J = 2.5$  Hz, 1H), 6.18 (ddd,  $J = 15.8$  Hz, 5.3, 5.3 Hz, 1H), 5.81 (d,  $J = 15.6$  Hz, 1H), 5.68 (d,  $J = 2.8$  Hz, 1H), 5.46 (dd,  $J = 3.2, 3.0$  Hz, 1H), 5.09 (ddd,  $J = 6.0, 6.0, 2.6$  Hz, 1H), 4.46 (sept.,  $J = 6.0$  Hz, 1H), 4.20 (d,  $J = 4.8$  Hz, 2H), 3.82 (s, 3H), 3.73 (s, 3H), 3.50 (d,  $J = 6.3$  Hz, 2H), 2.97 (s, 3H), 2.32 (dd,  $J = 14.7, 7.1$  Hz, 1H), 2.17 (dd,  $J = 14.7, 2.0$  Hz, 1H), 1.65 (ddd,  $J = 12.2, 12.2, 4.7$  Hz, 1H), 1.55 (ddd,  $J = 11.9, 11.9, 5.1$  Hz, 1H), 1.31 (s, 3H), 1.30 (s, 3H), 1.29-1.17 (m, 2H), 0.90 (dd,  $J = 7.3, 7.3$  Hz, 3H);  $^{13}\text{C}$  NMR (100 MHz,  $\text{CDCl}_3$ ):  $\delta$  165.5, 154.3, 153.5, 149.4, 144.2, 140.9, 132.0, 131.1, 126.9, 121.0, 119.7, 107.6, 100.7, 75.9, 71.5, 70.3, 68.0, 63.4, 60.9, 55.7, 41.8, 38.7, 37.6, 33.1, 22.1, 16.8, 14.4; IR (film)  $\nu_{\max}$  3419, 2965, 2936, 1717, 1597, 1356, 1176  $\text{cm}^{-1}$ ; HRMS (ESI)  $m/z$  calcd. for  $\text{C}_{28}\text{H}_{40}\text{NaO}_{10}\text{S} [\text{M}+\text{Na}]^+$  591.2234, found 591.2244.



To a solution of **5.38** (25 mg, 0.0440 mmol, 1.0 eq) in  $\text{CH}_2\text{Cl}_2$  (879  $\mu\text{L}$ ) at 0 °C was added DMAP (catalytic, 2 mg) then  $\text{Ac}_2\text{O}$  (6  $\mu\text{L}$ , 0.0659 mmol, 1.5 eq) and pyridine (5  $\mu\text{L}$ , 0.0659 mmol, 1.5 eq) and the reaction was stirred at 0 °C for 15 min. To the reaction was added saturated aqueous  $\text{NH}_4\text{Cl}$  (10 mL) and the mixture was extracted with  $\text{CH}_2\text{Cl}_2$  (3 x 10 mL). The combined organic layers were dried ( $\text{MgSO}_4$ ), filtered, and concentrated, and purification by flash column chromatography (40-60% EtOAc/hexanes) provided **5.39** as a light yellow oil (20 mg, 0.0327 mmol, 74%).  $[\alpha]_{\text{D}}^{20} +98.0$  ( $c$  0.15,  $\text{CHCl}_3$ );  $^1\text{H}$  NMR (400 MHz,  $\text{CDCl}_3$ ):  $\delta$  7.17 (ddd,  $J$  = 15.6, 6.7, 6.6 Hz, 1H), 6.39 (d,  $J$  = 2.8 Hz, 1H), 6.34 (d,  $J$  = 15.8 Hz, 1H), 6.21 (d,  $J$  = 2.7 Hz, 1H), 6.10 (ddd,  $J$  = 15.7, 6.1, 6.1 Hz, 1H), 5.81 (d,  $J$  = 15.6 Hz, 1H), 5.69 (d,  $J$  = 2.5 Hz, 1H), 5.45 (dd,  $J$  = 3.1, 3.0 Hz, 1H), 5.10 (dd,  $J$  = 3.4, 3.2 Hz, 1H), 4.60 (d,  $J$  = 5.9 Hz, 2H), 4.46 (sept.,  $J$  = 6.1 Hz, 1H), 3.82 (s, 3H), 3.73 (s, 3H), 3.50 (d,  $J$  = 6.3 Hz, 2H), 2.97 (s, 3H), 2.32 (dd,  $J$  = 14.8, 6.7 Hz, 1H), 2.16 (dd,  $J$  = 14.8, 1.8 Hz, 1H), 2.07 (s, 3H), 1.64 (ddd,  $J$  = 12.2, 12.2, 4.7 Hz, 1H), 1.54 (ddd,  $J$  = 12.0, 12.0, 5.0 Hz, 1H), 1.39-1.12 (m, 2H), 1.31 (s, 3H), 1.30 (s, 3H), 0.90 (dd,  $J$  = 7.3, 7.1 Hz, 3H);  $^{13}\text{C}$  NMR (100 MHz,  $\text{CDCl}_3$ ):  $\delta$  170.7, 165.5, 154.3, 153.5, 149.5, 143.7, 140.9, 131.1, 130.0, 126.6, 120.9, 120.6, 107.6, 100.7, 75.9, 71.3, 70.3, 68.1, 64.7, 60.8, 55.7, 41.7, 38.7, 37.7, 33.1, 22.1, 20.9, 16.8, 14.3; IR (film)  $\nu_{\text{max}}$  3500, 2963, 2936, 1724, 1651, 1596, 1358, 1177  $\text{cm}^{-1}$ ; HRMS (ESI)  $m/z$  calcd. for  $\text{C}_{30}\text{H}_{42}\text{NaO}_{11}\text{S}$   $[\text{M}+\text{Na}]^+$  633.2340, found 633.2319.

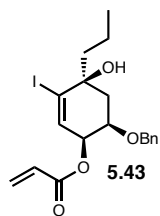


To a slurry of NaH (60% in mineral oil, 405 mg, 10.1 mmol, 2.2 eq) in THF (12 mL) at 0 °C was added a solution of **5.17** (1.90 g, 4.61 mmol, 1.0 eq) in THF (11 mL) via cannula causing vigorous gas evolution. After gas evolution had ceased (~15 min), BnBr (603  $\mu$ L, 5.07 mmol, 1.1 eq) was added dropwise and the reaction was stirred at 0 °C for 20 min and at RT for 4.25 h. To the reaction was added saturated aqueous NH<sub>4</sub>Cl (100 mL) and the mixture was extracted with CH<sub>2</sub>Cl<sub>2</sub> (3 x 75 mL). The combined organic layers were dried (MgSO<sub>4</sub>), filtered, and concentrated. Purification by flash column chromatography (3-6% EtOAc/hexanes) yielded **5.41** as a clear oil that solidified at 0 °C (1.54 g, 3.06 mmol, 66%). MP: 41-45 °C;  $[\alpha]_D^{20}$  +31.6 (*c* 0.26, CHCl<sub>3</sub>); <sup>1</sup>H NMR (400 MHz, CDCl<sub>3</sub>):  $\delta$  7.40-7.28 (m, 5H), 6.32 (dd, *J* = 1.4, 1.3 Hz, 1H), 4.92 (d, *J* = 12.0 Hz, 1H), 4.65 (d, *J* = 12.1 Hz, 1H), 4.23 (dd, *J* = 3.3, 1.8 Hz, 1H), 3.94-3.88 (m, 2H), 2.26 (dd, *J* = 14.4, 4.8 Hz, 1H), 1.91 (dd, *J* = 14.3, 1.0 Hz, 1H), 1.58-1.50 (m, 2H), 1.29-1.15 (m, 2H), 0.94 (dd, *J* = 7.4, 7.0 Hz, 3H), 0.94 (s, 9H), 0.11 (s, 6H); <sup>13</sup>C NMR (100 MHz, CDCl<sub>3</sub>):  $\delta$  140.7, 137.9, 128.3, 127.6 (2C), 112.6, 76.1, 73.6, 72.9, 72.7, 44.7, 34.4, 25.7, 18.1, 16.9, 14.2, -4.8, -4.9; IR (film)  $\nu_{\max}$  3506, 2954, 2859, 1463, 1364, 1255, 1113 cm<sup>-1</sup>; HRMS (ESI) *m/z* calcd. for C<sub>22</sub>H<sub>35</sub>INaO<sub>3</sub>Si [M+Na]<sup>+</sup> 525.1292, found 525.1287.



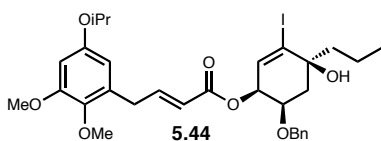
To a solution of **5.41** (1.54 g, 3.06 mmol, 1.0 eq) in THF (15 mL) at 0 °C was added TBAF (6.13 mL, 6.13 mmol, 2.0 eq) and the reaction was stirred at 0 °C for 1 h. To the reaction was added saturated aqueous NH<sub>4</sub>Cl (50 mL) and the mixture was extracted with CH<sub>2</sub>Cl<sub>2</sub> (3 x 50 mL). The combined organic layers were dried (MgSO<sub>4</sub>), filtered, and concentrated. Purification by flash column

chromatography (20-50% EtOAc/hexanes) yielded **5.42** as a light yellow oil (962 mg, 2.48 mmol, 81%).  $[\alpha]_{\text{D}}^{20} -6.1$  (*c* 0.34, CHCl<sub>3</sub>); <sup>1</sup>H NMR (400 MHz, CDCl<sub>3</sub>): δ 7.44-7.29 (m, 5H), 6.41 (dd, *J* = 1.9, 0.9 Hz, 1H), 4.76 (d, *J* = 11.1 Hz, 1H), 4.57 (d, *J* = 11.1 Hz, 1H), 4.09 (br. s, 1H), 3.98 (dd, *J* = 4.5, 4.4 Hz, 1H), 3.34 (br. s, 1H), 2.64 (br. s, 1H), 2.40 (dd, *J* = 14.8, 4.9 Hz, 1H), 1.93 (dd, *J* = 14.7, 1.5 Hz, 1H), 1.60-1.51 (m, 2H), 1.29-1.16 (m, 2H), 0.95 (dd, *J* = 7.3, 7.2 Hz, 3H); <sup>13</sup>C NMR (100 MHz, CDCl<sub>3</sub>): δ 140.7, 136.7, 128.8, 128.5, 128.4, 113.5, 75.7, 73.0, 72.8, 69.9, 44.9, 32.8, 17.0, 14.3; IR (film)  $\nu_{\text{max}}$  3429, 2958, 2931, 2871, 1619, 1455, 1389, 1099 cm<sup>-1</sup>; HRMS (ESI) *m/z* calcd. for C<sub>16</sub>H<sub>21</sub>INaO<sub>3</sub> [M+Na]<sup>+</sup> 411.0428, found 411.0414.

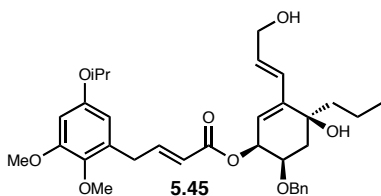


To a solution of **5.42** (100 mg, 0.266 mmol, 1.0 eq) in CH<sub>2</sub>Cl<sub>2</sub> (1.1 mL) at -78 °C was added DIPEA (351 μL, 2.13 mmol, 8.0 eq) then acryloyl chloride (129 μL, 1.59 mmol, 6.0 eq) and the reaction was stirred at -78 °C for 30 min and at 0 °C for 1.5 h. To the reaction was added saturated aqueous NH<sub>4</sub>Cl (15 mL) and the mixture was extracted with CH<sub>2</sub>Cl<sub>2</sub> (3 x 15 mL). The combined organic layers were dried (MgSO<sub>4</sub>), filtered, and concentrated. Purification by flash column chromatography (30-50% EtOAc/hexanes) provided **5.43** as a clear oil (100 mg, 0.232 mmol, 87%).  $[\alpha]_{\text{D}}^{20} +40.0$  (*c* 0.34, CHCl<sub>3</sub>); <sup>1</sup>H NMR (400 MHz, CDCl<sub>3</sub>): δ 7.38-7.26 (m, 5H), 6.47 (dd, *J* = 17.3, 1.0 Hz, 1H), 6.36 (dd, *J* = 1.4, 1.4 Hz, 1H), 6.17 (dd, *J* = 17.3, 10.4 Hz, 1H), 5.92 (dd, *J* = 10.4, 1.0 Hz, 1H), 5.31 (dd, *J* = 3.5, 2.6 Hz, 1H), 4.69 (d, *J* = 11.8 Hz, 1H), 4.58 (d, *J* = 11.8 Hz, 1H), 4.12 (ddd, *J* = 3.8, 3.8, 1.7 Hz, 1H), 3.60 (br. s, 1H), 2.32 (dd, *J* = 14.5, 5.5 Hz, 1H), 2.04 (dd, *J* = 14.5, 1.6 Hz, 1H), 1.61-1.52 (m, 2H), 1.30-1.15 (m, 2H), 0.94 (dd, *J* = 7.4, 7.2 Hz, 3H); <sup>13</sup>C NMR (100 MHz, CDCl<sub>3</sub>): δ 165.3,

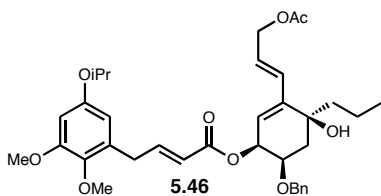
137.3, 135.6, 132.1, 128.6, 128.1, 127.9, 127.8, 115.4, 73.3 (2C), 73.2, 72.4, 44.6, 34.1, 16.9, 14.3; IR (film)  $\nu_{\max}$  3485, 2959, 1723, 1405, 1188  $\text{cm}^{-1}$ ; HRMS (ESI)  $m/z$  calcd. for  $\text{C}_{19}\text{H}_{23}\text{INaO}_4$   $[\text{M}+\text{Na}]^+$  465.0533, found 465.0559.



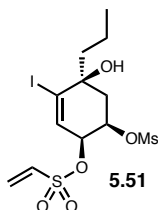
To a solution of **5.43** (96 mg, 0.217 mmol, 1.0 eq) in  $\text{CH}_2\text{Cl}_2$  (3.6 mL) was added **5.5** (154 mg, 0.651 mmol, 3.0 eq) and Hoveyda-Grubbs second generation catalyst (14 mg, 0.0217 mmol, 0.1 eq) and the reaction was heated via microwave irradiation at 100 °C for 1.5 h. The reaction mixture was concentrated, and purification by flash column chromatography (10-25% EtOAc/hexanes) yielded **5.44** as a yellow oil (76 mg, 0.117 mmol, 54%).  $[\alpha]_{\text{D}}^{20} +21.9$  ( $c$  2.13,  $\text{CHCl}_3$ );  $^1\text{H}$  NMR (600 MHz,  $\text{CDCl}_3$ ):  $\delta$  7.34-7.22 (m, 5H), 7.17 (ddd,  $J = 15.5, 6.6, 6.5$  Hz, 1H), 6.41 (d,  $J = 2.7$  Hz, 1H), 6.33 (dd,  $J = 1.5, 1.1$  Hz, 1H), 6.24 (d,  $J = 2.7$  Hz, 1H), 5.85 (d,  $J = 15.6$  Hz, 1H), 5.28 (dd,  $J = 3.4, 2.5$  Hz, 1H), 4.67 (d,  $J = 11.9$  Hz, 1H), 4.56 (d,  $J = 11.8$  Hz, 1H), 4.45 (sept.,  $J = 6.1$  Hz, 1H), 4.10 (ddd,  $J = 3.4, 3.4, 1.8$  Hz, 1H), 3.83 (s, 3H), 3.75 (s, 3H), 3.62 (s, 1H), 3.53 (d,  $J = 6.2$  Hz, 2H), 2.29 (dd,  $J = 14.5, 5.5$  Hz, 1H), 2.02 (dd,  $J = 14.5, 1.1$  Hz, 1H), 1.59-1.51 (m, 2H), 1.31 (s, 3H), 1.30 (s, 3H), 1.25-1.16 (m, 2H), 0.94 (dd,  $J = 7.3, 7.2$  Hz, 3H);  $^{13}\text{C}$  NMR (150 MHz,  $\text{CDCl}_3$ ):  $\delta$  165.6, 154.3, 153.5, 149.2, 141.0, 137.3, 135.8, 131.1, 128.5, 128.0, 127.8, 121.2, 115.1, 107.6, 100.7, 73.3, 73.2, 73.1, 72.1, 70.2, 60.8, 55.7, 44.6, 34.1, 33.0, 22.1, 16.9, 14.3; IR (film)  $\nu_{\max}$  3503, 2963, 2934, 2873, 1717, 1596, 1492, 1265, 1150  $\text{cm}^{-1}$ ; HRMS (ESI)  $m/z$  calcd. for  $\text{C}_{31}\text{H}_{39}\text{INaO}_7$   $[\text{M}+\text{Na}]^+$  673.1633, found 673.1658.



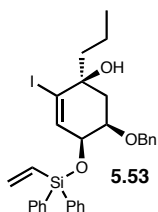
To a solution of **5.44** (76 mg, 0.117 mmol, 1.0 eq) in THF (2.0 mL) was added H<sub>2</sub>O (389  $\mu$ L), K<sub>2</sub>CO<sub>3</sub>•1.5H<sub>2</sub>O (58 mg, 0.350 mmol, 3.0 eq), **4.41** (60 mg, 0.234 mmol, 2.0 eq) and Pd(PPh<sub>3</sub>)<sub>4</sub> (27 mg, 0.0234 mmol, 0.2 eq) and the reaction was heated via microwave irradiation at 50 °C for 30 min. The reaction was diluted with EtOAc (10 mL) and washed with 1 N aqueous HCl (3 x 10 mL). The combined aqueous layers were extracted with EtOAc (2 x 10 mL), and the combined organic layers were dried (MgSO<sub>4</sub>), filtered, and concentrated. Purification by flash column chromatography (30-60% EtOAc/hexanes) provided **5.45** as a yellow oil (29 mg, 0.0499 mmol, 43%).  $[\alpha]_{\text{D}}^{20} +42.3$  (*c* 0.79, CHCl<sub>3</sub>); <sup>1</sup>H NMR (400 MHz, CDCl<sub>3</sub>):  $\delta$  7.33-7.22 (m, 5H), 7.16 (ddd, *J* = 15.6, 6.6, 6.6 Hz, 1H), 6.40 (d, *J* = 2.8 Hz, 1H), 6.30 (d, *J* = 15.6 Hz, 1H), 6.24 (d, *J* = 2.8 Hz, 1H), 6.12 (ddd, *J* = 15.8, 5.7, 5.6 Hz, 1H), 5.86 (d, *J* = 15.5 Hz, 1H), 5.65 (s, 1H), 5.40 (s, 1H), 4.66 (d, *J* = 11.8 Hz, 1H), 4.56 (d, *J* = 11.8 Hz, 1H), 4.45 (sept., *J* = 6.0 Hz, 1H), 4.18 (d, *J* = 5.5 Hz, 2H), 4.06 (ddd, *J* = 5.0, 5.0, 1.9 Hz, 1H), 3.83 (s, 3H), 3.74 (s, 3H), 3.52 (dd, *J* = 6.6, 0.9 Hz, 2H), 3.51 (s, 1H), 2.12 (dd, *J* = 14.7, 5.5 Hz, 1H), 1.87 (dd, *J* = 14.5, 1.0 Hz, 1H), 1.55 (ddd, *J* = 10.4, 10.4, 5.0 Hz, 2H), 1.31 (s, 3H), 1.29 (s, 3H), 1.22-1.06 (m, 2H), 0.88 (dd, *J* = 7.4, 7.2 Hz, 3H); <sup>13</sup>C NMR (100 MHz, CDCl<sub>3</sub>):  $\delta$  166.0, 154.3, 153.5, 148.7, 143.2, 141.0, 137.7, 131.3, 130.5, 128.4, 128.2, 127.8 (2C), 121.6, 121.3, 107.6, 100.7, 73.7, 73.0, 71.6, 71.4, 70.3, 63.7, 60.9, 55.7, 41.4, 36.4, 33.0, 24.8, 22.1, 16.9, 14.5; IR (film)  $\nu_{\text{max}}$  3423, 2964, 1713, 1650, 1596, 1492, 1268, 1151 cm<sup>-1</sup>; HRMS (ESI) *m/z* calcd. for C<sub>34</sub>H<sub>44</sub>NaO<sub>8</sub> [M+Na]<sup>+</sup> 603.2928, found 603.2928.



To a solution of **5.45** (7 mg, 0.0121 mmol, 1.0 eq) in CH<sub>2</sub>Cl<sub>2</sub> (241  $\mu$ L) at 0 °C was added DMAP (catalytic, 2 mg), Ac<sub>2</sub>O (2  $\mu$ L, 0.0181 mmol, 1.5 eq) and pyridine (1  $\mu$ L, 0.0181 mmol, 1.5 eq) and the reaction was stirred at 0 °C for 1 h and at RT for 3 h. To the reaction was added saturated aqueous NH<sub>4</sub>Cl (5 mL), and the mixture was extracted with CH<sub>2</sub>Cl<sub>2</sub> (3 x 5 mL). The combined organic layers were dried (MgSO<sub>4</sub>), filtered, and concentrated. Purification by flash column chromatography (30-50% EtOAc/hexanes) yielded **5.46** as a clear oil (7 mg, 0.0112 mmol, 93%).  $[\alpha]_D^{20} +46.5$  (*c* 0.28, CHCl<sub>3</sub>); <sup>1</sup>H NMR (400 MHz, CDCl<sub>3</sub>):  $\delta$  7.34-7.22 (m, 5H), 7.16 (ddd, *J* = 15.6, 6.6, 6.6 Hz, 1H), 6.40 (d, *J* = 2.8 Hz, 1H), 6.34 (d, *J* = 15.8 Hz, 1H), 6.24 (d, *J* = 2.8 Hz, 1H), 6.03 (ddd, *J* = 15.8, 6.3, 6.3 Hz, 1H), 5.86 (d, *J* = 15.7 Hz, 1H), 5.66 (s, 1H), 5.39 (s, 1H), 4.66 (d, *J* = 11.8 Hz, 1H), 4.62-4.53 (m, 3H), 4.45 (sept., *J* = 6.0 Hz, 1H), 4.07 (ddd, *J* = 4.1, 4.1, 1.7 Hz, 1H), 3.83 (s, 3H), 3.74 (s, 3H), 3.52 (dd, *J* = 5.2, 1.1 Hz, 2H), 2.12 (dd, *J* = 14.6, 5.4 Hz, 1H), 2.06 (s, 3H), 1.86 (d, *J* = 13.9 Hz, 1H), 1.54 (ddd, *J* = 15.9, 10.4, 4.5 Hz, 1H), 1.31 (s, 3H), 1.29 (s, 3H), 1.27-1.05 (m, 3H), 0.88 (dd, *J* = 7.3, 7.2 Hz, 3H); <sup>13</sup>C NMR (100 MHz, CDCl<sub>3</sub>):  $\delta$  170.8, 166.0, 154.3, 153.5, 148.8, 142.9, 141.0, 137.6, 131.3, 131.2, 128.5, 127.9, 127.8, 125.2, 122.0, 121.6, 107.6, 100.7, 73.7, 73.1, 71.6, 71.2, 70.3, 64.9, 60.9, 55.7, 41.4, 36.4, 33.0, 22.1, 21.0, 16.9, 14.5; IR (film)  $\nu_{\max}$  3613, 3541, 2962, 1717, 1596, 1492, 1227, 1024 cm<sup>-1</sup>; HRMS (ESI) *m/z* calcd. for C<sub>36</sub>H<sub>46</sub>NaO<sub>9</sub> [M+Na]<sup>+</sup> 645.3034, found 645.3037.



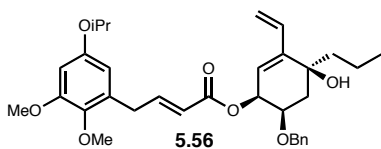
To a solution of **5.19** (30 mg, 0.0797 mmol, 1.0 eq) in CH<sub>2</sub>Cl<sub>2</sub> (797 μL) at –78 °C was added vinylsulfonyl chloride (15 μL, 0.159 mmol, 2.0 eq) then DIPEA (53 μL, 0.319 mmol, 4.0 eq) and the reaction was stirred at –78 °C for 1.5 h. To the reaction was added saturated aqueous NH<sub>4</sub>Cl (10 mL), and at RT, the mixture was extracted with CH<sub>2</sub>Cl<sub>2</sub> (3 x 10 mL). The combined organic layers were dried (MgSO<sub>4</sub>), filtered, and concentrated. Purification by flash column chromatography (30-50% EtOAc/hexanes) yielded **5.51** as a clear oil (29 mg, 0.0622 mmol, 78%). <sup>1</sup>H NMR (400 MHz, CDCl<sub>3</sub>): δ 6.64 (dd, *J* = 16.6, 9.8 Hz, 1H), 6.49 (s, 1H), 6.43 (dd, *J* = 4.2, 3.7 Hz, 1H), 5.05 (ddd, *J* = 8.3, 3.3, 3.1 Hz, 1H), 4.90 (dd, *J* = 3.8, 3.7 Hz, 1H), 3.13 (s, 3H), 2.46 (dd, *J* = 14.3, 8.5 Hz, 1H), 2.33 (dd, *J* = 14.4, 2.5 Hz, 1H), 2.17 (br. s, 1H), 1.67 (ddd, *J* = 12.2, 12.2, 5.0 Hz, 1H), 1.54 (ddd, *J* = 11.7, 11.7, 5.0 Hz, 1H), 1.39-1.24 (m, 2H), 0.96 (dd, *J* = 7.3, 7.3 Hz, 3H).



To a solution of **5.42** (187 mg, 0.482 mmol, 1.0 eq) in CH<sub>2</sub>Cl<sub>2</sub> (2.4 mL) and DMAP (2 mg, catalytic) at –78 °C was added DIPEA (119 μL, 0.722 mmol, 1.5 eq) then vinyltriphenylchlorosilane (128 μL, 0.578 mmol, 1.2 eq) dropwise, and the reaction was stirred at –78 °C for 10 min. To the mixture was added saturated aqueous NH<sub>4</sub>Cl (20 mL), and at RT, the mixture was extracted with CH<sub>2</sub>Cl<sub>2</sub> (3 x 20 mL). The combined organic layers were dried (MgSO<sub>4</sub>), filtered, and concentrated. Purification by flash column chromatography (5-15% EtOAc/hexanes) provided **5.53** as a clear oil (241 mg, 0.404 mmol, 84%). [α]<sub>D</sub><sup>20</sup> +28.4 (*c* 1.19, CHCl<sub>3</sub>); <sup>1</sup>H NMR (400 MHz, CDCl<sub>3</sub>): δ 7.62 (dd, *J* = 8.0, 7.2 Hz, 5H), 7.51-7.44 (m, 2H), 7.43-7.36 (m, 3H), 7.32-7.23 (m, 5H), 6.50 (dd, *J* = 20.2, 14.9 Hz, 1H), 6.40 (br. s, 1H), 6.33 (dd, *J*

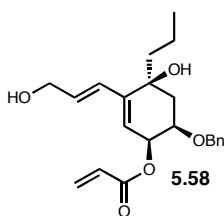


= 14.9, 3.7 Hz, 1H), 5.92 (dd,  $J$  = 20.2, 3.7 Hz, 1H), 4.83 (d,  $J$  = 11.9 Hz, 1H), 4.62 (d,  $J$  = 11.9 Hz, 1H), 4.40 (dd,  $J$  = 3.4, 2.2 Hz, 1H), 3.85 (dd,  $J$  = 4.3, 3.6 Hz, 1H), 3.82 (s, 1H), 2.22 (dd,  $J$  = 14.5, 5.1 Hz, 1H), 1.83 (app. d,  $J$  = 14.0 Hz, 1H), 1.56-1.46 (m, 2H), 1.16 (ddd,  $J$  = 14.8, 14.8, 7.3 Hz, 2H), 0.92 (dd,  $J$  = 7.4, 7.2 Hz, 3H);  $^{13}\text{C}$  NMR (100 MHz,  $\text{CDCl}_3$ ):  $\delta$  140.2, 138.1, 137.9, 135.0, 133.1, 130.3, 128.4, 128.0 (2C), 127.8, 127.7, 113.2, 75.7, 73.3, 73.1, 72.8, 44.7, 34.2, 16.9, 14.3; IR (film)  $\nu_{\text{max}}$  3502, 3050, 2958, 2871, 1428, 1114  $\text{cm}^{-1}$ ; HRMS (ESI)  $m/z$  calcd. for  $\text{C}_{30}\text{H}_{33}\text{INaO}_3\text{Si}$   $[\text{M}+\text{Na}]^+$  619.1136, found 619.1152.



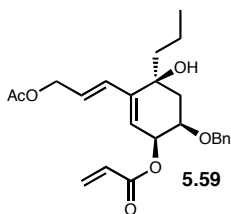
To a solution of **5.44** (15 mg, 0.0231 mmol, 1.0 eq) in THF (417  $\mu\text{L}$ ) was added  $\text{H}_2\text{O}$  (83  $\mu\text{L}$ ),  $\text{K}_2\text{CO}_3 \cdot 1.5\text{H}_2\text{O}$  (11 mg, 0.0692 mmol, 3.0 eq), **3.20** (4 mg, 0.0173 mmol, 0.75 eq) and  $\text{Pd}(\text{PPh}_3)_4$  (3 mg, 2.31  $\mu\text{mol}$ , 0.1 eq) and the reaction mixture was heated via microwave irradiation at 50  $^\circ\text{C}$  for 30 min. The reaction was diluted with EtOAc (10 mL), added to saturated aqueous  $\text{NH}_4\text{Cl}$  (10 mL), and extracted with EtOAc (3 x 10 mL). The combined organic layers were dried ( $\text{MgSO}_4$ ), filtered, and concentrated. Purification by flash column chromatography (10-25% EtOAc/hexanes) provided **5.56** as a yellow oil (5.0 mg, 9.08  $\mu\text{mol}$ , 39%).  $[\alpha]_{\text{D}}^{20}$  +51.8 ( $c$  0.19,  $\text{CHCl}_3$ );  $^1\text{H}$  NMR (400 MHz,  $\text{CDCl}_3$ ):  $\delta$  7.33-7.23 (m, 5H), 7.16 (ddd,  $J$  = 15.5, 6.7, 6.6 Hz, 1H), 6.41 (dd,  $J$  = 17.4, 11.0 Hz, 1H), 6.40 (d,  $J$  = 2.5 Hz, 1H), 5.87 (d,  $J$  = 15.7 Hz, 1H), 5.66 (s, 1H), 5.47 (d,  $J$  = 16.5 Hz, 1H), 5.40 (s, 1H), 5.09 (dd,  $J$  = 10.9, 1.0 Hz, 1H), 4.66 (d,  $J$  = 11.9 Hz, 1H), 4.57 (d,  $J$  = 11.9 Hz, 1H), 4.45 (sept.,  $J$  = 6.1 Hz, 1H), 4.07 (dd,  $J$  = 4.1, 3.8 Hz, 1H), 3.83 (s, 3H), 3.74 (s, 3H), 3.55-3.49 (m, 3H), 2.12 (dd,  $J$  = 14.6, 5.2 Hz, 1H), 1.86 (d,  $J$  = 13.9 Hz,

1H), 1.35-1.07 (m, 4H), 1.31 (s, 3H), 1.29 (s, 3H), 0.87 (dd,  $J = 7.4, 7.2$  Hz, 3H);  $^{13}\text{C}$  NMR (100 MHz,  $\text{CDCl}_3$ ):  $\delta$  166.0, 154.3, 153.5, 148.7, 144.3, 141.0, 137.7, 134.4, 131.3, 128.5, 127.9, 127.8, 121.7, 120.9, 115.8, 107.6, 100.7, 73.8, 73.0, 71.7, 71.2, 70.3, 60.9, 55.7, 41.4, 36.3, 33.0, 22.1, 16.9, 14.5; IR (film)  $\nu_{\text{max}}$  3512, 2963, 2934, 1715, 1596, 1492, 1151  $\text{cm}^{-1}$ ; HRMS (ESI)  $m/z$  calcd. for  $\text{C}_{33}\text{H}_{42}\text{NaO}_7$   $[\text{M}+\text{Na}]^+$  573.2823, found 573.2845.

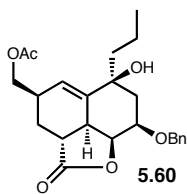


To a solution of **5.43** (287 mg, 0.649 mmol, 1.0 eq) in THF (10.8 mL) was added  $\text{H}_2\text{O}$  (2.2 mL) then  $\text{K}_2\text{CO}_3 \cdot 1.5\text{H}_2\text{O}$  (322 mg, 1.95 mmol, 3.0 eq), **4.41** (333 mg, 1.30 mmol, 2.0 eq) and  $\text{Pd}(\text{PPh}_3)_4$  (75 mg, 0.0649 mmol, 0.1 eq) and the reaction was heated via microwave irradiation at 50  $^\circ\text{C}$  for 1 h. The reaction was diluted with  $\text{CH}_2\text{Cl}_2$  (50 mL), added to 1 N aqueous HCl (50 mL) and extracted with  $\text{CH}_2\text{Cl}_2$  (3 x 50 mL). The combined organic layers were dried ( $\text{MgSO}_4$ ), filtered, and concentrated. Purification by flash column chromatography (20-80% EtOAc/hexanes) yielded **5.58** as an orange oil (114 mg, 0.306 mmol, 47%).  $[\alpha]_{\text{D}}^{20} +76.6$  ( $c$  0.24,  $\text{CHCl}_3$ );  $^1\text{H}$  NMR (400 MHz,  $\text{CDCl}_3$ ):  $\delta$  7.36-7.24 (m, 5H), 6.47 (dd,  $J = 17.3, 0.7$  Hz, 1H), 6.32 (d,  $J = 15.7$  Hz, 1H), 6.18 (dd,  $J = 17.5, 10.4$  Hz, 1H), 6.14 (ddd,  $J = 15.7, 5.8, 5.5$  Hz, 1H), 5.90 (dd,  $J = 10.5, 0.7$  Hz, 1H), 5.68 (s, 1H), 5.45 (s, 1H), 4.69 (d,  $J = 11.9$  Hz, 1H), 4.59 (d,  $J = 11.9$  Hz, 1H), 4.23-4.15 (m, 2H), 4.11-4.05 (m, 1H), 3.51 (s, 1H), 2.15 (dd,  $J = 14.4, 5.5$  Hz, 1H), 1.89 (dd,  $J = 14.5, 1.4$  Hz, 1H), 1.61-1.49 (m, 2H), 1.21-1.08 (m, 2H), 0.88 (dd,  $J = 7.3, 7.3$  Hz, 3H);  $^{13}\text{C}$  NMR (100 MHz,  $\text{CDCl}_3$ ):  $\delta$  165.7, 143.4, 137.6, 131.6, 130.7, 128.5, 128.2, 128.1, 127.9, 127.8, 120.9, 73.6, 72.9, 71.8, 71.4, 63.6, 41.4, 36.3, 24.8, 16.9, 14.5; IR (film)  $\nu_{\text{max}}$  3415, 2963, 2873, 1720,

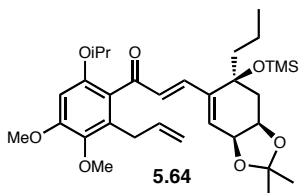
1406, 1195  $\text{cm}^{-1}$ ; HRMS (ESI)  $m/z$  calcd. for  $\text{C}_{22}\text{H}_{28}\text{NaO}_5$   $[\text{M}+\text{Na}]^+$  395.1829, found 395.1825.



To a solution of **5.58** (13 mg, 0.0349 mmol, 1.0 eq) in  $\text{CH}_2\text{Cl}_2$  (698  $\mu\text{L}$ ) at 0  $^\circ\text{C}$  was added  $\text{Ac}_2\text{O}$  (7  $\mu\text{L}$ , 0.0698 mmol, 2.0 eq) and pyridine (6  $\mu\text{L}$ , 0.0698 mmol, 2.0 eq) and the reaction was stirred at 0  $^\circ\text{C}$  for 1 h. To the reaction was added saturated aqueous  $\text{NH}_4\text{Cl}$  (10 mL) and the mixture was extracted with  $\text{CH}_2\text{Cl}_2$  (3 x 10 mL). The combined organic layers were dried ( $\text{MgSO}_4$ ), filtered, and concentrated. Purification by flash column chromatography (10-40% EtOAc/hexanes) provided **5.59** as a clear oil (10 mg, 0.0241 mmol, 69%).  $[\alpha]_{\text{D}}^{20} +89.0$  ( $c$  0.38,  $\text{CHCl}_3$ );  $^1\text{H}$  NMR (400 MHz,  $\text{CDCl}_3$ ):  $\delta$  7.36-7.27 (m, 5H), 6.47 (dd,  $J = 17.3, 1.0$  Hz, 1H), 6.36 (d,  $J = 15.7$  Hz, 1H), 6.18 (dd,  $J = 17.3, 10.5$  Hz, 1H), 6.05 (ddd,  $J = 15.8, 6.3, 6.1$  Hz, 1H), 5.91 (dd,  $J = 10.4, 1.0$  Hz, 1H), 5.69 (s, 1H), 5.44 (s, 1H), 4.69 (d,  $J = 11.9$  Hz, 1H), 4.63-4.56 (m, 3H), 4.10 (dd,  $J = 4.6, 2.3$  Hz, 1H), 3.55 (br. s, 1H), 2.15 (dd,  $J = 14.6, 5.3$  Hz, 1H), 2.06 (s, 3H), 1.88 (dd,  $J = 14.7, 1.4$  Hz, 1H), 1.63-1.48 (m, 2H), 1.22-1.05 (m, 2H), 0.89 (dd,  $J = 7.3, 7.3$  Hz, 3H);  $^{13}\text{C}$  NMR (100 MHz,  $\text{CDCl}_3$ ):  $\delta$  170.8, 165.7, 143.1, 137.6, 131.6, 131.2, 128.5, 128.2, 128.0, 127.8, 125.3, 121.7, 73.6, 73.1, 71.9, 71.3, 64.9, 41.5, 36.6, 21.0, 16.9, 14.4; IR (film)  $\nu_{\text{max}}$  3507, 2959, 2873, 1729, 1233, 1193  $\text{cm}^{-1}$ ; HRMS (ESI)  $m/z$  calcd. for  $\text{C}_{24}\text{H}_{30}\text{NaO}_6$   $[\text{M}+\text{Na}]^+$  437.1935, found 437.1927.



To a solution of **5.59** (8.0 mg, 0.0193 mmol, 1.0 eq) in toluene (1.0 mL) was added BHT (3 mg, catalytic) and the mixture was heated at 150 °C in a sealed tube for 96 h. At RT, the mixture was concentrated, and purification by flash column chromatography (10-50% EtOAc/hexanes) provided **5.60** as a light yellow oil (3.0 mg, 7.24 μmol, 38%).  $[\alpha]_{\text{D}}^{20} +18.5$  ( $c$  0.07, CHCl<sub>3</sub>); <sup>1</sup>H NMR (600 MHz, CDCl<sub>3</sub>): δ 7.37-7.23 (m, 5H), 5.68 (dd,  $J$  = 2.5, 2.5 Hz, 1H), 4.64 (d,  $J$  = 11.8 Hz, 1H), 4.62 (d,  $J$  = 11.7 Hz, 1H), 4.41 (dd,  $J$  = 9.1, 3.1 Hz, 1H), 4.20 (ddd,  $J$  = 4.4, 4.4, 2.0 Hz, 1H), 4.01 (dd,  $J$  = 10.8, 5.8 Hz, 1H), 3.94 (dd,  $J$  = 10.8, 7.2 Hz, 1H), 2.86-2.80 (m, 1H), 2.80 (dd,  $J$  = 12.7, 4.4 Hz, 1H), 2.72 (dddd,  $J$  = 12.9, 11.7, 2.5, 2.5 Hz, 1H), 2.45 (br. s, 1H), 2.25 (dd,  $J$  = 15.6, 4.6 Hz, 1H), 1.96 (ddd,  $J$  = 13.3, 4.4, 2.0 Hz, 1H), 1.94 (s, 3H), 1.84 (ddd,  $J$  = 12.8, 12.8, 9.3 Hz, 1H), 1.72 (dd,  $J$  = 15.6, 1.7 Hz, 1H), 1.60-1.52 (m, 2H), 1.37-1.23 (m, 2H), 0.91 (dd,  $J$  = 7.3, 7.2 Hz, 3H); <sup>13</sup>C NMR (150 MHz, CDCl<sub>3</sub>): δ 176.2, 171.1, 148.4, 137.4, 128.7, 128.1, 127.5, 123.5, 78.2, 75.1, 73.2, 72.2, 67.4, 46.0, 43.2, 40.4, 39.4, 35.3, 24.6, 20.8, 17.4, 14.3; IR (film)  $\nu_{\text{max}}$  3403, 2956, 1780, 1737, 1244, 1090 cm<sup>-1</sup>; HRMS (ESI)  $m/z$  calcd. for C<sub>24</sub>H<sub>30</sub>NaO<sub>6</sub> [M+Na]<sup>+</sup> 437.1935, found 437.1911.

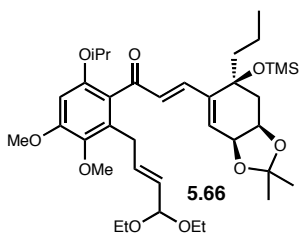


To a solution of **5.6** (736 mg, 2.34 mmol, 1.1 eq, dried by azeotropic removal of H<sub>2</sub>O with benzene 2x and on high-vac overnight) in THF (5.3 mL, dried over activated 4 Å MS overnight) at -78 °C was added *n*-BuLi (2.5 M in hexanes, 1.04 mL, 2.55 mmol, 1.2 eq) dropwise and the yellow mixture was stirred at -78 °C for 30 min. To the mixture at -78 °C was added a solution of **4.62** (719 mg, 2.12 mmol, 1.0 eq, dried by azeotropic removal

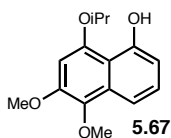
of H<sub>2</sub>O with benzene 2x and on high-vac for 2 h) in THF (5.3 mL, dried over activated 4 Å MS overnight) via cannula and the reaction was stirred at –78 °C for 30 min and at 0 °C for 1.5 h. To the reaction was added saturated aqueous NH<sub>4</sub>Cl (40 mL) and the mixture was extracted with CH<sub>2</sub>Cl<sub>2</sub> (3 x 40 mL). The combined organic layers were dried (MgSO<sub>4</sub>), filtered, and concentrated. Purification by flash column chromatography (10-40% EtOAc/hexanes) provided **5.63** as an inseparable mixture of diastereomers as a yellow oil (992 mg, 1.73 mmol, 81%). The material was taken forward without characterization.

To a solution of **5.63** (992 mg, 1.73 mmol, 1.0 eq) in CH<sub>2</sub>Cl<sub>2</sub> (35 mL) was added MnO<sub>2</sub> (3.00 g, 34.5 mmol, 20 eq) and the black slurry was stirred at RT for 6 h. The reaction was diluted with CH<sub>2</sub>Cl<sub>2</sub> (50 mL) and filtered through a plug of Celite with CH<sub>2</sub>Cl<sub>2</sub> washes. The filtrate was concentrated, and purification by flash column chromatography (10-30% EtOAc/hexanes) provided **5.64** as a yellow oil (860 mg, 1.50 mmol, 87%).  $[\alpha]_{\text{D}}^{20} +73.9$  (*c* 0.22, CDCl<sub>3</sub>); <sup>1</sup>H NMR (400 MHz, C<sub>6</sub>D<sub>6</sub>): δ 7.39 (d, *J* = 16.2 Hz, 1H), 7.09 (d, *J* = 16.2 Hz, 1H), 6.26 (s, 1H), 6.15 (dddd, *J* = 17.0, 10.1, 6.4, 6.4 Hz, 1H), 6.00 (d, *J* = 3.9 Hz, 1H), 5.18 (ddd, *J* = 17.0, 3.3, 1.5 Hz, 1H), 5.01 (ddd, *J* = 10.0, 1.8, 1.2 Hz, 1H), 4.17-4.08 (m, 2H), 4.05 (sept., *J* = 5.6 Hz, 1H), 3.77-3.64 (m, 2H), 3.71 (s, 3H), 3.34 (s, 3H), 2.27 (dd, *J* = 11.8, 5.5 Hz, 1H), 1.97 (dd, *J* = 11.5, 11.4 Hz, 1H), 1.57 (ddd, *J* = 12.8, 12.8, 4.1 Hz, 1H), 1.49 (s, 3H), 1.46-1.32 (m, 2H), 1.32-1.24 (m, 1H), 1.29 (s, 3H), 1.11 (d, *J* = 6.1 Hz, 3H), 1.08 (d, *J* = 6.1 Hz, 3H), 0.81 (dd, *J* = 7.3, 7.3 Hz, 3H), 0.12 (s, 9H); <sup>13</sup>C NMR (150 MHz, C<sub>6</sub>D<sub>6</sub>): δ 195.9, 154.3, 152.1, 147.2, 142.8, 141.6, 137.6, 133.1, 132.0, 125.3, 115.8, 109.5, 99.9, 77.1, 72.4, 72.3, 71.4, 60.6, 55.6, 43.5, 40.0, 31.8, 28.5,

25.9, 22.3, 22.2, 17.2, 14.6, 2.1; IR (film)  $\nu_{\max}$  2962, 2874, 2279, 1653, 1593, 1323, 1255  $\text{cm}^{-1}$ ; HRMS (ESI)  $m/z$  calcd. for  $\text{C}_{32}\text{H}_{49}\text{O}_7\text{Si}$   $[\text{M}+\text{H}]^+$  573.3242, found 573.3266.

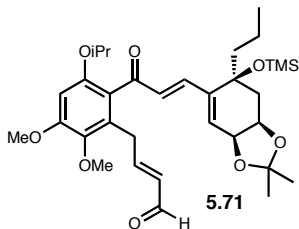


To a solution of **5.64** (26 mg, 0.0454 mmol, 1.0 eq) in  $\text{CH}_2\text{Cl}_2$  (454  $\mu\text{L}$ ) was added acrolein diethyl acetal (**5.65**, 173  $\mu\text{L}$ , 1.13 mmol, 25 eq) and Hoveyda-Grubbs second generation catalyst (3.0 mg, 4.54  $\mu\text{mol}$ , 0.1 eq) and the reaction was heated via microwave irradiation at 50  $^\circ\text{C}$  for 1 h. The reaction mixture was concentrated, and purification by flash column chromatography (10-40% EtOAc/hexanes) yielded **5.66** as a yellow oil (11 mg, 0.0163 mmol, 36%).  $[\alpha]_{\text{D}}^{20} +51.0$  ( $c$  0.78,  $\text{CDCl}_3$ );  $^1\text{H}$  NMR (400 MHz,  $\text{C}_6\text{D}_6$ ):  $\delta$  7.40 (d,  $J$  = 16.2 Hz, 1H), 7.08 (d,  $J$  = 16.2 Hz, 1H), 6.28 (ddd,  $J$  = 15.9, 7.1, 6.6 Hz, 1H), 6.24 (s, 1H), 6.02 (d,  $J$  = 3.8 Hz, 1H), 5.83 (dd,  $J$  = 15.6, 5.0 Hz, 1H), 4.92 (d,  $J$  = 5.0 Hz, 1H), 4.17 (dd,  $J$  = 6.4, 4.0 Hz, 1H), 4.15-4.03 (m, 2H), 3.75 (s, 3H), 3.71-3.55 (m, 4H), 3.41 (ddd,  $J$  = 16.4, 7.1, 1.5 Hz, 2H), 3.32 (s, 3H), 2.27 (dd,  $J$  = 11.8, 5.4 Hz, 1H), 1.96 (dd,  $J$  = 11.4, 11.4 Hz, 1H), 1.56 (ddd,  $J$  = 12.9, 12.9, 4.4 Hz, 1H), 1.49 (s, 3H), 1.45-1.35 (m, 2H), 1.28 (s, 6H), 1.23-1.16 (m, 1H), 1.15-1.04 (m, 9H), 0.82 (dd,  $J$  = 7.3, 7.2 Hz, 3H), 0.13 (s, 9H);  $^{13}\text{C}$  NMR (100 MHz,  $\text{C}_6\text{D}_6$ ):  $\delta$  195.8, 154.3, 152.0, 147.0, 143.0, 141.6, 133.0, 132.9, 131.9, 129.9, 125.5, 125.2, 109.5, 101.6, 100.1, 77.1, 72.5, 72.3, 71.5, 60.6, 60.5, 55.5, 43.6, 40.2, 30.6, 28.5, 25.8, 22.2, 17.2, 15.6, 14.6, 2.2; IR (film)  $\nu_{\max}$  2970, 2935, 2874, 1653, 1594, 1254, 1050  $\text{cm}^{-1}$ ; HRMS (ESI)  $m/z$  calcd. for  $\text{C}_{37}\text{H}_{58}\text{NaO}_9\text{Si}$   $[\text{M}+\text{Na}]^+$  697.3742, found 697.3773.



From the above reaction, **5.67** was formed (7 mg, 0.0267 mmol, 59%).  $^1\text{H}$

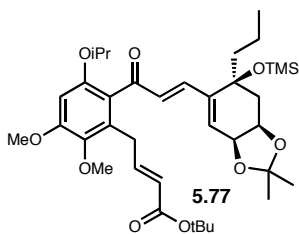
NMR (400 MHz,  $\text{CDCl}_3$ ):  $\delta$  9.64 (s, 1H), 7.54 (d,  $J$  = 8.4 Hz, 1H), 7.33 (dd,  $J$  = 8.0, 8.0 Hz, 1H), 6.73 (d,  $J$  = 7.6 Hz, 1H), 6.64 (s, 1H), 4.81 (sept.,  $J$  = 6.1 Hz, 1H), 3.97 (s, 3H), 3.90 (s, 3H), 1.51 (s, 3H), 1.50 (s, 3H);  $^{13}\text{C}$  NMR (100 MHz,  $\text{CDCl}_3$ ):  $\delta$  154.9, 150.8, 147.9, 137.8, 131.7, 128.0, 112.2 (2C), 108.4, 98.1, 73.5, 61.0, 57.3, 22.0; IR (film)  $\nu_{\text{max}}$  3370, 2978, 2935, 1611, 1387, 1108  $\text{cm}^{-1}$ ; HRMS (ESI)  $m/z$  calcd. for  $\text{C}_{15}\text{H}_{19}\text{O}_4$   $[\text{M}+\text{H}]^+$  263.1278, found 263.1256.



To a solution of **5.66** (10 mg, 0.0148 mmol, 1.0 eq) in  $\text{CH}_2\text{Cl}_2$  (500  $\mu\text{L}$ ) at  $-78^\circ\text{C}$  was added  $\text{BF}_3\cdot\text{OEt}_2$  (9  $\mu\text{L}$ , 0.0741 mmol, 5.0 eq) and the reaction was stirred at  $-78^\circ\text{C}$  for 45 min. To the reaction was added saturated aqueous  $\text{NaHCO}_3$  (5 mL) and the

mixture was extracted with  $\text{CH}_2\text{Cl}_2$  (3 x 10 mL). The combined organic layers were dried ( $\text{MgSO}_4$ ), filtered, and concentrated. Purification by flash column chromatography (20-50% EtOAc/hexanes) provided **5.71** as a yellow oil (4.0 mg, 6.66  $\mu\text{mol}$ , 45%).  $[\alpha]_{\text{D}}^{20} +2.1$  ( $c$  0.23,  $\text{CDCl}_3$ );  $^1\text{H}$  NMR (400 MHz,  $\text{CDCl}_3$ ):  $\delta$  9.43 (d,  $J$  = 7.9 Hz, 1H), 7.00 (d,  $J$  = 16.1 Hz, 1H), 6.89 (ddd,  $J$  = 15.6, 6.6, 6.4 Hz, 1H), 6.85 (d,  $J$  = 16.0 Hz, 1H), 6.46 (s, 1H), 6.09 (d,  $J$  = 3.8 Hz, 1H), 6.02 (dd,  $J$  = 15.5, 7.9 Hz, 1H), 4.53 (dd,  $J$  = 6.6, 3.9 Hz, 1H), 4.42 (sept.,  $J$  = 6.1 Hz, 1H), 4.29 (ddd,  $J$  = 12.0, 12.0, 6.0 Hz, 1H), 3.88 (s, 3H), 3.76 (s, 3H), 3.57 (ddd,  $J$  = 15.5, 7.8, 1.1 Hz, 1H), 3.50 (ddd,  $J$  = 15.6, 6.3, 1.3 Hz, 1H), 2.24 (dd,  $J$  = 11.9, 5.5 Hz, 1H), 1.74 (dd,  $J$  = 11.7, 11.4 Hz, 1H), 1.47 (s, 3H), 1.42-1.31 (m, 2H), 1.37 (s, 3H), 1.30-1.18 (m, 2H), 0.87 (dd,  $J$  = 7.1, 7.1 Hz, 3H), 0.02 (s, 9H);  $^{13}\text{C}$  NMR (150 MHz,  $\text{CDCl}_3$ ):  $\delta$  196.7, 193.9, 156.5, 154.0, 152.0, 147.2, 143.1, 141.6, 133.4,

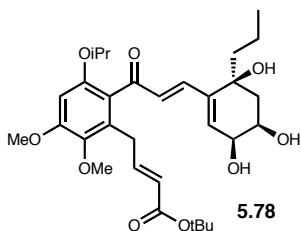
131.0, 129.5, 125.8, 123.5, 109.6, 99.1, 72.1, 72.0, 71.0, 60.9, 55.9, 43.1, 39.3, 30.7, 29.7, 28.0, 25.6, 22.2, 16.8, 14.3, 2.0; IR (film)  $\nu_{\max}$  3386, 2931, 1690, 1593, 1453, 1250, 1048  $\text{cm}^{-1}$ ; HRMS (ESI)  $m/z$  calcd. for  $\text{C}_{33}\text{H}_{48}\text{NaO}_8\text{Si}$   $[\text{M}+\text{Na}]^+$  623.3011, found 623.3023.



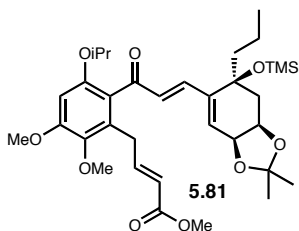
To **5.64** (41 mg, 0.0716 mmol, 1.0 eq) at RT was added *t*-butyl acrylate (**5.76**, 524  $\mu\text{L}$ , 3.58 mmol, 50 eq) then Hoveyda-Grubbs second generation catalyst (7.16  $\mu\text{mol}$ , 0.1 eq) and the reaction was stirred at RT for 5 h. The reaction was loaded

directly onto a silica gel column, and purification by flash column chromatography (10-30% EtOAc/hexanes) yielded **5.77** as a yellow oil (31 mg, 0.0461 mmol, 64%).  $[\alpha]_{\text{D}}^{20} +50.0$  ( $c$  0.45,  $\text{CDCl}_3$ );  $^1\text{H}$  NMR (400 MHz,  $\text{C}_6\text{D}_6$ ):  $\delta$  7.39 (d,  $J = 16.4$  Hz, 1H), 7.32 (ddd,  $J = 15.6, 6.5, 6.5$  Hz, 1H), 7.09 (d,  $J = 16.1$  Hz, 1H), 6.22 (s, 1H), 6.05-5.97 (m, 2H), 4.20 (dd,  $J = 6.3, 4.0$  Hz, 1H), 4.13-4.03 (m, 2H), 3.67-3.58 (m, 2H), 3.63 (s, 3H), 3.28 (s, 3H), 2.29 (dd,  $J = 11.8, 5.4$  Hz, 1H), 1.97 (dd,  $J = 11.5, 11.4$  Hz, 1H), 1.69-1.54 (m, 2H), 1.49 (s, 3H), 1.37 (s, 9H), 1.32-1.13 (m, 2H), 1.29 (s, 3H), 1.09 (d,  $J = 6.0$  Hz, 3H), 1.06 (d,  $J = 6.1$  Hz, 3H), 0.85 (dd,  $J = 7.3, 7.2$  Hz, 3H), 0.15 (s, 9H);  $^{13}\text{C}$  NMR (100 MHz,  $\text{C}_6\text{D}_6$ ):  $\delta$  195.4, 165.7, 154.3, 152.2, 147.2, 146.1, 142.9, 141.9, 131.8, 131.3, 125.7, 125.5, 124.6, 109.5, 100.4, 79.4, 77.1, 72.6, 72.3, 71.5, 60.5, 55.5, 43.5, 40.1, 30.2, 28.5, 28.2 (2C), 25.8, 22.2, 17.3, 14.6, 2.2; IR (film)  $\nu_{\max}$  2964, 1712, 1653, 1593, 1453, 1254, 1150  $\text{cm}^{-1}$ ; HRMS (ESI)  $m/z$  calcd. for  $\text{C}_{37}\text{H}_{57}\text{O}_9\text{Si}$   $[\text{M}+\text{H}]^+$  673.3766, found 673.3758.





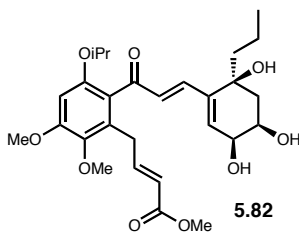
To a solution of **5.77** (12 mg, 0.0178 mmol, 1.0 eq) in THF (400  $\mu$ L) at 0  $^{\circ}$ C was added H<sub>2</sub>O (100  $\mu$ L) then TFA (27  $\mu$ L, 0.357 mmol, 20 eq) and the reaction was stirred at 0  $^{\circ}$ C for 15 min and at RT for 48 h. To the reaction was added EtOAc (10 mL) and the mixture was washed with saturated aqueous NaHCO<sub>3</sub> (2 x 10 mL). The combined aqueous layers were extracted with EtOAc (2 x 10 mL), and the combined organic layers were washed with saturated aqueous NH<sub>4</sub>Cl (1 x 10 mL), then dried (MgSO<sub>4</sub>), filtered, and concentrated. Purification by flash column chromatography (40-100% EtOAc/hexanes) provided **5.78** as a yellow oil (6.0 mg, 0.0107 mmol, 60%).  $[\alpha]_{\text{D}}^{20} +24.0$  (*c* 0.30, CDCl<sub>3</sub>); <sup>1</sup>H NMR (600 MHz, CDCl<sub>3</sub>):  $\delta$  7.01 (d, *J* = 16.0 Hz, 1H), 6.84 (ddd, *J* = 15.6, 6.7, 6.7 Hz, 1H), 6.76 (d, *J* = 16.0 Hz, 1H), 6.43 (s, 1H), 5.88 (s, 1H), 5.57 (d, *J* = 15.4 Hz, 1H), 4.42 (sept., *J* = 6.1 Hz, 1H), 4.20 (br. m, 1H), 4.14 (br. m, 1H), 3.88 (s, 3H), 3.77 (s, 3H), 3.71 (s, 1H), 3.62 (br. s, 1H), 3.44 (ddd, *J* = 15.4, 6.5, 1.5 Hz, 1H), 3.37 (ddd, *J* = 15.2, 7.1, 0.9 Hz, 1H), 3.06 (br. s, 1H), 2.13 (dd, *J* = 14.8, 5.0 Hz, 1H), 1.81 (dd, *J* = 14.7, 1.5 Hz, 1H), 1.61-1.53 (m, 2H), 1.46-1.35 (m, 2H), 1.42 (s, 9H), 1.26 (d, *J* = 6.1 Hz, 3H), 1.24 (d, *J* = 6.2 Hz, 3H), 0.87 (dd, *J* = 7.3, 7.2 Hz, 3H); <sup>13</sup>C NMR (150 MHz, CDCl<sub>3</sub>):  $\delta$  196.7, 166.5, 153.9, 151.7, 145.8, 144.5, 141.5, 141.3, 131.2, 131.0, 130.0, 124.0, 123.5, 98.8, 80.6, 71.8, 71.1, 69.0, 67.9, 60.9, 55.8, 42.1, 37.3, 29.8, 28.1, 22.2, 22.0, 17.1, 14.4; IR (film)  $\nu_{\text{max}}$  3424, 2930, 1710, 1652, 1592, 1324, 1152 cm<sup>-1</sup>; HRMS (ESI) *m/z* calcd. for C<sub>31</sub>H<sub>44</sub>NaO<sub>9</sub> [M+Na]<sup>+</sup> 583.2878, found 583.2886.



To **5.64** (149 mg, 0.260 mmol, 1.0 eq) was added methyl acrylate (**5.80**, 1.17 mL, 13.0 mmol, 50 eq) and Hoveyda-Grubbs second generation catalyst (16 mg, 0.0260 mmol, 0.1 eq) and the reaction was stirred at RT for 22 h. The reaction mixture was

added directly to silica gel column, and purification by flash column chromatography (10-40% EtOAc/hexanes) provided **5.81** as a yellow oil (129 mg, 0.204 mmol, 79%). [ $\alpha$ ]

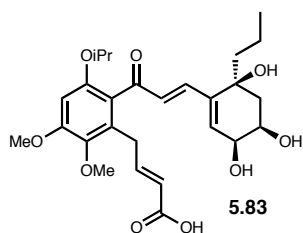
$^{20}_{\text{D}}$  +52.7 ( $c$  0.61,  $\text{CDCl}_3$ );  $^1\text{H}$  NMR (400 MHz,  $\text{CDCl}_3$ ):  $\delta$  6.98 (ddd,  $J = 15.8, 7.0, 6.0$  Hz, 2H), 6.82 (d,  $J = 16.2$  Hz, 1H), 6.43 (s, 1H), 6.07 (d,  $J = 3.8$  Hz, 1H), 5.69 (d,  $J = 15.7$  Hz, 1H), 4.51 (dd,  $J = 6.5, 3.9$  Hz, 1H), 4.40 (sept.,  $J = 6.1$  Hz, 1H), 4.28 (ddd,  $J = 11.6, 11.6, 5.9$  Hz, 1H), 3.87 (s, 3H), 3.75 (s, 3H), 3.63 (s, 3H), 3.42 (d,  $J = 6.4$  Hz, 2H), 2.23 (dd,  $J = 11.8, 5.6$  Hz, 1H), 1.73 (dd,  $J = 11.6, 11.4$  Hz, 1H), 1.54 (ddd,  $J = 13.1, 13.1, 4.8$  Hz, 1H), 1.46 (s, 3H), 1.36 (s, 3H), 1.34-1.25 (m, 3H), 1.25 (d,  $J = 6.0$  Hz, 3H), 1.23 (d,  $J = 6.0$  Hz, 3H), 0.86 (dd,  $J = 7.5, 7.1$  Hz, 3H), 0.01 (s, 9H);  $^{13}\text{C}$  NMR (100 MHz,  $\text{CDCl}_3$ ):  $\delta$  196.7, 166.8, 153.9, 151.8, 147.3, 147.1, 143.0, 141.6, 131.2, 130.0, 125.6, 123.7, 121.8, 109.5, 99.0, 76.6, 72.0 (2C), 71.0, 60.9, 55.9, 51.2, 43.1, 39.3, 29.9, 28.0, 25.6, 22.1 (2C), 16.8, 14.3, 1.9; IR (film)  $\nu_{\text{max}}$  2960, 2874, 1724, 1654, 1594, 1452, 1267, 1048  $\text{cm}^{-1}$ ; HRMS (ESI)  $m/z$  calcd. for  $\text{C}_{34}\text{H}_{51}\text{O}_9\text{Si}$   $[\text{M}+\text{H}]^+$  631.3297, found 631.3270.



To **5.81** (116 mg, 0.184 mmol, 1.0 eq) at RT was added  $\text{H}_2\text{O}$  (2.8 mL) then AcOH (6.4 mL) and the mixture was stirred at RT for 22 h. The mixture was diluted with EtOAc (30 mL) and carefully washed with saturated aqueous  $\text{NaHCO}_3$  (3 x 25 mL).

The combined aqueous layers were extracted with EtOAc (1 x 25 mL), and the combined

organic layers were dried (MgSO<sub>4</sub>), filtered, and concentrated. The material was taken forward crude except for characterization purposes, for which purification by flash column chromatography (60-100% EtOAc/hexanes) provided **5.82** as a yellow oil.  $[\alpha]_D^{20} +77.0$  (*c* 1.19, CDCl<sub>3</sub>); <sup>1</sup>H NMR (400 MHz, CDCl<sub>3</sub>): δ 6.99 (d, *J* = 16.3 Hz, 1H), 6.95 (ddd, *J* = 15.6, 6.6, 6.4 Hz, 1H), 6.74 (d, *J* = 16.0 Hz, 1H), 6.43 (s, 1H), 5.84 (s, 1H), 5.65 (ddd, *J* = 15.6, 1.5, 1.3 Hz, 1H), 4.41 (sept., *J* = 6.1 Hz, 1H), 4.18 (br. m, 1H), 4.12 (br. m, 1H), 3.87 (s, 3H), 3.75 (s, 3H), 3.63 (s, 3H), 3.47 (ddd, *J* = 15.6, 6.3, 1.6 Hz, 1H), 3.39 (ddd, *J* = 15.5, 6.8, 1.4 Hz, 1H), 3.21 (br. s, 1H), 2.10 (dd, *J* = 14.7, 5.0 Hz, 1H), 1.79 (dd, *J* = 14.7, 1.5 Hz, 1H), 1.58-1.50 (m, 2H), 1.24 (d, *J* = 6.1 Hz, 3H), 1.23 (d, *J* = 6.1 Hz, 3H), 1.19-1.03 (m, 2H), 0.84 (dd, *J* = 7.3, 7.2 Hz, 3H); <sup>13</sup>C NMR (100 MHz, CDCl<sub>3</sub>): δ 196.7, 167.4, 153.9, 151.8, 147.5, 144.3, 141.4, 141.2, 131.2, 130.9, 129.8, 123.5, 121.8, 98.9, 71.8, 71.1, 69.0, 67.9, 60.9, 55.8, 51.5, 41.9, 37.4, 29.8, 22.2, 22.0, 17.0, 14.4; IR (film)  $\nu_{\max}$  3425, 2961, 1719, 1652, 1593, 1451, 1274 cm<sup>-1</sup>; HRMS (ESI) *m/z* calcd. for C<sub>28</sub>H<sub>38</sub>NaO<sub>9</sub> [M+Na]<sup>+</sup> 541.2408, found 541.2403.



To a solution of **5.82** (95 mg crude, 0.184 mmol, 1.0 eq) in THF (6.9 mL) at 4 °C was added a solution of LiOH (44 mg, 1.84 mmol, 10 eq) in H<sub>2</sub>O (2.3 mL) and the reaction was stirred at 4 °C for 22 h. The reaction was added directly to a silica gel

column, and purification by flash column chromatography (5-15% MeOH/CH<sub>2</sub>Cl<sub>2</sub>) yielded **5.83** as a brown oil (53 mg, 0.105 mmol, 57% two steps). IR (film)  $\nu_{\max}$  3411, 2934, 2250, 1703, 1652, 1592, 1323, 1235, 1113 cm<sup>-1</sup>; HRMS (ESI) *m/z* calcd. for C<sub>27</sub>H<sub>37</sub>O<sub>9</sub> [M+H]<sup>+</sup> 505.2432, found 505.2447.

## References

1. Romaine, I. M.; Hempel, J. E.; Shanmugam, G.; Hori, H.; Igarashi, Y.; Polavarapu, P. L.; Sulikowski, G. A. "Assignment and stereocontrol of hibarimicin atropoisomers" *Org. Lett.*, **2011**, *13*, 4538-4541.
2. Hori, H.; Igarashi, Y.; Kajiura, T.; Sato, S.; Furumai, T.; Higashi, K.; Ishiyama, T.; Uehara, Y.; Oki, T. "Structure, biosynthesis and biological activities of v-Src tyrosine specific protein kinase inhibitor, hibarimicins" *Tennen Yuki Kagobutsu Toronkai Koen Yoshishu*, **2004**, *46*, 49-54.
3. Tatsuta, K.; Fukuda, T.; Ishimori, T.; Yachi, R.; Yoshida, S.; Hashimoto, H.; Hosokawa, S. "The first total synthesis of hibarimicinone, a potent v-Src tyrosine kinase inhibitor" *Tet. Lett.*, **2012**, *53*, 422-425.
4. Park, Y. S.; Grove, C. I.; González-López, M.; Urgaonkar, S.; Fettingner, J. C.; Shaw, J. T. "Synthesis of (–)-viriditoxin: a 6,6'-binaphthopyran-2-one that targets the bacterial cell division protein FtsZ" *Angew. Chem. Int. Ed.*, **2011**, *50*, 3730-3733.
5. Gross, P. J.; Hartmann, C. E.; Nieger, M.; Bräse, S. "Synthesis of methoxyfumimycin with 1,2-addition to ketimines" *J. Org. Chem.*, **2010**, *75*, 229-232.
6. Roy, A.; Reddy, K. R.; Mohanta, P. K.; Ila, H.; Junjappat, H. "Hydrogen peroxide/boric acid: an efficient system for oxidation of aromatic aldehydes and ketones to phenols" *Synth. Commun.*, **1999**, *29*, 3781-3791.
7. Oppolzer, W.; Mirza, S. "Stereospecific, R<sub>2</sub>AlCl-promoted intramolecular ene reaction of a 1,6-dienoate: evidence for a concerted mechanism" *Helv. Chim. Acta*, **1984**, *67*, 730-738.
8. Bolster, M. G.; Jansen, B. J. M.; de Groot, A. "The synthesis of Ambrox<sup>®</sup>-like compounds starting from (+)-larixol" *Tetrahedron*, **2001**, *57*, 5663-5679.
9. Sharpless, K. B.; Michaelson, R. C. "High stereo- and regioselectivities in the transition-metal catalyzed epoxidations of olefinic alcohols by *tert*-butyl hydroperoxide" *J. Am. Chem. Soc.*, **1973**, *95*, 6136-6137.
10. Wang, Z.; Cui, Y.-T.; Xu, Z.-B.; Qu, J. "Hot water-promoted ring-opening of epoxides and aziridines by water and other nucleophiles" *J. Org. Chem.*, **2008**, *73*, 2270-2274.

11. Dumortier, L.; Van der Eycken, J.; Vandewalle, M. "The synthesis of chiral isopropylidene derivatives of 1,2,3-cyclohexanetriols by enzymatic differentiation" *Tet. Lett.*, **1989**, *30*, 3201-3204.
12. Kennedy, J. W. J.; Hall, D. G. "Lewis acid catalyzed allylboration: discovery, optimization, and application to the formation of stereogenic quaternary carbon centers" *J. Org. Chem.*, **2004**, *69*, 4412-4428.
13. Ishihara, K.; Kubota, M.; Kurihara, H.; Yamamoto, H. "Scandium trifluoromethanesulfonate as an extremely active lewis acid catalyst in acylation of alcohols with acid anhydrides and mixed anhydrides" *J. Org. Chem.*, **1996**, *61*, 4560-4567.
14. Lee, H. M.; Nieto-Oberhuber, C.; Shair, M. D. "Enantioselective synthesis of (+)-cortistatin A, a potent and selective inhibitor of endothelial cell proliferation" *J. Am. Chem. Soc.*, **2008**, *130*, 16864-16866.
15. Schauer, D. J.; Helquist, P. "Mild zinc-promoted Horner-Wadsworth-Emmons reactions of diprotic phosphonate reagents" *Synthesis*, **2006**, *21*, 3654-3660.
16. Chatterjee, A. K.; Choi, T.-L.; Sanders, D. P.; Grubbs, R. H. "A general model for selectivity in olefin cross metathesis" *J. Am. Chem. Soc.*, **2003**, *125*, 11360-11370.
17. Dai, M.; Sarlah, D.; Yu, M.; Danishefsky, S. J.; Jones, G. O.; Houk, K. N. "Highly selective Diels-Alder reactions of directly connected enyne dienophiles" *J. Am. Chem. Soc.*, **2007**, *129*, 645-657.
18. Pietraszuk, C.; Fischer, H.; Rogalski, S.; Marciniak, B. "The effect of substituents at silicon on the cross-metathesis of trisubstituted vinylsilanes with olefins" *J. Organometallic Chem.*, **2005**, *690*, 5912-5921.
19. Sieburth, S. M.; Fensterbank, L. "An intramolecular Diels-Alder reaction of vinylsilanes" *J. Org. Chem.*, **1992**, *57*, 5279-5281.
20. Metz, P.; Fleischer, M.; Fröhlich, R. "Intramolecular Diels-Alder reaction of vinylsulfonates derived from hydroxyalkyl substituted 1,3-dienes and oxidative desulfurization of the resultant sultones" *Tetrahedron*, **1995**, *51*, 711-732.
21. Krenske, E. H.; Perry, E. W.; Jerome, S. V.; Maimone, T. J.; Baran, P. S.; Houk, K. N. "Why a proximity-induced Diels-Alder reaction is so fast" *Org. Lett.*, **2012**, *14*, 3016-3019.

22. Wang, Y.; Janjic, J.; Kozmin, S. A. "Synthesis of leucascandrolide A via a spontaneous macrolactolization" *J. Am. Chem. Soc.*, **2002**, *124*, 13670-13671.
23. Li, J.; Todaro, L.; Mootoo, D. R. "Synthesis of an A'B' precursor to angelmicin B: Product diversification in the Suárez lactol fragmentation" *Eur. J. Org. Chem.*, **2011**, 6281-6287.
24. Still, W. C.; Kahn, M.; Mitra, A. "Rapid chromatographic technique for preparative separations with moderate resolution" *J. Org. Chem.*, **1978**, *43*, 2923-2925.

## **Appendix A3:**

### **Spectra Relevant to Chapter V.**

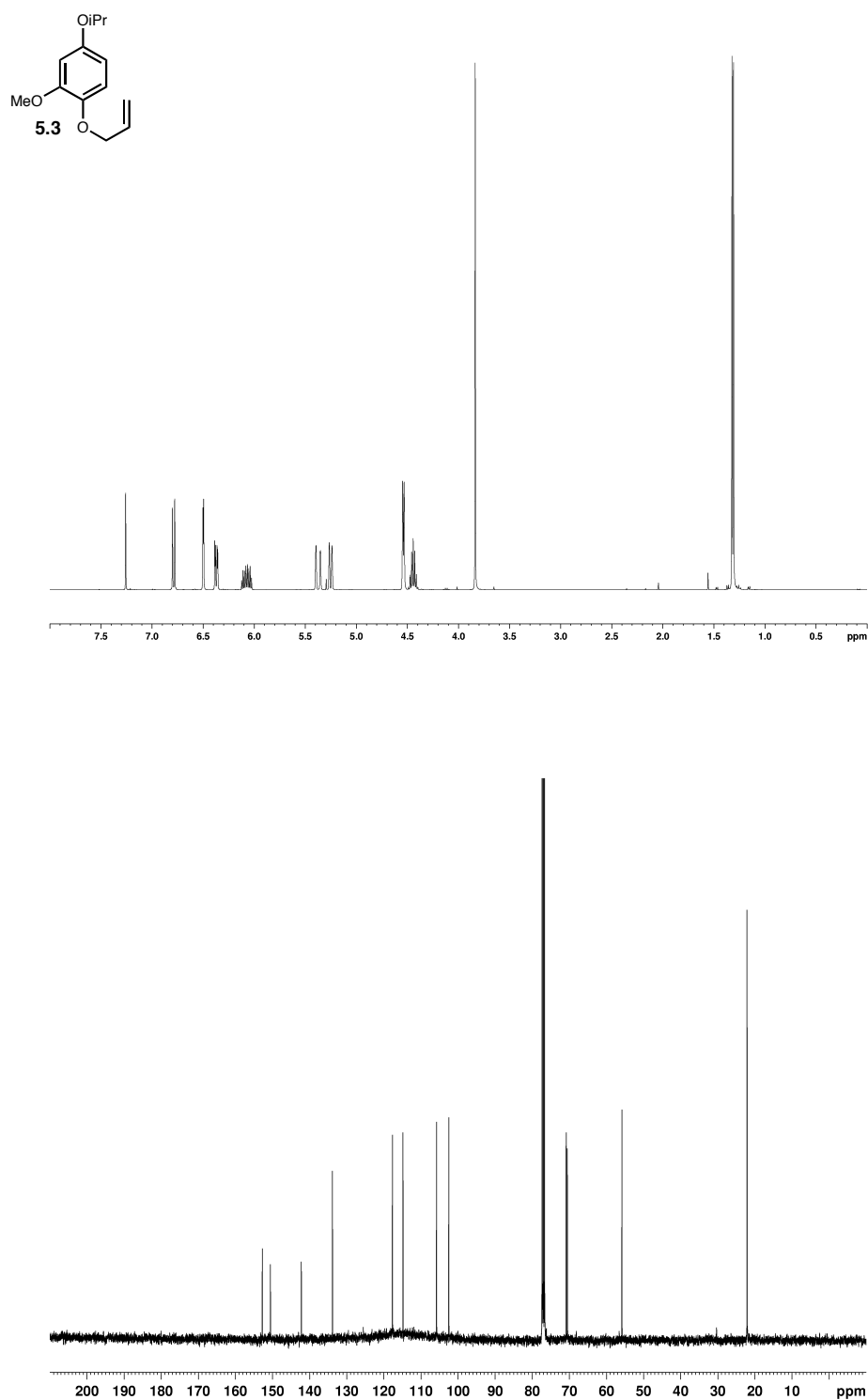


**Figure A3.1.** <sup>1</sup>H NMR spectrum (400 MHz, CDCl<sub>3</sub>) and <sup>13</sup>C NMR spectrum (100 MHz, CDCl<sub>3</sub>) of compound **5.3**.



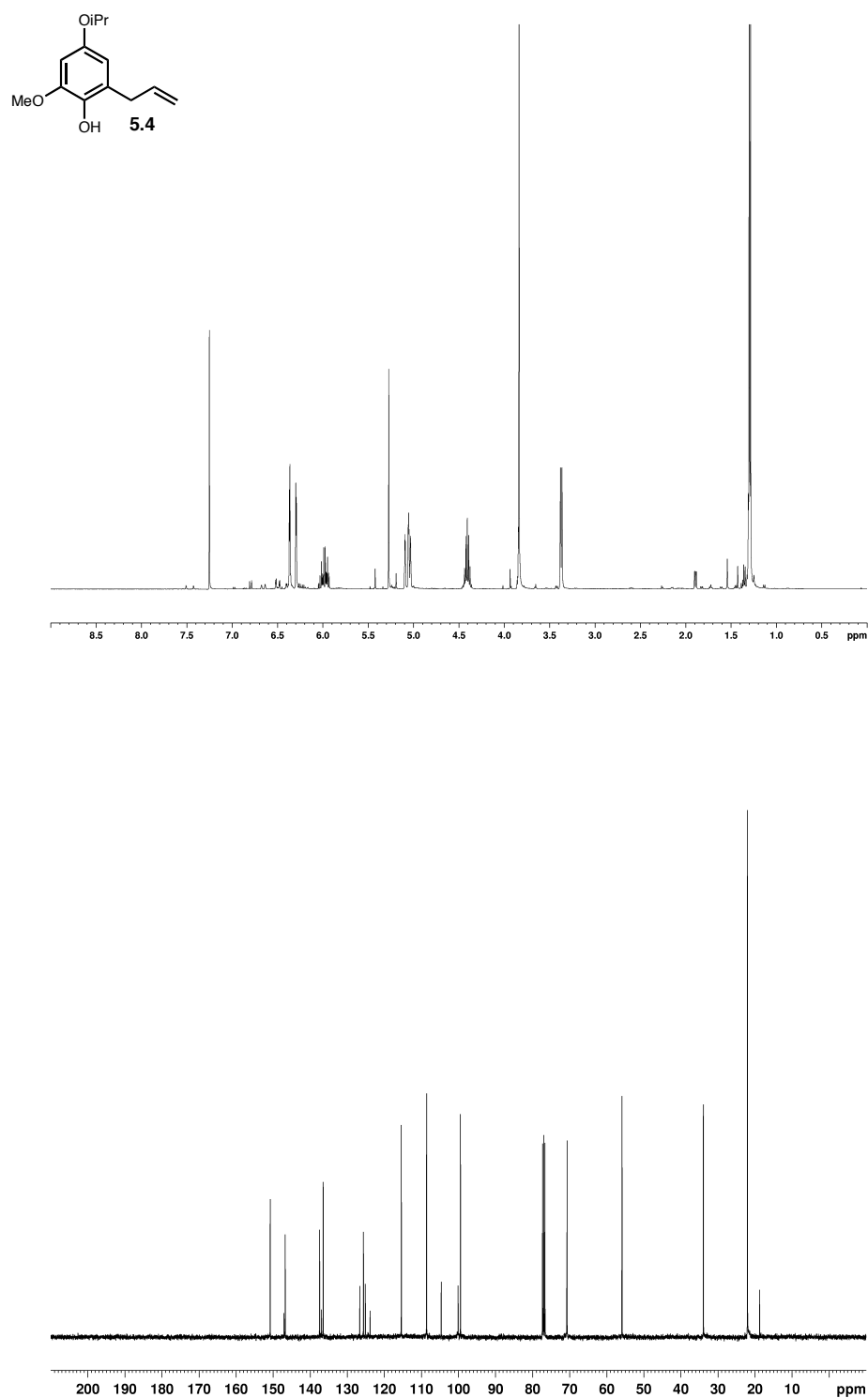


**Figure A3.2.**  $^1\text{H}$  NMR spectrum (400 MHz,  $\text{CDCl}_3$ ) and  $^{13}\text{C}$  NMR spectrum (100 MHz,  $\text{CDCl}_3$ ) of compound **5.4**.

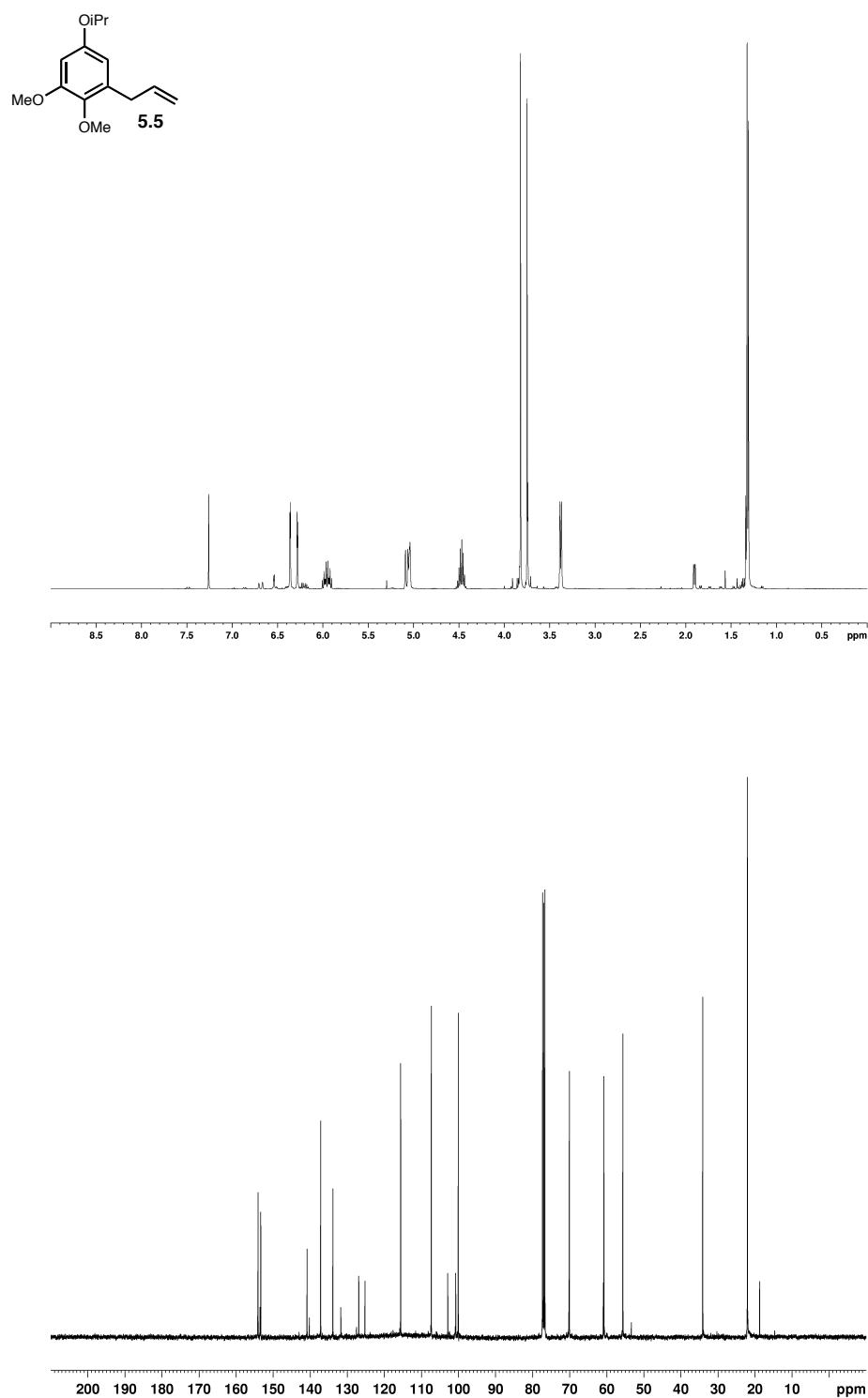


**Figure A3.3.**  $^1\text{H}$  NMR spectrum (400 MHz,  $\text{CDCl}_3$ ) and  $^{13}\text{C}$  NMR spectrum (100 MHz,  $\text{CDCl}_3$ ) of compound **5.5**.

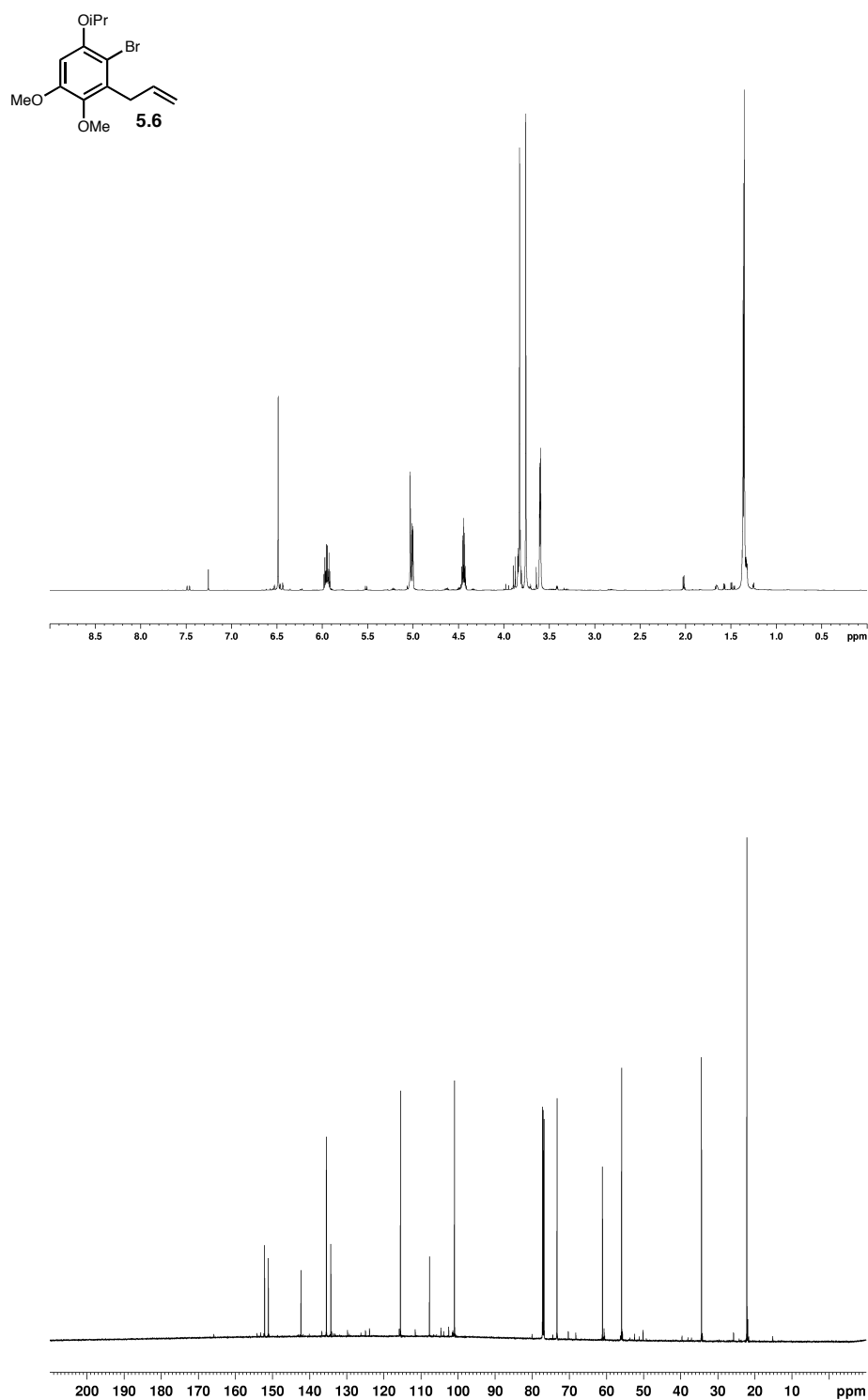


**Figure A3.4.**  $^1\text{H}$  NMR spectrum (600 MHz, CDCl<sub>3</sub>) and  $^{13}\text{C}$  NMR spectrum (150 MHz, CDCl<sub>3</sub>) of compound **5.6**.

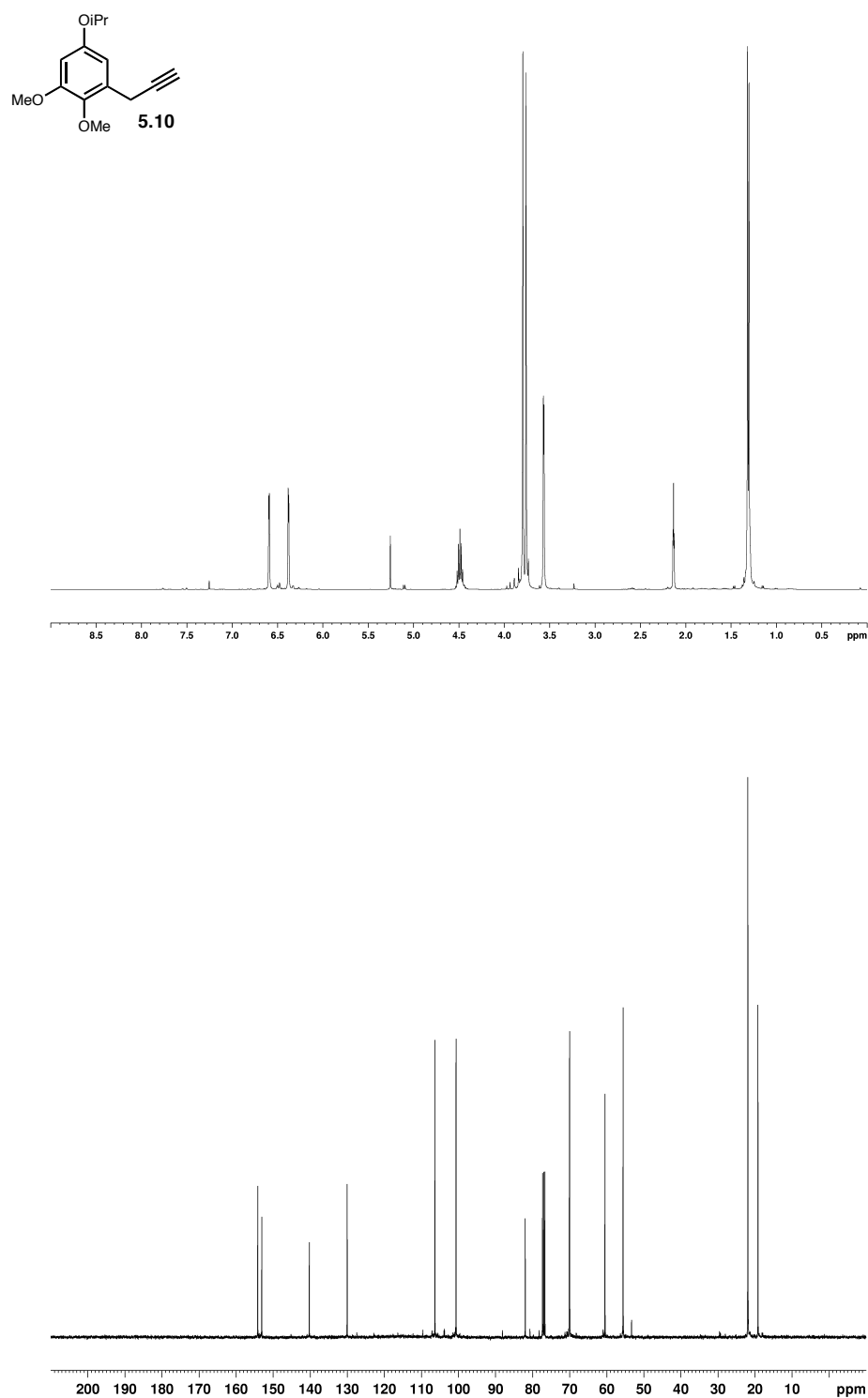


**Figure A3.5.**  $^1\text{H}$  NMR spectrum (400 MHz,  $\text{CDCl}_3$ ) and  $^{13}\text{C}$  NMR spectrum (100 MHz,  $\text{CDCl}_3$ ) of compound **5.10**.

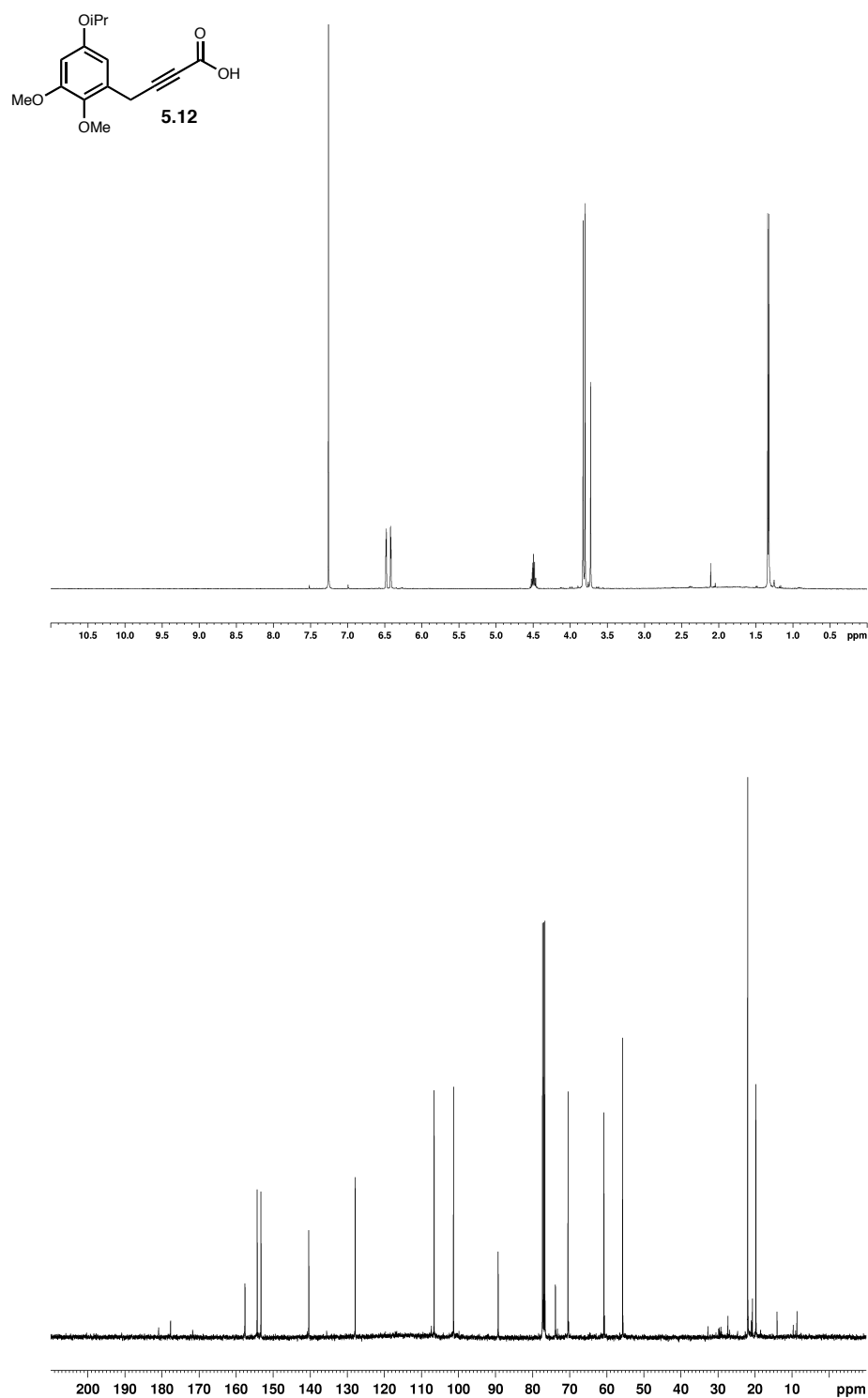


**Figure A3.6.**  $^1\text{H}$  NMR spectrum (400 MHz,  $\text{CDCl}_3$ ) and  $^{13}\text{C}$  NMR spectrum (100 MHz,  $\text{CDCl}_3$ ) of compound **5.12**.

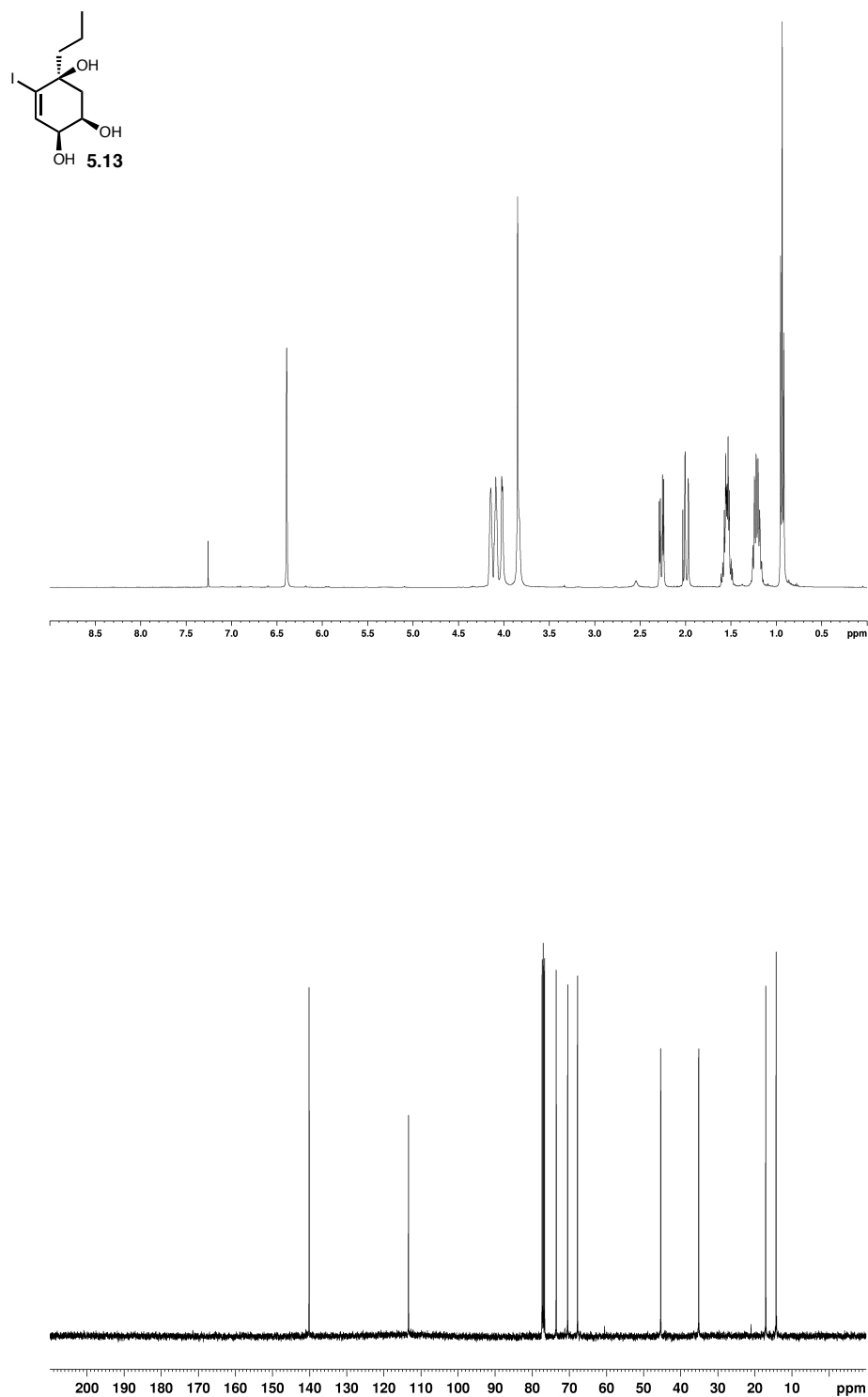


**Figure A3.7.**  $^1\text{H}$  NMR spectrum (400 MHz,  $\text{CDCl}_3$ ) and  $^{13}\text{C}$  NMR spectrum (100 MHz,  $\text{CDCl}_3$ ) of compound **5.13**.

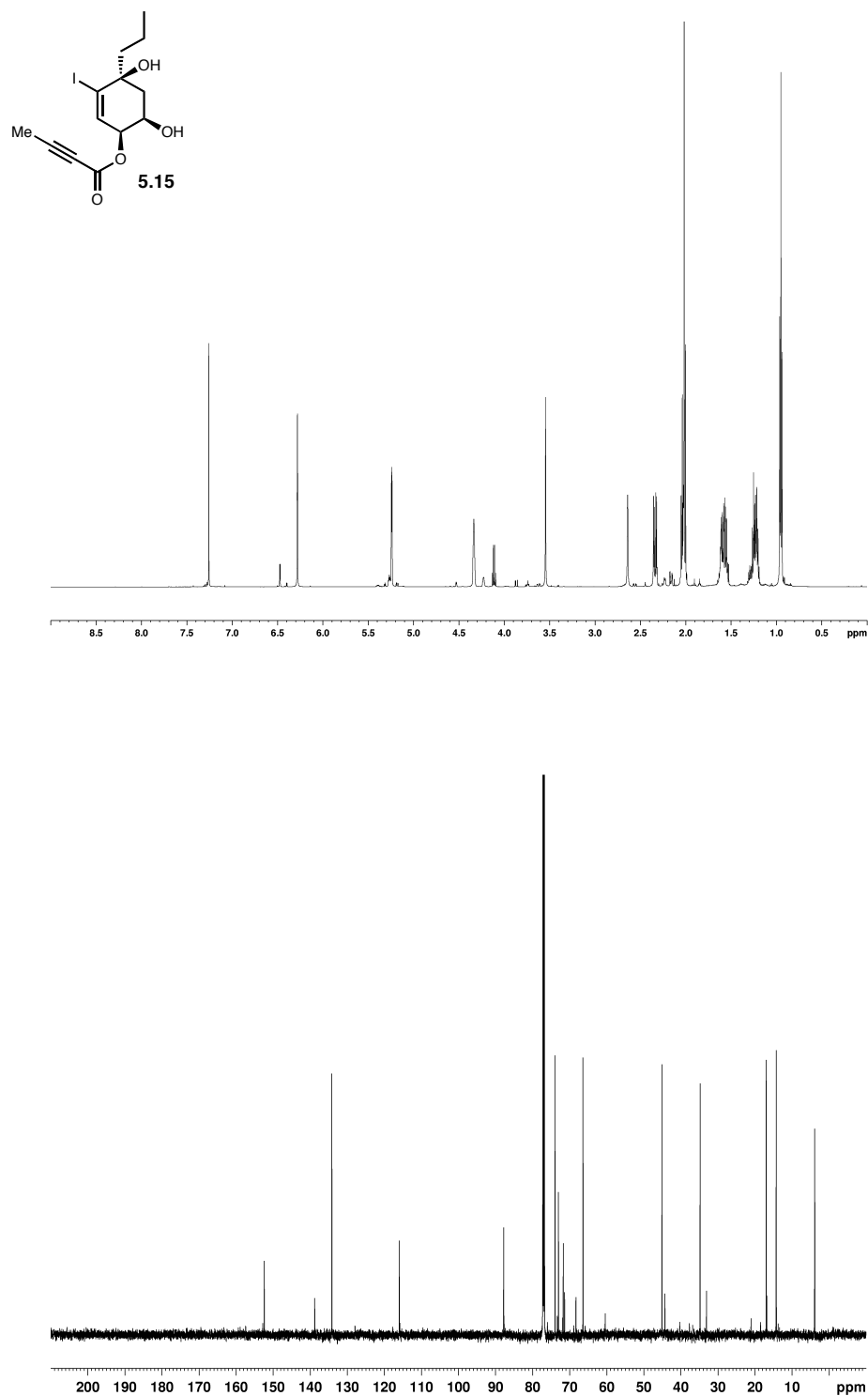


**Figure A3.8.**  $^1\text{H}$  NMR spectrum (600 MHz,  $\text{CDCl}_3$ ) and  $^{13}\text{C}$  NMR spectrum (150 MHz,  $\text{CDCl}_3$ ) of compound **5.15**.

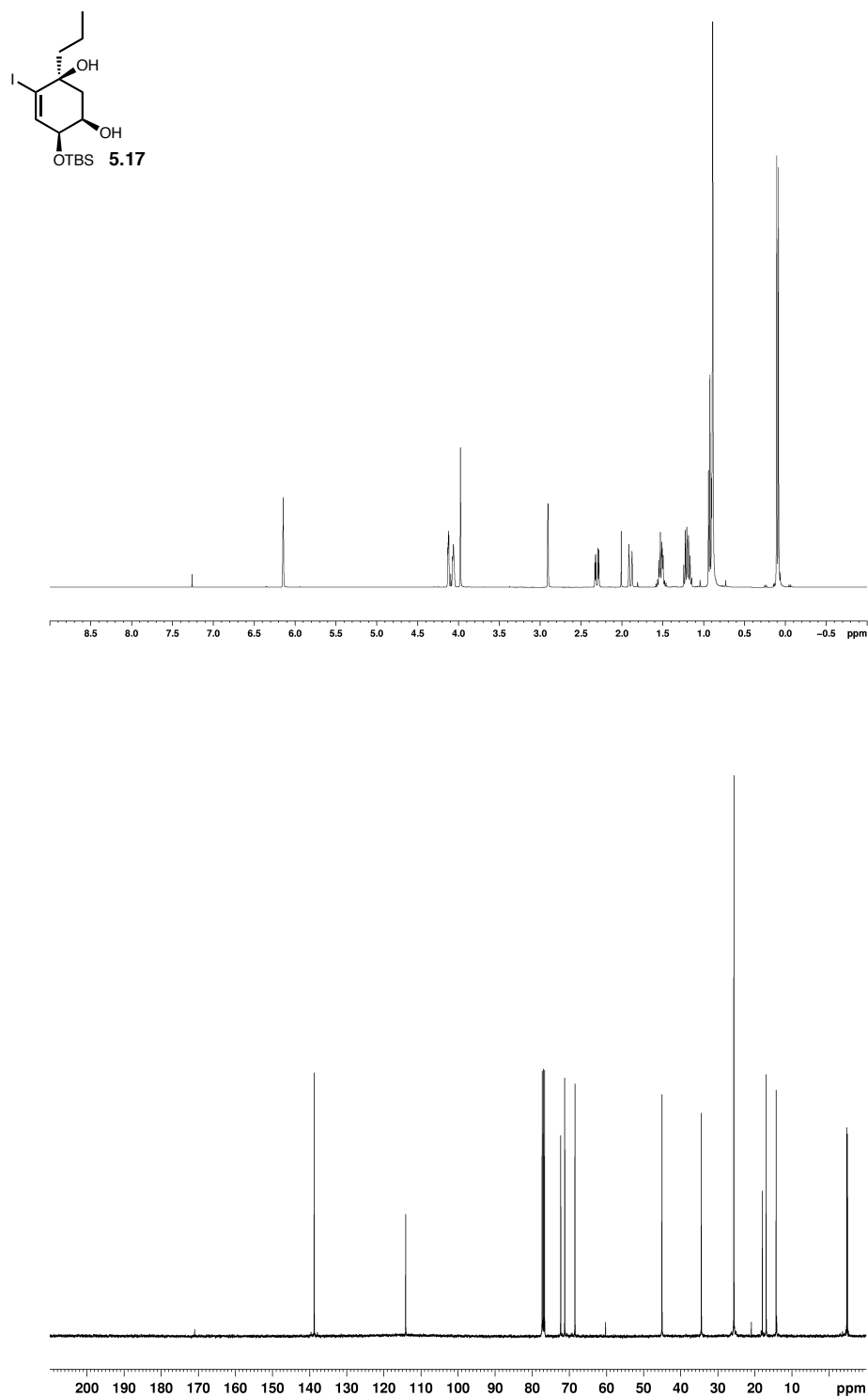


**Figure A3.9.**  $^1\text{H}$  NMR spectrum (400 MHz,  $\text{CDCl}_3$ ) and  $^{13}\text{C}$  NMR spectrum (100 MHz,  $\text{CDCl}_3$ ) of compound **5.17**.



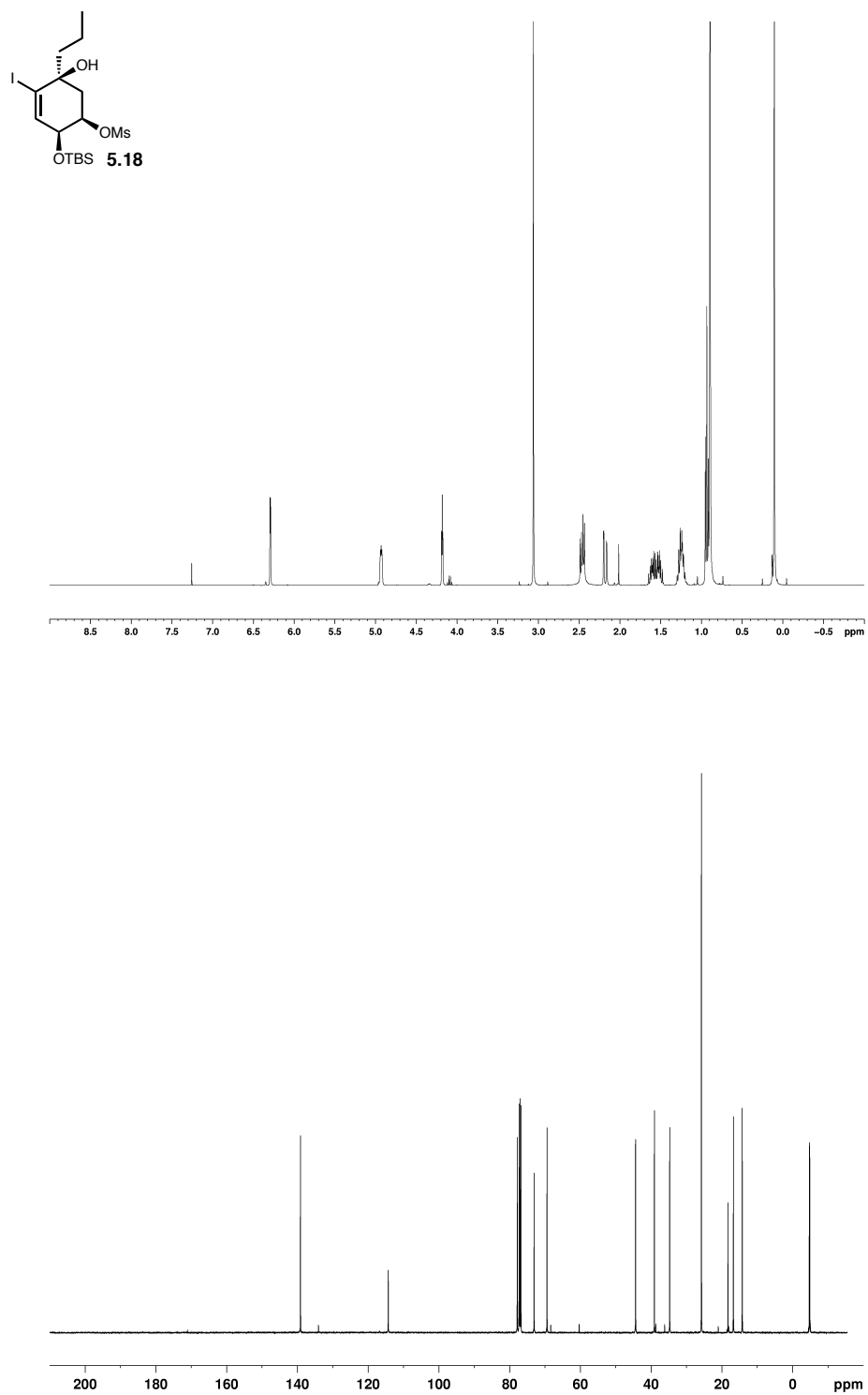


**Figure A3.10.**  $^1\text{H}$  NMR spectrum (400 MHz,  $\text{CDCl}_3$ ) and  $^{13}\text{C}$  NMR spectrum (125 MHz,  $\text{CDCl}_3$ ) of compound **5.18**.

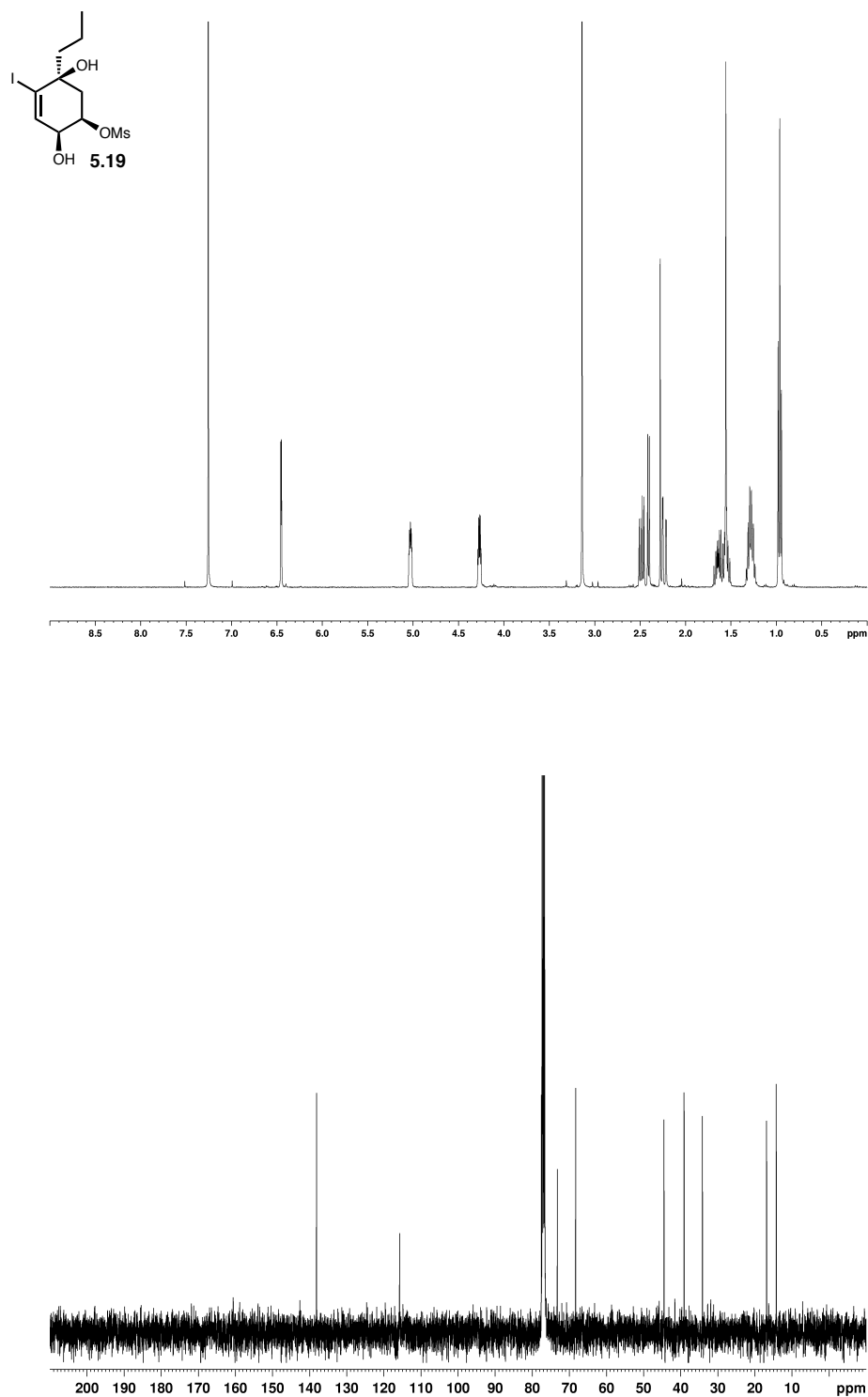


**Figure A3.11.**  $^1\text{H}$  NMR spectrum (400 MHz,  $\text{CDCl}_3$ ) and  $^{13}\text{C}$  NMR spectrum (100 MHz,  $\text{CDCl}_3$ ) of compound **5.19**.

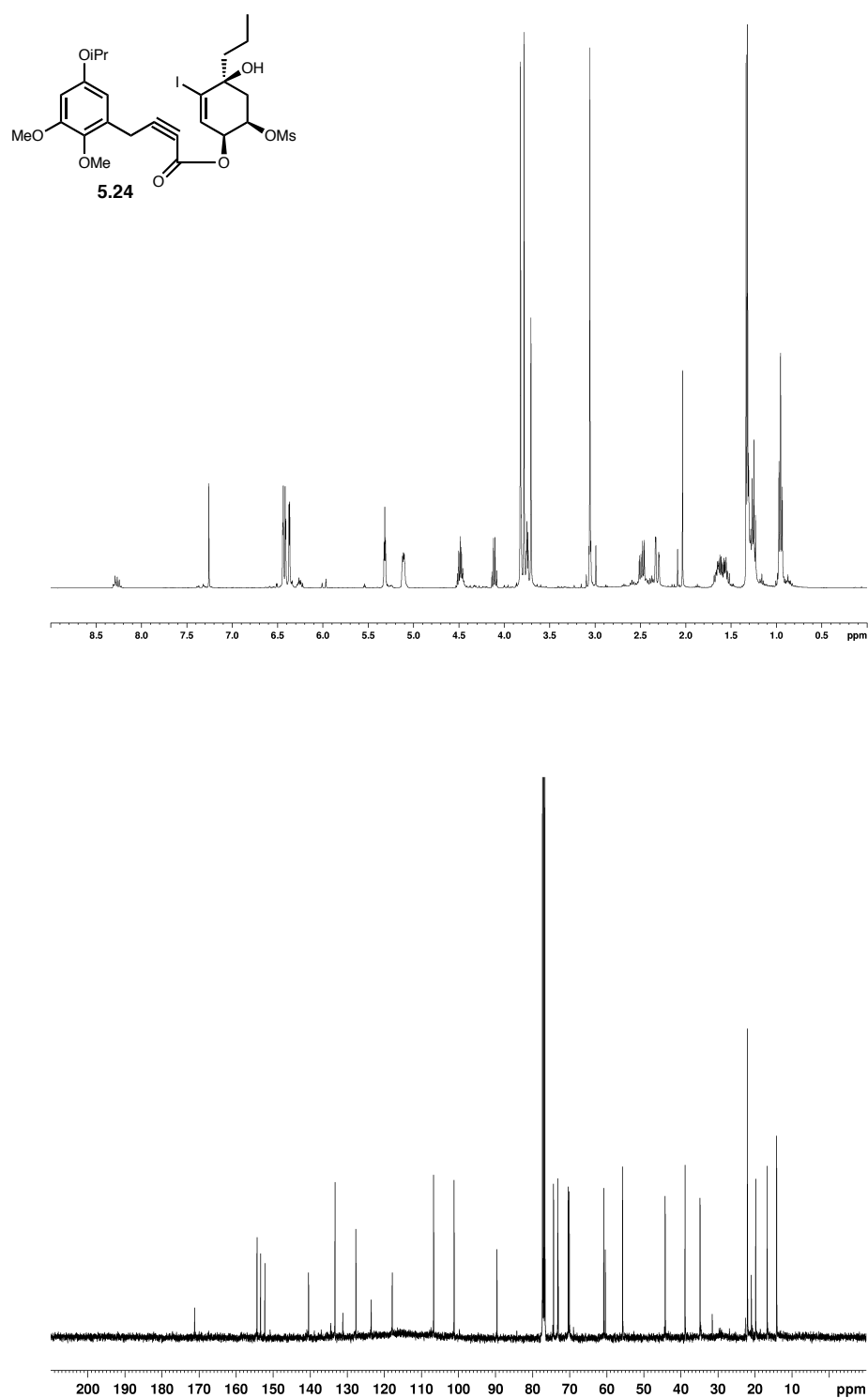


**Figure A3.12.**  $^1\text{H}$  NMR spectrum (400 MHz,  $\text{CDCl}_3$ ) and  $^{13}\text{C}$  NMR spectrum (100 MHz,  $\text{CDCl}_3$ ) of compound **5.24**.

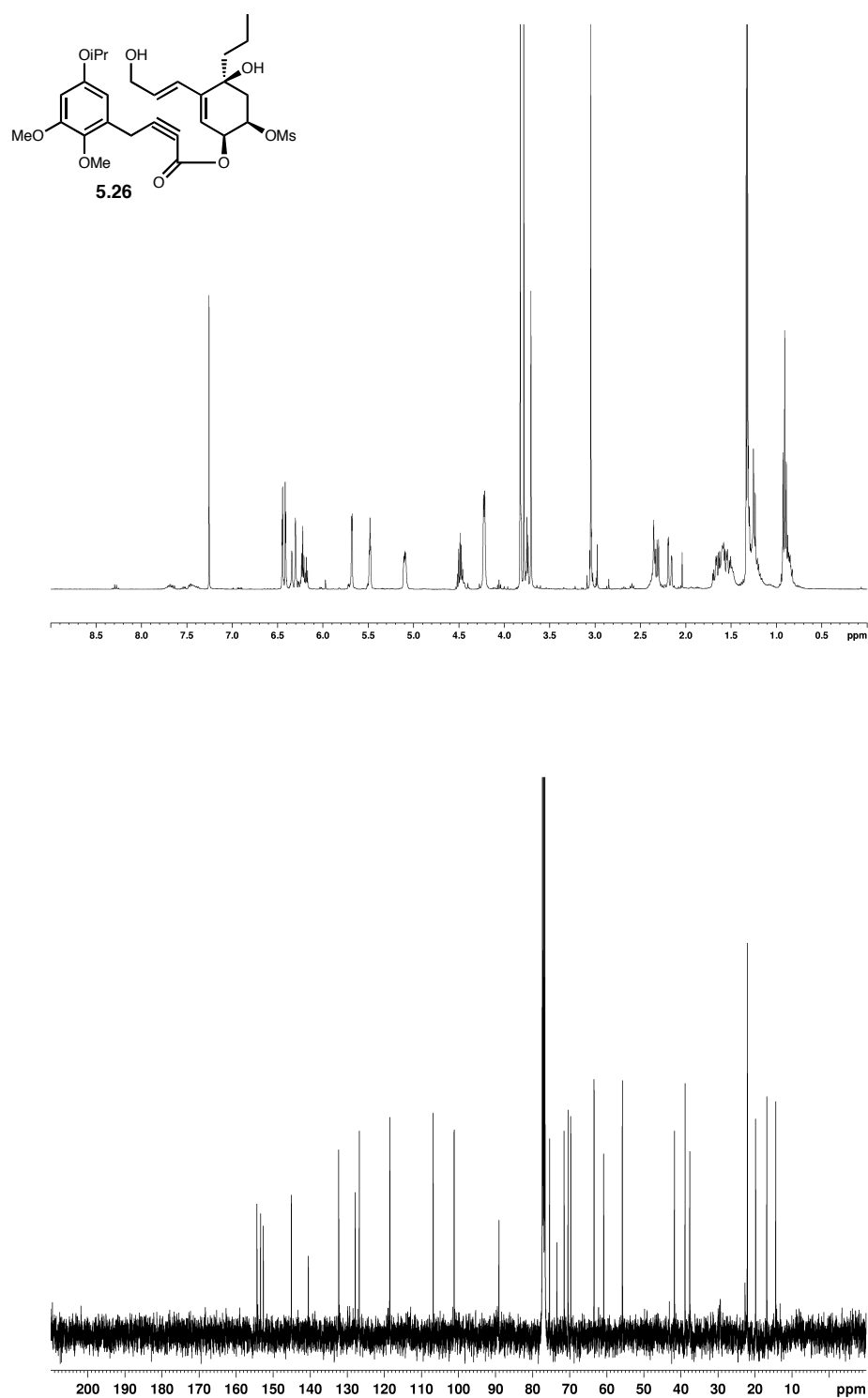


**Figure A3.13.**  $^1\text{H}$  NMR spectrum (400 MHz,  $\text{CDCl}_3$ ) and  $^{13}\text{C}$  NMR spectrum (100 MHz,  $\text{CDCl}_3$ ) of compound **5.26**.

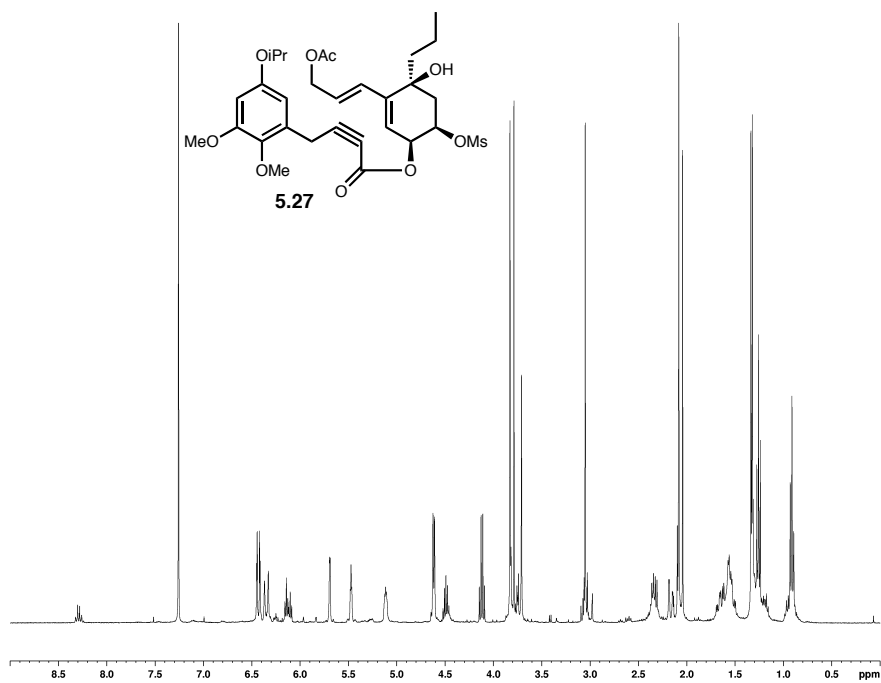


**Figure A3.14.**  $^1\text{H}$  NMR spectrum (400 MHz,  $\text{CDCl}_3$ ) of compound 5.27.

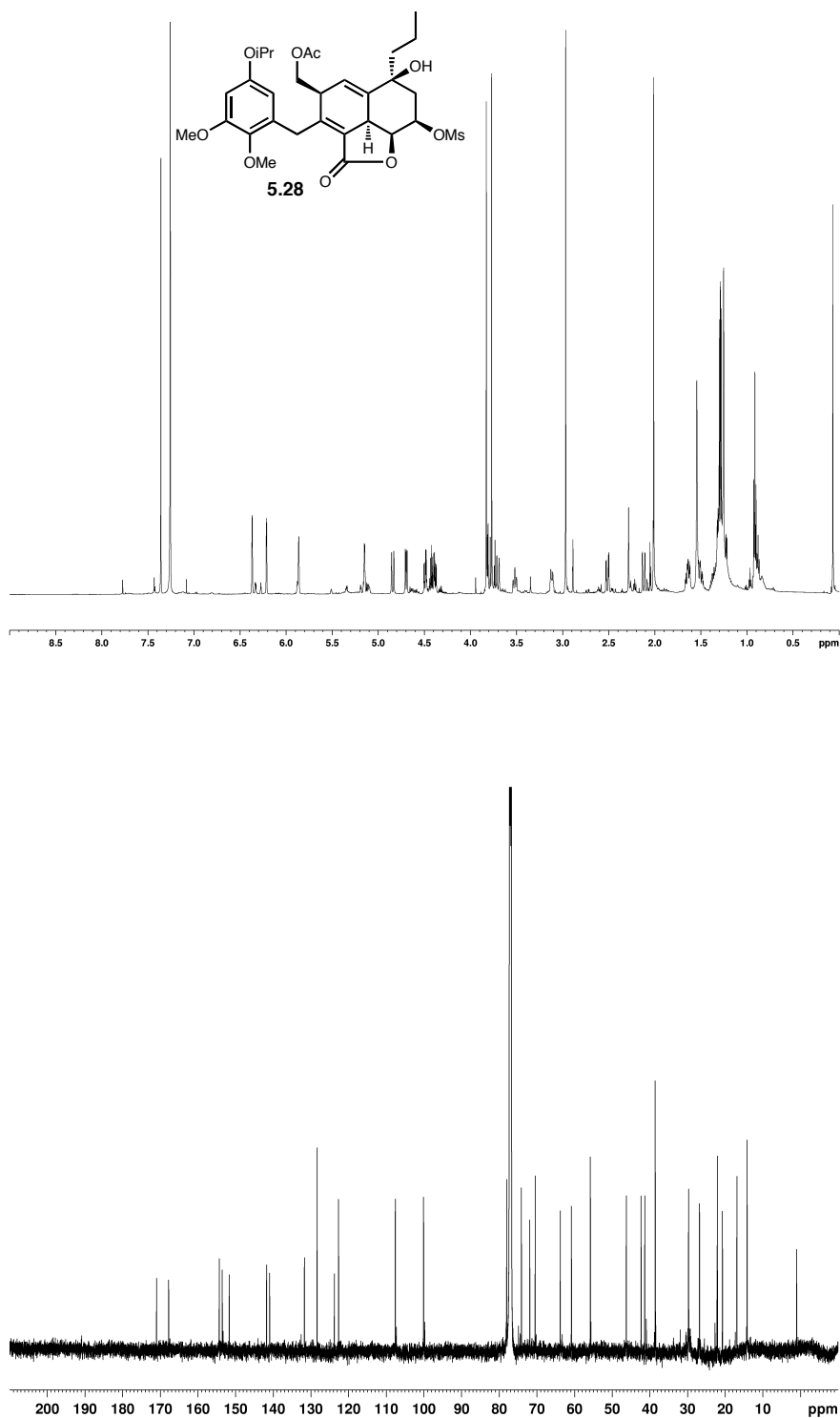


**Figure A3.15.**  $^1\text{H}$  NMR spectrum (600 MHz,  $\text{CDCl}_3$ ) and  $^{13}\text{C}$  NMR spectrum (150 MHz,  $\text{CDCl}_3$ ) of compound **5.28**.

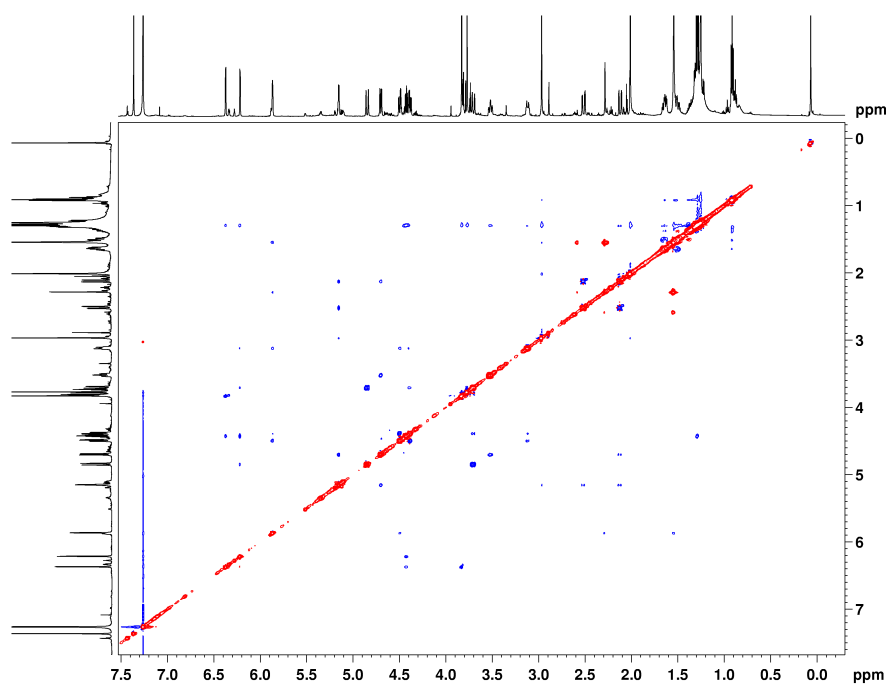
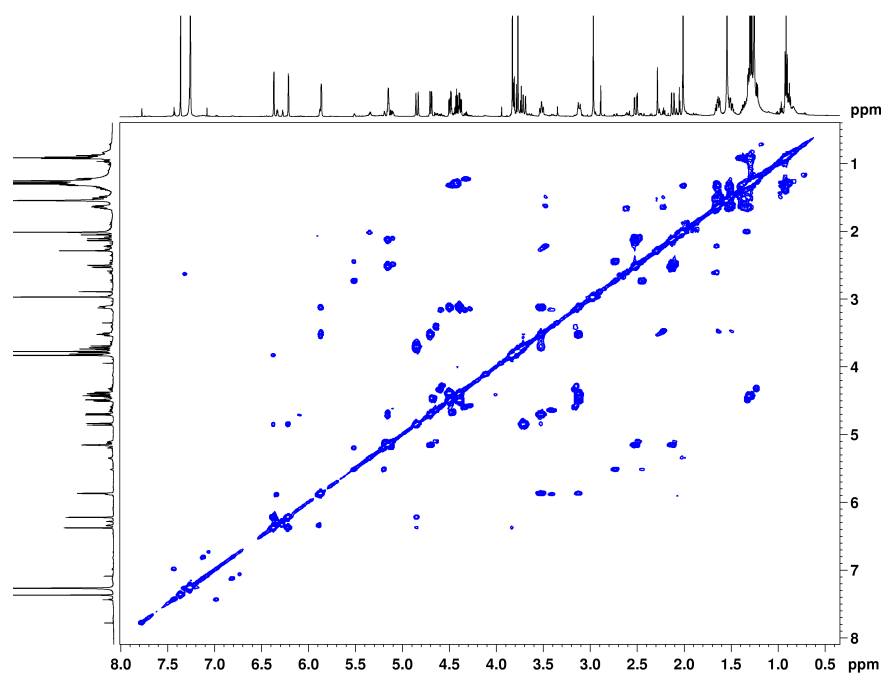


**Figure A3.16.** COSY spectrum (600 MHz, CDCl<sub>3</sub>) and NOESY spectrum (600 MHz, CDCl<sub>3</sub>) of compound **5.28**.

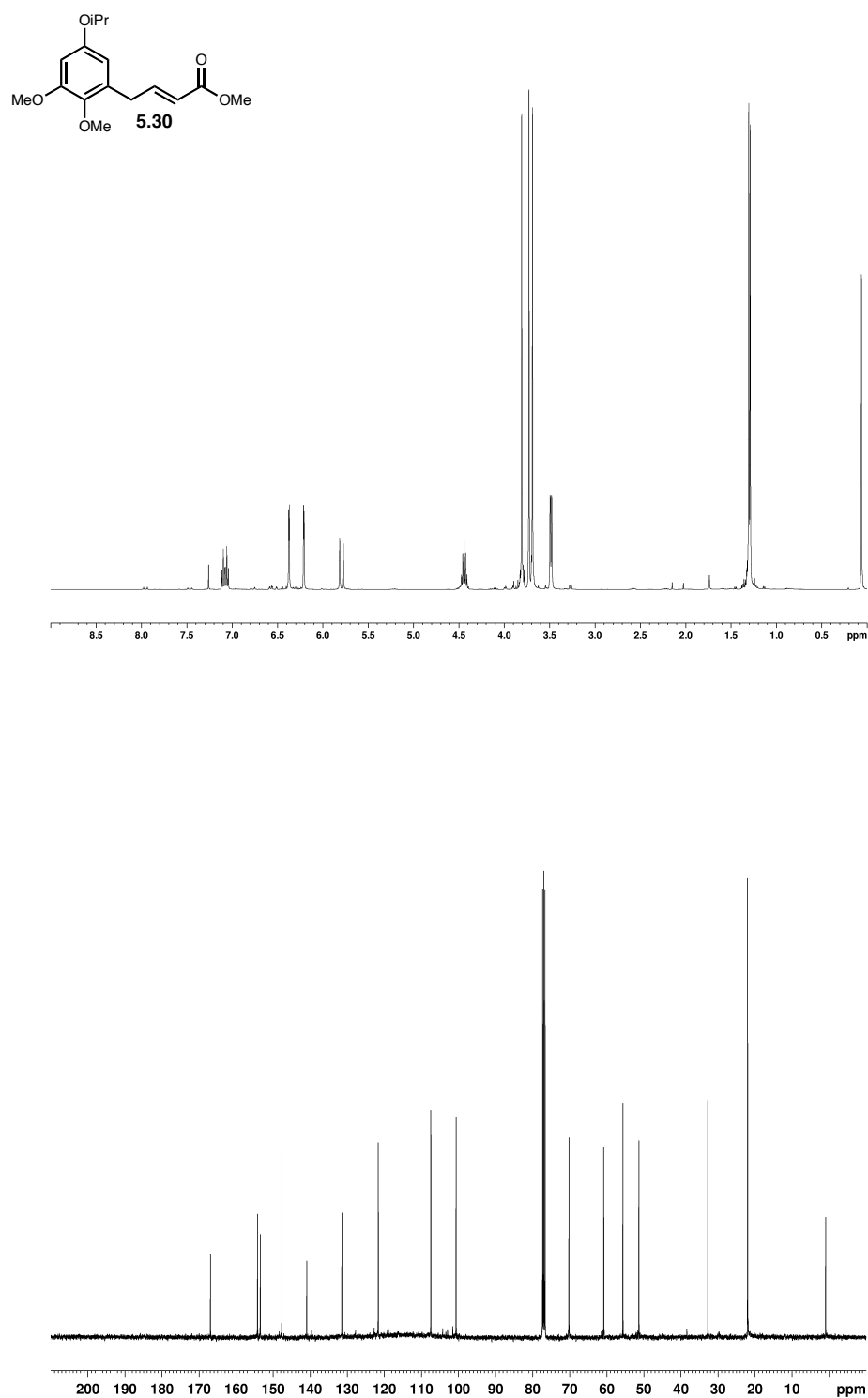


**Figure A3.17.**  $^1\text{H}$  NMR spectrum (400 MHz,  $\text{CDCl}_3$ ) and  $^{13}\text{C}$  NMR spectrum (100 MHz,  $\text{CDCl}_3$ ) of compound **5.30**.



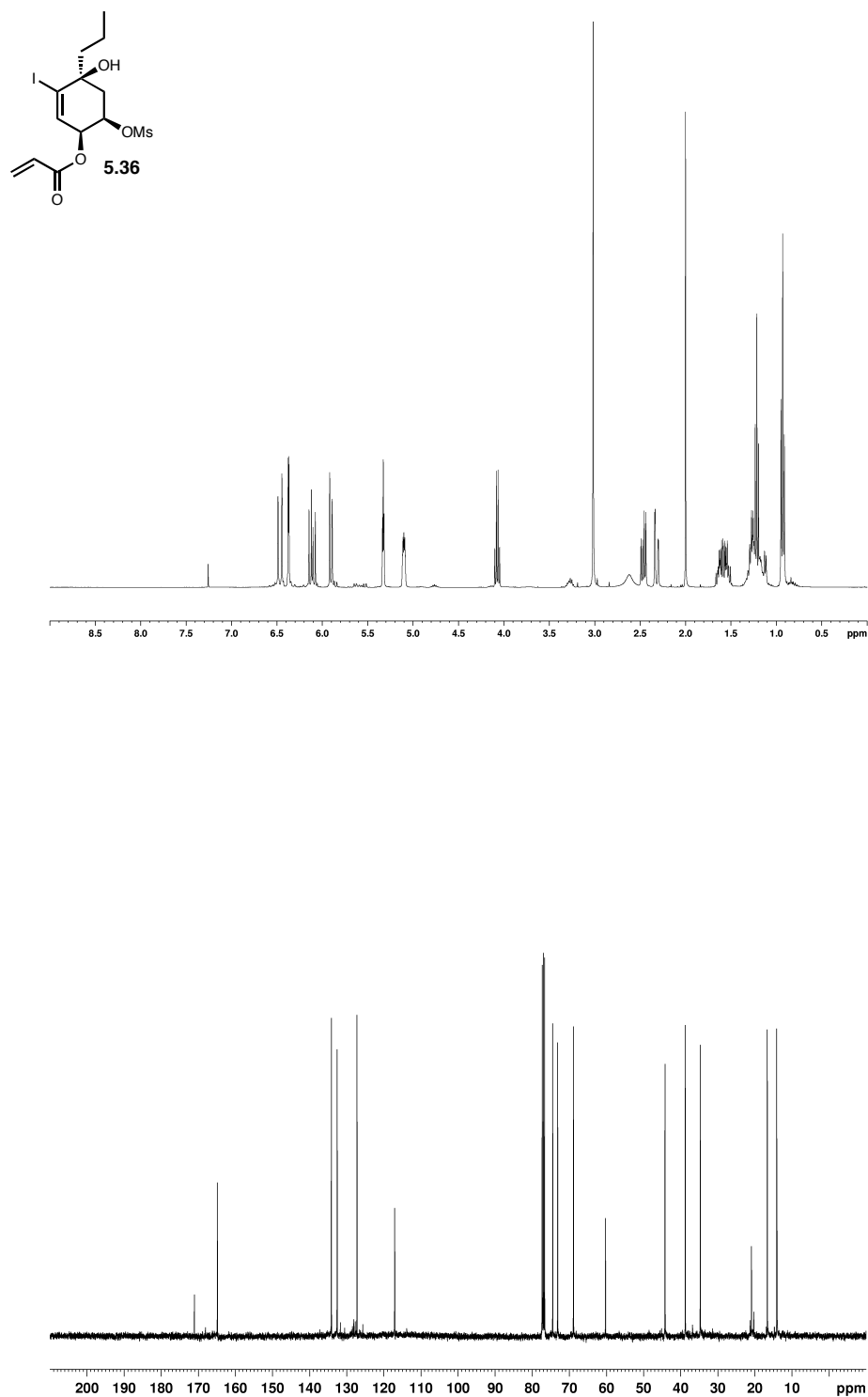


**Figure A3.18.**  $^1\text{H}$  NMR spectrum (400 MHz,  $\text{CDCl}_3$ ) and  $^{13}\text{C}$  NMR spectrum (100 MHz,  $\text{CDCl}_3$ ) of compound **5.36**.

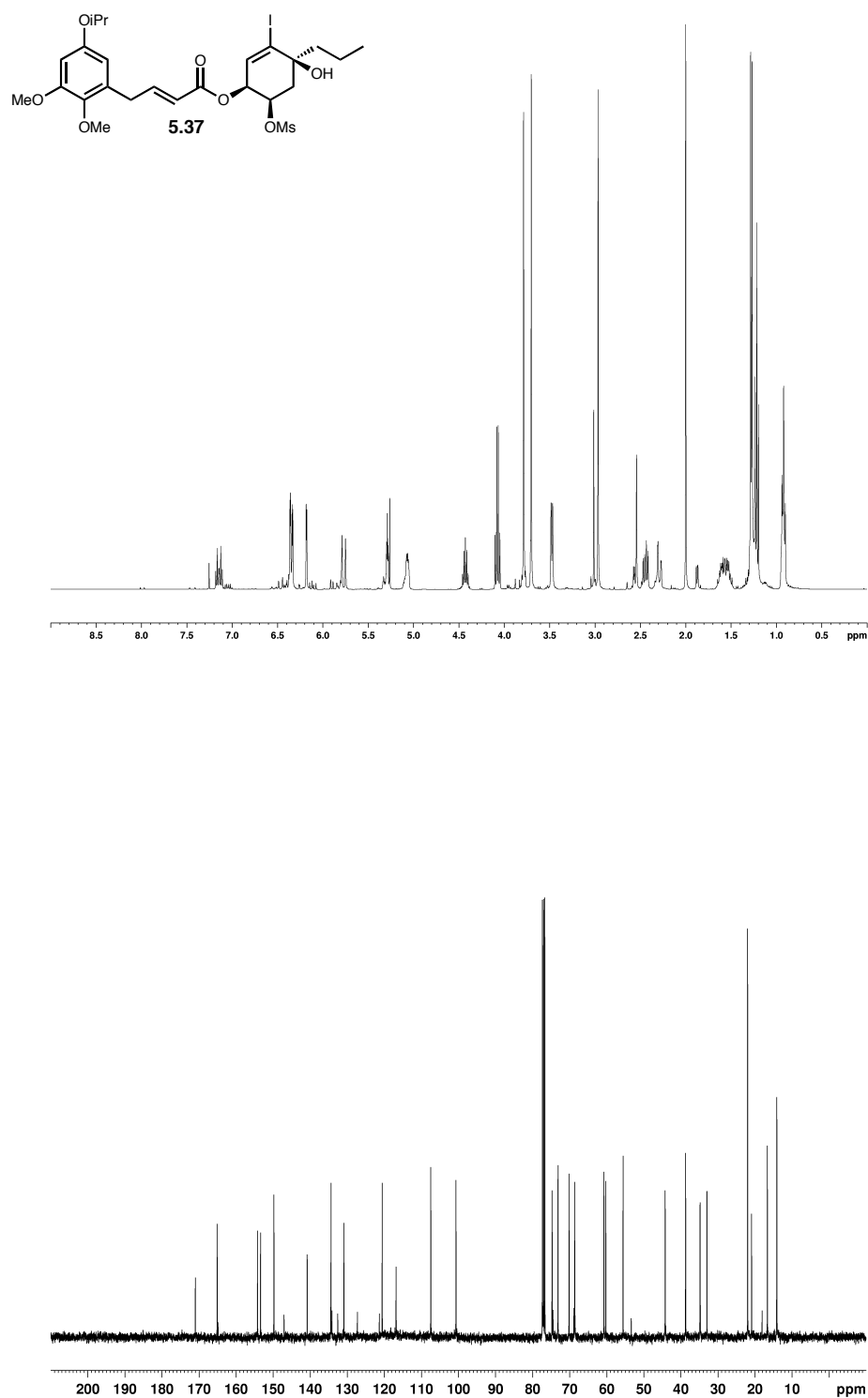


**Figure A3.19.**  $^1\text{H}$  NMR spectrum (400 MHz,  $\text{CDCl}_3$ ) and  $^{13}\text{C}$  NMR spectrum (100 MHz,  $\text{CDCl}_3$ ) of compound **5.37**.

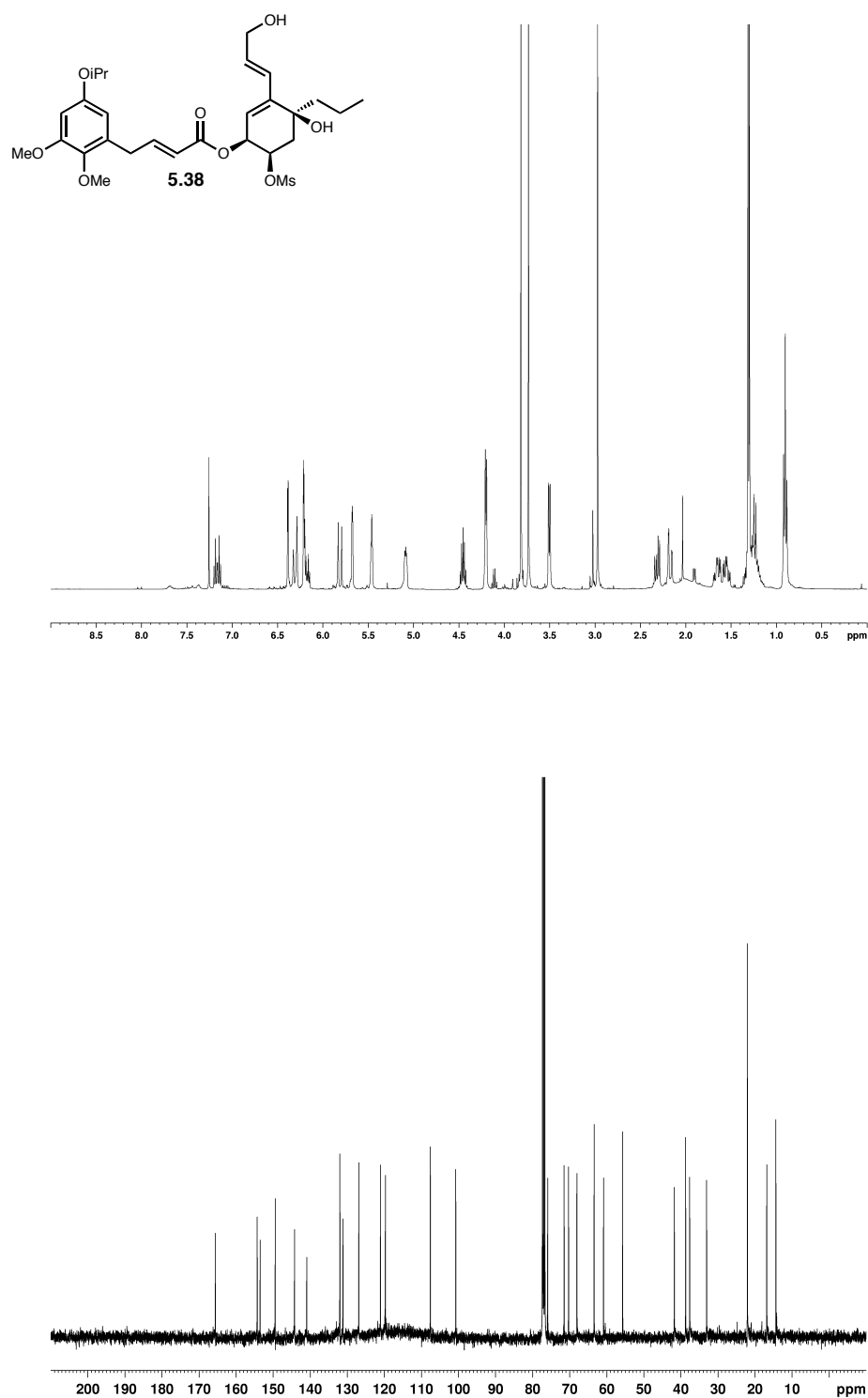


**Figure A3.20.**  $^1\text{H}$  NMR spectrum (400 MHz,  $\text{CDCl}_3$ ) and  $^{13}\text{C}$  NMR spectrum (100 MHz,  $\text{CDCl}_3$ ) of compound **5.38**.

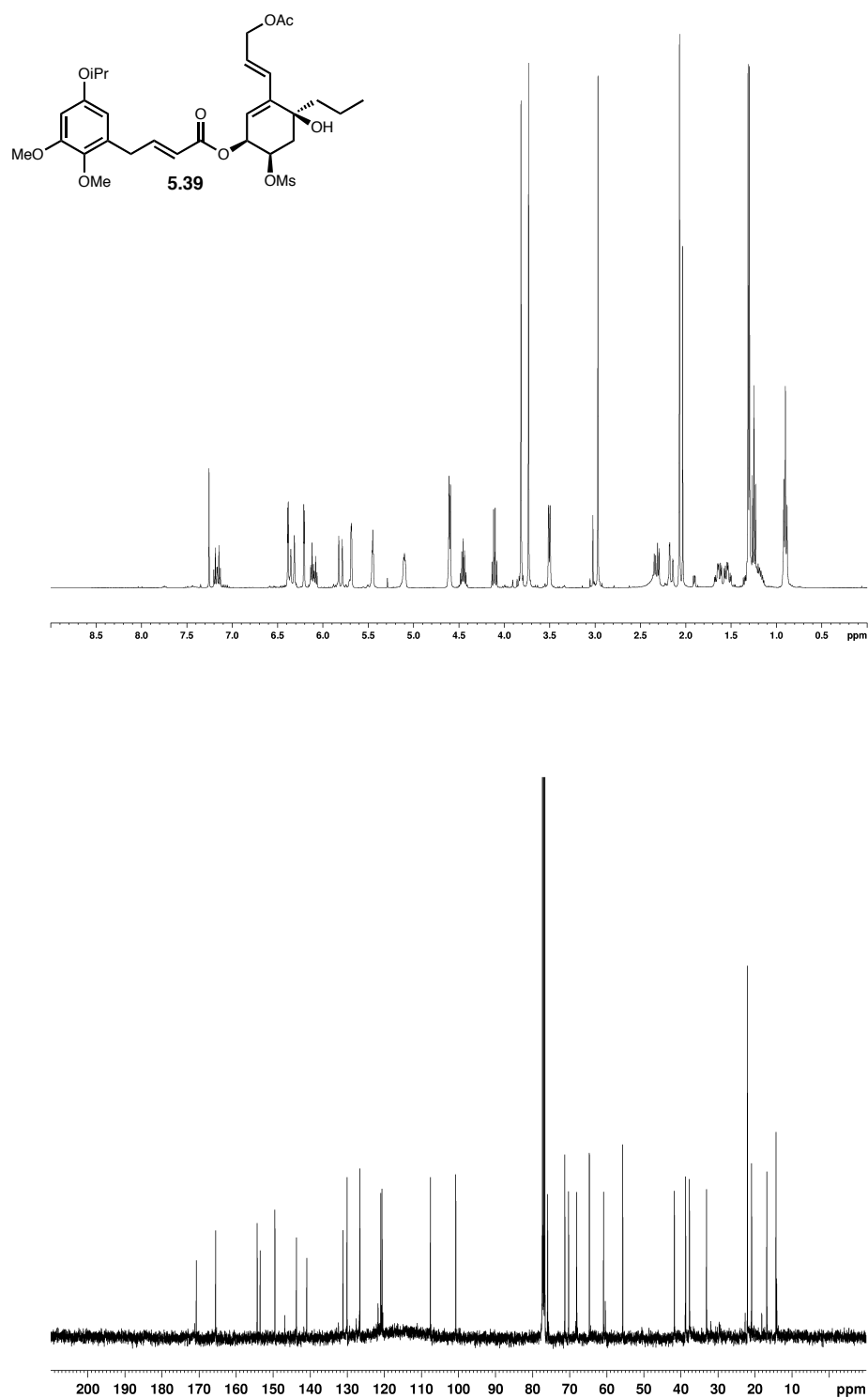


**Figure A3.21.**  $^1\text{H}$  NMR spectrum (400 MHz,  $\text{CDCl}_3$ ) and  $^{13}\text{C}$  NMR spectrum (100 MHz,  $\text{CDCl}_3$ ) of compound **5.39**.

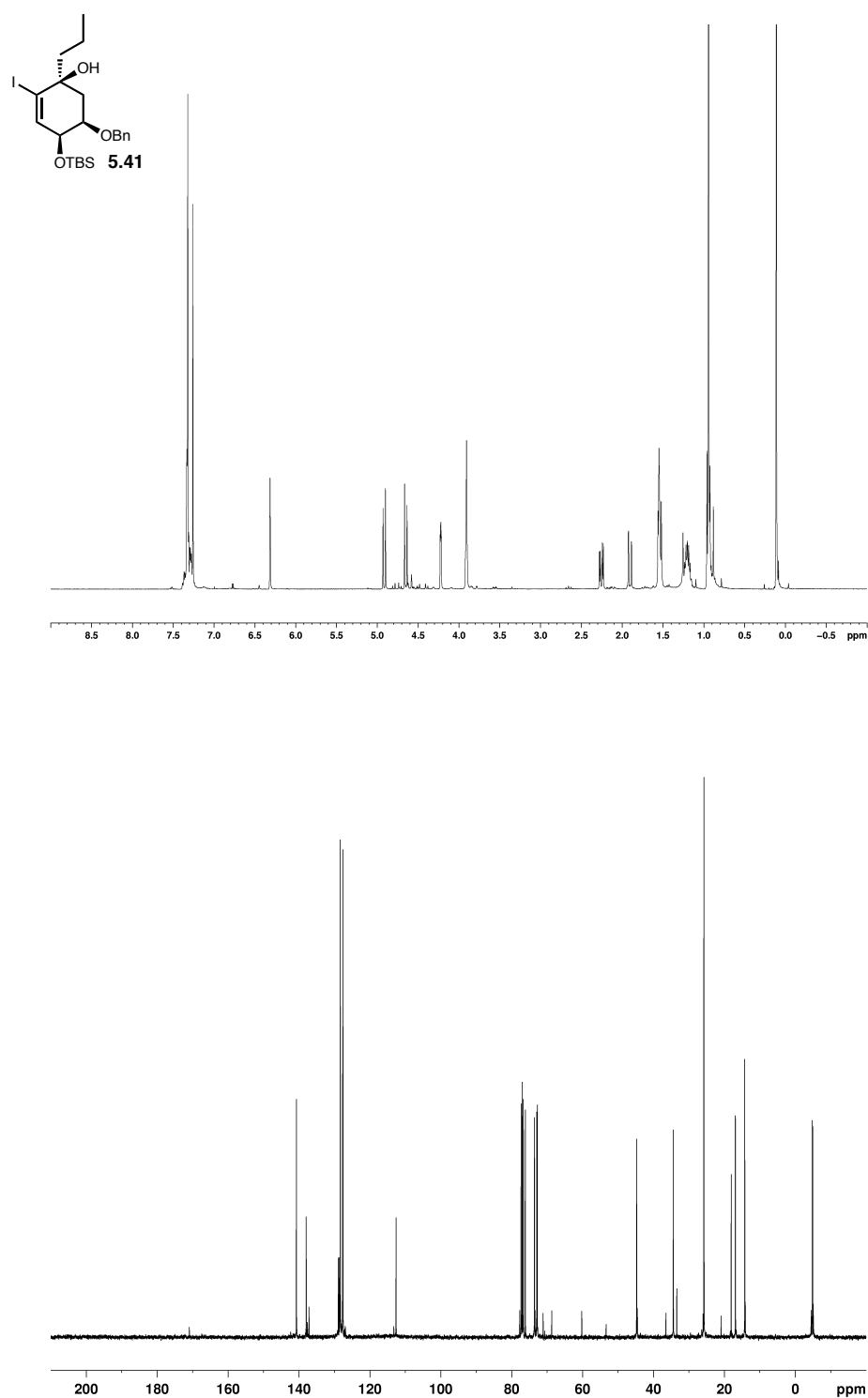


**Figure A3.22.**  $^1\text{H}$  NMR spectrum (400 MHz,  $\text{CDCl}_3$ ) and  $^{13}\text{C}$  NMR spectrum (100 MHz,  $\text{CDCl}_3$ ) of compound **5.41**.

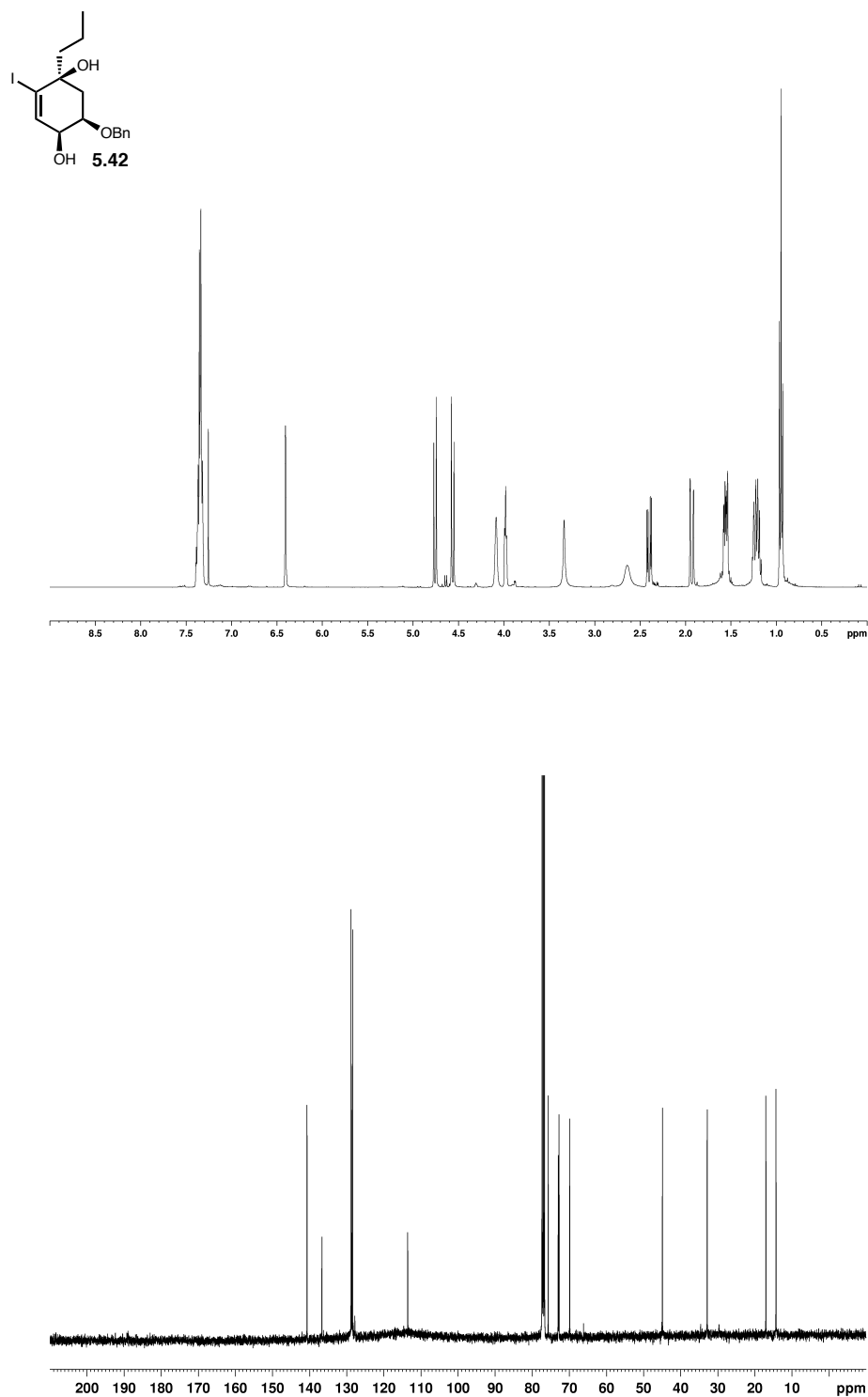


**Figure A3.23.**  $^1\text{H}$  NMR spectrum (400 MHz,  $\text{CDCl}_3$ ) and  $^{13}\text{C}$  NMR spectrum (100 MHz,  $\text{CDCl}_3$ ) of compound **5.42**.

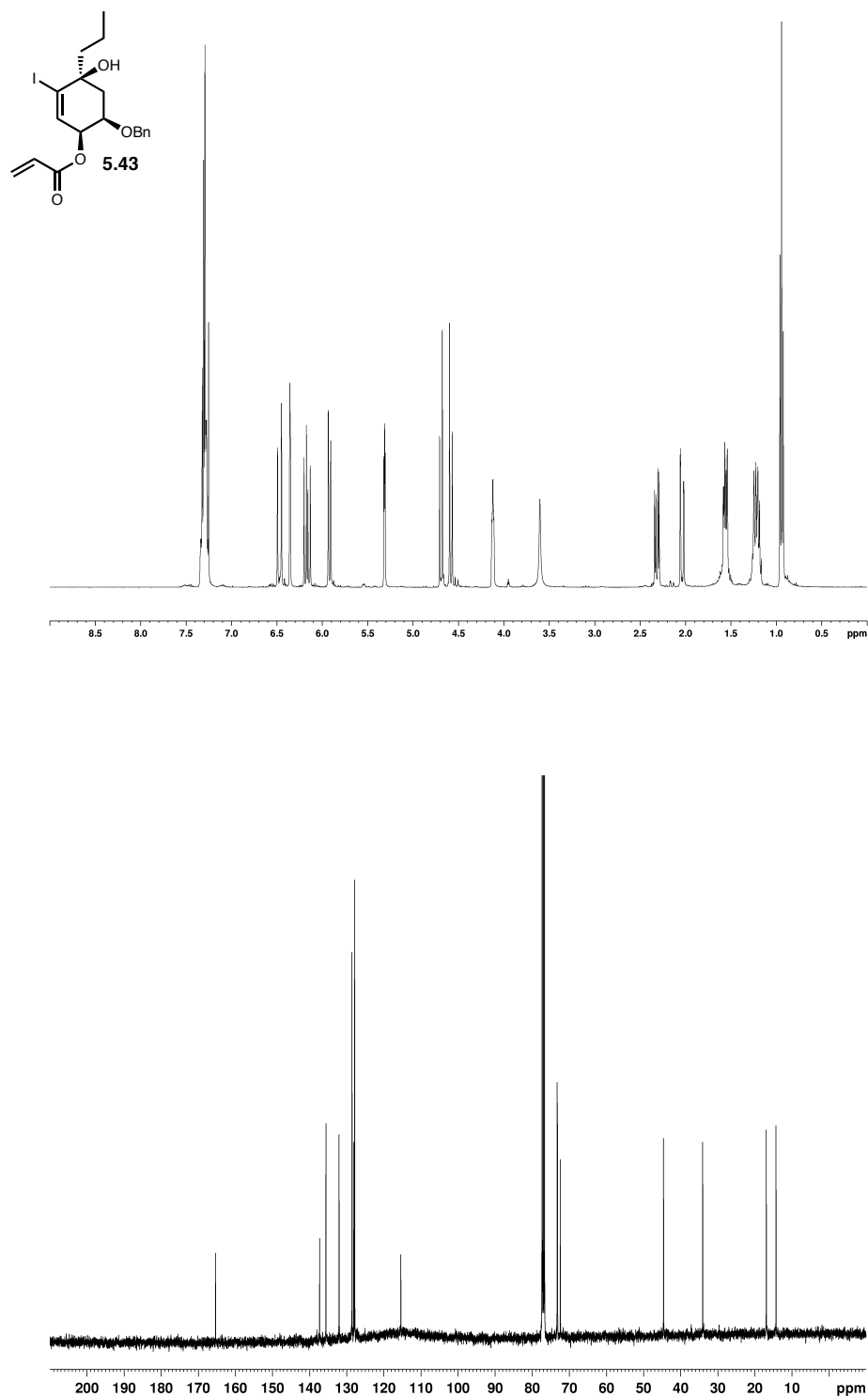


**Figure A3.24.**  $^1\text{H}$  NMR spectrum (400 MHz,  $\text{CDCl}_3$ ) and  $^{13}\text{C}$  NMR spectrum (100 MHz,  $\text{CDCl}_3$ ) of compound **5.43**.

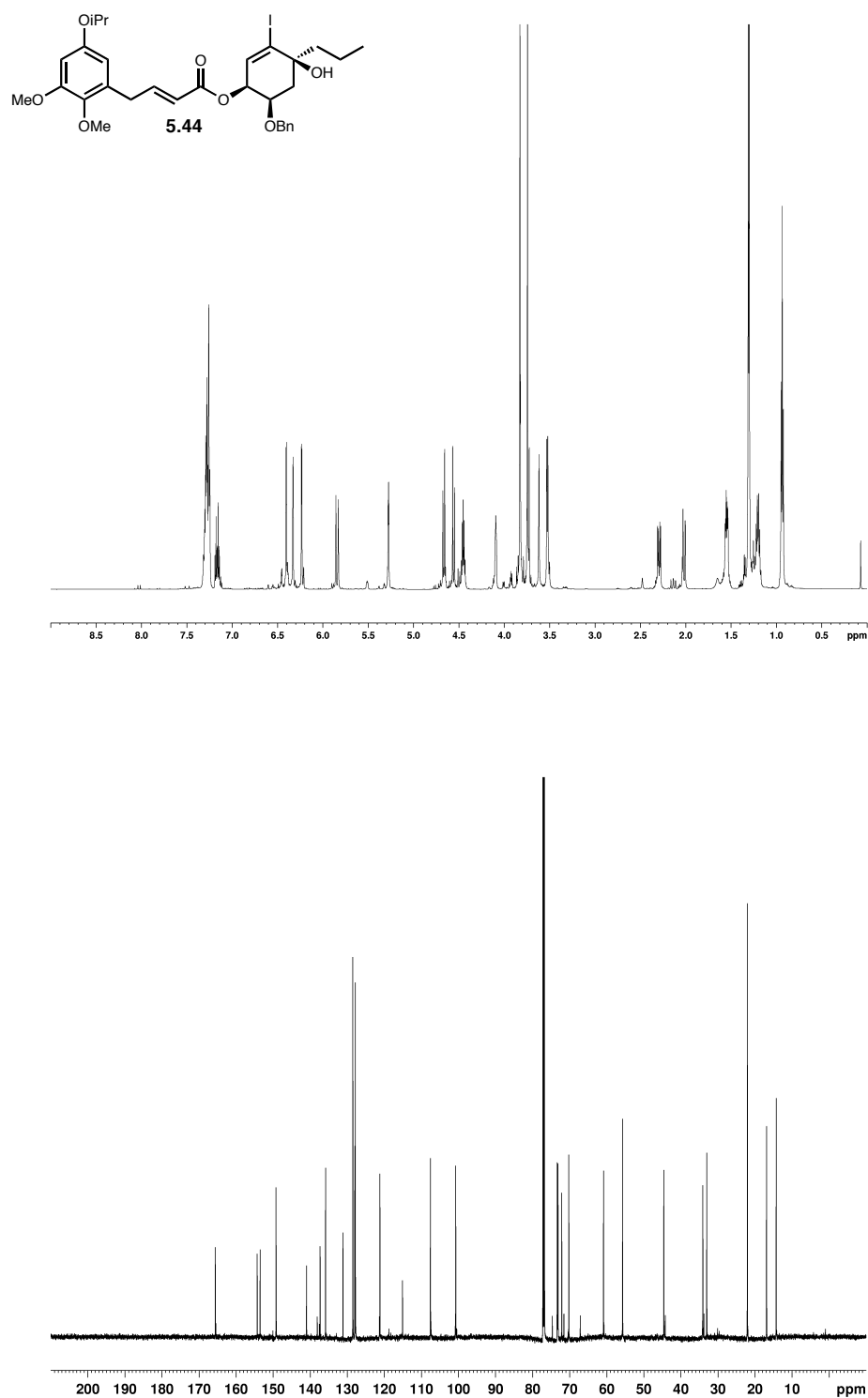


**Figure A3.25.**  $^1\text{H}$  NMR spectrum (600 MHz,  $\text{CDCl}_3$ ) and  $^{13}\text{C}$  NMR spectrum (150 MHz,  $\text{CDCl}_3$ ) of compound **5.44**.



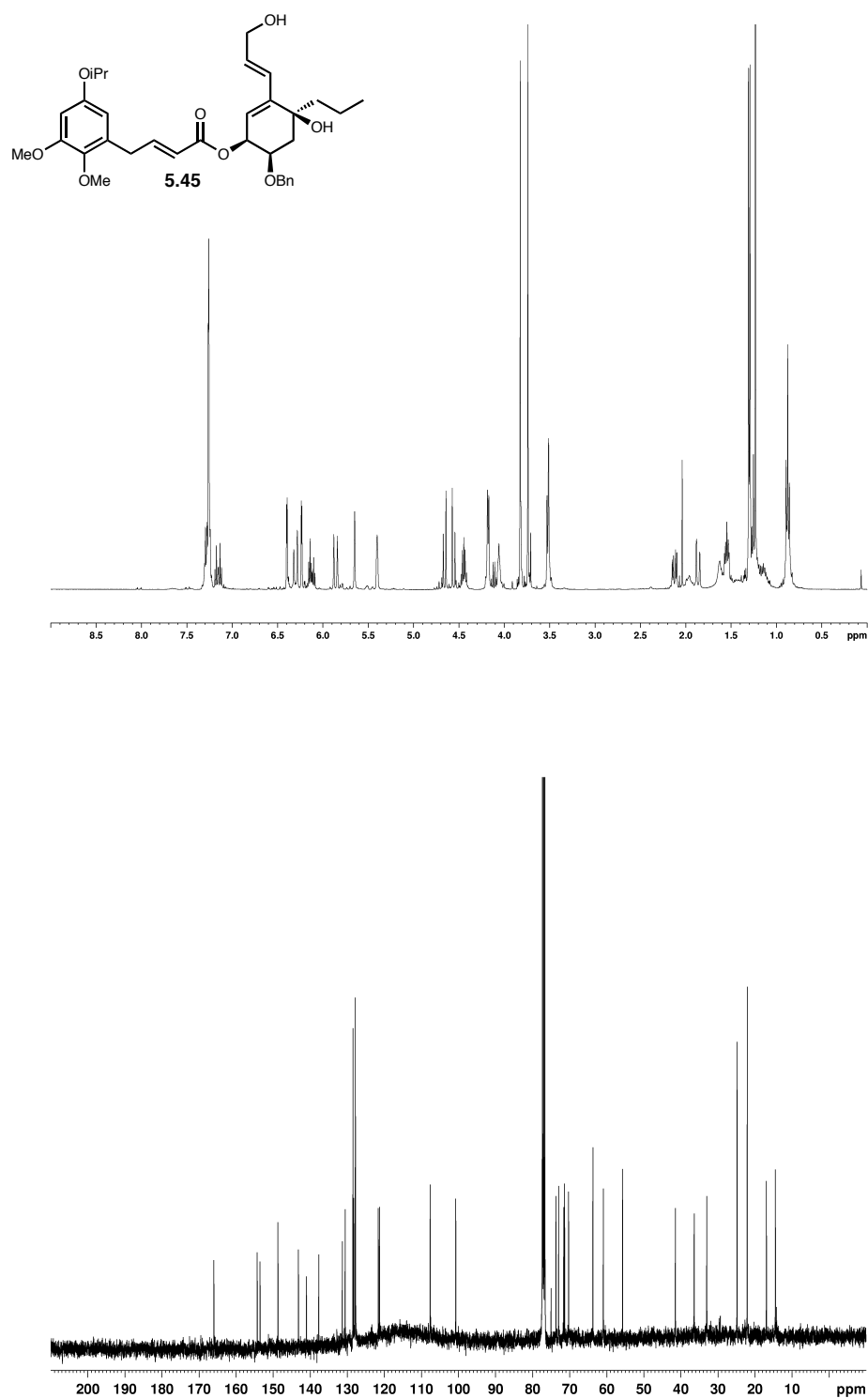


**Figure A3.26.**  $^1\text{H}$  NMR spectrum (400 MHz,  $\text{CDCl}_3$ ) and  $^{13}\text{C}$  NMR spectrum (100 MHz,  $\text{CDCl}_3$ ) of compound **5.45**.

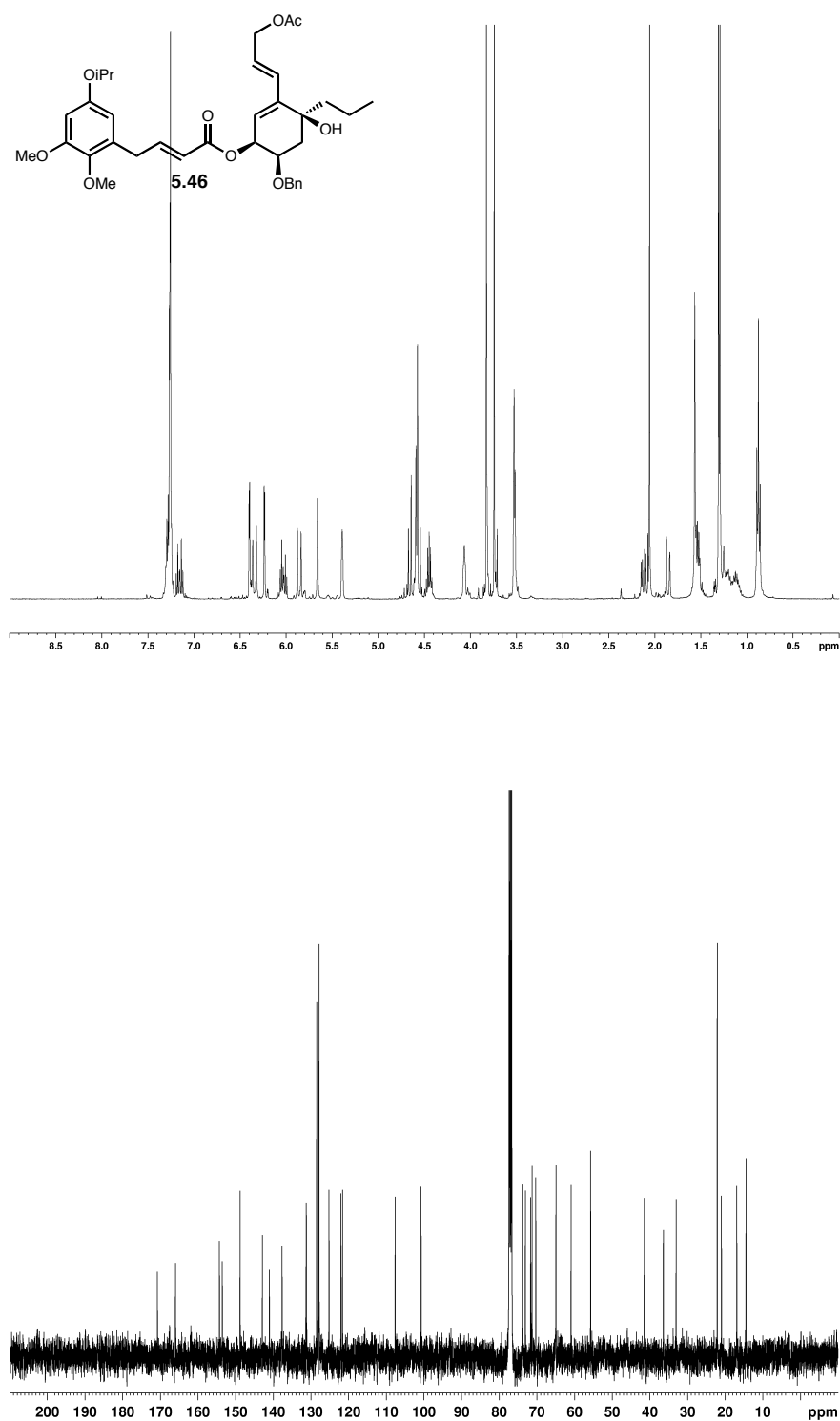


**Figure A3.27.**  $^1\text{H}$  NMR spectrum (400 MHz,  $\text{CDCl}_3$ ) and  $^{13}\text{C}$  NMR spectrum (100 MHz,  $\text{CDCl}_3$ ) of compound **5.46**.

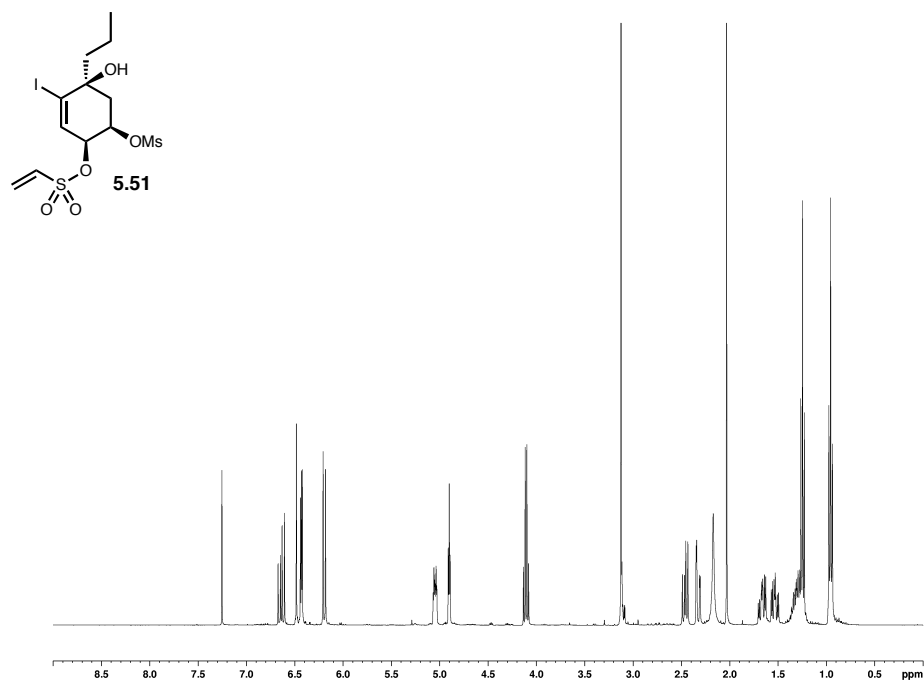


**Figure A3.28.**  $^1\text{H}$  NMR spectrum (400 MHz,  $\text{CDCl}_3$ ) of compound **5.51**.

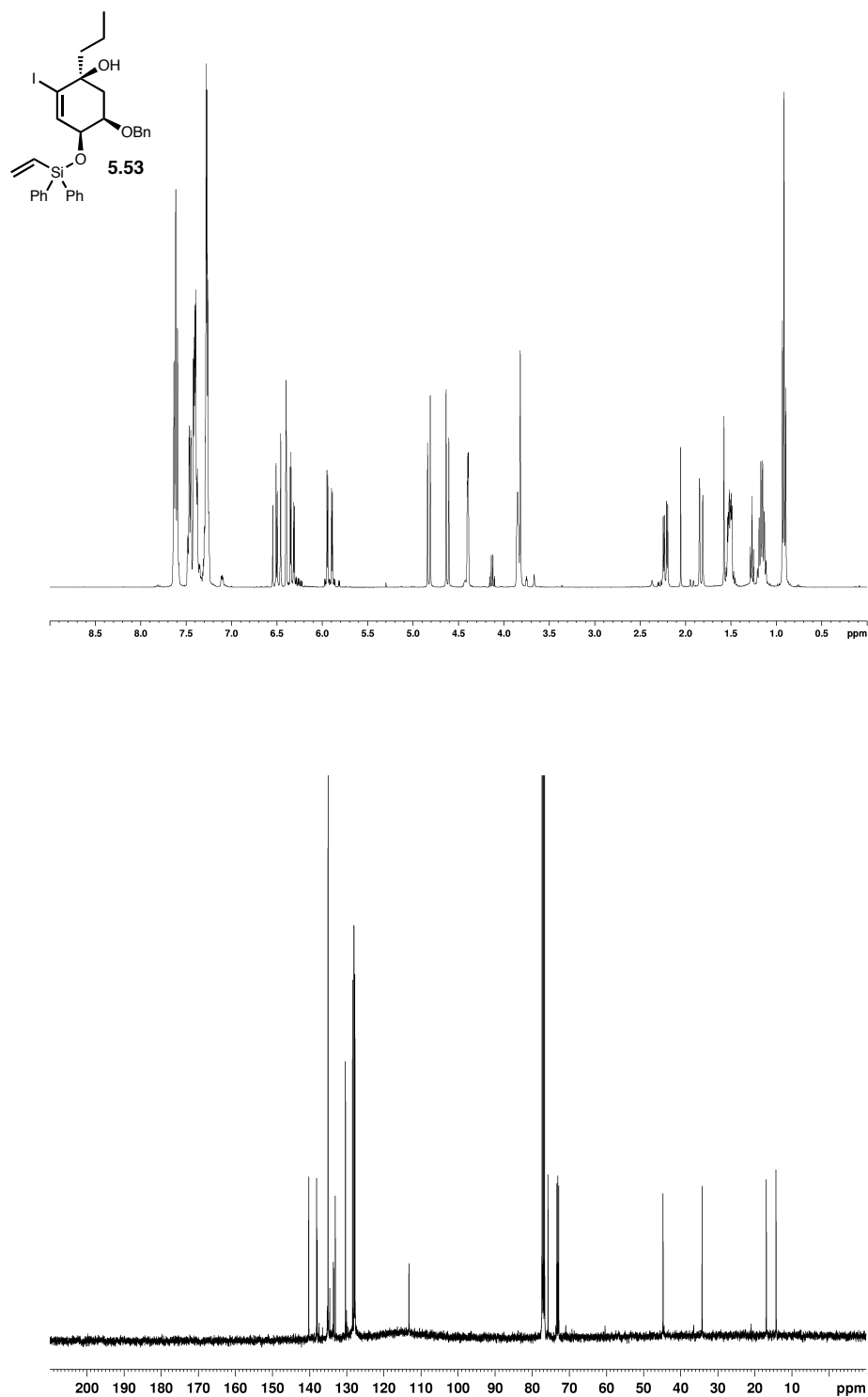


**Figure A3.29.**  $^1\text{H}$  NMR spectrum (400 MHz,  $\text{CDCl}_3$ ) and  $^{13}\text{C}$  NMR spectrum (100 MHz,  $\text{CDCl}_3$ ) of compound **5.53**.

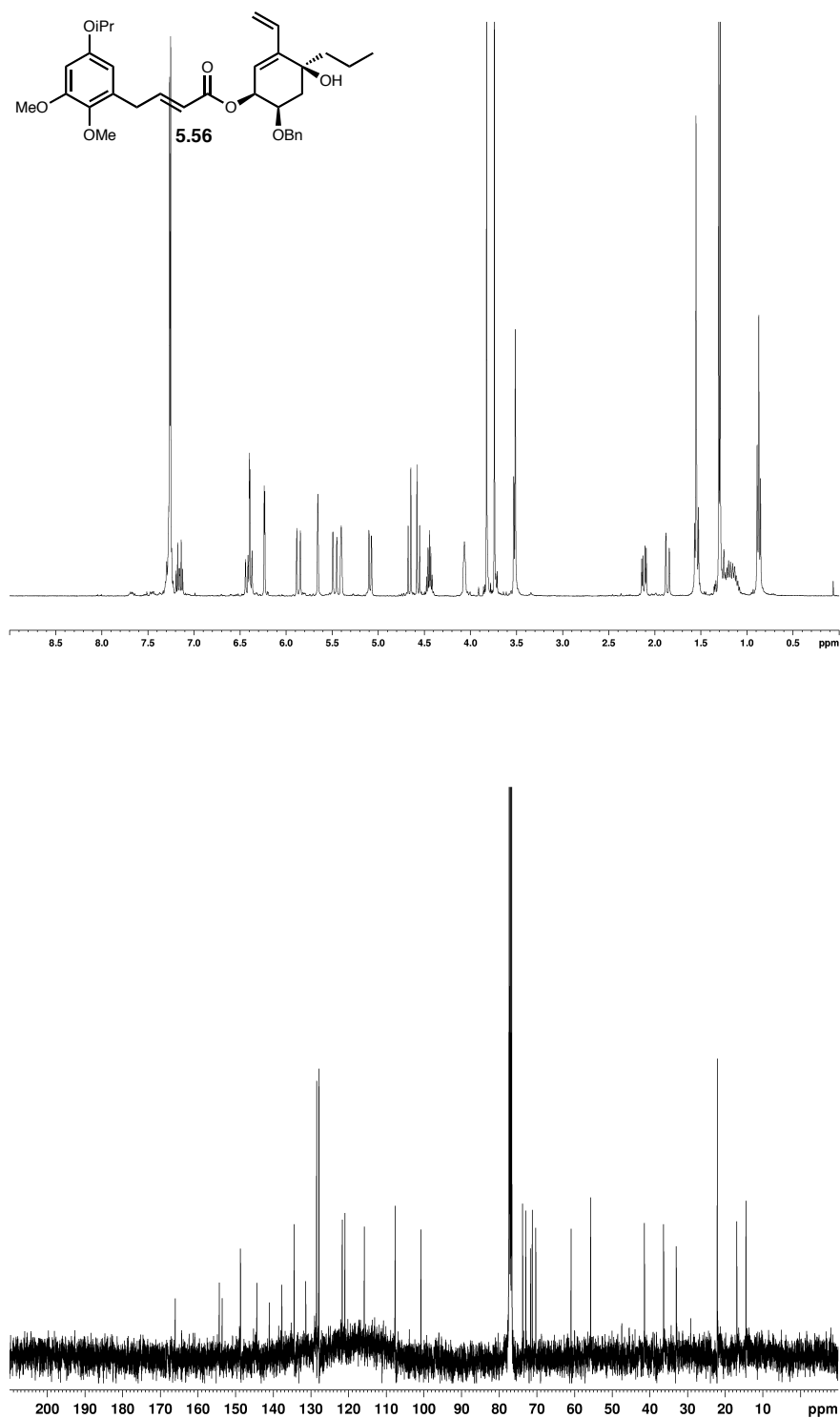


**Figure A3.30.**  $^1\text{H}$  NMR spectrum (400 MHz,  $\text{CDCl}_3$ ) and  $^{13}\text{C}$  NMR spectrum (100 MHz,  $\text{CDCl}_3$ ) of compound **5.56**.



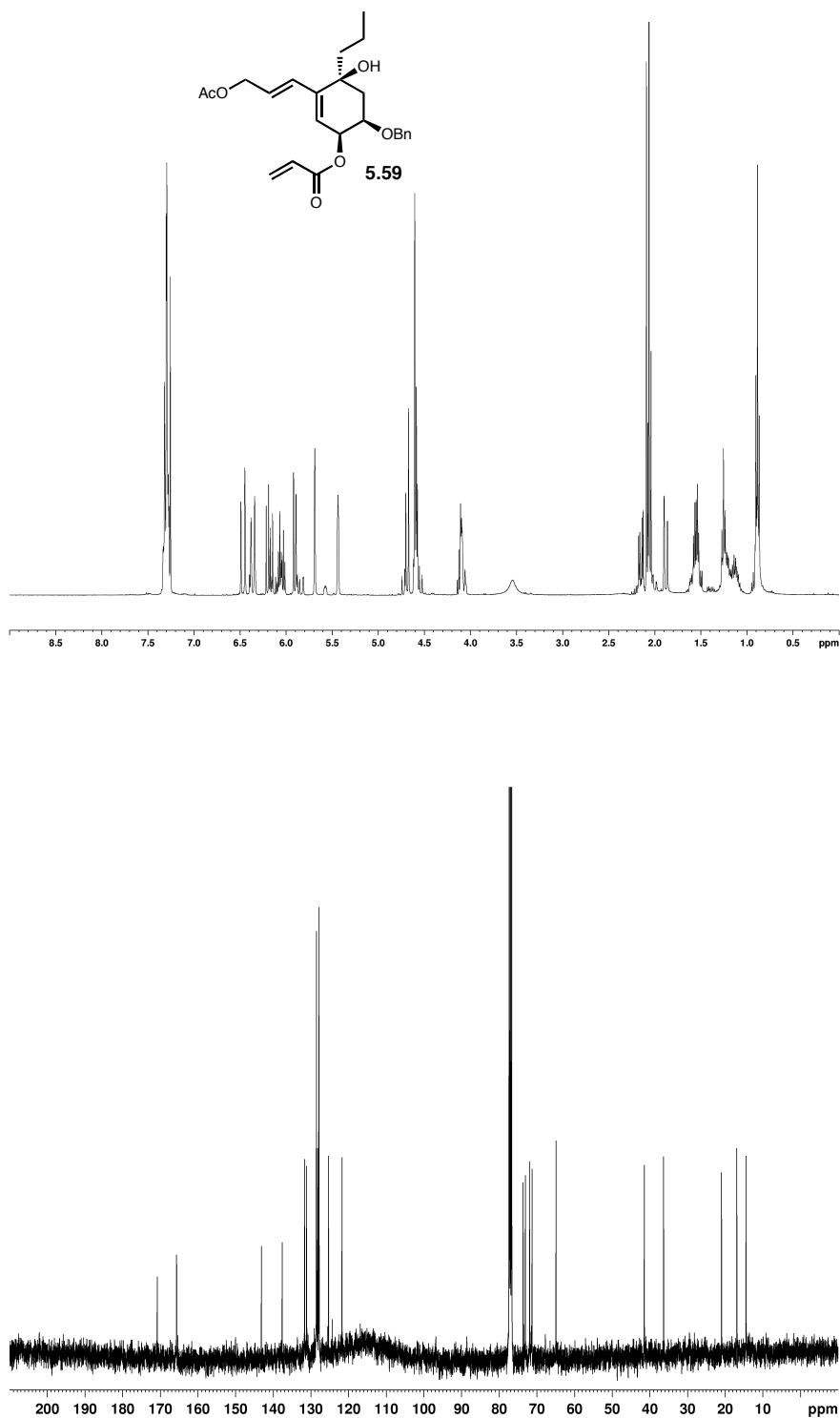


**Figure A3.32.** <sup>1</sup>H NMR spectrum (400 MHz, CDCl<sub>3</sub>) and <sup>13</sup>C NMR spectrum (100 MHz, CDCl<sub>3</sub>) of compound 5.59.

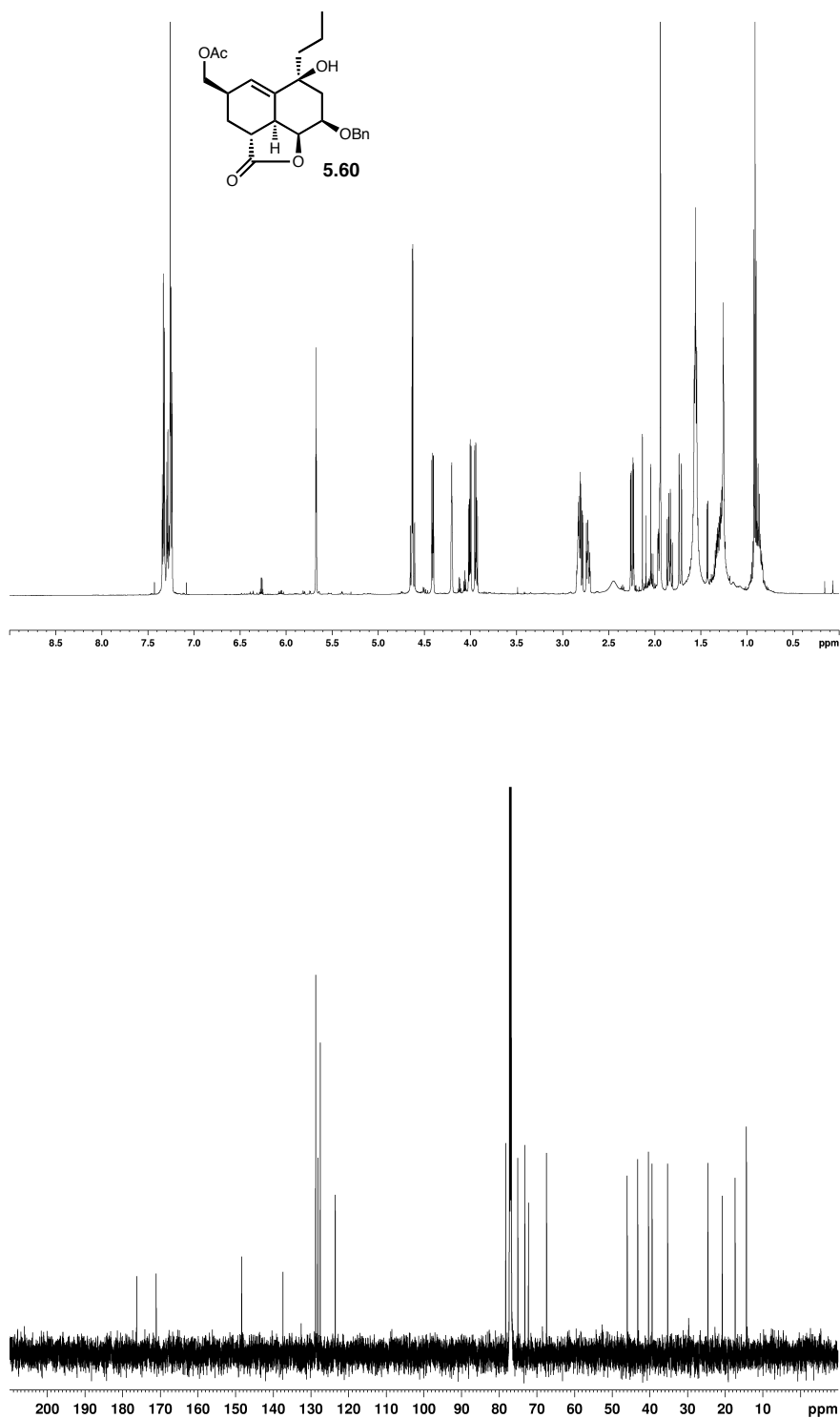


**Figure A3.33.**  $^1\text{H}$  NMR spectrum (600 MHz,  $\text{CDCl}_3$ ) and  $^{13}\text{C}$  NMR spectrum (150 MHz,  $\text{CDCl}_3$ ) of compound **5.60**.



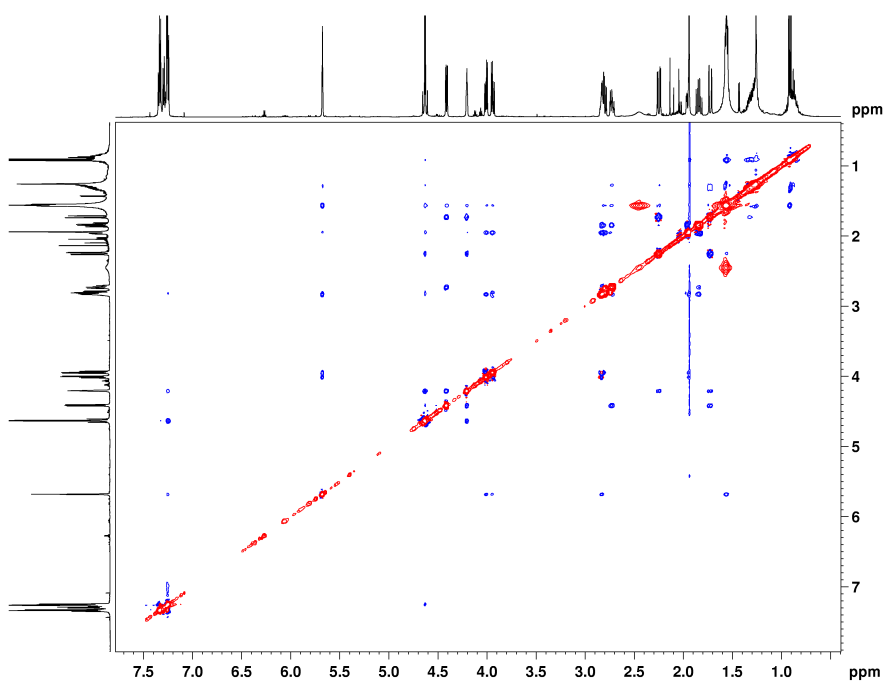
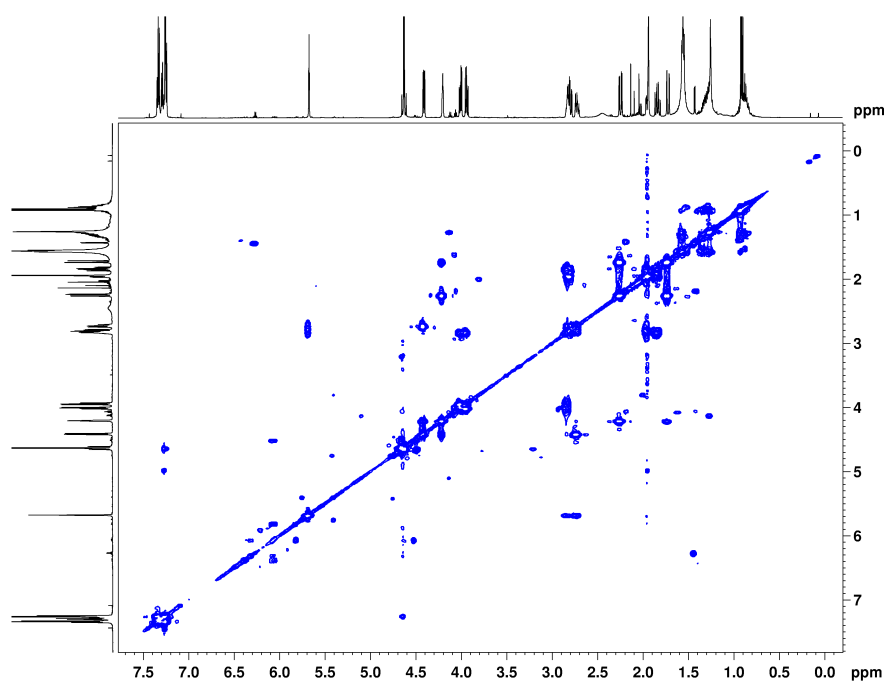


**Figure A3.34.** COSY spectrum (600 MHz,  $\text{CDCl}_3$ ) and NOESY spectrum (600 MHz,  $\text{CDCl}_3$ ) of compound **5.60**.

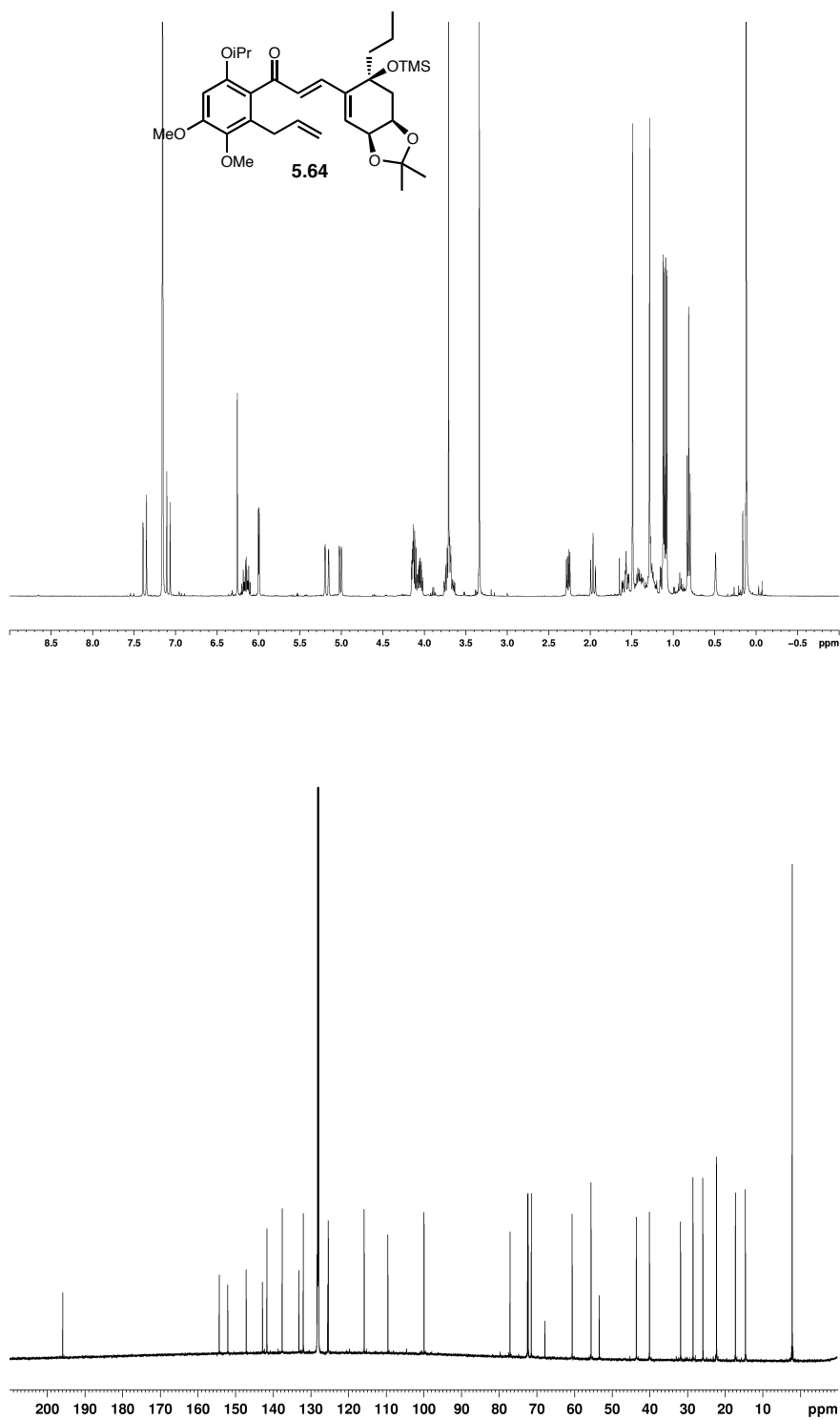


**Figure A3.35.**  $^1\text{H}$  NMR spectrum (400 MHz,  $\text{C}_6\text{D}_6$ ) and  $^{13}\text{C}$  NMR spectrum (150 MHz,  $\text{C}_6\text{D}_6$ ) of compound **5.64**.

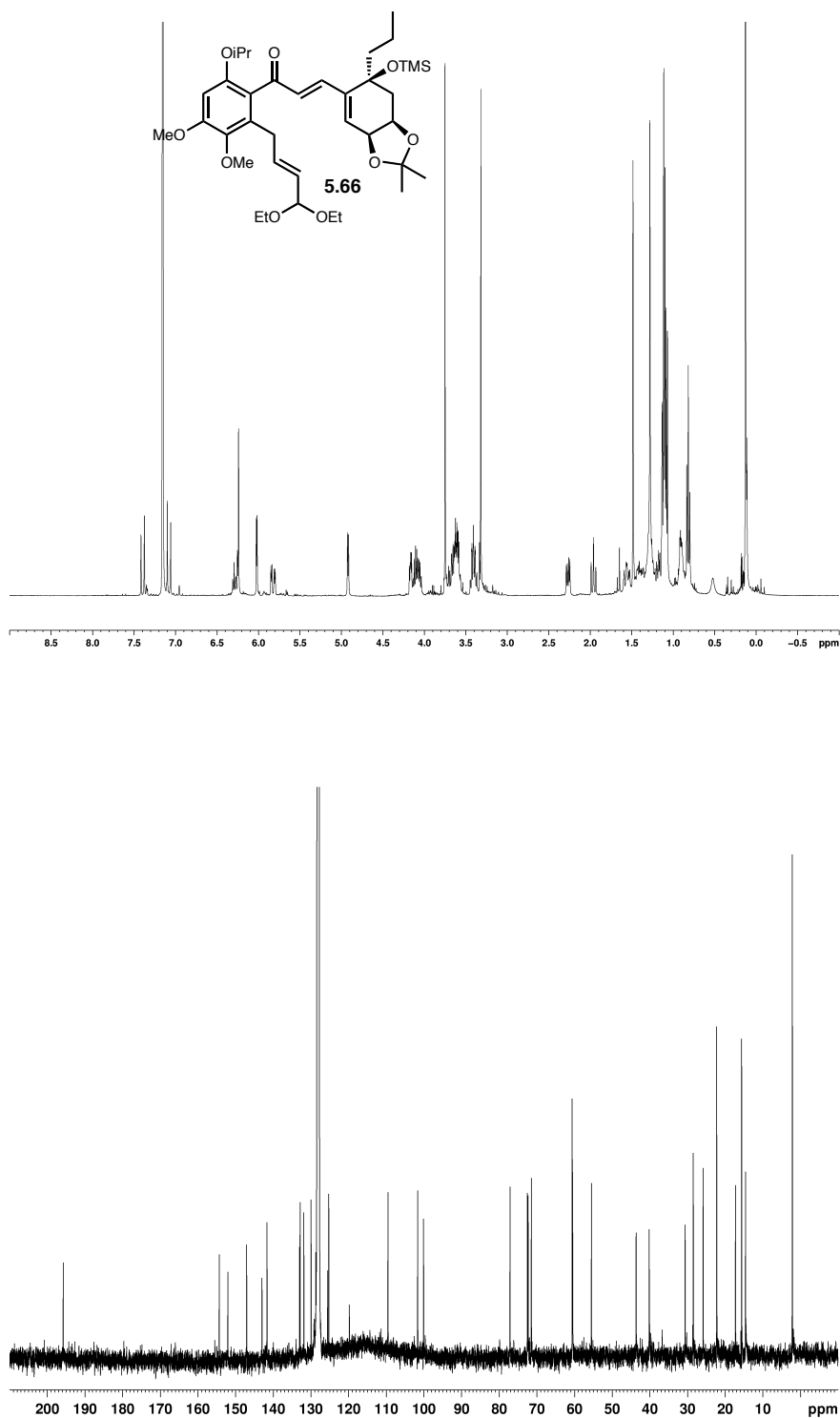


**Figure A3.36.**  $^1\text{H}$  NMR spectrum (400 MHz,  $\text{C}_6\text{D}_6$ ) and  $^{13}\text{C}$  NMR spectrum (100 MHz,  $\text{C}_6\text{D}_6$ ) of compound **5.66**.

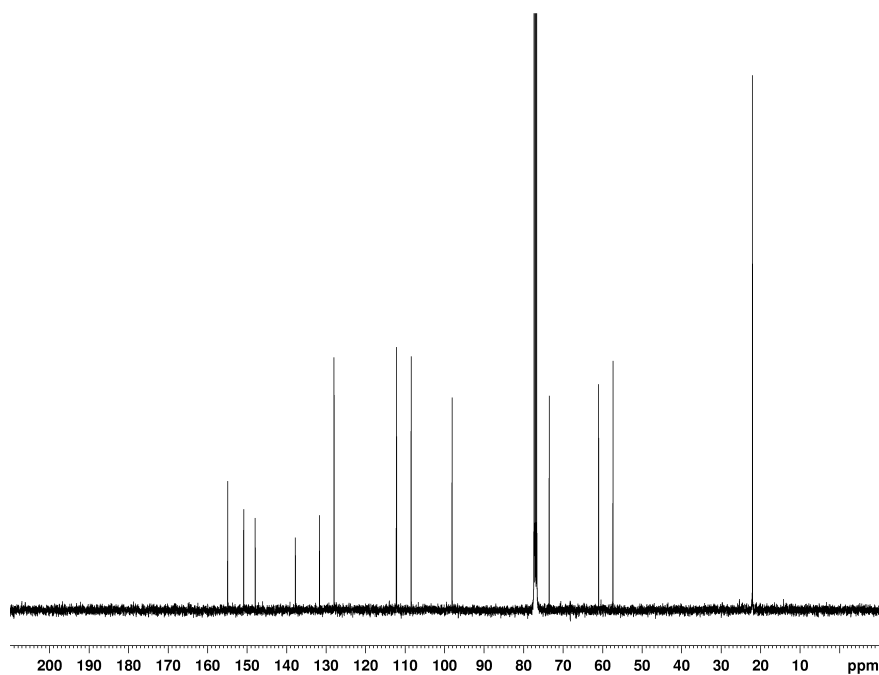
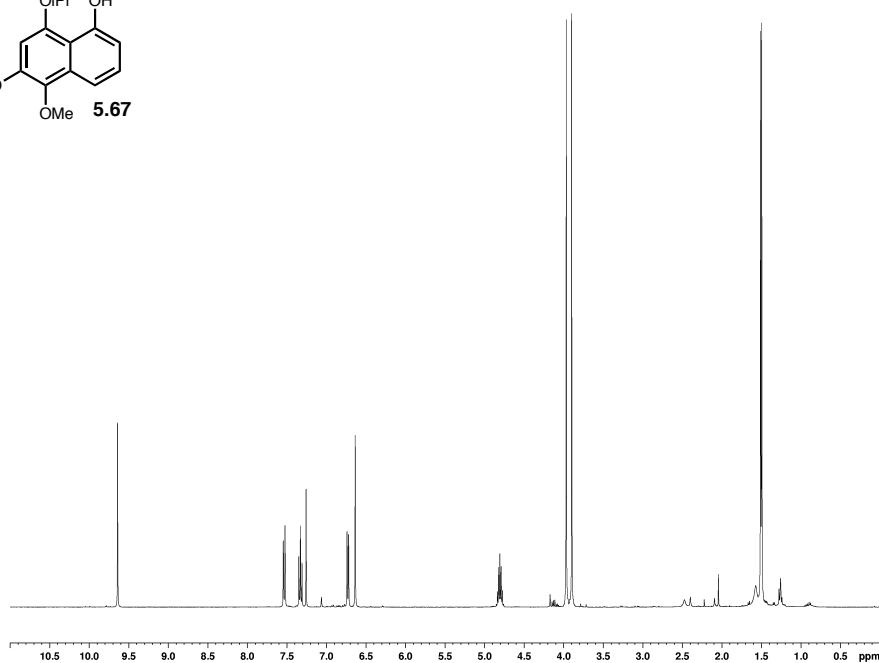
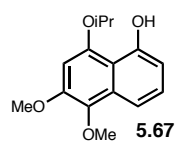


**Figure A3.37.**  $^1\text{H}$  NMR spectrum (400 MHz,  $\text{CDCl}_3$ ) and  $^{13}\text{C}$  NMR spectrum (100 MHz,  $\text{CDCl}_3$ ) of compound **5.67**.

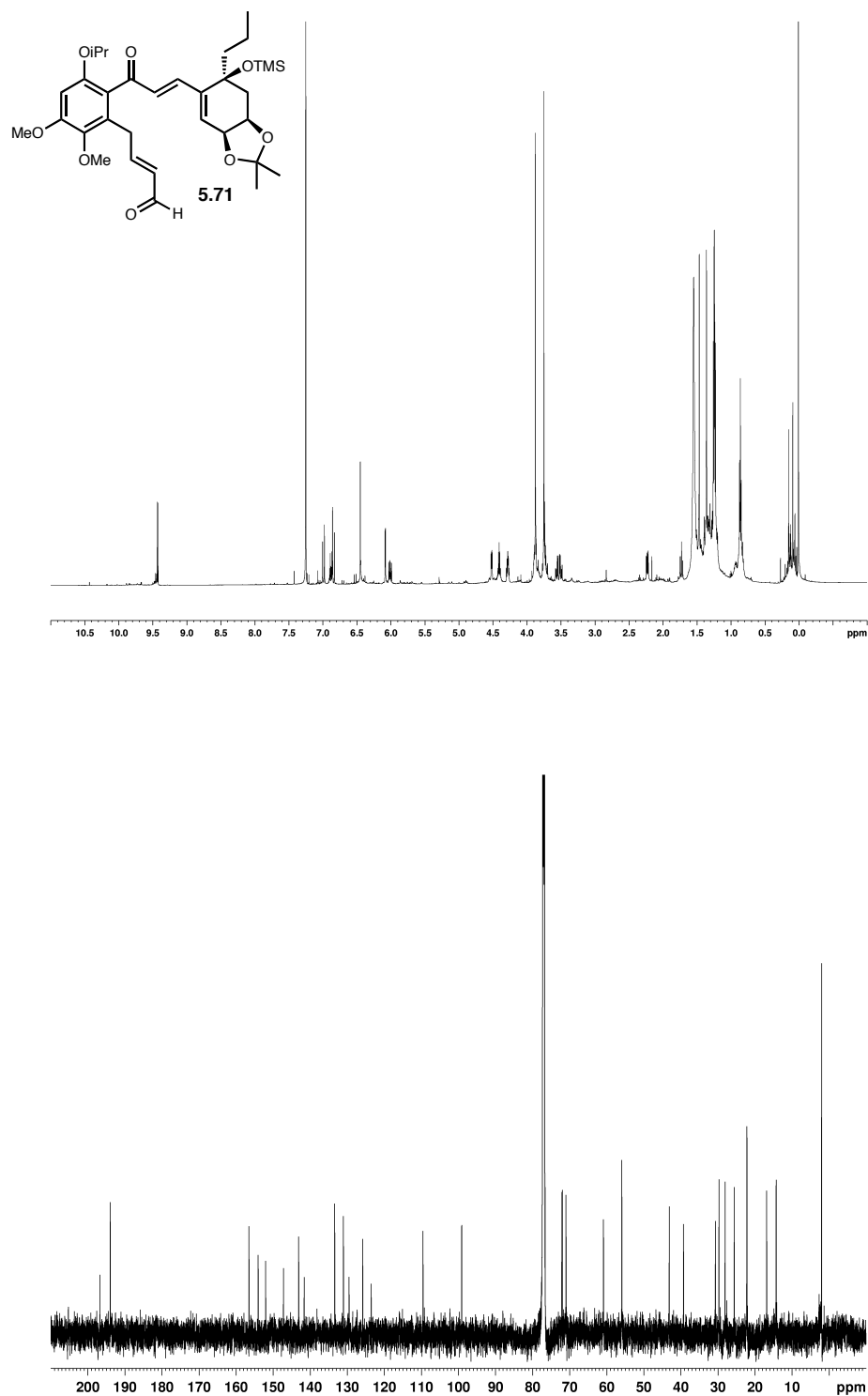


**Figure A3.38.**  $^1\text{H}$  NMR spectrum (400 MHz,  $\text{CDCl}_3$ ) and  $^{13}\text{C}$  NMR spectrum (150 MHz,  $\text{CDCl}_3$ ) of compound **5.71**.

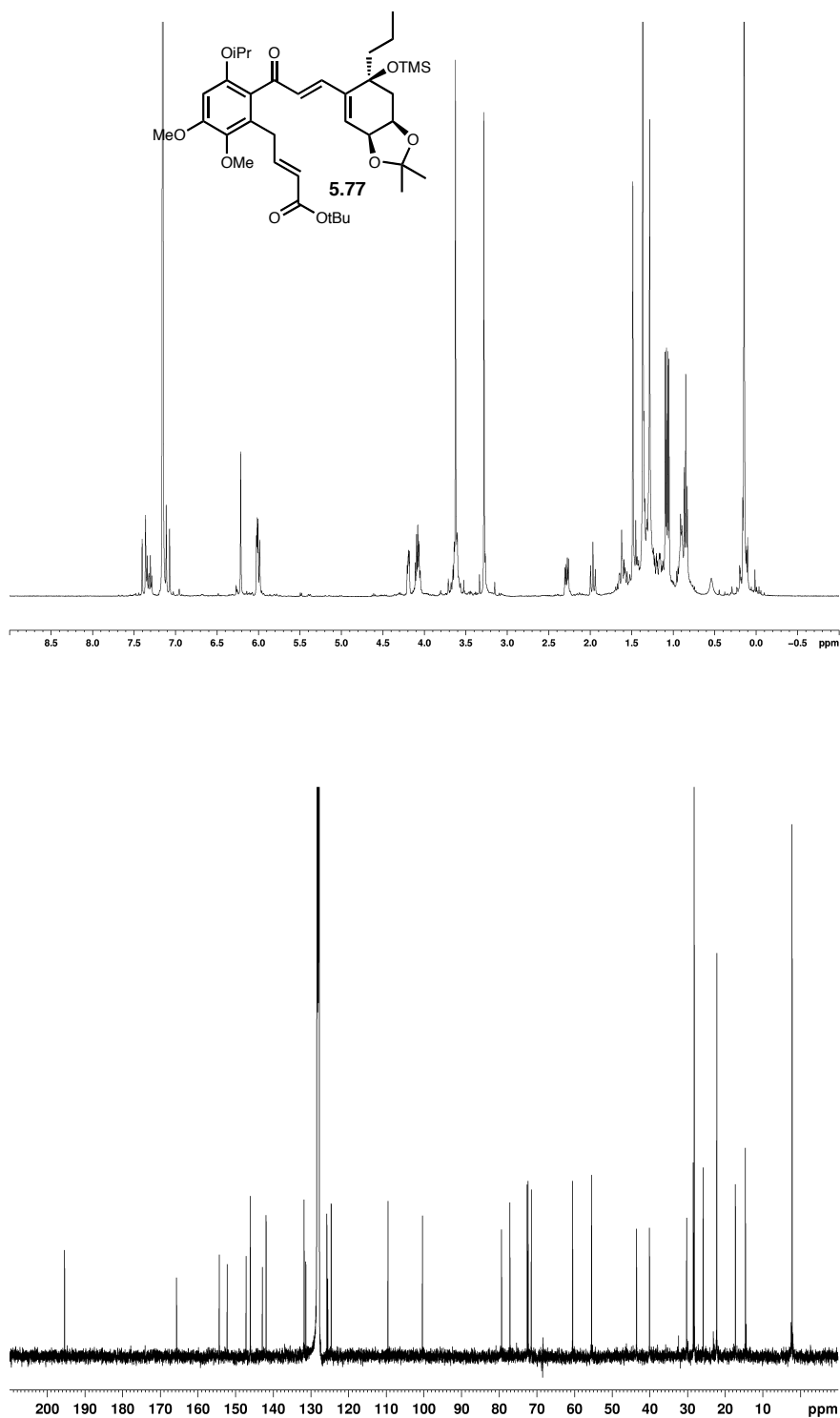


**Figure A3.39.**  $^1\text{H}$  NMR spectrum (400 MHz,  $\text{C}_6\text{D}_6$ ) and  $^{13}\text{C}$  NMR spectrum (100 MHz,  $\text{C}_6\text{D}_6$ ) of compound 5.77.



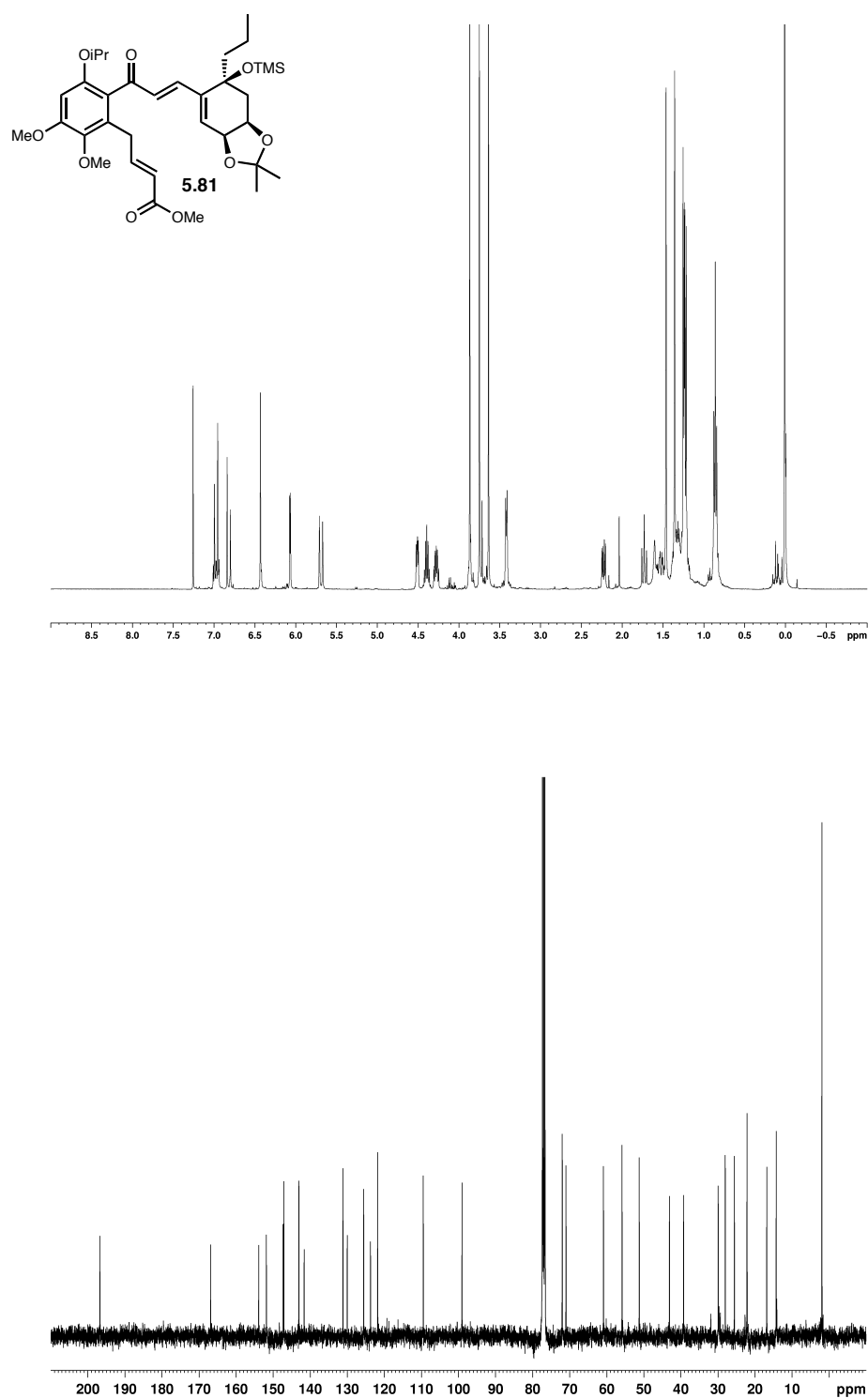


**Figure A3.41.**  $^1\text{H}$  NMR spectrum (400 MHz,  $\text{CDCl}_3$ ) and  $^{13}\text{C}$  NMR spectrum (100 MHz,  $\text{CDCl}_3$ ) of compound **5.81**.



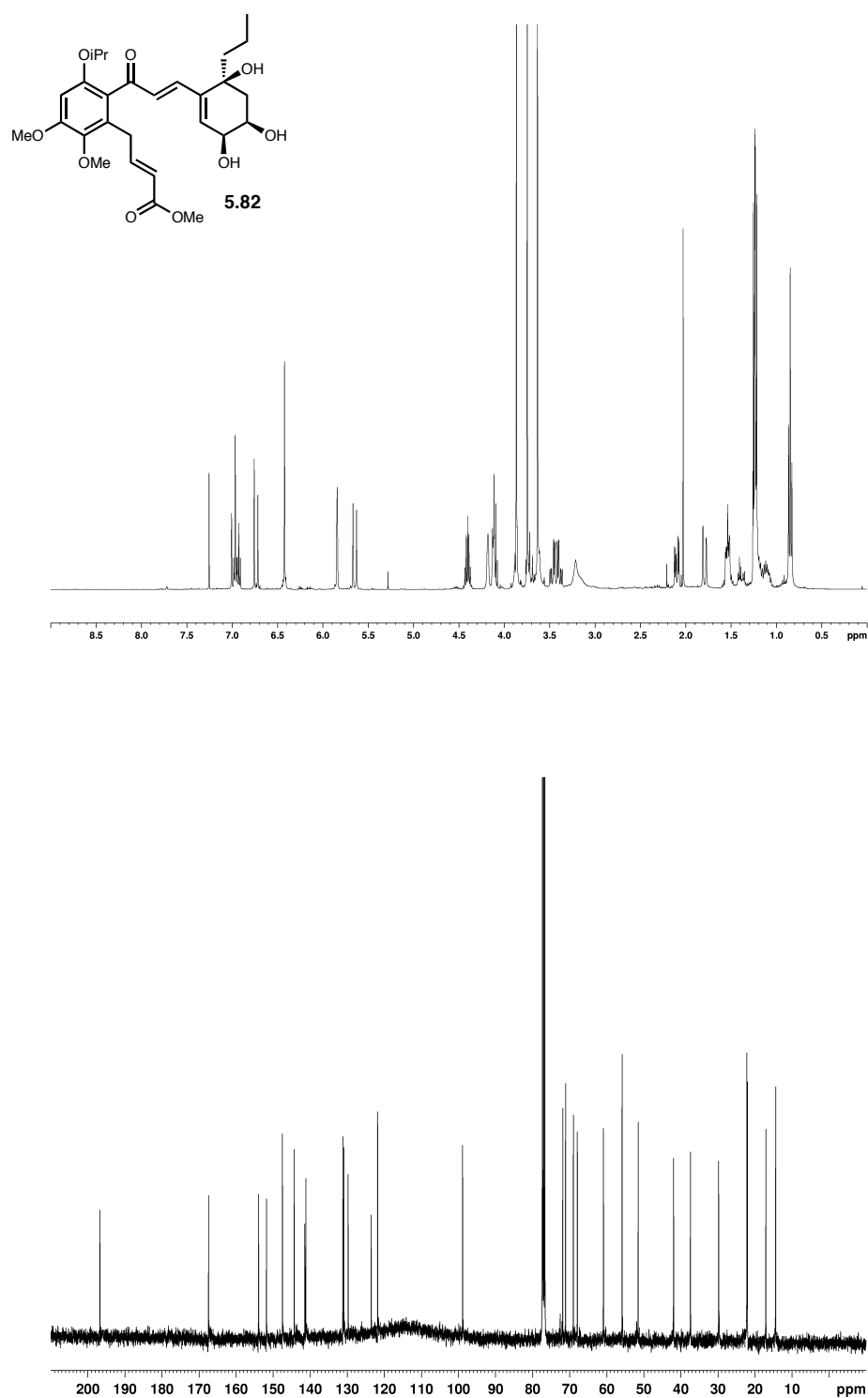


**Figure A3.42.**  $^1\text{H}$  NMR spectrum (400 MHz,  $\text{CDCl}_3$ ) and  $^{13}\text{C}$  NMR spectrum (100 MHz,  $\text{CDCl}_3$ ) of compound **5.82**.